UNIVERSITY OF CALIFORNIA

Santa Barbara

Synthesis, Characterization, and Reactivity of "Masked" Terminal Nickel Sulfides

A dissertation submitted in partial satisfaction of the

requirements for the degree Doctor of Philosophy

in Chemistry

by

Nathaniel J. Hartmann

Committee in charge:

Professor Trevor W. Hayton, Chair

Professor Peter C. Ford

Professor Susannah L. Scott

Professor Javier Read de Alaniz

September 2018

The dissertation of Nathaniel J. Hartmann is approved.

_____

Professor Peter C. Ford

_____

Professor Susannah L. Scott

_____

Professor Javier Read de Alaniz

_____

Professor Trevor W. Hayton, Committee Chair

June 2018

Synthesis, Characterization, and Reactivity of "Masked" Terminal Nickel Sulfides

Nathaniel J. Hartmann

Acknowledgements

I would like to begin by thanking my undergraduate research advisor, Prof. Benjamin Lovaasen, for giving me my initial opportunity to get into the lab and try my hand at inorganic synthesis and for getting me excited about research. Of course, none of the work that I have done here at UCSB would have been possible without the patient guidance of my boss, Prof. Trevor Hayton, who always pushed me to do my best and taught me to critically assess my own work. I am grateful to him for having helped shape me into the chemist I am today. I would also like to thank my thesis committee members, Prof. Peter Ford, Prof, Susannah Scott, and Prof. Javier Read de Alaniz, for their advice and support throughout my graduate school career.

Thanks to the former Hayton group members, Dr. Ellie Owens, Dr. Danil Smiles, and Ed Paul, for welcoming me into the group and Dr. Bi Nguyen and Dr. Peter Damon, for sharing glove box space and supervising me as I learned how to repair vacuum pumps.

For financial support of this work, I would like to thank the National Science Foundation (CHE 1361654). This research made use of the SQUID Magnetometer of the Materials Research Laboratory, an NSF MRSEC (DMR 1121053), and the 400 MHz NMR Spectrometer of the Chemistry Department, an NIH SIG (1S10OD012077-01A1).

Finally, I would like to thank my family and friends (special shout-out to Andre for helping me track down Javier) for supporting me throughout my many years of education.

Vita of Nathaniel J Hartmann

June 2018

EDUCATION

Doctor of Philosophy in Chemistry (expected) June 2018
University of California, Santa Barbara
Advisor: Professor Trevor W. Hayton
Dissertation: "Synthesis, Characterization, and Reactivity of "Masked" Terminal Nickel Sulfides"

Bachelor of Science, Chemistry May 2013
Wheaton College, Wheaton, IL
Advisor: Professor Benjamin Lovaasen

PROFESSIONAL EMPLOYMENT

12/13-Present	Graduate Student Researcher, Dept. of Chemistry, UCSB
09/13-06/18	Teaching Assistant, Dept. of Chemistry, UCSB
01/12-12/12	Undergraduate Researcher, Dept. of Chemistry, Wheaton College
08/08-05/11	Teaching Assistant, Dept. of Chemistry, Wheaton College

PUBLICATIONS

N. J. Hartmann, G. Wu, T. W. Hayton, Trapping of an Ni^{II} Sulfide by a Co^{I} Fulvene Complex, *Organometallics,* **2017**, *36*, 1765.

N. J. Hartmann, G. Wu, T. W. Hayton, Reactivity of a Nickel Sulfide with Carbon Monoxide and Nitric Oxide, *Journal of the American Chemical Society,* **2016**, *138*, 12352.

N. J. Hartmann, G. Wu, T. W. Hayton, Activation of CS_2 by a "Masked" Terminal Nickel Sulfide, *Dalton Transactions,* **2016**, *45*, 14508.

N. J. Hartmann, G. Wu, T. W. Hayton, Synthesis of a "Masked" Terminal Nickel(II) Sulfide by Reductive Deprotection and its Reaction with Nitrous Oxide, *Angewandte Chemie International Edition*, **2015**, *54*, 14956.

AWARDS

- Paul Wright Medal and Prize in Chemistry: October 2012
- President's Award: June 2009

Major Field: Inorganic Chemistry

Studies in Transition Metal Coordination Chemistry

Abstract

Synthesis, Characterization, and Reactivity of "Masked" Terminal Nickel Sulfides

by

Nathaniel J. Hartmann

Treatment of the Ni(II) chloride complexes, $[L^{R}Ni^{II}Cl]$ (L^{R} = {(2,6-$^{i}Pr_2C_6H_3$)NC(R)}$_2$CH, R = Me, ^{t}Bu) with 1 equiv of $KSCPh_3$ affords the Ni(II) triphenylmethylthiolate complexes, $[L^{R}Ni^{II}(SCPh_3)]$, in good yields. The reaction of $[L^{R}Ni^{II}(SCPh_3)]$ with 2 equiv of KC_8 and L (L = 18-crown-6 or 2,2,2-cryptand) affords both $[K(L)][L^{R}Ni^{II}(S)]$ and $[K(L)][CPh_3]$ via reductive deprotection of the triphenylmethyl group. Treatment of $[K(18\text{-crown-6})][L^{tBu}Ni^{II}(S)]$ with Ph_2SiH_2 affords a Ni(I) SH^- complex, $[K(18\text{-crown-6})][L^{tBu}Ni^{I}(SH)]$. Treatment of $[K(18\text{-crown-6})][L^{tBu}Ni^{II}(S)]$ with Me_3SiOTf affords a Ni(II) trimethylsilanethiolato complex $[L^{tBu}Ni^{II}(SSiMe_3)]$.

Treatment of $[L^{tBu}Ni^{II}(SCPh_3)]$ with 2 equiv of decamethylcobaltocene (Cp^*_2Co) generates a transient Ni^{II} sulfide complex, $[Cp^*_2Co][L^{tBu}Ni^{II}(S)]$. A subsequent deprotonation of $[Cp^*_2Co]^+$ by $[CPh_3]^-$ gives the Co^{I} fulvenyl complex, $[Cp^*Co(C_5Me_4CH_2)]$, which couples with the sulfide ligand in $[Cp^*_2Co][L^{tBu}Ni^{II}(S)]$ to form a Ni(I) cobaltocenium thiolate complex, $[L^{tBu}Ni^{I}(SCH_2Me_4C_5)Co(Cp^*)]$, concomitant with the reduction of the cobaltocenium cation.

Treatment of [K(18-crown-6)][$L^{tBu}Ni^{II}$(S)] with CS_2 yields the Ni(II) trithiocarbonate complex, [K(18-crown-6)][$L^{tBu}Ni^{II}$(*S*,*S*:κ_2-CS_3)]. Treatment of [K(2,2,2-cryptand)][$L^{tBu}Ni^{II}$(S)] with CS_2 generates the double insertion product, a Ni(II) trithiocarbonate dithiocarboxylate complex, [K(2,2,2-cryptand)][(*S*,*S*:κ_2-CS_3)Ni^{II}{*S*,*S*:κ_2-CS_2(L^{tBu})}].

Treatment of [K(18-crown-6)][$L^{tBu}Ni^{II}$(S)] with CO affords a Ni(II) carbonyl sulfide complex, [K(18-crown-6)][$L^{tBu}Ni^{II}$(*S*,*C*:η_2-SCO]. Treatment of [K(18-crown-6)][$L^{tBu}Ni^{II}$(S)] with NO yields a nickel nitrosyl complex, [L^{tBu}Ni(NO)], and a perthionitrite salt, [K(18-crown-6)][SSNO].

Treatment of [K(18-crown-6)][$L^{tBu}Ni^{II}$(S)] with N_2O yields an unprecedented Ni(II) thiohyponitrite complex, [K(18-crown-6)][$L^{tBu}Ni^{II}$(κ^2-SNNO)]. Gentle thermolysis of [K(18-crown-6)][$L^{tBu}Ni^{II}$(κ^2-SNNO)] results in extrusion of N_2 and formation of a thioperoxide complex, [K(18-crown-6)][$L^{tBu}Ni^{II}$(η^2-SO)]. Treatment of [K(18-crown-6)][$L^{tBu}Ni^{II}$(η^2-SO)] with CO, forms [K(18-crown-6)][$L^{tBu}Ni^{II}$(S)] along with CO_2, via O-atom abstraction. The Ni(II) sulfide then reacts with CO or CO_2 to form [K(18-crown-6)][$L^{tBu}Ni^{II}$(η^2-SCO)] and [K(18-crown-6)][L^{tBu}Ni(*S*,*O*:κ^2-SCO_2)], respectively. The thioperoxide complex, [K(18-crown-6)][$L^{tBu}Ni^{II}$(η^2-SO)], can also react with the newly formed CO_2 to form a putative monothiopercarbonate complex, [K(18-crown-6)][$L^{tBu}Ni^{II}$(κ^2-$SOCO_2$)], which can then transfer an S atom to CO, forming COS and [K(18-crown-6)][$L^{tBu}Ni^{II}$(κ^2-CO_3)].

Table of Contents

List of Figures

List of Schemes

List of Tables

List of Abbreviations

°	degree
°C	degree Celsius
ε	extinction coefficient *or* bond critical point ellipticity
Δ	heat *or* difference
δ	chemical shift, ppm
η^n	hapticity of order n
κ^n	denticity of order n
μ	micro or denotes bridging atom
ν	stretching frequency, cm^{-1}
ρ	bond critical point electron density
Å	angstrom, 10^{-10} m
Ar	aryl
av.	average
BCP	bond critical point
BDE	bond dissociation energy
br	broad
Bu	butyl
calcd.	calculated
$^{13}C\{^1H\}$	carbon-13 proton decoupled
ca.	circa
Cp^*	η^5-C_5Me_5
Cp	η^5-C_5H_5
cm^{-1}	wavenumber
CV	cyclic voltammetry
d	doublet *or* day(s)
d_n	deuterated in *n* positions
deg	degree
DFT	density functional theory
DME	1,2-dimethoxyethane
$E_{1/2}$	average wave potential, $(E_{p,a} + E_{p,c})/2$
$E_{p,a}$	anodic half-wave potential
$E_{p,c}$	cathodic half-wave potential
e^-	electron
equiv	equivalent
Et_2O	diethyl ether
Et	ethyl
$^{19}F\{^1H\}$	fluorine-19 proton decoupled
Fc	ferrocene

FTIR	Fourier transform infrared
g	gram(s)
GOF	goodness of fit
H	enthalpy *or* bond critical point energy density
^{1}H	hydrogen-1
^{1}H{^{31}P}	hydrogen-1 phosphorus decoupled
h	hour(s)
Hz	Hertz
$i_{p,a}$	anodic half-wave current
$i_{p,c}$	cathodic half-wave current
^{i}Pr	isopropyl
IR	infrared
J	NMR coupling constant
K	Kelvin
L	liter *or* ligand
^{7}Li{^{1}H}	lithium-7 proton decoupled
M	Molar
m	meter *or* multiplet *or* medium
m	meta
Me	methyl
min	minute(s)
mL	milliliter(s)
mmol	millimole(s)
mol	mole(s)
^{n}Bu	n-butyl
NMR	nuclear magnetic resonance
o	ortho
ORTEP	Oak Ridge Thermal Ellipsoid Program
OTf	triflate, $[CF_3SO_3]^-$
p	para
^{31}P{^{1}H}	phosphorus-31 proton decoupled
Ph	phenyl
ppm	parts per million
py	pyridine
q	quartet
R	alkyl
redox	reduction-oxidation
RT	room temperature
s	singlet *or* strong *or* second(s)
sh	shoulder

t	triplet
^{t}Bu	*tert*-butyl
THF	tetrahydrofuran
UV	ultraviolet
V	Volt
vis	visible
VT	variable temperature
w	weak
xs	excess

Chapter 1 Introduction

Table of Contents

1.1 Metal-Ligand Multiple Bonds and The Oxo Wall

Transition metal complexes containing oxo (O^{2-}), sulfide (S^{2-}), imido (NR^{2-}), nitrido (N^{3-}), and carbene (CR_2^{2-}) ligands play important roles throughout inorganic chemistry.[1] For example, metal oxos have applications for both H-atom abstraction and O-atom transfer reactions[2–5] and have been shown to be a key intermediate in the catalytic cycle of cytochrome P450.[6] While metal sulfides are known to serve both structural[7–11] and catalytic[12,13] roles in the active sites of biological enzymes such as NiFe and MoCu CO dehydrogenases (CODH), the "orange protein complex", and N_2O reductase (N_2OR); and are likely intermediates in heterogeneous hydrodesulfurization catalysis.[14–16] Finally, metal nitridos and imidos are thought to be important intermediates in the critical N_2 fixation processes carried out biologically by the iron-molybdenum cofactor (FeMoco) nitrogenase enzyme and industrially using the Haber-Bosch process.[17–23]

Complexes with metal-ligand (M=L) multiple bonds are numerous for the early and mid-transition metals (groups 4-8).[24–28] However, only a small handful of late transition metal (groups 9, 10, and 11) complexes containing M=L multiple bonds have been isolated. The small number of these species can be attributed to the electronic and structural requirements for the formation of stabilizing M=L multiple bonds. The ligand field theory behind the requirements for the formation of M=L multiple bonds was first put forth by Ballhausen and Gray in 1963, and predicts the presence of a so called "oxo wall" between groups 8 and 9 on the periodic table (Figure 1.1).[29,30]

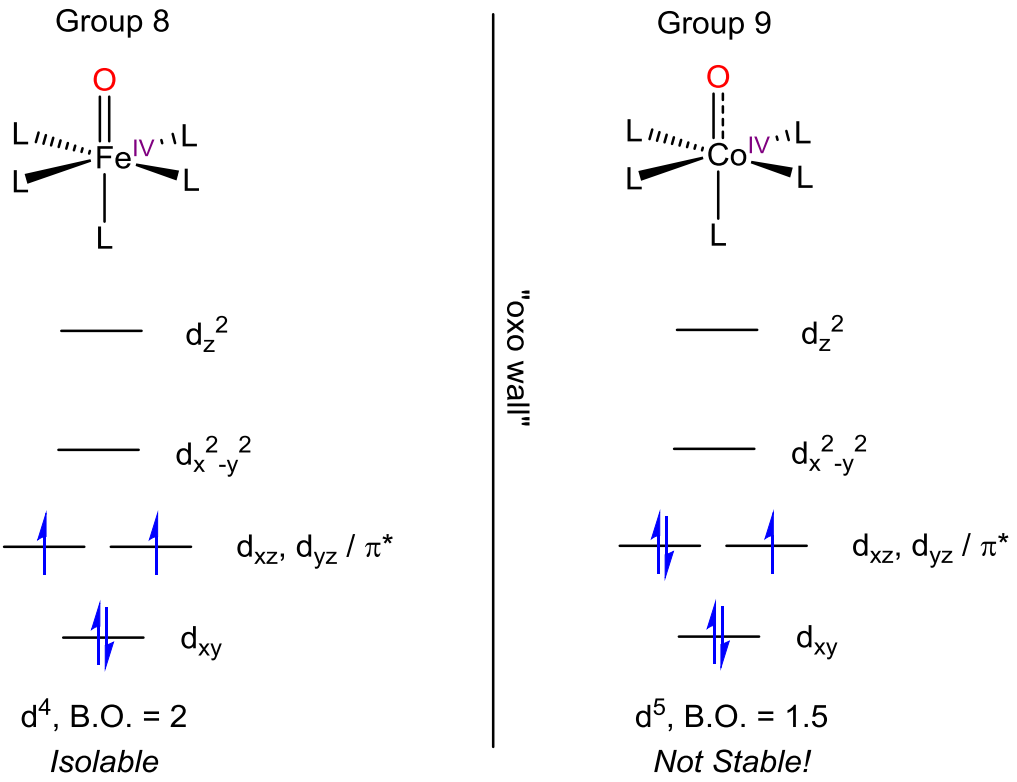

Figure 1.1. Effects of d-electron count on the stability of M=O bonds in tetragonal complexes

According to this theory, the ability of a tetragonal (C_{4v}) transition metal complex to form an M-O double bond is dependent upon the occupancy of the of the M=O π* orbitals. As represented in Figure 1.1, the d^4 $[Fe^{IV}(L)_5(O)]$ system would be predicted to contain a stable Fe=O double bond, while the analogous d^5 $[Co^{IV}(L)_5(O)]$ system is predicted to be unstable due to the population of the π* orbitals with an additional electron. However, since the oxo wall theory is formulated for tetragonal systems, it can be circumvented by reducing the coordination number of the metal center. Which makes additional d orbitals available for M=O multiple bonding.

There are two examples of late metal terminal oxos, $[Ir^{V}(O)(Mes)_3]$ (Mes = 2,4,6-$Me_3C_6H_2$) and $[Pt^{IV}(O)(PCN)][BF_4]$ (PCN = $C_6H_3[CH_2P(tBu)_2](CH_2CH_2NMe_2)$), whose

stability can be rationalized by this mechanism, specifically by reduction of metal coordination number from 6 to 4.[31,32] A proposed d-orbital splitting diagram for [Ir^{V}(O)$(Mes)_3$] is presented in Figure 1.2. Notably, the change from tetragonal (C_{4v}) to trigonal (C_{3v}) symmetry results in a reordering of the d-orbitals such that an additional non-bonding orbital becomes lower in energy than the M=O π* orbitals.[33] Consequently, this complex has only 2 π* electrons, resulting in the presence of a stable Ir=O double bond. As noted above, this complex is not in violation of the oxo wall. Moreover, it illustrates the importance of reduced metal coordination number for the synthesis of late transition M=L multiple bonds.

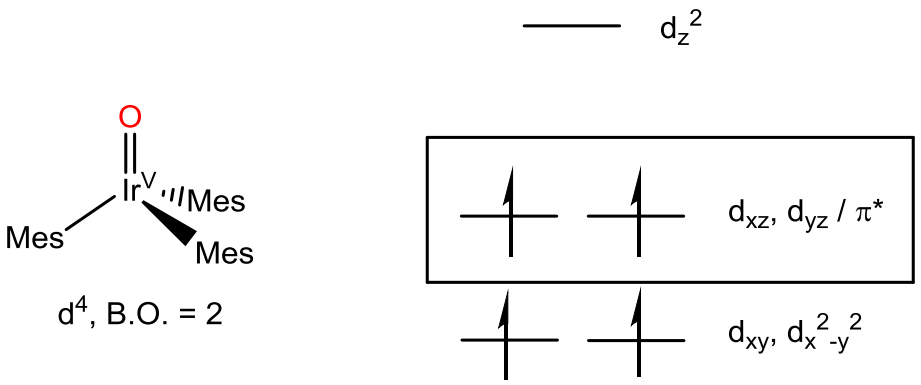

Figure 1.2. Proposed electronic structure of [Ir^{V}(O)$(Mes)_3$]

Building off of the initial success of this strategy for the synthesis of four-coordinate Ir oxo and imido complexes in the late '80s and early '90s,[31,34,35] there has been a notable growth in the number of late transition metal complexes with terminal M=L multiple bonds. In addition to the two oxo complexes mentioned above,[31,32] terminal nitride,[36–38] imido,[39–56] phosphido (PR^{2-}),[57–62] and carbene[63–66] complexes have also been reported (Figure 1.3).[62,67] Like [Ir^{V}(O)$(Mes)_3$] and [Pt^{IV}(O)(PCN)][BF_4], all of these complexes feature reduced metal coordination numbers (2-5), that allow for the formation of stable M=L multiple bonds.

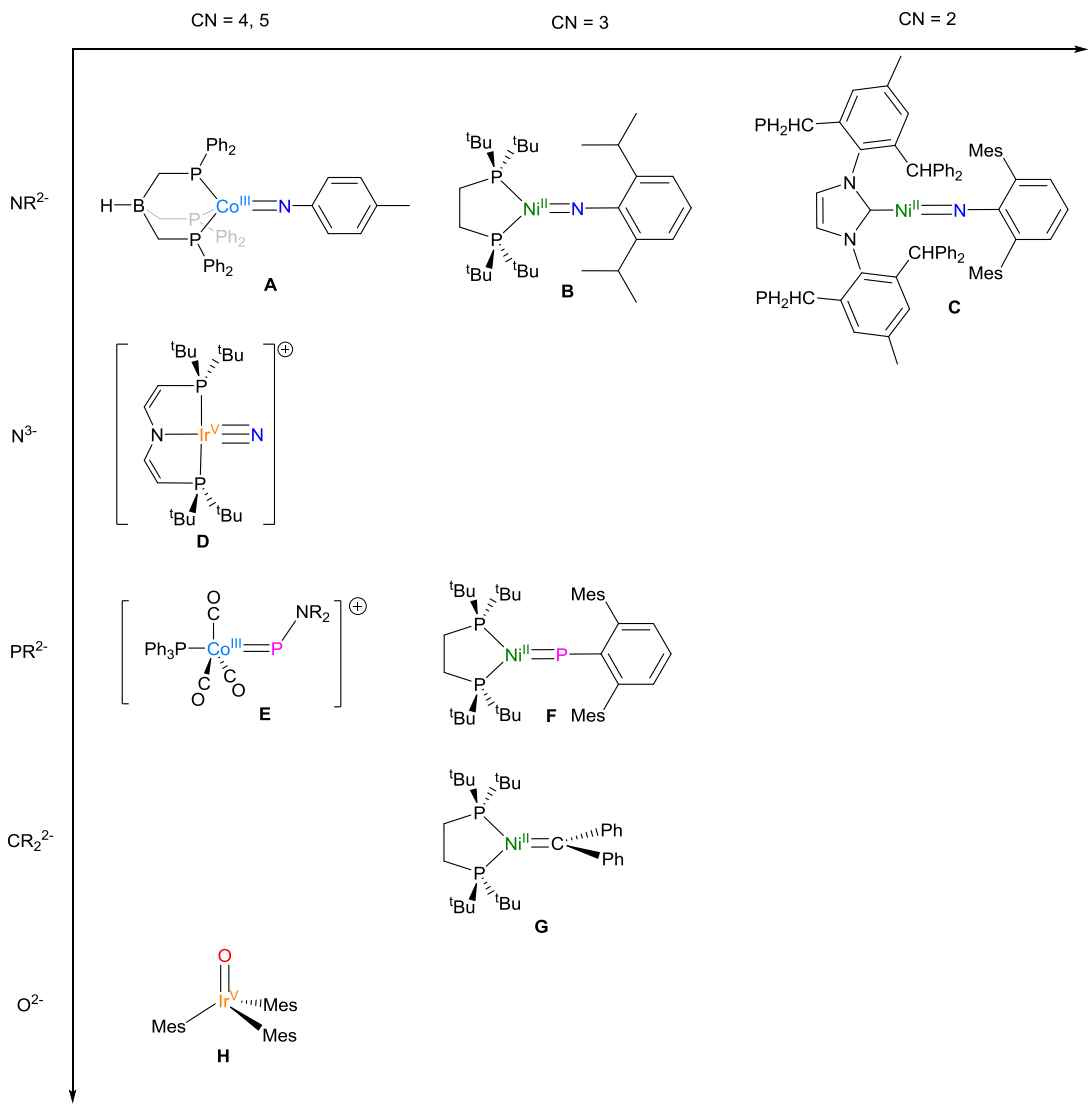

Figure 1.3. Examples of isolated late transition metal complexes with M=L multiple bonds. **A**, Ref. 39; **B**, Ref. 68; **C,** Ref. 50; **D**, Ref. 37; **E**, Ref. 58; **F**, Ref. 57, **G**, Ref. 64, **H**, Ref 31

1.2 Synthesis and Reactivity of Late Metal-Ligand Multiple Bond Containing Complexes

A growing understanding of the steric and electronic requirements for the synthesis of late transition metal complexes with M=L multiple bonds has led to the isolation a variety of these species. Representative examples of reported synthetic procedures can be found in Scheme 1.1. Late metal oxo complexes have been prepared by reactions with O_2 or oxo

transfer regents such as Me_3NO and dimethyloxirane (Scheme 1.1 A). The two reported terminal Ir nitride complexes were prepared via elimination of N_2 from the corresponding Ir azido (N_3^-) species (Scheme 1.1 B). Terminal imido complexes are most commonly prepared via a 2 electron nitrene group transfer using aryl or alkyl azides (RN_3) (Scheme 1.1 C). Late metal imidos and phosphidos have also been successfully synthesized via both H-atom abstraction or deprotonation of metal amide (NHR^-) and phosphide (PHR^-) species, respectively (Scheme 1.1 D-E). While, phosphinidene complexes have been prepared via the dehalogenation of a chloroaminophosphido ($PClNR_2^-$) ligand and via dehydroalogenation of primary phosphines (PH_2R) (Scheme 1.1 F-G). Finally, terminal carbenes have been isolated via N_2 elimination from diazoalkanes (N_2CR_2) (Scheme 1.1 H). This family of complexes is highly reactive and they are capable of effecting CO oxidation,[39,41,55,69] C-H and Si-H bond activation,[40,42,44,45,50,51,60,62,70–72] and [2+2] cycloaddition reactions.[43,46] Consequently, there is much interest in the synthesis of complexes with novel M=L linkages in order to further probe the reactivity of these rare species.

Scheme 1.1. Synthesis of late transition metal complexes with M=L multiple bonds

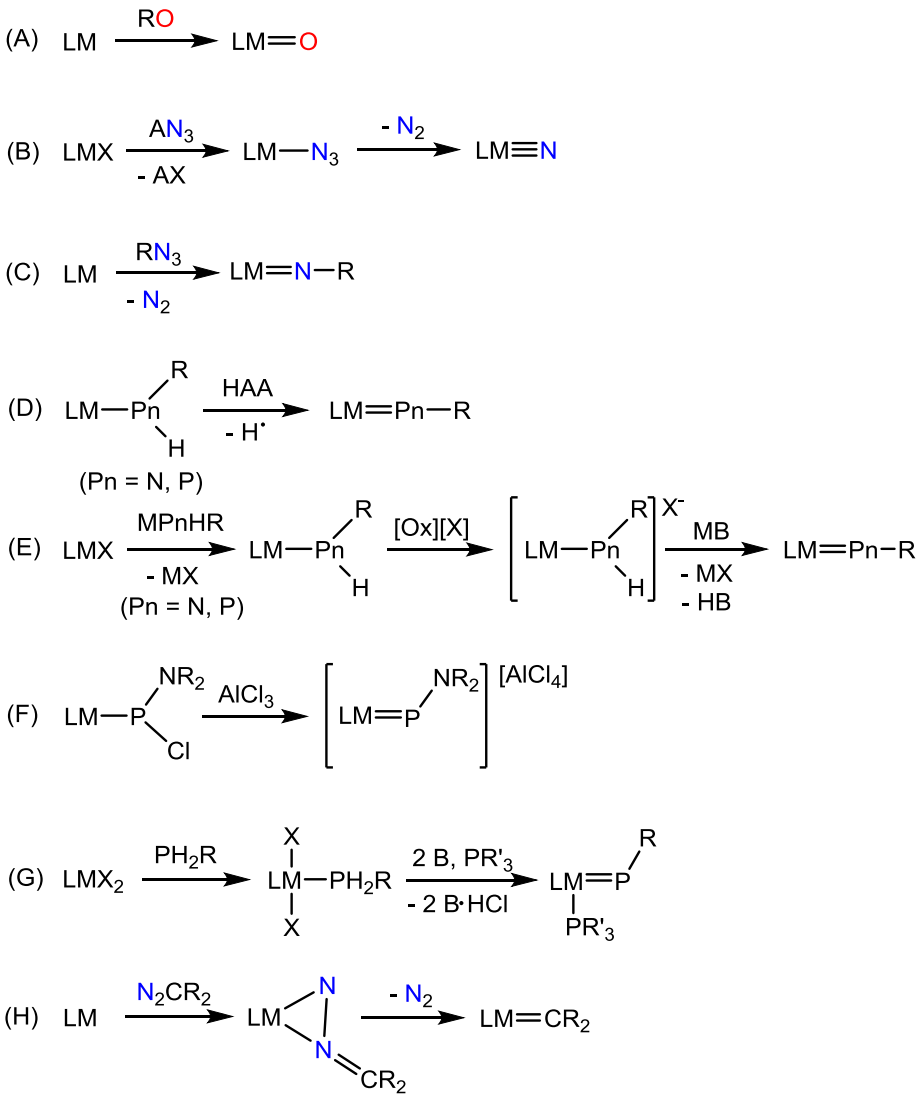

In spite of clear advances in the synthesis of late metal complexes with M=L multiple bonds, the number of terminal chalcogenide (O, S, Se) complexes remains very low – with no examples among first row metals (Co, Ni, Cu) − highlighting the need for the development of new approaches for the synthesis of these elusive species.

In this regard, one of the key challenges to overcome in the synthesis of late metal terminal chalcogenides is their tendency to form bridging bimetallic species. For example, Jones and co-workers reported that elimination of C_6H_6 from [(dippe)Ni^{II}(SH)(C_6H_5)] (dippe

= 1,2-bis(diisoproylphosphino)ethane) under mild heating resulted in the transient formation of a nickel terminal sulfide, [(dippe)Ni^{II}(S)]. However, the nickel sulfide complex rapidly dimerizes to form a bridged sulfide species, [{(dippe)Ni^{II}}$_2$(μ^2-S)$_2$] (Scheme 1.2).[73] Similar results have been observed with a wide range of different methods and supporting ligand systems.[74–77]

Scheme 1.2. Dimerization of [(dippe)Ni^{II}(S)] to form [{(dippe)Ni^{II}}$_2$(μ^2-S)$_2$]

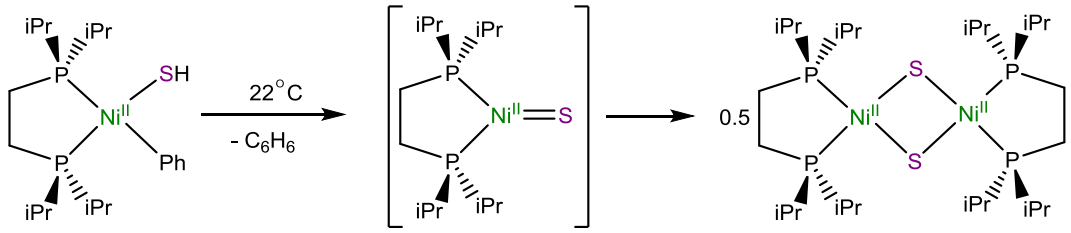

1.3 Reductive Deprotection

In order to address the above-mentioned challenge for the synthesis of terminal chalcogenide complexes, the Hayton group has developed the reductive deprotection strategy.[78,79] This approach makes use of protecting groups, such as triphenylmethyl (trityl), that have been developed in the field of synthetic organic chemistry[80] and applies them to the synthesis of terminal chalcogenide ligands. The reductive deprotection protocol involves the installation of "protected" oxo or sulfide moieties to the desired metal center followed by reductive cleavage of the O/S-protecting group bond to yield the desired terminal oxo or sulfide ligand (Scheme 1.3).

Scheme 1.3. General mechanism for reductive deprotection

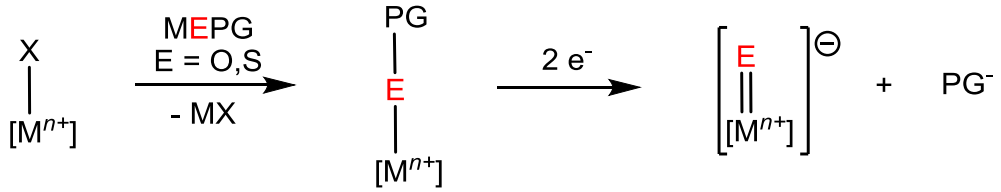

PG = protecting group

In addition to disfavoring the formation of dimers, reductive deprotection is also advantageous because it does not require a change in the oxidation state of the metal center. For example, in the synthesis of the Th^{IV} oxo complex, $[K(18\text{-crown-6})][Th^{IV}(O)(NR_2)_3]$, the first step is installation of the "trityl protected oxo" via a salt metathesis with $KOCPh_3$ and $[Th^{IV}(I)(NR_2)_3]$. This is followed by the 2 electron reductive cleavage of the O-C trityl bond in the presence of 18-crown-6 to yield the desired Th terminal oxo complex, $[K(18\text{-crown-6})][Th^{IV}(O)(NR_2)_3]$, and the trityl anion, $[K(18\text{-crown-6})][CPh_3]$ (Scheme 1.4).[79]

Scheme 1.4. Synthesis of actinide oxo complexes via reductive deprotection

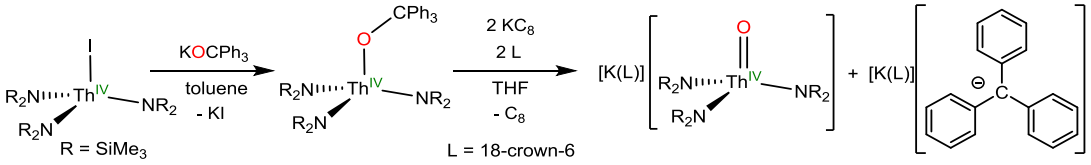

Notably, Th remains in the +4 oxidation state throughout all stages of the synthesis. In contrast other O-and S-atom transfer reagents, this pathway does not require an oxidative addition. This makes it well suited to first row transition metals which do not readily undergo 2 electron processes.[24]

1.4 General Remarks

The overall goal of this research is the application of the reductive deprotection protocol towards the synthesis of first-row late transition metal complexes with M=L multiple bonds.

Chapter 2 describes the synthesis of Ni^{II} "masked" terminal sulfide complexes via the reductive deprotection protocol and describes their reactivity with diphenylsilane (Ph_2SiH_2) and trimethylsilyl triflate (Me_3SiOTf) in order to probe the nucleophilicity of the sulfide ligand.

Chapter 3 details the reductive deprotection of a nickel tritylthiolate complex with decamethylcobaltocene (Cp^*_2Co), which unexpectedly leads to the generation of a Ni^{I}

cobaltocenium thiolate complex. The Ni^{I} complex likely forms via the reaction of a putative nickel sulfide with deprotonated decamethylcobaltocenium, ($CoCp^{*}(C_5Me_4{=}CH_2)$). These results expand the scope of late metal sulfide reactivity.

Chapter 4 describes the reactions of carbon disulfide (CS_2) with the nickel sulfide complexes, described in chapter 2, to yield trithiocarbonate ($[CS_3]^{2-}$) complexes and expands the known reactivity of late metal sulfides.

Chapter 5 details the reactivity of a "masked" terminal nickel sulfide complex, synthesized in chapter 2, with carbon monoxide (CO) and nitric oxide (NO) further advancing understanding of the fundamental chemistry of these small molecules with metal sulfides.

Chapter 6 describes the reaction of a nickel sulfide with nitrous oxide (N_2O) to yield an unprecedented thiohyponitrite ($[SN{=}NO]^{2-}$) complex. Also detailed is the extrusion of N_2 from $SN{=}NO^{2-}$ to yield a thioperoxide ($[SO]^{2-}$) complex. The thioperoxide complex reacts with carbon monoxide (CO) to yield CO_2 and regenerate nickel sulfide. On the whole, this work shows a new route to N_2O reduction via sulfur based redox chemistry.

Chapter 7 details efforts to extend the scope of the reductive deprotection reaction to the synthesis of other late transition metal (Fe, Co, Ni) complexes with oxo, sulfide, and imido ligands.

1.5 References

(1) Nugent, W. A.; Mayer, J. M. *Metal-Ligand Multiple Bonds*; John Wiley & Sons: New York, 1988.

(2) Meyer, T. J. Metal Oxo Complexes and Oxygen Activation. In *Oxygen Complexes and Oxygen Activation by Transition Metals*; Springer US: Boston, MA, 1988; pp 33–47.

(3) Costas, M.; Mehn, M. P.; Jensen, M. P.; Que, L. Dioxygen Activation at Mononuclear Nonheme Iron Active Sites: Enzymes, Models, and Intermediates. *Chem. Rev.* **2004**, *104* (2), 939.

(4) Krebs, C.; Galonić Fujimori, D.; Walsh, C. T.; Bollinger, J. M. Non-Heme Fe(IV)–Oxo Intermediates. *Acc. Chem. Res.* **2007**, *40* (7), 484.

(5) Baik, M. H.; Newcomb, M.; Friesner, R. A.; Lippard, S. J. Mechanistic Studies on the Hydroxylation of Methane by Methane Monooxygenase. *Chem. Rev.* **2003**, *103* (6), 2385.

(6) Meunier, B.; de Visser, S. P.; Shaik, S. Mechanism of Oxidation Reactions Catalyzed by Cytochrome P450 Enzymes. *Chem. Rev.* **2004**, *104* (9), 3947.

(7) Can, M.; Armstrong, F. A.; Ragsdale, S. W. Structure, Function, and Mechanism of the Nickel Metalloenzymes, CO Dehydrogenase, and Acetyl-CoA Synthase. *Chem. Rev.* **2014**, *114* (8), 4149.

(8) George, G. N.; Pickering, I. J.; Yu, E. Y.; Prince, R. C.; Bursakov, S. A.; Gavel, O. Y.; Moura, I.; Moura, J. J. G. A Novel Protein-Bound Copper−Molybdenum Cluster. *J. Am. Chem. Soc.* **2000**, *122* (34), 8321.

(9) Pomowski, A.; Zumft, W. G.; Kroneck, P. M. H.; Einsle, O. N_2O Binding at a [4Cu:2S] Copper-Sulphur Cluster in Nitrous Oxide Reductase. *Nature* **2011**, *477* (7363), 234.

(10) Brown, K.; Djinovic-Carugo, K.; Haltia, T.; Cabrito, I.; Saraste, M.; Moura, J. G.; Moura, I.; Tegoni, M.; Cambillau, C. Revisiting the Catalytic CuZ Cluster of Nitrous Oxide (N_2O) Reductase: Evidence of a Bridging Inorganic Sulfur. *J. Biol. Chem.* **2000**, *275* (52), 41133.

(11) Dobbek, H.; Svetlitchnyi, V.; Gremer, L.; Huber, R.; Meyer, O. Crystal Structure of a Carbon Monoxide Dehydrogenase Reveals a [Ni-4Fe-5S] Cluster. *Science* **2001**, *293* (5533), 1281.

(12) Dobbek, H.; Gremer, L.; Kiefersauer, R.; Huber, R.; Meyer, O. Catalysis at a Dinuclear [CuSMo(O)OH] Cluster in a CO Dehydrogenase Resolved at 1.1-Å Resolution. *Proc. Natl. Acad. Sci.* **2002**, *99* (25), 15971.

(13) Stiefel, E. I. Transition Metal Sulfur Chemistry and Its Relevance to Molybdenum and Tungsten Enzymes. *Pure Appl. Chem.* **1998**, *70* (4), 889.

(14) Prins, R.; Egorova, M.; Röthlisberger, A.; Zhao, Y.; Sivasankar, N.; Kukula, P. Mechanisms of Hydrodesulfurization and Hydrodenitrogenation. *Catal. Today* **2006**, *111* (1–2), 84.

(15) Chang-long, Y.; Xi-ping, Z.; Lei-yan, Z.; Chen-guang, L. Mechanism of Hydrodesulfurization of Dibenzothiophenes on Unsupported NiMoW Catalyst. *J. Fuel Chem. Technol.* **2013**, *41* (8), 991.

(16) *Transition Metal Sulphides*; Weber, T., Prins, R., Santen, R. A., Eds.; Springer Netherlands: Dordrecht, 1998.

(17) Smil, V. *Enriching the Earth : Fritz Haber, Carl Bosch, and the Transformation of World Food Production*; MIT Press, 2001.
(18) Seefeldt, L. C.; Hoffman, B. M.; Dean, D. R. Mechanism of Mo-Dependent Nitrogenase. *Annu. Rev. Biochem.* **2009**, *78* (1), 701.
(19) Hoffman, B. M.; Lukoyanov, D.; Yang, Z.-Y.; Dean, D. R.; Seefeldt, L. C. Mechanism of Nitrogen Fixation by Nitrogenase: The Next Stage. *Chem. Rev.* **2014**, *114* (8), 4041.
(20) Yandulov, D. V.; Schrock, R. R. Reduction of Dinitrogen to Ammonia at a Well-Protected Reaction Site in a Molybdenum Triamidoamine Complex. *J. Am. Chem. Soc.* **2002**, *124* (22), 6252.
(21) Yandulov, D. V; Schrock, R. R. Catalytic Reduction of Dintrogen to Ammonia at a Sngle Molybdenum Center. *Science (80-.).* **2003**, *301*, 76.
(22) McWilliams, S. F.; Holland, P. L. Dinitrogen Binding and Cleavage by Multinuclear Iron Complexes. *Acc. Chem. Res.* **2015**, *48* (7), 2059.
(23) Rittle, J.; Peters, J. C. An Fe-N_2 Complex That Generates Hydrazine and Ammonia via Fe=NNH_2 : Demonstrating a Hybrid Distal-to-Alternating Pathway for N_2 Reduction. *J. Am. Chem. Soc.* **2016**, *138* (12), 4243.
(24) Ray, K.; Heims, F.; Pfaff, F. F. Terminal Oxo and Imido Transition-Metal Complexes of Groups 9–11. *Eur. J Inorg. Chem.* **2013**, 3784.
(25) Sharp, P. R. Late Transition Metal Oxo and Imido Chemistry. *Comments Inorg. Chem.* **1999**, *21* (1–3), 85.
(26) Berry, J. F. Terminal Nitrido and Imido Complexes of the Late Transition Metals. *Comments Inorg. Chem.* **2009**, *30* (1–2), 28.
(27) Mayer, J. M. Why Are There No Terminal Oxo Complexes of the Late Transition Metals? Or The Importance of Metal–Ligand π Antibonding Interactions. *Comments Inorg. Chem.* **1988**, *8* (4), 125.
(28) Trnka, T. M.; Parkin, G. A Survey of Terminal Chalcogenido Complexes of the Transition Metals : Trends in Their Distribution and the Variation of Their M=E Bond Lengths. *Polyhedron* **1997**, *16* (7), 1031.
(29) Ballhausen, C. J.; Gray, H. B. The Electronic Structure of the Vanadyl Ion. *Inorg. Chem.* **1962**, *1* (1), 111.
(30) Winkler, J. R.; Gray, H. B. Electronic Structures of Oxo-Metal Ions. In *Molecular Electronic Structures of Transition Metal Complexes I*; Mingos, D. M. P., Day, P., Dahl, J. P., Eds.; Springer Berlin Heidelberg, 2012; Vol. 142, pp 17–28.
(31) Hay-Motherwell, R. S.; Wilkinson, G.; Hussain-Bates, B.; Hursthouse, M. B. Synthesis and X-Ray Crystal Structure of Oxotrimesityliridium(V). *Polyhedron* **1993**, *12* (16), 2009.
(32) Poverenov, E.; Efremenko, I.; Frenkel, A. I.; Ben-David, Y.; Shimon, L. J. W.; Leitus, G.; Konstantinovski, L.; Martin, J. M. L.; Milstein, D. Evidence for a Terminal Pt(IV)-Oxo Complex Exhibiting Diverse Reactivity. *Nature* **2008**, *455* (7216), 1093.
(33) Saouma, C. T.; Peters, J. C. ME and ME Complexes of Iron and Cobalt That Emphasize Three-Fold Symmetry (E=O, N, NR). *Coord. Chem. Rev.* **2011**, *255* (7–8), 920.
(34) Glueck, D. S.; Hollander, F. J.; Bergman, R. G. Synthesis, Structure, and Reactivity of a Monomeric Pentamethylcyclopentadienyliridium(III) Imido Complex. *J. Am.*

Chem. Soc. **1989**, *111* (7), 2719.
(35) Glueck, D. S.; Wu, J.; Hollander, F. J.; Bergman, R. G. Monomeric (Pentamethylcyclopentadienyl)Iridium Imido Compounds: Synthesis, Structure, and Reactivity. *J. Am. Chem. Soc.* **1991**, *113* (6), 2041.
(36) Schöffel, J.; Rogachev, A. Y.; DeBeer George, S.; Burger, P. Isolation and Hydrogenation of a Complex with a Terminal Iridium–Nitrido Bond. *Angew. Chem. Int. Ed.* **2009**, *48* (26), 4734.
(37) Scheibel, M. G.; Askevold, B.; Heinemann, F. W.; Reijerse, E. J.; de Bruin, B.; Schneider, S. Closed-Shell and Open-Shell Square-Planar Iridium Nitrido Complexes. *Nat. Chem.* **2012**, *4* (7), 552.
(38) Zolnhofer, E. M.; Käß, M.; Khusniyarov, M. M.; Heinemann, F. W.; Maron, L.; van Gastel, M.; Bill, E.; Meyer, K. An Intermediate Cobalt(IV) Nitrido Complex and Its N-Migratory Insertion Product. *J. Am. Chem. Soc.* **2014**, *136* (42), 15072.
(39) Jenkins, D. M.; Betley, T. A.; Peters, J. C. Oxidative Group Transfer to Co(I) Affords a Terminal Co(III) Imido Complex. *J. Am. Chem. Soc.* **2002**, *124* (38), 11238.
(40) Shay, D. T.; Yap, G. P. A.; Zakharov, L. N.; Rheingold, A. L.; Theopold, K. H. Intramolecular CH Activation by an Open-Shell Cobalt(III) Imido Complex. *Angew. Chem. Int. Ed.* **2005**, *44* (10), 1508.
(41) Mindiola, D. J.; Hillhouse, G. L. Isocyanate and Carbodiimide Synthesis by Nitrene-Group-Transfer from a Nickel(II) Imido Complex. *Chem. Commun.* **2002**, No. 17, 1840.
(42) Jones, C.; Schulten, C.; Rose, R. P.; Stasch, A.; Aldridge, S.; Woodul, W. D.; Murray, K. S.; Moubaraki, B.; Brynda, M.; La Macchia, G.; et al. Amidinato– and Guanidinato–Cobalt(I) Complexes: Characterization of Exceptionally Short Co–Co Interactions. *Angew. Chem. Int. Ed.* **2009**, *48* (40), 7406.
(43) Mindiola, D. J.; Waterman, R.; Iluc, V. M.; Cundari, T. R.; Hillhouse, G. L. Carbon–Hydrogen Bond Activation, C–N Bond Coupling, and Cycloaddition Reactivity of a Three-Coordinate Nickel Complex Featuring a Terminal Imido Ligand. *Inorg. Chem.* **2014**, *53* (24), 13227.
(44) King, E. R.; Sazama, G. T.; Betley, T. A. Co(III) Imidos Exhibiting Spin Crossover and C–H Bond Activation. *J. Am. Chem. Soc.* **2012**, *134* (43), 17858.
(45) Iluc, V. M.; Miller, A. J. M.; Anderson, J. S.; Monreal, M. J.; Mehn, M. P.; Hillhouse, G. L. Synthesis and Characterization of Three-Coordinate Ni(III)-Imide Complexes. *J. Am. Chem. Soc.* **2011**, *133* (33), 13055.
(46) Kogut, E.; Wiencko, H. L.; Zhang, L.; Cordeau, D. E.; Warren, T. H. A Terminal Ni(III)-Imide with Diverse Reactivity Pathways. *J. Am. Chem. Soc.* **2005**, *127* (32), 11248.
(47) Hu, X.; Meyer, K. Terminal Cobalt(III) Imido Complexes Supported by Tris(Carbene) Ligands: Imido Insertion into the Cobalt−Carbene Bond. *J. Am. Chem. Soc.* **2004**, *126* (50), 16322.
(48) Dai, X.; Kapoor, P.; Warren, T. H. [Me2NN]Co(H6-Toluene): O=O, N=N, and O=N Bond Cleavage Provides β-Diketiminato Cobalt μ-Oxo and Imido Complexes. *J. Am. Chem. Soc.* **2004**, *126* (15), 4798.
(49) Waterman, R.; Hillhouse, G. L. η^2-Organoazide Complexes of Nickel and Their Conversion to Terminal Imido Complexes *via* Dinitrogen Extrusion. *J. Am. Chem. Soc.* **2008**, *130* (38), 12628.

(50) Laskowski, C. A.; Miller, A. J. M.; Hillhouse, G. L.; Cundari, T. R. A Two-Coordinate Nickel Imido Complex That Effects C−H Amination. *J. Am. Chem. Soc.* **2011**, *133* (4), 771.
(51) Wiese, S.; McAfee, J. L.; Pahls, D. R.; McMullin, C. L.; Cundari, T. R.; Warren, T. H. C–H Functionalization Reactivity of a Nickel–Imide. *J. Am. Chem. Soc.* **2012**, *134* (24), 10114.
(52) Wiese, S.; Aguila, M. J. B.; Kogut, E.; Warren, T. H. β-Diketiminato Nickel Imides in Catalytic Nitrene Transfer to Isocyanides. *Organometallics* **2013**, *32* (8), 2300.
(53) Zhang, L.; Liu, Y.; Deng, L. Three-Coordinate Cobalt(IV) and Cobalt(V) Imido Complexes with N-Heterocyclic Carbene Ligation: Synthesis, Structure, and Their Distinct Reactivity in C–H Bond Amination. *J. Am. Chem. Soc.* **2014**, *136* (44), 15525.
(54) Du, J.; Wang, L.; Xie, M.; Deng, L. A Two-Coordinate Cobalt(II) Imido Complex with NHC Ligation: Synthesis, Structure, and Reactivity. *Angew. Chemie Int. Ed.* **2015**, *54* (43), 12640.
(55) Liu, Y.; Du, J.; Deng, L. Synthesis, Structure, and Reactivity of Low-Spin Cobalt(II) Imido Complexes $[(Me_3P)_3Co(NAr)]$. *Inorg. Chem.* **2017**, *56* (14), 8278.
(56) Cowley, R. E.; Bontchev, R. P.; Sorrell, J.; Sarracino, O.; Feng, Y.; Wang, H.; Smith, J. M. Formation of a Cobalt(III) Imido from a Cobalt(II) Amido Complex. Evidence for Proton-Coupled Electron Transfer. **2007**.
(57) Melenkivitz, R.; Mindiola, D. J.; Hillhouse, G. L. Monomeric Phosphido and Phosphinidene Complexes of Nickel. *J. Am. Chem. Soc.* **2002**, *124* (15), 3846.
(58) Sánchez-Nieves, J.; Sterenberg, B. T.; Udachin, K. A.; Carty, A. J. A Thermally Stable and Sterically Unprotected Terminal Electrophilic Phosphinidene Complex of Cobalt and Its Conversion to an η^1-Phosphirene. *J. Am. Chem. Soc.* **2003**, *125* (9), 2404.
(59) Termaten, A. T.; Aktas, H.; Schakel, M.; Ehlers, A. W.; Lutz, M.; Spek, A. L.; Lammertsma, K. Terminal Phosphinidene Complexes CpR(L)M=PAr of the Group 9 Transition Metals Cobalt, Rhodium, and Iridium. Synthesis, Structures, and Properties. *Organometallics* **2003**, *22* (9), 1827.
(60) Cundari, T. R.; Jimenez-Halla, J. O. C.; Morello, G. R.; Vaddadi, S. Catalytic Tuning of a Phosphinoethane Ligand for Enhanced C−H Activation. *J. Am. Chem. Soc.* **2008**, *130* (39), 13051.
(61) Kessler, J. A.; Iluc, V. M. NI(Ii) Phosphine and Phosphide Complexes Supported by a PNP-Pyrrole Pincer Ligand. *Dalt. Trans.* **2017**, *46* (36), 12125.
(62) Iluc, V. M.; Hillhouse, G. L. Hydrogen-Atom Abstraction from Ni(I) Phosphido and Amido Complexes Gives Phosphinidene and Imide Ligands. *J. Am. Chem. Soc.* **2010**, *132* (43), 15148.
(63) Iluc, V. M.; Hillhouse, G. L. Three-Coordinate Nickel Carbene Complexes and Their One-Electron Oxidation Products. *J. Am. Chem. Soc.* **2014**, *136* (17), 6479.
(64) Mindiola, D. J.; Hillhouse, G. L. Synthesis, Structure, and Reactions of a Three-Coordinate Nickel-Carbene Complex, {1,2-Bis(Di-Tert-Butylphosphino)Ethane}$NiCPh_2$. *J. Am. Chem. Soc.* **2002**, *124* (34), 9976.
(65) Dai, X.; Warren, T. H. Discrete Bridging and Terminal Copper Carbenes in Copper-Catalyzed Cyclopropanation. *J. Am. Chem. Soc.* **2004**, *126* (32), 10085.
(66) Bellow, J. A.; Stoian, S. A.; Van Tol, J.; Ozarowski, A.; Lord, R. L.; Groysman, S.

Synthesis and Characterization of a Stable High-Valent Cobalt Carbene Complex. *J. Am. Chem. Soc.* **2016**, *138* (17), 5531.
(67) Waterman, R.; Hillhouse, G. L. Group Transfer from Nickel Imido, Phosphinidene, and Carbene Complexes to Ethylene with Formation of Aziridine, Phosphirane, and Cyclopropane Products. *J. Am. Chem. Soc.* **2003**, *125* (44), 13350.
(68) Mindiola, D. J.; Hillhouse, G. L. Terminal Amido and Imido Complexes of Three-Coordinate Nickel. *J. Am. Chem. Soc.* **2001**, *123* (19), 4623.
(69) Kogut, E.; Wiencko, H. L.; Zhang, L.; Cordeau, D. E.; Warren, T. H. A Terminal Ni(III)-Imide with Diverse Reactivity Pathways. *J. Am. Chem. Soc.* **2005**, *127* (32), 11248.
(70) Sieh, D.; Burger, P. Si–H Activation in an Iridium Nitrido Complex—A Mechanistic and Theoretical Study. *J. Am. Chem. Soc.* **2013**, *135* (10), 3971.
(71) Mehn, M. P.; Brown, S. D.; Jenkins, D. M.; Peters, J. C.; Que, L. Vibrational Spectroscopy and Analysis of Pseudo-Tetrahedral Complexes with Metal Imido Bonds. *Inorg. Chem.* **2006**, *45* (18), 7417.
(72) Pierpont, A. W.; Cundari, T. R. Computational Study of Methane C−H Activation by First-Row Late Transition Metal LnM═E (M: Fe, Co, Ni) Complexes. *Inorg. Chem.* **2010**, *49* (5), 2038.
(73) Vicic, D. A.; Jones, W. D. Evidence for the Existence of a Late-Metal Terminal Sulfido Complex. *J. Am. Chem. Soc.* **1999**, *121* (16), 4070.
(74) Kubas, G. J.; Vergamini, P. J. Synthesis, Characterization, and Reactions of Iron-Sulfur Clusters Containing the S_2 Ligand. *Inorg. Chem.* **1981**, *20* (8), 2667.
(75) Wachter, J. Synthesis, Structure and Reactivity of Sulfur-Rich Cyclopentadienyl-Transition Metal Complexes: Sulfur Chemistry from an Organometallic Point of View. *Angew. Chemie Int. Ed. English* **1989**, *28* (12), 1613.
(76) Bag, B.; Mondal, N.; Mitra, S.; Rosair, G. The First Thermally-Stable Singly Oxo-Bridged Dinuclear Ni(III) Complex. *Chem. Commun.* **2000**, *0* (18), 1729.
(77) Cho, J.; Van Heuvelen, K. M.; Yap, G. P. A.; Brunold, T. C.; Riordan, C. G. New Synthetic Routes to a Disulfidodinickel(II) Complex: Characterization and Reactivity of a $Ni_2(\mu\text{-}\eta^2\text{:}\eta^2\text{-}S_2)$ Core. *Inorg. Chem.* **2008**, *47* (10), 3931.
(78) Smiles, D. E.; Wu, G.; Hayton, T. W. Synthesis of Uranium–Ligand Multiple Bonds by Cleavage of a Trityl Protecting Group. *J. Am. Chem. Soc.* **2014**, *136* (1), 96.
(79) Smiles, D. E.; Wu, G.; Kaltsoyannis, N.; Hayton, T. W. Thorium-Ligand Multiple Bonds via Reductive Deprotection of a Trityl Group. *Chem. Sci.* **2015**, *6* (6), 3891.
(80) Wuts, P. G. M.; Greene, T. W. *Greene's Protective Groups in Organic Synthesis*; John Wiley & Sons, Inc.: Hoboken, NJ, USA, 2006.

Chapter 2 Synthesis of a Ni^{II} "Masked" Terminal Sulfide via Reductive Deprotection

Portions of this work were published in:

Nathaniel J. Hartmann , Guang Wu, Trevor W. Hayton

Angew. Chem. Int. Ed., **2015**, *54*, 14956-14959.

Table of Contents

2.1 Introduction

Metal-ligand multiple bonding in the late metals (groups 9, 10, 11) is relatively rare.[1,2] This observation can be rationalized by the "oxo wall" concept,[3] which postulates that a tetragonal complex with a d^5 configuration (or greater) cannot form stable multiple bonds because of occupation of the M=E π^* orbitals. While no exceptions to the "oxo wall" concept are currently known, it can be circumvented by reducing the coordination number at the metal center. For example, two late metal oxos have been reported, namely $[Ir(O)(Mes)_3]$ (**A**, Mes = 2,4,6-$Me_3C_6H_2$) and $[Pt(O)(PCN)][BF_4]$ (PCN = $C_6H_3[CH_2P(tBu)_2](CH_2CH_2NMe_2)$), and both feature four coordinate geometries.[4,5] Two recently isolated Ir nitride complexes also feature four coordinate geometries.[6,7] Similarly, a handful of isolable cobalt, nickel, and copper nitrenes are known, such as $[(Me_2NN)Co(NAd)]$ (Me_2NN = $(\{2,6\text{-}Me_2C_6H_3)NC(Me)\}_2CH$), $[(dtbpe)Ni^{II}(N(2,6\text{-}{}^iPr_2C_6H_3)]$ (**B**, dtbpe = $P^tBu_2CH_2CH_2P^tBu_2$), $[(IPr^*)Ni(N(2,6\text{-}(Mes)_2C_6H_3)]$, and $[\{(Me_3NN)Cu\}_2(\mu\text{-}NAd)]$ (Me_3NN = $\{(2,4,6\text{-}Me_3C_6H_2)NC(Me)\}_2CH$), which also feature low coordination numbers (2-4).[8–11] Also of note are the closely related nickel carbene and phosphinidene complexes, $[(dtbpe)Ni^{II}(E)]$ (E = CPh_2, $P[2,6\text{-}Mes_2C_6H_3]$), reported by Hillhouse and co-workers.[12–14] This class of materials is highly reactive and is capable of effecting CO oxidation,[15] C-H activation,[16–23] and [2+2] cycloaddition, demonstrating their utility for small molecule activation.[24,25]

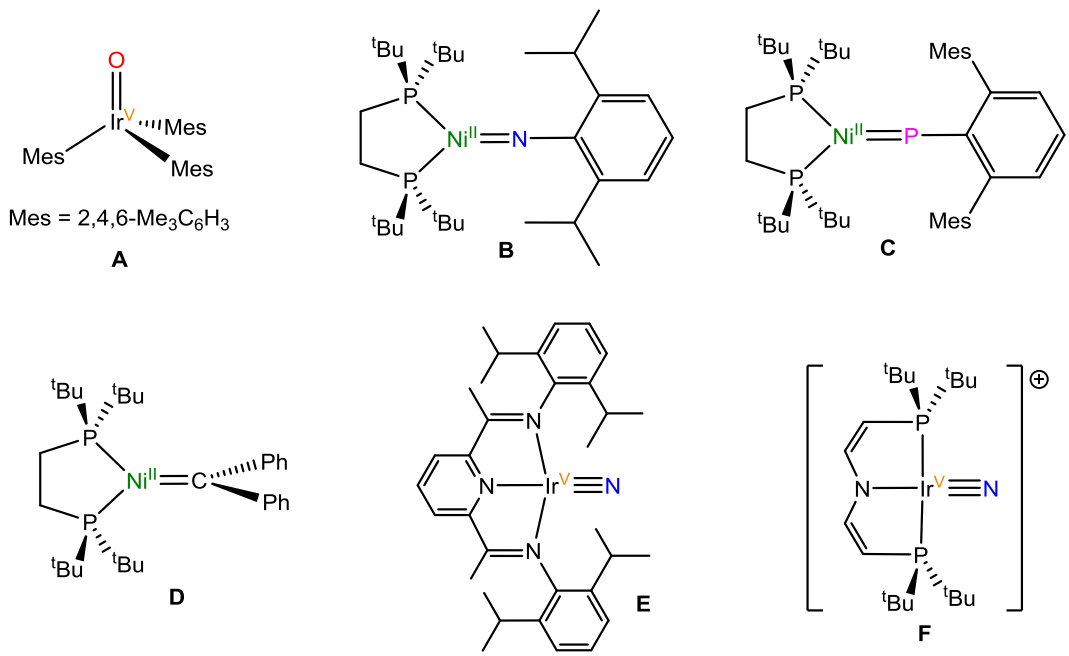

Figure 2.1. Previously reported complexes containing late metal-ligand multiple bonds. **A**, Ref. 4; **B**, Ref. 9; **C**, Ref. 13; **D**, Ref. 12; **E**, Ref. 6; **F**, Ref. 7.

In contrast to the above-mentioned success with C, O, N, and P-donor multiple bonds, attempts to synthesize a stable late metal terminal sulfide have been unsuccessful. For example, Driess and co-workers postulated that reaction of $[L^{R}Ni^{II}(\eta^{2}\text{-}S_2)]$ (L^{R} = {(2,6-$^{i}Pr_2C_6H_3$)NC(R)}$_2$CH, R = Me) with Ph_3P resulted in transient formation of $[L^{R}Ni^{III}(S)]$, but it rapidly dimerizes to form a bridged disulfide complex (Figure 2.2).[26] Similarly, Jones and co-workers reported the transient formation of $[(dippe)Ni^{II}(S)]$, which could be trapped by a variety of nitrones(Figure 2.2).[27]

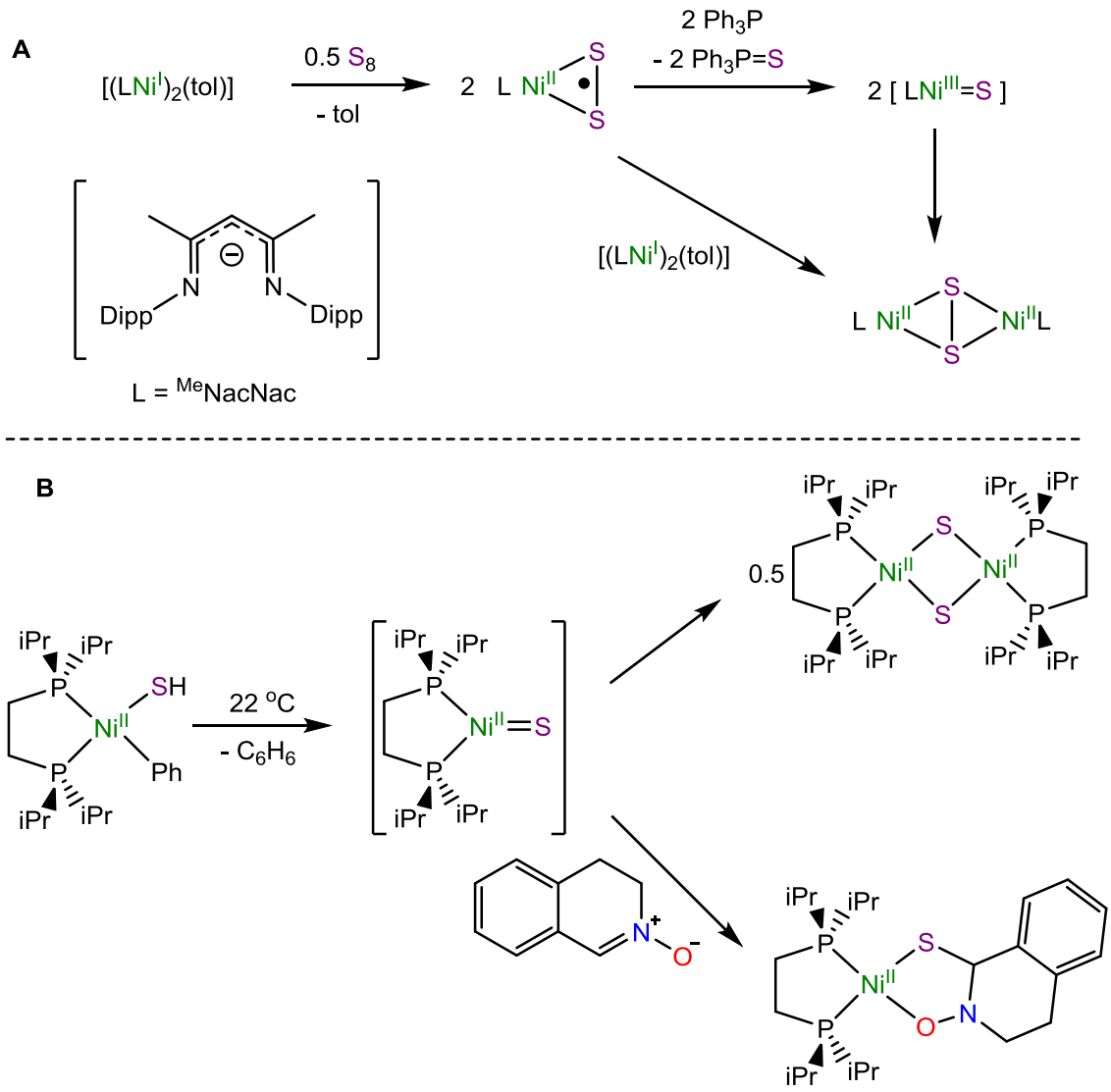

Figure 2.2. Previously reported transient nickel sulfides. **A**, Ref. 26; **B**, Ref. 27.

Late metal (Ni and Cu) sulfides are found in a variety of metalloenzyme active sites, including the NiFe and MoCu CO dehydrogenases (CODH),[28,29] the "orange protein complex",[30] and N_2O reductase (N_2OR).[31–33] The sulfide ligands in these enzymes can play either a catalytic role, as in the case of MoCu CODH,[29] or a structural role, as in the case of NiFe CODH and N_2OR.[31,34] Not surprisingly, given the role that late metal sulfides play in biology, there has been a long standing interest in synthesis of Ni and Cu sulfide model

complexes. For example, Tolman and co-workers reported the synthesis of $[\{(Me_3tacn)Cu\}_3(\mu_3\text{-}\eta^2,\eta^1,\eta^1\text{-}S_2)]^{2+}$, [35,36] which functions as a N_2O reduction catalyst. More recently, Mankad and co-workers reported the synthesis of two Cu clusters that feature rare examples of the $\mu_4\text{-}S^{2-}$ ligand.[37,38] Despite these successes, it is clear that controlling the binding mode of the sulfide ligand, and the nuclearity of the resulting complex, is still a synthetic challenge. Accordingly, the discovery of new methods to deliver a sulfur atom (or atoms) to a metal ion would be beneficial to the development of this class of materials.

The Hayton group has recently reported the synthesis of a Th(IV) sulfide complex, $[K(18\text{-crown-6})][Th(S)(NR_2)_3]$ (R = $SiMe_3$), via reductive removal of the trityl protecting group (Scheme 2.1).[39] In an effort to discern the scope of this 'reductive deprotection' reaction, I began to explore its applicability to other systems, especially late metal sulfides. The research reported herein describes the synthesis of a Ni^{II} "masked" terminal sulfide via the 'reductive deprotection' protocol and describes its reactivity with diphenylsilane (Ph_2SiH_2) and trimethylsilyl triflate (Me_3SiOTf) in order to probe the nucleophilicity of the sulfide ligand.

Scheme 2.1 Reductive deprotection of a thorium tritylthiolate complex

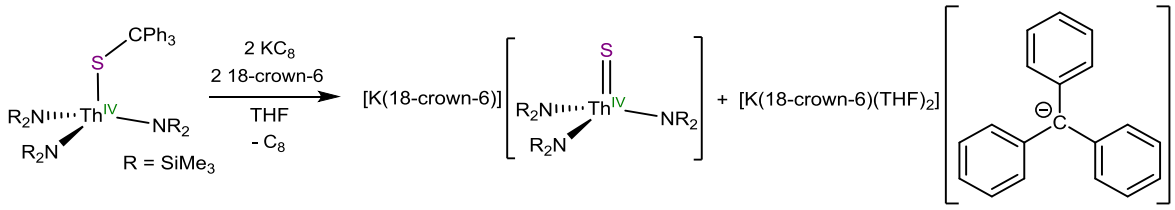

2.2 Results and Discussion

2.2.1 Synthesis and Characterization of [$L^{Me}Ni^{II}(SCPh_3)$] (2.1) and [$L^{tBu}Ni^{II}(SCPh_3)$] (2.2)

Addition of 1 equiv of $KSCPh_3$ to [$L^{R}Ni^{II}Cl$] (R = Me, ^{t}Bu)[40] in C_6H_6 results in the formation of [$L^{R}Ni^{II}(SCPh_3)$] (**2.1**, R = Me; **2.2**, R = ^{t}Bu). Complex **2.1** can be isolated as dark purple blocks from hexanes in 78% yield, while complex **2.2** can be isolated as dark blue blocks in 81% yield (Scheme 2.2).

Scheme 2.2 Synthesis of [$L^{Me}Ni^{II}(SCPh_3)$] (**2.1**) and [$L^{tBu}Ni^{II}(SCPh_3)$] (**2.2**)

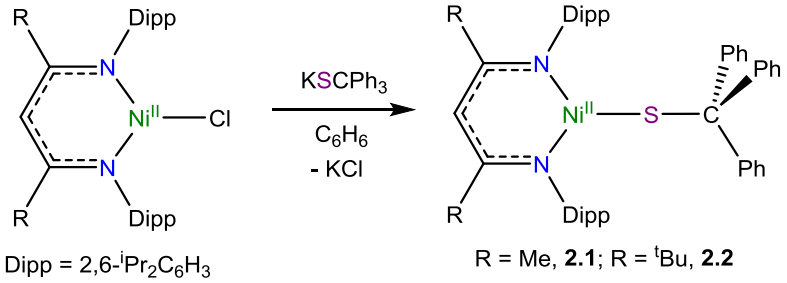

Dipp = 2,6-$^{i}Pr_2C_6H_3$

R = Me, **2.1**; R = ^{t}Bu, **2.2**

Their formulations were confirmed by elemental analysis and X-ray crystallography the solid state molecular structures of **2.1** and **2.2** are shown in Figure 2.3. Complexes **2.1** and **2.2** feature three coordinate Ni^{II} centers ligated by a tritylthiolate moiety. The Ni-S and C-S bond lengths in **2.1** are 2.1523(5) and 1.8647(2) Å, respectively, and are both consistent with single bonds.[41] Notably, complex **2.1** appears to contain an agostic interaction between Ni1 and H40c (Ni1-H40c = 2.61 Å, Figure 2.4), and is probably best described as featuring a pseudo-tetrahedral geometry (Σ(L-Ni-L) = 342.3°). In contrast to complex **2.1**, the geometry of complex **2.2** is best described as trigonal planar (Σ(L-Ni-L) = 356.5°). Additionally, complex **2.2** features a shortened Ni-S bond length of 2.0959(1) Å, and slightly lengthened S-C bond length of 1.892(4) Å, relative to **2.1**. These changes in geometry may explain the

differing magnetic behavior of complex **2.2** vs. complex **2.1** which are discussed in the following section.

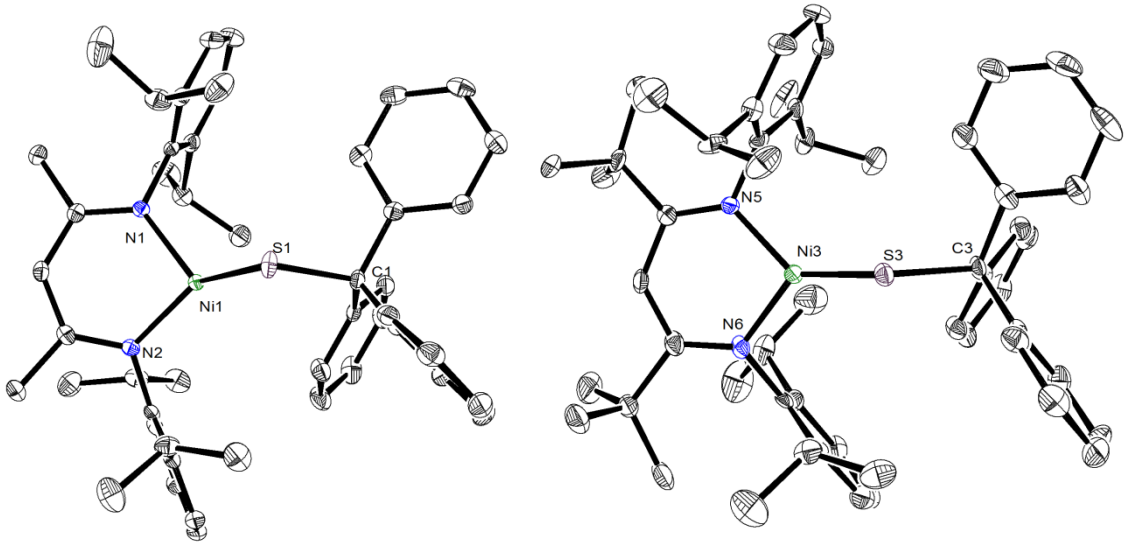

Figure 2.3. ORTEP diagrams of $[L^{Me}Ni^{II}(SCPh_3)]\cdot 0.5C_6H_6$ (**2.1**$\cdot 0.5C_6H_6$, left) and $[L^{tBu}Ni^{II}(SCPh_3)]\cdot 0.33C_5H_{12}$ (**2.2**$\cdot 0.33C_5H_{12}$, right) with 50% probability ellipsoids. Hydrogen atoms and solvate molecules have been omitted for clarity. Selected bond lengths and angles: (**2.1**) Ni1-S1 2.1523(5) Å, C1-S1 1.8647(2) Å, N1-Ni1-N2 96.65(6)°, N1-Ni1-S1 113.98(4)°, N2-Ni1-S1 131.67(4)°, Ni1-S1-C1 113.09(5)°; (**2.2**) Ni3-S3 2.0959(1) Å, C3-S3 1.892(4) Å, N5-Ni3-N6 96.97(1)°, N5-Ni3-S3 129.97(1)°, N6-Ni3-S3 129.60(1)°, Ni3-S3-C3 131.25(1)°.

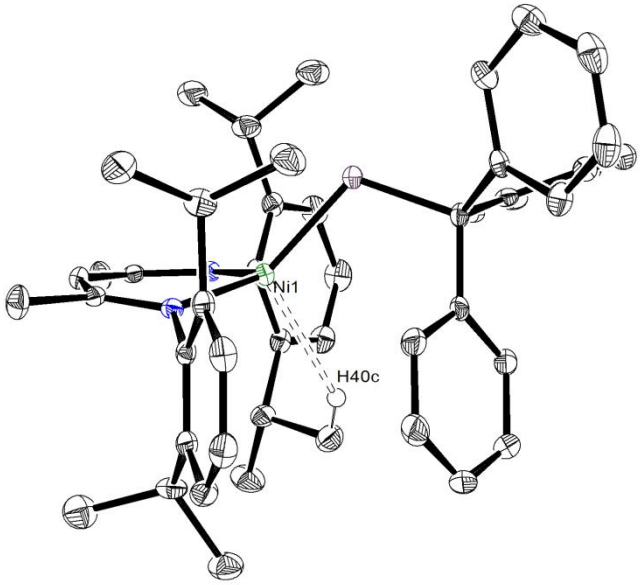

Figure 2.4. ORTEP diagram of $[L^{Me}Ni^{II}(SCPh_3)]\cdot 0.5C_6H_6$ (**2.1**$\cdot 0.5C_6H_6$) shown with 50% probability ellipsoids.

The ^{1}H NMR spectra of **2.1** and **2.2** are similar to those reported for other Ni^{II} β-diketiminate thiolate complexes, such as $[L^{tBu}Ni^{II}(SPh)]$ and $[L^{tBu}Ni^{II}(SEt)]$,[41,42] although I should note that **2.2** features a much smaller chemical shift range than that observed for **2.1**. The solution effective magnetic moment of **2.1** (μ_{eff} = 2.87 B.M. at 298 K), as determined by Evans' method,[43] is consistent with the expected S = 1 ground state.[40,41,44] However, the solution effective magnetic moment of **2.2** (μ_{eff} = 1.74 B.M. at 298 K), as determined by Evans' method, is much too low for an S = 1 ground state. Moreover, its solution magnetic moment was found to decrease to 1.23 B.M. upon cooling to 233 K (Figure 2.5). In addition, the magnetic susceptibility of **2.2** at 300 K, as determined by SQUID magnetometry (χ_M = -0.000578 $cm^3\cdot mol^{-1}$), is indicative of a diamagnetic ground state in the solid state (Figure 2.6). This is a somewhat surprising observation, as the singlet state in the related nickel thiolate, $[L^{tBu}Ni^{II}(SR)]$ (R = Et, Ph), is calculated to be ca. 21 $kJ\cdot mol^{-1}$ higher in energy than

the triplet state.[41] To explain these data, I suggest that the $S = 1$ and $S = 0$ states in **2.2** are very close in energy, but it is not immediately apparent why this would be the case.

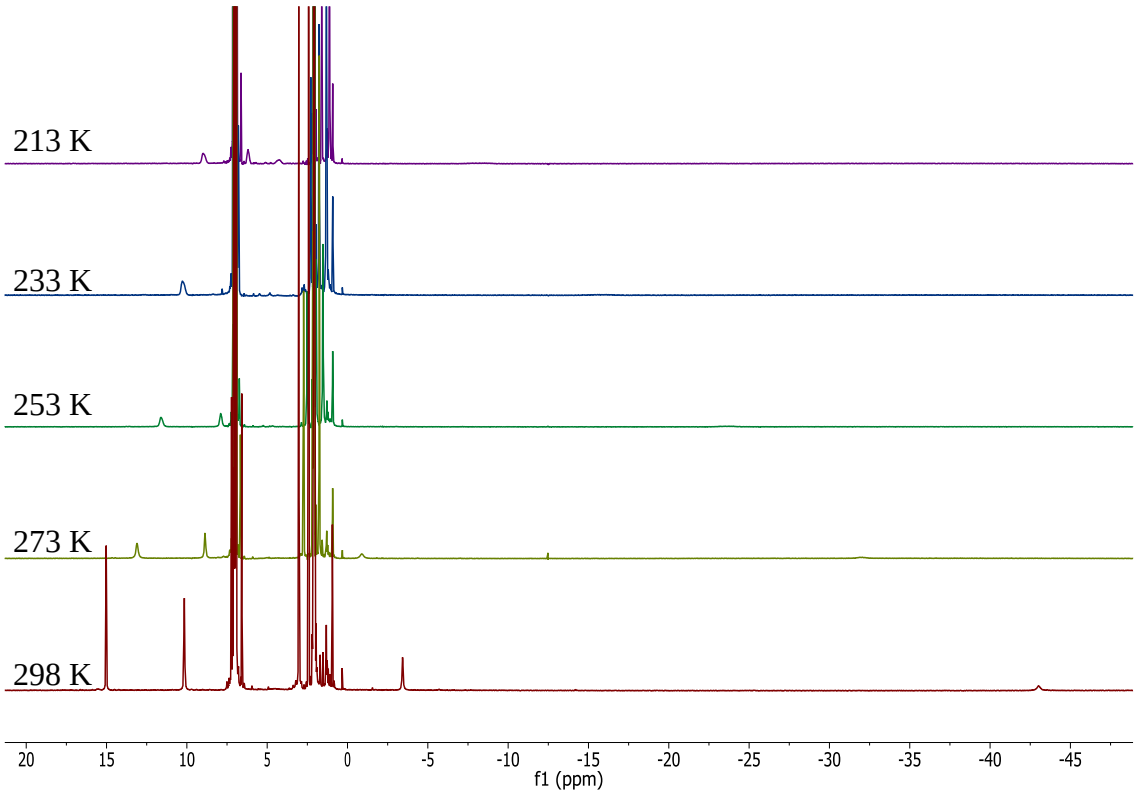

Figure 2.5. Variable temperature ^{1}H NMR spectra of [$L^{tBu}Ni^{II}(SCPh_3)$] (**2.2**) in toluene-d_8.

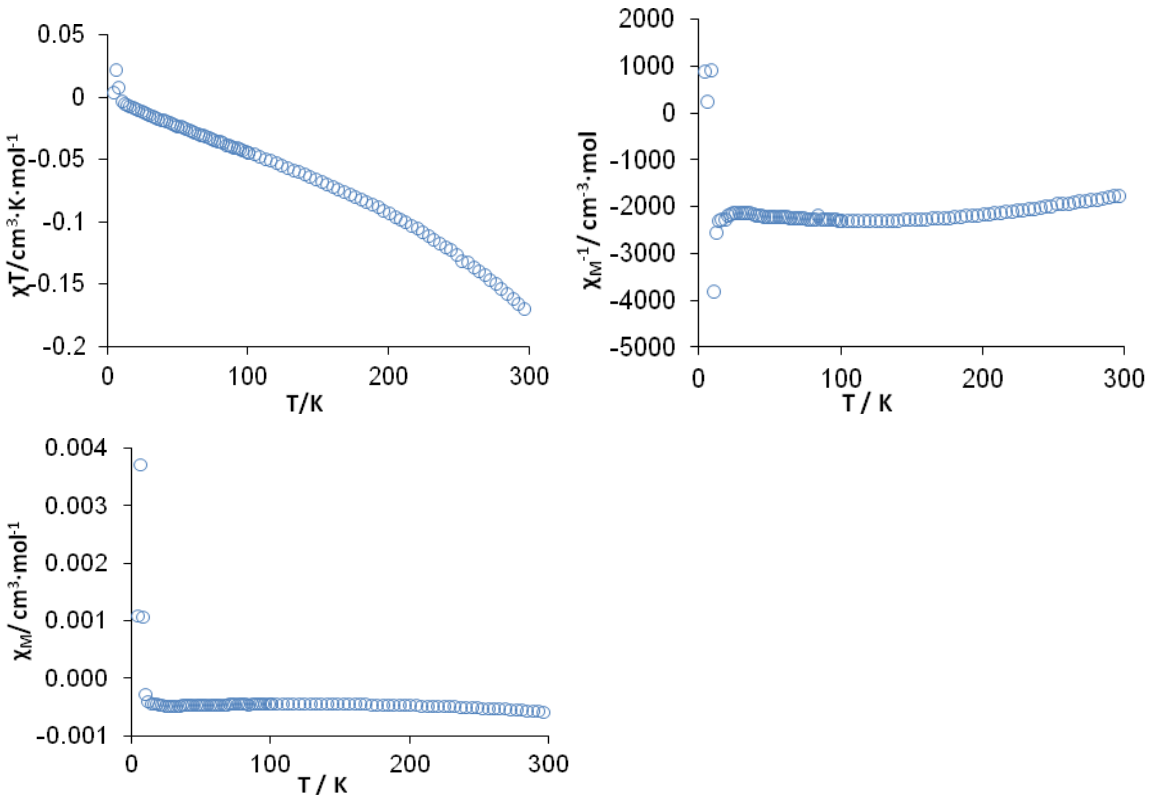

Figure 2.6. Temperature dependent, solid state magnetic susceptibility data for [$L^{tBu}Ni^{II}(SCPh_3)$] (**2.2**). $\chi_{dia} = -5.504 \times 10^{-4}$ $cm^3 \cdot mol^{-1}$, mass = 38.3 mg, M = 833.1 g/mol.

Interestingly, complex **2.2** has been observed to undergo a spontaneous C-S bond homolysis upon prolonged storage in solution. In contrast, this transformation has not been observed to occur spontaneously for complex **2.1**. I hypothesize that this difference is due the greater steric pressure exerted by the Dipp groups on -CPh_3 in complex **2.2**.[45] The homolysis of the C-S bond in **2.2** results in the formation of a dimeric Ni disulfide complex, [{*N*,*N*:κ^2-L^{tBu}}Ni^{II}(μ_2-η^2-η^2-S_2)Ni^{II}{*N*,*C*:κ^2-L^{tBu}}] (**2.3**) which was isolate as dark green plates in 40% yield. The formation of Gomberg's dimer[46] in the reaciton was confirmed by ^{1}H NMR spectroscopy (Scheme 2.3).

Scheme 2.3 Homolysis of [$L^{tBu}Ni^{II}(SCPh_3)$] (**2.2**) to yield [{*N*,*N*:κ^2-L^{tBu}}Ni^{II}(μ_2-η^2-η^2-S_2)Ni^{II}{*N*,*C*:κ^2-L^{tBu}}] (**2.3**)

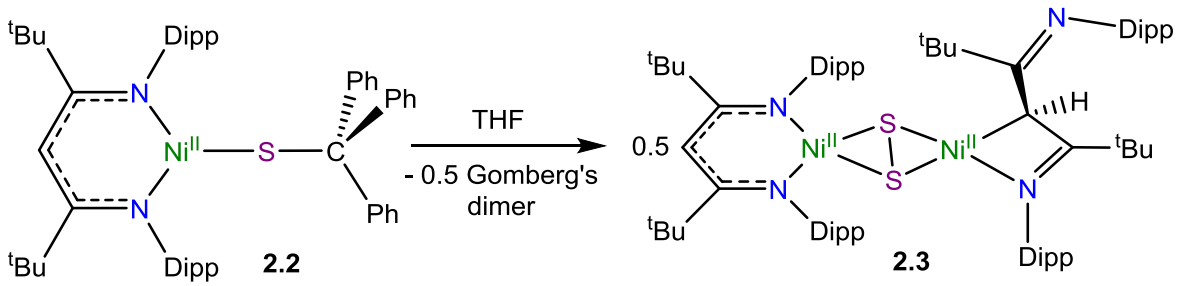

The formulation of complex **2.3** has been confirmed by elemental analysis, ^{1}H NMR spectroscopy, X-ray crystallography. The solid state molecular structure of **2.3** is shown in Figure 2.7. The S-S bond length in **2.3** is 2.039(6) Å and is consistent with the single bond present in the S_2^{2-} ligand.[26,47–53] The coordination geometry of each Ni center is square planar, with Σ(L-Ni-L) = 358.5° for Ni1 and Σ(L-Ni-L) = 359.3° for Ni2, consistent with the observed diamagnetism of **2.3**. The ^{1}H NMR spectrum of complex **2.3** in C_6D_6 is characteristic of a diamagnetic, square planar Ni^{II} β-diketiminate complex where the β-diketiminate proton environments are asymmetrical due to the abnormal binding mode of the *N*,*C*:κ^2-L^{tBu} ligand coordinated to Ni1. The formation of complex **2.3** likely proceeds via the dimerizaiton of an intermediate Ni^{II} thiyl ($S^{\bullet-}$) species and is similar to a reaction previously reported by Riordan and co-workers. In particular, they observe that thermolysis of the Ni tritylthiolate complex, [{$PhB(CH_2S^tBu)_3Ni(SCPh_3)$], results in the formation of [{$PhB(CH_2S^tBu)_3Ni]_2(\mu_2$-η^2,η^2-$S_2$) and Gomberg's dimer.[49]

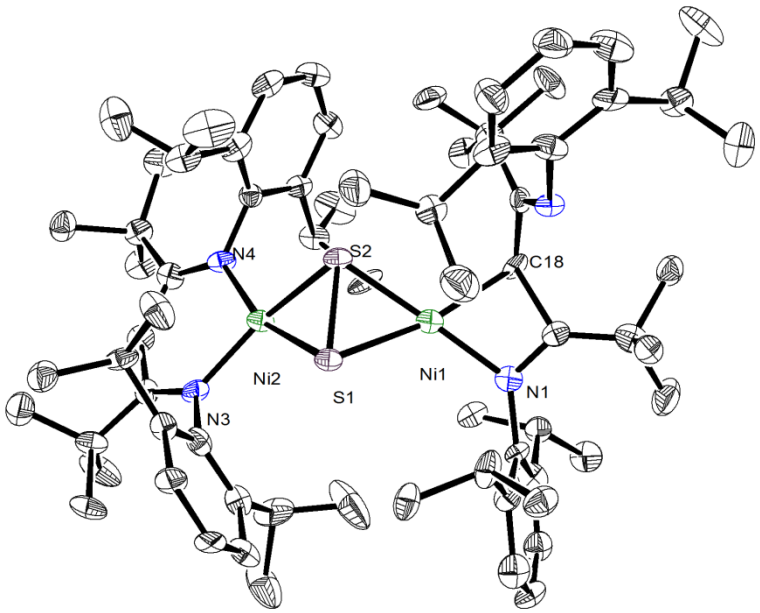

Figure 2.7. ORTEP diagram of [{*N*,*N*:κ^2-L^{tBu}}Ni^{II}(μ$_2$-η^2-η^2-S$_2$)Ni^{II}{*N*,*C*:κ^2-L^{tBu}}]·C$_6$H$_{18}$O$_2$Si (**2.3**· C$_6$H$_{18}$O$_2$Si) with 50% probability ellipsoids. Hydrogen atoms and a C$_6$H$_{18}$O$_2$Si solvate molecule have been omitted for clarity. Selected bond lengths and angles: S1-S2 2.039(6) Å, Ni1-S1 2.222(4) Å, Ni1-S2 2.167(5) Å, Ni2-S1 2.231(5) Å, Ni2-S2 2.203(4) Å, Ni1-N1 1.90(1) Å, Ni1-C18 2.00(1) Å, Ni2-N3 1.91(1) Å, Ni2-N4 1.90(2) Å, N1-Ni1-C18 68.9(6)°, N1-Ni1-S1 120.7(4)°, S1-Ni1-S2 55.4(2)°, N3-Ni2-N4 96.9(5)°, N3-Ni2-S1 102.7(4)°, S1-Ni2-S2 54.76(16)°.

2.2.2 Synthesis and Characterization of [K(18-crown-6)][L^{R}Ni^{II}(S)] (2.4, R = Me; 2.5, R = ^{t}Bu) and [K(2,2,2-crypt)][L^{iBu}Ni^{II}(S)] (2.6)

Subsequent reduction of **2.1** and **2.2** with 2 equiv of KC$_8$, in cold (-25 °C) Et$_2$O, in the presence of 2 equiv of 18-crown-6, results in the formation of [K(18-crown-6)][L^{R}Ni^{II}(S)] (**2.4**, R = Me; **2.5**, R = ^{t}Bu). Complex **2.4** can be isolated as dark green blocks from hexanes/C$_6$H$_6$ in 66% yield, while complex **2.5** can be isolated as dark brown plates from toluene/isooctane in 88% yield (Scheme 2.3). Similarly, use of 2,2,2-cryptand in place of

18-crown-6 affords [K(2,2,2-cryptand)][$L^{tBu}Ni^{II}(S)$] (**2.6**), which can be isolated as brown needles in 89% yield after crystallization from hexanes (Scheme 2.3). The syntheses of **2.4**, **2.5**, and **2.6** also produce one equiv of [K(L)][CPh_3] (L = 18-crown-6, **2.7**; 2,2,2-cryptand, **2.8**), which precipitates from the reaction mixtures as a bright red solid that can be separated from the Ni-containing products via filtration (Scheme 2.4).

Scheme 2.4 Synthesis of [K(18-crown-6)][$L^{R}Ni^{II}(S)$] (**2.4**, R = Me; **2.5**, R = ^{t}Bu) and [K(2,2,2-crypt)][$L^{iBu}Ni^{II}(S)$] (**2.6**) via reductive deprotection

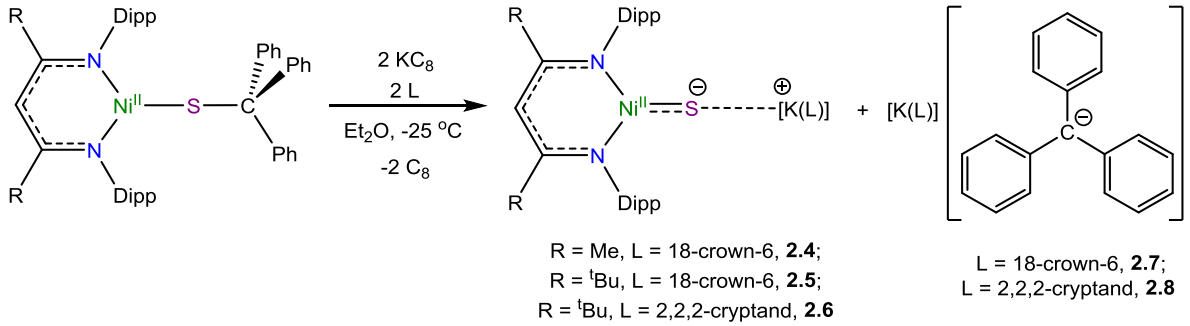

R = Me, L = 18-crown-6, **2.4**;
R = ^{t}Bu, L = 18-crown-6, **2.5**;
R = ^{t}Bu, L = 2,2,2-cryptand, **2.6**

L = 18-crown-6, **2.7**;
L = 2,2,2-cryptand, **2.8**

I should also note that reaction of **2.2** with only one equivalent of KC_8, in the presence of 18-crown-6, still provides **2.5** in good yield (67%). However, under these conditions, triphenylmethane, and not $[CPh_3]^-$, is formed as the reaction by-product. This suggests that the Ph_3C-S cleavage can also proceed via a radical process as proposed in Scheme 2.5. C-S homolysis has previously been observed for a Ni tritylthiolate complex.[49,54] For example, Riordan and co-workers reported the formation of [{$PhB(CH_2S^tBu)_3Ni]_2(\mu_2$-$\eta^2,\eta^2$-$S_2$) and $\cdot CPh_3$ upon thermal decomposition of [{$PhB(CH_2S^tBu)_3Ni(SCPh_3)$].[49]

Scheme 2.5 Synthesis of **2.5** via one electron reduction

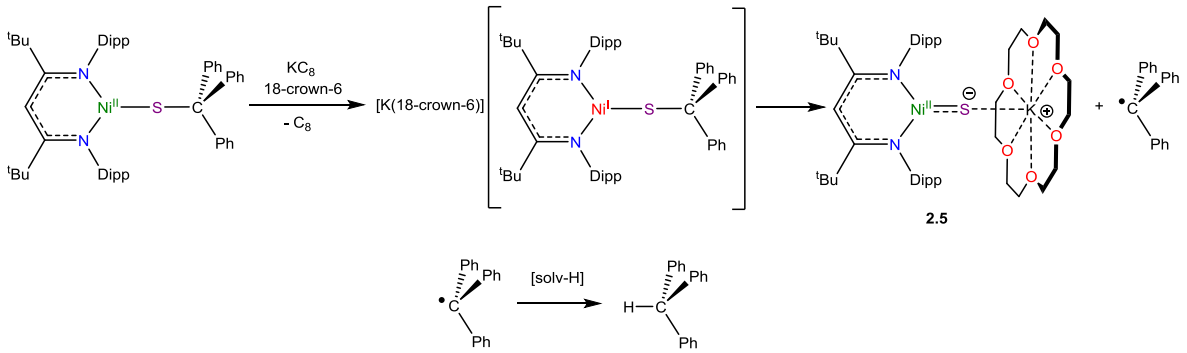

The formulations of complexes **2.4**, **2.5**, and **2.6** were confirmed through elemental analysis, ^{1}H NMR spectroscopy, and X-ray crystallography. The solid-state structures of **2.4**, **2.5**, and **2.6** are shown in Figure 2.8, while selected metrical parameters can be found in Table 2.1.

Table 2.1 Selected Bond Lengths and Angles for **2.4**, **2.5**, and **2.6**

bond (Å) / angle(°)	**2.4**	**2.5**	**2.6**
Ni1-S1	2.0635(6)	2.0643(2)	2.0843(1)
S1-K1	3.1212(7)	3.094(1)	3.3795(1)
Ni1-N1	1.9466(2)	1.938(5)	1.931(3)
Ni1-N2	1.9444(2)	1.928(5)	1.933(3)
Ni1-S1-K1	153.74(3)	177.95(8)	170.08(5)
N1-Ni1-S1	136.28(5)	134.08(2)	131.01(9)
N2-Ni1-S1	130.53(5)	130.37(2)	133.18(9)
N1-Ni1-N2	93.02(7)	95.5(2)	95.78(1)

Complexes **2.4**, **2.5** and **2.6** feature identical coordination environments about their Ni centers. In the solid state, each exhibits a planar (Σ(L-Ni-L) ~ 360°), Y-shaped geometry. The Ni-S bond lengths in **2.4-2.6** range from 2.0635(6)-2.0843(1) Å. All three complexes feature weak S-K interactions,[39,54] which range from 3.094(2)-3.3795(1) Å. Not surprisingly, complex **2.6**, which features the strongest K^{+} chelator (2,2,2-cryptand), exhibits

the longest S-K interaction. Interestingly, the Ni-S-K angles vary widely, from 153.73(3)° (for **2.4**) to 177.9(1)° (for **2.5**), a disparity I ascribe to crystal packing. Also of note, complex **2.5** exists as a dimer in the solid state; its monomer units are connected via bridging interactions between the $[K(18\text{-crown-6}]^+$ cations (Figure 2.8). Finally, the Ni-N distances in **2.4**-**2.6** are typical of those found in other three coordinate Ni^{II} β-diketiminate complexes.[40–42,44]

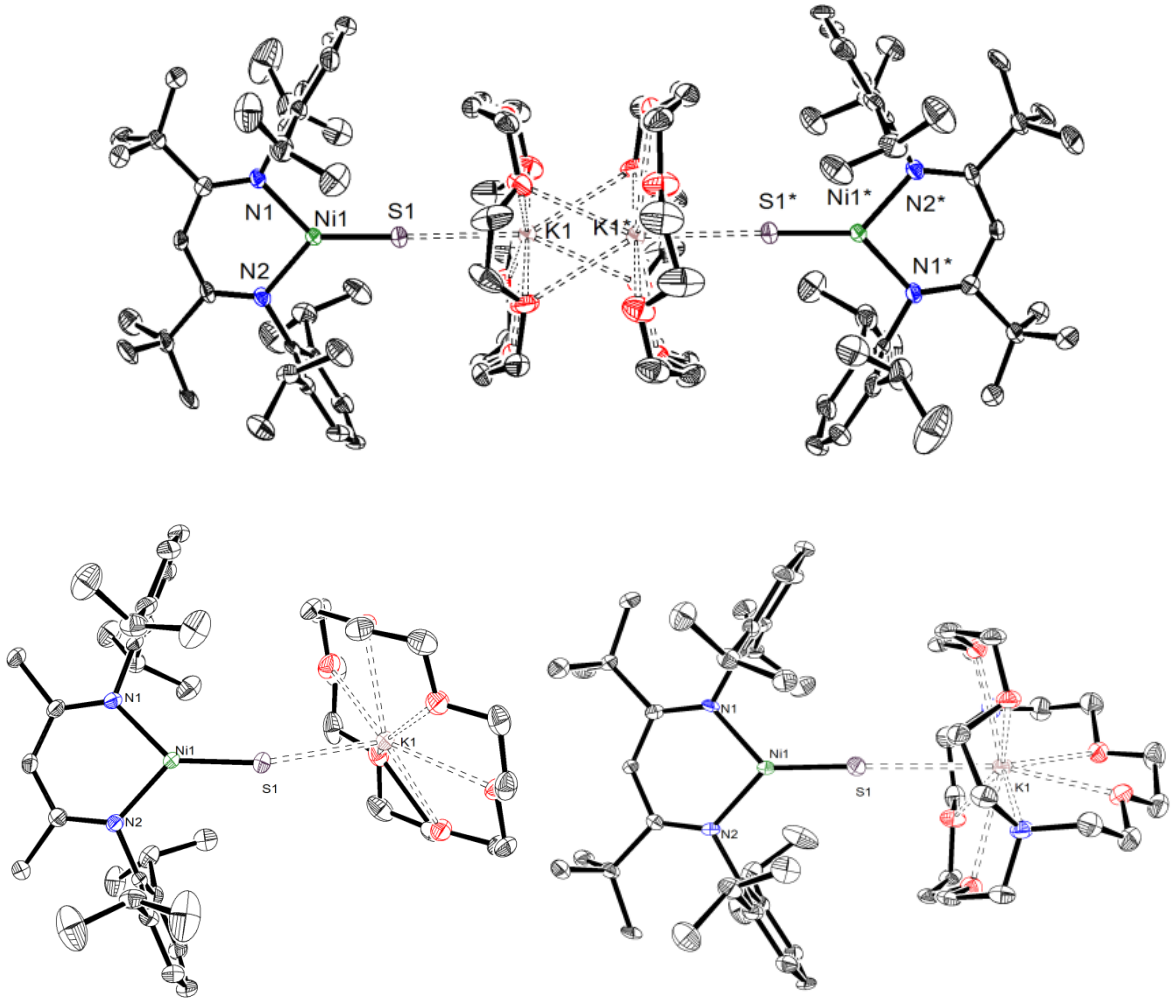

Figure 2.8. ORTEP diagrams of $[K(18\text{-crown-6})][L^{tBu}Ni^{II}(S)]\cdot C_8H_{18}$ (**2.5**$\cdot 0.5C_8H_{18}$) (top), $[K(18\text{-crown-6})][L^{Me}Ni^{II}(S)]\cdot 2.5C_6H_6$ (**2.4**$\cdot 2.5C_6H_6$) (bottom left), and [K(2,2,2-

cryptand)][$L^{tBu}Ni^{II}(S)$] (**2.6**) (bottom right) with 50% probability ellipsoids. Hydrogen atoms and solvate molecules have been omitted for clarity.

Most significantly, the Ni-S bond lengths in complexes **2.4**, **2.5**, and **2.6** are amongst the shortest known, and are intermediate between the additive covalent radii projected for nickel-sulfur single (2.13 Å) and double bonds (1.95 Å).[55] Moreover, the Ni-S bond length in **2.4** is shorter than that observed in the parent thiolate, **2.2** (2.1523(5) Å), as expected for a bond with partial multiple bond character. For further comparison, $[L^{tBu}Ni]_2(\mu\text{-}S)$,[42] $\{(IPr)Ni\}_2(\mu\text{-}S)_2$ (IPr = 1,3-bis(2,6-diisopropylphenyl)imidazol-2-ylidene),[52] and $[(PhB\{CH_2S^tBu\}_3)Ni]_2(\mu\text{-}S)_2$,[49] possess comparable Ni-S bond lengths of 2.0651(7), 2.0972(6), and 2.0714(4) Å, respectively, despite each possessing a bridging S^{2-} ligand. Overall, this suggests similar magnitudes of π-bonding in both classes of materials.

The ^{1}H NMR spectra of complexes **2.4-2.6** in C_6D_6 are typical of those observed for other three coordinate, high spin Ni^{II} β-diketiminate complexes.[42,46] Notably, the resonances assignable to the $[K(18\text{-crown-}6)]^+$ cations are broad and shifted to 1.18 and 0.28 for **2.4** and **2.5**, respectively. The 2,2,2,-cryptand resonances for **2.6** are similarly broadened and shifted. These data suggest that the $[K(L)]^+$ cations form a contact pair with the $[L^RNi^{II}(S)]^-$ anions in solution. These complexes are highly soluble in THF, Et_2O, benzene, and toluene, but sparing solubility in hexane and pentane; **2.6** is notably more soluble in the former, presumably due to the ability of 2,2,2-cryptand to better encapsulate the K+ ion. Complexes **2.4-2.6** do not show any appreciable decomposition upon prolonged storage in the solid state under inert atmosphere at -25 °C. However, **2.4** and **2.5** have been observed to decompose in THF solutions to yield a mixture of nickel-sulfur compounds. In THF, complex **2.4** decomposes more quickly (hours) than **2.5** (days) necessitating the use of Et_2O as the

reaction solvent in its synthesis. The products of this decomposition reaction are discussed below. Interestingly, oxidation of complex **2.6** with one equiv of silver triflate (AgOTf) resulted in the formation of the previously reported complex [{$L^{tBu}Ni^{II}$}$_2$(μ^2-S)],[42] with elemental sulfur formed as a likely byproduct (Scheme 2.6).

Scheme 2.6 Oxidation of **2.6** to yield [{$L^{tBu}Ni^{II}$}$_2$(μ^2-S)]

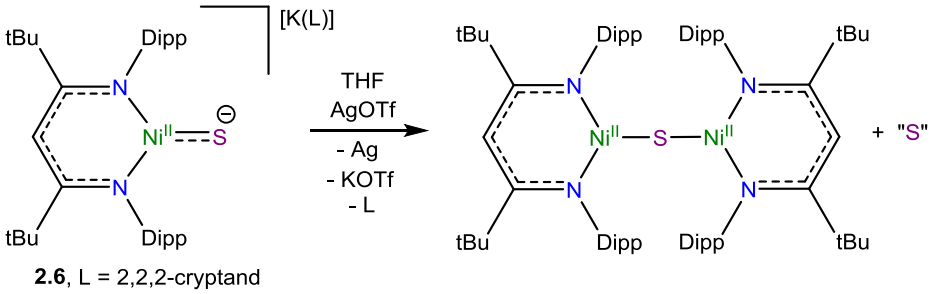

2.6, L = 2,2,2-cryptand

In the solid state, complexes **2.4** and **2.5** exhibit effective magnetic moments of 2.80 B.M. at 300 K (D = 91 cm^{-1}) and 2.98 B.M. at 300 K (D = 94 cm^{-1}), respectively (Figure 2.9). This behavior is consistent with that anticipated for a Y-shaped Ni^{II} complex with an S = 1 ground state.[56] Overall, the solid state molecular structures and magnetic properties of **2.4**-**2.6** confirm my Ni^{II} oxidation state assignments, and exclude the possibility that the sulfur atom is protonated, as this would require nickel to be in the +1 oxidation state. Intriguingly, the related Ni^{II} imido, carbene, and phosphinidene complexes, e.g., [(dtbpe)Ni^{II}(E)], are diamagnetic.[9,12,13] This change in spin state may reflect differing amounts of π-bonding between the two classes of molecules.

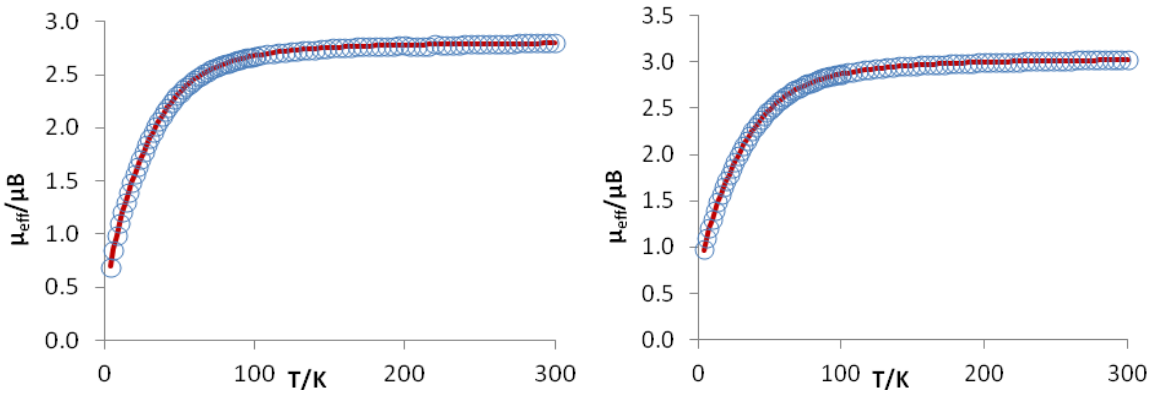

Figure 2.9. Temperature dependent, solid state magnetic susceptibility data for [K(18-crown-6)][$L^{Me}Ni^{II}$(S)] (left) (**2.4**) and [K(18-crown-6)][$L^{tBu}Ni^{II}$(S)] (right) (**2.5**).

On the basis of DFT calculations performed by Ghosh and co-workers for the related Ni^{III} imido complex, [L^{R}Ni(NPh)], I predict a $(d_z^2)^2(d_x^2\text{-}_y^2)^2(d_{yz})^2(b_1)^2(b_2)^2(b_2*)^1(b_1*)^1$ electronic configuration for complexes **2.4-2.6** (Figure 2.10),[1,57] wherein b_1 and b_2 are the π-bonds formed between the sulfur lone pairs and the d_{xz} and d_{yz} orbitals, respectively. If true, this electronic structure would suggest a formal Ni-S bond order of 2, a prediction that is somewhat inconsistent with the observed Ni-S bond lengths in **2.4-2.6**, which is perhaps a function of coordination of K^+ to the sulfide ligand.

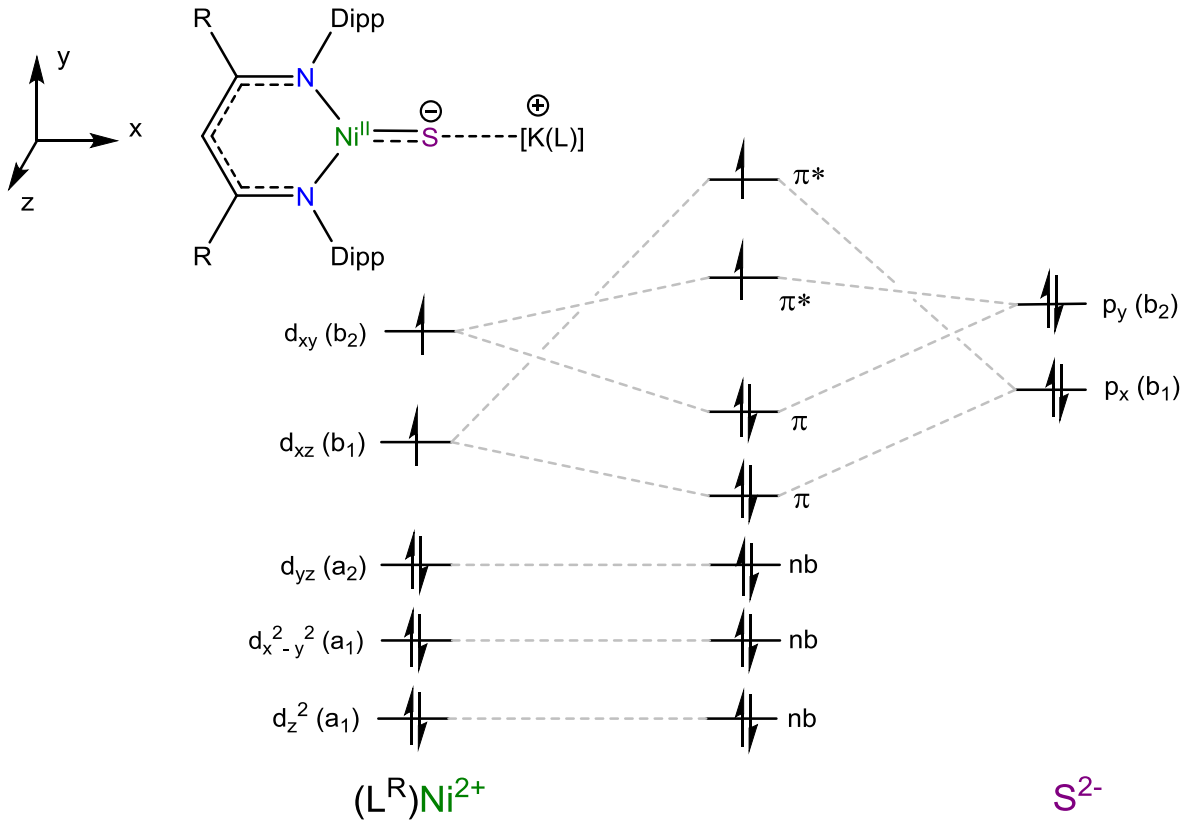

Figure 2.10. Proposed molecular orbital diagram for the Ni-S bonding interaction in complexes **2.4-2.6**.

2.2.3 The Decomposition of [K(18-crown-6)][$L^{Me}Ni^{II}$(S)] (2.4) to yield [K(18-crown-6)][{$L^{Me}Ni$}$_2$(μ^2-S)] (2.9) and [K(18-crown-6)][{$L^{Me}Ni$}$_2$(μ^2-S)$_2$] (2.10)

As mentioned above, complex **2.4** has been observed to decompose upon storage in THF. While the mechanism of this process has not been worked out, I have been able to characterize the main Ni containing products of this transformation as [K(18-crown-6)][{$L^{Me}Ni$}$_2$(μ^2-S)] (**2.9**) and [K(18-crown-6)][{$L^{Me}Ni$}$_2$(μ^2-η^2-η^2-S_2)] (**2.10**) (Scheme 2.7).

Scheme 2.7 Decomposition of **2.4** to yield **2.9** and **2.10**

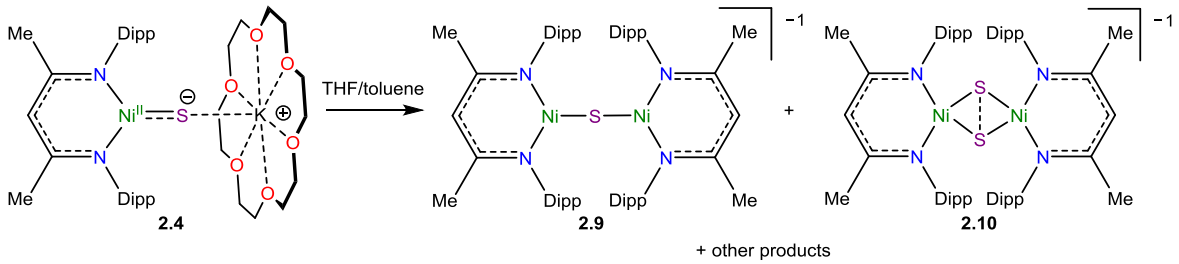

Isolation and full characterization of these products has proven to be very challenging as they possess near identical solubility and spectroscopic characteristics and co-crystallize in the same unit cell. An initial single crystal containing co-crystallized **2.9** and **2.10** was isolated from the supernatant (THF layered with hexane) of the crystallization of **2.4**. This crystal contained **2.9** and **2.10** in a 1:4 ratio. Further experiments are needed to assess the relative ratios of formation of **2.9** and **2.10** in the supernatant. The solid state molecular structures of **2.9** and **2.10** are shown in Figure 2.11. Due to co-crystallization, the bond lengths and angles present in this structure should be considered estimates; however, they do allow for a preliminary assignment of the sulfur and nickel oxidation states. It appears that complex **2.9** is a mixed-valent $Ni^{I/II}$ complex with a μ^2-S^{2-} ligand. While, complex **2.10** can be described as either containing two Ni^{II} centers with a μ^2-η^2-η^2-subsufide (S_2^{3-}) ligand, or a mixed valent $Ni^{II/III}$ complex with two μ^2-S^{2-} ligands.

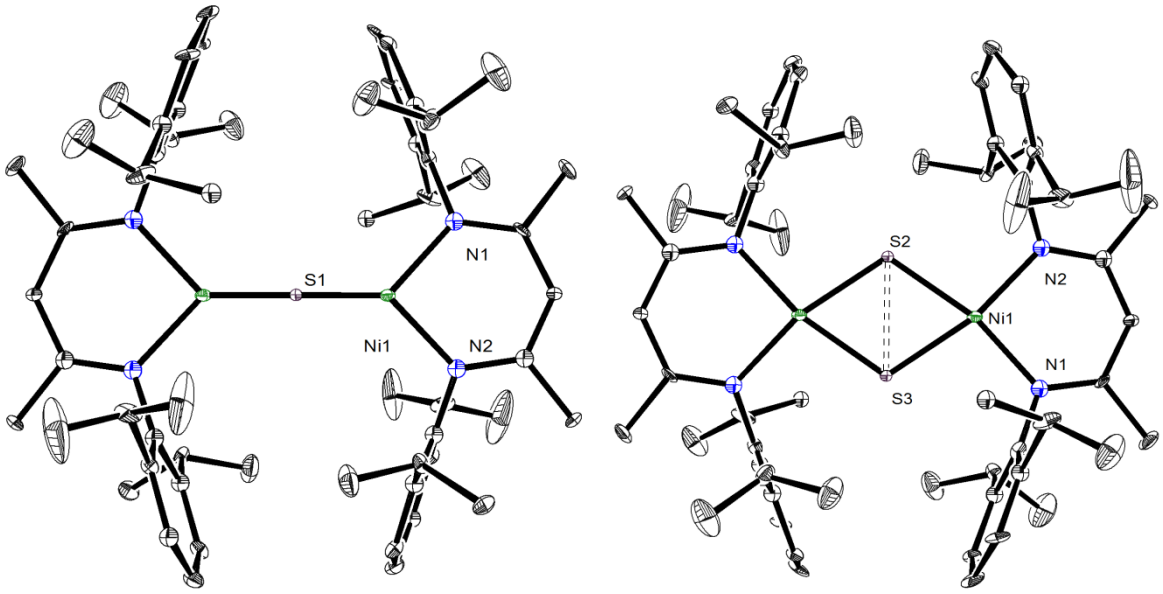

Figure 2.11. ORTEP diagrams of [K(18-crown-6)][{L^{Me}Ni}$_2$(μ^2-S)]·C_4H_8O (**2.9**·C_4H_8O, left) and [K(18-crown-6)][{L^{Me}Ni}$_2$(μ^2-η^2-η^2-S_2)]·C_4H_8O (**2.10**·C_4H_8O, right) with 50% probability ellipsoids. These diagrams represent the two disordered species present in the solid state molecular structure in 21:79 (**2.9**:**2.10**) ratio. Hydrogen atoms, $[K(18\text{-crown-6})]^+$, and C_4H_8O solvate molecules have been omitted for clarity.

I have been able to isolate single crystals of **2.10** from the decomposition of **2.4** in cold (- 25 °C) THF/toluene in 49% yield. The solid-state molecular structure of pure **2.10** is shown in Figure 2.12. The S-S distance in **2.10** is 2.522(5) Å (about 0.1 Å longer that the S-S bond length observed in the mixed structure Figure 2.11) and is much longer than a S-S single bond,[26,47–53] being approximately on the order of S-S distances observed in subsulfide complexes.[58–63] The Ni-S distances in **2.10** are consistent with single bonds and the coordination geometry of each Ni center is square planar, with Σ(L-Ni-L) = 360.1°. The ^{1}H NMR spectrum of complex **2.10** in THF-d_8 contains apparently paramagnetically broadened resonances that are, however, not significantly shifted from what would be expected for a square planar Ni^{II} β-diketiminate complex. For example, the spectrum contains β-

diketiminate methyl and γ-H resonances at 0.77 and 5.50 ppm, respectively. Based upon these observations, I believe that **2.10** contains two Ni^{II} centers bridged by a μ^2-η^2-η^2-subsufide (S_2^{3-}) ligand, where the unpaired electron is localized on the subsulfide moiety and not on the Ni centers.

Metal subsulfide complexes are quite rare and only a few examples have been reported to date, including $[\{(C_5H\textit{i}Pr_4)Ni\}_2(S_2)]$, $[L^{Me}Ni(S_2)Pt(PPh_3)_2]$ and $[L^{Me}Ni(S_2)Fe(dmpe)_2]$ (dmpe = 1,2-bis(dimethylphosphino)ethane).[58,61,62] To rationalize formation of **2.9** and **2.10** in this reaction, I propose that a by-product containing oxidized sulfur (S^0 or K_2S_2) is being formed. Notable previous examples of Ni sulfide dimerization resulted in the formation different products. For example Limberg and co-workers reported the isolation of a bimetallic Ni^{II} μ^2-η^2-η^2-disufide, $[\{L^{Me}Ni^{II}\}_2(\eta^2\text{-}S_2)]$, via a proposed Ni^{III} terminal sulfide intermediate. The formation of a disulfide in this reaction can be rationalized by the Ni centers in this system each being reduced by one e^- to facilitate the S-S bond forming reaciton.[26] In the example reported by Jones and co-workers, formation of a bimetallic Ni^{II} bis(μ^2-sulfide) complex, $[\{(dippe)Ni^{II}\}_2(S)_2]$, results from the dimerization of a proposed Ni^{II} terminal sulfide intermediate.[27] I hypothesize that a similar bimetallic Ni^{II} bis(μ^2-sulfide) product is not observed in this reaction because the formation of this dianionic species is disfavored and results in spontaneous disproportionation to generate **2.9** and **2.10**.

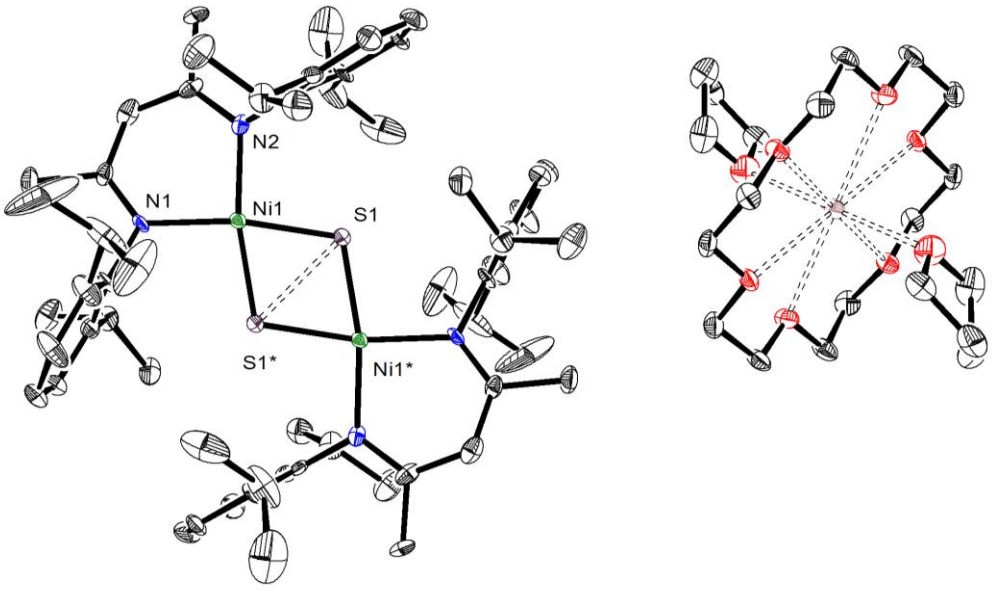

Figure 2.12. ORTEP diagram of [K(18-crown-6)][{L^{Me}Ni}$_2$(μ^2-η^2-η^2-S_2)]·C_4H_8O (**2.10**·C_4H_8O) with 50% probability ellipsoids. Hydrogen atoms and a C_4H_8O solvate molecule have been omitted for clarity. Selected bond lengths and angles: S1-S1* 2.522(5) Å, Ni1-S1 2.151(4) Å, Ni1-S1* 2.167(4) Å, Ni1-N1 1.990(7) Å, Ni1-N2 1.970(7) Å, N1-Ni1-N2 93.3(3)°, N1-Ni1-S1* 97.8(2)°, N2-Ni1-S1 97.5(2)°, S1-Ni1-S1* 71.5(2)°.

2.2.4 Synthesis of [K(18-crown-6)][$L^{tBu}Ni^{I}$(SH)] (2.11)

While the use crystallographic and magnetism data were used to rule out the protonation of the sulfur atom in cmopelxes **2.4** -**2.6**, I was still interested in pursuing a method to access a Ni hydrosulfide complex. The sulfide ligand in these complexes does not react with H-atom donors such as 1,4-cyclohexadiaene and 2,9-dihydroanthracene. However, **2.5** was found to react with diphenylsilane (Ph_2SiH_2) to afford [K(18-crown-6)][$L^{tBu}Ni^{I}$(SH)] (**2.11**) (Scheme 2.8). Complex **2.11** was isolated in low yields as this reaction is not clean. To date, I have been unable to identify the silicon containing byproduct of this reaction, However it is likely $Ph_2HSiSiHPh_2$.

Scheme 2.8 Synthesis of [K(18-crown-6)][L^{tBu}Ni^{I}(SH)] (**2.11**)

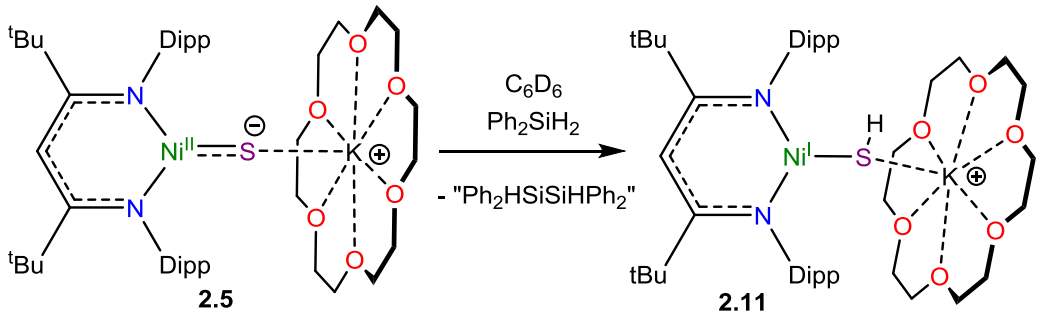

Complex **2.11** was characterized by ^{1}H NMR spectroscopy and X-ray crystallography. The solid state molecular structure of **2.11** is shown in Figure 2.13. Complex **2.11** features a three coordinate Ni^{I} center ligated by a hydrosulfide (SH^{-}) moiety with an Ni-S bond length of 2.176(3) Å which longer than the Ni-S bond in the starting material, **2.5** (2.0643(2) Å), and is consistent with a single bond.[41] The coordination geometry of the Ni center in **2.11** is planar (Σ(L-Ni-L) = 360.0°) and is best described as Y-shaped. The ^{1}H NMR spectrum of **2.11** in C_6D_6 contains paramagnetically shifted resonances similar to those of other three coordinate Ni^{I} *β*-diketiminate complexes. For example, **2.11** features a broad *tert*-butyl resonance at -1.03 ppm.[41,64–66] To my knowledge, complex **2.11** is only the fourth structurally characterized Ni SH^{-} complex and the first example of a Ni^{I} SH^{-} complex.[48,67]

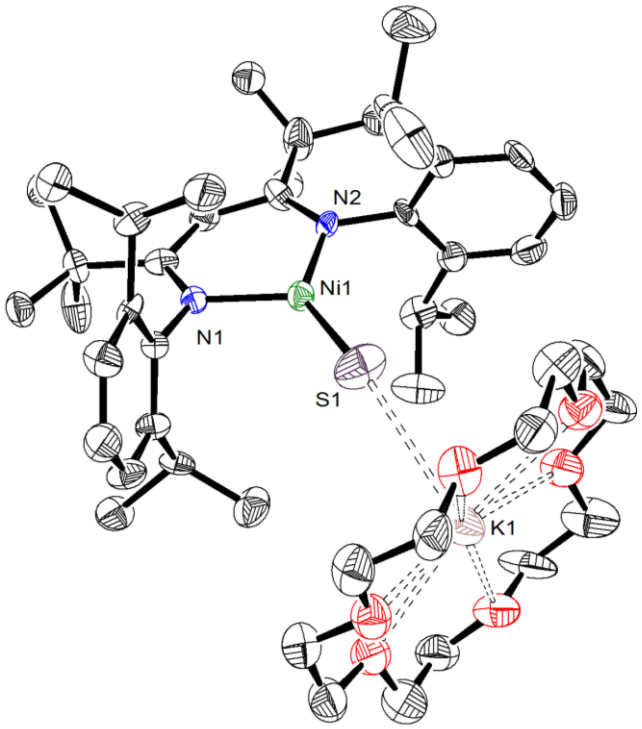

Figure 2.13 ORTEP diagram of [K(18-crown-6)][$L^{tBu}Ni^{I}(SH)$]·$C_4H_{10}O$ (**2.11**·$C_4H_{10}O$) with 50% probability ellipsoids. Hydrogen atoms and Et_2O solvate molecule omitted for clarity. Selected bond lengths and angles: Ni1-S1 2.176(3) Å, S1-K1 3.170(4) Å, Ni1-N1 1.895(6) Å, Ni1-N2 1.882(6) Å, Ni1-S1-K1 142.3(1)°, N1-Ni1-N2 98.7(3)°, N1-Ni1-S1 123.5(2)°, N2-Ni1-S1 137.8(2)°.

2.2.5 Synthesis of [$L^{tBu}Ni^{II}(SSiMe_3)$] (2.12)

The sulfide ligand in complexes **2.4-2.6** would be anticipated to be a potent nucleophile. Consequently, I endeavored to test this hypothesis by reacting complex **2.5** with the strong electrophile, trimethylsilyl triflate (Me_3SiOTf). Reaction of a C_6H_6 solution of **2.5** with one equiv of Me_3SiOTf results in the formation of a trimethylsilanethiolato complex [$L^{tBu}Ni^{II}(SSiMe_3)$] (**2.12**) with concomitant loss of [K][OTf] (Scheme 2.9).

Scheme 2.9 Synthesis of [$L^{tBu}Ni^{II}(SSiMe_3)$] (**2.12**)

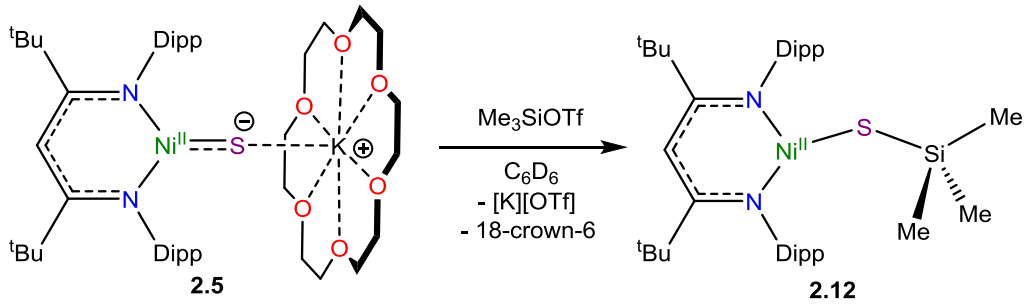

Complex **2.12** was isolated as red plates in 70% yield and characterized by ^{1}H NMR spectroscopy and X-ray crystallography. The solid state molecular structure of **2.12** is shown in Figure 2.14. Complex **2.12** features a three coordinate Ni^{II} center ligated by a trimethylsilanethiolato moiety with a Ni-S bond length of 2.177(1) Å which is longer than the Ni-S bond in the starting material (2.0643(2) Å) and is consistent with a single bond.[41] The coordination geometry of Ni center remains planar (Σ(L-Ni-L) = 358.25°). However, the C_{2v} symmetry present in **2.5** has been lost. The ^{1}H NMR spectrum of **2.12** in C_6D_6 contains paramagnetically shifted resonances similar to those of other three coordinate Ni^{II} *β*-diketiminate complexes.[40,41] Complex **2.12** is a rare example of a Ni silanethilato ($SSiR_3$) complex and the first three coordinate Ni($SSiR_3$) complex. Other examples reported by Tatsumi and coworkers were synthesized via salt metathesis of M($SSiR_3$) and $LNiCl_2$ to yield [(dppe)Ni($SSiMe_2R)_2$] (R = Me, ^{t}Bu, dppe = $PPh_2CH_2CH_2PPh_2$) and [(tmeda)Ni(SSiPh3)2] (tmeda = NMe2CH2CH2NMe2).[68,69] Additionally, formation of the SSiMe3 product, is reminiscent of the reaction of Me3SiCl and Na2S to give Me3SiSNa,[70] this result confirms the nucleophilicity of the sulfide ligand and suggests that "masked" terminal nickel sulfide complexes may be capable of effecting more challenging transformations.

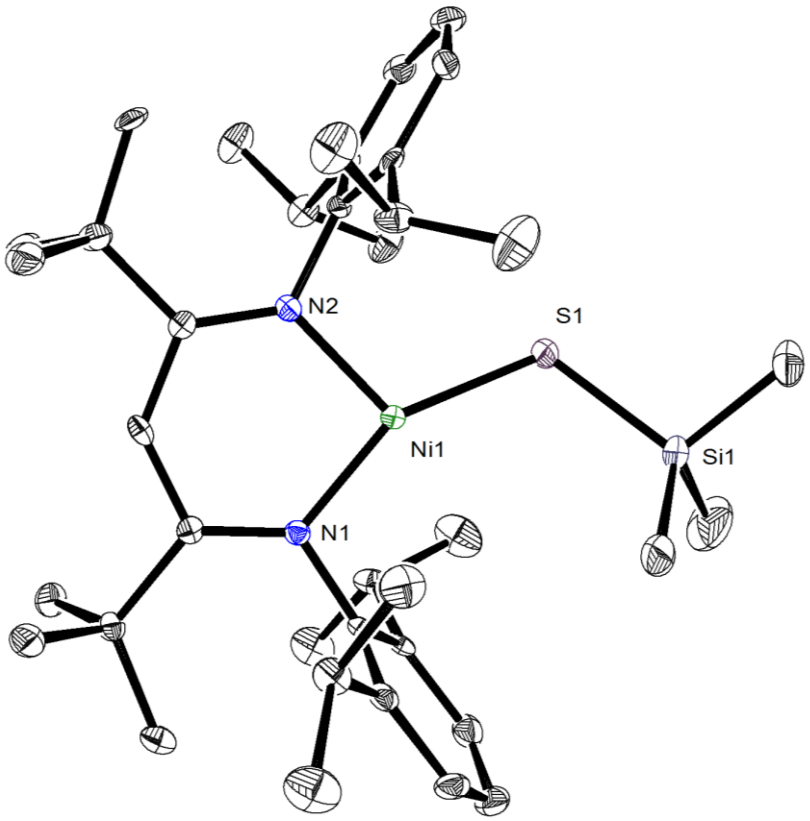

Figure 2.14. ORTEP diagram of [$L^{tBu}Ni^{II}(SSiMe_3)$] (2.12) with 50% probability ellipsoids. Hydrogen atoms and a second independent molecule of [$L^{tBu}Ni^{II}(SSiMe_3)$] omitted for clarity. Selected bond lengths and angles: (2.1) Ni1-S1 2.177(1) Å, Si1-S1 2.116(2) Å, N1-Ni1-N2 95.9(1)°, N1-Ni1-S1 149.7(1)°, N2-Ni1-S1 112.9(1)°, Ni1-S1-Si1 115.27(6)°.

2.3 Summary

The results outlined in Chapter 2 demonstrate that reductive deprotection, initially used for the synthesis of actinide chalcogenide multiple bonds, is also applicable to a late transition metal system. Reaction of [$L^{R}Ni^{II}Cl$] (R = Me, ^{t}Bu) with $KSCPh_3$ yields the nickel tritylthiolates, [$L^{R}Ni^{II}(SCPh_3)$] (**2.1**, R = Me; **2.2**, R = ^{t}Bu). Subsequent application of the reductive deprotection protocol to these complexes results in cleavage of the tritylthiolate C-S bond and affords the first family of "masked" terminal Ni^{II} sulfides, [K(L)][$L^{R}Ni^{II}(S)$]

(**2.4**, R = Me, L = 18-crown-6; **2.5**, R = ^{t}Bu, L = 18-crown-6; **2.6**, R = ^{t}Bu, L = 2,2,2-cryptand). Structural characterization of these complexes reveals that the Ni-S distances in this class of materials are amongst the shortest observed, suggesting the presence of partial multiple bond character, critical for the stabilization of the Ni-S bond. Furthermore, [K(18-crown-6)][$L^{tBu}Ni^{II}$(S)] (**2.5**) reacts with Ph_2SiH_2 to form a SH^- complex, [K(18-crown-6)][$L^{tBu}Ni^{I}$(SH)] (**2.10**), and Me_3SiOTf to form a trimethylsilanethiolato complex [$L^{tBu}Ni^{II}$($SSiMe_3$)], (**2.12**) confirming the nucleophilicity of the sulfide ligand. The stability of these nickel sulfide complexes should allow for further investigations of the reactivity of the sulfide ligand with other electrophilic substrates.

The reductive deprotection method is particularly attractive for late transition metal systems as it leads to the controlled installation of a single sulfide ligand at the metal center, retaining the low coordination number needed to stabilize the metal-ligand multiple bond. A final beneficial facet of this method, is the presence of $[K(L)]^+$ as a capping countercation in the nickel sulfide complexes. This fragment it appears to protect the sulfide ligand from unwanted side reactions such as dimerization. Thus, allowing me to explore the reactivity of Ni sulfide with small molecules, which will be discussed in chapters 4, 5, and 6.

2.4 Experimental Procedures

2.4.1 General Methods

All reactions and subsequent manipulations were performed under anaerobic and anhydrous conditions under an atmosphere of nitrogen. Hexanes, diethyl ether (Et_2O), toluene, and tetrahydrofuran (THF) were dried using a Vacuum Atmospheres DRI-SOLV Solvent Purification system and stored over 3Å sieves for 24 h prior to use. Benzene-d_6, tetrahydrofuran-d_8, toluene-d_8, and C_8H_{18} (isooctane) were dried over 3Å molecular sieves

for 24 h prior to use. L^{Me} (L = {(2,6-$^{i}Pr_2C_6H_3$)NC(R)}$_2$CH), R = Me),[71] L^{tBu} (L = {(2,6-$^{i}Pr_2C_6H_3$)NC(R)}$_2$CH), R = ^{t}Bu),[72] L^{Me}Li,[73] L^{tBu}Li,[72] $L^{Me}Ni^{II}Cl$,[44] $L^{tBu}Ni^{II}Cl$,[40] $KSCPh_3$,[74] and $KOCPh_3$[75] were synthesized according to the previously reported procedures. All other reagents were purchased from commercial suppliers and used as received.

^{1}H and $^{13}C\{^{1}H\}$ NMR spectra and Evans' method determinations[43] were recorded on a Agilent Technologies 400-MR DD2 400 MHz spectrometer or a Varian UNITY INOVA 500 MHz spectrometer. ^{1}H and $^{13}C\{^{1}H\}$ NMR spectra were referenced to external $SiMe_4$ using the residual protio solvent peaks as internal standards.[76,77] IR spectra were recorded on a Nicolet 6700 FT-IR spectrometer with a NXR FT Raman Module. Elemental analyses were performed by the Micro-Mass Facility at the University of California, Berkeley.

2.4.2 Magnetism Measurements

Magnetism data were recorded using a Quantum Design MPMS 5XL SQUID magnetometer. The experiment was performed between 4 - 300 K using 20-50 mg of powdered, crystalline solid. The solids were loaded into an NMR tube, which was subsequently flame sealed. The solids were kept in place with approximately 100 mg of quartz wool packed on either side of the sample. The data was corrected for the contribution of the NMR tube holder and the quartz wool. The experiments were performed using a 0.5 T field. Diamagnetic corrections (χ_{dia} = -5.504×10^{-4} $cm^3 \cdot mol^{-1}$ for **2,** χ_{dia} = -5.518×10^{-4} $cm^3 \cdot mol^{-1}$ for **3**, and χ_{dia} = -6.143×10^{-4} $cm^3 \cdot mol^{-1}$ for **4**) were made using Pascal's constants.[78] Data were fit using the JulX program (v. 1.4.1).[79]

2.4.3 Synthesis of [$L^{Me}Ni^{II}(SCPh_3)$] (2.1)

To a dark blue, stirring suspension of $L^{Me}Ni^{II}Cl$ (200 mg, 0.391 mmol) in C_6H_6 (3 mL) was added a suspension of $KSCPh_3$ (125 mg, 0.397 mmol) in C_6H_6 (2 mL). After addition,

the color of the solution gradually transformed from dark blue to dark purple, concomitant with the deposition of a fine white precipitate (KCl). This solution was allowed to stir for 45 min, whereupon the reaction mixture was filtered through a Celite column supported on glass wool (0.5 cm × 2 cm). The solvent was removed from the filtrate *in vacuo*, and the dark purple residue was extracted into hexanes (3 mL) and filtered through a Celite column supported on glass wool (0.5 cm × 2 cm). This yielded a dark purple filtrate. The volume of this solution was reduced *in vacuo* to 2 mL. Storage of the solution at -25 °C for 24 h resulted in the deposition of dark purple blocks, which were isolated by decanting off the solution (253 mg, 78%). Anal. Calcd for: $C_{48}H_{56}N_2NiS \cdot 0.5C_6H_6$: C, 77.46; H, 7.52; N, 3.54. Found: C, 77.15; H, 7.77; N, 3.65. ^{1}H NMR (400 MHz, 25 °C, benzene-d_6): δ = 28.78 (m, 4H, Ar-*m***H**, dipp), 18.70 (6H, Ar-*m***H**, CPh_3), 18.09 (4H, C**H**$(CH_3)_2$), 6.03 (t, $^3J_{HH}$, = 6.8 Hz, 3H, Ar-*p***H**, CPh_3), 5.54 (d, $^3J_{HH}$, = 6.3 Hz, 6H, Ar-*o***H**, CPh_3), 4.54 (12H, CH(C**H**$_3)_2$), 3.69 (12H, CH(C**H**$_3)_2$), -12.97 (2H, Ar-*p***H**, dipp), -47.08 (6H, C(C**H**$_3$)), -136.44 (1H, γ-**H**) ppm. Evans' method (C_6D_6, 400 MHz, 25 °C, 0.058 M): 2.87 B.M. IR (KBr Pellet, cm^{-1}): 1527 (m), 1485 (m), 1479 (s), 1458 (s), 1435 (s), 1433 (m), 1381 (s), 1369 (s), 1354 (s), 1313 (s), 1282 (m), 1257 (s), 1186 (m), 1172 (s), 1153 (m), 1095 (m), 1076 (m), 1053 (s), 1030 (s), 1018 (m), 931 (m), 858 (m), 841 (m), 796 (s), 781 (s), 758 (s), 754 (s), 749 (s), 700 (s), 686 (s), 667 (m), 632 (m), 623 (s), 615 (s), 524 (m), 513(m), 501 (m), 438 (w), 420 (s), 413 (m).

2.4.4 Synthesis of [L^{tBu}Ni^{II}(SCPh$_3$)] (2.2)

To a dark green, stirring suspension of L^{tBu}Ni^{II}Cl (130 mg, 0.219 mmol) in C_6H_6 (3 mL) was added dropwise a suspension of $KSCPh_3$ (70.3 mg, 0.224 mmol) in C_6H_6 (2 mL). After addition, the color of the solution gradually transformed from dark green to dark blue, concomitant with the deposition of a fine white precipitate (KCl). This solution was allowed

to stir for 45 min, whereupon the reaction mixture was filtered through a Celite column supported on glass wool (0.5 cm × 2 cm). The solvent was removed from the filtrate *in vacuo*, and the blue residue was extracted into pentane (3 mL) and filtered through a Celite column supported on glass wool (0.5 cm × 2 cm). This yielded a deep blue filtrate. The filtrate was stored at - 25 °C for 15 min, filtered through a Celite column supported on glass wool (0.5 cm × 2 cm), concentrated to 1 mL *in vacuo*, and stored at -25 °C for 24 h, which led to the deposition of dark blue blocks. These were isolated by decanting off the supernatant (148 mg, 81%). Anal. Calcd for $C_{54}H_{68}N_2NiS$: C, 77.59; H, 8.20; N, 3.35. Found: C, 77.91; H, 8.26; N, 3.06. ^{1}H NMR (400 MHz, 25 °C, benzene-d_6): δ = 14.17 (br s, 4H, Ar-*m***H**, dipp), 9.62 (4H, C**H**$(CH_3)_2$), 7.14 (6H, Ar-*o***H**, CPh_3), 7.00 (t, J_{HH}, = 6.9 Hz, 6H, Ar-*m***H**, CPh_3), 6.59 (t, $^3J_{HH}$, = 7.3 Hz, 3H, Ar-*p***H**, CPh_3), 2.91 (12H, CH(C**H**$_3)_2$), 2.27 (12H, CH(C**H**$_3)_2$), 1.88 (18H, C(C**H**$_3)_3$), -2.33 (2H, Ar-*p***H**, dipp), -38.38 (1H, γ-**H**) ppm. Evans' method (C_6D_6, 400 MHz, 25 °C, 0.060 M): 1.73 B.M. IR (KBr Pellet, cm^{-1}): 1635 (m), 1622 (s), 1585(s), 1560 (s), 1533 (s), 1527 (w), 1487 (s), 1477 (m), 1458 (s), 1438 (s), 1430 (m), 1394 (m), 1381 (s), 1359 (s), 1313 (s), 1269 (w), 1260 (m), 1252 (s), 1224 (w), 1215 (m), 1203 (m), 1176 (s), 1155 (s), 1110 (m), 1093 (m), 1054 (s), 1033 (s), 1020 (w), 997 (s), 970 (w), 931 (s), 916 (s), 885 (m), 858 (s), 842 (s), 819 (s), 798 (s), 779 (s), 758 (s), 737 (s), 723 (s), 696 (s), 669 (s), 624 (s), 615 (s), 593 (m), 578 (m), 532 (w), 516 (m), 484 (s), 455 (m), 441 (w), 426 (m), 403 (m), 401 (s).

2.4.5 Variable temperature NMR spectroscopy and temperature dependent, solution magnetic susceptibility of (2.2)

To an NMR tube containing a capillary tube of toluene-d_8 was added a toluene-d_8 (0.75 mL) solution of **2.2** (12.2 mg, 0.0146 mmol). The sample was cooled to -60 °C in a 500

MHz NMR spectrometer. ^{1}H NMR spectra were collected at ca. 20 C° intervals. Note: at -60 °C the reference and solution toluene-d_8 resonances converge so the magnetic susceptibility could not be calculated. The temperature dependent, solution magnetic susceptibility data is shown in Figure S4. ^{1}H NMR (500 MHz, 25 °C, toluene-d_8): δ = 15.02 (4H, Ar-*m***H**, dipp), 10.16 (4H, C**H**$(CH_3)_2$), 7.23 (6H, Ar-*o***H**, CPh_3), 6.90-7.10 (6H, Ar-*m***H**, CPh_3), 6.58 (t, $^{3}J_{HH}$, = 7.3 Hz, 3H, Ar-*p***H**, CPh_3), 3.03 (12H, CH(C**H**$_3)_2$), 2.42 (12H, CH(C**H**$_3)_2$), 2.05 (18H, C(C**H**$_3)_3$), -3.43 (2H, Ar-*p***H**, dipp), -43.03 (1H, γ-**H**) ppm. Evans' method (toluene-d_8, 500 MHz, 25 °C, 0.060 M): 1.74 B.M. ^{1}H NMR (500 MHz, 0 °C, toluene-d_8): δ = 13.12 (4H, Ar-*m***H**, dipp), 8.87 (4H, C**H**$(CH_3)_2$), 6.90-7.10 (12H, Ar-*o***H** and Ar-*m***H**, CPh_3), 6.67 (t, $^{3}J_{HH}$, = 7.3 Hz, 3H, Ar-*p***H**, CPh_3), 2.73 (12H, CH(C**H**$_3)_2$), 2.16 (12H, CH(C**H**$_3)_2$), 1.76 (18H, C(C**H**$_3)_3$), -0.89 (2H, Ar-*p***H**, dipp), -32.00 (1H, γ-**H**) ppm. Evans' method (toluene-d_8, 500 MHz, 0 °C, 0.060 M): 1.57 B.M. ^{1}H NMR (500 MHz, -20 °C, toluene-d_8): δ = 11.66 (4H, Ar-*m***H**, dipp), 7.89 (4H, C**H**$(CH_3)_2$), 6.90-7.10 (12H, Ar-*o***H** and Ar-*m***H**, CPh_3), 6.74 (br s, 3H, Ar-*p***H**, CPh_3), 2.51 (12H, CH(C**H**$_3)_2$), 1.97 (12H, CH(C**H**$_3)_2$), 1.95 (2H, Ar-*p***H**, dipp), 1.53 (18H, C(C**H**$_3)_3$), -23.61 (1H, γ-**H**) ppm. Evans' method (toluene-d_8, -20 °C, 500 MHz, 0.060 M): 1.37 B.M. ^{1}H NMR (500 MHz, -40 °C, toluene-d_8): δ = 10.27 (4H, Ar-*m***H**, dipp), 6.90-7.10 (16H, Ar-*o***H**, CPh_3, Ar-*m***H**, CPh_3, and C**H**$(CH_3)_2$), 6.79 (br s, 3H, Ar-*p***H**, CPh_3), 2.29 (12H, CH(C**H**$_3)_2$), 1.77 (12H, CH(C**H**$_3)_2$1.31 (18H, C(C**H**$_3)_3$), -15.95 (1H, γ-**H**) ppm. Note that the Ar-*p***H** dipp resonance was not observed. Evans' method (toluene-d_8, 500 MHz, -40 °C, 0.060 M): 1.23 B.M. ^{1}H NMR (500 MHz, -60 °C, toluene-d_8): δ = 8.98 (4H, Ar-*m***H**, dipp), 6.90-7.10 (12H, Ar-*o***H** and Ar-*m***H**, CPh_3), 6.87 (2H, Ar-*p***H**, dipp), 6.63 (br s, 3H, Ar-*p***H**, CPh_3), 6.19 (4H, C**H**$(CH_3)_2$), 2.08 (12H, CH(C**H**$_3)_2$), 1.60 (12H, CH(C**H**$_3)_2$), 1.12 (18H, C(C**H**$_3)_3$), -8.23 (1H, γ-**H**) ppm.

2.4.6 Isolation of [{*N*,*N*:κ^2-L^{tBu}}Ni^{II}(μ$_2$-η^2-η^2-S$_2$)Ni^{II}}{*N*,*C*:κ^2-L^{tBu}}] (2.3)

Storage of a dark blue solution of [L^{tBu}Ni^{II}(SCPh$_3$)] (**2.2**) (130 mg, 0.157 mmol) in THF at -25 °C for 24 h results in a color change of the solution to dark green. The volatiles were removed *in vacuo* to produce a dark green residue. This residue was extracted into hexane (5 mL) and stored at - 25 °C for 24 h. This resulted in the deposition of colorless blocks of Gomberg's dimer[46] which were isolated by decanting off the supernatant and indentified by ^{1}H NMR spectroscopy (24 mg). The dark green supernatant was then concentrated *in vacuo* to 3 mL and filtered through a Celite column supported on glass wool (0.5 cm × 2 cm) to yield a dark green filtrate. Then, 1 mL of hexamethyldisiloxide (HMDSO) was added and the resulting solution was stored at - 25 °C for 48 h. This resulted in the deposition of colorless blocks of Gomberg's dimer[46] which were isolated by decanting off the supernatant and indentified by ^{1}H NMR spectroscopy (10 mg; total yield: 34 mg, 89%). The volatiles were then removed from the dark green supernatant *in vacuo* resulting in a green residue. This residue was then extracted into HMDSO (2 mL), filtered through a Celite column supported on glass wool (0.5 cm × 2 cm), concentrated *in vacuo* to 0.25 mL, and stored at -25 °C for 72 h. This result in the deposition of green-brown plates that were isolated by decanting off the supernatant (37 mg, 40% yield). Anal. Calcd for $C_{70}H_{106}N_4Ni_2S_2$: C, 70.94; H, 9.01; N, 4.73. Found: C, 70.71; H, 8.84; N, 4.56. ^{1}H NMR (400 MHz, 25 °C, benzene-d_6): δ = 7.11-6.68 (m, 12H, Ar-**H**), 5.50 (s, 1H, γ-**H**), 4.75 (sept, 1H, C**H**(CH$_3$)$_2$), 4.43 (sept, 1H, C**H**(CH$_3$)$_2$), 4.37 (sept, 1H, C**H**(CH$_3$)$_2$), 4.01 (sept, 1H, C**H**(CH$_3$)$_2$), 3.85 (sept, 1H, C**H**(CH$_3$)$_2$), 3.33 (sept, 1H, C**H**(CH$_3$)$_2$), 3.23 (sept, 1H, C**H**(CH$_3$)$_2$), 2.99 (sept, 1H, C**H**(CH$_3$)$_2$), 2.71 (d, 3H, CH(C**H**$_3$)$_2$), 2.35 (d, 3H, CH(C**H**$_3$)$_2$), 2.20 (d, 3H, CH(C**H**$_3$)$_2$), 1.87 (d, 3H, CH(C**H**$_3$)$_2$), 1.65 (d, 3H, CH(C**H**$_3$)$_2$), 1.46 (d, 3H, CH(C**H**$_3$)$_2$), 1.44 (d, 3H,

CH(C**H**$_3$)$_2$), 1.41 (d, 3H, CH(C**H**$_3$)$_2$), 1.39 (d, 3H, CH(C**H**$_3$)$_2$), 1.38 (d, 3H, CH(C**H**$_3$)$_2$), 1.28 (d, 3H, CH(C**H**$_3$)$_2$), 1.24 (d, 3H, CH(C**H**$_3$)$_2$), 1.12 (d, 3H, CH(C**H**$_3$)$_2$), 1.10 (s, 9H, C(C**H**$_3$)$_3$), 1.04 (s, 9H, C(C**H**$_3$)$_3$), 1.03 (d, 3H, CH(C**H**$_3$)$_2$), 0.98 (d, 3H, CH(C**H**$_3$)$_2$), 0.95 (s, 9H, C(C**H**$_3$)$_3$), 0.80 (s, 9H, C(C**H**$_3$)$_3$), 0.16 (d, 3H, CH(C**H**$_3$)$_2$), ppm. Crystallographic details: Triclinic, P-1, a = 13.075(9), b = 15.20(1), c = 19.41(1), α = 91.76(2), β = 103.87(2), γ = 105.231(2), V = 3595(4) g/cm^3, Z = 2.

2.4.7 Synthesis of [K(18-crown-6)][L^{Me}Ni^{II}(S)] (2.4)

To a deep purple, cold (-25 °C), stirring solution of **2.1** (25 mg, 0.0332 mmol) and 18-crown-6 (17.6 mg, 0.0665 mmol), in Et_2O (2 mL), was added KC_8 (9.1 mg, 0.0672 mmol). This resulted in immediate formation of a dark red-brown mixture. This mixture was allowed to warm to room temperature with stirring, during which time the solution transformed to dark green concomitant with the deposition of a red solid. This solution was allowed to stir for 15 min, whereupon the reaction mixture was filtered through a Celite column supported on glass wool (0.5 cm × 2 cm), which afforded a large plug of bright red solid and a dark green filtrate. The volatiles were removed *in vacuo* to produce a bright green residue. This residue was extracted into 1:1 hexanes (0.5 mL)/benzene (0.5 mL) and stored at -25 °C for 24 h. This resulted in the deposition of dark green blocks, which were isolated by decanting off the supernatant (22.1 mg, 66% yield). The red solid was identified as [K(18-crown-6)][CPh_3][54] by its ^{1}H NMR spectrum. Anal. Calcd for $C_{41}H_{65}KN_2NiO_6S\cdot0.5C_6H_6$: C, 62.11; H, 8.05; N, 3.29. Found: C, 62.46; H, 8.09; N, 3.03. ^{1}H NMR (400 MHz, 25 °C, benzene-d_6): 28.06 (4H, Ar-*m***H**), 26.98 (4H, C**H**(CH$_3$)$_2$), 14.89 (12H, CH(C**H**$_3$)$_2$), 5.32 (12H, CH(C**H**$_3$)$_2$), 1.18 (24H, 18-crown-6), -9.60 (2H, Ar-*p***H**), -47.34 (6H, C(C**H**$_3$)), -107.29 (1H, γ-**H**) ppm. Evans' method (C_6D_6, 400 MHz, 25 °C, 0.036

M): 2.68 B.M. IR (KBr Pellet, cm^{-1}): 1657 (w), 1620 (w), 1585 (w), 1552 (s), 1527 (s), 1463 (m), 1439 (m), 1407 (s), 1380 (s), 1359 (m), 1351 (s), 1319 (s), 1284 (m), 1251 (s), 1228 (s), 1178 (m), 1159 (s), 1145 (m), 1113 (vs), 1056 (m), 1033 (m), 962 (s), 939 (m), 896 (w), 872 (w), 838 (m), 798 (m), 763 (m), 740 (m), 721 (w), 698 (w), 684 (s), 667 (s), 630 (w), 619 (m), 576 (m), 551 (w), 532 (m), 432 (m), 408 (m).

2.4.8 Reaction of [K(18-crown-6)][$L^{Me}Ni^{II}$(S)] (2.4) with 18-crown-6

To a deep green, C_6D_6 (0.5 mL) solution of **2.4** (15 mg, 0.0168 mmol) was added solid 18-crown-6 (4.1 mg, 0.0168 mmol). There was no visible change observed upon addition; however, inspection of the ^{1}H NMR spectrum of the resulting reaction mixture (Figure S6) shows that the 18-crown-6 resonance, which was initially broad and located at 1.18 ppm, sharpened and shifted to 2.87 ppm. ^{1}H NMR (400 MHz, 25 °C, benzene-d_6): 27.97 (4H, Ar-*m***H**), 26.89 (4H, C**H**$(CH_3)_2$), 14.83 (12H, CH(C**H**$_3)_2$), 5.27 (12H, CH(C**H**$_3)_2$), 2.87 (18-crown-6), -9.57 (2H, Ar-*p***H**), -47.33 (6H, C(C**H**$_3$)), -107.16 (1H, γ-**H**) ppm.

2.4.9 Synthesis of [K(18-crown-6)][$L^{tBu}Ni^{II}$(S)] (2.5)

To a deep blue, cold (-25 °C), stirring solution of **2.2** (100 mg, 0.120 mmol) and 18-crown-6 (63.5 mg, 0.240 mmol), in Et_2O (5 mL), was added KC_8 (32.8 mg, 0.242 mmol). This resulted in immediate formation of a dark red-brown mixture. This mixture was allowed to warm to room temperature with stirring, during which time the solution transformed to dark brown concomitant with the deposition of a red solid. This solution was allowed to stir for 10 min, whereupon the reaction mixture was filtered through a Celite column supported on glass wool (0.5 cm × 2 cm), which afforded a large plug of bright red solid and a dichroic filtrate, which was green to transmitted light and dark brown to reflected light. The volatiles were removed from the filtrate *in vacuo* to produce a dark brown residue.

This residue was extracted into toluene (2 mL) and the resulting solution was layered with isooctane (1 mL) and stored at -25 °C for 24 h. This resulted in the deposition of dark brown plates, which were isolated by decanting off the supernatant (113 mg, 88% yield). The red solid was identified as [K(18-crown-6)][CPh_3][54] by its ^{1}H NMR spectrum. Anal. Calcd for: $C_{47}H_{77}KN_2NiO_6S$: C, 63.00; H, 8.66; N, 3.13. Found: C, 63.36; H, 8.96; N, 3.02. ^{1}H NMR (400 MHz, 25 °C, benzene-d_6): 28.53 (4H, Ar-*m***H**), 26.42 (4H, C**H**$(CH_3)_2$), 16.25 (12H, CH(C**H**$_3)_2$), 6.76 (12H, CH(C**H**$_3)_2$), 0.28 (24H, 18-crown-6), -0.79 (18H, C(C**H**$_3)_3$) -18.97 (2H, Ar-*p***H**), -115.21 (1H, γ-**H**) ppm. Evans' Method (C_6D_6, 400 MHz, 25 °C, 0.039 M): 3.06 B.M. IR (KBr Pellet, cm^{-1}): 1629 (w), 1581 (w), 1537 (m), 1510 (m), 1466 (m), 1446 (m), 1444 (m), 1411 (s), 1383 (m), 1376 (m), 1351 (m), 1319 (m), 1286 (w), 1251 (m), 1216 (m), 1191 (w), 1159 (s), 1110 (vs), 1056 (w), 1033 (w), 960 (s), 943 (w), 834 (w), 806 (w), 782 (w), 761 (w), 730 (w), 696 (w), 667 (s), 617 (w), 577 (w), 528 (w), 462 (w).

2.4.10 Reaction of [$L^{tBu}Ni^{II}(SCPh_3)$] (2.2) with one equiv of KC_8 and 18-crown-6

To a deep blue, cold (-25 °C), stirring solution of **2.2** (50 mg, 0.060 mmol) and 18-crown-6 (15.8 mg, 0.060 mmol), in THF (2 mL), was added KC_8 (8.2 mg, 0.060 mmol). This resulted in immediate formation of a dark green-brown mixture. This mixture was allowed to warm to room temperature with stirring. After 10 min, the reaction mixture was filtered through a Celite column supported on glass wool (0.5 cm × 2 cm), which afforded a plug of black solid (C_8) and a dichroic (green to transmitted light and dark brown to reflected light) filtrate. The volatiles were removed *in vacuo* to provide a dark brown residue. This residue was extracted into Et_2O (2 mL) and subsequent storage at - 25 °C for 1 h resulted in the deposition of colorless, partially crystalline solid (13 mg). The dark brown supernatant was then filtered through a Celite column supported on glass wool (0.5 cm × 2

cm), concentrated to 0.5 mL *in vacuo*, and stored at -25 °C for 24 h. This resulted in the deposition of dark brown plates, which were isolated by decanting off the supernatant (38 mg, 67% yield). This material was identified as **2.5** by comparison of its ^{1}H NMR spectrum with authentic material (Figure A 2.10). The colorless product was identified as triphenylmethane by its ^{1}H NMR spectrum (Figure A 2.11).[80] Complex **2.5**: ^{1}H NMR (400 MHz, 25 °C, benzene-d_6): 28.40 (4H, Ar-*m***H**), 26.29 (4H, C**H**$(CH_3)_2$), 16.12 (12H, CH(C**H**$_3)_2$), 6.72 (12H, CH(C**H**$_3)_2$), 0.30 (24H, 18-crown-6), -0.76 (18H, C(C**H**$_3)_3$) -18.85 (2H, Ar-*p***H**), -114.31 (1H, γ-**H**) ppm. Ph_3CH: ^{1}H NMR (400 MHz, 25 °C, benzene-d_6): 7.02-7.09 (15H, aryl), 5.37 (1H, **H**CPh_3) ppm.

2.4.11 Synthesis of [K(2,2,2-cryptand)][L^{tBu}Ni^{II}(S)] (2.6)

To a deep blue, cold (-25 °C), stirring solution of **2.2** (88.5 mg, 0.106 mmol) and 2,2,2-cryptand (80 mg, 0.212 mmol), in 1:10 THF/Et_2O (5 mL total volume), was added KC_8 (29 mg, 0.215 mmol). This resulted in immediate formation of a dark red-brown mixture. This mixture was allowed to warm to room temperature with stirring, during which time the solution transformed to dark brown concomitant with the deposition of a red solid. This solution was allowed to stir for 25 min, whereupon the reaction mixture was filtered through a Celite column supported on glass wool (0.5 cm × 2 cm), which afforded a large plug of bright red solid and a dichroic filtrate, which was green to transmitted light and dark brown to reflected light. The volatiles were removed *in vacuo* to provide a dark green-brown residue. This residue was extracted into hexanes (5 mL), filtered through a Celite column supported on glass wool (0.5 cm × 2 cm), and concentrated to 2 mL *in vacuo*. Storage of this solution at -25 °C for 24 h resulted in the deposition of dark brown needles, which were isolated by decanting off the supernatant (95 mg, 89% yield). The red solid was identified as

[K(2,2,2-cryptand)][CPh_3][54] by its ^{1}H NMR spectrum. Anal. Calcd for $C_{53}H_{89}KN_4NiO_6S$: C, 63.14; H, 8.90; N, 5.56. Found: C, 63.51; H, 8.87; N, 5.78. ^{1}H NMR (400 MHz, 25 °C, benzene-d_6): 27.45 (4H, Ar-*m***H**), 24.25 (4H, C**H**$(CH_3)_2$), 16.46 (12H, CH(C**H**$_3)_2$), 6.56 (12H, CH(C**H**$_3)_2$), 1.40 (12H, 2,2,2-cryptand), 0.97 (12H, 2,2,2-cryptand), -0.87 (18H, C(C**H**$_3)_3$), -1.04 (12H, 2,2,2-cryptand) -17.50 (2H, Ar-*p***H**), -110.49 (1H, γ-**H**) ppm. Evans' Method (C_6D_6, 400 MHz, 25 °C, 0.041 M): 3.10 B.M. IR (KBr pellet, cm^{-1}): 1629 (w), 1579 (w), 1535 (m), 1519 (m), 1477 (m), 1457 (m), 1446 (m), 1412 (s), 1359 (m), 1353 (m), 1319 (m), 1299 (w), 1259 (m), 1238 (m), 1223 (w), 1193 (w), 1157 (s), 1132 (s), 1105 (vs), 1079 (s), 1056 (m), 1029 (m), 950 (m), 933 (m), 808 (m), 781 (w), 761 (w), 721 (w), 698 (w), 663 (m), 615 (w), 575 (w), 526 (w), 455 (w), 418 (w), 406 (w).

2.4.12 Isolation of [K(18-crown-6)][{L^{Me}Ni}$_2$(μ^2-η^2-η^2-S_2)] 2.10 from the decomposition of [K(18-crown-6)][$L^{Me}Ni^{II}$(S)] (2.4)

Storage of a solution of [K(18-crown-6)][$L^{Me}Ni^{II}$(S)] (**2.4**, 15 mg, 0.0185 mmol) in a THF/toluene (0.5:0.5 mL) at - 25 °C for 24 h resulted in the deposition of bright red plates of [K(18-crown-6)][{L^{Me}Ni}$_2$(μ^2-η^2-S_2)] which were isolated by decanting off the supernatant (6 mg, 49% yield). ^{1}H NMR (400 MHz, 25 °C, THF-d_8): δ = 7.29 (s, 4H, Ar-**H**), 6.55 (br s, 8H, Ar-**H**), 5.50 (s, 2H, γ-**H**), 5.12 (br s, 4H, C**H**$(CH_3)_2$), 4.79 (br s, 4H, C**H**$(CH_3)_2$), 3.60 (s, 24H, 18-crown-6), 1.28 (br s, 24H, CH(C**H**$_3)_2$), 1.02 (br s, 24H, CH(C**H**$_3)_2$), 0.77 (br s, 12H, C(C**H**$_3$)) ppm. Crystallographic details: Triclinic, P-1, a = 12.93(2), b = 13.03(3), c = 13.73(3), α = 104.98(5), β = 109.76(7), γ = 97.99(6), V = 2036(7) g/cm^3, Z = 4.

2.4.13 Synthesis of [K(18-crown-6)][$L^{tBu}Ni^{I}$(SH)] (2.11)

A NMR tube was charged with a brown solution of [K(18-crown-6)][$L^{tBu}Ni^{II}$(S)] (**2.5**) (15 mg, 0.0167 mmol) in C_6D_6 (0.6 mL) to this solution was added diphenylsilane (Ph_2SiH_2, 3.1 μL, 0.0167 mmol). After addition, the color of the mixture slowly changes to dark red. The reaction was followed by ^{1}H NMR spectroscopy for 3 h, after which all of the starting material had been consumed. The NMR tube was then bought back into a glove box, whereupon the volatiles were removed from the filtrate *in vacuo* yielding a dark red residue that was washed with pentane (1 mL × 2). The residue was then extracted into Et_2O (2 mL) and filtered through a Celite column supported on glass wool (0.5 cm × 2 cm) yielding a dark red filtrate. The volume of this solution was reduced *in vacuo* to 0.25 mL causing some colorless solid to crash out. This solution was then filtered through a Celite column supported on glass wool (0.5 cm × 2 cm) and subsequent storage of the solution at -25 °C for 72 h resulted in the deposition of bright red blocks, which were isolated by decanting off the supernatant (4 mg, 27%). ^{1}H NMR (400 MHz, 25 °C, benzene-d_6): δ = 24.49 (br s), 20.53 (br s), 13.81 (br s), 4.05 (br s), 3.14 (br s), 3.05 (br s), -1.03 (br s) ppm. Crystallographic details: Triclinic, P-1, a = 12.653(6), b = 12.971(6), c = 17.775(8), α = 78.11 (1), β = 82.90(1), γ = 70.47(1), V = 2686(2) g/cm^3, Z = 2.

2.4.14 Synthesis of [$L^{tBu}Ni^{II}(SSiMe_3)$] (2.12)

A NMR tube was charged with a brown solution of [K(18-crown-6)][$L^{tBu}Ni^{II}$(S)] (**2.5**) (22 mg, 0.0250 mmol) in C_6D_6 (0.6 mL) to this solution was added Me_3SiOTf (4.52 μL, 0.0250 mmol). After addition, the color of the mixture quickly transformed to dark red, concomitant with the deposition of a fine white precipitate ([K][OTf]). A ^{1}H NMR spectrum taken 10 minutes after addition, confirmed complete consumption of **2.5**. The NMR tube

was then bought back into a glove box, whereupon the reaction mixture was filtered through a Celite column supported on glass wool (0.5 cm × 2 cm). Volatiles were removed from the filtrate *in vacuo*, and the resulting dark red residue was extracted into hexanes (1 mL) and filtered through a Celite column supported on glass wool (0.5 cm × 2 cm). This yielded a dark red filtrate. The volume of this solution was reduced *in vacuo* to 0.25 mL. Storage of the solution at -25 °C for 48 h resulted in the deposition of dark red plates, which were isolated by decanting off the supernatant (11 mg, 70%). ^{1}H NMR (400 MHz, 25 °C, benzene-d_6): δ = 53.56 (s, 4H, Ar-*m***H**, dipp), 34.38 (s, 4H, C**H**$(CH_3)_2$, dipp), 8.61 (s, 12H, CH(C**H**$_3)_2$, dipp), 8.57 (s, 12H, CH(C**H**$_3)_2$, dipp), 5.26 (s, 18H, C(C**H**$_3)_3$), 3.35 (s, 9H, Si(C**H**$_3)_3$), -45.1 (2H, Ar-*p***H**, dipp) ppm. Note: the γ-**H** resonance was not observable in the range of 250 to -250 ppm.

2.4.15 X-ray Crystallography

Data for **2.1**-**2.6** and **2.12** were collected on a Bruker KAPPA APEX II diffractometer equipped with an APEX II CCD detector using a TRIUMPH monochromator with a Mo Kα X-ray source (α = 0.71073 Å). The crystals were mounted on a cryoloop under Paratone-N oil, and all data were collected at 100(2) K using an Oxford nitrogen gas cryostream. Data were collected using ω scans with 0.5° frame widths. Frame exposures of 10 seconds were used for **2.1** and **2.6**. Frame exposures of 15 seconds were used for **2.2** and **2.4** and **2.12**. Frame exposures of 20 seconds were used for **2.5**. Data collection and cell parameter determination were conducted using the SMART program.[81] Integration of the data frames and final cell parameter refinement were performed using SAINT software.[82] Absorption correction of the data was carried out using the multi-scan method SADABS.[83] Subsequent calculations were carried out using SHELXTL.[84] Structure determination was done using

direct or Patterson methods and difference Fourier techniques. All hydrogen atom positions were idealized, and rode on the atom of attachment. Structure solution, refinement, graphics, and creation of publication materials were performed using SHELXTL.[84]

In complex **4**, the C_8H_{18} solvate molecule exhibited mild positional disorder; however, alternate positions were not found. The C–C bonds were constrained to 1.5 Å using the DFIX command. Hydrogen atoms were not added to disordered carbon atoms. Further crystallographic details for complexes **2.1**-**2.6** and **2.12** can be found in Tables Table 2.2 and Table 2.3.

Table 2.2. X-ray Crystallographic Data for Complexes 2.1, 2.2, and 2.4.

	2.1·0.5C_6H_6	**2.2**·0.33C_5H_{12}	**2.4**·2.5C_6H_6
empirical formula	$C_{48}H_{56}N_2NiS·0.5C_6H_6$	$C_{54}H_{68}N_2NiS·0.33C_5H_{12}$	$C_{41}H_{65}KN_2NiO_6S·2.5C_6H_6$
crystal habit, color	Block, Purple	Block, Blue	Block, Green
crystal size (mm)	0.15 × 0.15 × 0.15	0.2 × 0.15 × 0.05	0.7 × 0.7 × 0.25
crystal system	Monoclinic	triclinic	Triclinic
space group	*P2(1)/c*	*P-1*	*P-1*
volume ($Å^3$)	4281.6(3)	7264(3)	2821.1(5)
a (Å)	13.0333(6)	12.686(3)	13.194(1)
b (Å)	16.6343(7)	19.394(5)	13.298(1)
c (Å)	19.8726(9)	30.321(8)	16.695(2)
α (deg)	90	88.294(5)	88.621(2)
β (deg)	96.392(2)	80.235(5)	74.520(2)
γ (deg)	90	81.137(5)	88.213(2)
Z	4	2	2
formula weight (g/mol)	790.77	859.88	1007.09
density (calculated)	1.227	1.179	1.186
absorption coefficient	0.539	0.481	0.502
F_{000}	1692	2784	1082
total no. reflections	26749	75714	24286
unique reflections	8819	29695	12841
R_{int}	0.0421	0.1482	0.0227
final R indices (I >2σ(I)]	R_1 = 0.0328 wR_2 = 0.0729	R_1 = 0.0698 wR_2 = 0.0944	R_1 = 0.0397 wR_2 = 0.1098
largest diff. peak and	0.311 and -0.353	0.425 and -0.446	0.604 and -0.531
GOF	1.013	0.963	0.860

Table 2.3. X-ray Crystallographic Data for Complexes 2.5, 2.6, and 2.12.

	2.5·0.5C_8H_{18}	**2.6**	**2.12**
empirical formula	$C_{47}H_{77}KN_2NiO_6S$·0.5C_8H_{18}	$C_{53}H_{89}KN_4NiO_6S$	$C_{38}H_{62}N_2NiSSi$
crystal habit, color	Plate, Brown	Plate, Brown	Plate, Dark Red
crystal size (mm)	0.15 × 0.1 × 0.05	0.5 × 0.4 × 0.1	0.2 × 0.1 × 0.05
crystal system	Monoclinic	Monoclinic	Monoclinic
space group	*P2(1)/n*	*P2(1)/n*	*P2(1)/n*
volume ($Å^3$)	5911.2(5)	5606.2(5)	7787.1(8)
a (Å)	18.5580(9)	12.7125(6)	15.3665(9)
b (Å)	16.8220(8)	22.493(1)	26.029(2)
c (Å)	19.055(1)	20.053(1)	19.619(1)
α (deg)	90.00	90	90
β (deg)	96.441(3)	102.126(4)	97.105(4)
γ (deg)	90.00	90	90
Z	2	4	8
formula weight (g/mol)	1906.14	1008.15	665.74
density (calculated) (Mg/m^3)	1.071	1.194	1.136
absorption coefficient (mm^{-1})	0.475	0.506	0.609
F_{000}	2068	2184	2896.0
total no. reflections	25946	35206	15946
unique reflections	12111	11559	8254
R_{int}	0.1058	0.1187	0.1217
final R indices (I >2σ(I)]	R_1 = 0.0845 wR_2 = 0.2132	R_1 = 0.0601 wR_2 = 0.1175	R_1 = 0.0591 wR_2 = 0.1240
largest diff. peak and hole (e^-	1.279 and -0.485	0.816 and -0.590	0.343 and -0.411
GOF	1.012	0.964	0.946

2.5 Appendix

2.5.1 NMR Spectra

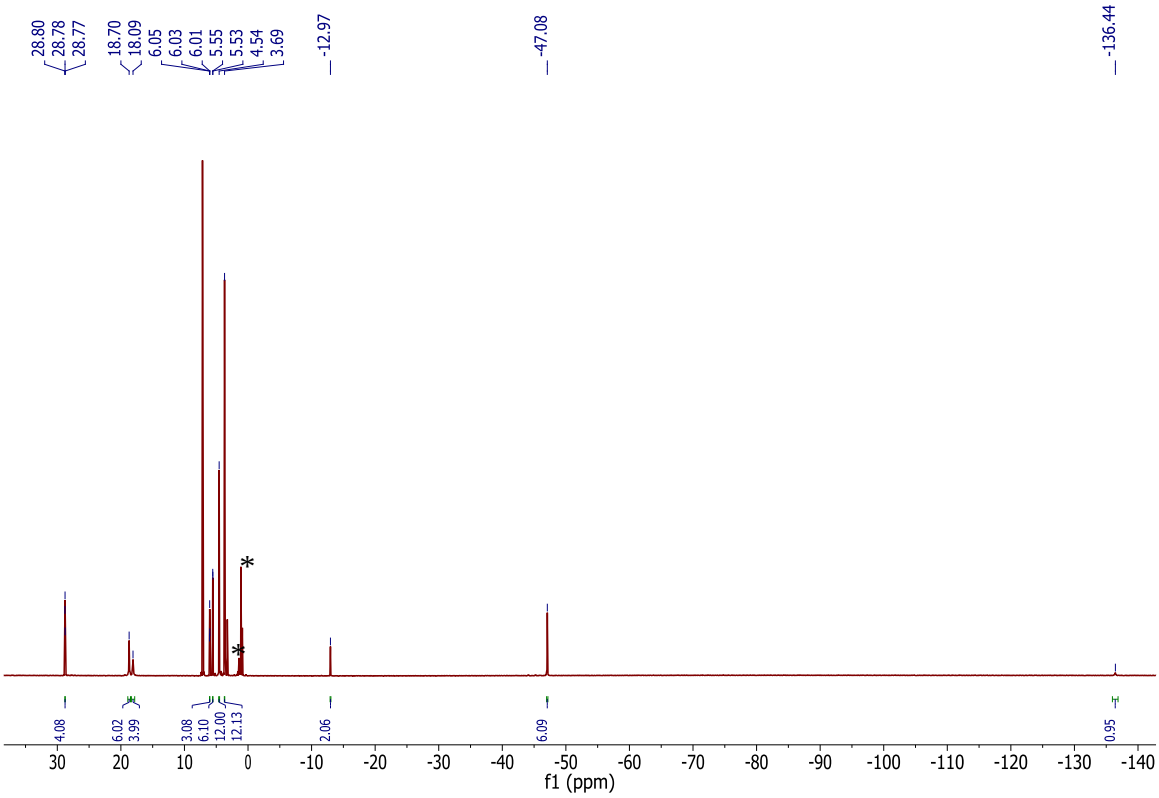

Figure A 2.1. ^{1}H NMR spectrum of [$L^{Me}Ni^{II}(SCPh_3)$] (**2.1**) in benzene-d_6. (*) indicates the presence of Et_2O.

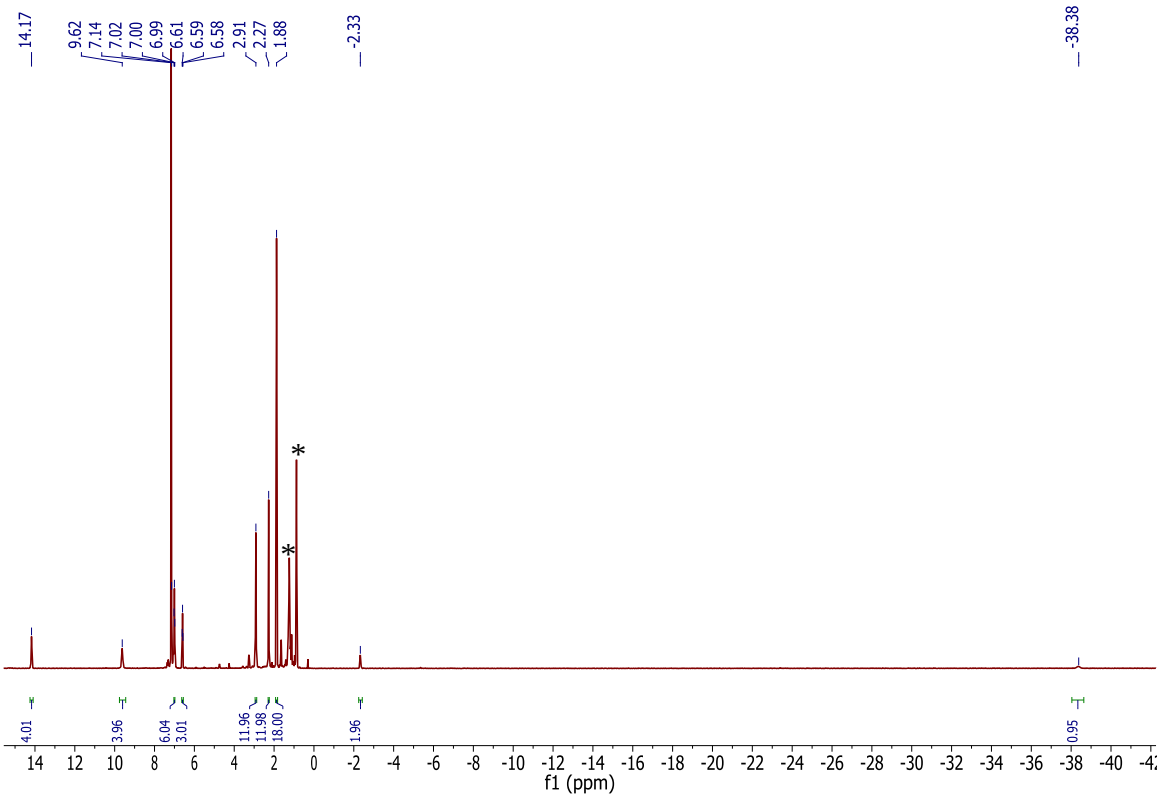

Figure A 2.2. ^{1}H NMR spectrum of [$L^{tBu}Ni^{II}(SCPh_3)$] (**2.2**) in benzene-d_6. (*) indicates the presence of hexanes and pentane.

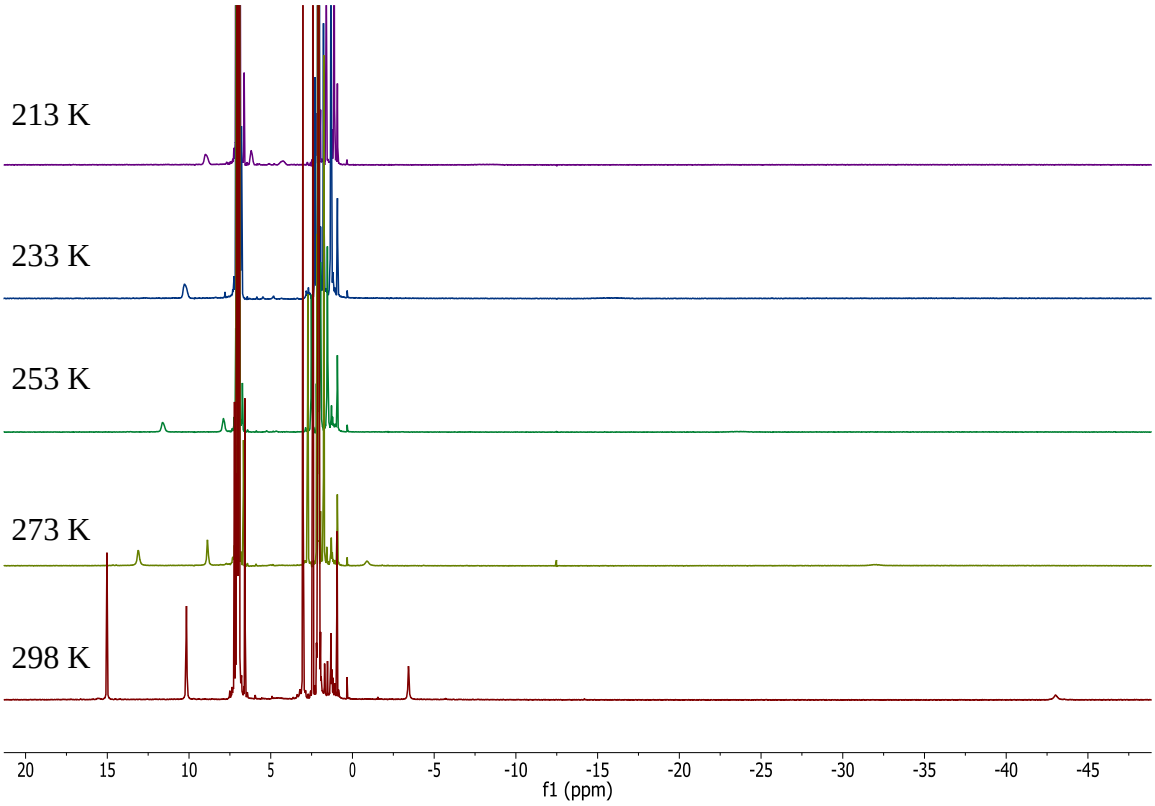

Figure A 2.3. Variable temperature ^{1}H NMR spectra of [$L^{tBu}Ni^{II}(SCPh_3)$] (**2.2**) in toluene-d_8.

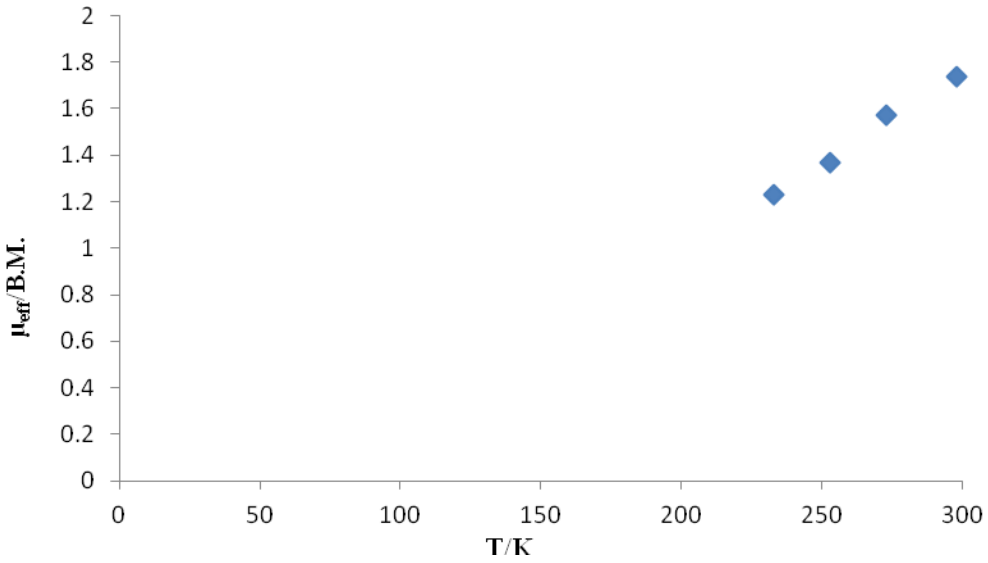

Figure A 2.4. Temperature dependent, solution magnetic susceptibility of complex **2.2** as determined by Evans' method.

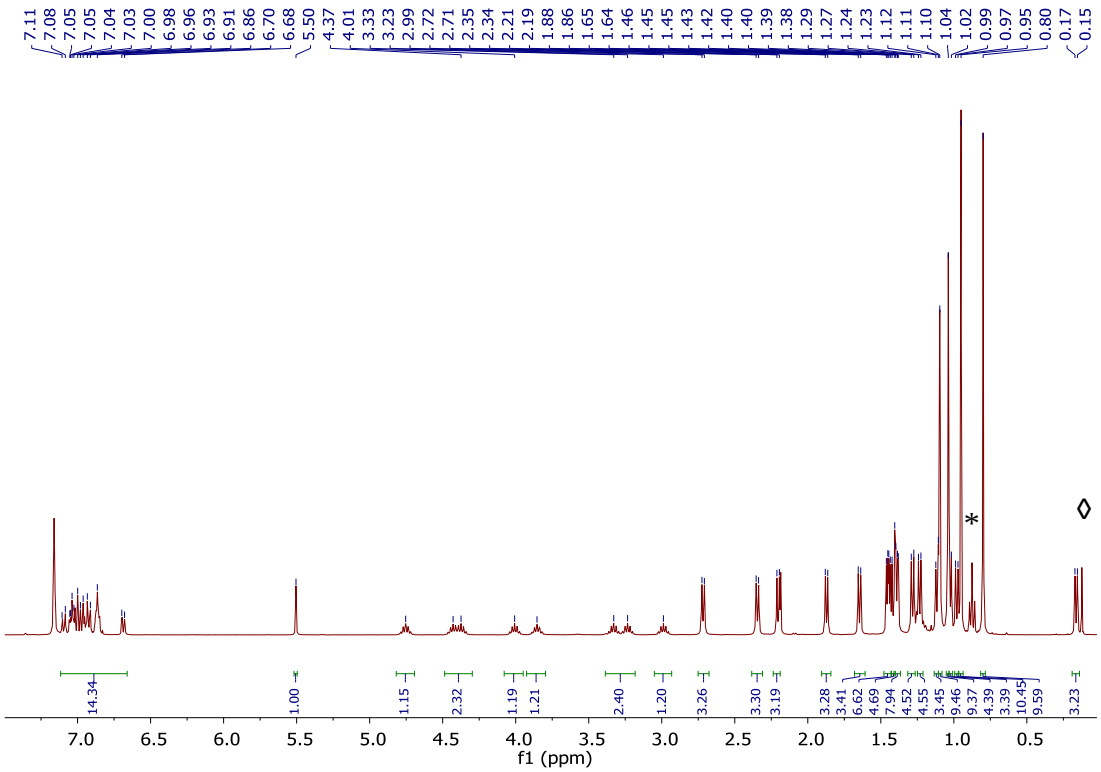

Figure A 2.5. ^{1}H NMR spectrum of [K(18-crown-6)][L^{Me}Ni^{II}(S)] (**2.4**) in benzene-d_6. (*) indicates the presence of pentane and (◊) indicates the presence of HMDSO.

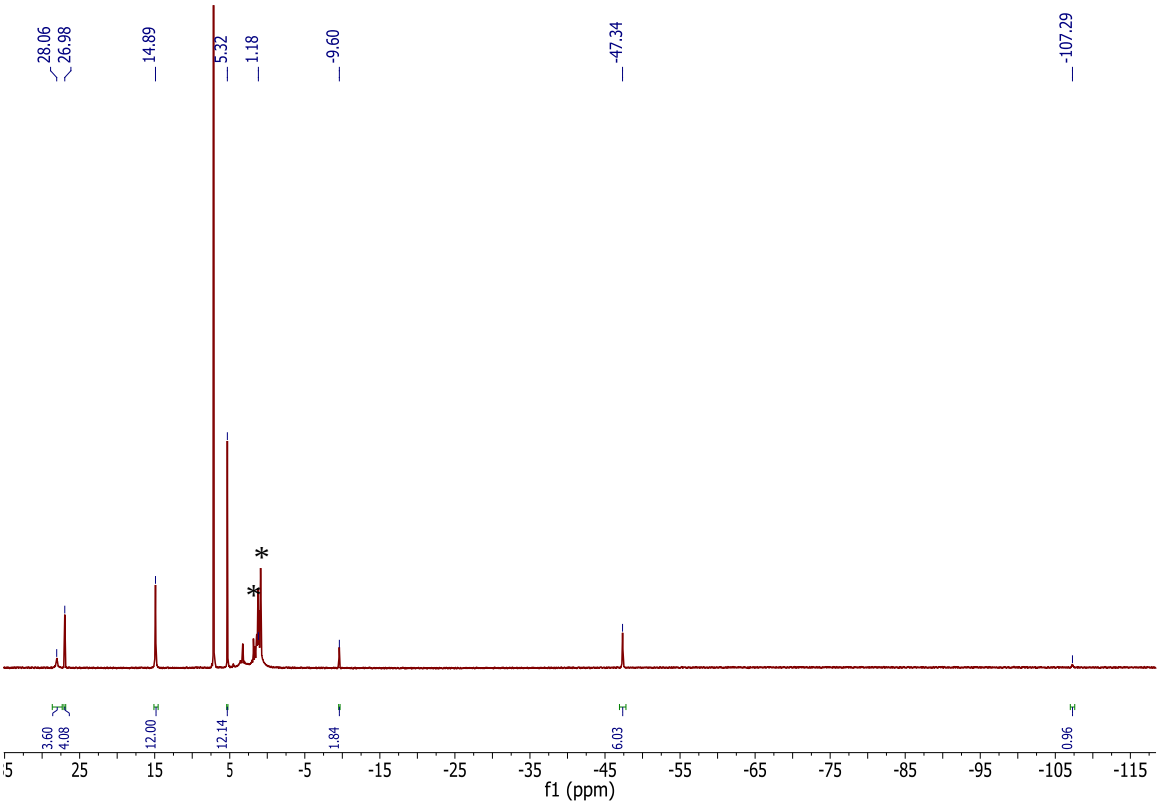

Figure A 2.6. ^{1}H NMR spectrum of [K(18-crown-6)][L^{Me}Ni^{II}(S)] (**2.4**) in benzene-d_6. (*) indicates the presence of hexanes.

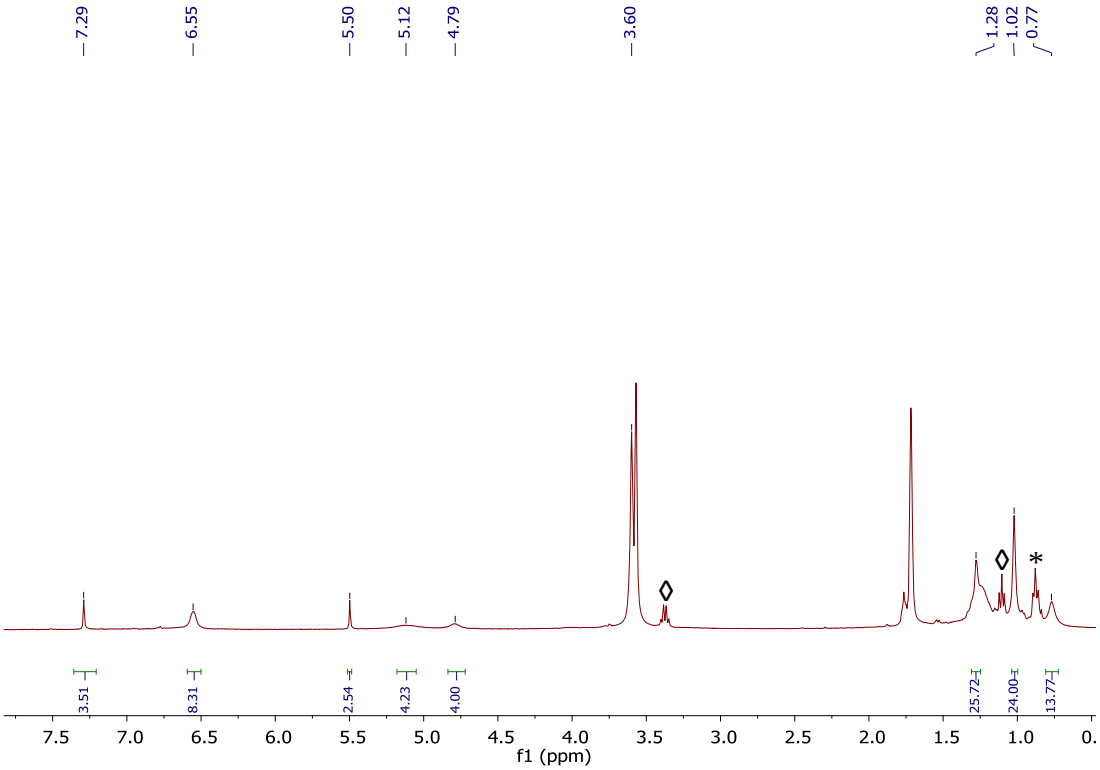

Figure A 2.7. ^{1}H NMR spectrum of [K(18-crown-6)][{L^{Me}Ni}$_2$(μ^2-η^2-η^2-S_2)] (**2.10**) in THF-d_8. (*) indicates the presence of hexanes and (◊) indicates the presence of Et_2O.

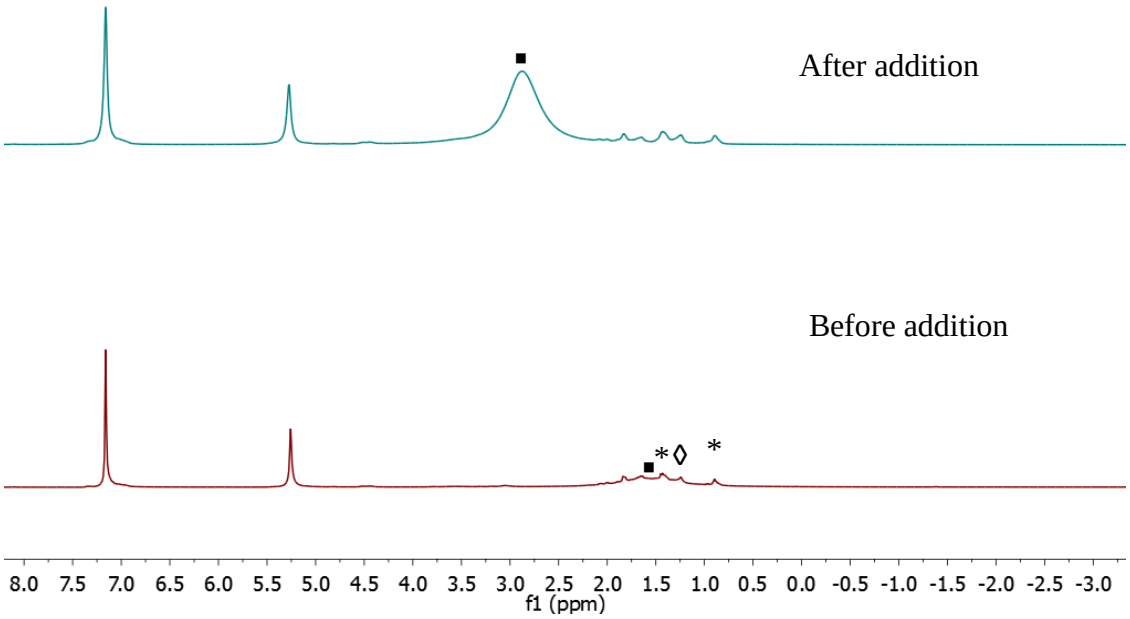

Figure A 2.8. Partial ^{1}H NMR spectrum of the addition of 1 equiv of 18-crown-6 to [K(18-crown-6)][$L^{Me}Ni^{II}(S)$] (**2.4**) in benzene-d_6. (▪) indicates the 18-crown-6 resonance, (*) indicates the presence of hexanes and (◊) indicates the presence of Et_2O.

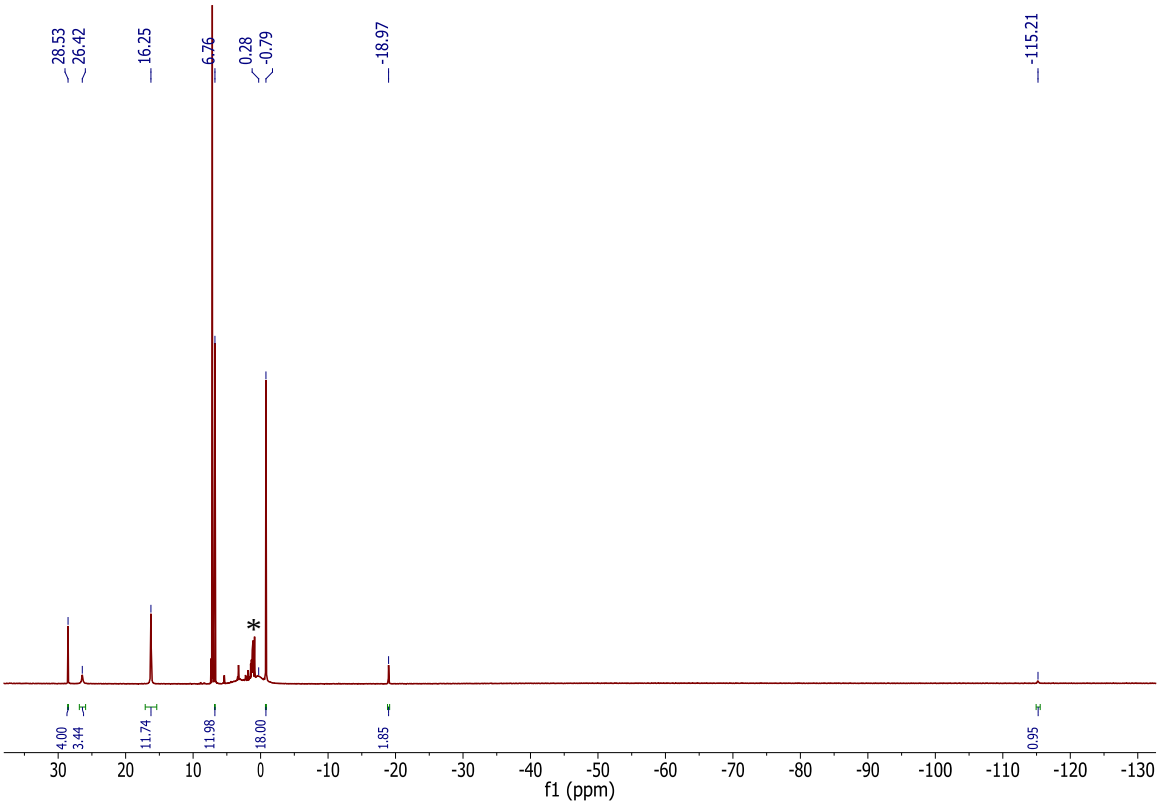

Figure A 2.9. ^{1}H NMR spectrum of [K(18-crown-6)][L^{tBu}Ni^{II}(S)] (**2.4**) in benzene-d_6. (*) indicates the presence of isooctane.

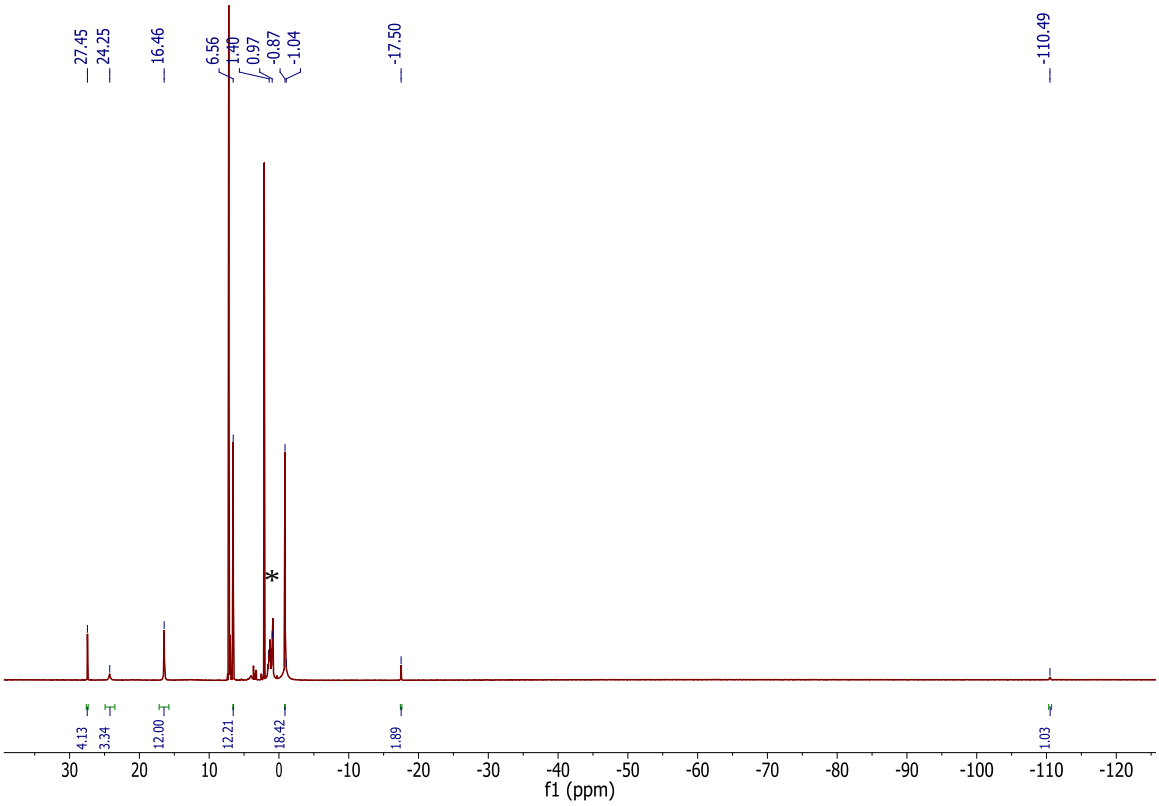

Figure A 2.10. ^{1}H NMR spectrum of [K(2,2,2-cryptand)][L^{tBu}Ni^{II}(S)] (**2.6**) in benzene-d_6. (*) indicates the presence of toluene.

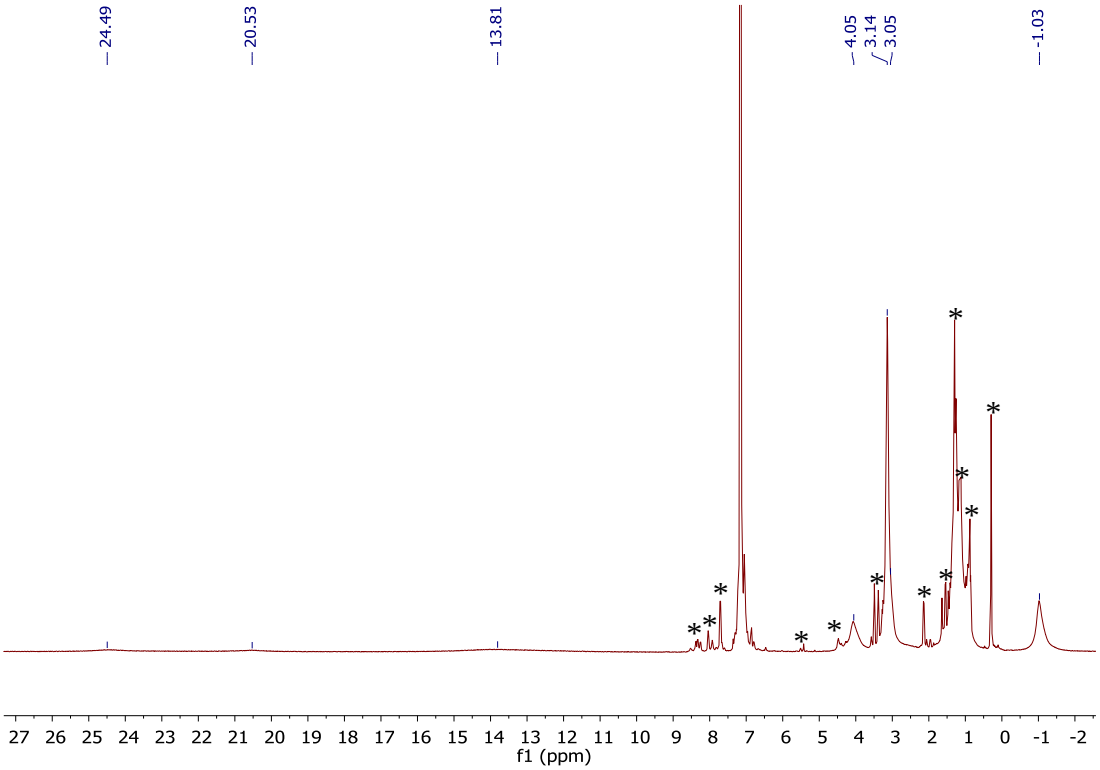

Figure A 2.11. ^{1}H NMR spectrum of [K(18-crown-6)][L^{tBu}Ni^{I}(SH)] (**2.11**) in benzene-d_6. (*) indicates the presence of unidentified diamagnetic impurities.

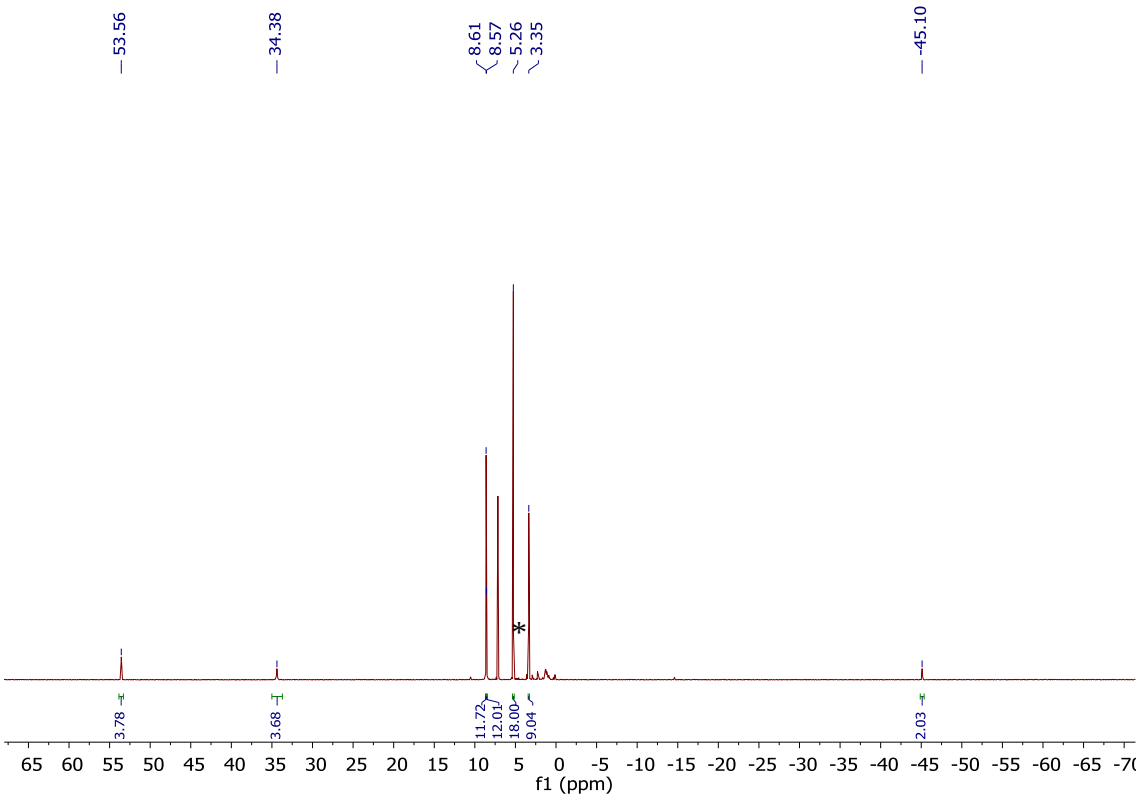

Figure A 2.12. ^{1}H NMR spectrum of [L^{tBu}Ni^{II}(SSiMe$_3$)] (**2.12**) in benzene-d_6. (*) indicates the presence of hexane.

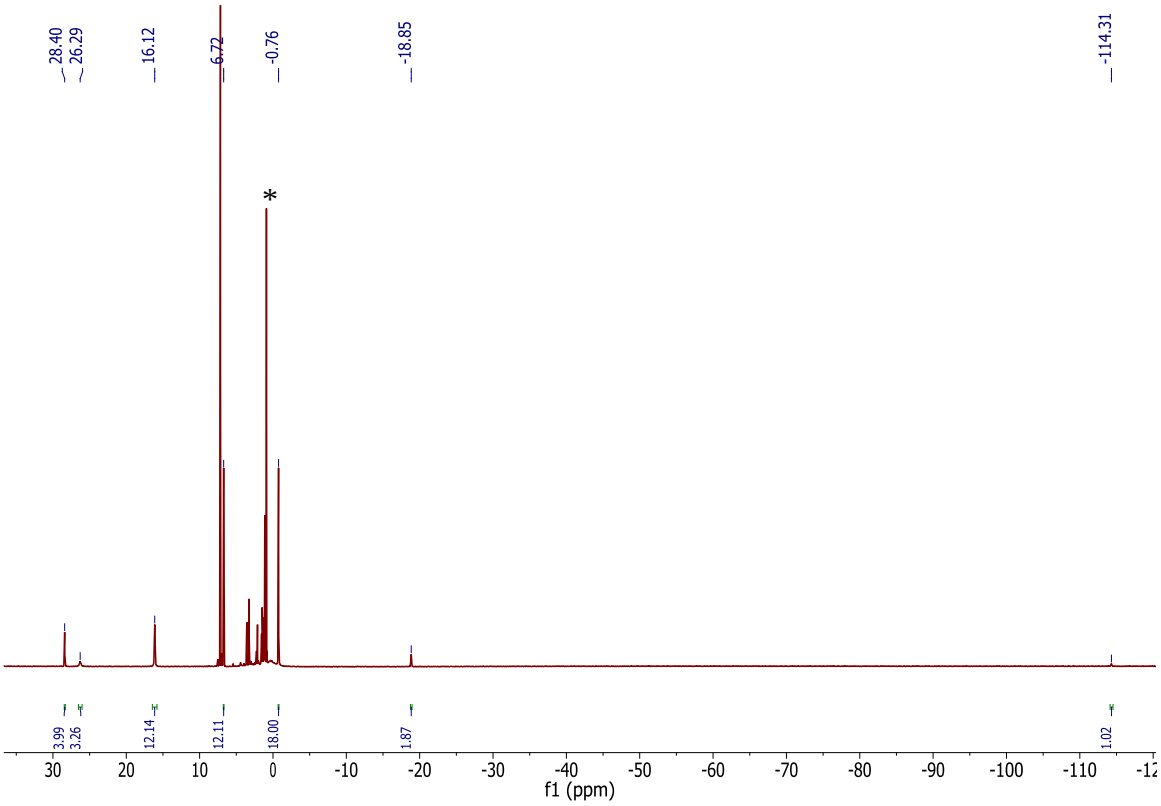

Figure A 2.13. ^{1}H NMR spectrum of [K(18-crown-6)][L^{tBu}Ni^{II}(S)] (**2.4**), formed by reaction of **2.2** with 1 equiv of KC_8. (*) indicates the presence of isooctane.

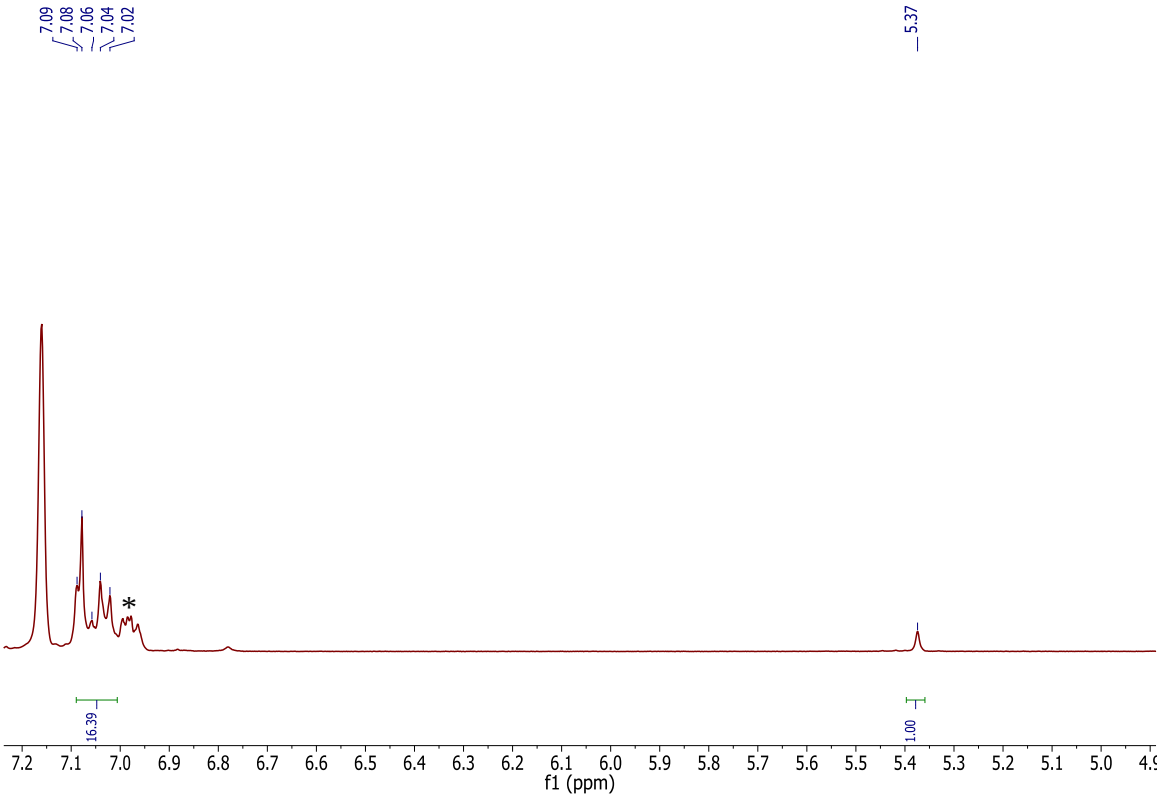

Figure A 2.14. Partial ^{1}H NMR spectrum of triphenylmethane, formed as a by-product upon reaction of **2.2** with 1 equiv of KC_8. (*) indicates the presence of toluene.

2.5.2 IR Spectra

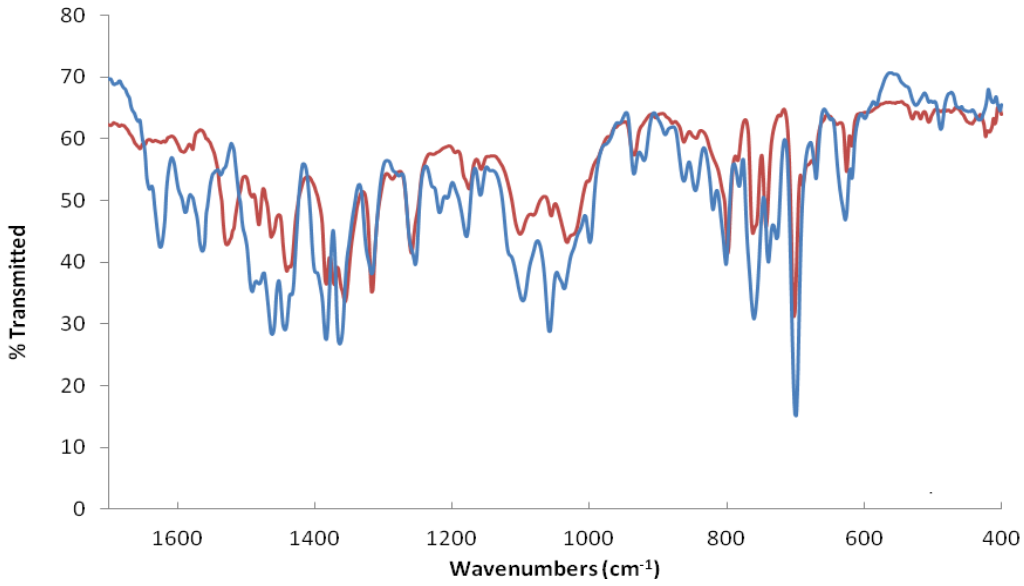

Figure A 2.15. Partial IR spectra of complexes **2.1** (red) and **2.2** (blue) (KBr pellets).

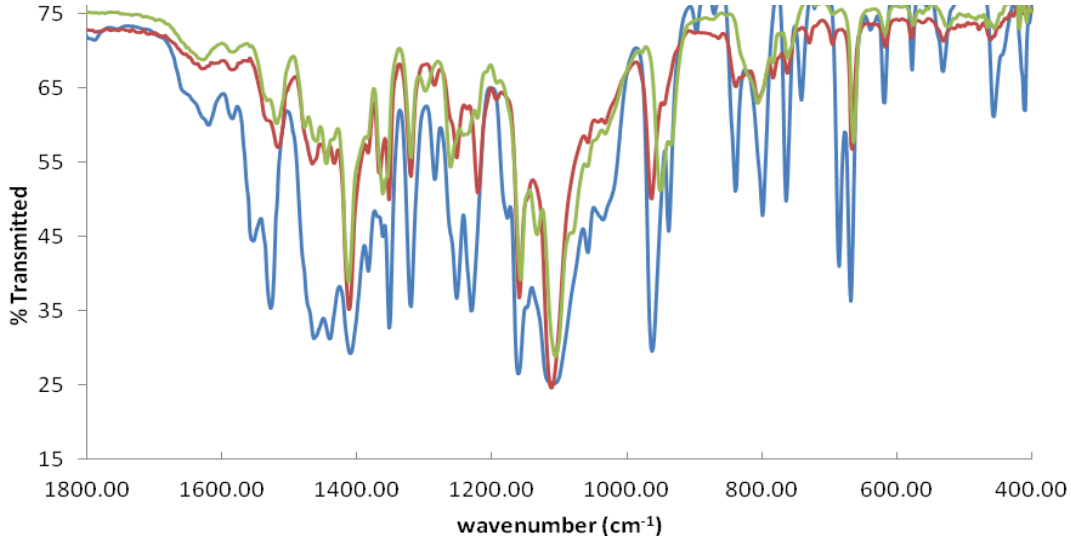

Figure A 2.16. Partial IR spectra of complexes **2.4** (blue) **2.5** (red), and **2.6** (green) (KBr pellets).

2.5.3 Magnetization Data

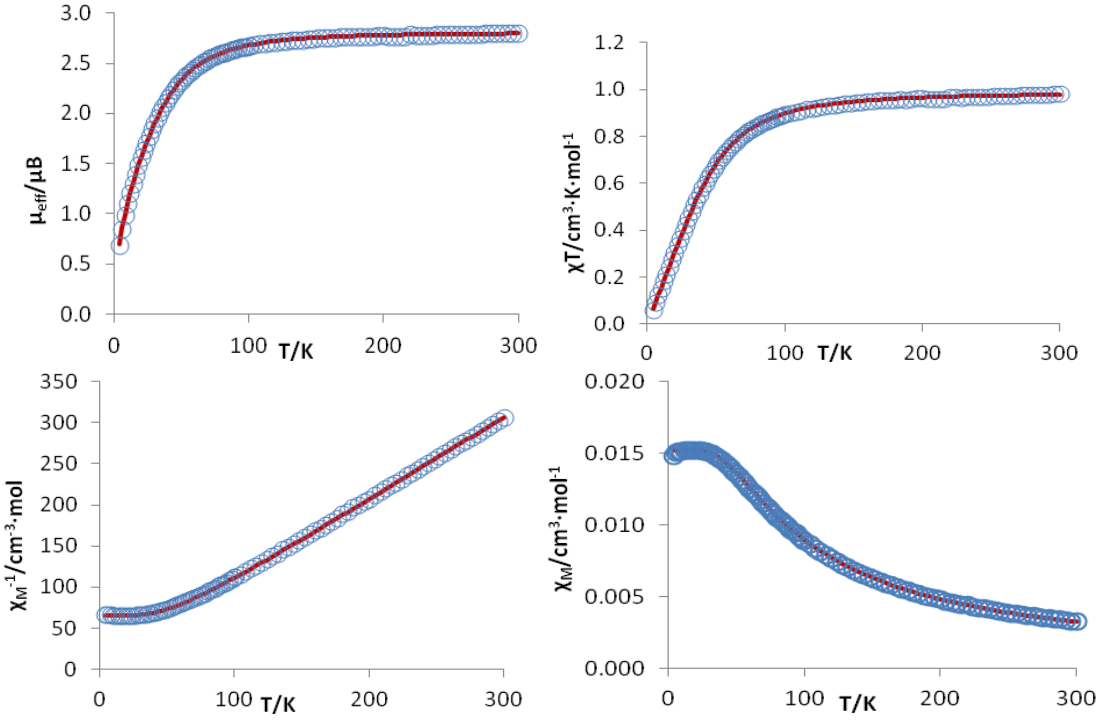

Figure A 2.17. Temperature dependent, solid state magnetic susceptibility data for [K(18-crown-6)][$L^{Me}Ni^{II}(S)$] (**2.4**). χ_{dia} = -5.518 × 10^{-4} $cm^3 \cdot mol^{-1}$, mass = 42.0 mg, M = 888.94 g/mol. Variables used to fit the data were *g*, D, and Temperature Independent Paramagnetism (TIP). Simulation of the data with JulX provided the following fit parameters: *g* = 1.981, D = 90.506 cm^{-1}, and TIP = 593.7 × 10^{-6} emu. Data is shown as circles and fits are shown as red lines.

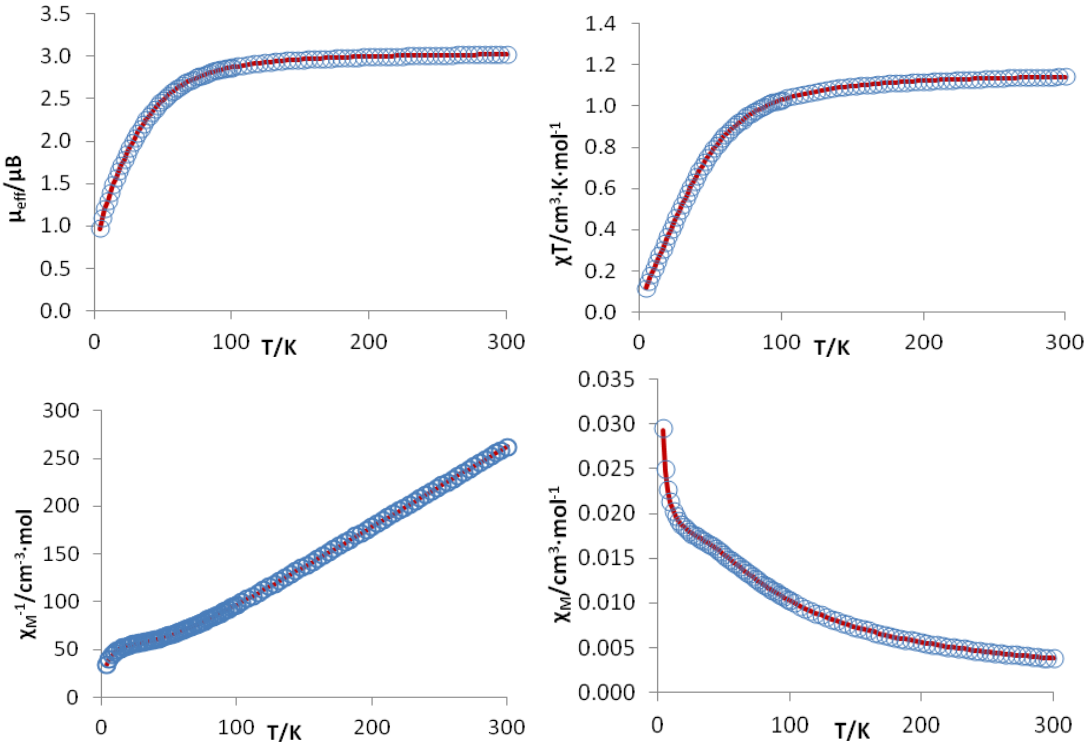

Figure A 2.18. Temperature dependent, solid state magnetic susceptibility data for [K(18-crown-6)][$L^{tBu}Ni^{II}(S)$] (**2.5**). χ_{dia} = -6.143 × 10^{-4} $cm^3 \cdot mol^{-1}$, mass = 24.0 mg, M =953.11 g/mol. Variables used to fit the data were *g*, D, and Temperature Independent Paramagnetism (TIP). The data was also fit with a minor *S* = 1 impurity (3.5%). Simulation of the data with JulX provided the following fit parameters: *g* = 2.091, D = 88.358 cm^{-1}, and TIP = 243.1 × 10^{-6} emu. Data is shown as circles and fits are shown as red lines.

2.6 References

(1) Berry, J. F. Terminal Nitrido and Imido Complexes of the Late Transition Metals. *Comments Inorg. Chem.* **2009**, *30* (1–2), 28.

(2) Ray, K.; Heims, F.; Pfaff, F. F. Terminal Oxo and Imido Transition-Metal Complexes of Groups 9–11. *Eur. J Inorg. Chem.* **2013**, 3784.

(3) Winkler, J. R.; Gray, H. B. Electronic Structures of Oxo-Metal Ions. In *Molecular Electronic Structures of Transition Metal Complexes I*; Mingos, D. M. P., Day, P., Dahl, J. P., Eds.; Springer Berlin Heidelberg, 2012; Vol. 142, pp 17–28.

(4) Hay-Motherwell, R. S.; Wilkinson, G.; Hussain-Bates, B.; Hursthouse, M. B. Synthesis and X-Ray Crystal Structure of Oxotrimesityliridium(V). *Polyhedron* **1993**, *12* (16), 2009.

(5) Poverenov, E.; Efremenko, I.; Frenkel, A. I.; Ben-David, Y.; Shimon, L. J. W.; Leitus, G.; Konstantinovski, L.; Martin, J. M. L.; Milstein, D. Evidence for a Terminal Pt(IV)-Oxo Complex Exhibiting Diverse Reactivity. *Nature* **2008**, *455* (7216), 1093.

(6) Schöffel, J.; Rogachev, A. Y.; DeBeer George, S.; Burger, P. Isolation and Hydrogenation of a Complex with a Terminal Iridium–Nitrido Bond. *Angew. Chem. Int. Ed.* **2009**, *48* (26), 4734.

(7) Scheibel, M. G.; Askevold, B.; Heinemann, F. W.; Reijerse, E. J.; de Bruin, B.; Schneider, S. Closed-Shell and Open-Shell Square-Planar Iridium Nitrido Complexes. *Nat. Chem.* **2012**, *4* (7), 552.

(8) Dai, X.; Kapoor, P.; Warren, T. H. $[Me_2NN]Co(\eta^6$-Toluene): O=O, N=N, and O=N Bond Cleavage Provides β-Diketiminato Cobalt μ-Oxo and Imido Complexes. *J. Am. Chem. Soc.* **2004**, *126* (15), 4798.

(9) Mindiola, D. J.; Hillhouse, G. L. Terminal Amido and Imido Complexes of Three-Coordinate Nickel. *J. Am. Chem. Soc.* **2001**, *123* (19), 4623.

(10) Laskowski, C. A.; Miller, A. J. M.; Hillhouse, G. L.; Cundari, T. R. A Two-Coordinate Nickel Imido Complex That Effects C−H Amination. *J. Am. Chem. Soc.* **2011**, *133* (4), 771.

(11) Badiei, Y. M.; Dinescu, A.; Dai, X.; Palomino, R. M.; Heinemann, F. W.; Cundari, T. R.; Warren, T. H. Copper–Nitrene Complexes in Catalytic C-H Amination. *Angew. Chem. Int. Ed.* **2008**, *47* (51), 9961.

(12) Mindiola, D. J.; Hillhouse, G. L. Synthesis, Structure, and Reactions of a Three-Coordinate Nickel-Carbene Complex, {1,2-Bis(Di-Tert-Butylphosphino)Ethane}$NiCPh_2$. *J. Am. Chem. Soc.* **2002**, *124* (34), 9976.

(13) Melenkivitz, R.; Mindiola, D. J.; Hillhouse, G. L. Monomeric Phosphido and Phosphinidene Complexes of Nickel. *J. Am. Chem. Soc.* **2002**, *124* (15), 3846.

(14) Iluc, V. M.; Hillhouse, G. L. Three-Coordinate Nickel Carbene Complexes and Their One-Electron Oxidation Products. *J. Am. Chem. Soc.* **2014**, *136* (17), 6479.

(15) Jenkins, D. M.; Betley, T. A.; Peters, J. C. Oxidative Group Transfer to Co(I) Affords a Terminal Co(III) Imido Complex. *J. Am. Chem. Soc.* **2002**, *124* (38), 11238.

(16) Shay, D. T.; Yap, G. P. A.; Zakharov, L. N.; Rheingold, A. L.; Theopold, K. H. Intramolecular CH Activation by an Open-Shell Cobalt(III) Imido Complex. *Angew. Chem. Int. Ed.* **2005**, *44* (10), 1508.

(17) Jones, C.; Schulten, C.; Rose, R. P.; Stasch, A.; Aldridge, S.; Woodul, W. D.; Murray,

K. S.; Moubaraki, B.; Brynda, M.; La Macchia, G.; et al. Amidinato– and Guanidinato–Cobalt(I) Complexes: Characterization of Exceptionally Short Co–Co Interactions. *Angew. Chem. Int. Ed.* **2009**, *48* (40), 7406.

(18) King, E. R.; Sazama, G. T.; Betley, T. A. Co(III) Imidos Exhibiting Spin Crossover and C–H Bond Activation. *J. Am. Chem. Soc.* **2012**, *134* (43), 17858.

(19) Mehn, M. P.; Brown, S. D.; Jenkins, D. M.; Peters, J. C.; Que, L. Vibrational Spectroscopy and Analysis of Pseudo-Tetrahedral Complexes with Metal Imido Bonds. *Inorg. Chem.* **2006**, *45* (18), 7417.

(20) Cundari, T. R.; Jimenez-Halla, J. O. C.; Morello, G. R.; Vaddadi, S. Catalytic Tuning of a Phosphinoethane Ligand for Enhanced C−H Activation. *J. Am. Chem. Soc.* **2008**, *130* (39), 13051.

(21) Pierpont, A. W.; Cundari, T. R. Computational Study of Methane C−H Activation by First-Row Late Transition Metal LnM═E (M: Fe, Co, Ni) Complexes. *Inorg. Chem.* **2010**, *49* (5), 2038.

(22) Iluc, V. M.; Hillhouse, G. L. Hydrogen-Atom Abstraction from Ni(I) Phosphido and Amido Complexes Gives Phosphinidene and Imide Ligands. *J. Am. Chem. Soc.* **2010**, *132* (43), 15148.

(23) Iluc, V. M.; Miller, A. J. M.; Anderson, J. S.; Monreal, M. J.; Mehn, M. P.; Hillhouse, G. L. Synthesis and Characterization of Three-Coordinate Ni(III)-Imide Complexes. *J. Am. Chem. Soc.* **2011**, *133* (33), 13055.

(24) Mindiola, D. J.; Waterman, R.; Iluc, V. M.; Cundari, T. R.; Hillhouse, G. L. Carbon–Hydrogen Bond Activation, C–N Bond Coupling, and Cycloaddition Reactivity of a Three-Coordinate Nickel Complex Featuring a Terminal Imido Ligand. *Inorg. Chem.* **2014**, *53* (24), 13227.

(25) Kogut, E.; Wiencko, H. L.; Zhang, L.; Cordeau, D. E.; Warren, T. H. A Terminal Ni(III)-Imide with Diverse Reactivity Pathways. *J. Am. Chem. Soc.* **2005**, *127* (32), 11248.

(26) Yao, S.; Milsmann, C.; Bill, E.; Wieghardt, K.; Driess, M. From a Paramagnetic, Mononuclear Supersulfidonickel(II) Complex to a Diamagnetic Dimer with a Four-Sulfur Two-Electron Bond. *J. Am. Chem. Soc.* **2008**, *130* (41), 13536.

(27) Vicic, D. A.; Jones, W. D. Evidence for the Existence of a Late-Metal Terminal Sulfido Complex. *J. Am. Chem. Soc.* **1999**, *121* (16), 4070.

(28) Can, M.; Armstrong, F. A.; Ragsdale, S. W. Structure, Function, and Mechanism of the Nickel Metalloenzymes, CO Dehydrogenase, and Acetyl-CoA Synthase. *Chem. Rev.* **2014**, *114* (8), 4149.

(29) Dobbek, H.; Gremer, L.; Kiefersauer, R.; Huber, R.; Meyer, O. Catalysis at a Dinuclear [CuSMo(O)OH] Cluster in a CO Dehydrogenase Resolved at 1.1-Å Resolution. *Proc. Natl. Acad. Sci.* **2002**, *99* (25), 15971.

(30) George, G. N.; Pickering, I. J.; Yu, E. Y.; Prince, R. C.; Bursakov, S. A.; Gavel, O. Y.; Moura, I.; Moura, J. J. G. A Novel Protein-Bound Copper−Molybdenum Cluster. *J. Am. Chem. Soc.* **2000**, *122* (34), 8321.

(31) Pomowski, A.; Zumft, W. G.; Kroneck, P. M. H.; Einsle, O. N_2O Binding at a [4Cu:2S] Copper-Sulphur Cluster in Nitrous Oxide Reductase. *Nature* **2011**, *477* (7363), 234.

(32) Brown, K.; Djinovic-Carugo, K.; Haltia, T.; Cabrito, I.; Saraste, M.; Moura, J. G.; Moura, I.; Tegoni, M.; Cambillau, C. Revisiting the Catalytic CuZ Cluster of Nitrous

Oxide (N_2O) Reductase: Evidence of a Bridging Inorganic Sulfur. *J. Biol. Chem.* **2000**, *275* (52), 41133.
(33) Brown, K.; Tegoni, M.; Prudencio, M.; Pereira, A. S.; Besson, S.; Moura, J. J.; Moura, I.; Cambillau, C. A Novel Type of Catalytic Copper Cluster in Nitrous Oxide Reductase. *Nat. Struct. Biol.* **2000**, *7* (3), 191.
(34) Dobbek, H.; Svetlitchnyi, V.; Gremer, L.; Huber, R.; Meyer, O. Crystal Structure of a Carbon Monoxide Dehydrogenase Reveals a [Ni-4Fe-5S] Cluster. *Science* **2001**, *293* (5533), 1281.
(35) Bar-Nahum, I.; Gupta, A. K.; Huber, S. M.; Ertem, M. Z.; Cramer, C. J.; Tolman, W. B. Reduction of Nitrous Oxide to Dinitrogen by a Mixed Valent Tricopper-Disulfido Cluster. *J. Am. Chem. Soc.* **2009**, *131* (8), 2812.
(36) Tolman, W. B. Binding and Activation of N_2O at Transition-Metal Centers: Recent Mechanistic Insights. *Angew. Chem. Int. Ed.* **2010**, *49* (6), 1018.
(37) Johnson, B. J.; Antholine, W. E.; Lindeman, S. V; Mankad, N. P. A Cu_4S Model for the Nitrous Oxide Reductase Active Sites Supported Only by Nitrogen Ligands. *Chem. Commun.* **2015**.
(38) Johnson, B. J.; Lindeman, S. V; Mankad, N. P. Assembly, Structure, and Reactivity of Cu_4S and Cu_3S Models for the Nitrous Oxide Reductase Active Site, CuZ*. *Inorg. Chem.* **2014**, *53* (19), 10611.
(39) Smiles, D. E.; Wu, G.; Kaltsoyannis, N.; Hayton, T. W. Thorium-Ligand Multiple Bonds via Reductive Deprotection of a Trityl Group. *Chem. Sci.* **2015**, *6* (6), 3891.
(40) Holland, P. L.; Cundari, T. R.; Perez, L. L.; Eckert, N. A.; Lachicotte, R. J. Electronically Unsaturated Three-Coordinate Chloride and Methyl Complexes of Iron, Cobalt, and Nickel. *J. Am. Chem. Soc.* **2002**, *124* (48), 14416.
(41) Horn, B.; Limberg, C.; Herwig, C.; Braun, B. Three-Coordinate Nickel(II) and Nickel(I) Thiolate Complexes Based on the β-Diketiminate Ligand System. *Inorg. Chem.* **2014**, *53* (13), 6867.
(42) Holze, P.; Horn, B.; Limberg, C.; Matlachowski, C.; Mebs, S. The Activation of Sulfur Hexafluoride at Highly Reduced Low-Coordinate Nickel Dinitrogen Complexes. *Angew. Chem. Int. Ed.* **2014**, *53* (10), 2750.
(43) Evans, D. F. The Determination of the Paramagnetic Susceptibility of Substances in Solution by Nuclear Magnetic Resonance. *J. Chem. Soc.* **1959**, 2003.
(44) Eckert, N. A.; Bones, E. M.; Lachicotte, R. J.; Holland, P. L. Nickel Complexes of a Bulky Beta-Diketiminate Ligand. *Inorg. Chem.* **2003**, *42* (5), 1720.
(45) Chen, C.; Bellows, S. M.; Holland, P. L. Tuning Steric and Electronic Effects in Transition-Metal [Small Beta]-Diketiminate Complexes. *Dalt. Trans.* **2015**.
(46) Gomberg, M. An Instance of Trivalent Carbon: Triphenylmethyl. *J. Am. Chem. Soc.* **1900**, *22* (11), 757.
(47) Mealli, C.; Midollini, S.; Sacconi, L. Transition-Metal Complexes with Sulfur Atom as Ligand. 2. Synthesis, Properties, and Structural Characterization of Thio, Mercapto, and Methylthio Complexes of Cobalt(I) and Nickel(I) and -(II) with Poly(Tertiary Phosphines). *Inorg. Chem.* **1978**, *17* (3), 632.
(48) Pleus, R. J.; Waden, H.; Saak, W.; Haase, D.; Pohl, S. Preparation of the First Sulfur-Containing Cobalt and Nickel Complexes Stabilised by the Macrocyclic Cyclam Ligand; Observation of S–H Bond Activation. *J. Chem. Soc. Dalt. Trans.* **1999**, *0* (15), 2601.

(49) Cho, J.; Van Heuvelen, K. M.; Yap, G. P. A.; Brunold, T. C.; Riordan, C. G. New Synthetic Routes to a Disulfidodinickel(II) Complex: Characterization and Reactivity of a $Ni_2(\mu\text{-}\eta^2\text{:}\eta^2\text{-}S_2)$ Core. *Inorg. Chem.* **2008**, *47* (10), 3931.

(50) Inosako, M.; Kunishita, A.; Kubo, M.; Ogura, T.; Sugimoto, H.; Itoh, S. ($\mu\text{-}\eta^2\text{:}\eta^2$-Disulfido)Dinickel(II) Complexes Supported by 6-Methyl-TPA Ligands. *Dalt. Trans.* **2009**, No. 43, 9410.

(51) Iluc, V. M.; Laskowski, C. A.; Brozek, C. K.; Harrold, N. D.; Hillhouse, G. L. Monomeric and Dimeric Disulfide Complexes of Nickel(II). *Inorg. Chem.* **2010**, *49* (15), 6817.

(52) Olechnowicz, F.; Hillhouse, G. L.; Jordan, R. F. Synthesis and Reactivity of NHC-Supported $Ni_2(\mu^2\text{-}\eta^2,\eta^2\text{-}S_2)$-Bridging Disulfide and $Ni_2(\mu\text{-}S)_2$-Bridging Sulfide Complexes. *Inorg. Chem.* **2015**, *54* (6), 2705.

(53) Yao, S.; Xiong, Y.; Zhang, X.; Schlangen, M.; Schwarz, H.; Milsmann, C.; Driess, M. Facile Dissociation of $[(LNi^{II})_2E_2]$ Dichalcogenides: Evidence for $[LNi^{II}E_2]$ Superselenides and Supertellurides in Solution. *Angew. Chem. Int. Ed.* **2009**, *48* (25), 4551.

(54) Smiles, D. E.; Wu, G.; Hayton, T. W. Synthesis of Uranium–Ligand Multiple Bonds by Cleavage of a Trityl Protecting Group. *J. Am. Chem. Soc.* **2014**, *136* (1), 96.

(55) Pyykkö, P. Additive Covalent Radii for Single-, Double-, and Triple-Bonded Molecules and Tetrahedrally Bonded Crystals: A Summary. *J. Phys. Chem. A* **2015**, *119* (11), 2326.

(56) Laskowski, C. A.; Morello, G. R.; Saouma, C. T.; Cundari, T. R.; Hillhouse, G. L. Single-Electron Oxidation of N-Heterocyclic Carbene-Supported Nickel Amides Yielding Benzylic C-H Activation. *Chem. Sci.* **2013**, *4* (1), 170.

(57) Ghosh, A.; Gonzalez, E.; Tangen, E.; Roos, B. O. Mapping the D−d Excited-State Manifolds of Transition Metal β-Diiminato−Imido Complexes. Comparison of Density Functional Theory and CASPT2 Energetics†. *J. Phys. Chem. A* **2008**, *112* (50), 12792.

(58) Sitzmann, H.; Saurenz, D.; Wolmershäuser, G.; Klein, A.; Boese, R. Bis(Tetraisopropylcyclopentadienylnickel)Dichalcogenides: Complexes of the Novel [{CpME}2] Type (E = S, Se, Te). *Organometallics* **2001**, *20* (4), 700.

(59) Brown, E. C.; York, J. T.; Antholine, W. E.; Ruiz, E.; Alvarez, S.; Tolman, W. B. [Cu3(μ-S)2]3+ Clusters Supported by N-Donor Ligands: Progress toward a Synthetic Model of the Catalytic Site of Nitrous Oxide Reductase. *J. Am. Chem. Soc.* **2005**, *127* (40), 13752.

(60) Berry, J. F. A Definitive Answer to a Bonding Quandary? The Role of One-Electron Resonance Structures in the Bonding of a {Cu3S2}3+ Core. *Chem. - A Eur. J.* **2010**, *16* (9), 2719.

(61) Yao, S.; Hrobárik, P.; Meier, F.; Rudolph, R.; Bill, E.; Irran, E.; Kaupp, M.; Driess, M. A Heterobimetallic Approach To Stabilize the Elusive Disulfur Radical Trianion (“Subsulfide”) ${{\rm S}{{{{\bullet}}3- \hfill \atop 2\hfill}}}$. *Chem. Eur. J.* **2013**, *19* (4), 1246.

(62) Rudolph, R.; Blom, B.; Yao, S.; Meier, F.; Bill, E.; van Gastel, M.; Lindenmaier, N.; Kaupp, M.; Driess, M. Synthesis, Reactivity, and Electronic Structure of a Bioinspired Heterobimetallic [Ni(μ-S $_2$)Fe] Complex with Disulfur Monoradical Character. *Organometallics* **2014**, *33* (12), 3154.

(63) Berry, J. F. Two-Center/Three-Electron Sigma Half-Bonds in Main Group and Transition Metal Chemistry. *Acc. Chem. Res.* **2016**, *49* (1), 27.
(64) Holland, P. L.; Cundari, T. R.; Perez, L. L.; Eckert, N. a; Lachicotte, R. J. Electronically Unsaturated Three-Coordinate Chloride and Methyl Complexes of Iron, Cobalt, and Nickel. *J. Am. Chem. Soc.* **2002**, *124* (48), 14416.
(65) Hartmann, N. J.; Wu, G.; Hayton, T. W. Trapping of an Ni^{II} Sulfide by a Co^{I} Fulvene Complex. *Organometallics* **2017**, *36* (9), 1765.
(66) Köthe, C.; Braun, B.; Herwig, C.; Limberg, C. Synthesis, Characterization, and Interconversion of β-Diketiminato Nickel N_xH_y Complexes. *Eur. J Inorg. Chem.* **2014**, *2014* (31), 5296.
(67) Huang, D.; Deng, L.; Sun, J.; Holm, R. H. Cleavage of Ni-(μ_2-S)-Ni Bridges in Dinuclear Nickel(II) Dithiolate Pincer Complexes and Related Reactions. *Inorg. Chem.* **2009**, *48* (13), 6159.
(68) Komuro, T.; Hiroyuki Kawaguchi; Tatsumi, K. Synthesis and Reactions of Triphenylsilanethiolato Complexes of Manganese(II), Iron(II), Cobalt(II), and Nickel(II). **2002**.
(69) Komuro, T.; Matsuo, T.; Kawaguchi, H.; Tatsumi, K. Synthesis and Structural Characterization of Silanethiolato Complexes Having Tert-Butyldimethylsilyl and Trimethylsilyl Groups. *Dalt. Trans.* **2004**, *0* (10), 1618.
(70) Shiao, M. J.; Lai, L. L.; Ku, W. S.; Lin, P. Y.; Hwu, J. R. Chlorotrimethylsilane in Combination with Sodium Sulfide as the Equivalent of Sodium Trimethylsilanethiolate in Organic Reactions. *J. Org. Chem.* **1993**, *58* (17), 4742.
(71) Feldman, J.; McLain, S. J.; Parthasarathy, A.; Marshall, W. J.; Calabrese, J. C.; Arthur, S. D. Electrophilic Metal Precursors and a β-Diimine Ligand for Nickel(II)- and Palladium(II)-Catalyzed Ethylene Polymerization. *Organometallics* **1997**, *16* (8), 1514.
(72) M. Budzelaar, P. H.; van Oort, A. B.; Orpen, A. G. β-Diiminato Complexes of VIII and TiIII – Formation and Structure of Stable Paramagnetic Dialkylmetal Compounds. *Eur. J Inorg. Chem.* **1998**, *1998* (10), 1485.
(73) Smith, J. M.; Lachicotte, R. J.; Holland, P. L. Tuning Metal Coordination Number by Ancillary Ligand Steric Effects: Synthesis of a Three-Coordinate Iron(II) Complex. *Chem. Commun.* **2001**, *0* (17), 1542.
(74) Chadwick, S.; Englich, U.; Ruhlandt-Senge, K. Lewis Base Coordination versus Cation−π Interaction in Monomeric and Hexameric Potassium Thiolates. *Organometallics* **1997**, *16* (26), 5792.
(75) Poulton, J. T.; Sigalas, M. P.; Folting, K.; Streib, W. E.; Eisenstein, O.; Caulton, K. G. $RuHX(CO)(PR_3)_2$: Can ν_{CO} Be a Probe for the Nature of the Ru-X Bond? *Inorg. Chem.* **1994**, *33* (7), 1476.
(76) Harris Robin, K.; Becker Edwin, D.; Cabral de Menezes Sonia, M.; Goodfellow, R.; Granger, P. NMR Nomenclature: Nuclear Spin Properties and Conventions for Chemical Shifts. IUPAC Recommendations 2001. International Union of Pure and Applied Chemistry. Physical Chemistry Division. Commission on Molecular Structure and Spectroscopy. *Pure Appl. Chem.* **2002**, *40* (7), 489.
(77) Harris Robin, K.; Becker Edwin, D.; Cabral De Menezes Sonia, M.; Granger, P.; Hoffman Roy, E.; Zilm Kurt, W. Further Conventions for NMR Shielding and Chemical Shifts. *Pure Appl. Chem.* **2008**, *80*, 59.

(78) Bain, G. A.; Berry, J. F. Diamagnetic Corrections and Pascal's Constants. *J. Chem. Educ.* **2008**, *85* (4), 532.
(79) Bill, E. JulX. *julX*. 1.4.1. http://ewww.mpi-muelheim.mpg.de/bac/logins/bill/julX_en.php 2008.
(80) Dunsford, J. J.; Clark, E. R.; Ingleson, M. J. Direct $C(Sp^2)$-$C(Sp^3)$ Cross-Coupling of Diaryl Zinc Reagents with Benzylic, Primary, Secondary, and Tertiary Alkyl Halides. *Angew. Chem. Int. Ed.* **2015**, *54* (19), 5688.
(81) SMART Apex II. Bruker AXS Inc.: Madison, WI 2005.
(82) SAINT Software User's Guide. Bruker AXS Inc.: Madison, WI 2005.
(83) Sheldrick, G. M. SADABS. University of Gottingen: Germany 2005.
(84) SHELXTL PC. Bruker AXS Inc.: Madison, WI 2005.

Chapter 3 Trapping of an Ni^{II} sulfide by a Co^{I} fulvene complex

Portions of this work were published in:

Nathaniel J. Hartmann , Guang Wu, Trevor W. Hayton

Organometallics, **2017**, *36*, 1765-1769.

Table of Contents

3.1 Introduction

The synthesis of late transition metal (groups 9-11) terminal chalcogenides (especially oxygen and sulfur) has long been a target of synthetic inorganic chemists.[1] This class of compounds tends to be highly reactive,[2–4] and as a result, only a few well characterized late metal terminal chalcogenides are known, including $[Ir^{V}(O)(Mes)_3]$ (Mes = 2,4,6-$Me_3C_6H_2$) and $[Pt^{IV}(O)(PCN)][BF_4]$ (PCN = $C_6H_3[CH_2P(tBu)_2](CH_2CH_2NMe_2)$).[5,6] A number of late transition metal carbene (CR_2^{2-}),[7] nitrene (NR^{2-}),[8–15] nitride (N^{3-}),[16,17] and phosphinidene (PR^{2-})[18,19] complexes have also been reported in recent years.[20,21] While a few of these complexes have been isolated, they tend to be extremely reactive, and often can only be observed spectroscopically.[17,22–24] Nonetheless, it is clear that synthetic chemists are now beginning to identify the combination of ligand requirements and synthetic procedures that can successfully generate late-metal ligand multiple bonds.

In Chapter 2, I detailed the synthesis of Ni^{II} sulfides, $[K(L)][L^{R}Ni^{II}(S)]$ (**2.4**, R = Me, L = 18-crown-6; **2.5**, R = ^{t}Bu, L = 18-crown-6; **2.6**, R = ^{t}Bu, L = 2,2,2-cryptand),[25] by $2e^{-}$ reduction of Ni^{II} triylthiolate complexes, $[L^{R}Ni^{II}(SCPh_3)]$ (**2.1**, R = Me; **2.2**, R = ^{t}Bu), using KC_8. This reaction results in the selective cleavage of the S-C bond and release of $[CPh_3]^{-}$, a strategy that the Hayton group has coined "reductive deprotection". A preliminary reactivity study, highlighted in Chapter 2, shows that **2.5** can react with Me_3SiOTf to form a trimethylsilanethiolato complex $[L^{tBu}Ni^{II}(SSiMe_3)]$ (**2.12**), demonstrating the nucleophilicity of the sulfide ligand. Importantly, however, the presence of the coordinating $[K(L)]^{+}$ cation likely tempers the reactivity of the sulfide ligand, and possibly limits the extent of reactivity of this functional group. Consequently, I have sought to perform the "reductive

deprotection" reaction with a reducing agent that generates a non-coordinating cation, and, in particular, I identified Cp^*_2Co as an ideal choice for this application.

The research in this chapter details the reductive deprotection of $[L^{tBu}Ni^{II}(SCPh_3)]$ (**2.2**) with Cp^*_2Co, which unexpectedly leads to the generation of a Ni^I cobaltocenium thiolate complex, $[L^{tBu}Ni^I(SCH_2Me_4C_5)Co(Cp^*)]$ that likely forms via the reaction of a putative nickel sulfide, $[Cp^*_2Co][\ L^{tBu}Ni^{II}(S)]$, with deprotonated decamethylcobaltocenium, $[CoCp^*(C_5Me_4{=}CH_2)]$.

3.2 Results and Discussion

3.2.1 Synthesis of $[L^{tBu}Ni^I(SCH_2Me_4C_5)Co(Cp^*)]$ (3.1)

Addition of 2 equiv of Cp^*_2Co to a stirring, deep blue solution of $[L^{tBu}Ni^{II}(SCPh_3)]$ (**2.2**) in cold (-25 °C) THF, results in a rapid color change to deep red-brown (Scheme 3.1). The reaction mixture was stirred for 3 h, and following work-up, $[L^{tBu}Ni^I(SCH_2Me_4C_5)Co(Cp^*)]$ (**3.1**) was successfully isolated as dark brown plates in 69% yield. Interestingly, the reaction of $[L^{tBu}Ni^{II}(SCPh_3)]$ with Cp_2Co results in no reaction, demonstrating that this reagent is not sufficiently reducing to initiate the required C-S bond cleavage.

Scheme 3.1 Synthesis of **3.1**

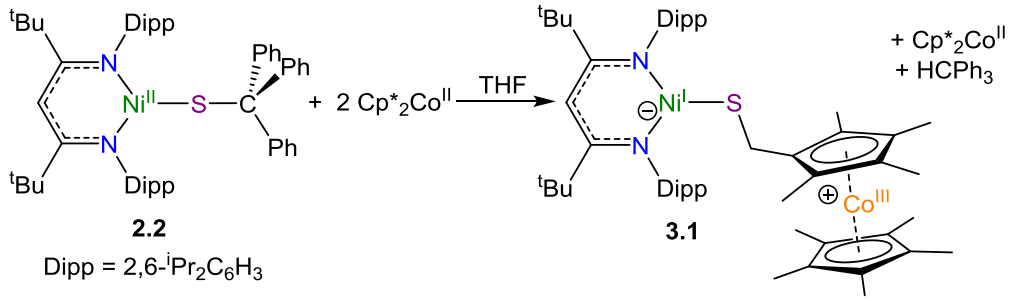

Complex **3.1** crystallizes in the monoclinic space group *P2₁/c*, and its solid state molecular structure is shown in Figure 3.1. It features a three coordinate Ni^I center ligated by a cobaltocenium thiolate moiety. The Ni-S and C-S bond lengths of 2.181(2) Å and

1.870(7) Å, respectively, are both consistent with single bonds.[25,26] For comparison, the Ni-S bond length in the starting material is markedly shorter (2.0869(1) Å).[25] The Ni-N bond lengths in **3.1** (1.901(4) and 1.902(5) Å) are also longer than those found in the Ni^{II} starting material (1.863(3) and 1.862(3) Å), consistent with the larger ionic radius anticipated for Ni^{I} vs. Ni^{II}. Moreover, the Ni-N bond lengths in **3.1** are consistent with those of other $L^{tBu}Ni^{I}$ complexes.[26,27] Finally, the average distance from the Co atom to the ring carbon atoms of the Cp* ligand is 2.033 Å, which is characteristic of Cp^*Co^{III} complexes.[28,29]

The ^1H NMR spectrum of **3.1** in C_6D_6 is typical of those reported for other Ni^{I} β-diketiminate complexes.[26,27,30] It features a very broad resonance at -0.8 ppm, which is assignable to the ^{t}Bu groups on the backbone of the β-diketiminate ligand. Additionally, a broad singlet at 0.7 ppm is assignable methyl groups of the Cp* ligand attached to Co^{III}, while resonances at 0.3 and 3.9 ppm are assignable to the two unique methyl environments of the $SCH_2Me_4C_5$ ring. Complex **3.1** exhibits an effective magnetic moment of 1.67 B.M., as determined by Evans' method.[31] This value is consistent with that anticipated for a Ni^{I} complex with an $S = 1/2$ ground state.[26,27]

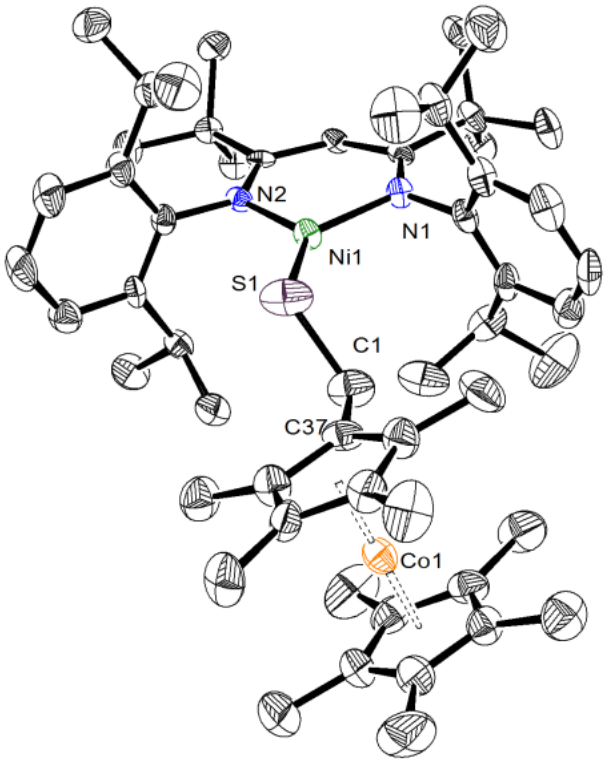

Figure 3.1. ORTEP drawing of $[L^{tBu}Ni^{I}(SCH_2Me_4C_5)Co(Cp^*)]\cdot C_4H_{10}O$ (**3.1**$\cdot C_4H_{10}O$) shown with 50% thermal ellipsoids. Hydrogen atoms and a $C_4H_{10}O$ solvate molecule have been omitted for clarity. Selected metrical parameters: Ni1-N1 1.910(4), Ni1-N2 1.902(5), Ni1-S1 2.181(2), S1-C1 1.870(7), C1-C37 1.498(8), N1-Ni1-N2 98.2(2)°, N1-Ni1-S1 130.5(2)°, N2-Ni1-S1 131.2(1)°, Ni1-S1-C1 107.2(2)°.

3.2.2 Probing the formation of $[L^{tBu}Ni^{I}(SCH_2Me_4C_5)Co(Cp^*)]$ (3.1) using ^{1}H NMR Spectroscopy

In an effort to better understand the formation of **3.1**, I monitored the reaction of $[L^{tBu}Ni^{II}(SCPh_3)]$ with Cp^*_2Co by ^{1}H NMR spectroscopy. Addition of 2 equiv of Cp^*_2Co to $[L^{tBu}Ni^{II}(SCPh_3)]$ in THF-d_8 in a NMR tube, results in a rapid color change from deep blue to dark red-brown. A ^{1}H NMR spectrum of the reaction mixture, taken 5 min after the addition of Cp^*_2Co, reveals the complete consumption of both $[L^{tBu}Ni^{II}(SCPh_3)]$ and Cp^*_2Co, concomitant with the formation of a new Ni^{II} complex (Figure 3.2, Figures A 3.1-

3.2). I have tentatively identified this complex as the Ni^{II} sulfide, $[Cp^*_2Co][L^{tBu}Ni^{II}(S)]$ (**3.2**). My assignment was made on the basis of the similarity of its ^1H NMR resonances with those of the previously characterized Ni^{II} sulfide, $[K(18\text{-crown-6})][L^{tBu}Ni^{II}(S)]$.[25] For example, complex **3.2** features resonances at -101.97, -1.37, and 15.93 ppm, which are assignable to the γ-proton of the L^{tBu} ligand, its ^{t}Bu substituents, and one environment of its diastereotopic ^{i}Pr methyl groups, respectively. For comparison, these resonances appear at -115.21, -0.88, and 16.25 ppm, respectively, for the original Ni^{II} sulfide, $[K(18\text{-crown-6})][L^{tBu}Ni^{II}(S)]$.[25] Also present in the 5 min spectrum are resonances assignable to the Co^I fulvene complex, $[CoCp^*(C_5Me_4CH_2)]$ (**3.3**) (Figure 3.2, Figures A 3.1-3.2),[32] as well as resonances assignable to $HCPh_3$.[33]

After 30 min, the resonances assignable to complexes **3.2** and **3.3** decrease in intensity, while those assignable to complex **3.1** begin to appear. After 3 h, only trace amounts of complex **3.2** can be detected in the ^1H NMR spectrum of the reaction mixture, while those assignable to **3.1** have grown in intensity. Curiously, I also observe a broad resonance at 21.0 ppm in the 3 h spectrum, which I have assigned to Cp^*_2Co. These spectra also feature a broad singlet at about -1.6 ppm, which I have assigned to the ^{t}Bu groups of an as-yet-unidentified Ni^I β-diketiminate complex. This assignment was made on the basis of its chemical shift along with the broadness of the resonance. This complex is present in an approximately 2:5 ratio, relative to complex **3.1** (Figure A 3.7). Unfortunately, my efforts to isolate and structurally characterize this material have been unsuccessful; however, given the similarity of its ^1H NMR spectrum to that of **3.1**, I conclude that it is similar in structure, e.g., $[L^{tBu}Ni^I(X)]^-$.

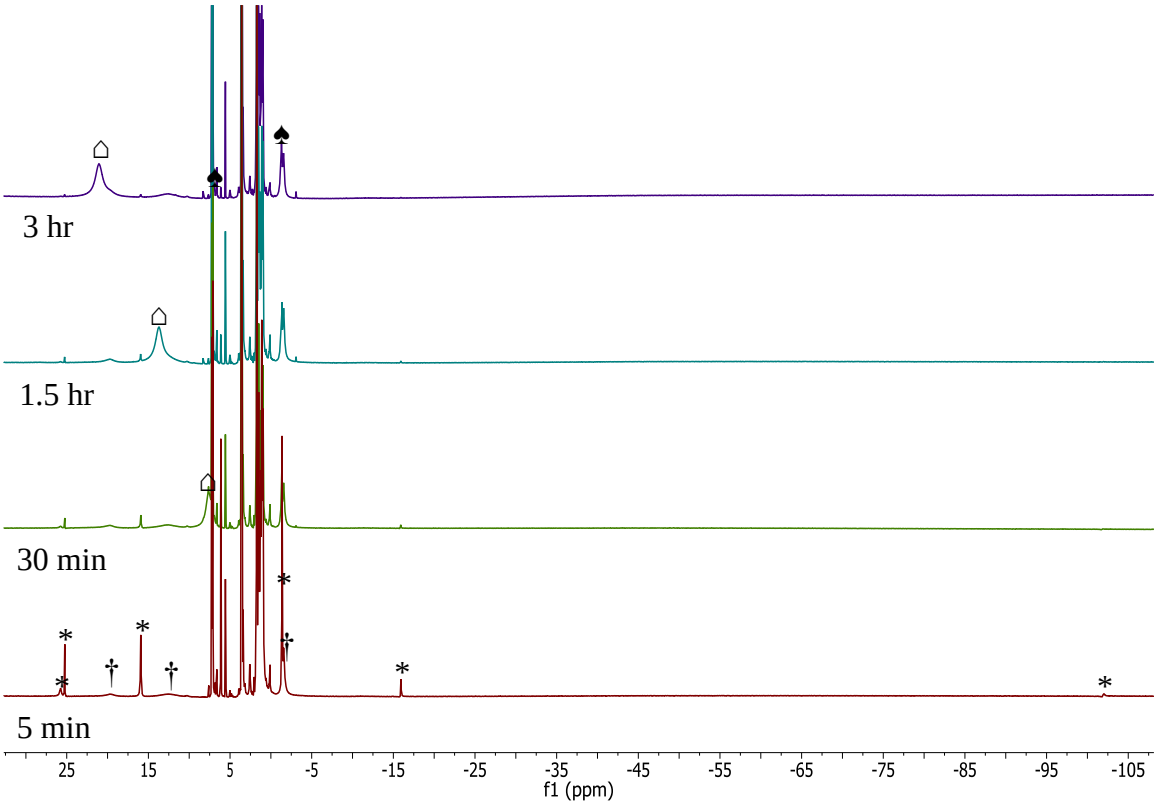

Figure 3.2. ^{1}H NMR spectra of the reaction of [$L^{tBu}Ni^{II}(SCPh_3)$] (**2.2**) with two equiv. of Cp^*_2Co in THF-d_8. (*) indicates the presence of **3.2**, (⌂) indicates the presence of Cp^*_2Co, (†) indicates the presence of an unknown Ni^{I}-containing product, and (♠) indicates the presence of **3.1**.

3.2.3 Mechanistic Considerations

To rationalize my observations, I hypothesize that reduction of [$L^{tBu}Ni^{II}(SCPh_3)$] (**2.2**) with two equiv of Cp^*_2Co results in formation of **3.2** and one equiv of [$Cp^*_2Co^{III}$][CPh_3] (Scheme 3.2). Deprotonation of [Cp^*_2Co]$^+$ by [CPh_3]$^-$ subsequently generates [$CoCp^*(C_5Me_4CH_2)$] (**3.3**)[32] and $HCPh_3$. Finally, coupling of the nucleophilic terminal sulfide ligand in **3.2** with the methylene carbon of **3.3** results in formation complex **3.1**, concomitant with reduction of the [Cp^*_2Co]$^+$ counterion. The latter observation is somewhat surprising given the high reduction potential of [Cp^*_2Co] (1.94 V vs. Fc/Fc$^+$ in

CH_2Cl_2).[34] Formally, the C-S bond forming reaction results in a $2e^-$ oxidation of the Co^I center in **3.3**. One of the electrons is transferred to the Ni center in $[L^{tBu}Ni^{II}(S)]^-$, while the other is transferred to $[Cp^*_2Co^{III}]^+$, reforming $Cp^*_2Co^{II}$.

For comparison, there are several other examples of C-S bond formation mediated by nucleophilic metal sulfides.[35–40] For example, $[ReS_4]^-$ reacts with norbornene to form the dithiolate complex, $[ReS_2(S_2C_7H_{10})]^-$. Similarly, $[Mo_3(\mu_3\text{-}S)(\mu\text{-}S)_3(H_2O)_9]^{4+}$ reacts with alkynes to generate a dithiolene ligand by formation of two new C-S bonds.[41] Also of note, $[CpMo(\mu\text{-}S)]_2(S_2CH_2)$ has been reported to catalyze the hydrogenation of acetylene and CS_2, via a dithiolene intermediate.[42] My proposed reaction pathway is also consistent with the known chemical reactivity of $[Cp^*Co(C_5Me_4CH_2)]$ (**3.3**). For example, reaction of $[Cp^*Co(C_5Me_4CH_2)]$ (**3.3**) with 1-mesityl-2,3,4,5-tetraphenylborole ($MesBC_4Ph_4$) results in rapid C-B bond formation and generation of a zwitterionic cobaltocenium borate, $[Cp^*Co(C_5Me_4CH_2B(Mes)\{C_4Ph_4\}]$.[32] Similarly, reaction of an $[Fe_8S_7]$ cluster with $[Cp^*Co(C_5Me_4CH_2)]$ has been shown to result in Fe-C bond formation.[28]

Scheme 3.2 Proposed mechanism for the formation of **3.1**

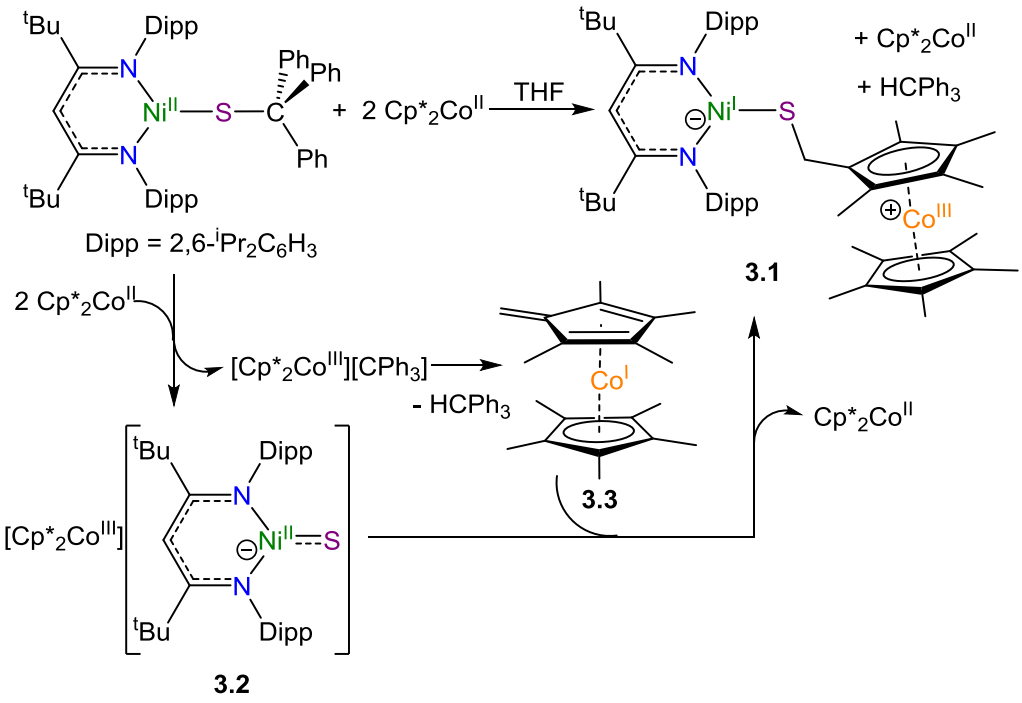

To test my mechanistic hypothesis, I monitored the reaction of independently prepared [Cp*$_2$Co][PF$_6$] with [K(18-crown-6)][CPh$_3$]. Upon mixing in pyridine I observe rapid formation of **3.3** and HCPh$_3$ (Scheme 3.3) (Figure A 3.6). Given this result, in addition to the appearance of **3.3** in the *in situ* ^{1}H NMR experiment, I believe that the proposed intermediacy of [Cp*Co(C$_5$Me$_4$CH$_2$)] (**3.3**) in the formation of **3.1** is reasonable.

Scheme 3.3 Deprotonation of [Cp*$_2$Co^{III}]$^+$ with [CPh$_3$]$^-$

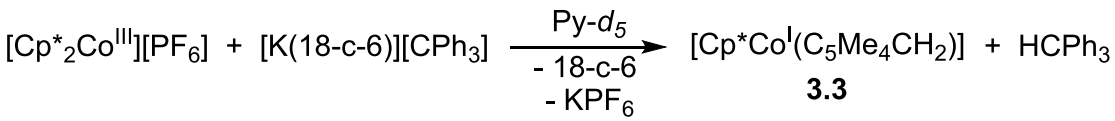

I also monitored the reaction of [L^{tBu}Ni^{II}(SCPh$_3$)] with Cp*$_2$Co by ^{1}H NMR spectroscopy in the presence of an internal standard. Under these conditions, the yield of HCPh$_3$ was determined to be 88% (Figure A 3.5), which is also consistent with the proposed mechanism.

The solution phase redox properties of **3.1** were investigated by cyclic voltammetry. In THF at room temperature, the cyclic voltammogram of **3.1** displays one quasi-reversible redox feature and one reversible redox feature, at -2.20 V and -1.38 V (vs. Fc/Fc^{+}), respectively (Figure 3.3). The feature at -2.20 V is tentatively attributed to the Co^{II}/Co^{III} redox couple, while the feature at -1.38 V is tentatively attributed to the Ni^{II}/Ni^{I} redox couple. The Co^{II}/Co^{III} couple was assigned to be quasi-reversible on the basis of the large $i_{p,a}/i_{p,c}$ ratios observed at high scan rates (Table 3.2). In support of my assignments, I note that my Ni^{II}/Ni^{I} redox potential agrees well with those previously reported for $[L^{tBu}Ni^{II}(SR)]$ (R = Et, -1.40 V; Ph -1.60 V, vs. Fc/Fc^{+}).[26] In addition, the Co^{III}/Co^{II} couple in **3.1** is more negative than that reported for $[Cp^{*}_{2}Co]^{0/+}$ (-1.94 V vs. Fc/Fc^{+} in CH_2Cl_2),[34] demonstrating that $[\mathbf{3.1}]^{-}$, in fact, can reduce $[Cp^{*}_{2}Co]^{+}$ as proposed in Scheme 3.2.

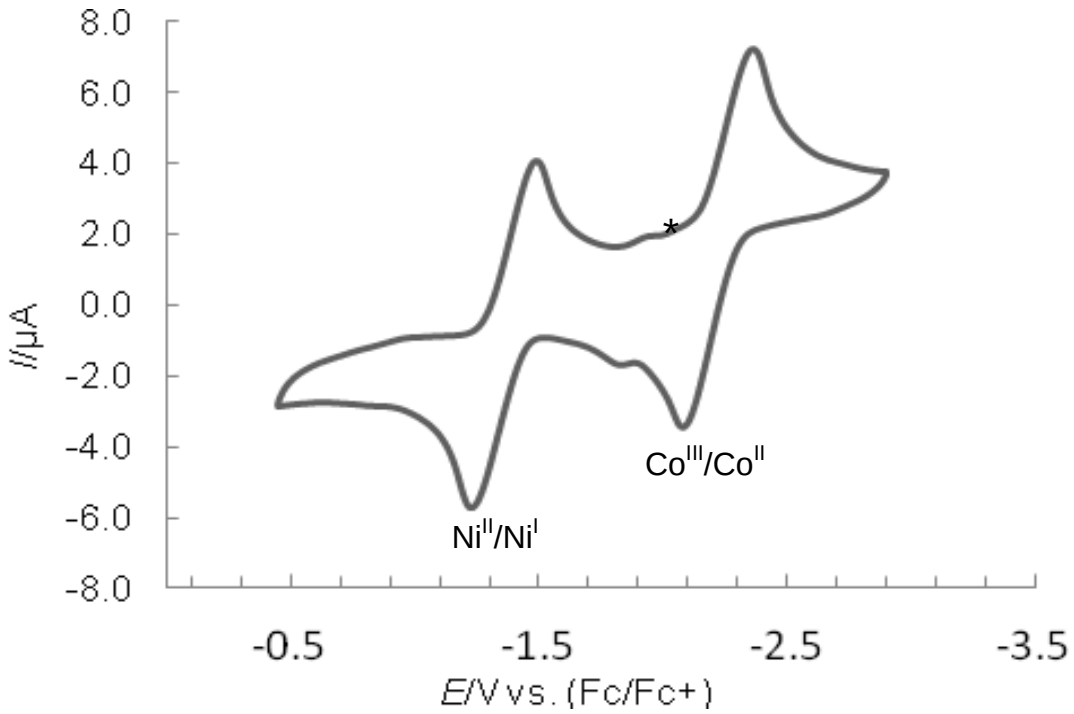

Figure 3.3. Cyclic voltammogram of complex **3.1** (200 mV/s, vs. Fc/Fc^{+}). Measured in THF with 0.1 M $[NBu_4][PF_6]$ as the supporting electrolyte. (*) indicates a feature tentatively assigned to Cp^*_2Co, which is present as a minor impurity.

Finally, to explore the generality of this transformation, I monitored the reaction of $[K(18\text{-crown-6})][L^{tBu}Ni^{II}(S)]$ with a variety of olefins, including cyclohexene, norbornene, and styrene, by ^1H NMR spectroscopy. In each case, I observe no reaction, demonstrating that common olefins, alone, will not couple with the sulfide ligand in $[L^{tBu}Ni^{II}(S)]^-$. Likewise, addition of **3.3** to $[K(18\text{-crown-6})][L^{tBu}Ni^{II}(S)]$ also results in no reaction. Thus, it appears that the C-S bond forming reaction likely requires the presence of both a redox-active counter-cation (i.e., $[Cp^*_2Co]^+$) and a formally redox-active olefin (i.e., $[Cp^*Co(C_5Me_4CH_2)]$) to proceed.

3.3 Summary

In this chapter, I have demonstrated that the reduction of the nickel triphenylmethythiolate complex [$L^{tBu}Ni^{II}(SCPh_3)$] (**2.2**) with Cp^*_2Co generates a transient Ni^{II} sulfide complex, $[Cp^*_2Co][L^{tBu}Ni^{II}(S)]$ (**3.2**). A subsequent deprotonation of $[Cp^*_2Co]^+$ by $[CPh_3]^-$ gives the Co^I fulvenyl complex, $[Cp^*Co(C_5Me_4CH_2)]$ (**3.3**), which couples with the sulfide ligand in $[Cp^*_2Co][L^{tBu}Ni^{II}(S)]$ to form a Ni^I cobaltocenium thiolate complex, $[L^{tBu}Ni^I(SCH_2Me_4C_5)Co(Cp^*)]$ (**3.1**), concomitant with the reduction of the cobaltocenium cation.

Due to unexpected side reactions, this application of the reductive deprotection protocol did not lead to the isolation of the desired terminal nickel sulfide complex. Nevertheless, this result expands the scope of late metal sulfide reactivity from the preliminary study discussed in Chapter 2, and suggests that the sulfide ligand in these complexes may be capable of other S-C bond forming reactions. This result also demonstrates that "reductive deprotection" is possible with a variety of reducing agents, not just KC_8 as previously demonstrated,[25,43,44] suggesting a broader scope of this transformation than hitherto recognized.

3.4 Experimental Procedures

3.4.1 General Methods

All reactions and subsequent manipulations were performed under anaerobic and anhydrous conditions under an atmosphere of nitrogen. Hexanes, tetrahydrofuran, diethyl ether (Et_2O), and toluene were dried using a Vacuum Atmospheres DRI-SOLV Solvent Purification system and stored over 3Å sieves for 24 h prior to use. Benzene-d_6, THF-d_8, pyridine-d_5, and pentane, were dried over 3Å molecular sieves for 24 h prior to use. Decamethylcobaltocene (Cp^*_2Co) was purified by recrystallization from hexanes at -25 °C.

$[L^{tBu}Ni^{II}SCPh_3]$, $[K(18\text{-crown-6})][L^{tBu}Ni(S)]$, $[Cp^*_2Co][PF_6]$, $(CH_2C_5Me_4)Co(Cp^*)$, and $[K(18\text{-crown-6})][CPh_3]$ were synthesized according to the previously reported procedures.[25,32,43,45] All other reagents were purchased from commercial suppliers and used as received.

^1H and ^{19}F NMR spectra, and Evans' method determinations,[31] were recorded on a Agilent Technologies 400-MR DD2 400 MHz spectrometer or a Varian UNITY INOVA 500 MHz spectrometer. ^1H and ^{19}F NMR spectra were referenced to external $SiMe_4$ using the residual protio solvent peaks as internal standards.[46,47] IR spectra were recorded on a Nicolet 6700 FT-IR spectrometer. Electronic absorption spectra were recorded on a Shimadzu UV3600 UV-NIR Spectrometer. Elemental analyses were performed by the Micro-Mass Facility at the University of California, Berkeley.

3.4.2 Cyclic Voltammetry Measurements.

CV experiments were performed with a CH Instruments 600c Potentiostat, and the data were processed using CHI software (version 6.29). All experiments were performed in a glove box using a 20 mL glass vial as the cell. The working electrode consisted of a platinum disk embedded in glass (2 mm diameter), the counter electrode and the reference electrode were a platinum wire. Solutions employed for CV studies were typically 1 mM in analyte, and 0.1 M in $[NBu_4][PF_6]$. All potentials are reported versus the $[Cp_2Fe]^{0/+}$ couple.

3.4.3 Preparative scale reaction of $[L^{tBu}Ni^{II}(SCPh_3)]$ with Cp^*_2Co to yield $[L^{tBu}Ni^{I}(SCH_2Me_4C_5)Co(Cp^*)]$ (3.1)

To a deep blue, cold (-25 °C), stirring solution of $[L^{tBu}Ni^{II}(SCPh_3)]$ (50.0 mg, 0.0598 mmol) in THF (2 mL) was added Cp^*_2Co (39.4 mg, 0.1196 mmol) in cold (-25 °C) THF (1 mL). This resulted in immediate formation of a dark red-brown solution. This mixture was

allowed to warm to room temperature with stirring. During this time the solution transformed to dark brown. This solution was allowed to stir for 3 h, whereupon the reaction mixture was filtered through a Celite column supported on glass wool (0.5 cm × 2 cm), which afforded a small plug of black solid and a brown-red filtrate. The volatiles were removed from the filtrate *in vacuo* to produce a dark brown residue. This residue was washed with hexanes (1 mL × 2), extracted into toluene (1 mL), filtered through a Celite column supported on glass wool (0.5 cm × 2 cm), concentrated to ca. 0.5 mL, and layered with pentane (1 mL). Storage of this solution at -25 °C for 48 h resulted in the deposition of dark brown needles of $[L^{tBu}Ni^{I}(SCH_2Me_4C_5)Co(Cp^*)]$ (**3.1**), which were isolated by decanting off the supernatant (17 mg). The supernatant was concentrated in vacuo to 0.25 mL and layered with pentane (2 mL). Further storage of this solution at -25 °C for 48 h led to the deposition of more crystals (21 mg), which were isolated by decanting off the supernatant (combined yield: 38 mg, 69%). Anal. Calcd for: $C_{55}H_{82}CoN_2NiS$: C, 71.73; H, 8.97; N, 3.04. Found: C, 71.90; H, 8.80; N, 2.73. ^{1}H NMR (400 MHz, 25 °C, C_6D_6): δ 20.4 (br s), 13.0 (br s), 3.9 (br s, 6H, $CH_2C_5Me_4$, C**H**$_3$), 0.7 (br s, 15 H, Cp*), 0.3 (br s, 6H, $CH_2C_5Me_4$, C**H**$_3$), -0.8 (br s, 18 H, C(C**H**$_3$)$_3$), -12.0 (br s). Of the eleven unique proton enviornments expected for **3.1**, only seven resonances are observed in the ^{1}H NMR spectrum. We suggest that the unobserved resonances are either too broad to be obsevered or are overlapping with other peaks. Evans' method (C_6D_6, 400 MHz, 25 °C, 0.0054 M): 1.67 B.M. IR (KBr Pellet, cm^{-1}): 1624 (w), 1510 (m), 1477 (m), 1446 (s), 1414 (s), 1385 (s), 1363 (s), 1319 (s), 1254 (w), 1219 (w), 1192 (w), 1182 (w), 1155 (m), 1095 (m), 1059 (w), 1024 (m), 937 (w), 920 (w), 897 (w), 852 (w), 802 (w), 781 (m), 762 (m), 729 (m), 700 (s),

665 (w), 638 (m), 619 (w), 590 (w), 467 (m), 447 (m), 407 (w). UV-vis (C_6H_6, 1.0 mM, 25 °C): 443 nm (ε = 5770 $L \cdot mol^{-1} \cdot cm^{-1}$), 527 nm ($\varepsilon$ = 1020 $L \cdot mol^{-1} \cdot cm^{-1}$).

3.4.4 NMR scale reaction of [$L^{tBu}Ni^{II}(SCPh_3)$] with Cp^*_2Co in THF-d_8

To a J-Young NMR tube containing [$L^{tBu}Ni^{II}(SCPh_3)$] (30 mg, 0.0359 mmol) in THF-d_8 (0.5 mL) was added Cp^*_2Co (23.6 mg, 0.0718 mmol). After addition, the color of the solution quickly changed from blue to red-brown. An *in situ* ^{1}H NMR spectrum taken shortly after addition of Cp^*_2Co, revealed the presence of [Cp^*_2Co][$L^{tBu}Ni^{II}(S)$] (**3.2**), $HCPh_3$, an unidentified Ni^I containing product (**3.I**), and ($CH_2Me_4C_5$)Co(Cp*) (**3.3**). An *in situ* ^{1}H NMR spectrum taken after 3 h revealed the disappearance of peaks assignable to **3.2** and a decrease in the intensity of the resonances assignable to **3.3**, and appearance of new resonances assignable to **3.1** and free Cp^*_2Co. The NMR tube was then bought into a glovebox and the solution was transferred to a 20 mL scintillation vial. The volatiles were removed *in vacuo*. The resulting brown residue was rinsed with hexanes (1 mL × 2), the rinsings were collected, and the volatiles were removed *in vacuo* to give a brown solid. A ^{1}H NMR spectrum of this material, taken in C_6D_6, revealed the presence of $HCPh_3$, as indicated by the appearance of the methine proton resonance at 5.50 ppm,[33] and Cp^*_2Co, as indicated by a broad resonance at 46.7 ppm. The hexanes-insoluble solid was then extracted into THF (1 mL), filtered through a Celite column supported on glass wool (0.5 cm × 2 cm), concentrated to ca. 0.25 mL, and layered with Et_2O (2 mL). Storage of this solution at -25 °C for 72 h resulted in the deposition of dark brown plates of [$L^{tBu}Ni^I(SCH_2Me_4C_5)$Co(Cp*)], which were isolated by decanting off the supernatant (22 mg, 67% yield). ^{1}H NMR (400 MHz, 25 °C, THF-d_8): **5 min**: δ 25.75 (s, **3.2**), 25.24 (s, **3.2**), 19.6 (br s, **3.I**), 15.93 (s, **3.2**), 12.5 (br s, **3.I**), 7.3-7.05 (15 H, $HCPh_3$, Ar-**H**), 6.13 (s, **3.2**),

5.57 (s, 1H, **H**CPh$_3$), 2.59 (br s, 2H, **3.3**, C**H**$_2$), 1.78 (br s, 6H, **3.3**, C**H**$_3$), 1.49 (br s, 15H, **3.3**, Cp* C**H**$_3$), 1.03 (br s, 6H, **3.3**, C**H**$_3$), 0.2 (br s, **3.I**), -1.37 (s, **3.2**), -1.6 (br s, **I**), -11.3 (br s, **3.I**), -15.93 (s, **3.2**), -101.97 (s, **3.2**). **30 min**: δ 25.71 (s, **3.2**), 25.23 (s, **3.2**), 19.6 (overlapping br s, **3.1** and **3.I**), 15.92 (s, **3.2**), 12.5 (overlapping br s, **3.1** and **3.I**), 7.6 (br s, Cp*$_2$Co), 7.3-7.05 (15 H, HCPh$_3$, Ar-**H**), 6.13 (s, **3.2**), 5.57 (s, 1H, **H**CPh$_3$), 2.6 (br s, 2H, **3.3**, C**H**$_2$), 1.8 (br s, 6H, **3.3**, C**H**$_3$), 1.5 (br s, 15H, **3.3**, Cp* C**H**$_3$), 1.4 (br s, **3.1**), 1.0 (br s, 6H, **3.3**, C**H**$_3$), 0.2 (br s, **3.I**), -1.3 (br s, **3.1**), -1.35 (s, **3.2**), -1.6 (br s, **3.I**), -11.4 (overlapping br s, **3.1** and **3.I**), -15.90 (s, **3.2**), -101.80 (s, **3.2**). **1.5 hr**: δ 25.76 (s, **3.2**), 25.26 (s, **3.2**), 19.7 (overlapping br s, **3.1** and **3.I**), 15.93 (s, **3.2**), 13.7 (br s, Cp*$_2$Co), 7.3-7.05 (15 H, HCPh$_3$, Ar-**H**), 6.14 (s, **3.2**), 5.57 (s, 1H, **H**CPh$_3$), 3.5 (br s, **3.1**), 2.6 (br s, 2H, **3.3**, C**H**$_2$), 1.8 (br s, 6H, **3.3**, C**H**$_3$), 1.5 (br s, 15H, **3.3**, Cp* C**H**$_3$), 1.4 (br s, **3.1**), 1.0 (br s, 6H, **3.3**, C**H**$_3$), 0.2 (br s, **3.I**), -1.3 (br s, **3.1**), -1.35 (s, **3.2**), -1.6 (br s, **3.I**), -11.3 (overlapping br s, **3.1** and **3.I**), -15.92 (s, **3.2**), -101.96 (s, **3.2**). **3 hr**: δ 25.71 (s, **3.2**), 21.0 (br s, Cp*$_2$Co), 20.0 (overlapping br s, **3.1** and **3.I**), 15.93 (s, **3.2**), 12.6 (overlapping br s, **3.1** and **3.I**), 7.3-7.05 (15 H, HCPh$_3$, Ar-**H**), 6.14 (s, **3.2**), 5.57 (s, 1H, **H**CPh$_3$), 3.5 (br s, **3.1**), 2.6 (br s, 2H, **3.3**, C**H**$_2$), 1.8 (br s, 6H, **3.3**, C**H**$_3$), 1.5 (br s, 15H, **3.3**, Cp* C**H**$_3$), 1.4 (br s, **3.1**), 1.0 (br s, 6H, **3.3**, C**H**$_3$), 0.2 (br s, **3.I**), -1.3 (br s, **3.1**), -1.30 (s, **3.2**), -1.6 (br s, **3.I**), -11.6 (overlapping br s, **3.1** and **3.I**) ppm.

3.4.5 NMR scale reaction of [L^{tBu}Ni^{II}(SCPh$_3$)] with Cp*$_2$Co in THF-*d*$_8$ to quantify the yield of HCPh$_3$.

To an NMR tube containing [L^{tBu}Ni^{II}(SCPh$_3$)] (**2.2**, 10 mg, 0.012 mmol) and hexamethyldisiloxane (HMDSO) (2.5 μL, 0.012 mmol) in THF-*d*$_8$ (0.3 mL) was added Cp*$_2$Co (7.8 mg, 0.024 mmol) in THF-*d*$_8$ (0.3 mL). After addition, the color of the solution

quickly changed from blue to red-brown. An ^{1}H NMR spectrum taken after 4 h reveals the presence of **3.1**, **3.3**, $HCPh_3$, an unidentified Ni^{I} containing product (**3.I**), and Cp^*_2Co. The yield of $HCPh_3$ was determined to be 88% by integration of the methine proton resonance of $HCPh_3$ against the HMDSO internal standard. ^{1}H NMR (400 MHz, 25 °C, THF-d_8): δ 19.9 (overlapping br s, **3.1** and **I**), 17.6 (Cp^*_2Co), 12.5(overlapping br s, **3.1** and **3.I**), 7.25-7.09 (15 H, $HCPh_3$, Ar-**H**), 5.57 (s, 1H, **H**CPh_3), 3.5 (br s, **3.1**), 2.6 (br s, 2H, **3.3**, C**H**$_2$), 1.8 (br s, 6H, **3.3**, C**H**$_3$), 1.5 (br s, 15H, **3.3**, Cp* C**H**$_3$), 1.4 (br s, **3.1**), 1.1 (br s, 6H, **3.3**, C**H**$_3$), 0.1 (br s, **3.I**), 0.07 (s, 18H, HMDSO), -1.3 (br s, **3.1**), -1.5 (br s, **3.I**), -11.7 (overlapping br s, **3.1** and **3.I**) ppm.

3.4.6 Reaction of $[Cp^*_2Co][PF_6]$ and $[K(18\text{-crown-}6)][CPh_3]$ to yield $(CH_2Me_4C_5)Co(Cp^*)$ (3.3) and $HCPh_3$

To an NMR tube containing $[Cp^*_2Co][PF_6]$ (10.0 mg, 0.0183 mmol) in pyridine-d_5 (0.3 mL) was added $[K(18\text{-crown-}6)][CPh_3]$ (8.7 mg, 0.0183 mmol) in pyridine-d_5 (0.3 mL). Upon mixing, the deep red color of $[K(18\text{-crown-}6)][CPh_3]$ rapidly disappeared and the solution became pale brown-green in color. An ^{1}H NMR spectrum of the reaction mixture revealed the formation of both $(CH_2Me_4C_5)Co(Cp^*)$ (**3.3**) and $HCPh_3$, based upon a comparison of the observed resonances with the reported literature spectra for **3.3** and $HCPh_3$.[32,33] ^{1}H NMR (400 MHz, 25 °C, pyridine-d_5): δ 7.15-7.05 (s, 15 H, $HCPh_3$, Ar-**H**), 5.51 (s, 1H, **H**CPh_3), 3.27 (s, 24H, 18-crown-6), 1.46 (br s, 6H, **3.3**, $CH_2C_5Me_4$, C**H**$_3$), 1.34 (br s, 6H, **3.3**, $CH_2C_5Me_4$, C**H**$_3$), 1.28 (br s, 15H, **3.3**, Cp*), 0.90 (br s, 2H, **3.3**, C**H**$_2$) ppm. ^{19}F NMR (376 MHz, 25 °C, pyridine-d_5): δ -72.97 (d, $^{1}J_{FP}$, = 706 Hz, PF_6^-) ppm.

3.4.7 NMR scale reaction of [$L^{tBu}Ni^{II}(SCPh_3)$] with Cp^*_2Co in THF-d_8 to determine yield of unidentified Ni(I) product

To a 20 mL scintillation vial containing [$L^{tBu}Ni^{II}(SCPh_3)$] (19.7 mg, 0.0235 mmol) and HMDSO (5 μL, 0.0235 mmol) in cold, stirring THF-d_8 (0.3 mL) was added dropwise a solution of Cp^*_2Co (15.5 mg, 0.0470 mmol) in THF-d_8 (0.3 mL). After addition, the color of the solution quickly changed from blue to red-brown. The solution was then transferred to an NMR tube. A ^{1}H NMR spectrum taken after 4 h revealed the presence of resonances assignable to **3.3**, **3.1**, the unidentified Ni^I-containing product, and free Cp^*_2Co. Integration of the peaks assigned to complex **3.1** and the unidentified Ni^I-containing product revealed that they are present in an approximately 5:2 ratio (Figure A 3.7). ^{1}H NMR (400 MHz, 25 °C, THF-d_8): δ 20.0 (overlapping br s, **3.1** and **3.I**), 11.70 (br s, Cp^*_2Co), 7.3-7.05 (15 H, $HCPh_3$, Ar-**H**), 6.14 (s, **3.2**), 5.56 (s, 1H, **H**CPh_3), 3.5 (br s, **3.1**), 2.6 (br s, 2H, **3.3**, C**H**$_2$), 1.5 (br s, 15H, **3.3**, Cp* C**H**$_3$), 1.4 (br s, **3.1**), 0.2 (br s, **3.I**), 0.07 (HMDSO), -1.3 (br s, **3.1**), -1.6 (br s, **3.I**), -11.9 (overlapping br s, **3.1** and **3.I**).

3.4.8 X-ray Crystallography

Data for complex **3.1**·$C_4H_{10}O$ was collected on a Bruker KAPPA APEX II diffractometer equipped with an APEX II CCD detector using a TRIUMPH monochromator with a Mo Kα X-ray source (α = 0.71073 Å). The crystals were mounted on a cryoloop under Paratone-N oil, and all data were collected at 100(2) K using an Oxford nitrogen gas cryostream. Data were collected using ω scans with 0.5° frame widths and frame exposures of 20 seconds. Data collection and cell parameter determination were conducted using the SMART program.[48] Integration of the data frames and final cell parameter refinement were performed using SAINT software.[49] Absorption correction of the data was carried out using

the multi-scan method SADABS.[50] Subsequent calculations were carried out using SHELXTL.[51] Structure determination was done using the direct method and difference Fourier techniques. All hydrogen atom positions were idealized, and rode on the atom of attachment. Structure solution, refinement, graphics, and creation of publication materials were performed using SHELXTL. [51]

Further crystallographic details for complex **3.1**·$C_4H_{10}O$ can be found in Table 3.1.

Table 3.1. X-ray Crystallographic Data for Complex 3.1·$C_4H_{10}O$.

	3.1·$C_4H_{10}O$
empirical formula	$C_{55}H_{82}CoN_2NiS \cdot C_4H_{10}$
crystal habit, color	Plate, Brown
crystal size (mm)	0.25 × 0.10 × 0.05
crystal system	Monoclinic
space group	*P21/c*
volume (Å^3)	5546.8(7)
a (Å)	12.2784(8)
b (Å)	25.957(2)
c (Å)	17.836(1)
α (deg)	90
β (deg)	102.645(5)
γ (deg)	90
Z	4
formula weight	995.04
density (calculated)	1.192
absorption coefficient	0.715
F_{000}	2156
total no. reflections	11410
unique reflections	5043
R_{int}	0.1760
final R indices (]	R_1 = 0.0802
largest diff. peak and	1.217 and -0.684
GOF	0.984

3.5 Appendix

3.5.1 NMR Spectra

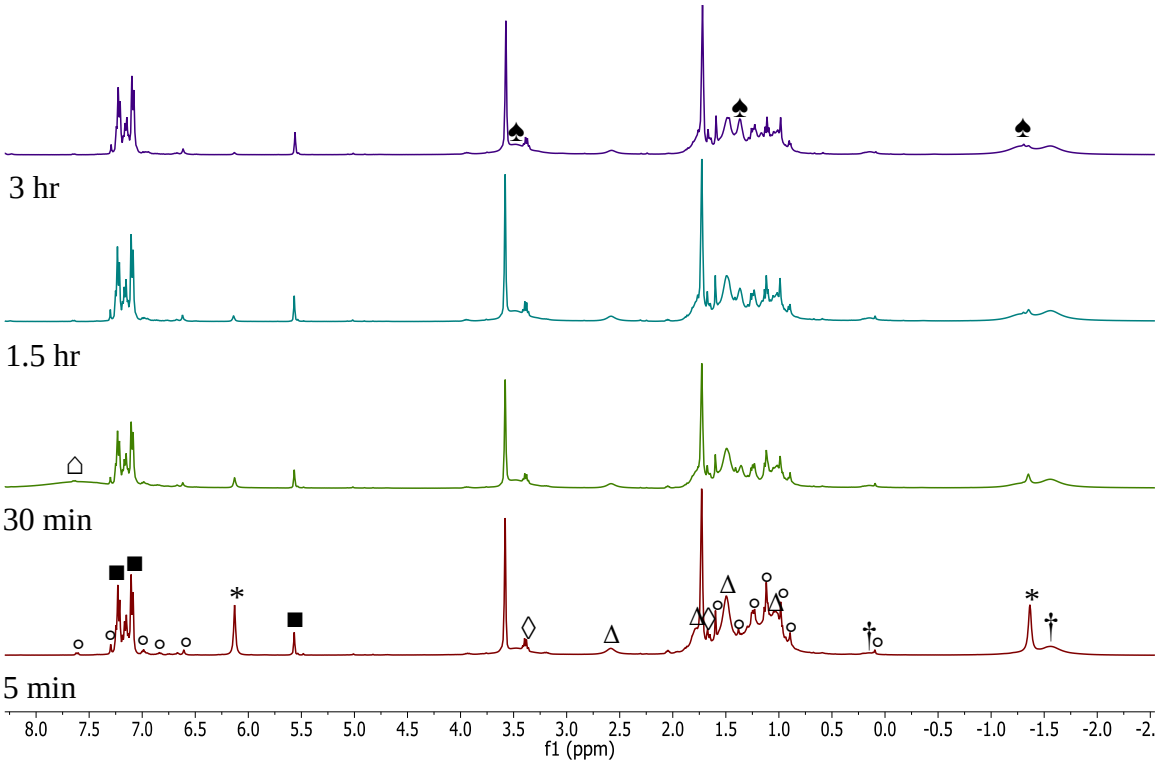

Figure A 3.1. Partial ^{1}H NMR spectra of the reaction of [L^{tBu}Ni(SCPh$_3$)] with two equiv. of Cp*$_2$Co in THF-d_8. (*) indicates the presence of **3.2**, (Δ) indicates the presence of **3.3**, (♠) indicates the presence of **3.1**, (⌂) indicates the presence of Cp*$_2$Co, (■) indicates the presence of HCPh$_3$, (†) indicates the presence of an unidentified Ni^{I}-containing product, (◊) indicates the presence of Et$_2$O, and (°) indicates the presence of unidentified decomposition products.

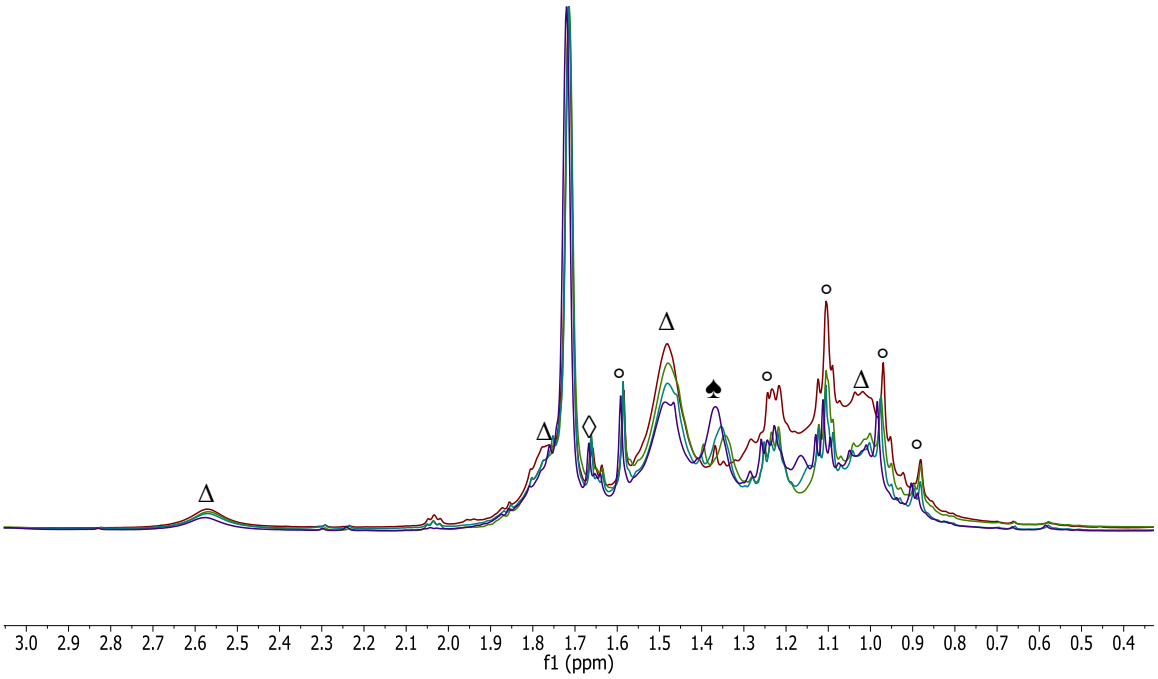

Figure A 3.2. Partial ^{1}H NMR spectra of the reaction of [L^{tBu}Ni(SCPh$_3$)] with two equiv. of Cp*$_2$Co in THF-d_8: red (5 min), green (30 min), cyan (1.5 h), and purple (3 h). (Δ) indicates the presence of **3.3**, (♠) indicates the presence of **3.1**, (◊) indicates the presence of Et_2O, and (°) indicates the presence of unidentified decomposition product. These spectra, which are normalized to the THF-d_8 resonance at 1.72 ppm, clearly demonstrate a decrease in the intensity of the peaks assignable to complex **3.3** as the reaction progresses. It is important to note, however, that, because of the formation of the unidentified Ni(I) by-product, we do not expect full consumption of complex **3.3** during this reaction.

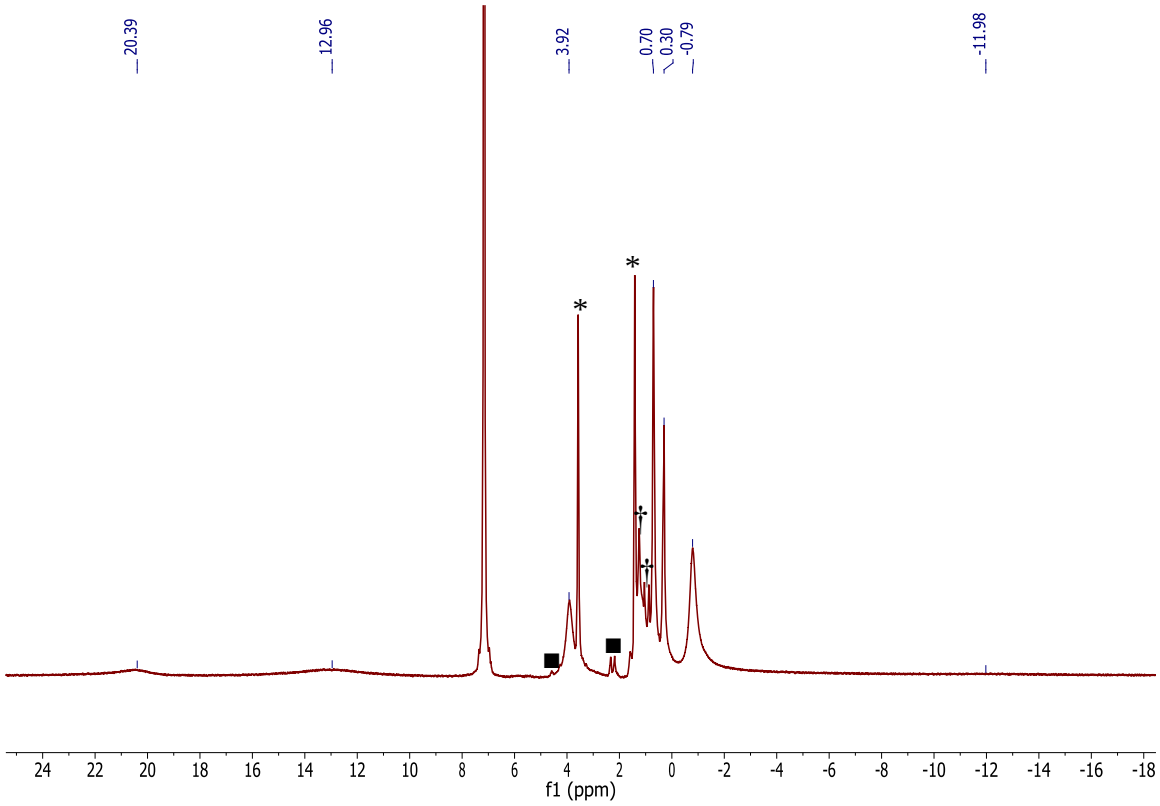

Figure A 3.3. ^{1}H NMR spectrum of **3.1** in C_6D_6. (*) indicates the presence THF, (†) indicates the presence of pentane, (■) indicates the presence of an unidentified impurity.

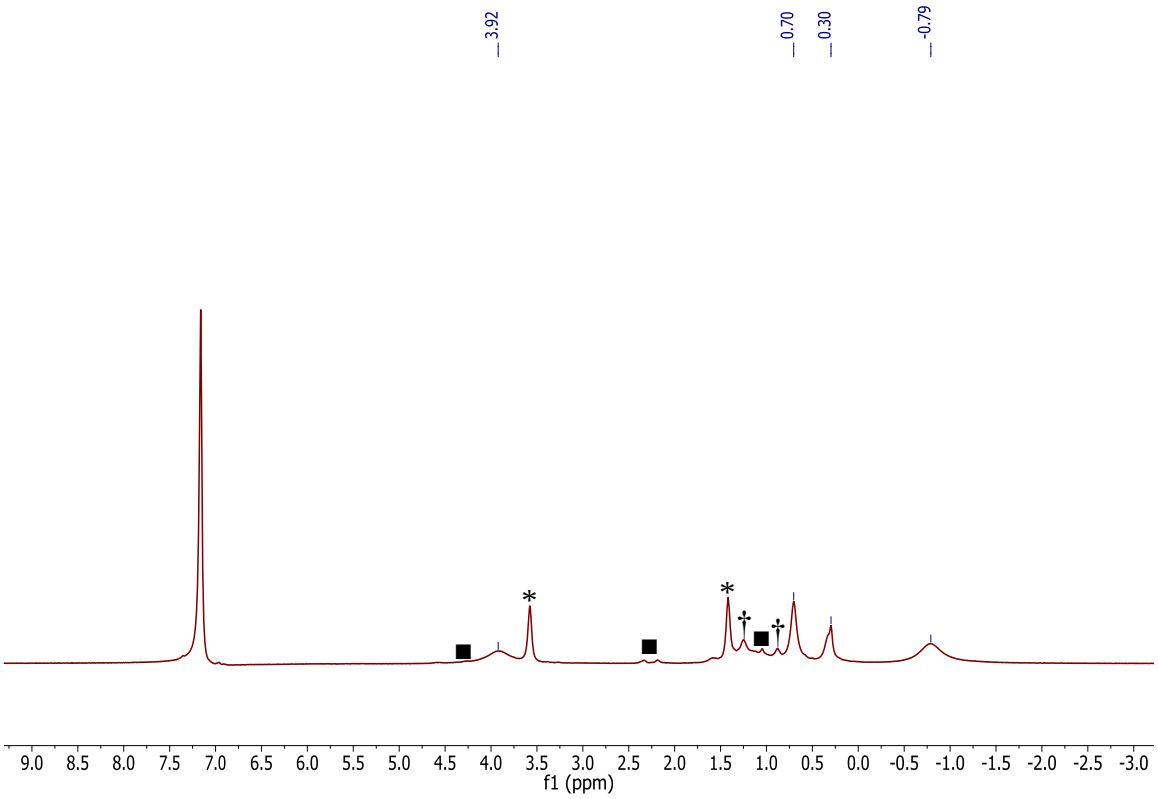

Figure A 3.4. Partial ^{1}H NMR spectrum of **3.1** in C_6D_6. (*) indicates the presence THF, (†) indicates the presence of pentane, (■) indicates the presence of an unidentified impurity.

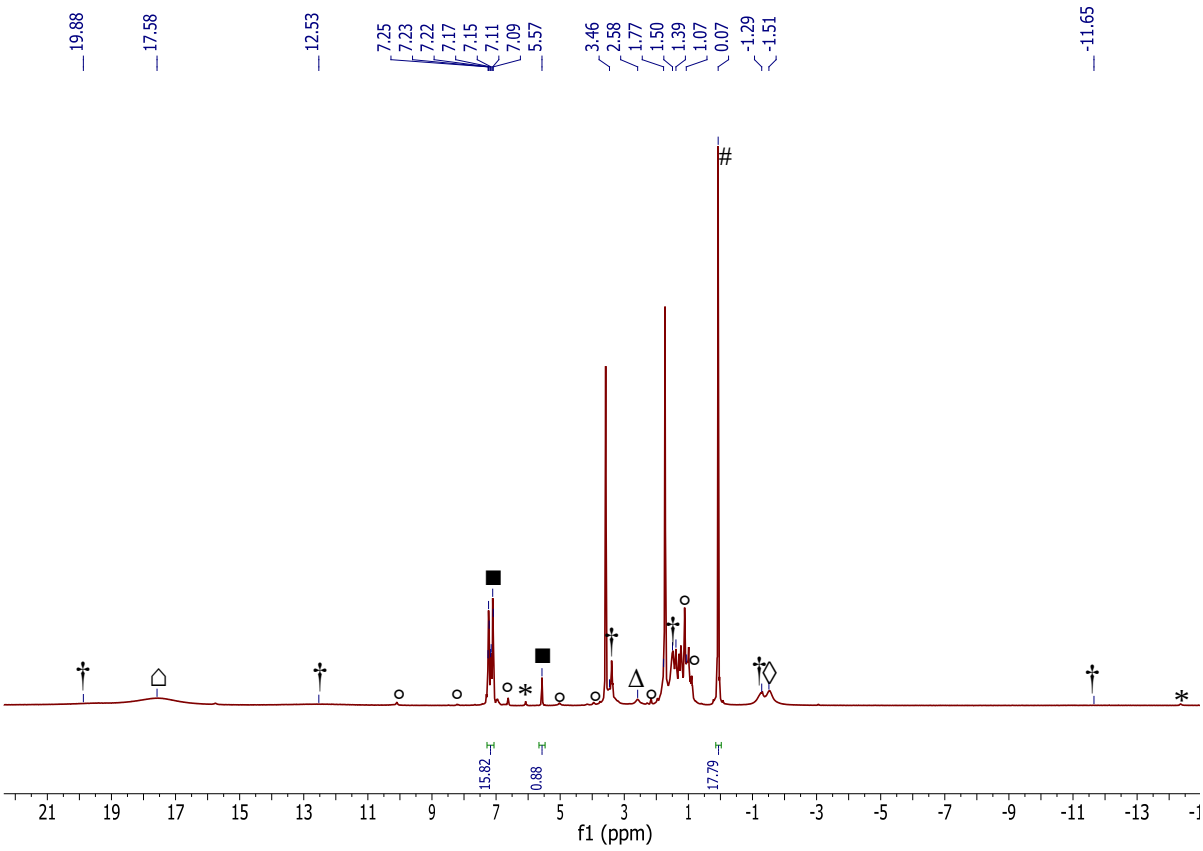

Figure A 3.5. ^{1}H NMR spectrum of the reaction of [L^{tBu}Ni(SCPh$_3$)] with two equiv. of Cp*$_2$Co in THF-d_8 with HMDSO as an internal standard. (†) indicates the presence of **1**, (■) indicates the presence of HCPh$_3$, (Δ) indicates the presence of **3.3**, (⌂) indicates the presence of Cp*$_2$Co, (◊) indicates the presence of an unidentified Ni^{I}-containing product, (#) indicates the presence HMDSO, (*) indicates the presence of **3.2**, and (°) indicates the presence of unidentified decomposition products.

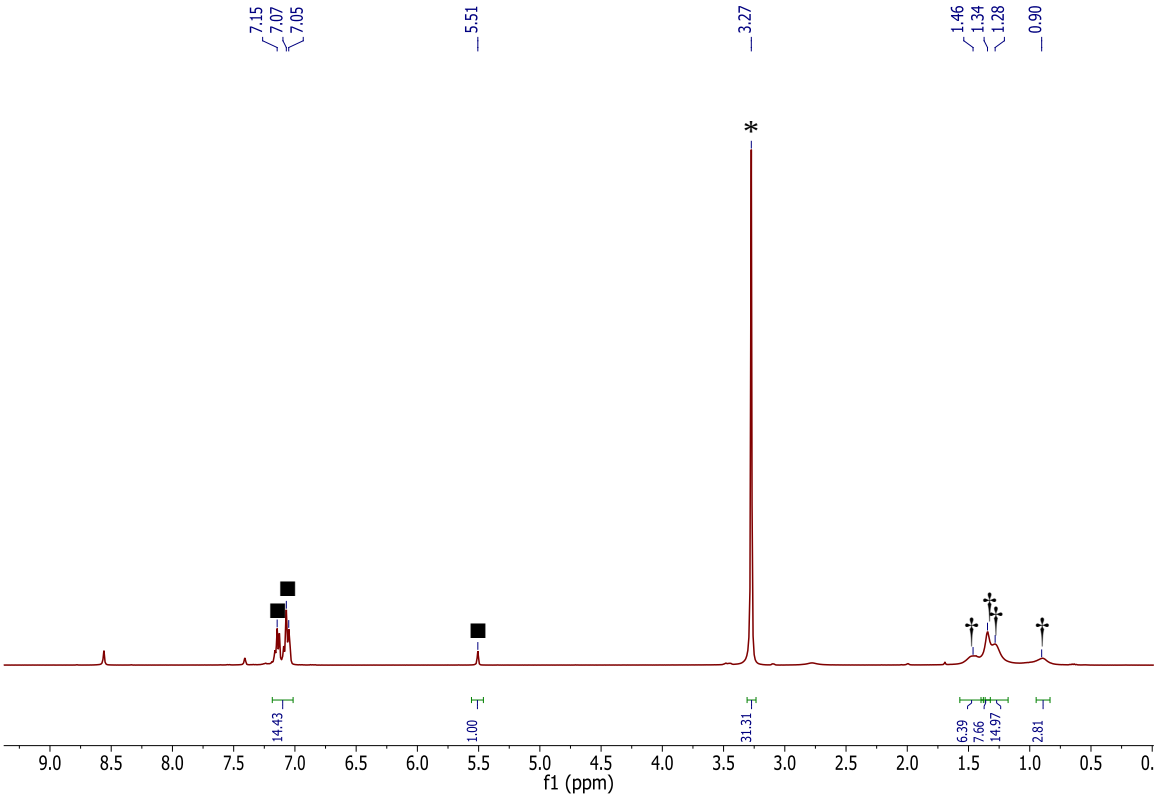

Figure A 3.6. ^{1}H NMR spectrum of the reaction of $[Cp^*_2Co][PF_6]$ and [K(18-crown-6)][CPh_3] in pyridine-d_5. (*) indicates the presence of 18-crown-6, (†) indicates the presence of **3.3**, (■) indicates the presence of $HCPh_3$.

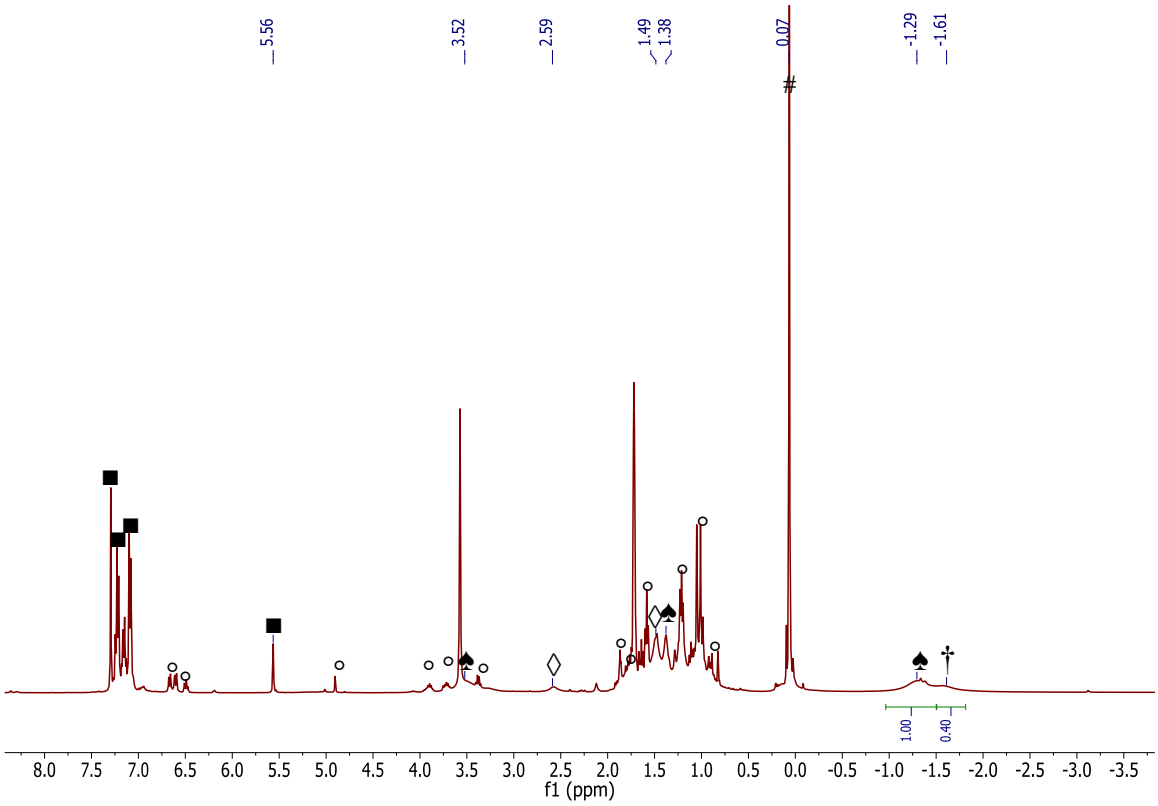

Figure A 3.7. Partial ^{1}H NMR spectra of the reaction of [L^{tBu}Ni(SCPh$_3$)] with two equiv. of Cp*$_2$Co in THF-d_8. (†) indicates the presence of an unknown Ni^{I} product, (■) indicates the presence of HCPh$_3$, (#) indicates the presence HMDSO, (♠) indicates the presence of **3.1**, (◊) indicates the presence of **3.3**, and (°) indicates the presence of unidentified decomposition products.

3.5.2 IR Spectra

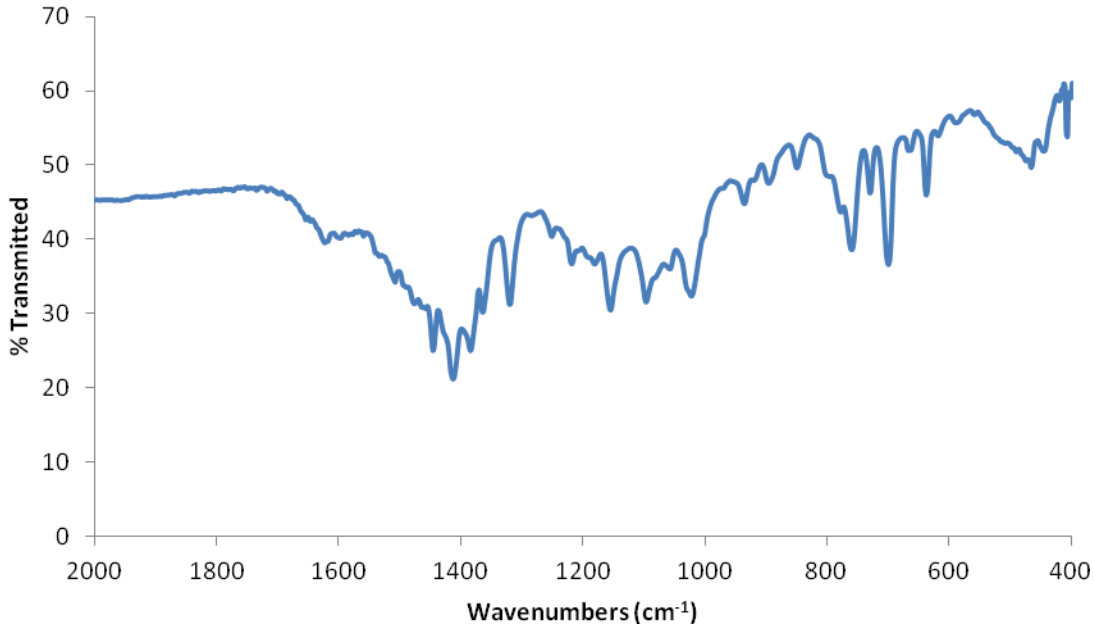

Figure A 3.8. Partial IR spectrum of complex **3.1** (KBr pellet).

3.5.3 UV-Vis Spectra

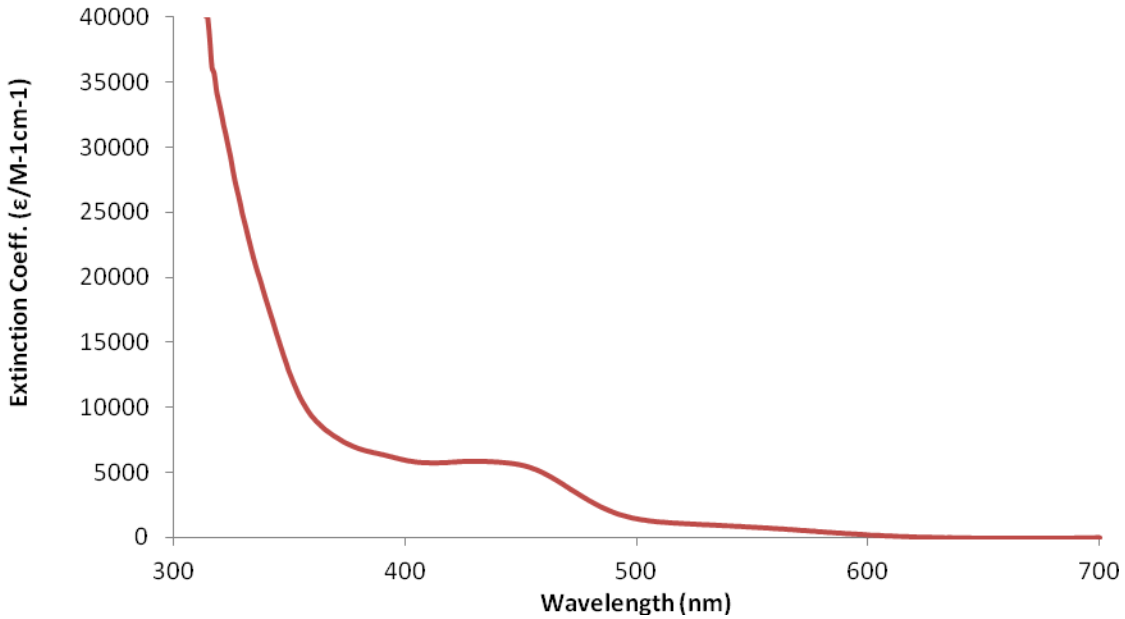

Figure A 3.9. UV-vis spectrum of complex **3.1** (1.0 mM in C_6H_6).

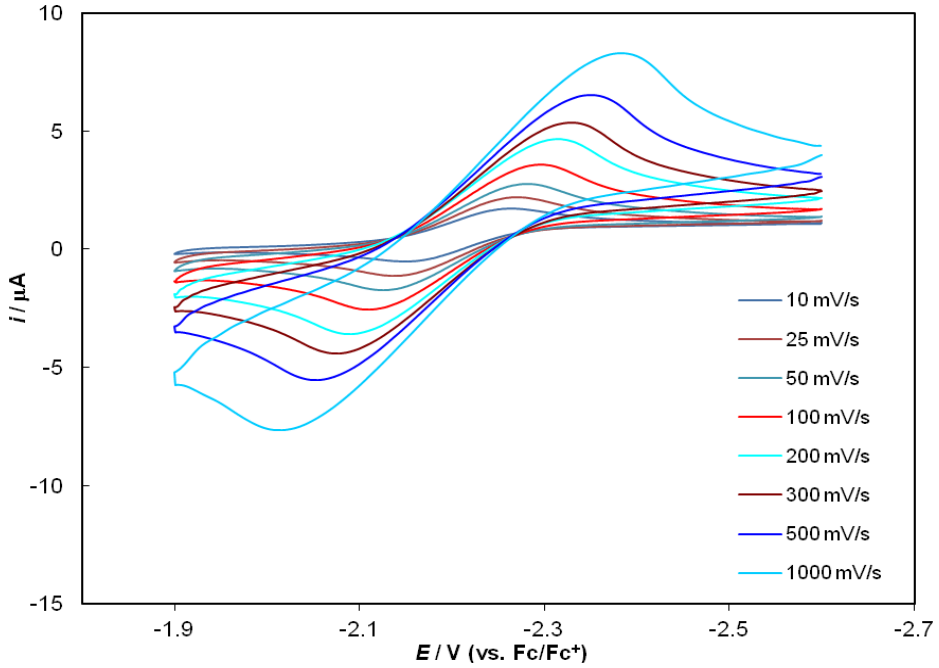

Figure A 3.10. Cyclic voltammogram of the Co(III)/Co(II) redox feature of complex **3.1** measured in THF with 0.1 M $[NBu_4][PF_6]$ as the supporting electrolyte (vs. Fc/Fc^+).

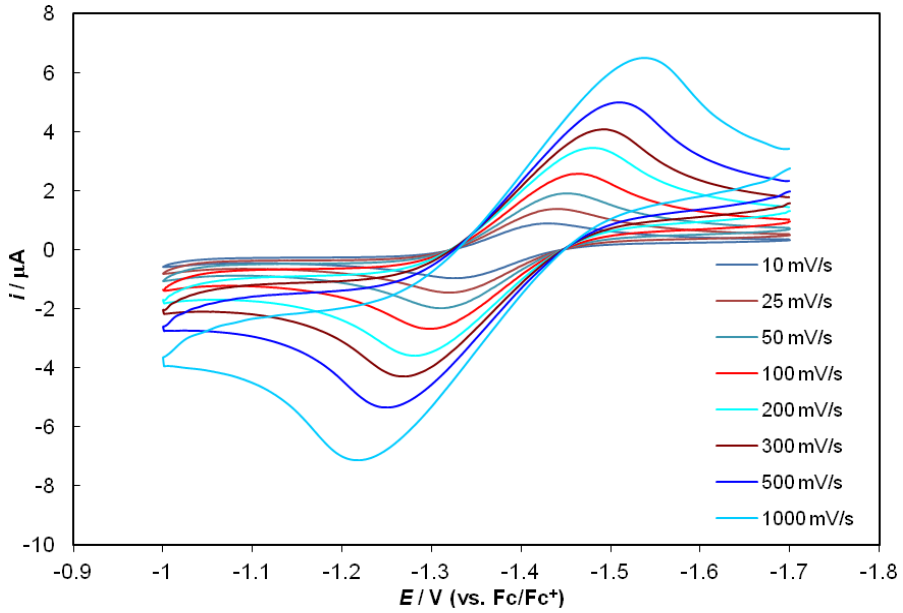

Figure A 3.11. Cyclic voltammogram of the Ni(II)/Ni(I) redox feature of complex **3.1** measured in THF with 0.1 M $[NBu_4][PF_6]$ as the supporting electrolyte (vs. Fc/Fc^+).

Table 3.2. Electrochemical parameters for [$L^{tBu}Ni^{I}(SCH_2Me_4C_5)Co(Cp^*)$] (**3.1**) in THF (vs. Fc/Fc^+, $[NBu_4][PF_6]$ as the supporting electrolyte).

Co(III)/Co(II) Feature	**Scan rate, V/s**	**$E_{p,c}$, V**	**$E_{p,a}$, V**	**ΔE_p [a]**	**$i_{p,a}/i_{p,c}$**
	0.010	-2.264	-2.150	0.114	0.99
	0.025	-2.275	-2.139	0.136	1.05
	0.050	-2.281	-2.124	0.157	1.13
	0.100	-2.296	-2.111	0.185	1.21
	0.200	-2.319	-2.094	0.225	1.25
	0.300	-2.329	-2.076	0.253	1.48
	0.500	-2.347	-2.053	0.294	1.46
	1.000	-2.381	-2.021	0.36	1.77
Ni(II)/Ni(I) Feature	**Scan rate, V/s**	**$E_{p,c}$, V**	**$E_{p,a}$, V**	**ΔE_p [a]**	**$i_{p,a}/i_{p,c}$**
	0.010	-1.426	-1.325	0.101	0.94
	0.025	-1.441	-1.314	0.127	0.95
	0.050	-1.446	-1.309	0.137	0.97
	0.100	-1.462	-1.295	0.167	1.00
	0.200	-1.473	-1.280	0.193	1.01
	0.300	-1.490	-1.265	0.225	1.01
	0.500	-1.505	-1.247	0.258	1.01
	1.000	-1.531	-1.220	0.311	1.03

[a] ΔE_p is defined as the potential difference between the anodic wave and the cathodic wave generated after the change in sweep direction.

3.6 References

(1) Winkler, J. R.; Gray, H. B. Electronic Structures of Oxo-Metal Ions. In *Molecular Electronic Structures of Transition Metal Complexes I*; Mingos, D. M. P., Day, P., Dahl, J. P., Eds.; Springer Berlin Heidelberg, 2012; Vol. 142, pp 17–28.

(2) Vicic, D. A.; Jones, W. D. Evidence for the Existence of a Late-Metal Terminal Sulfido Complex. *J. Am. Chem. Soc.* **1999**, *121* (16), 4070.

(3) Berry, J. F. Terminal Nitrido and Imido Complexes of the Late Transition Metals. *Comments Inorg. Chem.* **2009**, *30* (1–2), 28.

(4) Ray, K.; Heims, F.; Pfaff, F. F. Terminal Oxo and Imido Transition-Metal Complexes of Groups 9–11. *Eur. J Inorg. Chem.* **2013**, 3784.

(5) Hay-Motherwell, R. S.; Wilkinson, G.; Hussain-Bates, B.; Hursthouse, M. B. Synthesis and X-Ray Crystal Structure of Oxotrimesityliridium(V). *Polyhedron* **1993**, *12* (16), 2009.

(6) Poverenov, E.; Efremenko, I.; Frenkel, A. I.; Ben-David, Y.; Shimon, L. J. W.; Leitus, G.; Konstantinovski, L.; Martin, J. M. L.; Milstein, D. Evidence for a Terminal Pt(IV)-Oxo Complex Exhibiting Diverse Reactivity. *Nature* **2008**, *455* (7216), 1093.

(7) Iluc, V. M.; Hillhouse, G. L. Three-Coordinate Nickel Carbene Complexes and Their One-Electron Oxidation Products. *J. Am. Chem. Soc.* **2014**, *136* (17), 6479.

(8) Jenkins, D. M.; Betley, T. A.; Peters, J. C. Oxidative Group Transfer to Co(I) Affords a Terminal Co(III) Imido Complex. *J. Am. Chem. Soc.* **2002**, *124* (38), 11238.

(9) Shay, D. T.; Yap, G. P. A.; Zakharov, L. N.; Rheingold, A. L.; Theopold, K. H. Intramolecular CH Activation by an Open-Shell Cobalt(III) Imido Complex. *Angew. Chem. Int. Ed.* **2005**, *44* (10), 1508.

(10) Mindiola, D. J.; Hillhouse, G. L. Isocyanate and Carbodiimide Synthesis by Nitrene-Group-Transfer from a Nickel(II) Imido Complex. *Chem. Commun.* **2002**, No. 17, 1840.

(11) Jones, C.; Schulten, C.; Rose, R. P.; Stasch, A.; Aldridge, S.; Woodul, W. D.; Murray, K. S.; Moubaraki, B.; Brynda, M.; La Macchia, G.; et al. Amidinato– and Guanidinato–Cobalt(I) Complexes: Characterization of Exceptionally Short Co–Co Interactions. *Angew. Chem. Int. Ed.* **2009**, *48* (40), 7406.

(12) Mindiola, D. J.; Waterman, R.; Iluc, V. M.; Cundari, T. R.; Hillhouse, G. L. Carbon–Hydrogen Bond Activation, C–N Bond Coupling, and Cycloaddition Reactivity of a Three-Coordinate Nickel Complex Featuring a Terminal Imido Ligand. *Inorg. Chem.* **2014**, *53* (24), 13227.

(13) King, E. R.; Sazama, G. T.; Betley, T. A. Co(III) Imidos Exhibiting Spin Crossover and C–H Bond Activation. *J. Am. Chem. Soc.* **2012**, *134* (43), 17858.

(14) Iluc, V. M.; Miller, A. J. M.; Anderson, J. S.; Monreal, M. J.; Mehn, M. P.; Hillhouse, G. L. Synthesis and Characterization of Three-Coordinate Ni(III)-Imide Complexes. *J. Am. Chem. Soc.* **2011**, *133* (33), 13055.

(15) Kogut, E.; Wiencko, H. L.; Zhang, L.; Cordeau, D. E.; Warren, T. H. A Terminal Ni(III)-Imide with Diverse Reactivity Pathways. *J. Am. Chem. Soc.* **2005**, *127* (32), 11248.

(16) Schöffel, J.; Rogachev, A. Y.; DeBeer George, S.; Burger, P. Isolation and Hydrogenation of a Complex with a Terminal Iridium–Nitrido Bond. *Angew. Chem.*

Int. Ed. **2009**, *48* (26), 4734.
(17) Scheibel, M. G.; Askevold, B.; Heinemann, F. W.; Reijerse, E. J.; de Bruin, B.; Schneider, S. Closed-Shell and Open-Shell Square-Planar Iridium Nitrido Complexes. *Nat. Chem.* **2012**, *4* (7), 552.
(18) Melenkivitz, R.; Mindiola, D. J.; Hillhouse, G. L. Monomeric Phosphido and Phosphinidene Complexes of Nickel. *J. Am. Chem. Soc.* **2002**, *124* (15), 3846.
(19) Cundari, T. R.; Jimenez-Halla, J. O. C.; Morello, G. R.; Vaddadi, S. Catalytic Tuning of a Phosphinoethane Ligand for Enhanced C−H Activation. *J. Am. Chem. Soc.* **2008**, *130* (39), 13051.
(20) Waterman, R.; Hillhouse, G. L. Group Transfer from Nickel Imido, Phosphinidene, and Carbene Complexes to Ethylene with Formation of Aziridine, Phosphirane, and Cyclopropane Products. *J. Am. Chem. Soc.* **2003**, *125* (44), 13350.
(21) Iluc, V. M.; Hillhouse, G. L. Hydrogen-Atom Abstraction from Ni(I) Phosphido and Amido Complexes Gives Phosphinidene and Imide Ligands. *J. Am. Chem. Soc.* **2010**, *132* (43), 15148.
(22) Scheibel, M. G.; Wu, Y.; Stückl, A. C.; Krause, L.; Carl, E.; Stalke, D.; de Bruin, B.; Schneider, S. Synthesis and Reactivity of a Transient, Terminal Nitrido Complex of Rhodium. *J. Am. Chem. Soc.* **2013**, *135* (47), 17719.
(23) Zolnhofer, E. M.; Käß, M.; Khusniyarov, M. M.; Heinemann, F. W.; Maron, L.; van Gastel, M.; Bill, E.; Meyer, K. An Intermediate Cobalt(IV) Nitrido Complex and Its N-Migratory Insertion Product. *J. Am. Chem. Soc.* **2014**, *136* (42), 15072.
(24) Vreeken, V.; Siegler, M. A.; de Bruin, B.; Reek, J. N. H.; Lutz, M.; van der Vlugt, J. I. C-H Activation of Benzene by a Photoactivated NiII(Azide): Formation of a Transient Nickel Nitrido Complex. *Angew. Chem. Int. Ed.* **2015**, *54* (24), 7055.
(25) Hartmann, N. J.; Wu, G.; Hayton, T. W. Synthesis of a "Masked" Terminal Nickel(II) Sulfide by Reductive Deprotection and Its Reaction with Nitrous Oxide. *Angew. Chem. Int. Ed.* **2015**, *54* (49), 14956.
(26) Horn, B.; Limberg, C.; Herwig, C.; Braun, B. Three-Coordinate Nickel(II) and Nickel(I) Thiolate Complexes Based on the β-Diketiminate Ligand System. *Inorg. Chem.* **2014**, *53* (13), 6867.
(27) Holland, P. L.; Cundari, T. R.; Perez, L. L.; Eckert, N. A.; Lachicotte, R. J. Electronically Unsaturated Three-Coordinate Chloride and Methyl Complexes of Iron, Cobalt, and Nickel. *J. Am. Chem. Soc.* **2002**, *124* (48), 14416.
(28) Ohki, Y.; Murata, A.; Imada, M.; Tatsumi, K. C−H Bond Activation of Decamethylcobaltocene Mediated by a Nitrogenase Fe_8S_7 P-Cluster Model. *Inorg. Chem.* **2009**, *48* (10), 4271.
(29) Heise, H.; Köhler, F. H.; Herker, M.; Hiller, W. Inter- and Intramolecular Spin Transfer in Molecular Magnetic Materials. Solid-State NMR Spectroscopy of Paramagnetic Metallocenium Ions. *J. Am. Chem. Soc.* **2002**, *124* (36), 10823.
(30) Köthe, C.; Braun, B.; Herwig, C.; Limberg, C. Synthesis, Characterization, and Interconversion of β-Diketiminato Nickel N_xH_y Complexes. *Eur. J Inorg. Chem.* **2014**, *2014* (31), 5296.
(31) Evans, D. F. The Determination of the Paramagnetic Susceptibility of Substances in Solution by Nuclear Magnetic Resonance. *J. Chem. Soc.* **1959**, 2003.
(32) Bauer, J.; Braunschweig, H.; Hörl, C.; Radacki, K.; Wahler, J. Synthesis of Zwitterionic Cobaltocenium Borate and Borata-Alkene Derivatives from a Borole-

Radical Anion. *Chem. Eur. J.* **2013**, *19* (40), 13396.
(33) Prakash, G. K. S.; Panja, C.; Shakhmin, A.; Shah, E.; Mathew, T.; Olah, G. A. BF_3−H_2O Catalyzed Hydroxyalkylation of Aromatics with Aromatic Aldehydes and Dicarboxaldehydes: Efficient Synthesis of Triarylmethanes, Diarylmethylbenzaldehydes, and Anthracene Derivatives. *J. Org. Chem.* **2009**, *74* (22), 8659.
(34) Connelly, N. G.; Geiger, W. E. Chemical Redox Agents for Organometallic Chemistry. *Chem. Rev.* **1996**, *96* (2), 877.
(35) Herrmann, W. A.; Rohrmann, J.; Schäfer, A. Mehrfachbindungen Zwischen Hauptgruppenelementen Und Übergangsmetallen. *J. Organomet. Chem.* **1984**, *265* (1), c1.
(36) Angelici, R. J.; Gingerich, R. G. W. Reactions of the SH^- and S_2^- Ligands in $W(CO)_5(SH)^-$ and μ-$S[W(CO)_5]_2^{2-}$ with Organic Electrophiles. *Organometallics* **1983**, *2* (1), 89.
(37) Venturelli, A.; Rauchfuss, T. B.; Verma, A. K. Sulfido−Persulfido Equilibria in Sulfur-Rich Metal Clusters: The Case of $(C_5Me_5)_3RhRu_2S_4^{2+}$. *Inorg. Chem.* **1997**, *36* (7), 1360.
(38) Goodman, J. T.; Rauchfuss, T. B. Binding of Alkenes to ReS_4. *J. Am. Chem. Soc.* **1999**, *121* (21), 5017.
(39) Kawaguchi, H.; Tatsumi, K. Facile Route to the Trithiotungsten(VI) Complex $(PPh_4)[(C_5Me_5)W(S)_3]$ via Carbon-Sulfur Bond Cleavage of Ethanedithiolate and Its Reactions with Alkyl Halides and Alkynes. *J. Am. Chem. Soc.* **1995**, *117* (13), 3885.
(40) Kawaguchi, H.; Yamada, K.; Lang, J.-P.; Tatsumi, K. A New Entry into Molybdenum/Tungsten Sulfur Chemistry: Synthesis and Reactions of Mononuclear Sulfido Complexes of Pentamethylcyclopentadienyl−Molybdenum(VI) and −Tungsten(VI). *J. Am. Chem. Soc.* **1997**, *119* (43), 10346.
(41) Pino-Chamorro, J. Á.; Algarra, A. G.; Fernández-Trujillo, M. J.; Hernández-Molina, R.; Basallote, M. G. Kinetic and DFT Studies on the Mechanism of C–S Bond Formation by Alkyne Addition to the $[Mo_3S_4(H_2O)_9]^{4+}$ Cluster. *Inorg. Chem.* **2013**, *52* (24), 14334.
(42) DuBois, M. R. Catalytic Applications of Transition-Metal Complexes with Sulfide Ligands. *Chem. Rev.* **1989**, *89* (1), 1.
(43) Smiles, D. E.; Wu, G.; Hayton, T. W. Synthesis of Uranium–Ligand Multiple Bonds by Cleavage of a Trityl Protecting Group. *J. Am. Chem. Soc.* **2014**, *136* (1), 96.
(44) Smiles, D. E.; Wu, G.; Kaltsoyannis, N.; Hayton, T. W. Thorium-Ligand Multiple Bonds via Reductive Deprotection of a Trityl Group. *Chem. Sci.* **2015**, *6* (6), 3891.
(45) Hamada, S.; Funasako, Y.; Mochida, T.; Kuwahara, D.; Yoza, K. Phase Transitions and Thermal Properties of Decamethylferrocenium Salts with Perfluoroalkyl-Sulfonate and -Carboxylate Anions Exhibiting Disorder. *J. Organomet. Chem.* **2012**, *713*, 35.
(46) Harris Robin, K.; Becker Edwin, D.; Cabral de Menezes Sonia, M.; Goodfellow, R.; Granger, P. NMR Nomenclature: Nuclear Spin Properties and Conventions for Chemical Shifts. IUPAC Recommendations 2001. International Union of Pure and Applied Chemistry. Physical Chemistry Division. Commission on Molecular Structure and Spectroscopy. *Pure Appl. Chem.* **2002**, *40* (7), 489.
(47) Harris Robin, K.; Becker Edwin, D.; Cabral De Menezes Sonia, M.; Granger, P.;

Hoffman Roy, E.; Zilm Kurt, W. Further Conventions for NMR Shielding and Chemical Shifts. *Pure Appl. Chem.* **2008**, *80*, 59.
(48) SMART Apex II. Bruker AXS Inc.: Madison, WI 2005.
(49) SAINT Software User's Guide. Bruker AXS Inc.: Madison, WI 2005.
(50) Sheldrick, G. M. SADABS. University of Gottingen: Germany 2005.
(51) SHELXTL PC. Bruker AXS Inc.: Madison, WI 2005.

Chapter 4 Activation of CS_2 by a "Masked" Terminal Nickel Sulfide

Portions of this work were published in:

Nathaniel J. Hartmann , Guang Wu, Trevor W. Hayton

Dalton Trans., **2016**, *45*, 14508-14510.

Table of Contents

4.1 Introduction

There are now a number of reports on the synthesis and reactivity of late transition metal (groups 9, 10, and 11) complexes containing terminal imido (NR^{2-}),[1–8] phosphido (PR^{2-}),[9,10] and carbene (CR_2^{2-})[11] ligands.[12,13] In contrast, the synthesis and reactivity of late transition metal complexes containing terminal chalcogenide ligands (O, S, Se, Te) remains largely unexplored. This is due, in part, to the paucity of this class of materials. Only a handful of late metal oxo complexes have been reported,[14,15] including the Pt^{IV} terminal oxo (O^{2-}) complex, [Pt(O)(PCN)][BF_4] (PCN = $C_6H_3[CH_2P(t\text{Bu})_2](CH_2CH_2NMe_2)$), which can perform inter- and intramolecular electrophilic O-atom transfer. In Chapter 2, I described the synthesis and characterization of a family of "masked" terminal nickel sulfides, [K(L)][L^RNi^{II}(S)] (**2.4**-**2.6**). Preliminary reactivity studies suggest that the sulfide ligand in these comlpexes is nucleophilic. For example, [K(18-crown-6)][$L^{tBu}Ni^{II}$(S)] (**2.5**) readily reacts with trimethylsilyltriflate (Me_3SiOTf), via nucleophilic attack, to form a trimethylsilylthiolato ($[SSiMe_3]^-$) complex (**2.12**) and the the putative nickel sulfide [Cp^*_2Co][$L^{tBu}Ni^{II}$(S)] (**3.2**) couples with the methylene carbon of [$CoCp^*(C_5Me_4CH_2)$] (**3.3**) to form [$L^{tBu}Ni^{I}(SCH_2Me_4C_5)Co(Cp^*)$] (**3.1**) (Scheme 4.1).

Scheme 4.1 Nucleophilicity of the sulfide ligand

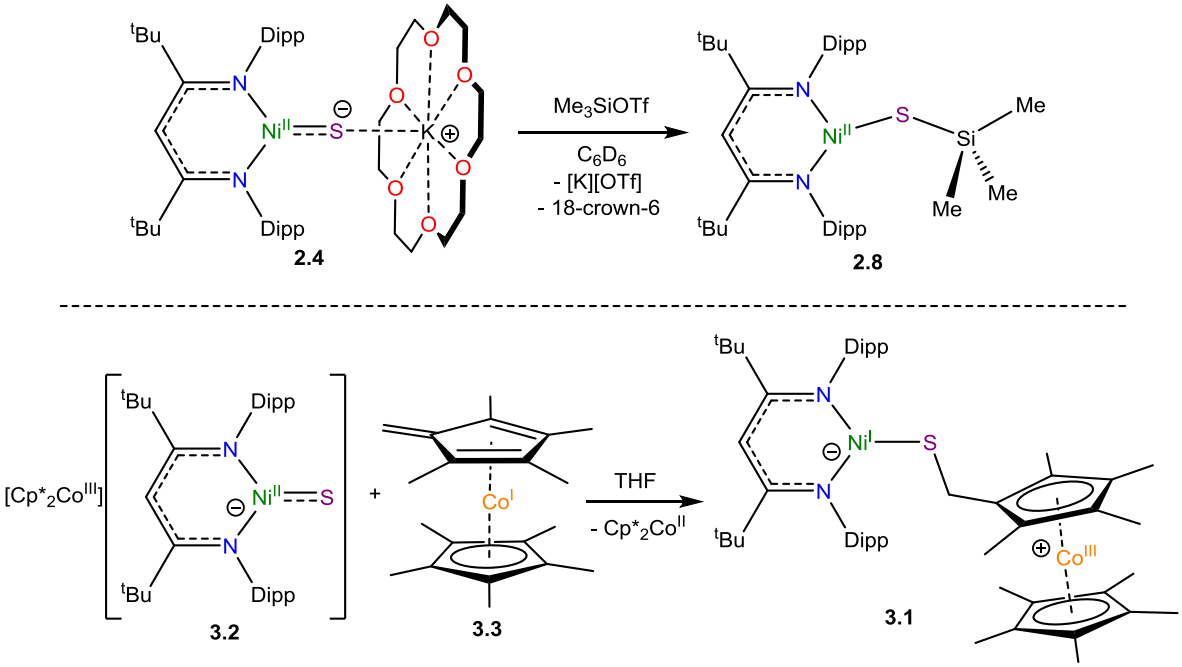

While our understanding of late metal sulfide reactivity is still relatively limited, early transition metal sulfides are widely known to react with carbon disulfide (CS_2) to yield trithiocarbonate complexes. For example, $[V(\eta_2\text{-}S_2)(S)_2(SPh)]^{2-}$ yields $[V_2(\mu_2\text{-}S_2)_2(S,S\text{:}\kappa_2\text{-}CS_3)_4]^{4-}$, $[MS_4]^n$ (M = Mo, n = 2-; M = Re, n = 1-) yields $[M(S,S\text{:}\kappa_2\text{-}CS_3)_4]^{3-}$, and $[Mo_2S_6]^{2-}$ yields $[Mo_2(S)_2(\mu\text{-}S)_2(S,S\text{:}\kappa_2\text{-}CS_3)_2]^{2-}$, upon reaction with CS_2 (Figure 4.1).[16–20] The research reported herein, describes the reactions of carbon disulfide (CS_2) with the sulfide ligand of $[L^{tBu}Ni^{II}(S)]^-$ and expands the known reactivity of late metal sulfides.

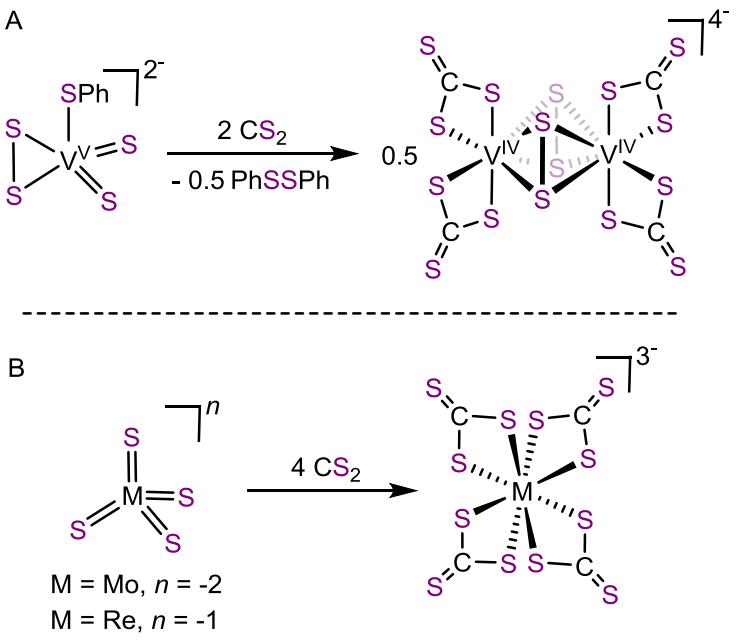

Figure 4.1. Previously reported activations of CS_2 by transition metal sulfides. **A**, Ref. 16; **B**, Ref. 17,18.

4.2 Results and Discussion

4.2.1 Synthesis and Characterization of [K(18-crown-6)][L^{tBu}Ni^{II}(CS$_3$)] (4.1)

Treatment of [K(18-crown-6)][L^{tBu}Ni^{II}(S)] (**2.5**) with one equivalent of CS_2 in toluene affords a yellow-orange solution from which orange plates of [K(18-crown-6)][L^{tBu}Ni^{II}(κ_2-CS$_3$)] (**4.1**) could be isolated in 76% yield (Scheme 4.2).

Scheme 4.2 Synthesis of **4.1**

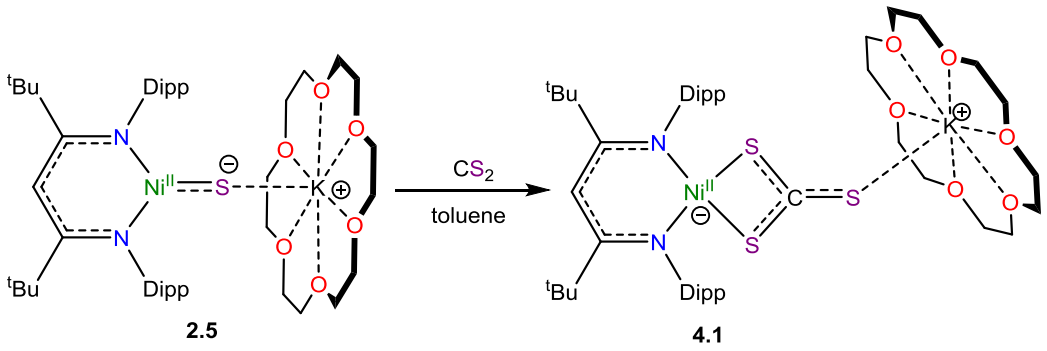

Complex **4.1** was shown by X-ray crystallography to contain a κ_2-trithiocarbonate (CS_3^{2-}) ligand coordinated to nickel (Figure 4.2). In the solid state, the Ni^{II} ion features a square planar (Σ(L-Ni-L) = 360°) coordination environment with Ni-N and Ni-S bond lengths that are typical of Ni^{II}.[21–25] The C-S bond lengths in **4.1** (C-S = 1.666(4), 1.697(4), 1.696(4) Å) are intermediate between C-S single and double bonds, consistent with a trithiocarbonate moiety.[26] In addition, the terminal sulfur atom of the trithiocarbonate ligand is weakly interacting with the [K(18-crown-6)] cation as evidenced by the S-K bond distance of 3.172(4) Å. Two other nickel $[CS_3]^{2-}$ complexes are known, namely, [(dmpe)Ni(*S*,*S*:κ_2-CS$_3$)] (dmpe = PMe$_2$CH$_2$CH$_2$PMe$_2$) and [Et$_4$N]$_2$[(*S*,*S*:κ_2-CS$_3$)Ni(μ-SEt)$_2$Ni(*S*,*S*:κ_2-CS$_3$)], and each features comparable Ni-S and C-S metrical parameters.[22,23]

The ^{1}H NMR spectrum of **4.1** in C_6D_6 is consistent with a C_{2v} symmetric, square planar Ni^{II} complex. For example, this spectrum features only one *tert*-butyl resonance, at 1.26 ppm. Likewise, the spectrum displays only two methyl resonances for the isopropyl substituents, which appear as doublets at 1.48 and 2.09 ppm.

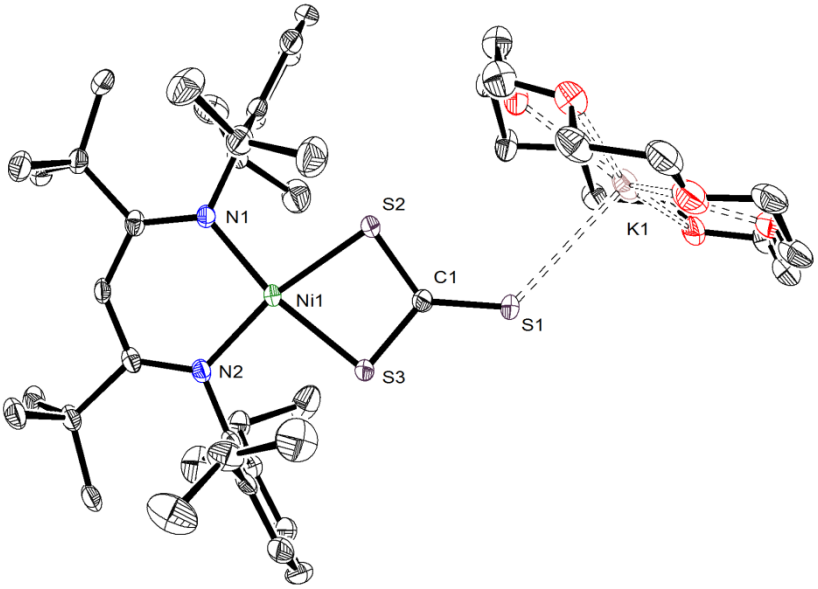

Figure 4.2. ORTEP diagram of [K(18-crown-6)][$L^{tBu}Ni^{II}$(*S*,*S*:κ_2-CS_3)] (**4.1**·C_7H_8) with 50% probability ellipsoids. Hydrogen atoms and a toluene solvate molecule have been omitted for clarity. Selected bond lengths and angles: Ni1-N1 1.929(3), Ni1-N2 1.940(3), Ni1-S2 2.235(1), Ni1-S3 2.210(1), S1-C1 1.666(4), S2-C1 1.697(4), S3-C1 1.696(4), S1-K1 3.172(4), N1-Ni1-N2 96.6(1)°, N1-Ni1-S2 94.93(9)°, N2-Ni1-S3 94.14(9)°, S2-Ni1-S3 74.29(4)°, S2-C1-S3 104.5(2)°, S2-C1-S1 129.5(2)°, S3-C1-S1 125.9(2)°.

4.2.2 Synthesis and Characterization of [K(2,2,2-cryptand)][(*S*,*S*:κ_2-CS_3)Ni^{II}{*S*,*S*:κ_2-CS_2(L^{tBu})}] (4.2)

Treatment of [K(2,2,2-cryptand)][$L^{tBu}Ni^{II}$(S)] (**2.6**) with 1 equiv of CS_2 in benzene immediately affords a bright red solution that slowly turns purple on standing. From this

solution, [K(2,2,2-cryptand)][(*S*,*S*:κ$_2$-CS$_3$)Ni^{II}{*S*,*S*:κ$_2$-CS$_2$(L^{tBu})}] (**4.2**), the product of double CS_2 insertion, was isolated in 36% yield as a purple solid. Alternatively, complex **4.2** could be generated by reaction of [K(2,2,2-cryptand)][L^{tBu}Ni^{II}(S)] with 2 equiv of CS_2 in THF (Scheme 4.3).

Scheme 4.3 Synthesis of **4.2**

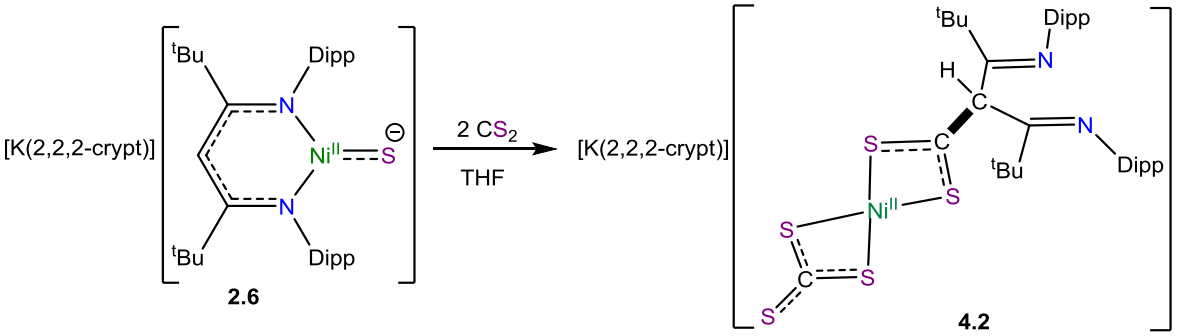

Under these conditions, complex **4.2** was isolated in 55% yield. The formulation of complex **4.2** was confirmed through elemental analysis, VT ^{1}H NMR spectroscopy, and X-ray crystallography. Complex **4.2** features a square planar Ni center ((Σ(L-Ni-L) = 360°) coordinated by a $[CS_3]^{2-}$ ligand and a dithiocarboxylate $[CS_2(L^{tBu})]^-$ ligand (Figure 4.3). The $[CS_3]^{2-}$ ligand in **4.2** possesses C-S bond lengths of 1.66(1), 1.72(1), and 1.72(1) Å; similar to those observed in complex **4.1**. The $[CS_2(L^{tBu})]^-$ ligand contains nearly identical C-S bond lengths of 1.662(9) and 1.682(9) Å, while the newly formed C-C bond is 1.54(1) Å, consistent with a C-C single bond. The Ni-S bonds in **4.2** are within the range expected for Ni^{II}-S single bonds.[22–24] Also of note is the angle between the two N-C(β)-C(^{t}Bu) planes in the β-diketiminate fragment, which is 66(1)° and contrasts to complex **4.1,** where the angle is only 1.4(7)°. This angle results in an overall C_1 symmetric complex. The ^{1}H NMR spectrum of **4.2** at 25 °C (thf-d_8) is relatively featureless, but upon cooling to -75 °C, the resonances sharpen considerably. This spectrum features two distinct *tert*-butyl resonances,

at 1.27 and 1.13 ppm, consistent with the low symmetry of the solid state structure. Also present in the spectrum is a resonance at 5.50 ppm, which I have assigned to the γ-CH environment (see Figures A 4.5 and A 4.6). Examination of the solid state molecular structure of complex **4.2** suggests that slow rotation about C3-C4 and C3-C21 bonds would explain the broadening observed in the room temperature ^{1}H NMR spectrum.

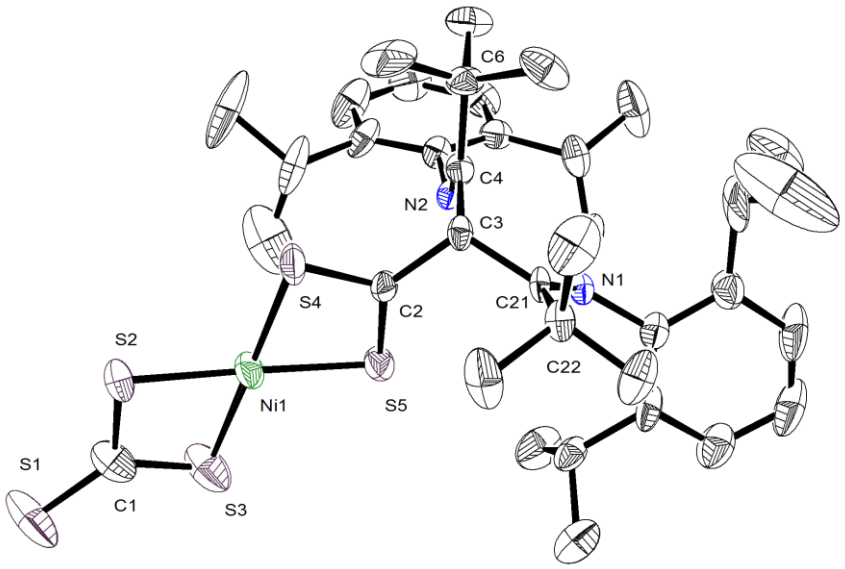

Figure 4.3. ORTEP diagram of [K(2,2,2-cryptand)][(*S*,*S*:κ$_2$-CS$_3$)Ni^{II}{*S*,*S*:κ$_2$-CS$_2$(L^{tBu})}] (**4.2**·C$_4$H$_{10}$O) shown with 50% thermal ellipsoids. Hydrogen atoms, [K(2,2,2-cryptand)]$^+$, and C$_4$H$_{10}$O solvate have been omitted for clarity. Selected metrical parameters: Ni1-S2 2.183(3), Ni1-S3 2.169(3), S1-C1 1.66(1), S2-C1 1.72(1), S3-C1 1.72(1), Ni1-S4 2.223(3), Ni1-S5 2.229(3), S4-C2 1.682(9), S5-C2 1.662(9), C2-C3 1.54(1), C3-C4 1.54(1), C3-C21 1.55(1), C4-N2 1.27(1), C21-N1 1.25(1), S1-C1-S2 126.0(7)°, S1-C1-S3 128.4(7)°, S2-C1-S3 105.6(6)°, S2-Ni1-S3 78.1(1)°, S2-Ni1-S4 101.5(1)°, S3-Ni1-S5 102.8(1)°, S4-Ni1-S5 77.7(1)°, S4-C2-S5 113.2(5)°.

In complex **4.2**, the $[CS_3]^{2-}$ moiety is the product of CS_2 activation by the sulfide ligand, while the dithiocarboxylate $[CS_2(L^{tBu})]^-$ ligand is the product of nucleophilic attack of a second equiv of CS_2 by the β-diketiminate γ-carbon. Nucleophilic bond forming reactions involving the β-diketiminate γ-carbon have been reported previously for O_2, NO, $OCCPh_2$, nitriles, and diazoacetate.[27–31] However, to my knowledge, this is the first example involving CS_2. Interestingly, reaction of [K(18-crown-6)][$L^{tBu}Ni^{II}$(S)] (**2.5**) with two equiv of CS_2 produces a product that I have tentatively identified as [K(18-crown-6)][(*S*,*S*:κ$_2$-CS_3)Ni^{II}{*S*,*S*:κ$_2$-$CS_2(L^{tBu})$}] (**4.3**) (i.e., the product of double CS_2 insertion) on the basis of the similarity of its ^{1}H NMR spectrum with that of complex **4.2** (See Figure A 4.7).

To rationalize the difference in reactivity between the 18-crown-6 and 2,2,2-cryptand salts, I suggest that the rate of CS_2 insertion into the putative intermediate, [K(2,2,2-cryptand)][$L^{tBu}Ni^{II}$(*S*,*S*:κ$_2$-CS_3)], is faster than the rate of CS_2 insertion into complex **4.1**. I hypothesize that the faster rate of insertion exhibited by [K(2,2,2-cryptand)][$L^{tBu}Ni^{II}$(*S*,*S*:κ$_2$-CS_3)] is due to the enhanced nucleophilicity of its β-diketiminate ligand, which results from the better separation of $[K(2,2,2\text{-cryptand})]^+$ cation from the anionic nickel fragment.

4.3 Summary

In summary, the "masked" terminal nickel sulfide complex, [K(18-crown-6)][$L^{tBu}Ni^{II}$(S)] (**2.5**), readily activates CS_2 to give the trithiocarbonate product, [K(18-crown-6)][$L^{tBu}Ni^{II}$(*S*,*S*:κ$_2$-CS_3)] (**4.1**). In contrast, [K(2,2,2-cryptand)][$L^{tBu}Ni^{II}$(S)] (**2.6**) preferentially reacts with CS_2 to generate the double insertion product, [K(2,2,2-cryptand)][(*S*,*S*:κ$_2$-CS_3)Ni^{II}{*S*,*S*:κ$_2$-$CS_2(L^{tBu})$}] (**4.2**). I attribute this difference in reactivity to the difference in the rate of the second CS_2 insertion reaction between the two systems. This work expands on the nucleophilic reactivity of the sulfide ligand in $[L^{tBu}Ni^{II}(S)]^-$

introduced in Chapters 2 and 3, and further expands the scope of reactivity for late metal terminal sulfide complexes. While the K^+ ion of the $[K(L)]^+$ (L = 18-crown-6, 2,2,2-cryptand) moiety is coordinated to the sulfide ligand of $[K(L)][L^{tBu}Ni^{II}(S)]$ in both the solid state and solution, the S^{2-} ligand in $[L^{tBu}Ni^{II}(S)]^-$ is able to readily activate CS_2, resulting in my classification of these complexes as a "masked" terminal sulfides. The nucleophilic activation of other small molecules (CO, NO, CO_2, and N_2O) by "masked" terminal nickel sulfides is detailed in Chapters 5 and 6.

4.4 Experimental Procedures

4.4.1 General Methods

All reactions and subsequent manipulations were performed under anaerobic and anhydrous conditions under an atmosphere of nitrogen. Hexanes, toluene, and tetrahydrofuran (THF) were dried using a Vacuum Atmospheres DRI-SOLV Solvent Purification system and stored over 3Å sieves for 24 h prior to use. Benzene-d_6, tetrahydrofuran-d_8, and C_8H_{18} (isooctane) were dried over 3Å molecular sieves for 24 h prior to use, and CS_2 was dried using CaH_2. $[K(18\text{-crown-6})][L^{tBu}Ni(S)]$ and $[K(2,2,2\text{-cryptand})][L^{tBu}Ni(S)]$ were synthesized according to the previously reported procedures.[21] All other reagents were purchased from commercial suppliers and used as received.

^1H and $^{13}C\{^1H\}$ NMR spectra were recorded on a Agilent Technologies 400-MR DD2 400 MHz spectrometer or a Varian UNITY INOVA 500 MHz spectrometer. ^1H and $^{13}C\{^1H\}$ NMR spectra were referenced to external $SiMe_4$ using the residual protio solvent peaks as internal standards.[32,33] IR spectra were recorded on a Nicolet 6700 FT-IR spectrometer with a NXR FT Raman Module. Elemental analyses were performed by the Micro-Mass Facility at the University of California, Berkeley.

4.4.2 Synthesis of [K(18-crown-6)][L^{tBu}Ni(*S*,*S*:κ$_2$-CS$_3$)] (4.1)

To a brown, stirring solution of [K(18-crown-6)][L^{tBu}Ni(S)] (**2.5**) (44.5 mg, 0.0497 mmol) in toluene (2 mL) was added CS_2 (3.0 μL, 0.0497 mmol). After addition, the color of the solution turned from brown to orange. This solution was allowed to stir for 10 min, whereupon the volatiles were removed *in vacuo*. The resulting orange residue was rinsed with hexanes (1 mL × 2), extracted into toluene (2 mL), and filtered through a Celite column supported on glass wool (0.5 cm × 2 cm). This yielded a yellow-orange filtrate. The volume of this solution was reduced *in vacuo* to 0.5 mL and the solution was layered with isooctane (2 mL). Storage of the solution at -25 °C for 24 h resulted in the deposition of yellow-orange plates of [K(18-crown-6)][L^{tBu}Ni(*S*,*S*:κ$_2$-CS$_3$)] (**4.1**), which were isolated by decanting off the supernatant (36.7 mg, 76%). Anal. Calcd for: $C_{48}H_{77}KN_2NiO_6S_3$: C, 59.30; H, 7.98; N, 2.88. Found: C, 59.60; H, 8.14; N, 2.69. ^{1}H NMR (400 MHz, 25 °C, benzene-d_6): δ = 6.99 (m, 6H, Ar-**H**), 5.56 (s, 1H, γ-**H**), 4.37 (sept, $^3J_{HH}$, = 6.7 Hz, 4H, C**H**(CH$_3$)$_2$), 3.09 (s, 24H, 18-crown-6), 2.09 (d, $^3J_{HH}$, = 6.8 Hz, 12H, CH(C**H**$_3$)$_2$), 1.48 (d, $^3J_{HH}$, = 6.9 Hz, 12H, CH(C**H**$_3$)$_2$), 1.26 (s, 18H, C(C**H**$_3$)$_3$). ^{13}C{^{1}H} NMR (125 MHz, 25 °C, benzene-d_6): δ = 166.55 (Ar-C), 150.50 (Ar-C), 142.85 (Ar-C), 124.26 (Ar C), 122.35 (Ar-C), 98.18 (γ-C), 70.20 (18-crown-6), 42.71 (**C**(CH$_3$)$_3$), 33.89 (C(**C**H$_3$)$_3$), 28.70 (CH(**C**H$_3$)$_2$), 25.66 (CH(**C**H$_3$)$_2$), 24.62 (**C**H(CH$_3$)$_2$). Note: a resonanace assignable to $[CS_3]^{2-}$ was not observed; it should appear around ca. 250 ppm.[4] IR (KBr Pellet, cm^{-1}): 1633 (w, br), 1541 (m), 1508 (s), 1464 (m), 1458 (m), 1435 (m), 1403 (s), 1379 (w), 1363 (m), 1348 (m), 1317 (s), 1280 (w), 1248 (m), 1215 (w), 1186 (w), 1178 (w), 1159 (w), 1105 (s), 1032 (s), 960 (m), 930 (w), 881 (w), 862 (w), 829 (w), 800 (w), 779 (w), 709 (w, br), 528 (w), 472 (w), 451 (w).

4.4.3 Synthesis of [K(2,2,2-cryptand)][(*S*,*S*:κ$_2$-CS$_3$)Ni{*S*,*S*:κ$_2$-CS$_2$(L^{tBu})}] (4.2)

To a brown, stirring solution of [K(2,2,2-cryptand)][L^{tBu}Ni(S)] (**2.6**) (48.0 mg, 0.0414 mmol) in THF (2 mL) was added CS_2 (5.0 μL, 0.0827 mmol). After addition, the color of the solution quickly changed from brown to red. This solution was allowed to stir for 1 hr, slowly becoming deep purple. The volatiles were removed *in vacuo* and the resulting purple residue was rinsed with hexanes (1 mL), extracted into THF (2 mL), and filtered through a Celite column supported on glass wool (0.5 cm × 2 cm). This yielded a purple filtrate. The volume of this solution was reduced *in vacuo* to 0.5 mL and the solution was layered with C_8H_{18} (2 mL). Storage of the solution at -25 °C for 24 h resulted in the deposition of purple needles of [K(2,2,2-cryptand)][(*S*,*S*:κ$_2$-CS$_3$)Ni{*S*,*S*:κ$_2$-CS$_2$(L^{tBu})}] (**4.2**), which were isolated by decanting off the supernatant (31.6 mg, 55%). Anal. Calcd for: $C_{55}H_{89}KN_4NiO_6S_5$: C, 56.93; H, 7.73; N, 4.38. Found: C, 57.02; H, 7.92; N, 4.42. ^{1}H NMR (400 MHz, 25 °C, benzene-d_6): δ = 6.97 - 6.79 (m, 6H, Ar-**H**, dipp), 5.53 (br s, 1H, γ-**H**), 3.62-3.57 (24H, 2,2,2-cryptand), 3.44 (br m, 2H, C**H**(CH$_3$)$_2$), 2.89 (br m, 2H, C**H**(CH$_3$)$_2$), 2.58 (12 H, 2,2,2-cryptand), 1.23 (br m, 42H, CH(C**H**$_3$)$_2$ & C(C**H**$_3$)$_3$). IR (KBr Pellet, cm^{-1}): 1658 (m, br), 1587 (w), 1537 (w), 1506 (w), 1473 (m), 1456 (m), 1440 (m), 1429 (m), 1400 (w), 1398 (w), 1376 (w), 1359 (m), 1319 (m), 1301 (m), 1257 (m), 1234 (w), 1205 (w), 1170 (w), 1128 (w), 1101 (s), 1076 (w), 1035 (s), 1008 (w, br), 995 (w), 964 (w), 946 (m), 931 (w), 887 (w), 858 (w), 825 (m), 792 (m), 755 (m), 748 (m), 619 (w, br), 520 (w), 476 (w), 416 (w).

4.4.4 Reaction of [K(2,2,2-cryptand)][L^{tBu}Ni(S)] with one equiv CS_2

To a J-Young NMR tube containing [K(2,2,2-cryptand)][L^{tBu}Ni(S)] (**2.6**) (15 mg, 0.0155 mmol) in C_6D_6 (0.5 mL) was added CS_2 (0.9 μL, 0.0155 mmol). After addition, the color of

the solution quickly changed from brown to red. This solution was allowed to stir for 1 hr, slowly becoming deep purple. The reaction mixture was then transferred to a 20 mL scintillation vial and volatiles were removed *in vacuo*. The resulting purple residue was extracted into THF (1 mL), filtered through a Celite column supported on glass wool (0.5 cm × 2 cm), concentrated *in vacuo* to 0.25 mL, and layered with Et_2O (1 mL). Storage of this solution at -25 °C for 12 h resulted in the deposition of purple plates of [K(2,2,2-cryptand)][(*S,S*:κ_2-CS_3)Ni{*S,S*:κ_2-$CS_2(L^{tBu})$}] (**4.2**), which were isolated by decanting off the supernatant (6.9 mg, 36%). ^{1}H NMR (400 MHz, 25 °C, thf-d_8): δ = 6.97-6.75 (br m, 6H, Ar-**H**), 5.53 (br s, 1H, γ-**H**), 3.57-3.53 (br m, 24H, 2,2,2-cryptand), 2.90 (br s, 2H, C**H**$(CH_3)_2$), 2.55 (br s, 12H, 2,2,2-cryptand), 1.23 (br m, 42H, C(C**H**$_3)_3$ & CH(C**H**$_3)_2$).

4.4.5 Variable temperature ^{1}H NMR spectra of [K(2,2,2-cryptand)][(*S,S*:κ_2-CS_3)Ni{*S,S*:κ_2-$CS_2(L^{tBu})$}] (4.2)

To an NMR tube was added a thf-d_8 (0.5 mL) solution of **4.2** (12.6 mg, 0.0109 mmol). ^{1}H NMR spectra were collected at ca. 20 °C intervals. ^{1}H NMR (500 MHz, 25 °C, thf-d_8): δ = 6.97-6.78 (m, 6H, Ar-**H**), 5.53 (br s, 1H, γ-**H**), 3.62-3.57 (24H, 2,2,2-cryptand), 3.48 (br m, 2H, C**H**$(CH_3)_2$), 2.89 (br m, 2H, C**H**$(CH_3)_2$), 2.59 (m, 12H, 2,2,2-cryptand), 1.23 (br, 42H, C(C**H**$_3)_3$ & CH(C**H**$_3)_2$). ^{1}H NMR (500 MHz, 0 °C, thf-d_8): δ = 6.97-6.79 (m, 6H, Ar-**H**), 5.54 (br s, 1H, γ-**H**), 3.61-3.57 (24H, 2,2,2-cryptand), 3.45 (br m, 1H, C**H**$(CH_3)_2$), 2.89 (br m, 2H, C**H**$(CH_3)_2$), 2.58 (m, 12H, 2,2,2-cryptand), 1.21 (br, 42H, C(C**H**$_3)_3$ & CH(C**H**$_3)_2$) . ^{1}H NMR (500 MHz, -20 °C, thf-d_8): δ = 6.97-6.76 (m, 6H, Ar-**H**), 5.52 (s, 1H, γ-**H**), 3.60-3.57 (24H, 2,2,2-cryptand), 3.46 (br m, 1H, C**H**$(CH_3)_2$), 3.40 (br m, 1H, C**H**$(CH_3)_2$), 2.91 (br m, 1H, C**H**$(CH_3)_2$), 2.83 (br m, 1H, C**H**$(CH_3)_2$), 2.57 (m, 12H, 2,2,2-cryptand), 2.09 (br d, 3H, CH(C**H**$_3)_2$), 1.28 (br s, 9H, C(C**H**$_3)_3$), 1.14 (br s, 9H, C(C**H**$_3)_3$), 0.63 (br d, 3H, $^3J_{HH}$,

= 5.1 Hz, CH(C**H**$_3$)$_2$). ^{1}H NMR (500 MHz, -40 °C, thf-d_8): δ = 6.99-6.74 (m, 6H, Ar-**H**), 5.51 (s, 1H, γ-**H**), 3.60-3.56 (24H, 2,2,2-cryptand), 3.48 (br m, 1H, C**H**(CH$_3$)$_2$), 3.39 (br m, 1H, C**H**(CH$_3$)$_2$), 2.90 (br m, 1H, C**H**(CH$_3$)$_2$), 2.82 (br m, 1H, C**H**(CH$_3$)$_2$), 2.56 (br m, 12H, 2,2,2-cryptand), 2.11 (br d, 3H, $^3J_{HH}$, = 6.0 Hz, CH(C**H**$_3$)$_2$), 1.31 (br d, 3H, CH(C**H**$_3$)$_2$), 1.28 (s, 9H, C(C**H**$_3$)$_3$), 1.24 (br d, 3H, $^3J_{HH}$, = 6.6 Hz, CH(C**H**$_3$)$_2$), 1.14 (s, 9H, C(C**H**$_3$)$_3$), 1.11 (br d, 3H, $^3J_{HH}$, = 6.5 Hz, CH(C**H**$_3$)$_2$), 1.06 (br d, 3H, $^3J_{HH}$, = 6.5 Hz, CH(C**H**$_3$)$_2$), 1.00 (br d, 3H, $^3J_{HH}$, = 6.9 Hz, CH(C**H**$_3$)$_2$), 0.93 (br d, 3H, $^3J_{HH}$, = 6.6 Hz, CH(C**H**$_3$)$_2$), 0.63 (br d, 3H, $^3J_{HH}$, = 6.0 Hz, CH(C**H**$_3$)$_2$). ^{1}H NMR (500 MHz, -75 °C, thf-d_8): δ = 7.01-6.74 (m, 6H, Ar-**H**), 5.50 (s, 1H, γ-**H**), 3.58-3.56 (24H, 2,2,2-cryptand), 3.47 (br m, 1H, C**H**(CH$_3$)$_2$), 3.38 (br m, 1H, C**H**(CH$_3$)$_2$), 2.88 (br m, 1H, C**H**(CH$_3$)$_2$), 2.82 (br m, 1H, C**H**(CH$_3$)$_2$), 2.53 (br, 12H, 2,2,2-cryptand), 2.14 (d, 3H, $^3J_{HH}$, = 7.1 Hz, CH(C**H**$_3$)$_2$), 1.30 (br d, 3H, $^3J_{HH}$, = 6.0 Hz CH(C**H**$_3$)$_2$), 1.27 (s, 9H, C(C**H**$_3$)$_3$), 1.24 (br d, 3H, $^3J_{HH}$, = 6.0 Hz CH(C**H**$_3$)$_2$), 1.13 (s, 9H, C(C**H**$_3$)$_3$), 1.10 (d, 3H, $^3J_{HH}$, = 6.6 Hz, CH(C**H**$_3$)$_2$), 1.05 (d, 3H, $^3J_{HH}$, = 6.6 Hz, CH(C**H**$_3$)$_2$), 0.99 (d, 3H, $^3J_{HH}$, = 7.1Hz, CH(C**H**$_3$)$_2$), 0.94 (d, 3H, $^3J_{HH}$, = 6.6 Hz, CH(C**H**$_3$)$_2$), 0.61 (d, 3H, $^3J_{HH}$, = 6.0 Hz, CH(C**H**$_3$)$_2$).

4.4.6 Reaction of [K(18-crown-6)][L^{tBu}Ni(S)] with two equiv CS_2

To a J-Young NMR tube containing [K(18-crown-6)][L^{tBu}Ni(S)] (**2.5**) (20.0 mg, 0.0223 mmol) in thf-d_8 (0.6 mL) was added CS_2 (2.7 μL, 0.0446 mmol). After addition, the color of the solution quickly changed from brown to red. This solution was allowed to stand for 1 hr, slowly becoming deep purple. An *in situ* ^{1}H NMR spectrum taken after 1 h reveals the formation of a new product which we have tentatively identified as [K(18-crown-6)][(*S*,*S*:κ$_2$-CS$_3$)Ni{*S*,*S*:κ$_2$-CS$_2$(L^{tBu})}] (**4.3**) (i.e., the product of double CS_2 insertion) on the basis of the similarity of its ^{1}H NMR spectrum with that of complex **4.2** (Figure A 3.7). ^{1}H

NMR (400 MHz, 25 °C, thf-d_8): δ = 6.98-6.78 (br m, 6H, Ar-**H**), 5.54 (br s, 1H, γ-**H**), 3.63 (br s, 24H, 18-crown-6), 3.46 (br m, 2H, C**H**$(CH_3)_2$), 2.90 (br m, 2H, C**H**$(CH_3)_2$), 1.23 (br m, 42H, CH(C**H**$_3)_2$ & C(C**H**$_3)_3$).

4.4.7 X-ray Crystallography

Data for **4.1** and **4.2** were collected on a Bruker KAPPA APEX II diffractometer equipped with an APEX II CCD detector using a TRIUMPH monochromator with a Mo Kα X-ray source (α = 0.71073 Å). The crystals were mounted on a cryoloop under Paratone-N oil, and all data were collected at 100(2) K using an Oxford nitrogen gas cryostream. Data were collected using ω scans with 0.5° frame widths. Frame exposures of 20 seconds were used for both **4.1** and **4.2**. Data collection and cell parameter determination were conducted using the SMART program.[34] Integration of the data frames and final cell parameter refinement were performed using SAINT software.[35] Absorption correction of the data was carried out using the multi-scan method SADABS.[36] Subsequent calculations were carried out using SHELXTL.[37] Structure determination was done using direct or Patterson methods and difference Fourier techniques. All hydrogen atom positions were idealized, and rode on the atom of attachment. Structure solution, refinement, graphics, and creation of publication materials were performed using SHELXTL.[37]

In complex **4.1**, the 18-crown-6 molecule is disordered over two positions. These two orientations were modelled in a 60:40 ratio using the FVAR, EADP, and PART commands in SHELXL. The C-C and C-O bonds in the 18-crown-6 molecule in complex **4.1** were constrained using the SADI command. Additionally, the positions of the C and O atoms in the 18-crown-6 molecule were restrained using the RIGU ADP command. In complex **4.2**, both the 2,2,2-cryptand moiety and the $C_4H_{10}O$ solvate are disordered. The $C_4H_{10}O$

molecule was found to be disordered over two positions. These two orientations each were modelled in a 56:44 ratio, using the FVAR and EADP commands in SHELXL. The C–C, C-N, C-O, and O-K bonds of 2,2,2-cryptand and $C_4H_{10}O$ were constrained using the SADI command. The disordered 2,2,2-cryptand molecule was further refined using the DELU and SIMU commands for the O atoms. Further crystallographic details for complexes **4.1**-**4.2** can be found in Table 4.1.

Table 4.1. X-ray Crystallographic Data for Complexes 4.1, 4.2.

	4.1·C_7H_8	**4.2**·$C_4H_{10}O$
empirical	$C_{48}H_{77}KN_2NiO_6S_3 \cdot C_7H_8$	$C_{55}H_{89}KN_4NiO_6S_5 \cdot C_4H_{10}$
crystal habit,	Plate, Yellow	Needle, Purple
crystal size	0.3 × 0.25 × 0.1	0.3 × 0.1 × 0.05
crystal system	Monoclinic	Monoclinic
space group	*P2(1)/c*	*P2(1)/c*
volume ($Å^3$)	5709.8(1)	6521.8(8)
a (Å)	17.647(2)	20.301(1)
b (Å)	17.840(2)	18.450(1)
c (Å)	18.241(2)	17.415(1)
α (deg)	90	90
β (deg)	96.149(6)	90.816(4)
γ (deg)	90	90
Z	4	4
formula	1064.23	1232.53
density	1.238	1.257
absorption	0.570	0.572
F_{000}	2288	2656
total no.	35379	27276
unique	11684	13438
R_{int}	0.1186	0.1144
final R indices	R_1 = 0.0629	R_1 = 0.1404
largest diff.	0.630 and -0.485	2.299 and -1.076
GOF	1.007	1.391

4.5 Appendix

4.5.1 NMR Spectra

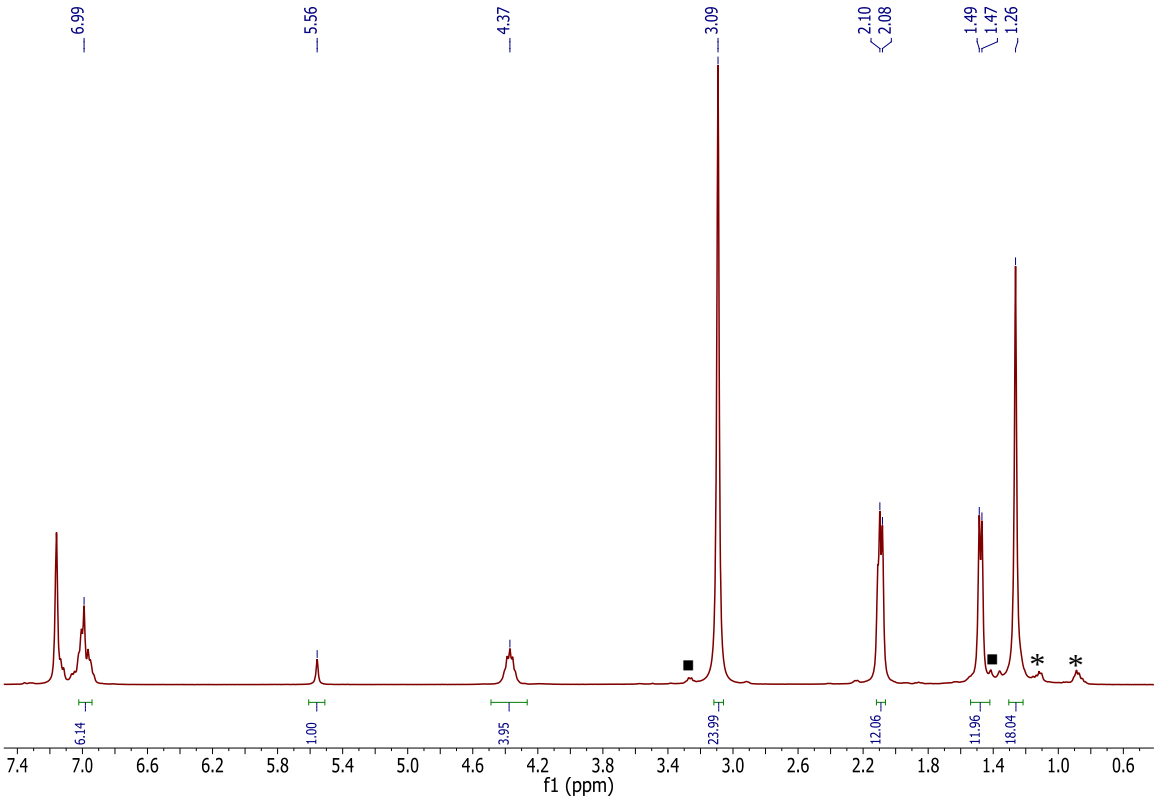

Figure A 4.1. ^{1}H NMR spectrum of [K(18-crown-6)][L^{tBu}Ni(*S*,*S*:κ_2-CS_3)] (**4.1**) in benzene-d_6. (*) indicates the presence of isooctane and (▪) indicates the presence of Et_2O.

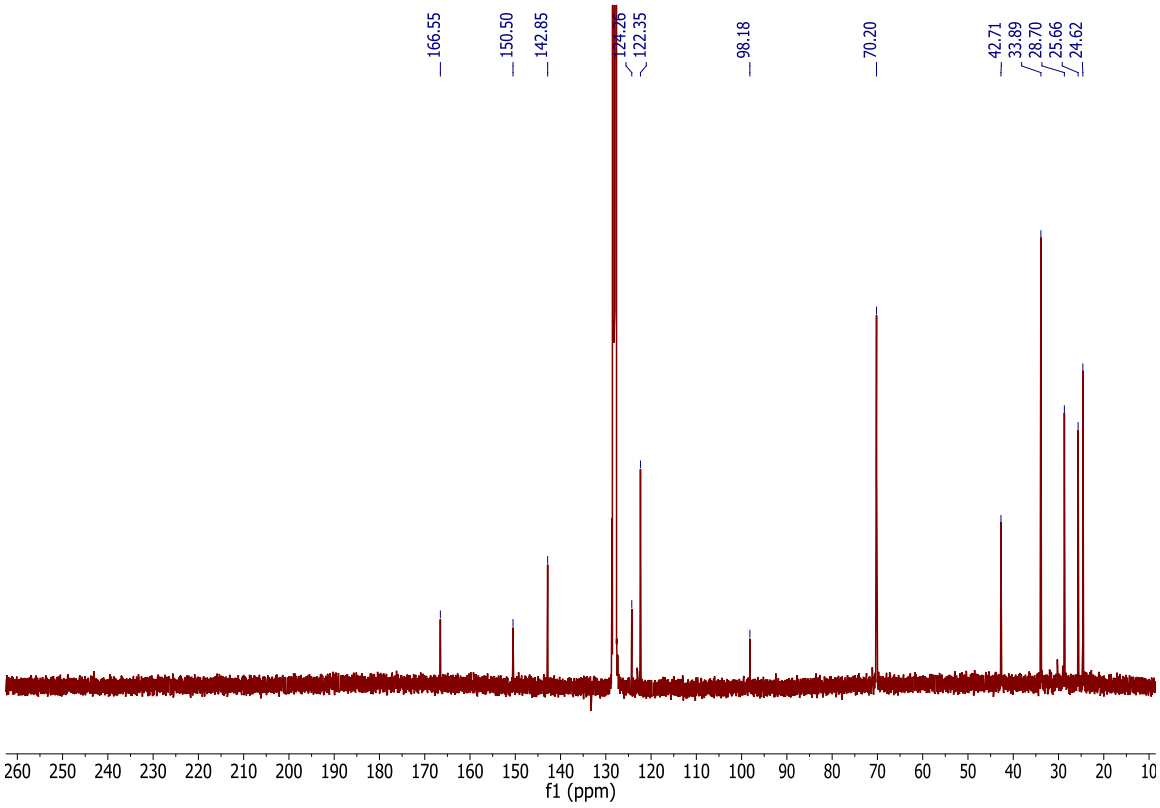

Figure A 4.2. $^{13}C\{^{1}H\}$ NMR spectrum of [K(18-crown-6)][L^{tBu}Ni(*S*,*S*:κ_2-CS_3)] (**4.1**) in benzene-d_6.

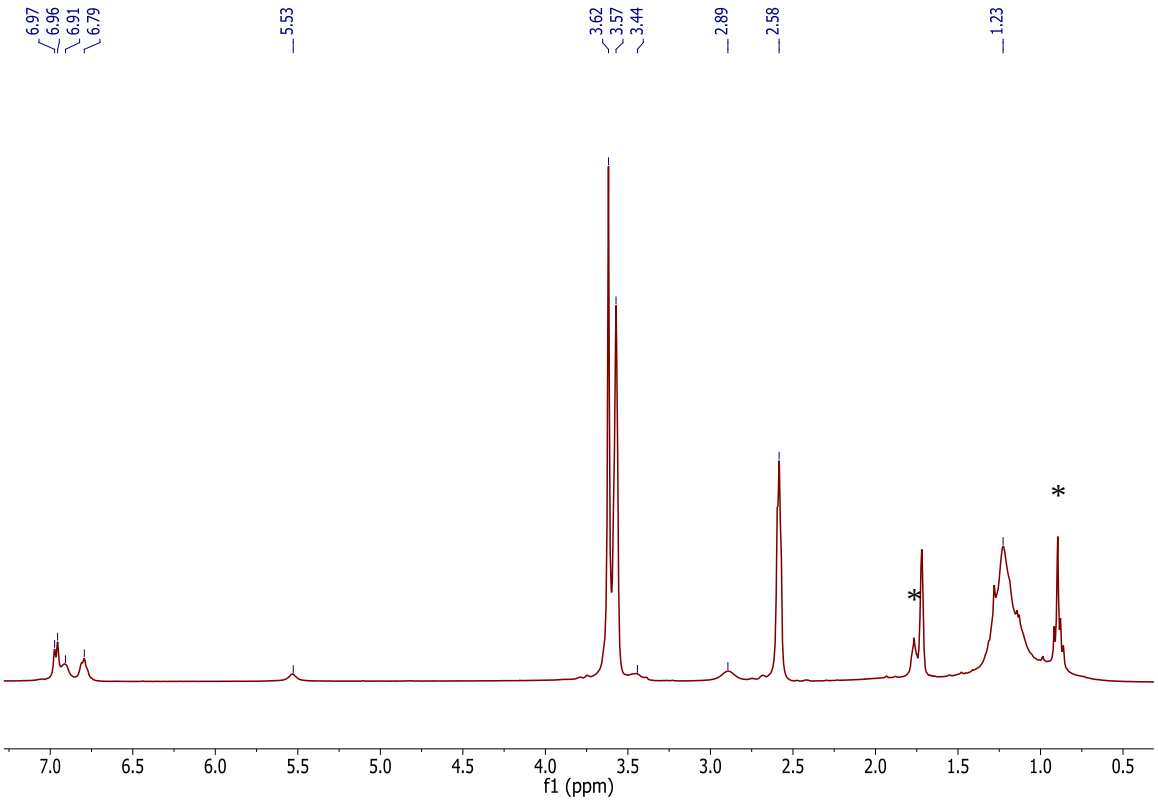

Figure A 4.3. ^{1}H NMR spectrum of [K(2,2,2-cryptand)][(*S*,*S*:κ$_2$-CS$_3$)Ni{*S*,*S*:κ$_2$-CS$_2$(L^{tBu})}] (**4.2**) in THF-d_8. (*) indicates the presence of isooctane.

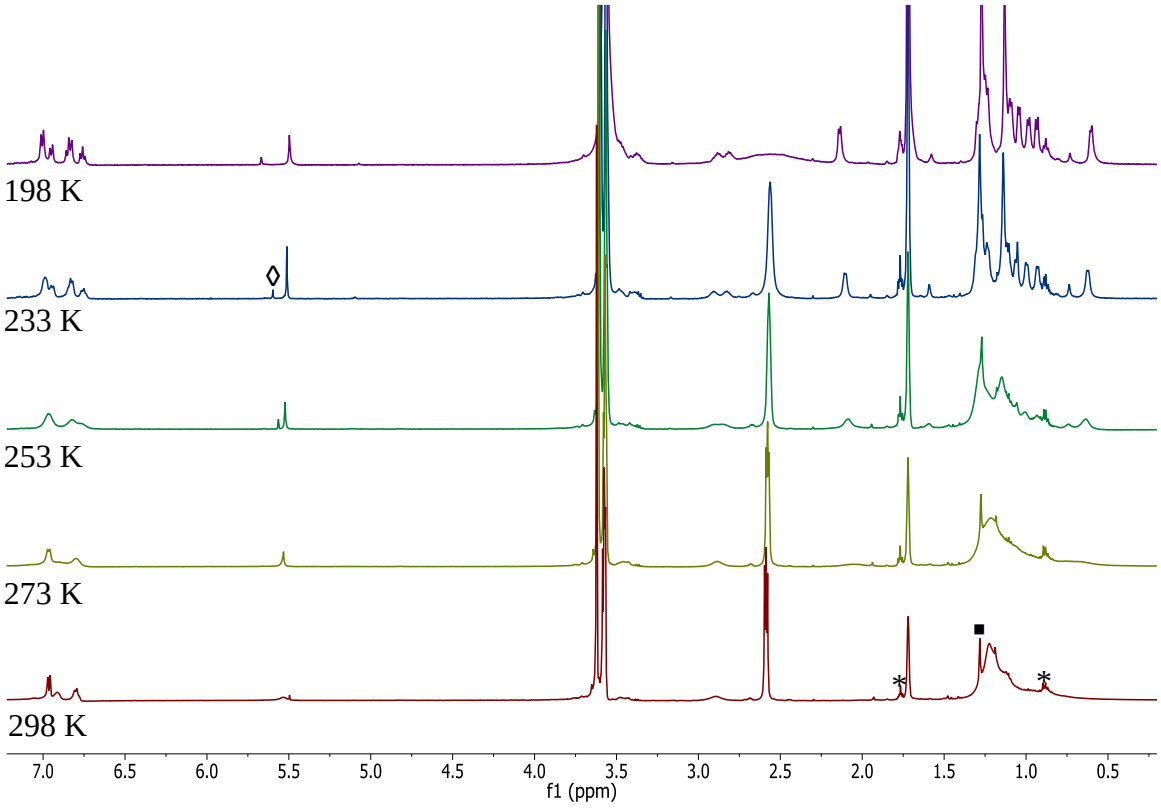

Figure A 4.4. Variable temperature ^{1}H NMR spectra of [K(2,2,2-cryptand)][(*S*,*S*:κ$_2$-CS$_3$)Ni{*S*,*S*:κ$_2$-CS$_2$(L^{tBu})}] (**4.2**) in THF-d_8. (*) indicates the presence of isooctane and (◊) indicates the presence of dichloromethane, and (▪) indicates the presence of an unidentified impurity.

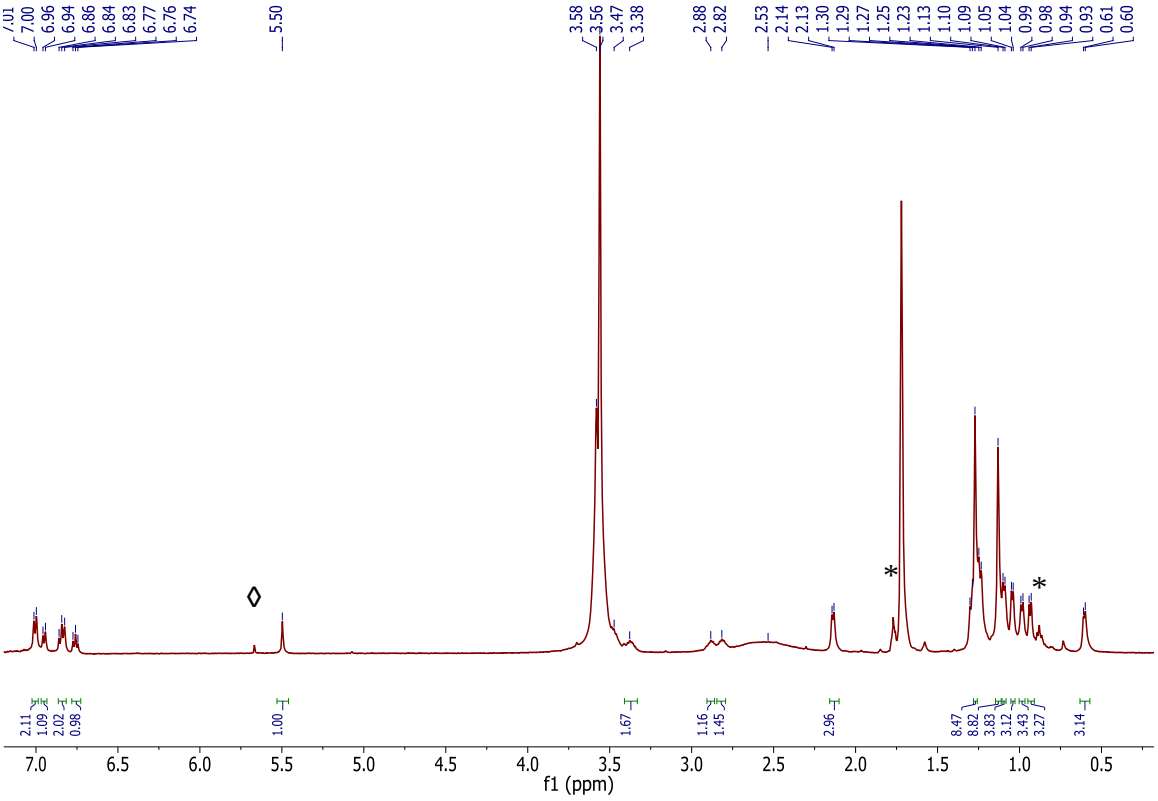

Figure A 4.5. ^{1}H NMR spectrum of [K(2,2,2-cryptand)][(*S*,*S*:κ$_2$-CS$_3$)Ni{*S*,*S*:κ$_2$-CS$_2$(L^{tBu})}] (**4.2**) at -75 °C in THF-d_8. (*) indicates the presence of isooctane and (◊) indicates the presence of dichloromethane.

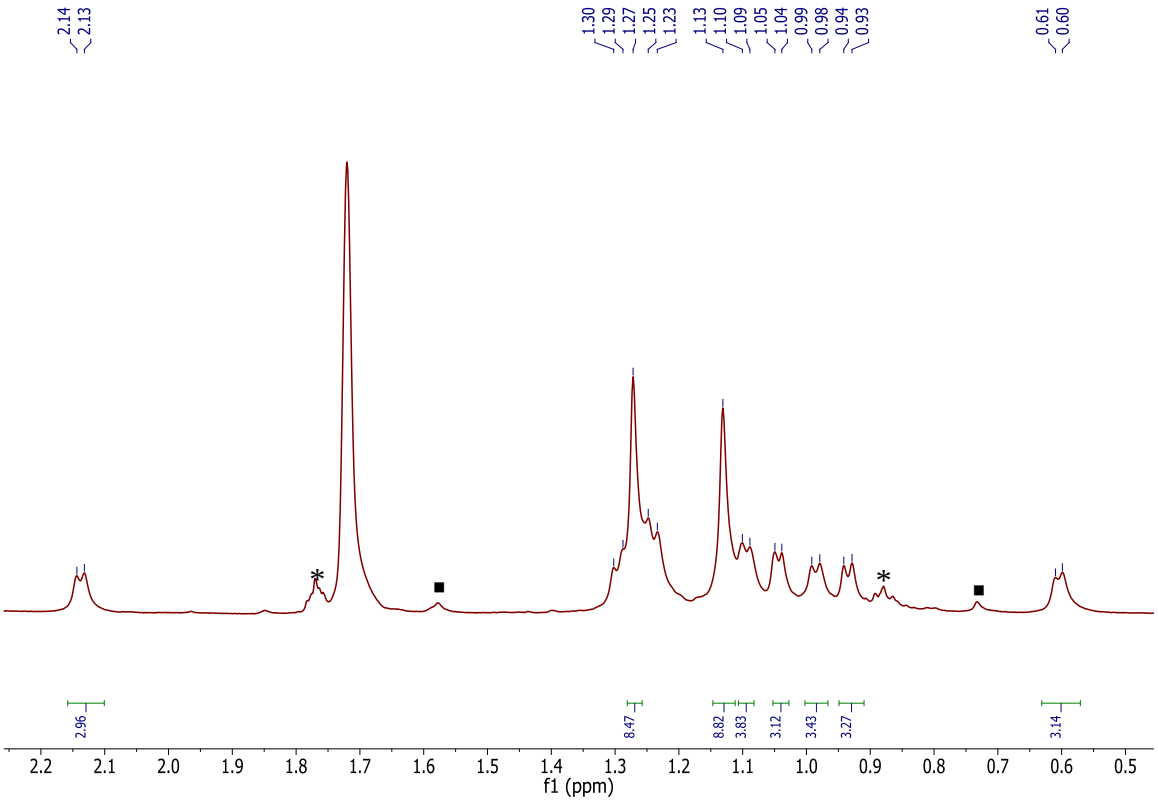

Figure A 4.6. Partial ^{1}H NMR spectrum of [K(2,2,2-cryptand)][(*S*,*S*:κ$_2$-CS$_3$)Ni{*S*,*S*:κ$_2$-CS$_2$(L^{tBu})}] (**4.2**) at -75 °C in THF-d_8. (*) indicates the presence of isooctane and (▪) indicates the presence of unknown impurities.

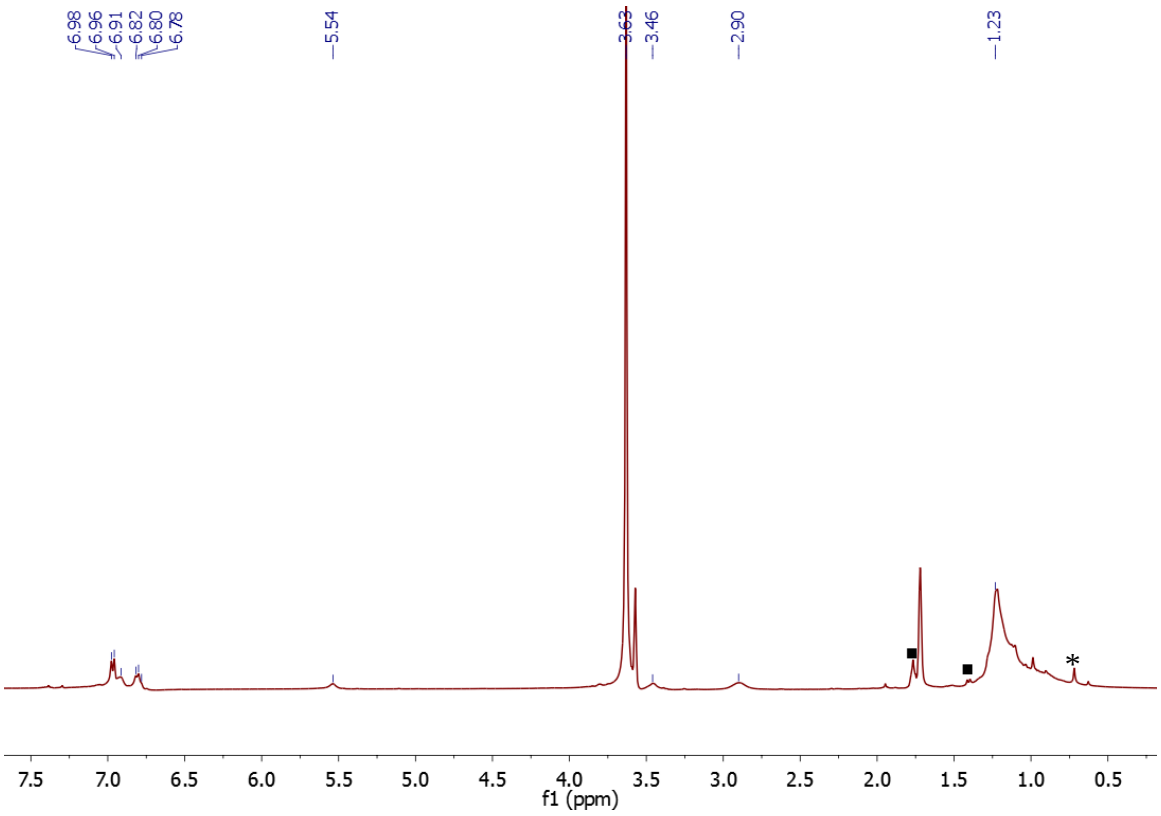

Figure A 4.7. In situ ^{1}H NMR spectrum of the reaction of [K(18-crown-6)][L^{tBu}Ni(S)] (**4.4**) with two equiv CS_2 in THF-d_8. (▪) indicate the presence of unidentified impurities and (*) indicates the presence of isooctane.

4.5.2 IR Spectra

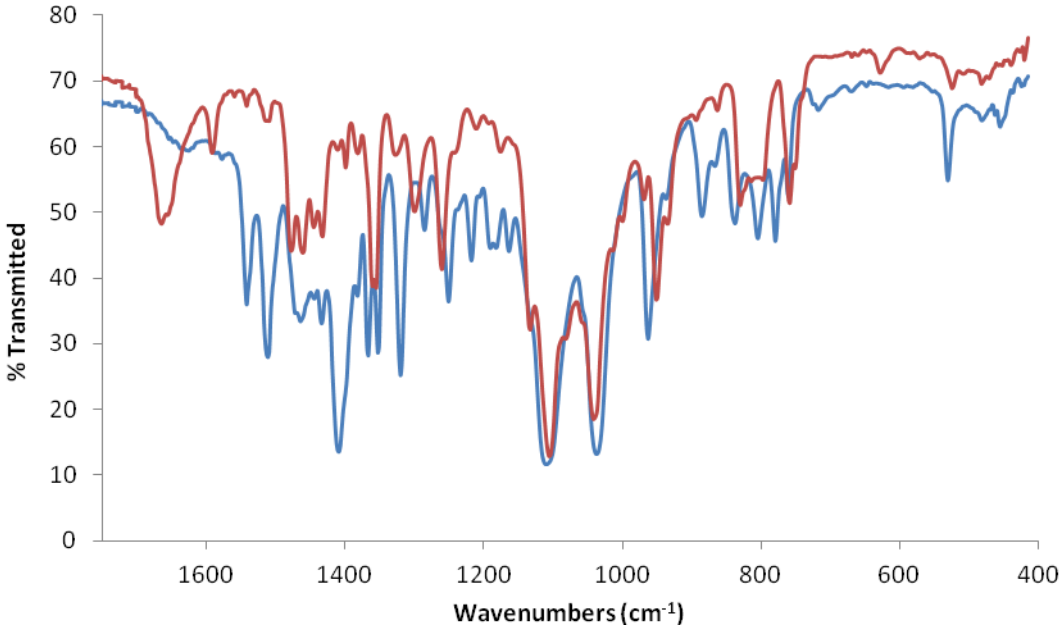

Figure A 4.8. Partial IR spectra of complexes **4.1** (blue) and **4.2** (red) (KBr pellets).

4.6 References

(1) Jenkins, D. M.; Betley, T. A.; Peters, J. C. Oxidative Group Transfer to Co(I) Affords a Terminal Co(III) Imido Complex. *J. Am. Chem. Soc.* **2002**, *124* (38), 11238.

(2) Shay, D. T.; Yap, G. P. A.; Zakharov, L. N.; Rheingold, A. L.; Theopold, K. H. Intramolecular CH Activation by an Open-Shell Cobalt(III) Imido Complex. *Angew. Chem. Int. Ed.* **2005**, *44* (10), 1508.

(3) Mindiola, D. J.; Hillhouse, G. L. Isocyanate and Carbodiimide Synthesis by Nitrene-Group-Transfer from a Nickel(II) Imido Complex. *Chem. Commun.* **2002**, No. 17, 1840.

(4) Jones, C.; Schulten, C.; Rose, R. P.; Stasch, A.; Aldridge, S.; Woodul, W. D.; Murray, K. S.; Moubaraki, B.; Brynda, M.; La Macchia, G.; et al. Amidinato– and Guanidinato–Cobalt(I) Complexes: Characterization of Exceptionally Short Co–Co Interactions. *Angew. Chem. Int. Ed.* **2009**, *48* (40), 7406.

(5) Mindiola, D. J.; Waterman, R.; Iluc, V. M.; Cundari, T. R.; Hillhouse, G. L. Carbon–Hydrogen Bond Activation, C–N Bond Coupling, and Cycloaddition Reactivity of a Three-Coordinate Nickel Complex Featuring a Terminal Imido Ligand. *Inorg. Chem.* **2014**, *53* (24), 13227.

(6) King, E. R.; Sazama, G. T.; Betley, T. A. Co(III) Imidos Exhibiting Spin Crossover and C–H Bond Activation. *J. Am. Chem. Soc.* **2012**, *134* (43), 17858.

(7) Iluc, V. M.; Miller, A. J. M.; Anderson, J. S.; Monreal, M. J.; Mehn, M. P.; Hillhouse, G. L. Synthesis and Characterization of Three-Coordinate Ni(III)-Imide Complexes. *J. Am. Chem. Soc.* **2011**, *133* (33), 13055.

(8) Kogut, E.; Wiencko, H. L.; Zhang, L.; Cordeau, D. E.; Warren, T. H. A Terminal Ni(III)-Imide with Diverse Reactivity Pathways. *J. Am. Chem. Soc.* **2005**, *127* (32), 11248.

(9) Melenkivitz, R.; Mindiola, D. J.; Hillhouse, G. L. Monomeric Phosphido and Phosphinidene Complexes of Nickel. *J. Am. Chem. Soc.* **2002**, *124* (15), 3846.

(10) Cundari, T. R.; Jimenez-Halla, J. O. C.; Morello, G. R.; Vaddadi, S. Catalytic Tuning of a Phosphinoethane Ligand for Enhanced C−H Activation. *J. Am. Chem. Soc.* **2008**, *130* (39), 13051.

(11) Iluc, V. M.; Hillhouse, G. L. Three-Coordinate Nickel Carbene Complexes and Their One-Electron Oxidation Products. *J. Am. Chem. Soc.* **2014**, *136* (17), 6479.

(12) Waterman, R.; Hillhouse, G. L. Group Transfer from Nickel Imido, Phosphinidene, and Carbene Complexes to Ethylene with Formation of Aziridine, Phosphirane, and Cyclopropane Products. *J. Am. Chem. Soc.* **2003**, *125* (44), 13350.

(13) Iluc, V. M.; Hillhouse, G. L. Hydrogen-Atom Abstraction from Ni(I) Phosphido and Amido Complexes Gives Phosphinidene and Imide Ligands. *J. Am. Chem. Soc.* **2010**, *132* (43), 15148.

(14) Hay-Motherwell, R. S.; Wilkinson, G.; Hussain-Bates, B.; Hursthouse, M. B. Synthesis and X-Ray Crystal Structure of Oxotrimesityliridium(V). *Polyhedron* **1993**, *12* (16), 2009.

(15) Poverenov, E.; Efremenko, I.; Frenkel, A. I.; Ben-David, Y.; Shimon, L. J. W.; Leitus, G.; Konstantinovski, L.; Martin, J. M. L.; Milstein, D. Evidence for a Terminal Pt(IV)-Oxo Complex Exhibiting Diverse Reactivity. *Nature* **2008**, *455* (7216), 1093.

(16) Sendlinger, S. C.; Nicholson, J. R.; Lobkovsky, E. B.; Huffman, J. C.; Rehder, D.; Christou, G. Reactivity Studies of Mononuclear and Dinuclear Vanadium-Sulfide-Thiolate Compounds. *Inorg. Chem.* **1993**, *32* (2), 204.

(17) Simonnet-Jégat, C.; Cadusseau, E.; Dessapt, R.; Sécheresse, F. Synthesis and Structural Characterizations of New Mononuclear and Dinuclear Molybdenum(V) Anions Containing Trithiocarbonate Ligands. *Inorg. Chem.* **1999**, *38* (10), 2335.

(18) Dessapt, R.; Simonnet-Jégat, C.; Riedel, S.; Marrot, J.; Sécheresse, F. $[Re(\eta^2\text{-}CS_3)_4]^{3-}$, a New Trithiocarbonate-Containing Rhenium(V) Dodecahedral Anion. *Trans. Met. Chem.* **2002**, *27* (2), 234.

(19) Coucouvanis, D.; Draganjac, M. E.; Koo, S. M.; Toupadakis, A.; Hadjikyriacou, A. I. Reactivity of the Molybdenum-Polysulfide Functional Groups in Thio- and Oxothiomolybdate Complexes toward Carbon Disulfide. Synthesis and Reactivity of Trithio- and Perthiocarbonate Complexes of Mo(IV) and Mo(V). *Inorg. Chem.* **1992**, *31* (7), 1186.

(20) Kim, B. J.; Park, J. W.; Koo, S. M. Niobium Persulfide Complexes: Synthesis and Structural Characterization of $[Et_4N][NbO(S_2)_2(bpy)]\cdot DMF$, $[PPN][NbO(CS_3)(S_2)(bpy)]$ and $[Et_4N][NbO(S_2C_2(CO_2Me)_2)(S_2)(bpy)]\cdot DMF$ Complexes. *Polyhedron* **2001**, *20* (18), 2279.

(21) Hartmann, N. J.; Wu, G.; Hayton, T. W. Synthesis of a "Masked" Terminal Nickel(II) Sulfide by Reductive Deprotection and Its Reaction with Nitrous Oxide. *Angew. Chem. Int. Ed.* **2015**, *54* (49), 14956.

(22) Campora, J.; Gutierrez, E.; Monge, A.; Palma, P.; Poveda, M. L.; Ruiz, C.; Carmona, E. Consecutive Insertion Reactions of Unsaturated Molecules into the Ni-C Bonds of the Nickelacycle [Cyclic] $(Me_3P)_2Ni(CH_2CHMe_2\text{-}o\text{-}C_6H_4)$. Formation of Heterocycles Derived from Seven-Membered Cyclic Acid Anhydrides. *Organometallics* **1994**, *13* (5), 1728.

(23) Choudhury, S. B.; Chakravorty, A. A Tris(Thioxanthate) of Nickel(II) and Its Transformation to a Dinuclear Trithiocarbonate Complex. Synthesis and Structure of $[Et_4N]_2[Ni_2(SEt)_2(CS_3)_2]$. *Inorg. Chem.* **1992**, *31* (6), 1055.

(24) Horn, B.; Limberg, C.; Herwig, C.; Braun, B. Three-Coordinate Nickel(II) and Nickel(I) Thiolate Complexes Based on the β-Diketiminate Ligand System. *Inorg. Chem.* **2014**, *53* (13), 6867.

(25) Yao, S.; Milsmann, C.; Bill, E.; Wieghardt, K.; Driess, M. From a Paramagnetic, Mononuclear Supersulfidonickel(II) Complex to a Diamagnetic Dimer with a Four-Sulfur Two-Electron Bond. *J. Am. Chem. Soc.* **2008**, *130* (41), 13536.

(26) Doherty, J.; Fortune, J.; Manning, A. R.; Stephens, F. S. Trithiocarbonate and Dithiocarbonate Complexes of [η]-Cyclopentadienyl Cobalt(III): X-Ray Crystal Structure of $[Co([\eta]\text{-}C_5H_5)(CNBut)(CS_3)]$. *J. Chem. Soc., Dalt. Trans.* **1984**, No. 6, 1111.

(27) Scheuermann, M. L.; Luedtke, A. T.; Hanson, S. K.; Fekl, U.; Kaminsky, W.; Goldberg, K. I. Reactions of Five-Coordinate Platinum(IV) Complexes with Molecular Oxygen. *Organometallics* **2013**, *32* (17), 4752.

(28) Kalita, A.; Kumar, V.; Mondal, B. C-Nitrosation of a β-Diketiminate Ligand in Copper(II) Complex. *RSC Adv.* **2015**, *5* (1), 643.

(29) Basuli, F.; Huffman, J. C.; Mindiola, D. J. Reactivity at the β-Diketiminate Ligand Nacnac$^-$ on Titanium(IV). Diimine-Alkoxo and Bis-Anilido Ligands Stemming from

the Nacnac$^-$ Skeleton. *Inorg. Chem.* **2003**, *42* (24), 8003.
(30) Yempally, V.; Fan, W. Y.; Arndtsen, B. A.; Bengali, A. A. Intramolecular C–C Bond Coupling of Nitriles to a Diimine Ligand in Group 7 Metal Tricarbonyl Complexes. *Inorg. Chem.* **2015**, *54* (23), 11441.
(31) Gregory, E. A.; Lachicotte, R. J.; Holland, P. L. A Cationic Three-Coordinate Iron(II) Complex and the Reaction of β-Diketiminate with Ethyl Diazoacetate. *Organometallics* **2005**, *24* (8), 1803.
(32) Harris Robin, K.; Becker Edwin, D.; Cabral de Menezes Sonia, M.; Goodfellow, R.; Granger, P. NMR Nomenclature: Nuclear Spin Properties and Conventions for Chemical Shifts. IUPAC Recommendations 2001. International Union of Pure and Applied Chemistry. Physical Chemistry Division. Commission on Molecular Structure and Spectroscopy. *Pure Appl. Chem.* **2002**, *40* (7), 489.
(33) Harris Robin, K.; Becker Edwin, D.; Cabral De Menezes Sonia, M.; Granger, P.; Hoffman Roy, E.; Zilm Kurt, W. Further Conventions for NMR Shielding and Chemical Shifts. *Pure Appl. Chem.* **2008**, *80*, 59.
(34) SMART Apex II. Bruker AXS Inc.: Madison, WI 2005.
(35) SAINT Software User's Guide. Bruker AXS Inc.: Madison, WI 2005.
(36) Sheldrick, G. M. SADABS. University of Gottingen: Germany 2005.
(37) SHELXTL PC. Bruker AXS Inc.: Madison, WI 2005.

Chapter 5 Reactivity of a Nickel Sulfide with Carbon Monoxide and Nitric Oxide

Portions of this work were published in:

Nathaniel J. Hartmann , Guang Wu, Trevor W. Hayton

J. Am. Chem. Soc., **2016**, *138*, 12352-12355.

Table of Contents

5.1 Introduction

There is a widespread interest in understanding the fundamental reactivity of late metal sulfides with small molecules, such as NO and CO, which are notable for their roles in biological signaling and the carbon cycle, respectively.[1–3] For example, the reactions of NO with the sulfide ligands in metallo-proteins can not only affect its bioavailability, but may also play an important regulatory role (e.g., NO/H_2S "cross talk").[4] In this regard, NO is known to react with iron sulfur clusters.[5,6] The sulfur-containing products from these reactions are S^0, S^{2-}, or H_2S. Other sulfur containing products, such as $[SNO]^-$, $[SSNO]^-$, and $[ONN(O)SO_3]^{2-}$ have not yet been observed from these reactions; however, these compounds have come under increasing scrutiny because they could function as both NO and sulfur reservoirs *in vivo*.[4,7,8] Similarly, CO is postulated to react with the sulfide ligands within metallo-enzymes. In particular, the first step of CO oxidation by MoCu CODH is thought to involve CO insertion into a Cu-S bond.[9]

In Chapter 2, I detailed the synthesis of the "masked" terminal Ni^{II} sulfides, $[K(L)][L^{tBu}Ni^{II}(S)]$, (**2.4**-**2.6**).[10] In Chapters 3 and 4, I demonstrated the nucleophilic reactivity of the sulfide ligand via its reactions with the methylene carbon of $[CoCp^*(C_5Me_4{=}CH_2)]$ and CS_2, respectively.[11,12] Given its potent reactivity, I hypothesized that $[K(L)][L^{tBu}Ni^{II}(S)]$ would be a good model for exploring the interactions of late metal sulfides with the biologically important small molecules, CO and NO. This survey is especially important because late metal (Ni and Cu) sulfides are found in a variety of metalloenzyme active sites, including the NiFe and MoCu CO dehydrogenases (CODH),[9,13] the "orange protein complex",[14] and N_2O reductase (N_2OR),[15–17] where they are known to play both catalytic[9] and structural roles,[15,18] yet our understanding of late metal sulfide (and

thiolate) reactivity is still relatively limited.[19–22] In this chapter, I describe the reactivity of [K(18-crown-6)][L^{tBu}Ni^{II}(S)] (**2.5**) with CO and NO in an effort to better understand the fundamental chemistry of these small molecules with metal sulfides.

5.2 Results and Discussion

5.2.1 Synthesis and Characterization of [K(18-crown-6)][L^{tBu}Ni^{II}(*S*,*C*:η^2-COS)] (5.1)

Exposure of a toluene solution of [K(18-crown-6)][L^{tBu}Ni^{II}(S)] (**2.5**) to excess carbon monoxide (CO) results in a rapid color change from dark brown to yellow. Work-up of the reaction mixture by crystallization from toluene/isooctane provides [K(18-crown-6)][L^{tBu}Ni^{II}(*S*,*C*:η^2-COS)] (**5.1**) as a orange crystalline solid in 88% yield (Scheme 5.1).

Scheme 5.1 Synthesis of [K(18-crown-6)][L^{tBu}Ni^{II}(*S*,*C*:η^2-COS)] (**5.1**)

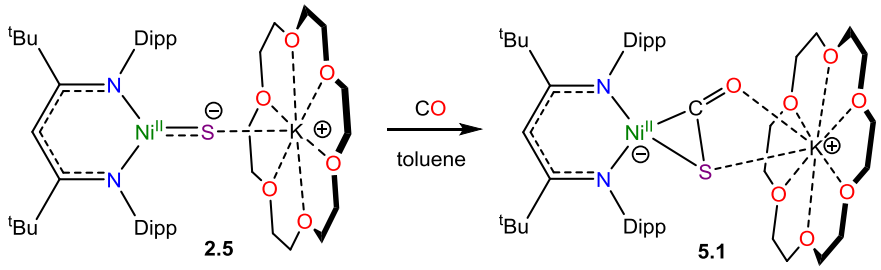

The solid state molecular structure of **5.1** is shown in Figure 5.1. Complex **5.1** features a rare carbonyl sulfide ([COS]$^{2-}$) ligand, formed by the activation of CO by the S^{2-} ligand. The [COS]$^{2-}$ ligand features a μ:η^2,κ^2 binding mode, wherein the carbon and sulfur atoms are coordinated to the Ni center, while the sulfur and oxygen atoms are coordinated to the K$^+$ center. The COS ligand is disordered over two positions, which are related by a C_2 rotation axis. This disorder could not be adequately resolved; consequently, the C-O bond length (1.07(1) Å) is anomalously short. A similar problem was observed in the only other structurally characterized COS complex, [(MeCp)$_2$Nb(*S*,*C*:η^2-COS)(CH$_2$SiMe$_3$)].[23] The Ni-S and Ni-C distances in **5.1** are 2.193(2) Å and 1.871(8) Å, while the K-S distance (3.250(4)

Å) is longer than that found in the starting material, [K(18-crown-6)][$L^{tBu}Ni^{II}$(S)], and is indicative of a rather weak dative interaction. The K-O (2.841(7) Å) distance is similarly long.[24,25] Finally, the Ni-N distances in **5.1** are comparable to those found in the starting material.[10]

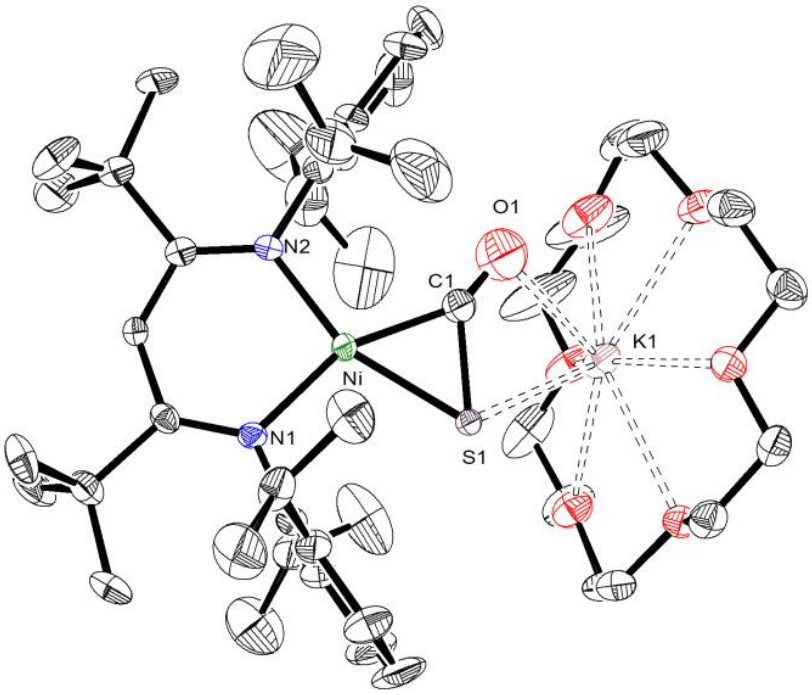

Figure 5.1. ORTEP drawing of [K(18-crown-6)][$L^{tBu}Ni^{II}$(*S*,*C*:η^2-SCO] (**5.1**·2C_6H_6) shown with 50% thermal ellipsoids. Hydrogen atoms, one orientation of the disordered COS moiety, and C_6H_6 solvate molecules have been omitted for clarity. Selected metrical parameters: Ni1-N1 1.929(4) Å, Ni1-N2 1.903(4) Å, Ni1-S1 2.193(2) Å, Ni1-C1 1.871(8) Å, S1-C1 1.791(8) Å, C1-O1 1.07(1) Å, S1-K1 3.250(4) Å, O1-K1 2.841(7) Å, N1-Ni1-N2 97.3(2)°, N1-Ni1-S1 104.7(1)°, N2-Ni1-C1 106.4(3)°, S1-C1-O1 136.6(7)°.

The ^{1}H NMR spectrum of **5.1** is consistent with its formulation as a C_s symmetric, diamagnetic, square planar Ni^{II} complex. For example, the ^{1}H NMR spectrum of **5.1** in C_6D_6 features two *tert*-butyl resonances at 1.43 and 1.41 ppm and a single γ-CH resonance at 5.48

ppm. Additionally, the ^{13}C NMR spectrum of **5.1** features a resonance at 214.72 ppm that I have assigned to the $[COS]^{2-}$ moiety. For comparison, this chemical shift is an exact average of the ^{13}C NMR chemical shifts observed for the CE_2 ligands in $[(dtbpe)Ni^{II}(\eta^2\text{-}CO_2)]$ (dtbpe = $^tBu_2PCH_2CH_2P^tBu_2$) and $[(dtbpe)Ni^{II}(\eta^2\text{-}CS_2)]$, which are found at 164.28 and 264.20 ppm, respectively.[26] The IR spectrum (KBr mull) of **5.1** shows a strong ν_{CO} mode at 1676 cm^{-1}, which is consentient with that expected for $[SCO]^{2-}$.[23]

The formation of **5.1** represents a rare example of attack of a S^{2-} ligand by CO, and highlights the potent nucleophilicity of the S^{2-} moiety in $[K(L)][L^{tBu}Ni^{II}(S)]$. Other examples of this transformation include the reaction of $[(Ph_3P)_4Pt_2(\mu\text{-}S)_2]$ with CO to make COS and $[(Ph_3P)_4Pt_2(\mu\text{-}S)]$, and the reaction of $[Cp^*Mo(\mu\text{-}S)\{N(^iPr)C(Ph)N(^iPr)\}]_2$ with CO and S_8 to make COS and $[Cp^*Mo(CO)(\eta^2\text{-}S_2)\{N(^iPr)C(Ph)N(^iPr)\}]$.[27,28] For further comparison, the previously mentioned COS complex, $[(MeCp)_2Nb(\eta^2\text{-}SCO)(CH_2SiMe_3)]$, was formed by reaction of $[(MeCp)_2Nb(CO)(CH_2SiMe_3)]$ with elemental sulfur.[23,29,30] Perhaps more importantly, the formation of **5.1** provides support for the first step in the proposed mechanism of MoCu CODH,[9] which is thought to involve insertion of CO into a Cu-S bond and formation of a thiocarbonate ligand, $[CO_2S]^{2-}$. Additionally, a metal-COS adduct may be a proposed intermediate in the catalytic cycle of thiocyanate hydrolase, which catalyzes the conversion of thiocyanate (SCN^-) to carbonyl sulfide.[31–33] Reaction of [K(18-crown-6)][$L^{tBu}Ni^{II}(S)$] with NO to yield [$L^{tBu}Ni(NO)$] (**5.2**) and [K(18-crown-6)][SSNO] (**5.3**).

Exposure of a toluene solution of [K(18-crown-6)][$L^{tBu}Ni^{II}(S)$] to an excess of nitric oxide (NO) results in a rapid color change from brown to brown-green. Work-up of the reaction mixture results in isolation of a nitrosyl complex, [$L^{tBu}Ni(NO)$] (**5.2**), along with a perthionitrite salt, [K(18-crown-6)][SSNO] (**5.3**) (Scheme 5.2).

Scheme 5.2 Synthesis of complexes **5.2** and **5.3**

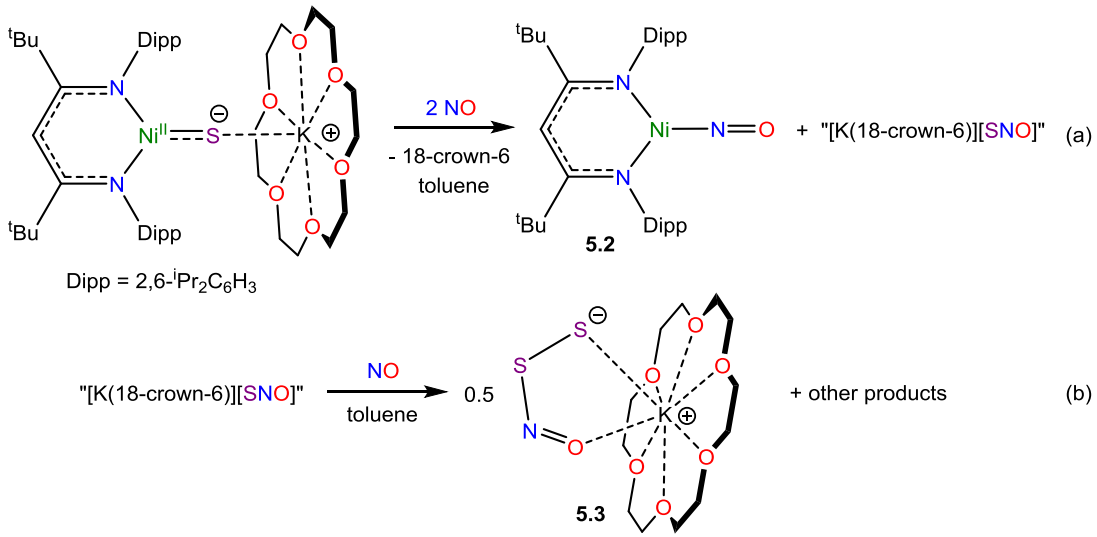

Complex **5.2** was isolated in an 80% yield and has been fully characterized by elemental analysis, X-ray crystallography (Figure 5.2), IR spectroscopy, and ^{1}H and ^{13}C NMR spectroscopy. Its structural and spectroscopic parameters are consistent with those previously reported for the related β-diketiminate nickel nitrosyl complex, [L^{Me}Ni(NO)] (L^{Me} = {(2,6-$^{i}Pr_2C_6H_3$)NC(Me)}$_2$CH), which was isolated from the reaction of [$L^{Me}Ni^{I}$(2,4-lutidine)] and NO.[34]

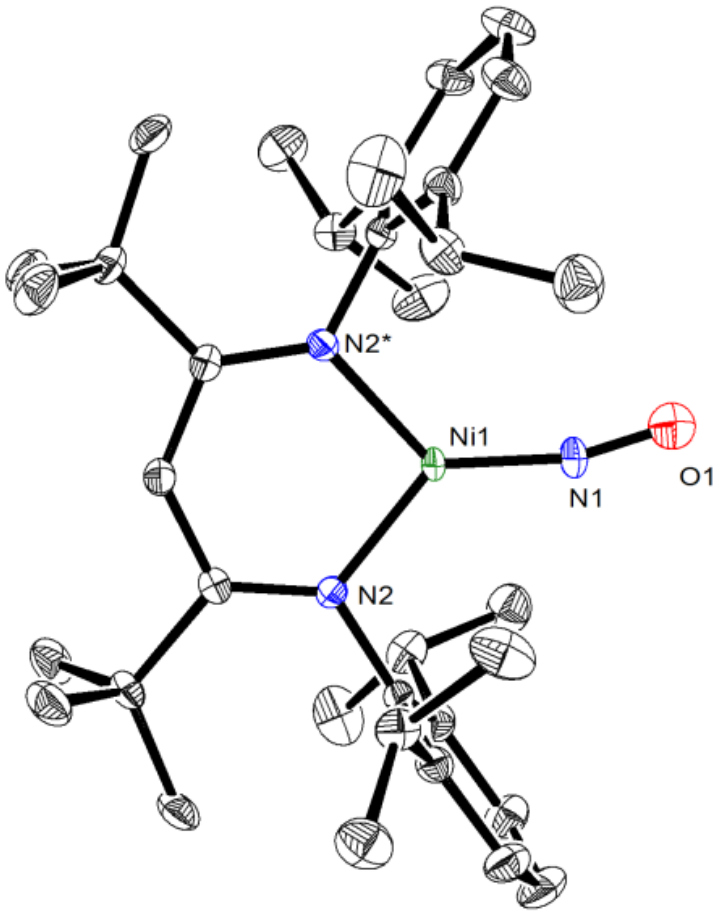

Figure 5.2. ORTEP drawing of [L^{tBu}Ni(NO)] (**5.2**) shown with 50% thermal ellipsoids. Hydrogen atoms have been omitted for clarity. Selected metrical parameters: Ni1-N2 1.874(2) Å, Ni1-N1 1.615(3) Å, N1-O1 1.187(7) Å, N2-Ni1-N1 130.61(5)°, Ni1-N1-O1 164.5(3)°.

Complex **5.3** was isolated in 86% yield as orange plates (based on sulfur). Its formulation was confirmed through X-ray crystallography, IR spectroscopy, and UV-Vis spectroscopy. Complex **5.3** crystallizes from CH_2Cl_2/pentane as a CH_2Cl_2 adduct (K1-Cl1 = 3.2674(8) Å) and features a perthionitrite $[SSNO]^-$ ligand coordinated to a $[K(18\text{-crown-6})]^+$ cation in a κ^2 fashion (Figure 5.3). The $[SSNO]^-$ moiety in complex **5.3** possesses O-N, N-S, and S-S bond lengths of 1.247(2), 1.669(2), and 1.9526(9) Å, respectively, which agree well

with those reported previously reported for [PNP][SSNO] (PNP = Ph_3PNPPh_3).[35] In addition, the K-S (3.2013(8) Å) and K-O (2.770(2) Å) bond lengths are comparable to those observed in **5.1**. The UV-vis spectrum of **5.3** in acetonitrile features an absorbance at 443 nm. For comparison, [PNP][SSNO] exhibits an absorbance of 448 nm in acetone.[35] The IR spectrum (KBr mull) of complex **5.3** reveals a ν_{NO} mode at 1313 cm^{-1}, which is somewhat lower than those observed for other $[SSNO]^-$ salts.[35,36] This lower value may be a consequence of the K···O dative interaction observed in the solid state molecular structure of **5.3**. Complex **5.3** is soluble in aromatic solvents, acetonitrile, and dichloromethane, and appears to be indefinitely stable when stored at -25 °C as a solid under inert atmosphere.

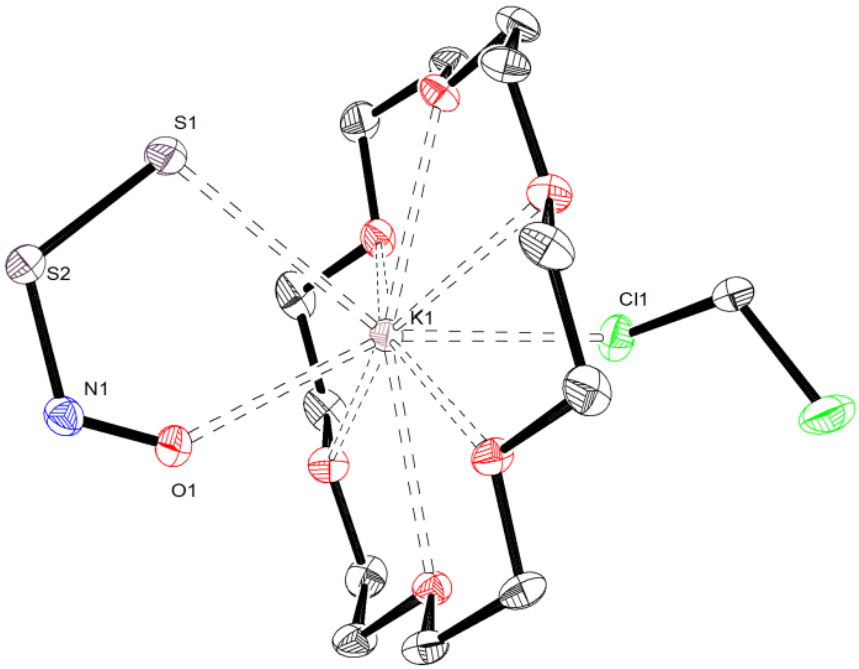

Figure 5.3. ORTEP drawing of [K(18-crown-6)][SSNO]·CH_2Cl_2 (**5.3**·CH_2Cl_2) shown with 50% thermal ellipsoids. Hydrogen atoms have been omitted for clarity. Selected metrical parameters: O1-N1 1.247(2) Å, N1-S2 1.669(2) Å, S2-S1 1.9526(9) Å, S1-K1 3.2013(8) Å, O1-K1 2.770(2) Å, Cl1-K1 3.2674(8) Å, O1-N1-S2 119.6(1)°, N1-S2-S1 113.27(7)°.

5.2.2 Mechanistic Considerations

The isolation of **5.3** from the reaction of [K(18-crown-6)][$L^{tBu}Ni^{II}$(S)] with NO demonstrates for the first time that a transition metal sulfide can react with NO to form $[SSNO]^-$, an observation that may have implications for our understanding of the reactions between NO and sulfur-containing metallo-proteins *in vivo*.[5,6] To account for the formation of **5.3**, I hypothesize that the first step of the transformation involves sulfur abstraction by NO, forming "[K(18-crown-6)][SNO]" and "[$L^{tBu}Ni^{I}$]". Subsequent reaction of "[$L^{tBu}Ni^{I}$]" with NO yields complex **5.2** (Scheme 5.2a), a transformation that has been observed previously.[34] Separately, reaction of "[K(18-crown-6)][SNO]" with NO results in formation of complex **5.3** (Scheme 5.2b). Alternatively, it is possible that the first step of the reaction yields a nickel-SNO adduct, e.g., [K(18-crown-6)][L^{tBu}Ni(SNO)], which subsequently reacts with NO to yield the final products. To test this hypothesis I monitored the reaction of [K(18-crown-6)][$L^{tBu}Ni^{II}$(S)] with only **5.1** equiv of NO, which resulted in only partial consumption of [K(18-crown-6)][$L^{tBu}Ni^{II}$(S)], and formation of complex **5.2** as the only identifiable Ni-containing product (Figures A 5.6-5.7). These two complexes are present in an approx. 1:2 ratio, respectively. The observation of unconsumed [K(18-crown-6)][$L^{tBu}Ni^{II}$(S)] is consistent with the proposed mechanism, assuming that the sulfide abstraction step is rate determining. In addition, I monitored the reaction of independently prepared [PNP][SNO] with nitric oxide by UV-vis spectroscopy (Scheme 5.3).

Scheme 5.3 Oxidation of SNO^- with NO to form $SNNO^-$

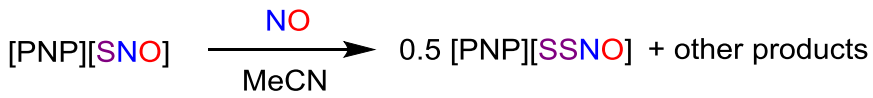

Thus, exposure of an MeCN solution of [PNP][SNO] to excess NO resulted in complete consumption of [PNP][SNO], as revealed by the loss of the absorption band at 334 nm, and

the generation of [PNP][SSNO], as revealed by the appearance of a new band at 445 nm (Figure 5.4). The other products generated in the transformation remain unidentified; however, I can rule out formation of N_2O as it could not be detected in reaction mixture by either gas chromatography or IR spectroscopy. While conversion of $[SSNO]^-$ to $[SNO]^-$ was previously reported,[35] this is the first demonstration that $[SNO]^-$ can be converted into $[SSNO]^-$ upon oxidation.

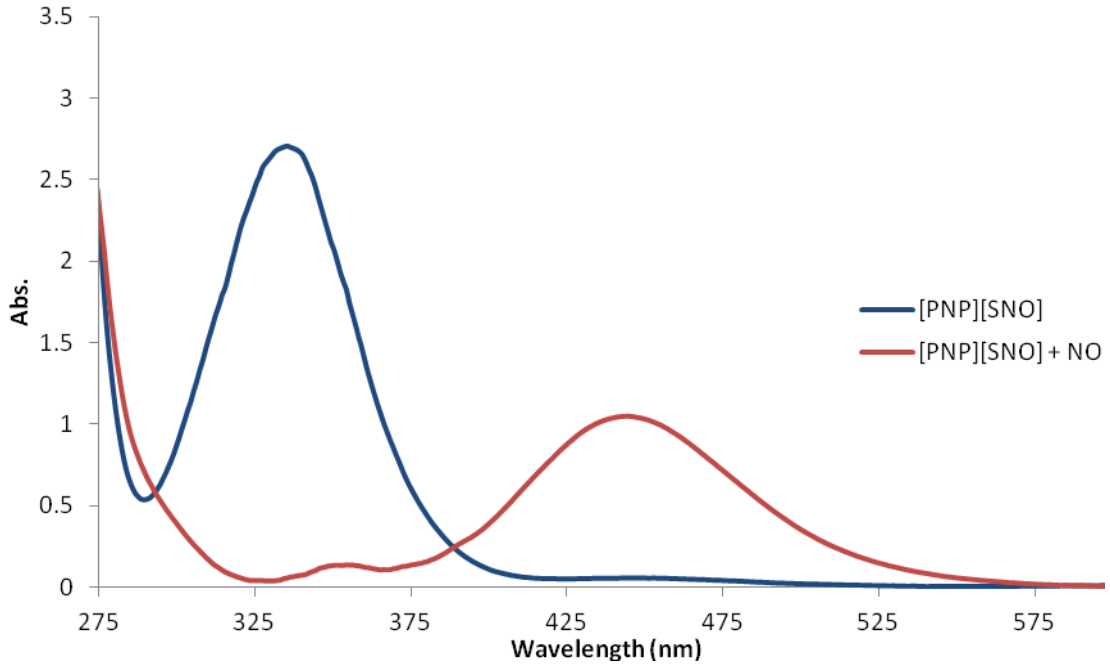

Figure 5.4. UV-vis spectrum of the reaction of [PNP][SNO] with excess NO in MeCN.[35]

5.3 Summary

In summary, the "masked" terminal nickel sulfide complex, [K(18-crown-6)][$L^{tBu}Ni^{II}$(S)] (**2.5**), readily activates CO to give a carbonyl sulfide complex, [K(18-crown-6)][$L^{tBu}Ni^{II}$(*S*,*C*:η_2-SCO] (**5.1**), via CO addition across the Ni-S bond. This result further highlights the high nucleophilicity of the sulfide ligand in [K(18-crown-6)][$L^{tBu}Ni^{II}$(S)], despite the K^+ capping moiety that is present in both solution and the solid-state. Moreover,

complex **5.1** represents a well-defined example of a late metal $[COS]^{2-}$ adduct.[9,31–33] The sulfide ligand in [K(18-crown-6)][$L^{tBu}Ni^{II}$(S)] also activates NO to generate a nickel nitrosyl, [L^{tBu}Ni(NO)] (**5.2**), and a perthionitrite salt, [K(18-crown-6)][SSNO] (**5.3**). This result represents the first confirmed generation of $[SSNO]^-$ from reaction of transition metal sulfide with NO. This observation is significant because it further confirms that metal sulfides can play a regulatory role *in vivo* with respect to NO availability (e.g., so-called NO/H_2S "cross talk").[4,37,38] I have also discovered that oxidation of $[SNO]^-$ with NO results in formation of $[SSNO]^-$. This represents a new route to $[SSNO]^-$, and provides us with a better understanding of the fundamental chemistry of this important, but poorly understood, ion.

5.4 Experimental Procedures

5.4.1 General Methods

All reactions and subsequent manipulations were performed under anaerobic and anhydrous conditions under an atmosphere of nitrogen. Hexanes, diethyl ether (Et_2O), and toluene were dried using a Vacuum Atmospheres DRI-SOLV Solvent Purification system and stored over 3Å sieves for 24 h prior to use. Acetonitrile, benzene-d_6, pentane, and C_8H_{18} (isooctane) were dried over 3Å molecular sieves for 24 h prior to use. Acetone was dried by distillation (twice) from B_2O_3. [K(18-crown-6)][L^{tBu}Ni(S)] and [PNP][NO_2] were synthesized according to the previously reported procedures.[10,39] Nitric oxide (NO) and carbon monoxide (CO) were supplied by Praxair and used as received. All other reagents were purchased from commercial suppliers and used as received.

^1H and $^{13}C\{^1H\}$ NMR spectra were recorded on a Agilent Technologies 400-MR DD2 400 MHz spectrometer or a Varian UNITY INOVA 500 MHz spectrometer. ^1H and

$^{13}C\{^{1}H\}$ NMR spectra were referenced to external $SiMe_4$ using the residual protio solvent peaks as internal standards.[40,41] IR spectra were recorded on a Nicolet 6700 FT-IR spectrometer. Electronic absorption spectra were recorded on a Shimadzu UV3600 UV-NIR Spectrometer. Elemental analyses were performed by the Micro-Mass Facility at the University of California, Berkeley.

5.4.2 Synthesis of [K(18-crown-6)][L^{tBu}Ni(*C*,*S*:η^2-C(O)S)] (5.1)

A 50 mL Schlenk flask, equipped with a Teflon rotoflow valve, was charged with a dark brown solution of [K(18-crown-6)][L^{tBu}Ni(S)] (**2.5**) (35.0 mg, 0.0391 mmol) in toluene (2 mL). The headspace was then evacuated and filled with CO gas (1 atm). After addition of CO, the solution rapidly changed from dark brown to pale yellow. After stirring the solution for one minute, the headspace was evacuated and replaced with N_2. The Schlenk flask was then transferred into a glovebox, and the reaction mixture was filtered through a Celite column supported on glass wool (0.5 cm × 2 cm). The filtrate was then concentrated to ca. 0.25 mL *in vacuo*. Addition of isooctane (1 mL) to this solution and subsequent storage at -25 °C for 48 h resulted in the deposition of orange plates of [K(18-crown-6)][L^{tBu}Ni(*C*,*S*:η^2-C(O)S)] (**1**), which were isolated by decanting off the supernatant (31.8 mg, 88% yield). Crystals suitable for X-ray diffraction were grown from concentrated solution of **1** in a ~1:1 mixture of hexanes and benzene that was stored at -25 °C for 24 h. Anal. Calcd for: $C_{48}H_{77}KN_2NiO_7S$: C, 62.39; H, 8.40; N, 3.03. Found: C, 62.02; H, 8.10; N, 2.95. ^{1}H NMR (400 MHz, 25 °C, benzene-d_6): δ 7.25-6.97 (m, 6H, Ar-**H**, dipp), 5.48 (s, 1H, γ-**H**), 4.24 (sept, $^3J_{HH}$, = 6.7 Hz, 2H, C**H**$(CH_3)_2$), 4.19 (sept, $^3J_{HH}$, = 6.7 Hz, 2H, C**H**$(CH_3)_2$), 2.99 (s, 24H, 18-crown-6), 2.01 (d, $^3J_{HH}$, = 6.8 Hz, 6H, CH(C**H**$_3)_2$), 1.80 (d, $^3J_{HH}$, = 6.8 Hz, 6H, CH(C**H**$_3)_2$), 1.55 (overlapping doublets, 12H, CH(C**H**$_3)_2$), 1.43 (s, 9H, C(C**H**$_3)_3$), 1.41 (s,

9H, C(C**H**$_3$)$_3$). ^{13}C NMR (125 MHz, 25 °C, benzene-d_6): δ 214.72 (S**C**(O)), 166.17 (Ar-C), 165.94 (Ar-C), 153.53 (Ar-C), 152.78 (Ar-C), 141.05 (Ar-C), 140.94 (Ar-C), 122.30 - 121.55 (Ar-C), 95.20 (γ-**C**), 69.43 (18-crown-6), 42.88 (**C**(CH$_3$)$_3$), 42.44 (**C**(CH$_3$)$_3$), 33.87 (C(**C**H$_3$)$_3$), 33.48 (C(**C**H$_3$)$_3$), 28.19 (CH(**C**H$_3$)$_2$), 27.85 (CH(**C**H$_3$)$_2$), 25.79 (CH(**C**H$_3$)$_2$), 24.36 (CH(**C**H$_3$)$_2$), 24.23 (**C**H(CH$_3$)$_2$), 23.85 (**C**H(CH$_3$)$_2$). IR (KBr Pellet, cm^{-1}): 1676 (s, ν_{CO}), 1624 (br w), 1535 (m), 1510 (s), 1473 (m), 1450 (m), 1444 (m), 1409 (s), 1385 (m), 1365 (m), 1352 (s), 1321 (s), 1286 (w), 1250 (w), 1221 (w), 1192 (w), 1160 (w), 1111 (s), 1057 (w), 964 (s), 937 (w), 896 (w), 839 (m), 804 (w), 776 (m), 758 (m), 642 (m), 579 (w), 530 (w).

5.4.3 Synthesis of [L^{tBu}Ni(NO)] (5.2) and [K(18-crown-6)][SSNO] (5.3)

A 50 mL Schlenk flask, equipped with a Teflon rotoflow valve, was charged with a dark brown solution of [K(18-crown-6)][L^{tBu}Ni(S)] (53.0 mg, 0.0592 mmol) in toluene (2 mL). The headspace was then evacuated and filled with NO gas (1 atm). After addition of NO, the solution rapidly changed from dark brown to brown-green. After stirring the solution for one minute, the headspace was evacuated and replaced with N_2. The Schlenk flask was then transferred to a glovebox, and the volatiles were removed *in vacuo* to give a pale brown solid. This solid was then washed with pentane (3 × 1 mL) and the washings were collected and filtered through a Celite column supported on glass wool (0.5 cm × 2 cm) to give a pale green solution, while leaving a yellow-orange solid on the Celite column. The volatiles were then removed from the green solution *in vacuo* to give a green-brown solid. The solid was extracted into Et_2O (0.5 mL) and transferred to a 5 mL vial. This vial was placed inside a 20 mL scintillation vial. Toluene (2 mL) was then added to the outer vial. Storage of this two vial system at -25 °C for 72 h resulted in the deposition of dichroic plates that appear to be

blue or orange depending upon their orientation relative to a light source. This solid was isolated by decanting off the supernatant (28.0 mg, 80% yield). Separately, the insoluble yellow-orange solid was extracted into dichloromethane (2 mL) to give an orange solution. This solution was concentrated to ca. 0.5 mL *in vacuo*, filtered through a Celite column supported on glass wool (0.5 cm × 2 cm), and transferred to a 5 mL vial. This vial was placed inside a 20 mL scintillation vial. Pentane (2 mL) was then added to the outer vial. Storage of this two vial system at -25 °C for 72 h resulted in the deposition of orange plates of [K(18-crown-6)][SSNO] (**5.3**), which were isolated by decanting off the supernatant (10.1 mg, 86% yield based on sulfur). Anal. Calcd for **5.2**: $C_{35}H_{53}N_3NiO$: C, 71.19; H, 9.05; N, 7.12. Found: C, 70.82; H, 9.02; N, 7.09. ^{1}H NMR (400 MHz, 25 °C, benzene-d_6): δ 7.21-7.11 (m, 6H, Ar-**H**, dipp), 4.91 (s, 1H, γ-**H**), 3.90 (sept, $^3J_{HH}$, = 6.7 Hz, 4H, C**H**$(CH_3)_2$), 1.67 (d, $^3J_{HH}$, = 6.8 Hz, 12H, CH(C**H**$_3)_2$), 1.42 (d, $^3J_{HH}$, = 6.8 Hz, 12H, CH(C**H**$_3)_2$) 1.10 (s, 18H, C(C**H**$_3)_3$). ^{13}C NMR (125 MHz, 25 °C, benzene-d_6): δ 169.59 (Ar-C), 152.66 (Ar-C), 141.66 (Ar-C), 126.00 (Ar-C), 123.66 (Ar-C), 93.74 (γ-**C**) 43.70 (**C**$(CH_3)_3$), 33.32 (C(**C**$H_3)_3$), 29.16 (CH(**C**$H_3)_2$), 25.83 (CH(**C**$H_3)_2$), 23.56 (**C**$H(CH_3)_2$). IR (KBr Pellet, cm^{-1}): 1784 (s, ν_{NO}), 1647 (br w), 1537 (m), 1508 (s), 1464 (s), 1446 (s), 1435 (s), 1387 (s), 1365 (s), 1321 (s), 1259 (m), 1252 (m), 1221 (s), 1196 (m), 1180 (m), 1157 (m), 1040 (m), 1101 (s), 1055 (m), 1032 (m), 966 (w), 931 (w), 897 (w), 820 (m), 802 (m), 779 (m), 756 (m), 723 (w), 687 (w), 615 (w), 532 (w), 476 (w), 455 (w), 436 (w). IR (C_6H_6, cm^{-1}): 1784 (s, ν_{NO}). Anal. Calcd for **5.3**: $C_{12}H_{24}KNO_7S_2$: C, 36.25; H, 6.08; N, 3.52. Found: Trial 1: C, 38.40; H, 6.33; N, 3.21; Trial 2: C, 37.93; H, 6.30; N, 3.34. The high carbon percentage is attributed to the presence of a small amount of free 18-crown-6, which could not be separated from **5.3** by crystallization. ^{1}H NMR (400 MHz, 25 °C, benzene-d_6): δ 3.20 (s, 24H, 18-crown-6). IR

(KBr Pellet, cm^{-1}): 1969 (w), 1778 (w), 1639 (br w), 1473 (m), 1456 (m), 1435 (w), 1385 (m), 1352 (s), 1313 (m, ν_{NO}), 1282 (m), 1252 (m), 1223 (m), 1107 (s), 1030 (m), 962 (s), 860 (w), 837 (m), 804 (br m), 690 (w), 669 (m), 553 (m), 532 (w), 492 (br m), 409 (w). UV-vis (MeCN, 1.0 mM, 25 °C): 443 nm (ε = 930 $L \cdot mol^{-1} \cdot cm^{-1}$).

5.4.4 Reaction of [K(18-crown-6)][L^{tBu}Ni(S)] with one equiv of NO

A 50 mL Schlenk flask, equipped with a septum, was charged with a dark brown solution of [K(18-crown-6)][L^{tBu}Ni(S)] (19 mg, 0.021 mmol) in toluene (2 mL) and cooled to 0 °C. Under an atmosphere of N_2, NO gas (0.52 mL, 0.021 mmol) was slowly bubbled into the solution using an airtight, volumetric syringe. Upon addition of NO, the solution rapidly changed from dark brown to pale brown. After stirring for 10 min, the volatiles were removed *in vacuo*, and the flask was transferred to the glove box. The reaction mixture was dissolved in C_6D_6 (0.5 mL) to give a green-brown solution and a ^{1}H NMR spectrum of this sample was recorded. This spectrum revealed that presence of a mixture of complex **5.2** and [K(18-crown-6)][L^{tBu}Ni(S)] (**I**) in a ~ 2:1 ratio, along with a small amount (less than 5%) of an unidentified diamagnetic product (Figure S6-S7). ^{1}H NMR (400 MHz, 25 °C, benzene-d_6): δ 28.38 (**I**, s, 4H, Ar-*m***H**), 26.26 (**I**, s, C**H**$(CH_3)_2$), 16.07 (**I**, 12H, CH(C**H**$_3)_2$), 7.21-7.11 (**5.2**, m, 6H, Ar-**H**, dipp), 6.71 (**I**, 12H, CH(C**H**$_3)_2$), 4.91 (**5.2**, s, 1H, γ-**H**), 3.90 (**5.2**, sept, $^3J_{HH}$, = 6.7 Hz, 4H, C**H**$(CH_3)_2$), 2.73 (18-crown-6), 1.67 (**5.2**, d, $^3J_{HH}$, = 6.8 Hz, 12H, CH(C**H**$_3)_2$), 1.42 (**5.2**, d, $^3J_{HH}$, = 6.8 Hz, 12H, CH(C**H**$_3)_2$) 1.10 (**5.2**, s, 18H, C(C**H**$_3)_3$), -0.74 (**I**, 18H, C(C**H**$_3)_3$), -18.83 (**I**, 2H, Ar-*p***H**) ppm.

5.4.5 Synthesis of [PNP][SSNO] from [PNP][NO_2] and S_8

The synthesis of [PNP][SSNO] was performed according to the previously reported procedure with slight modifications.[35] To a stirring suspension of S_8 (117.5 mg, 0.458

mmol) in acetone (1 mL) was added an acetone (15 mL) solution of [PNP][NO_2] (PNP = Ph_3PNPPh_3) (1.068 g, 1.832 mmol). The reaction mixture was protected from light and allowed to stir 24 h, whereupon the sulfur was consumed and the reaction mixture turned dark orange. The reaction mixture was then filtered through a Celite column supported on glass wool (0.5 cm × 2 cm) to give a dark orange solution. Storage of this solution at -25 °C for 48 h results in the deposition of dark orange blocks (306 mg, 26%) that were isolated by decanting off the supernatant. This product was identified as [PNP][SSNO] by comparison of its unit cell (Orthorhombic P; V = 3098 $Å^3$; a = 11.90 Å, b = 15.55 Å, c = 16.74 Å, α = 90.00°, β = 90.00°, γ = 90.00°) with the previously reported values, and by IR spectroscopy (ν_{NO} = 1350 cm^{-1}, KBr mull).[35]

5.4.6 Synthesis of [PNP][SNO] from [PNP][SSNO] and PPh_3

The synthesis of [PNP][SNO] was performed according to a previously reported procedure with slight modifications. [35] To a stirring solution of [PNP][SSNO] (57.0 mg, 0.0877 mmol) in acetone (5 mL) was added a solution of PPh_3 (28.7 mg, 0.1754 mmol) in acetone (1 mL). This mixture was protected from light and allowed to stir for 24 h. After 24 h, the reaction mixture was a pale green color. This solution was concentrated *in vacuo* to ca. 1 mL, and filtered through a Celite column supported on glass wool (0.5 cm × 2 cm) to give a pale green solution. This solution was then transferred to a 5 mL vial. This vial was placed inside a 20 mL scintillation vial. Et_2O (2 mL) was then added to the outer vial. Storage of this two vial system at -25 °C for 24 h resulted in the deposition of white crystals of $Ph_3P{=}S$ (identified by ^{31}P NMR spectroscopy, δ = 42.29 ppm)[42] which were isolated by decanting off the supernatant. The pale green supernatant was then filtered through a Celite column supported on glass wool (0.5 cm × 2 cm) and concentrated *in vacuo* to ca. 0.25 mL

and transferred into a 5 mL vial. This vial was placed inside a 20 mL scintillation vial. Et_2O (2 mL) was then added to the outer vial. Storage of this two vial system at -25 °C for 72 h resulted in the deposition of pale green blocks (34 mg, 63%) which were isolated by decanting off the supernatant. This product was identified as [PNP][SNO] by UV-vis spectroscopy (λ_{max} = 334 nm, 1.0 mM in MeCN).

5.4.7 Reaction of [PNP][SNO] with excess NO

A quartz UV-vis cell equipped with a Teflon rotoflow valve was charged with an MeCN solution of [PNP][SNO] (4 mL, 1.0 mmol). A UV-vis spectrum of this solution was recorded, which revealed a strong absorbance at 334 nm (Figure S14). The headspace was then evacuated and filled with NO gas (1 atm). After addition of NO, the solution rapidly changed from pale green to orange. A UV-vis spectrum of the reaction mixture was re-recorded. This spectrum revealed the complete consumption of the band assigned to [PNP][SNO], and the appearance of a new feature at 445 nm that is attributed to the presence of [PNP][SSNO] (Figure 5.4).[35]

5.4.8 X-ray Crystallography

Data for **5.1**-**5.3** were collected on a Bruker KAPPA APEX II diffractometer equipped with an APEX II CCD detector using a TRIUMPH monochromator with a Mo Kα X-ray source (α = 0.71073 Å). The crystals were mounted on a cryoloop under Paratone-N oil, and all data were collected at 100(2) K using an Oxford nitrogen gas cryostream. Data were collected using ω scans with 0.5° frame widths. Frame exposures of 15, 10, and 5 seconds were used for **5.1**, **5.2**, and **5.3**, respectively. Data collection and cell parameter determination were conducted using the SMART program.[43] Integration of the data frames and final cell parameter refinement were performed using SAINT software.[44] Absorption

correction of the data was carried out using the multi-scan method SADABS.[45] Subsequent calculations were carried out using SHELXTL.[46] Structure determination was done using direct or Patterson methods and difference Fourier techniques. All hydrogen atom positions were idealized, and rode on the atom of attachment. Structure solution, refinement, graphics, and creation of publication materials were performed using SHELXTL.[46]

In complex **5.1**, two of the C_6H_6 solvate molecules exhibited some positional disorder; alternate positions were found for both molecules: one was refined in a 50:50 ratio, and the second was modelled in a 57:43 ratio, using the FVAR command in SHELXL. The C-C bonds in the C_6H_6 molecules were constrained to 1.4 Å using the DFIX command. Hydrogen atoms were not added to disordered carbon atoms. Additionally, the $[SCO]^{2-}$ ligand was found to be disordered over two orientations, which were related by a C_2 rotation about the Ni-K vector. These two orientations were modelled in a 70:30 ratio using the FVAR command in SHELXL. In complex **5.2**, the O-atom in the NO ligand is disordered over two positions, which were modelled in a 50:50 ratio using the FVAR command in SHELXL. Additionally, the NO bond lengths were constrained using the SADI command in SHELXL. Further crystallographic details for complexes **5.1**-**5.3** can be found in Table 5.1.

Table 5.1. X-ray Crystallographic Data for Complexes 5.1, 5.2, and 5.3.

	5.1·$2C_6H_6$	**5.2**	**5.3**·CH_2Cl_2
empirical formula	$C_{48}H_{77}KN_2NiO_7S·2C_6H_6$	$C_{35}H_{53}N_3NiO$	$C_{12}H_{24}KNO_7S_2·CH_2Cl_2$
crystal habit, color	Plate, Orange	Plate, Blue-Orange	Plate, Orange
crystal size (mm)	0.15 × 0.1 × 0.05	0.2 × 0.15 × 0.05	0.5 × 0.4 × 0.1
crystal system	Triclinic	Monoclinc	Monoclinc
space group	*P-1*	*C2/c*	*P21/n*
volume ($Å^3$)	3071.9(9)	3414.4(4)	2205.4(5)
a (Å)	12.668(2)	16.832(1)	9.477(1)
b (Å)	13.370(2)	9.3700(6)	14.048(2)
c (Å)	20.680(3)	22.582(2)	16.771(3)
α (deg)	80.951(4)	90	90
β (deg)	88.335(4)	106.526(5)	98.978(4)
γ (deg)	62.771(3)	90	90
Z	2	4	4
formula weight (g/mol)	1080.18	590.51	482.47
density (calculated)	1.158	1.149	1.453
absorption coefficient	0.466	0.597	0.704
F_{000}	1146	1280	1008
total no. reflections	27019	12977	9506
unique reflections	12508	4835	4564
R_{int}	0.0559	0.0574	0.0280
final R indices (I >2σ(I)]	R_1 = 0.0791 wR_2 = 0.2006	R_1 = 0.0513 wR_2 = 0.1073	R_1 = 0.0343 wR_2 = 0.0676
largest diff. peak and hole	1.725 and -0.687	0.642 and -0.643	0.485 and -0.556
GOF	1.038	1.035	1.016

5.5 Appendix

5.5.1 NMR Spectra

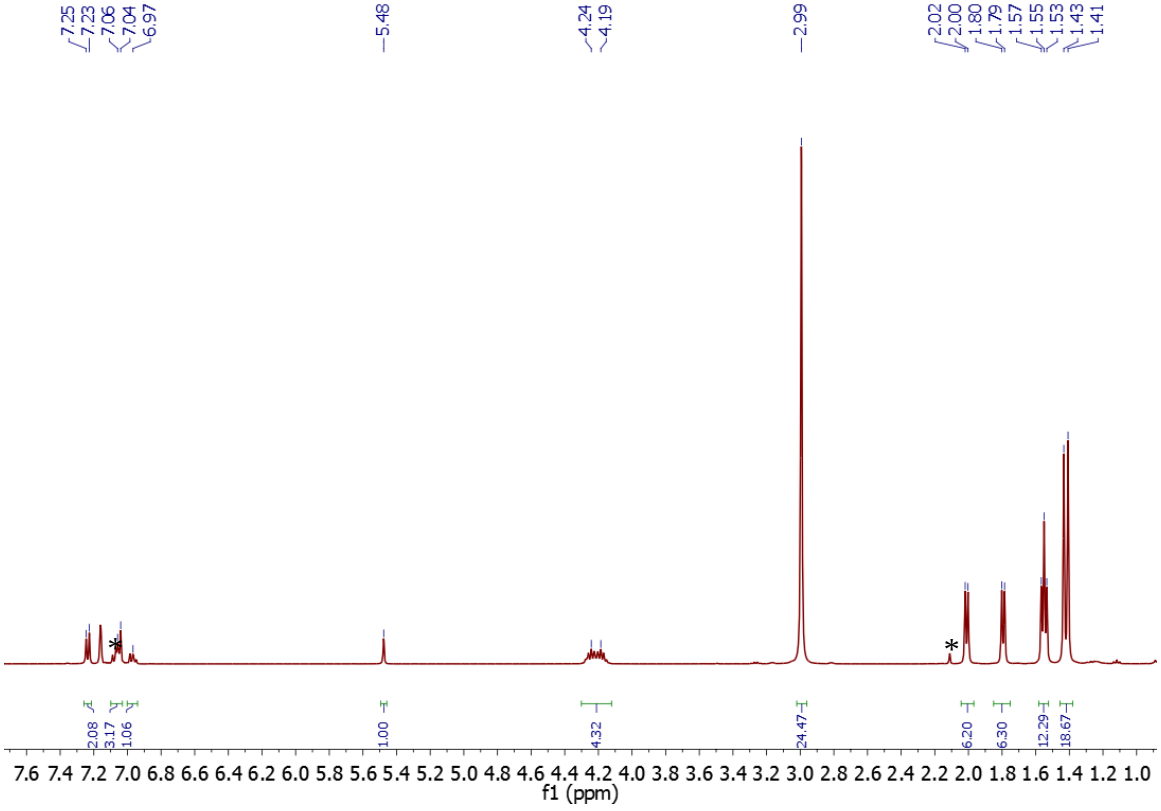

Figure A 5.1. ^{1}H NMR spectrum of [K(18-crown-6)][L^{tBu}Ni(*C*,*S*:η^{2}-C(O)S)] (**5.1**) in benzene-d_6. (*) indicates the presence of toluene.

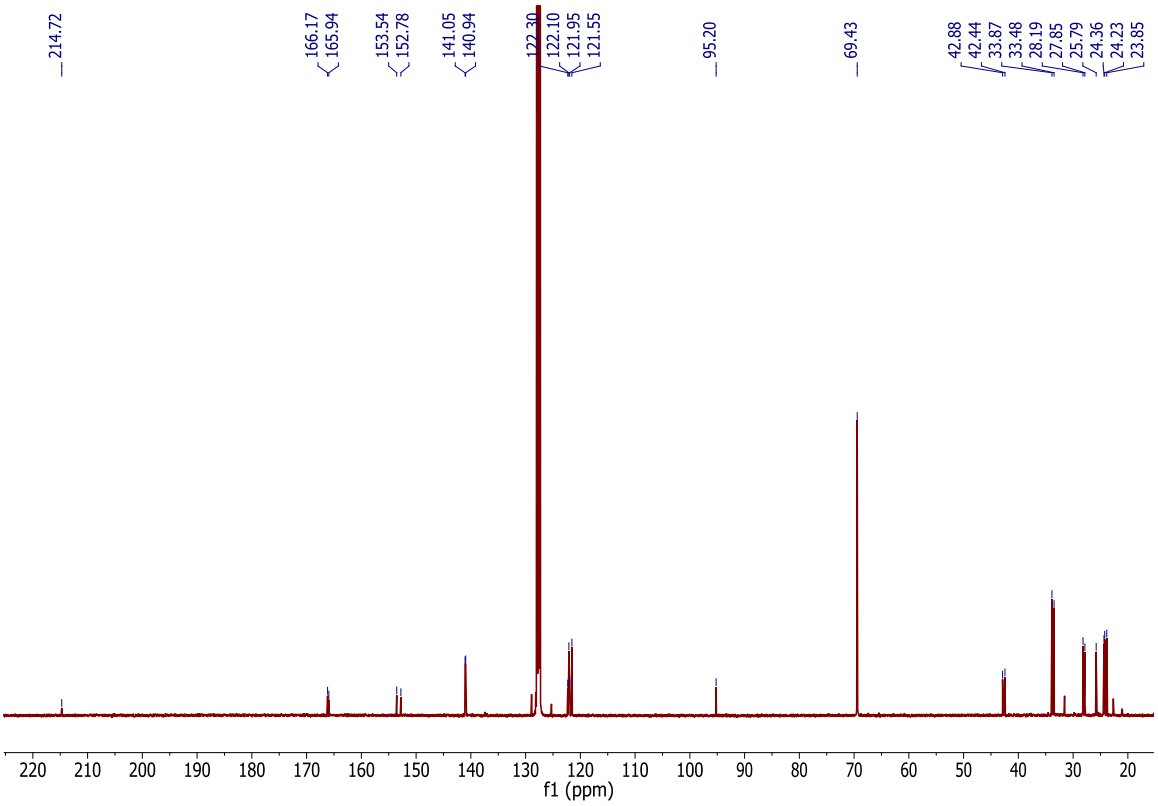

Figure A 5.2. ^{13}C NMR spectrum of [K(18-crown-6)][L^{tBu}Ni(*C*,*S*:η^2-C(O)S)] (**5.1**) in benzene-d_6.

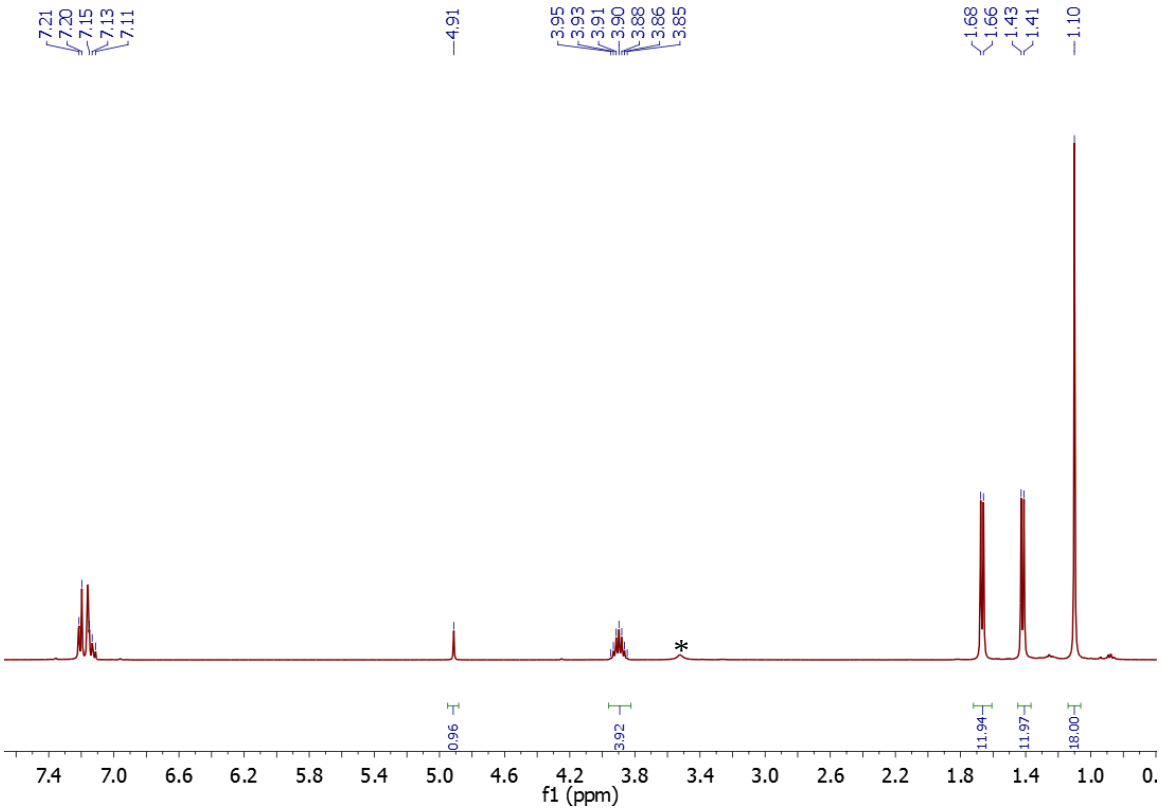

Figure A 5.3. ^{1}H NMR spectrum of [L^{tBu}Ni(NO)] (**5.2**) in benzene-d_6. (*) indicates the presence of free 18-crown-6.

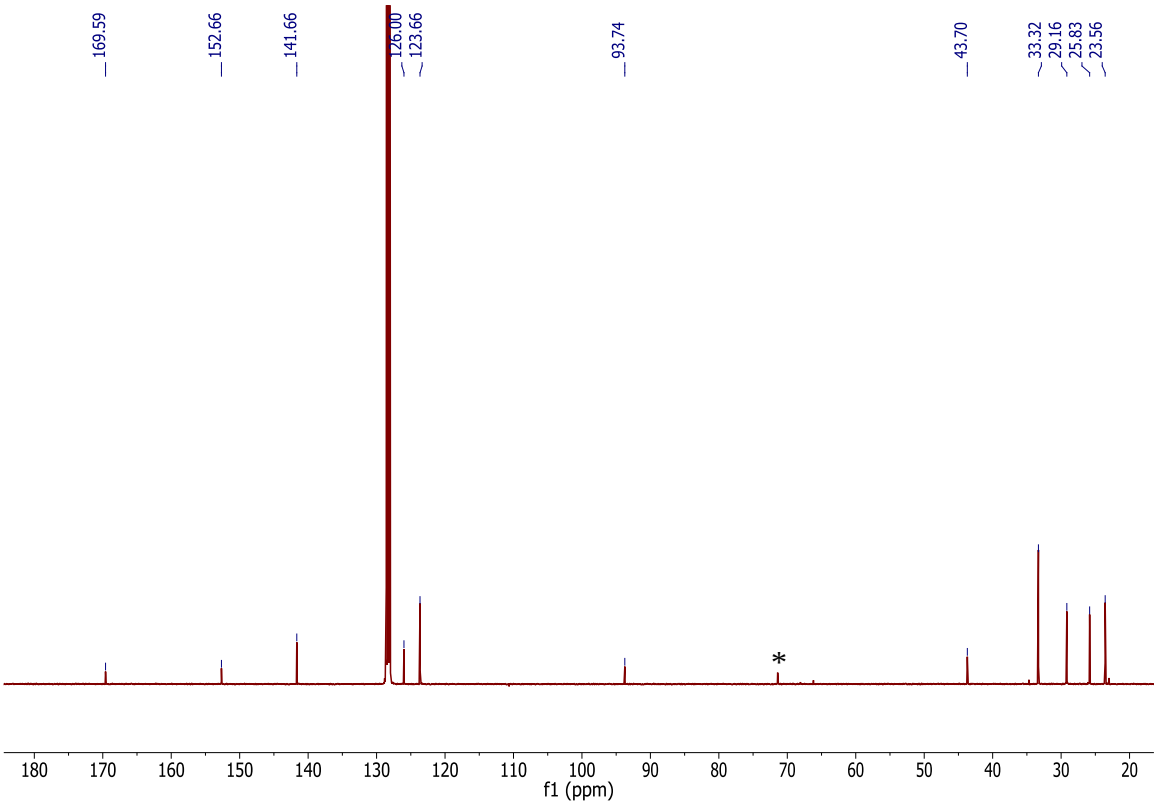

Figure A 5.4. ^{13}C NMR spectrum of [L^{tBu}Ni(NO)] (**5.2**) in benzene-d_6. (*) indicates the presence of free 18-crown-6.

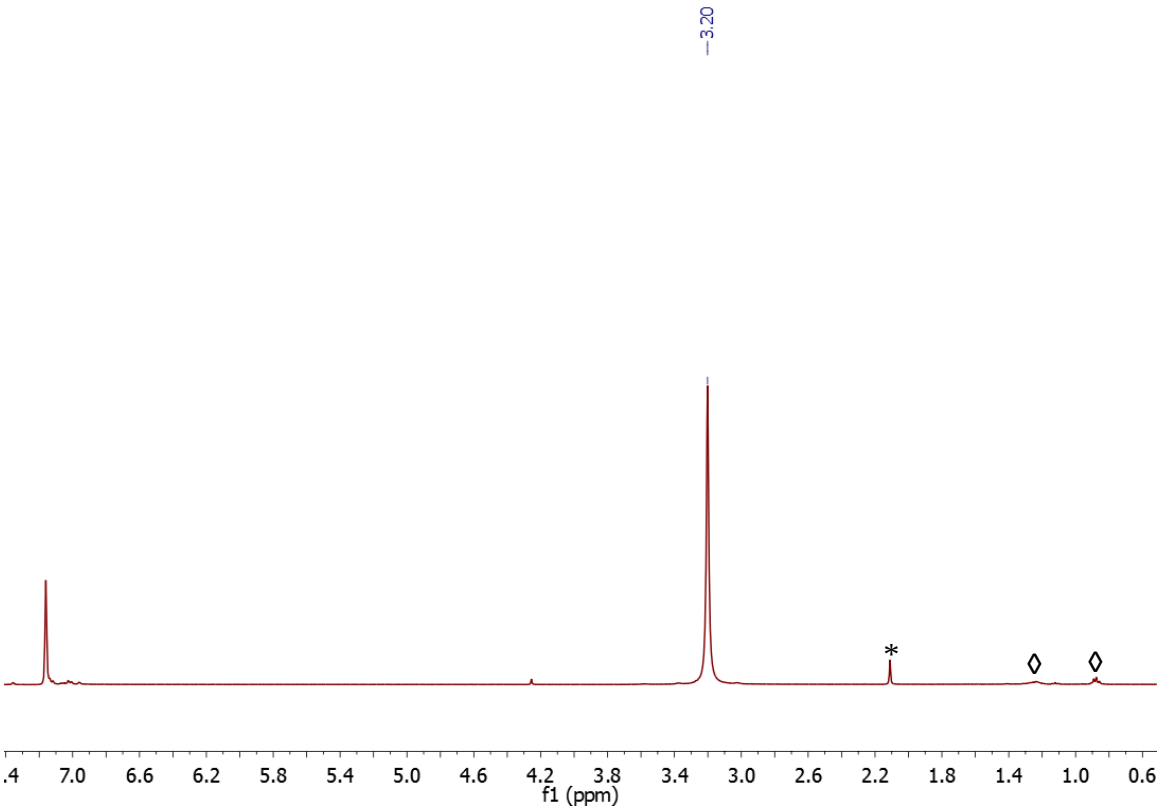

Figure A 5.5. ^{1}H NMR spectrum of [K(18-crown-6)][SSNO] (**5.3**) in C_6D_6. (*) indicates the presence of toluene and (◊) indicates the presence of pentane.

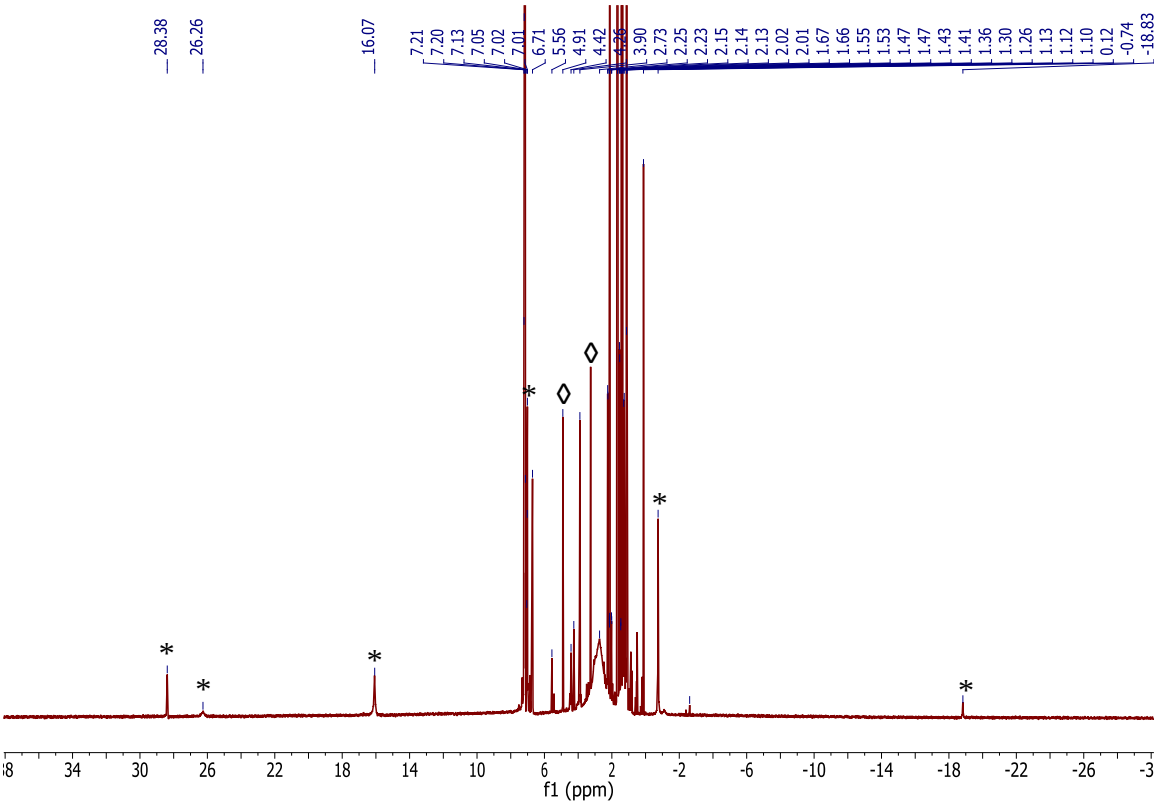

Figure A 5.6. ^{1}H NMR spectrum of reaction of [K(18-crown-6)][L^{tBu}Ni(S)] with one equiv of NO in benzene-d_6. (*) indicates the presence of [K(18-crown-6)][L^{tBu}Ni(S)] and (◊) indicates the presence of [L^{tBu}Ni(NO)] (**5.2**).

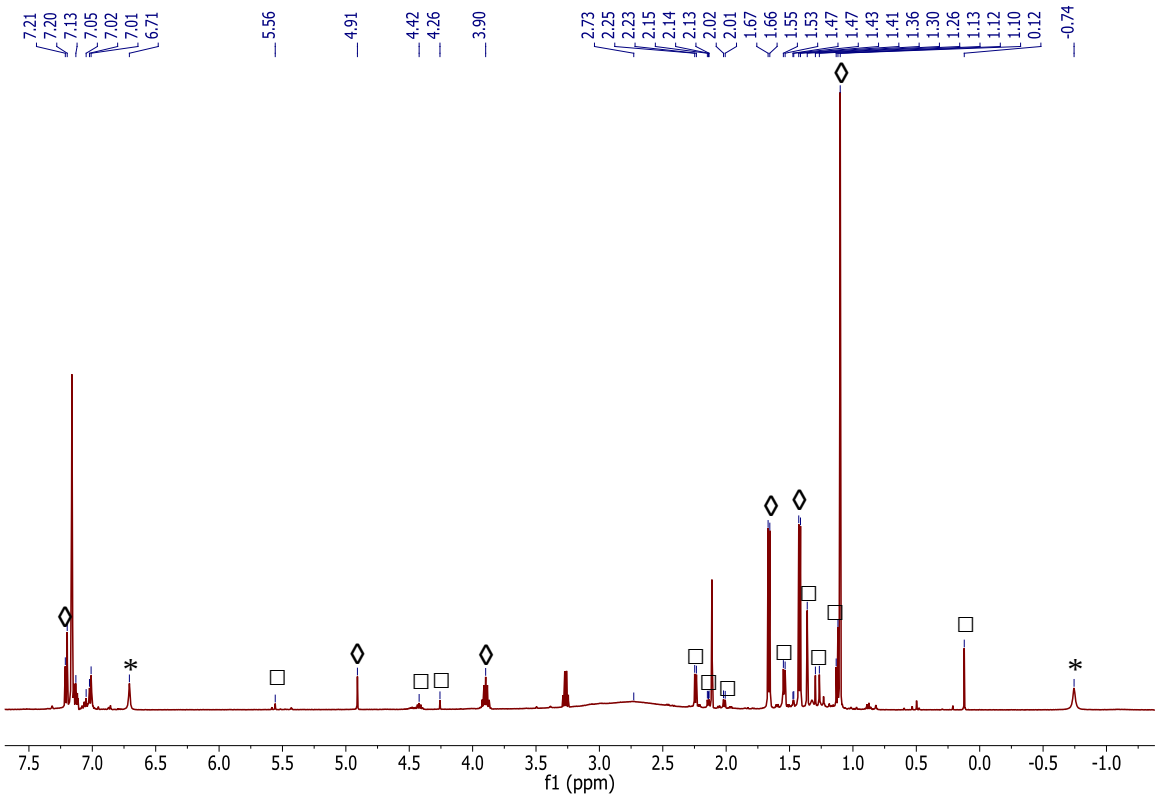

Figure A 5.7. Partial ^{1}H NMR spectrum of reaction of [K(18-crown-6)][L^{tBu}Ni(S)] with one equiv of NO in benene-d_6. (*) indicates the presence of [K(18-crown-6)][L^{tBu}Ni(S)], (◊) indicates the presence of [L^{tBu}Ni(NO)] (**5.2**), (□) indicates the presence of unidentified minor side products.

5.5.2 IR Spectra

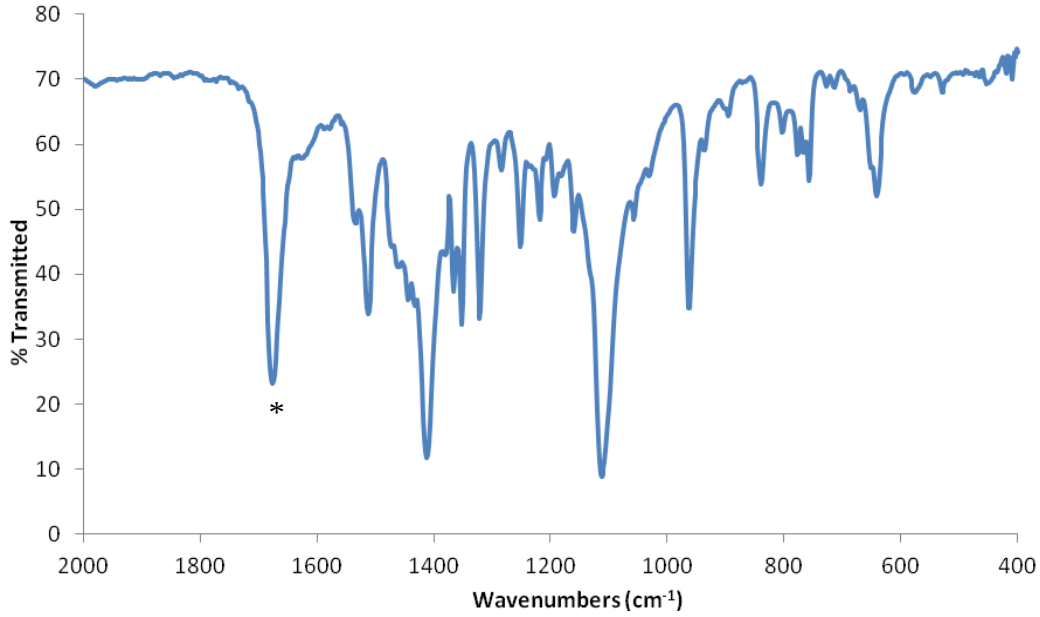

Figure A 5.8. Partial IR spectrum of complex **5.1** (KBr pellet). (*) indicates the ν_{CO} stretch (1676 cm^{-1}).

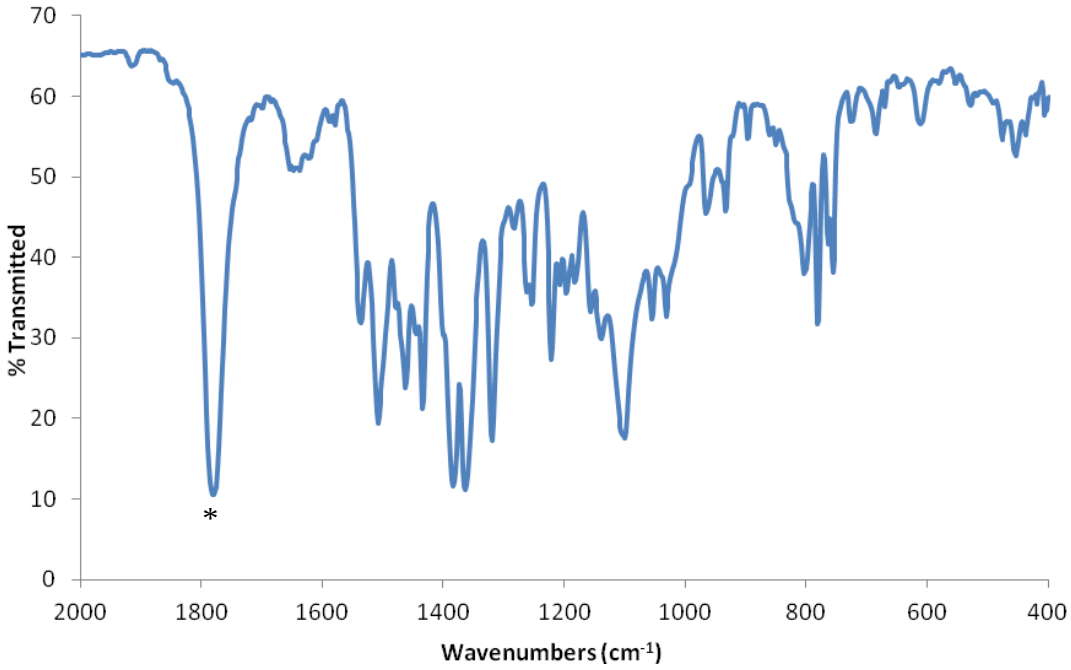

Figure A 5.9. Partial IR spectrum of complex **5.2** (KBr pellet). (*) indicates the ν_{NO} stretch (1784 cm^{-1}).

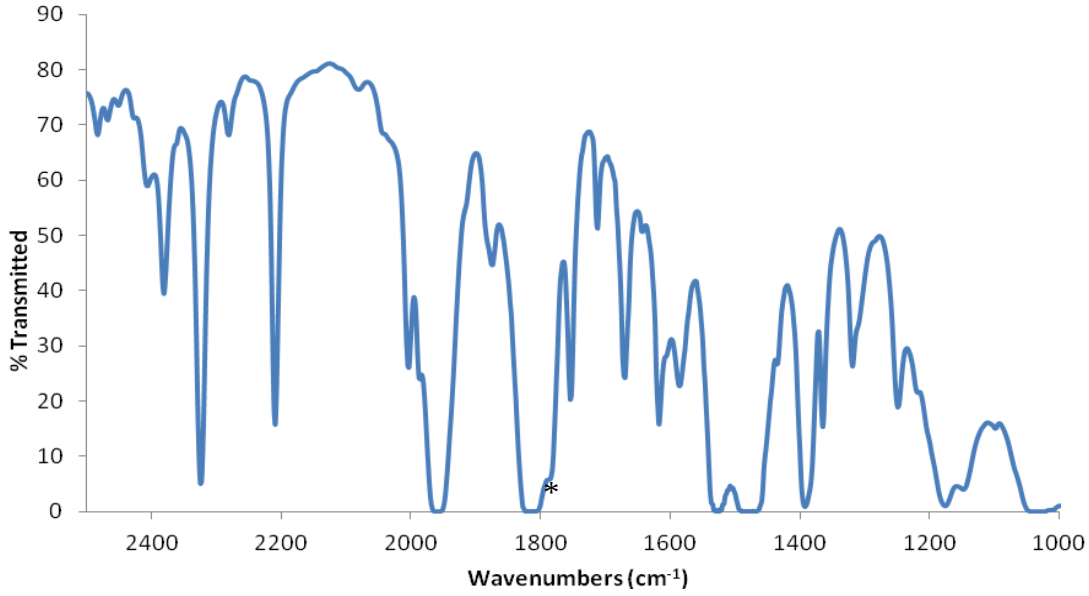

Figure A 5.10. Partial solution IR spectrum of complex **5.2** (C_6H_6, 25 ^{o}C). (*) indicates the ν_{NO} stretch (1784 cm^{-1}).

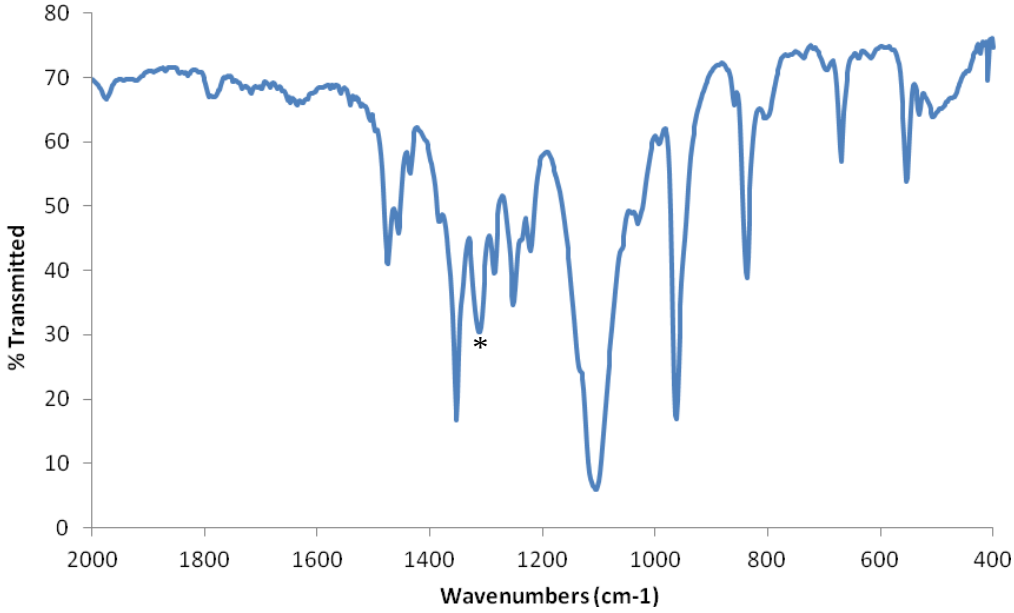

Figure A 5.11. Partial IR spectrum of complex **5.3** (KBr pellet). (*) indicates the ν_{NO} stretch (1313 cm^{-1}).

5.5.3 UV-Vis Data

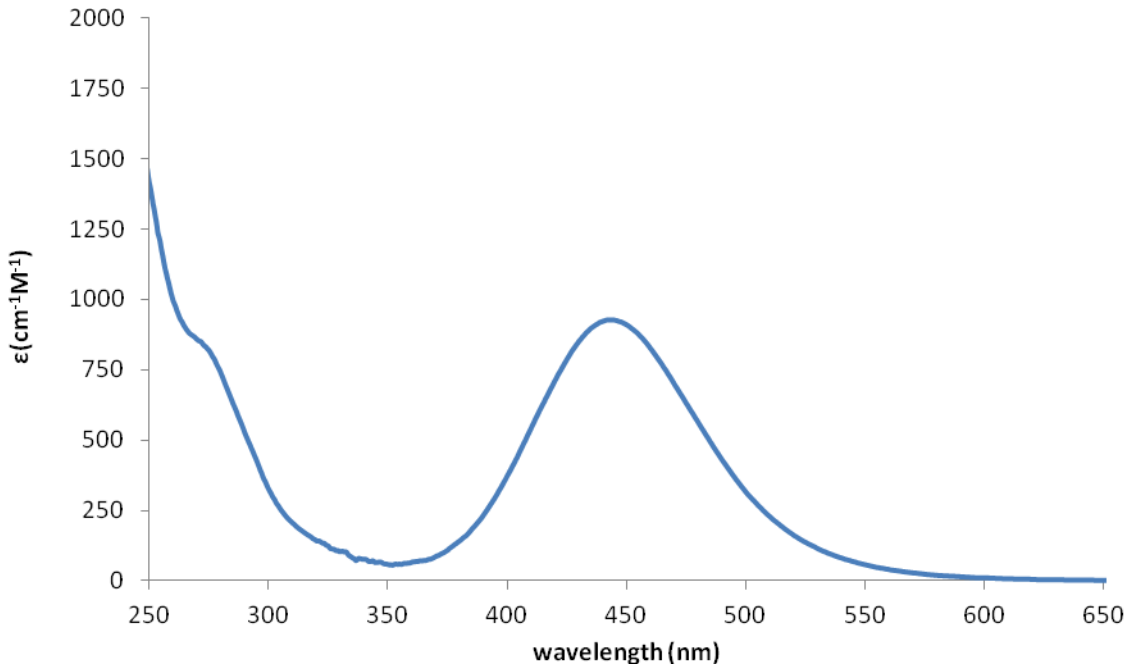

Figure A 5.12. UV-vis spectrum of complex **5.3** (1.0 mM in MeCN).

5.6 References

(1) Mustafa, A. K.; Gadalla, M. M.; Snyder, S. H. Signaling by Gasotransmitters. *Sci. Signal.* **2009**, *2* (68), re2.

(2) Wang, R. Gasotransmitters: Growing Pains and Joys. *Trends Biochem. Sci.* **2014**, *39* (5), 227.

(3) Chapin, F. S.; Woodwell, G. M.; Randerson, J. T.; Rastetter, E. B.; Lovett, G. M.; Baldocchi, D. D.; Clark, D. A.; Harmon, M. E.; Schimel, D. S.; Valentini, R.; et al. Reconciling Carbon-Cycle Concepts, Terminology, and Methods. *Ecosystems* **2006**, *9* (7), 1041.

(4) Cortese-Krott, M. M.; Kuhnle, G. G. C.; Dyson, A.; Fernandez, B. O.; Grman, M.; DuMond, J. F.; Barrow, M. P.; McLeod, G.; Nakagawa, H.; Ondrias, K.; et al. Key Bioactive Reaction Products of the NO/H_2S Interaction Are S/N-Hybrid Species, Polysulfides, and Nitroxyl. *Proc. Natl. Acad. Sci. U.S.A.* **2015**, *112* (34), E4651.

(5) Fitzpatrick, J.; Kim, E. Synthetic Modeling Chemistry of Iron–Sulfur Clusters in Nitric Oxide Signaling. *Acc. Chem. Res.* **2015**, *48* (8), 2453.

(6) Tran, C. T.; Williard, P. G.; Kim, E. Nitric Oxide Reactivity of [2Fe-2S] Clusters Leading to H_2S Generation. *J. Am. Chem. Soc.* **2014**, *136* (34), 11874.

(7) Cortese-Krott, M. M.; Fernandez, B. O.; Santos, J. L. T.; Mergia, E.; Grman, M.; Nagy, P.; Kelm, M.; Butler, A.; Feelisch, M. Nitrosopersulfide ($SSNO^-$) Accounts for Sustained NO Bioactivity of S-Nitrosothiols Following Reaction with Sulfide. *Redox Biol.* **2014**, *2*, 234.

(8) Wedmann, R.; Zahl, A.; Shubina, T. E.; Dürr, M.; Heinemann, F. W.; Bugenhagen, B. E. C.; Burger, P.; Ivanovic-Burmazovic, I.; Filipovic, M. R. Does Perthionitrite ($SSNO^-$) Account for Sustained Bioactivity of NO? A (Bio)Chemical Characterization. *Inorg. Chem.* **2015**, *54* (19), 9367.

(9) Dobbek, H.; Gremer, L.; Kiefersauer, R.; Huber, R.; Meyer, O. Catalysis at a Dinuclear [CuSMo(O)OH] Cluster in a CO Dehydrogenase Resolved at 1.1-Å Resolution. *Proc. Natl. Acad. Sci.* **2002**, *99* (25), 15971.

(10) Hartmann, N. J.; Wu, G.; Hayton, T. W. Synthesis of a "Masked" Terminal Nickel(II) Sulfide by Reductive Deprotection and Its Reaction with Nitrous Oxide. *Angew. Chem. Int. Ed.* **2015**, *54* (49), 14956.

(11) Hartmann, N. J.; Wu, G.; Hayton, T. W. Activation of CS_2 by a "Masked" Terminal Nickel Sulfide. *Dalt. Trans.* **2016**, *45*, 14508.

(12) Hartmann, N. J.; Wu, G.; Hayton, T. W. Trapping of an Ni II Sulfide by a Co I Fulvene Complex. *Organometallics* **2017**, *36* (9), 1765.

(13) Can, M.; Armstrong, F. A.; Ragsdale, S. W. Structure, Function, and Mechanism of the Nickel Metalloenzymes, CO Dehydrogenase, and Acetyl-CoA Synthase. *Chem. Rev.* **2014**, *114* (8), 4149.

(14) George, G. N.; Pickering, I. J.; Yu, E. Y.; Prince, R. C.; Bursakov, S. A.; Gavel, O. Y.; Moura, I.; Moura, J. J. G. A Novel Protein-Bound Copper−Molybdenum Cluster. *J. Am. Chem. Soc.* **2000**, *122* (34), 8321.

(15) Pomowski, A.; Zumft, W. G.; Kroneck, P. M. H.; Einsle, O. N_2O Binding at a [4Cu:2S] Copper-Sulphur Cluster in Nitrous Oxide Reductase. *Nature* **2011**, *477* (7363), 234.

(16) Brown, K.; Djinovic-Carugo, K.; Haltia, T.; Cabrito, I.; Saraste, M.; Moura, J. G.;

Moura, I.; Tegoni, M.; Cambillau, C. Revisiting the Catalytic CuZ Cluster of Nitrous Oxide (N_2O) Reductase: Evidence of a Bridging Inorganic Sulfur. *J. Biol. Chem.* **2000**, *275* (52), 41133.

(17) Brown, K.; Tegoni, M.; Prudencio, M.; Pereira, A. S.; Besson, S.; Moura, J. J.; Moura, I.; Cambillau, C. A Novel Type of Catalytic Copper Cluster in Nitrous Oxide Reductase. *Nat. Struct. Biol.* **2000**, *7* (3), 191.

(18) Dobbek, H.; Svetlitchnyi, V.; Gremer, L.; Huber, R.; Meyer, O. Crystal Structure of a Carbon Monoxide Dehydrogenase Reveals a [Ni-4Fe-5S] Cluster. *Science* **2001**, *293* (5533), 1281.

(19) Johnson, B. J.; Lindeman, S. V; Mankad, N. P. Assembly, Structure, and Reactivity of Cu_4S and Cu_3S Models for the Nitrous Oxide Reductase Active Site, CuZ*. *Inorg. Chem.* **2014**, *53* (19), 10611.

(20) Zhai, J.; Hopkins, M. D.; Hillhouse, G. L. Synthesis and Structure of a $Cu(I)_3S$ Cluster Unsupported by Other Bridging Ligands. *Organometallics* **2015**, *34* (19), 4637.

(21) Zhang, S.; Melzer, M. M.; Sen, S. N.; Çelebi-Ölçüm, N.; Warren, T. H. A Motif for Reversible Nitric Oxide Interactions in Metalloenzymes. *Nat. Chem.* **2016**, *8* (7), 663.

(22) Olechnowicz, F.; Hillhouse, G. L.; Jordan, R. F. Synthesis and Reactivity of NHC-Supported $Ni_2(\mu^2\text{-}\eta^2,\eta^2\text{-}S_2)$-Bridging Disulfide and $Ni_2(\mu\text{-}S)_2$-Bridging Sulfide Complexes. *Inorg. Chem.* **2015**, *54* (6), 2705.

(23) Fu, P. F.; Khan, M. A.; Nicholas, K. M. Facile Transformation of a Metal Carbonyl to a Metal Carbonyl Sulfide by Reaction with Elemental Sulfur. *Organometallics* **1993**, *12* (10), 3790.

(24) Smiles, D. E.; Wu, G.; Hayton, T. W. Synthesis of Uranium–Ligand Multiple Bonds by Cleavage of a Trityl Protecting Group. *J. Am. Chem. Soc.* **2014**, *136* (1), 96.

(25) Smiles, D. E.; Wu, G.; Kaltsoyannis, N.; Hayton, T. W. Thorium-Ligand Multiple Bonds via Reductive Deprotection of a Trityl Group. *Chem. Sci.* **2015**, *6* (6), 3891.

(26) Anderson, J. S.; Iluc, V. M.; Hillhouse, G. L. Reactions of CO_2 and CS_2 with 1,2-Bis(Di-Tert-Butylphosphino)Ethane Complexes of Nickel(0) and Nickel(I). *Inorg. Chem.* **2010**, *49* (21), 10203.

(27) Choon Hong, C.; Hor, T. S. A. Facile Reductive Excision of Sulfur from a $\{Pt_2S_2\}$ Core in $[Pt_2(PPh_3)_4(\mu\text{-}S)_2]$ to a $\{Pt_2S\}$ Triangle by Carbon Monoxide. *J. Organomet. Chem.* **1996**, *509* (1), 101.

(28) Farrell, W. S.; Zavalij, P. Y.; Sita, L. R. Metal-Catalyzed "On-Demand" Production of Carbonyl Sulfide from Carbon Monoxide and Elemental Sulfur. *Angew. Chem. Int. Ed.* **2015**, *54* (14), 4269.

(29) Pandey, K. K. Reactivities of Carbonyl Sulfide (COS), Carbon Disulfide (CS_2) and Carbon Dioxide(CO_2)with Transition Metal Complexes. *Coord. Chem. Rev.* **1995**, *140*, 37.

(30) Winkler, U.; Khan, M. A.; Nicholas, K. M. Atom Addition and Insertion Reactions of $(MeCp)_2Ta(H)CO$ with Sulfur, Tellurium, Carbonyl Sulfide and Carbon Disulfide. *Inorg. Chem. Comm.* **1998**, *1* (8), 317.

(31) Katayama, Y.; Narahara, Y.; Inoue, Y.; Amano, F.; Kanagawa, T.; Kuraishi, H. A Thiocyanate Hydrolase of Thiobacillus Thioparus. A Novel Enzyme Catalyzing the Formation of Carbonyl Sulfide from Thiocyanate. *J. Biol. Chem.* **1992**, *267* (13), 9170.

(32) Katayama, Y.; Matsushita, Y.; Kaneko, M.; Kondo, M.; Mizuno, T.; Nyunoya, H. Cloning of Genes Coding for the Three Subunits of Thiocyanate Hydrolase of Thiobacillus Thioparus THI 115 and Their Evolutionary Relationships to Nitrile Hydratase. *J. Bacteriol.* **1998**, *180* (10), 2583.
(33) Bezsudnova, E. Y.; Sorokin, D. Y.; Tikhonova, T. V; Popov, V. O. Thiocyanate Hydrolase, the Primary Enzyme Initiating Thiocyanate Degradation in the Novel Obligately Chemolithoautotrophic Halophilic Sulfur-Oxidizing Bacterium Thiohalophilus Thiocyanoxidans. *Biochim. Biophys. Acta* **2007**, *1774* (12), 1563.
(34) Puiu, S. C.; Warren, T. H. Three-Coordinate β-Diketiminato Nickel Nitrosyl Complexes from Nickel(I)−Lutidine and Nickel(II)−Alkyl Precursors. *Organometallics* **2003**, *22* (20), 3974.
(35) Seel, F.; Kuhn, R. G.; Simon, G.; Wagner, M.; Krebs, B.; Dartmann, M. PNP-Perthionitrite and PNP-Monothionitrite. *Z. Naturforsch. B* **1985**, *40*, 1607.
(36) Gao, Y.; Toubaei, A.; Kong, X.; Wu, G. Solving the 170-Year-Old Mystery About Red-Violet and Blue Transient Intermediates in the Gmelin Reaction. *Chem. Eur. J.* **2015**, *21* (48), 17172.
(37) Cortese-Krott, M. M.; Butler, A. R.; Woollins, J. D.; Feelisch, M. Inorganic Sulfur-Nitrogen Compounds: From Gunpowder Chemistry to the Forefront of Biological Signaling. *Dalt. Trans.* **2016**, *45*, 5908.
(38) Nava, M.; Martin-Drumel, M. A.; Lopez, C. A.; Crabtree, K. N.; Womack, C. C.; Nguyen, T. L.; Thorwirth, S.; Cummins, C. C.; Stanton, J. F.; McCarthy, M. C. Spontaneous and Selective Formation of HSNO, a Crucial Intermediate Linking H_2S and Nitroso Chemistries. *J. Am. Chem. Soc.* **2016**, *138* (36), 11441.
(39) Martinsen, A.; Songstad, J. Preparation and Properties of Some Bis(Triphenylphosphine)-Iminium Salts, $[(Ph_3P)_2N]X$. *Acta Chem. Scand. A* **1977**, *31*, 645.
(40) Harris Robin, K.; Becker Edwin, D.; Cabral de Menezes Sonia, M.; Goodfellow, R.; Granger, P. NMR Nomenclature: Nuclear Spin Properties and Conventions for Chemical Shifts. IUPAC Recommendations 2001. International Union of Pure and Applied Chemistry. Physical Chemistry Division. Commission on Molecular Structure and Spectroscopy. *Pure Appl. Chem.* **2002**, *40* (7), 489.
(41) Harris Robin, K.; Becker Edwin, D.; Cabral De Menezes Sonia, M.; Granger, P.; Hoffman Roy, E.; Zilm Kurt, W. Further Conventions for NMR Shielding and Chemical Shifts. *Pure Appl. Chem.* **2008**, *80*, 59.
(42) Baccolini, G.; Boga, C.; Mazzacurati, M. Highly Atom-Economic One-Pot Formation of Three Different C−P Bonds: General Synthesis of Acyclic Tertiary Phosphine Sulfides. *J. Org. Chem.* **2005**, *70* (12), 4774.
(43) SMART Apex II. Bruker AXS Inc.: Madison, WI 2005.
(44) SAINT Software User's Guide. Bruker AXS Inc.: Madison, WI 2005.
(45) Sheldrick, G. M. SADABS. University of Gottingen: Germany 2005.
(46) SHELXTL PC. Bruker AXS Inc.: Madison, WI 2005.

Chapter 6 Reduction of N_2O Mediated by a "Masked" Terminal Nickel(II) Sulfide

Portions of this work were published in:

Nathaniel J. Hartmann , Guang Wu, Trevor W. Hayton

Angew. Chem. Int. Ed., **2015**, *54*, 14956-14959.

Table of Contents

6.1 Introduction

Nitrous oxide (N_2O) features a long atmospheric lifetime and large global warming potential (ca. 300 times larger than CO_2), making it an important greenhouse gas.[1–4] Anthropogenic sources of N_2O include agriculture, fossil fuel combustion, adipic acid synthesis, and nitric acid production.[1,5] The latter two sources use on-site N_2O mitigation to remove N_2O from the effluent stream, either by decomposition to the elements[6] or reduction to N_2 and H_2O, but neither of these methods is completely effective and some N_2O is still released into the atmosphere.[7]

Given the above considerations, the development of new catalysts for N_2O reduction could help reduce its impact on global temperatures.[1,8] Not surprisingly, a large number of heterogeneous systems have been developed to catalyze this reaction.[9] Of most relevance to the current study are the catalyst systems used for automotive applications, which consist of nanoparticulate Pt and Rh on a ceramic support. This process uses partially oxidized fuel (i.e., CO) to reduce N_2O, forming N_2 and CO_2.[9] Sita and co-workers developed a *homogeneous* version of this transformation, mediated by the Mo(II) complex, $Cp^*Mo(NCN)(CO)_2$ (NCN = $^{i}PrNC(Me)N^{i}Pr$).[10] In this process, N_2O oxidizes $Cp^*Mo(NCN)(CO)_2$ to form a Mo(IV) oxo, $Cp^*Mo(NCN)(O)$, which then reacts with CO to form CO_2 and regenerate $Cp^*Mo(NCN)(CO)_2$. However, an N-N bond cleavage reaction, which results in irreversible formation of $Cp^*Mo(NCN)(NCO)(NO)$, was found to be competitive with oxo formation (Figure 6.1). Similarly, Limberg and co-workers reported the stoichiometric oxidation of a Ni(0) CO complex, $[K]_2[L^{tBu}Ni^{0}(CO)]_2$, with N_2O to form a carbonate complex, $[K]_6[L^{tBu}Ni^{II}(CO_3)]_6$, and N_2.[11] Subsequent release of carbonate from the metal center was not discussed. The homogeneous hydrogenation of N_2O has also been explored.[12,13] For example, in 2015 Piers and co-workers reported an Ir(III) pincer carbene

complex that could hydrogenate N_2O;[14] however, this system was not reported to be catalytic. More recently, Milstein and co-workers reported that the Ru pincer complex, (PNP)RuH(CO)(OH) (PNP = 2,6-$CH_2P^iPr_2(C_5H_3N)$), was an effective catalyst for the hydrogenation of N_2O, achieving a turnover number of ca. 400.[15]

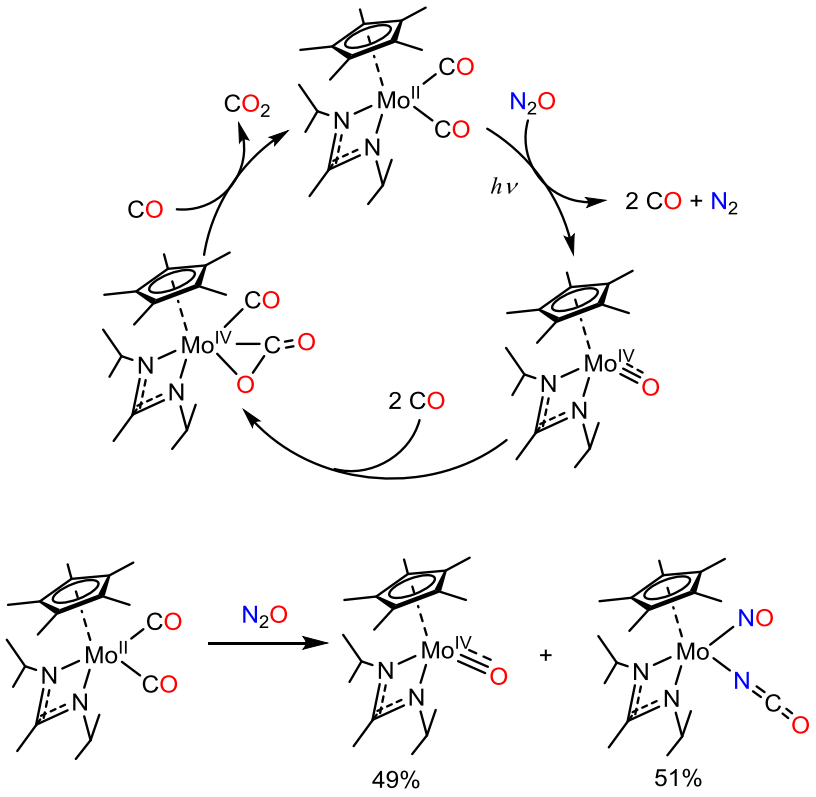

Figure 6.1. Homogeneous nitrous oxide reduction. Ref. 10.

In Chapters 2-5, I established the nucleophilic reactivity of "masked" terminal nickel sulfide complexes, [K(L)][L^RNi^{II}(S)] (**2.4-2.6**), with a variety of electrophiles (Me_3SiOTf, [CoCp*(C_5Me_4=CH_2)]) and small molecules (CS_2, CO, and NO). In Chapter 6, I will describe the reaction of [K(18-crown-6)][$L^{tBu}Ni^{II}$(S)] (**2.5**) with N_2O to yield an unprecedented thiohyponitrite complex, [K(18-crown-6)][$L^{tBu}Ni^{II}$(κ^2-SNNO)].[16] Given the challenge of activating N_2O,[17] and the novelty of the $[SNNO]^{2-}$ ligand, I also endeavored to

explore its reactivity in an effort to uncover new routes to N_2O reduction and better understand the chemistry of this enigmatic molecule.

6.2 Results and Discussion

6.2.1 Synthesis and Characterization of [K(18-crown-6)][L^{tBu}Ni(κ^2-SNNO)] (6.1)

Exposure of [K(18-crown-6)][$L^{tBu}Ni^{II}$(S)] (**2.5**) to an atmosphere of nitrous oxide (N_2O) results in a rapid color change from dark brown to yellow. Isolation of the resulting product via crystallization from toluene/isooctane provides [K(18-crown-6)][L^{tBu}Ni(κ^2-SNNO)] (**6.1**) as an orange crystalline solid in 62% yield (Scheme 6.1).

Scheme 6.1 Synthesis of [$L^{tBu}Ni^{II}$(κ^2-SNNO)] (**6.1**)

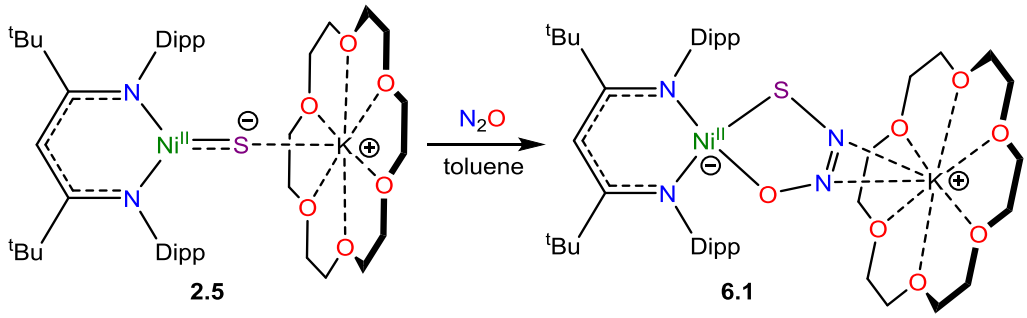

Complex **6.1** crystallizes in the triclinic space group *P-1*, and its solid state molecular structure is shown in Figure 6.2. Complex **6.1** features an unprecedented κ^2-thiohyponitrite ([SNNO]$^{2-}$) ligand, formed by [3 + 2] cycloaddition of N_2O across the Ni-S bond. The S-N and O-N distances in the [SNNO]$^{2-}$ moiety are 1.787(6) Å and 1.308(1) Å, respectively, are suggestive of single bonds, while the N-N bond length of 1.154(9) Å is indicative of a double bond. Finally, the [K(18-crown-6)]$^+$ moiety in **6.1** features a dative interaction with the thiohyponitrite ligand, and its N-K distances are 2.911(8) and 2.914(6) Å.

The ^{1}H NMR spectrum of **6.1** in C_6D_6 is indicative of a complex containing a diamagnetic S = 0 ground state. For example, the two isopropyl methyl resonances of the *β*-

diketiminate ligand are observed as doublets at 1.52 and 2.01 ppm, while the γ-CH resonance is observed at 5.43 ppm. Curiously, at both room temperature and -85 °C (toulene-d_8), only one resonance is observed for the ^{t}Bu substituents, which argues for a C_{2v} symmetric complex in solution, and not C_s, as is observed in the solid state. This suggests facile exchange of the sulfur and oxygen positions within the Ni coordination sphere. Similar behavior was observed in the alkyl-substituted hyponitrite complexes, [L^{Me}Ni(*O*N=N(R)*O*)] (R = Et, 3,5-$Me_2C_6H_3$),[18] which even at low temperatures feature equivalent *β*-diketiminate backbone methyl resonances in their ^{1}H NMR spectra.

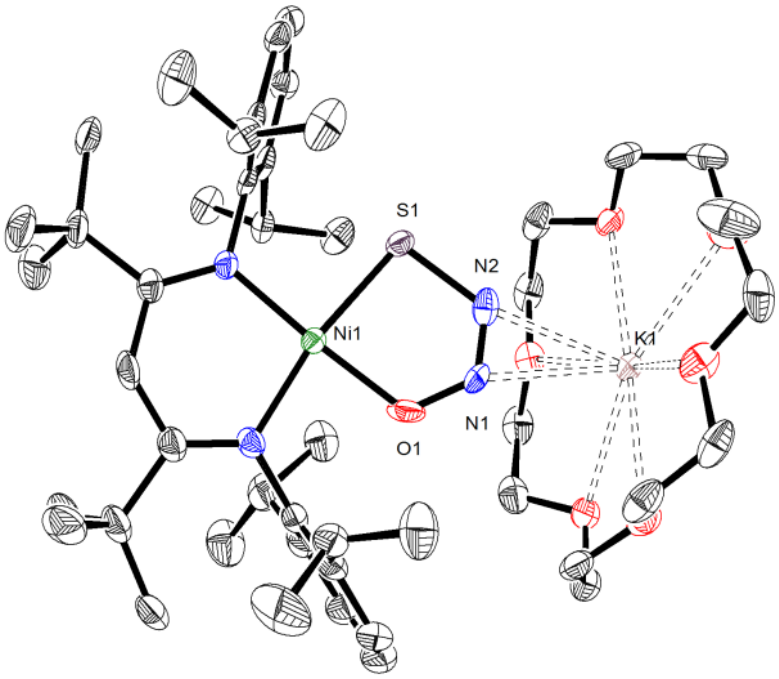

Figure 6.2. ORTEP drawing of [K(18-crown-6)][L^{tBu}Ni(κ^2-SNNO)] (**6.1**·1.5C_7H_8·0.5C_8H_{18}) shown with 50% thermal ellipsoids. Hydrogen atoms and C_7H_8 solvate molecules have been omitted for clarity.

Complex **6.1** is a rare example of a structurally characterized transition metal complex containing activated N_2O and features the first example of a thiohyponitrite ($[\kappa^2\text{-SNNO}]^{2-}$) ligand. Its formation is reminiscent of the Frustrated Lewis Pair (FLP) system, $^tBu_3P/B(C_6F_5)_3$, which reacts with N_2O to form $[^tBu_3P(NNO)B(C_6F_5)_3]$,[19] or the reaction of N_2O with Na_2O, which results in formation of *trans*-$[Na_2N_2O_2]$.[20,21] Also relevant is the reaction of IPr with N_2O to form IPr-N_2O (Figure 6.3).[22] These results support the conclusion that the $[SNNO]^{2-}$ ligand is formed by nucleophilic attack of N_2O by the sulfide ligand in **2.5**.[19,22,23]

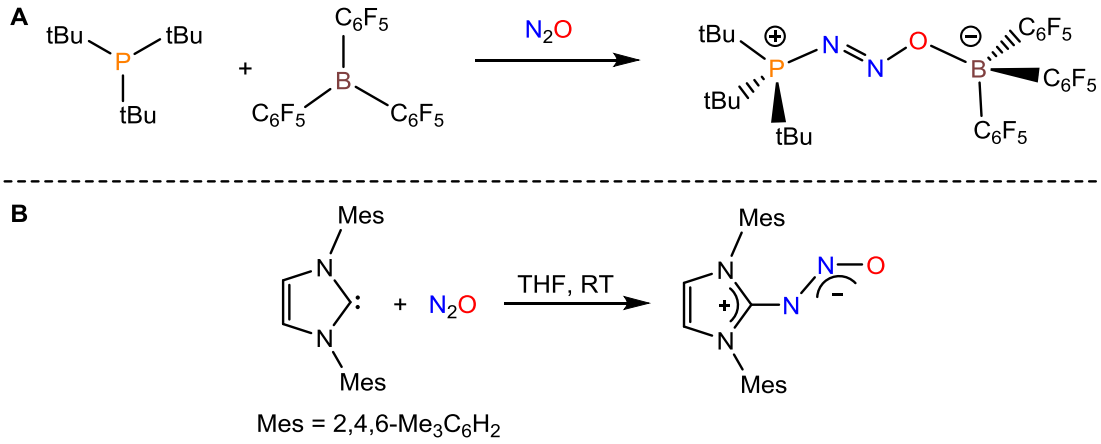

Figure 6.3. Nucleophilic activation of N_2O. **A**, Ref. 19; **B**, Ref. 22.

6.2.2 Synthesis and Characterization of [K(18-crown-6)][$L^{tBu}Ni^{II}(\eta^2\text{-SO})$] (6.2)

Gentle heating of a toluene-d_8 solution of [K(18-crown-6)][$L^{tBu}Ni^{II}(\kappa^2\text{-SNNO})$] (**6.1**) at 45 °C results in the complete thermolysis of **6.1** over the course of 6 d. A ^1H NMR spectrum of this reaction mixture reveals the presence of a new γ-CH resonance at 5.43 ppm (Figure A 6.5-6.6), which I have assigned to the thioperoxide complex, [K(18-crown-6)][$L^{tBu}Ni^{II}(\eta^2$-SO)] (**6.2**). Also present in this spectrum are two minor γ-CH resonances. The first, observed at 5.53 ppm, has been tentatively assigned to the disulfur dioxide complex, [K(18-

crown-6)][$L^{tBu}Ni^{II}(\eta^2$-OSSO)] (**6.3**), and the second resonance at 5.47 ppm, has been assigned to the disulfide complex, [K(18-crown-6)][$L^{tBu}Ni^{II}(\eta^2$-S_2)] (**6.4**). Work-up of the reaction mixture affords [K(18-crown-6)][$L^{tBu}Ni^{II}(\eta^2$-SO)] (**6.2**) as an orange crystalline solid in 82% yield (Scheme 6.2).

Scheme 6.2 Thermolysis of [K(18-crown-6)][$L^{tBu}Ni^{II}(\kappa^2$-SNNO)] (**6.1**)

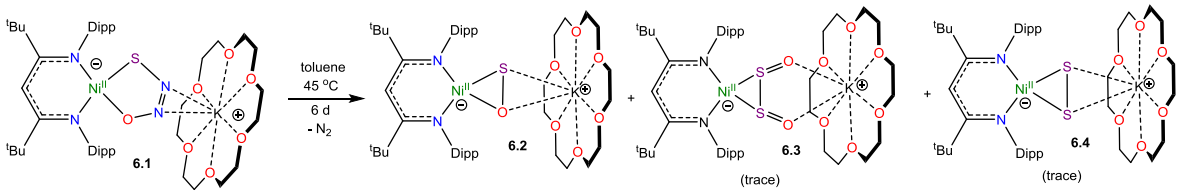

The solid state molecular structure of **6.2** is shown in Figure 6.4. Complex **6.2** features a rare example of the thioperoxide ($[\eta^2$-SO$]^{2-}$) ligand. It is formed via N_2 extrusion from the thiohyponitrite fragment. The $[\eta^2$-SO$]^{2-}$ ligand in **6.2** is disordered over two positions in a 97:3 ratio, which are related by a C_2 rotation about the Ni-K axis. The $[\eta^2$-SO$]^{2-}$ ligand in **6.2** is bound in a μ-η^2,η^2 fashion, wherein the sulfur and oxygen atoms are coordinated to both the Ni and K^+ centers. The $[\eta^2$-SO$]^{2-}$ ligand in complex **6.2** possesses an S-O bond length of 1.656(3) Å, consistent with an S-O single bond.[24] For comparison, the S-O distance in free S=O is substantially shorter (1.48108(8) Å), due to its higher bond order.[25] The Ni-S (2.127(1) Å) and Ni-O (1.954(3) Å) distances in **6.2** are both consistent with single bonds and are comparable with those found in the starting material (**6.1**), while the Ni-N bond lengths (1.881(4) and 1.900(4) Å) are similar to those observed in other square planar L^RNi^{II} complexes.[16,26]

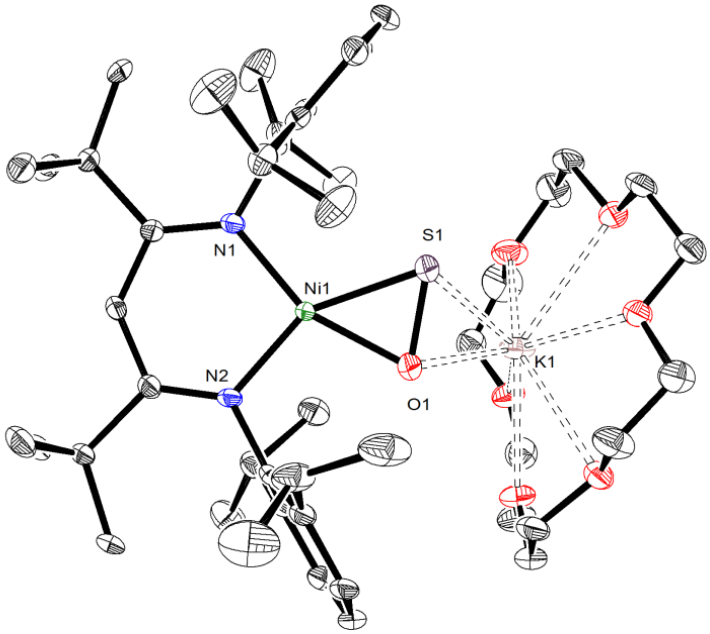

Figure 6.4. ORTEP drawing of [K(18-crown-6)][$L^{tBu}Ni^{II}(\eta^2$-SO)]·C_7H_8 (**6.2**·C_7H_8) shown with 50% thermal ellipsoids. Hydrogen atoms, a C_7H_8 solvate molecule, and one orientation of the disordered $[\eta^2$-SO$]^{2-}$ ligand have been omitted for clarity. Selected metrical parameters: S1-O1 1.656(3) Å, Ni1-S1 2.127(1) Å, Ni1-O1 1.954(3) Å, Ni1-N1 1.881(4) Å, Ni1-N2 1.900(4) Å, S1-K1 3.162(2) Å, O1-K1 2.881(3) Å, N1-Ni1-N2 99.2(2)°, N1-Ni1-S1 110.0(1)°, N2-Ni1-O1 103.2(1)°, S1-Ni1-O1 47.65(9)°.

The ^{1}H and ^{13}C{^{1}H} NMR spectra of **6.2** are consistent with its formulation as a C_s symmetric, diamagnetic, square planar Ni^{II} complex. The ^{1}H NMR spectrum of **6.2** in C_6D_6 features two *tert*-butyl resonances at 1.32 and 1.37 ppm and a single γ-CH resonance at 5.54 ppm. The IR spectrum (KBr pellet) of **6.2** reveals a strong ν_{SO} mode at 902 cm^{-1}, which is consistent with values reported for other bridging $[\eta^2$-SO$]^{2-}$ ligands (883, 873 cm^{-1}).[27,28] Only a handful of thioperoxide complexes are known, including [(triphos)Rh(μ-η^2,η^1-SO)$_2$Rh(triphos)][BPh_4]$_2$ (triphos = $CH_3C(CH_2PPh_2)_3$), [{RhCl(μ-η^2,η^1-SO)(PPh_3)$_2$}$_2$], and $Fe_3(\mu_3$-SO)(S)$(CO)_9$.[27,29,30] The iron example is notable because it can be prepared by O-

atom transfer to $Fe_3(S)_2(CO)_9$,[31] a manner of preparation that is similar to that of **6.2**. Interestingly, Mankad and co-workers suggest that a transient SO complex is formed upon reaction of $[(IPr^*)Cu]_2(\mu\text{-}S)$ with N_2O,[32] a transformation that parallels the conversion of **2.5** to **6.1** and then **6.2**.

As mentioned above, I also observe formation of $[K(18\text{-crown-6})][L^{tBu}Ni^{II}(\eta^2\text{-}OSSO)]$ (**6.3**), as a minor side product, during the conversion of $[K(18\text{-crown-6})][L^{tBu}Ni^{II}(\kappa^2\text{-}SNNO)]$ to **6.2**. Despite its presence in trace amounts, I have been able to obtain a few single crystals of **6.3** as orange plates from the reaction mixture. The solid state molecular structure of **6.3** is shown in Figure 6.5. It features the first example of a co-planar $[OSSO]^{2-}$ ligand (OSSO dihedral angle = 2°). The $[\eta^2\text{-}OSSO]^{2-}$ ligand in **6.3** is bound to the Ni center in an η^2 fashion, via both sulfur atoms, while the O atoms are bound to the $[K(18\text{-crown-6})]^+$ cation in a κ^2 fashion. Its S-S distance is 2.093(3) Å, while the S-O distances are 1.485(5) and 1.496(7) Å. For comparison, the S-S (2.0245(6) Å) and S-O (1.458(2) Å) distances in free S_2O_2 are shorter than those observed for **6.3**,[33–35] consistent with the reduced S-S and S-O bond orders anticipated for the $[OSSO]^{2-}$ fragment in the former.[33,36,37] Notably, complex **6.3** is only the third OSSO complex to be reported and only second to be structurally characterized.[31,38–40]

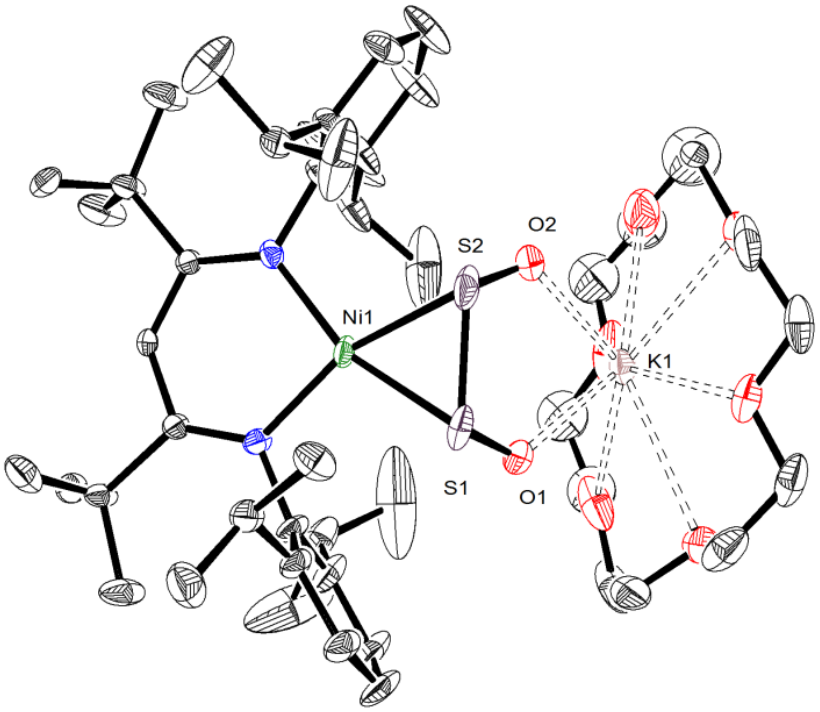

Figure 6.5. ORTEP drawing of [K(18-crown-6)][$L^{tBu}Ni^{II}(\eta^2$-OSSO)]·$2C_6H_{14}$ (**6.3**·$2C_6H_{14}$) shown with 50% thermal ellipsoids. Hydrogen atoms and C_6H_{14} solvate molecules have been omitted for clarity. Selected metrical parameters: S1-S2 2.093(3) Å, S1-O1 1.485(5) Å, S2-O2 1.496(7) Å, Ni1-S1 2.181(2) Å, Ni1-S2 2.173(2) Å, Ni1-N1 1.920(4) Å, Ni1-N2 1.925(4) Å, O1-K1 2.747(4) Å, O2-K1 2.777(6) Å, N1-Ni1-N2 97.3(2)°, N1-Ni1-S1 102.1(1)°, N2-Ni1-S2 102.9(1)°, O1-S1-S2 107.4(2)°, O2-S2-S1 107.4(2)°.

To account for the presence of **6.3** in the reaction mixture, I hypothesize that complex **6.2** undergoes a formal disproportionation, forming **6.3** and an equivalent of unobserved "[K(18-crown-6)][$L^{tBu}Ni^0$]". However, because of the low yield (typically less than 3% relative to complex **6.2**, as assessed by ^{1}H NMR spectroscopy), this transformation must be very inefficient.

6.2.3 Synthesis of [K(18-crown-6)][$L^{tBu}Ni^{II}(\eta^2\text{-}S_2)$] (6.4)

To further support the formation of the disulfide ($[\eta^2\text{-}S_2]^{2-}$) complex, [K(18-crown-6)][$L^{tBu}Ni^{II}(\eta^2\text{-}S_2)$] (**6.4**), during the synthesis of **6.2**, I endeavored to independently synthesize **6.4**. Several research groups have previously shown that terminal metal sulfides can react with S_8 to form metal disulfides.[41–43] Thus, I explored the reaction of [K(18-crown-6)][$L^{tBu}Ni^{II}(S)$] (**2.4**) with elemental sulfur. Addition of 0.125 equiv of S_8 to a toluene solution of [K(18-crown-6)][$L^{tBu}Ni^{II}(S)$] results in a rapid color change from brown to orange. Work-up of the reaction mixture affords [K(18-crown-6)][$L^{tBu}Ni^{II}(\eta^2\text{-}S_2)$] (**6.4**), as an orange crystalline solid in 81% yield (Scheme 6.3).

Scheme 6.3 Synthesis of [K(18-crown-6)][$L^{tBu}Ni^{II}(\eta^2\text{-}S_2)$] (**6.4**)

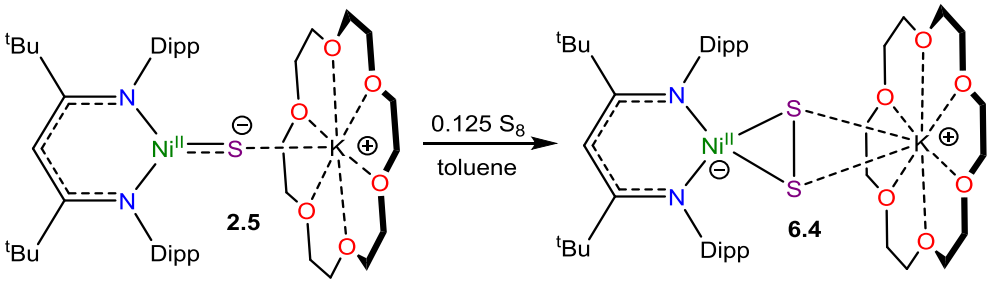

The solid state molecular structure of **6.4** is shown in Figure 6.6. The disulfide (S_2^{2-}) ligand in **6.4** has a S-S distance of 2.050(2) Å, consistent with a single bond.[24] This distance is comparable to those reported for other $Ni^{II}(\eta^2\text{-}S_2)$ complexes.[44–51] The Ni-S distances (2.202(2) and 2.199(2) Å) in **6.4** are consistent with single bonds, and are much longer than the Ni-S bond length in the starting material (**2.5**, 2.064(2) Å). Finally, the Ni-N bonds in **6.4** are similar to those found in other square planar Ni^{II} β-diketiminate complexes.[16,51,52]

The ^{1}H NMR spectrum of **6.4** in toluene-d_8 (Figure A 6.10) is consistent with a C_{2v} symmetric, diamagnetic, square planar Ni^{II} complex and features one *tert*-butyl resonance at 1.30 ppm and a single γ-CH resonance at 5.46 ppm. Importantly, this latter resonance is

also present in the *in situ* ^{1}H NMR spectrum of the thermolysis of **6.2** (Figure A 6.5), confirming the formation of **6.4** during that reaction, via an as-yet-unknown mechanism.

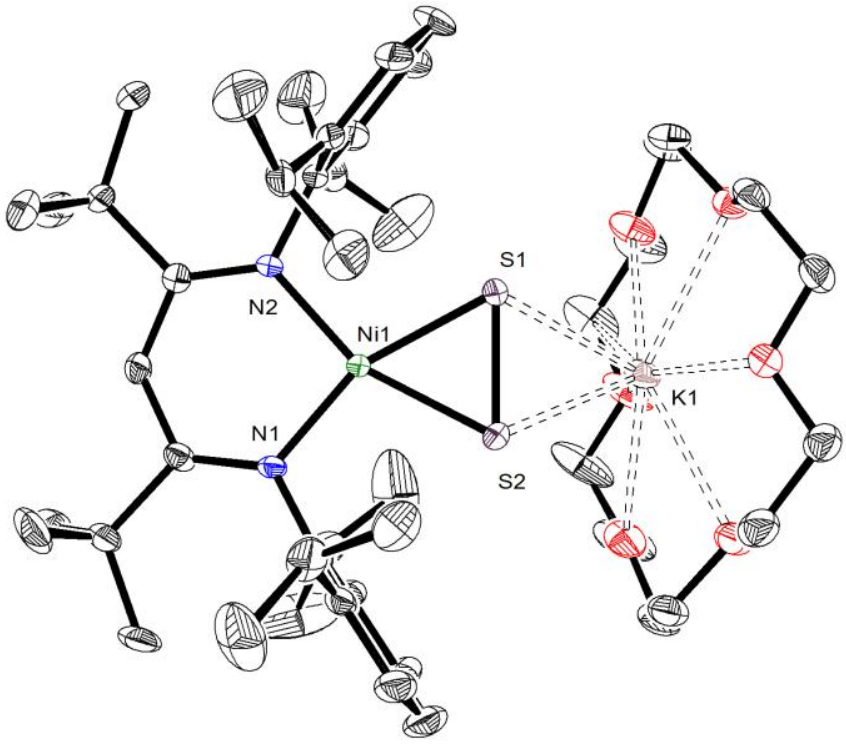

Figure 6.6. ORTEP drawing of [K(18-crown-6)][L^{tBu}Ni^{II}(η^2-S_2)]·2C_7H_8 (**6.4**·2C_7H_8) shown with 50% thermal ellipsoids. Hydrogen atoms and C_7H_8 solvate molecules have been omitted for clarity. Selected metrical parameters: S1-S2 2.050(2) Å, Ni1-S1 2.202(2) Å, Ni1-S2 2.199(2) Å, Ni1-N1 1.900(4) Å, Ni1-N2 1.906(4) Å, S1-K1 3.248(2) Å, S2-K1 3.249(2) Å, N1-Ni1-N2 98.0(2)°, N1-Ni1-S2 103.1(1)°, N2-Ni1-S1 103.4(1)°.

6.2.4 Reactivity of the (η^2-SO) Ligand

Not surprisingly, given the rarity of thioperoxide complexes, the reactivity of the SO moiety has not been well established. Previously, Schmid and co-workers reported that [(diphos)$_2$Ir(η^2-OSSO)][Cl] reacted with PPh_3 to form Ph_3PO, Ph_3PS, and [(diphos)$_2$IrCl].[38] More recently, Rauchfuss and co-workers demonstrated that $Cp_2Nb(S_2O)Cl$ reacted with Ph_3P to form $Cp_2Nb(O)Cl$ and two equiv of Ph_3PS.[31] Both transformations were presumed

to proceed through an unobserved SO intermediate, suggesting that S- or O-atom abstraction is a plausible reaction pathway for this ligand. However, the reactivity of the SO ligand with CO has not been studied explicitly. Accordingly, I explored the reactivity of [K(18-crown-6)][$L^{tBu}Ni^{II}(\eta^2$-SO)] (**6.2**) with this substrate. Thus, exposure of a C_6D_6 solution of complex **6.2** to an atmosphere of ^{13}CO results in complete consumption of **6.2** after 6 h. A $^{13}C\{^1H\}$ NMR spectrum (Figure A 6.14) of the reaction mixture reveals the formation of several ^{13}C-enriched products, indicating the incorporation of ^{13}CO. Specifically, this spectrum features resonances at 214.7, 177.3, 165.3, and 152.9 ppm, which are assignable to [K(18-crown-6)][$L^{tBu}Ni^{II}(\eta^2$-SCO)] (**5.1**),[53] [K(18-crown-6)][$L^{tBu}Ni^{II}(S,O:\kappa^2$-$SCO_2)$] (**6.5**), [K(18-crown-6)][$L^{tBu}Ni(\kappa^2$-$CO_3)$] (**6.6**), and SCO (**6.7**),[54] respectively (Scheme 6.4). This spectrum also features a minor ^{13}C-enriched resonance at 206.9 ppm, which I have tentatively assigned to [K(18-crown-6)][$L^{tBu}Ni^{II}(S_2CO)$] (**6.8**), on the basis of the similarity of its dithiocarbonate ($[S_2CO]^{2-}$) chemical shift with those reported for other dithiocarbonate complexes.[54–56]

Scheme 6.4 Reaction of [K(18-crown-6)][$L^{tBu}Ni^{II}(\eta^2$-SO)] (**6.2**) with CO

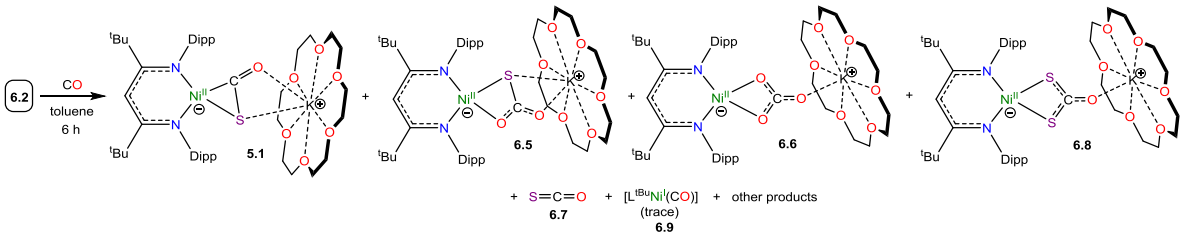

A ^1H NMR spectrum of the reaction mixture further supports these assignments. Specifically, an examination of the γ-CH region of this spectrum reveals overlapping resonances at 5.48 ppm (Figure A 6.13), which are assignable to [K(18-crown-6)][$L^{tBu}Ni^{II}(\eta^2$-SCO)] (**5.1**)[53] and [K(18-crown-6)][$L^{tBu}Ni^{II}(S,O:\kappa^2$-$SCO_2)$] (**6.5**), and a resonance at 5.42 ppm, assignable to [K(18-crown-6)][$L^{tBu}Ni(\kappa^2$-$CO_3)$] (**6.6**). This spectrum

also contains a minor resonance at 5.57 ppm that has been tentatively assigned to [K(18-crown-6)][$L^{tBu}Ni^{II}(S_2CO)$] (**6.8**). Interestingly, at short reaction times, I observe the presence of a paramagnetic intermediate in the reaction mixture (Figure A 6.12). I have tentatively identified this intermediate as the Ni^{II} sulfide, [K(18-crown-6)][$L^{tBu}Ni^{II}(S)$] (**2.5**), on the basis of the similarity of its ^{1}H NMR resonances with those of the previously characterized material.[16] For example, this intermediate features resonances at -130.25, -0.63, and 5.87 ppm, which are assignable to the γ-proton of the L^{tBu} ligand, its ^{t}Bu substituents, and one environment of its diastereotopic ^{i}Pr methyl groups, respectively. For comparison, these resonances appear at -115.21, -0.88, and 6.56 ppm, respectively, for authentic **2.5**.[16] This intermediate is quickly formed upon addition of ^{13}CO, but its signals immediately begin to decay, and they are completely absent after 6 h (Figure A 6.12).

I also characterized the products of the reaction of **6.2** and CO by IR spectroscopy. An IR spectrum of the reaction residue, dissolved in hexanes, reveals the presence of ν_{CO} modes at 2021, 1666, and 1620 cm^{-1} (Figure A 6.28), which are assignable to the ν_{CO} modes of [$L^{tBu}Ni^{I}(CO)$] (**6.9**),[57] [K(18-crown-6)[$L^{tBu}Ni^{II}(\eta^2$-SCO)] (**5.1**),[53] and [K(18-crown-6)][$L^{tBu}Ni^{II}(\kappa^2$-$CO_3)$] (**6.6**), respectively. Curiously, I do not observe any signals in the ^{1}H NMR spectrum of the reaction mixture that could be assigned to paramagnetic **6.9**, suggesting that it is only a minor product of the reaction. While I am uncertain as to how complex **6.9** is generated, I speculate that it may be formed via decomposition of the known Ni(0) carbonyl, [$L^{tBu}Ni^{0}(CO)]^-$,[57] which itself could be formed by sequential O- and S-atom transfer from **6.2**, although I do not observe [$L^{tBu}Ni^{0}(CO)]^-$ by either $^{13}C\{^1H\}$ or ^{1}H NMR spectroscopies, or by IR spectroscopy (Figures A 6.12-6.14, 6.28).

The ^{13}C NMR spectrum of the *in situ* reaction mixture also features a minor ^{13}C-enriched resonance at 178.5, as well as a major resonance at 191.4 ppm (Figure A 6.14). While these two resonances remain unassigned, I know that neither of the peaks is assignable to [K(18-crown-6)][$L^{tBu}Ni^{II}(\eta^2\text{-}CO_2)$] (**6.10**), as I have performed the independent synthesis of this complex for spectroscopic comparison (see below).

6.2.5 Synthesis and Characterization of [K(18-crown-6)][$L^{tBu}Ni^{II}(S,O{:}\kappa^2\text{-}SCO_2)$] (6.5)

To further support the presence of [K(18-crown-6)][$L^{tBu}Ni^{II}(S,O{:}\kappa^2\text{-}SCO_2)$] (**6.5**) in the reaction of **6.2** with CO, I pursued its synthesis via an independent route. Thus, exposure of a C_6D_6 solution of [K(18-crown-6)][$L^{tBu}Ni^{II}(S)$] (**2.5**) to excess carbon dioxide (CO_2) results in a rapid color change from dark brown to gold. The ^1H NMR spectrum of the reaction mixture taken 15 min after addition of CO_2 reveals full consumption of the starting material and formation of a new diamagnetic product whose spectroscopic signature is consistent with a square planar Ni^{II} complex.[53] Work-up of the reaction mixture provides **6.5** as a pale brown crystalline solid in 57% yield (Scheme 6.5).

Scheme 6.5 Synthesis of [K(18-crown-6)][$L^{tBu}Ni^{II}(S,O{:}\kappa^2\text{-}SCO_2)$] (**6.5**)

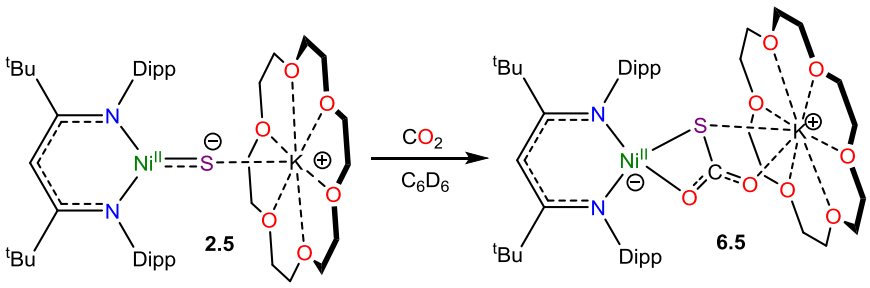

The solid state molecular structure of **6.5** is shown in Figure 6.7. The thiocarbonate ($[S,O{:}\kappa^2\text{-}SCO_2]^{2-}$) ligand in **6.5** features a $\mu{:}\kappa^2,\kappa^2$ binding mode. The $[S,O{:}\kappa^2\text{-}SCO_2]^{2-}$ ligand in **6.5** is disordered over two positions, which are related by a C_2 rotation about the Ni-K vector, in a 87:13 ratio. The S-C (1.756(4) Å) and O-C (1.279(5) and 1.238(4) Å) bond

lengths in **6.5** are consistent with those observed for previously reported $[SCO_2]^{2-}$ complexes.[58,59] The Ni-S and Ni-O distances in **6.5** are 2.234(1) Å and 1.922(3) Å, respectively, while the K-S and K-O distances are 3.531(1) Å and 2.715(3) Å, respectively, which are comparable to other K-S and K-O dative interactions.[60,61] Finally, the Ni-N distances in **6.5** are comparable to those found in the starting material.[16] To the best of my knowledge, complex **6.5** is the first structurally characterized transition metal complex containing the $[SCO_2]^{2-}$ ligand. Other structurally characterized thiocarbonate complexes include $[\{((^{Ad}ArO)_3N)U\}_2(\mu\text{-}\eta^1,(O):\kappa^2(O',S)SCO_2)]$ ($(^{Ad}ArO)_3N$ = N-[(2,4-adamantyl$_2$C$_6$H$_2$(CH$_2$)O]$_3$), prepared by reaction of $[\{((^{Ad}ArO)_3N)U\}_2(\mu\text{-}S)]$ with CO_2, and $[Cp^*_2Sm(\mu\text{-}\eta^1:\kappa^2\text{-}SCO_2)SmCp^*_2]$, prepared via reaction of $[(Cp^*_2Sm)_2(\mu\text{-}O)]$ with COS.[58,59]

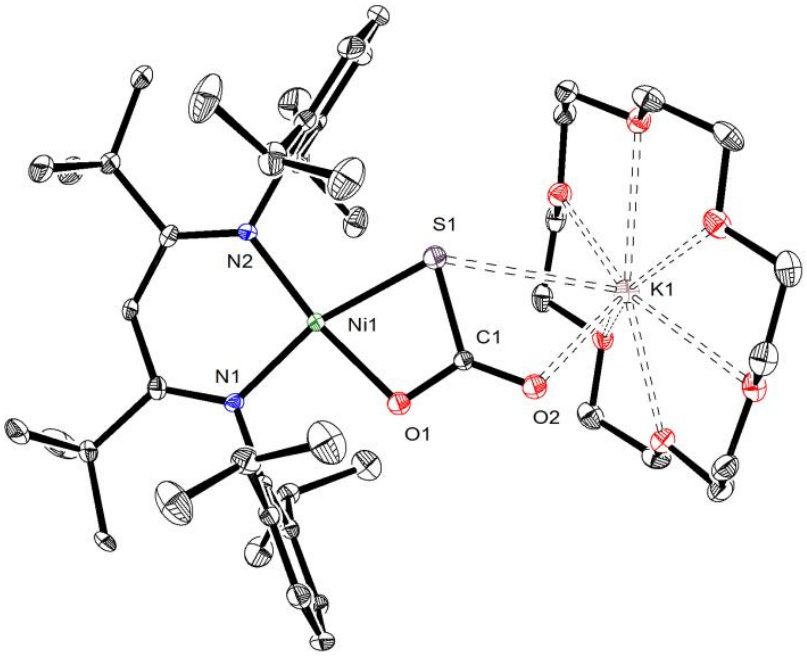

Figure 6.7. ORTEP drawing of $[K(18\text{-crown-6})][L^{tBu}Ni^{II}(S,O:\kappa^2\text{-}SCO_2)]\cdot 1.5C_7H_8$ (**6.5**$\cdot 1.5C_7H_8$) shown with 50% thermal ellipsoids. Hydrogen atoms, C_7H_8 solvate molecules, and one orientation of the disordered $[S,O:\kappa^2\text{-}SCO_2]^{2-}$ ligand have been omitted for clarity. Selected metrical parameters: S1-C1 1.756(4) Å, O1-C1 1.279(5) Å, O2-C1 1.238(4) Å,

Ni1-S1 2.234(1) Å, Ni1-O1 1.922(3) Å, Ni1-N1 1.904(3) Å, Ni1-N2 1.899(3) Å, S1-K1 3.531(1) Å, O2-K1 2.715(3) Å, S1-C1-O1 108.0(3)°, S1-C1-O2 126.2(3)°, O1-C1-O2 125.9(4)°, N1-Ni1-N2 96.7(1)°, N1-Ni1-O1 91.5(1)°, N2-Ni1-S1 99.22(9)°.

6.2.6 Synthesis and Characterization of [K(18-crown-6)][L^{tBu}Ni(κ^2-CO$_3$)] (6.6)

To further support the presence of [K(18-crown-6)][L^{tBu}Ni(κ^2-CO$_3$)] (**6.6**) in the reaction of **6.2** with CO, I pursued its synthesis via an independent route. The hexameric nickel carbonate complex, [K]$_6$[L^{tBu}Ni^{II}(κ^2-CO$_3$)]$_6$,[11] first reported by Limberg and coworkers in 2012, serves as a convenient starting material for the synthesis of [K(18-crown-6)][L^{tBu}Ni^{II}(κ^2-CO$_3$)] (**6.6**). Accordingly, addition of 6 equiv of 18-crown-6 to a suspension of [K]$_6$[L^{tBu}Ni^{II}(κ^2-CO$_3$)]$_6$ results in the formation of complex **6.6** in 52% yield (Scheme 6.6). Its solid state molecular structure of **6.6** is shown in Figure 6.8. The carbonate (CO_3^{2-}) ligand in **6.6** features a μ:κ^2,η^1 binding mode, identical to that observed for the trithiocarbonate (CS_3^{2-}) ligand in [K(18-crown-6)][L^{tBu}Ni(κ^2-CS$_3$)].[52] The O1-C1 (1.306(7) Å), O2-C1 (1.309(7) Å), and O3-C1 (1.242(7) Å) bond lengths in **6.6** are consistent with those reported for [K]$_6$[L^{tBu}Ni^{II}(κ^2-CO$_3$)]$_6$,[11] while the Ni-O1 and Ni-O2 distances in **6.6** are 1.882(4) and 1.901(4) Å, respectively, which are similar to those reported for the starting material.

Scheme 6.6 Synthesis of [K(18-crown-6)][L^{tBu}Ni(κ^2-CO$_3$)] (**6.6**)

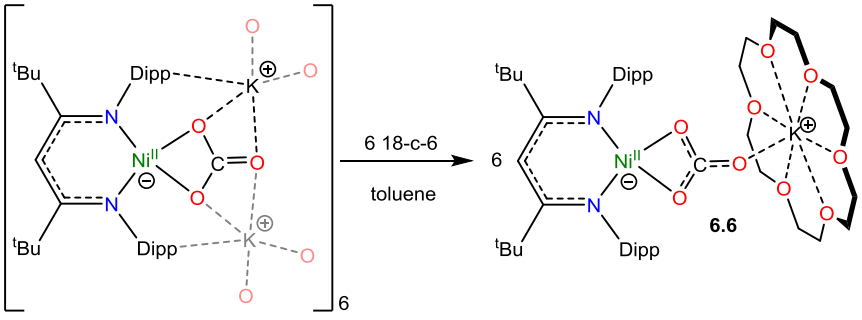

The $^{13}C\{^{1}H\}$ NMR spectrum of **6.6** in C_6D_6 features a resonance at 165.3 ppm, which is assignable to the $[CO_3]^{2-}$ moiety (Figure A 6.18). This chemical shift matches the resonance assigned to this complex in the *in situ* ^{13}C NMR spectrum of the reaction mixture of **6.2** and ^{13}CO (Figure A 6.14). In addition, the ^{1}H NMR spectrum of **6.6** in C_6D_6 features a γ-CH resonance at 5.42 ppm, which is present in the *in situ* ^{1}H NMR spectrum of the reaction mixture of **6.2** and ^{13}CO (Figure A 6.14). The IR spectrum (hexanes solution) of **6.6** features a strong ν_{CO} mode at 1620 cm^{-1}, which is also present in a solution IR spectrum of the reaction mixture formed upon addition of CO to **6.2** (Figure A 6.28). Overall, these data conclusively demonstrate that complex **6.6** is formed during reduction of [K(18-crown-6)][$L^{tBu}Ni^{II}(\eta^2$-SO)] (**6.2**) with CO.

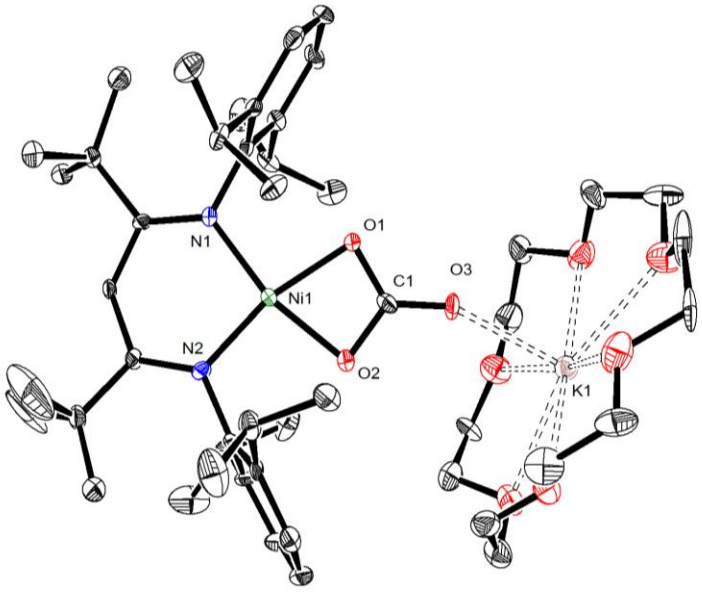

Figure 6.8. ORTEP drawing of [K(18-crown-6)][$L^{tBu}Ni^{II}(\kappa^2$-$CO_3)$]·0.5C_5H_{12} (**6.6**·0.5C_5H_{12}) shown with 50% thermal ellipsoids. Hydrogen atoms, a C_5H_{12} solvate molecule, and a second independent molecule of [K(18-crown-6)][$L^{tBu}Ni^{II}(\kappa^2$-$CO_3)$] have been omitted for clarity. Selected metrical parameters: C1-O1 1.306(7) Å, C1-O2 1.309(7) Å, C1-O3 1.242(7) Å, Ni1-O1 1.882(4) Å, Ni1-O2 1.901(4) Å, Ni1-N1 1.883(5) Å, Ni1-N2 1.879(5) Å, O3-K1

2.510(4) Å, O1-C1-O2 110.8(5)°, O1-C1-O3 125.0(6)°, N1-Ni1-N2 97.9(2)°, N1-Ni1-O1 96.6(2)°, N2-Ni1-O2 96.5(2)°.

6.2.7 Synthesis and Characterization of [K(18-crown-6)][$L^{tBu}Ni^{II}(\eta^2\text{-}CO_2)$] (6.10)

In an effort to assign the resonance at 191.4 ppm in the *in situ* $^{13}C\{^1H\}$ NMR spectrum of the reaction of **6.2** and ^{13}CO, I endeavored to independently synthesize the carbon dioxide complex, [K(18-crown-6)][$L^{tBu}Ni^{II}(\eta^2\text{-}CO_2)$] (**6.10**). I rationalized that **6.10** was a plausible reaction product, given the presence of CO_2 in the reaction mixture. Several previously reported Ni(CO_2) complexes have been synthesized by reaction of CO_2 with a Ni^0 precursor.[62–65] Gratifyingly, the Ni(0) N_2 complex, $[K]_2[L^{tBu}Ni^0(\mu\text{-}\eta^1\text{:}\eta^1\text{-}N_2)Ni^0L^{tBu}]$, previously reported by Limberg and co-workers in 2009,[66] was found to serve as an effective Ni^0 source for the synthesis of **6.10**. Thus, exposure of $[K]_2[L^{tBu}Ni^0(\mu\text{-}\eta^1\text{:}\eta^1\text{-}N_2)Ni^0L^{tBu}]$ to two equiv of CO_2, followed by addition of 18-crown-6, resulted in the formation of **6.10** (Scheme 6.7), which was isolated as pale orange plates in 41% yield after work-up. Its formulation was confirmed by X-ray crystallography and its solid state molecular structure is shown in Figure 6.9.

Scheme 6.7 Synthesis of [K(18-crown-6)][$L^{tBu}Ni^{II}(\eta^2\text{-}CO_2)$] (**6.10**)

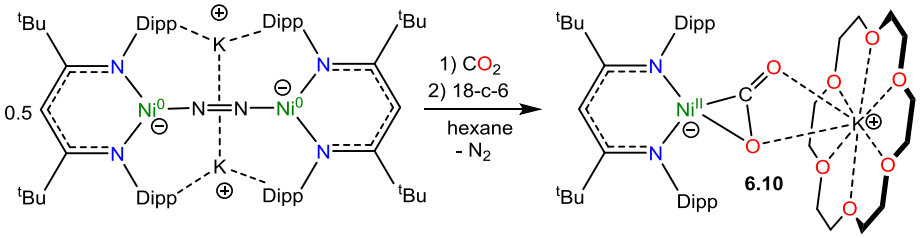

Complex **6.10** features a square planar Ni^{II} center ligated by the β-diketiminate ligand and a $[CO_2]^{2-}$ ligand. The $[CO_2]^{2-}$ ligand in **6.10** features a $\mu\text{:}\eta^2,\kappa^2$ binding mode, similar to that observed for the $[COS]^{2-}$ ligand in complex **5.1**. The $[CO_2]^{2-}$ ligand in **6.10** is disordered

over two positions, in a 76:24 ratio, which are related by a C_2 rotation axis about the Ni-K vector. The Ni1-O1 (1.897(6) Å) and Ni1-C1 (1.890(6) Å) distances are consistent with those previously reported for the Ni(η^2-CO_2) fragment.[62,64,65,67,68] Additionally, the Ni-N bonds in **6.10** are consistent with those found in other square planar Ni^{II} β-diketiminate complexes.[16,60,61]

The ^{1}H NMR spectrum of **6.10** in C_6D_6 is consistent with a C_s symmetric, square planar Ni^{II} complex. It features two *tert*-butyl resonances at 1.42 and 1.34 ppm, and a single γ-CH resonance at 5.42 ppm. Its $^{13}C\{^1H\}$ NMR spectrum in C_6D_6 features a resonance at 167.2 ppm, which I have assigned to the $[\eta^2$-$CO_2]^{2-}$ ligand. This chemical shift is consistent with those reported for previously isolated Ni(η^2-CO_2) complexes.[63–65] Most importantly, however, these resonances are not observed in the *in situ* $^{13}C\{^1H\}$ and ^{1}H NMR spectra of the reaction between **6.2** and ^{13}CO (Figures A 6.13-6.14). Thus, I can definitively conclude that complex **6.10** is not being formed in that reaction. Finally, complex **6.10** features a ν_{CO} mode at 1664 cm^{-1} in its IR spectrum (KBr pellet), which is similar to those reported for other nickel CO_2 complexes.[63–65] This vibration is also not present in the *in situ* IR spectrum (recorded in hexanes) of the reaction residue formed upon reaction of **1** with CO (Figure A 6.28).

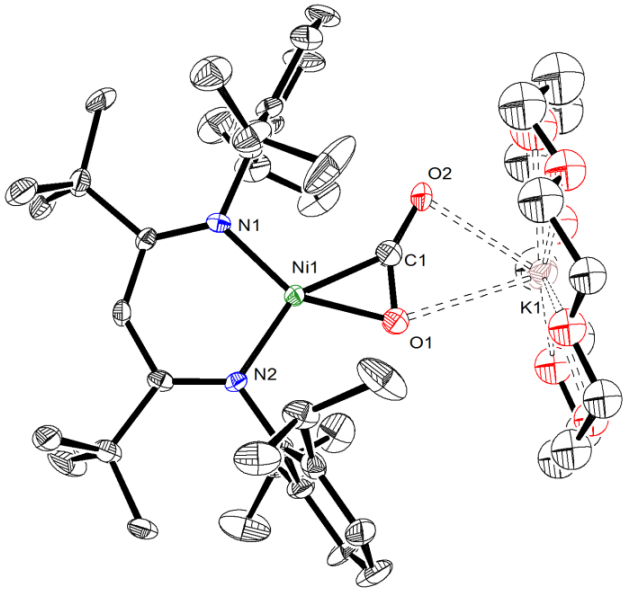

Figure 6.9. ORTEP drawing of $[K(18\text{-crown-6})][L^{tBu}Ni^{II}(\eta^2\text{-}CO_2)]\cdot 2C_6H_6$ (**6.10**$\cdot 2C_6H_6$) shown with 50% thermal ellipsoids. Hydrogen atoms, C_6H_6 solvate molecules, and second orientations of the CO_2 and 18-crown-6 fragments have been omitted for clarity. Selected metrical parameters: C1-O1 1.231(9) Å, C1-O2 1.22(1) Å, Ni1-C1 1.890(6) Å, Ni1-O1 1.897(6) Å, Ni1-N1 1.901(6) Å, Ni1-N2 1.896(5) Å, O1-K1 2.980(6) Å, O2-K1 2.71(1) Å, O1-C1-O2 144.0(8)°, N1-Ni1-N2 99.2(2)°, N1-Ni1-C1 112.2(3)°, N2-Ni1-O1 110.7(3)°.

I also attempted the synthesis of **6.10** via the reductive deprotection of the Ni trityl caboxylate complex, $[L^{tBu}Ni^{II}(O,O\text{:}\kappa^2\text{-}C(O)_2CPh_3)]$. However, reduction of this complex with KC_8 did not result in the desired deprotection reaction. While, I did not isolate the reduction product, it is likely the Ni^I complex, $[K(18\text{-crown-6})][L^{tBu}Ni^{I}(O,O\text{:}\kappa^2\text{-}C(O)_2CPh_3)]$ based on its ^{1}H NMR spectrum which features a broad *tert*-butyl resonance at -1.48 ppm.

6.2.8 Mechanistic Considerations.

To rationalize the formation of complexes **5.1** and **6.5**, I propose that CO initially reacts with **6.2** to form CO_2 and $[K(18\text{-crown-6})][L^{tBu}Ni^{II}(S)]$ (**2.5**) (Scheme 6.8). Complex **2.5**

then reacts with either CO or CO_2 to yield [K(18-crown-6)][$L^{tBu}Ni^{II}(\eta^2$-SCO)] (**5.1**) or [K(18-crown-6)][$L^{tBu}Ni^{II}(S,O:\kappa^2$-$SCO_2$)] (**6.5**), respectively. Significantly, their presence, along with the observation of [K(18-crown-6)][$L^{tBu}Ni^{II}$(S)] (**2.5**) in the reaction mixture, demonstrates the formal reduction of N_2O by CO, as originally envisioned. That said, the reaction rates of **2.5** with CO and CO_2 are qualitatively similar to the reaction rate of **2.5** with N_2O. As a consequence, **2.4** is unlikely to be an effective catalyst for N_2O reduction because off-cycle reaction pathways with CO and CO_2 would be competitive with the desired N_2O capture reaction (Scheme 6.8).

Scheme 6.8 Proposed Mechanism for Ni Sulfide Mediated N_2O Reduction

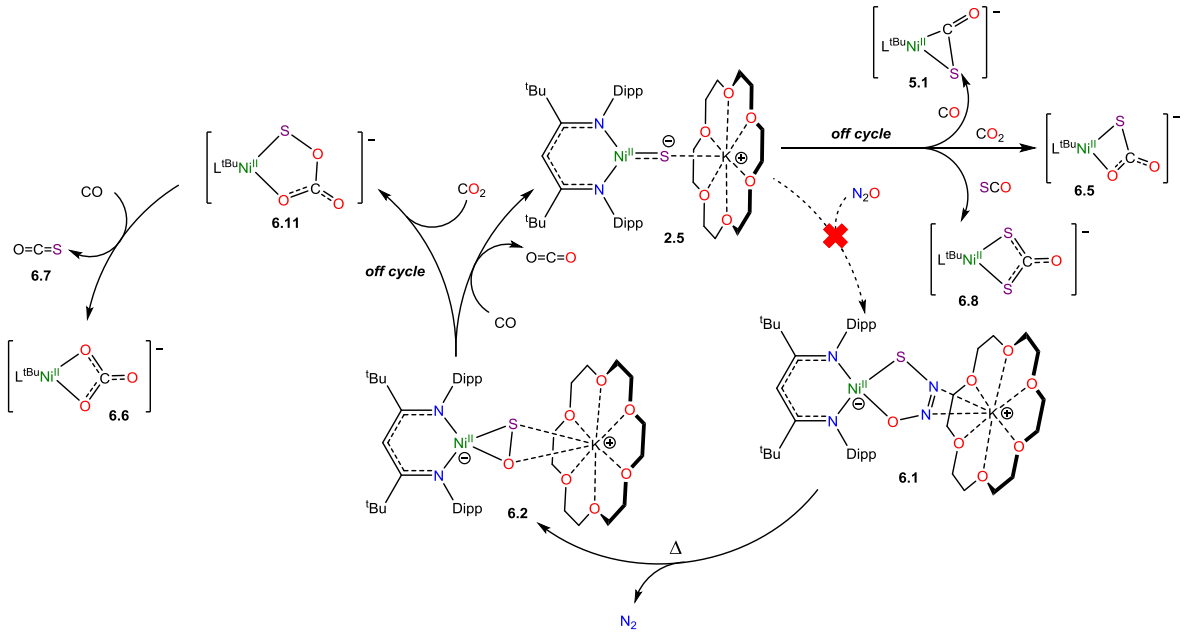

To rationalize the formation of complex **6.6** and COS, I propose that reaction of the newly formed CO_2 with unreacted **6.2** results in the formation of a transient, unobserved nickel monothiopercarbonate complex, [K(18-crown-6)][$L^{tBu}Ni^{II}(\kappa^2$-$SOCO_2$)] (**6.11**). Complex **6.11** then transfers a sulfur atom to CO to form [K(18-crown-6)][$L^{tBu}Ni^{II}(\kappa^2$-CO_3)] (**6.6**) and COS (**6.7**) (Scheme 6.8), both of which were confirmed to be present in the *in situ*

reaction mixture. This hypothesis also nicely explains the presence of [K(18-crown-6)][$L^{tBu}Ni^{II}(\kappa^2\text{-}S_2CO)$] (**6.8**), which could be formed via the reaction of **6.7** with **2.5** (Scheme 6.8). While the formation of a monothiopercarbonate complex has not been previously reported, the reaction of metal peroxides (O_2^{2-}) with CO_2 is known to yield peroxocarbonate ($[OOCO_2]^{2-}$) complexes.[69–71] Similarly, metal disulfides (S_2^{2-}) are known to react with CS_2 to form perthiocarbonates ($[SSCS_2]^{2-}$).[72,73] Moreover, peroxocarbonates are known to be very effective O-atom donors.[69,74–77]

Scheme 6.9 Reaction of [K(18-crown-6)][$L^{tBu}Ni^{II}(\eta^2\text{-}SO)$] (**6.2**) with CO_2

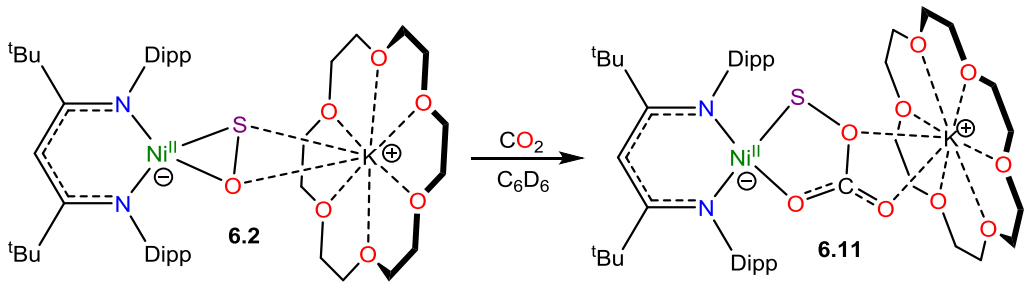

Consistent with my hypothesis, reaction of [K(18-crown-6)][$L^{tBu}Ni^{II}(\eta^2\text{-}SO)$] (**6.2**) with CO_2 in C_6D_6 results in the rapid formation of a new diamagnetic Ni^{II} complex, as evidenced by the appearance of diagnostic resonances at 4.49 ppm (γ-CH) and 1.20 ppm (*t*Bu) in the *in situ* ^{1}H NMR spectrum of the reaction mixture (Figure S18). I have assigned these resonances to the monothiopercarbonate complex [K(18-crown-6)][$L^{tBu}Ni^{II}(\kappa^2\text{-}SOCO_2)$] (**6.11**) (Scheme 6.9). Complex **6.11** is the only product observed in the reaction mixture. These results provide further support for the overall reaction mechanism proposed in Scheme 6.8 and suggest that $(SOCO_2)^{2-}$ could function as a very effective a S-atom transfer reagent.[78] Nonetheless, the off-cycle formation of **6.11** further reveals the unsuitability of **2.5** for catalytic N_2O reduction.

Complex **6.11** has proven to be quite thermally sensitive, and it decomposed in the freezer during an attempted crystallization. I have been able to identify a number of the decomposition products using ^{1}H NMR spectroscopy. For example, ^{1}H NMR resonances matching those for [K(18-crown-6)][$L^{tBu}Ni^{II}(\eta^2$-OSSO)] (**6.3**), [K(18-crown-6)][$L^{tBu}Ni^{II}(\eta^2$-S_2)] (**6.4**), [K(18-crown-6)][$L^{tBu}Ni^{II}(\kappa^2$-CO_3)] (**6.6**), [K(18-crown-6)][$L^{tBu}Ni^{II}(\kappa^2$-S_2CO)] (**6.8**), and [K(18-crown-6)][$L^{tBu}Ni^{II}(\eta^2$-CO_2)] (**6.10**) were observed in the ^{1}H NMR spectrum of the decomposition products in C_6D_6 (Figure 6.10). In addition, a new ^{1}H resonance at 5.54 ppm has been tentatively assigned to the γ-H of [K(18-crown-6)][$L^{tBu}Ni^{II}$(*S*,*S*:η^2-SSO)] **6.12** (see below). Notably, the formation of **6.6** in this reaction offers support for the presence of **6.11** as the product of CO_2 addition to **6.2**.

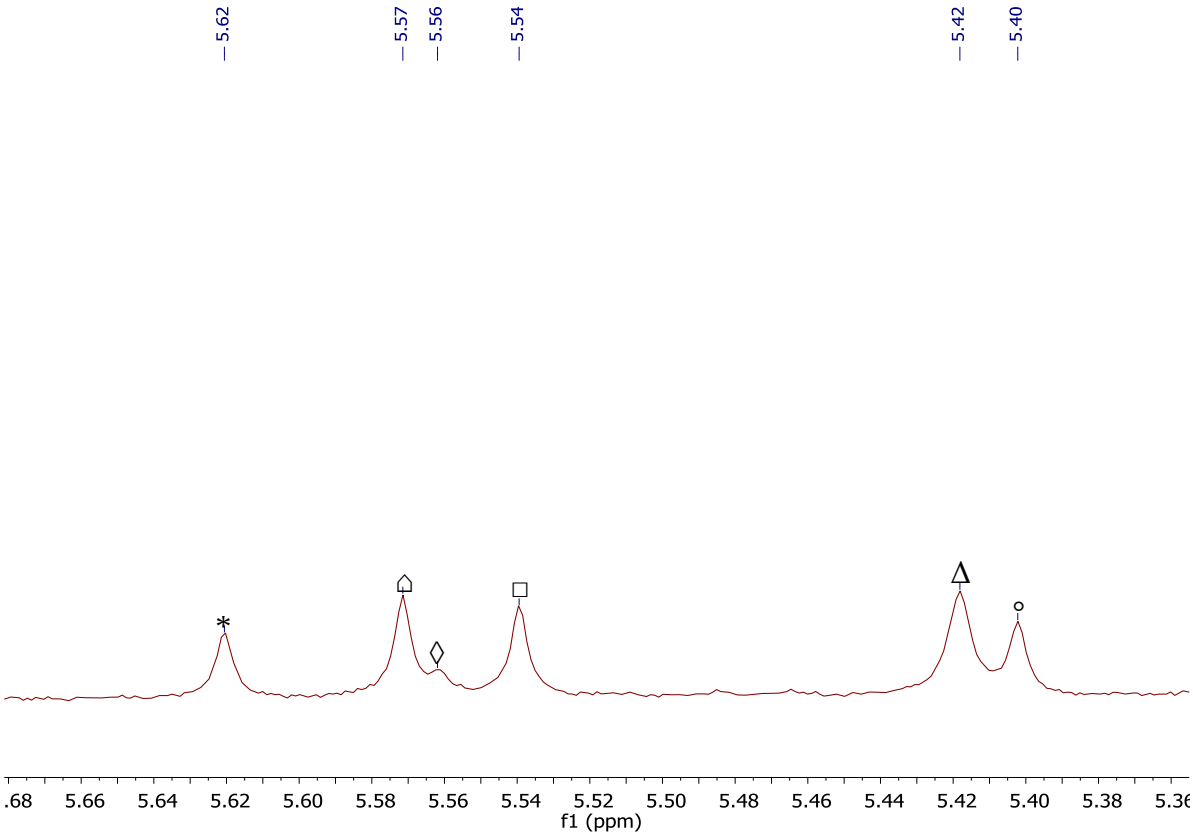

Figure 6.10. Partial ^{1}H NMR spectrum of the decomposition products of [K(18-crown-6)][L^{tBu}Ni^{II}(κ^2-SOCO$_2$)] (**6.11**) in C_6D_6. (*) [K(18-crown-6)][L^{tBu}Ni^{II}(η^2-OSSO)] (**6.3**), (◊) [K(18-crown-6)][L^{tBu}Ni^{II}(η^2-S$_2$)] (**6.4**), (Δ) [K(18-crown-6)][L^{tBu}Ni^{II}(κ^2-CO$_3$)] (**6.6**), (⌂) [K(18-crown-6)][L^{tBu}Ni^{II}(κ^2-S$_2$CO)] (**6.8**) (tentative), (°) [K(18-crown-6)][L^{tBu}Ni^{II}(η^2-CO$_2$)] (**6.10**), and (□) [K(18-crown-6)][L^{tBu}Ni^{II}(*S*,*S*:η^2-SSO)] (**6.12**) (tentative).

Interestingly, I was also able to obtain a single crystal of [K(18-crown-6)][L^{tBu}Ni^{II}(*S*,*S*:η^2-SSO)] (**6.12**) from this reaction. The solid state molecular structure of **6.12** is shown in Figure 6.11. It features a rare example of an [SSO]$^{2-}$ ligand. The [SSO]$^{2-}$ ligand in **6.12** is bound to the Ni center in an η^2 fashion, via both sulfur atoms, while the O atom is bound to the [K(18-crown-6)]$^{+}$ cation. The SSO ligand in **6.12** is disordered over two positions, which are related by a reflection across the plane that includes Ni, K and the

β-diketiminate γ-carbon atoms, in a 62:38 ratio. The S-S distance is 2.05(1) Å, which is consistent with an S-S single bond while the S-O distance is 1.16(2) Å appears to be anomalously short due to the disorder in the structure.[44–51] The related SSO complex, [(Cp*)(PMe_2Ph)Ir(SSO)], contains a similarly anomalously short S-O bond length of 1.162(9) Å, likely due to a related positional disorder.[79] To the best of my knowledge, complex **6.12** is the first structurally characterized nickel $[SSO]^{2-}$ complex. Other structurally characterized $[SSO]^{2-}$ complexes include [$(CO)_2$(Cp*)Mn(SSO)], prepared by the oxidation of [$(CO)_2$(Cp*)Mn(S_2)] with O_2, and [(Cp*)(PMe_2Ph)Ir(SSO)], prepared via reaction of [(Cp*)(PMe_2Ph)Ir(SH)(H)] with *p*-methyl-thionylanaline (PhNSO).[79–86]

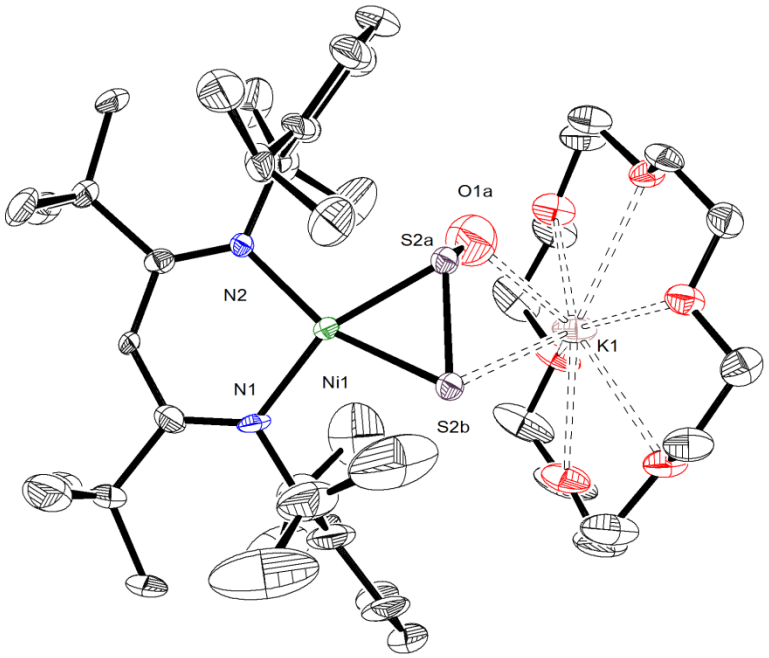

Figure 6.11. ORTEP drawing of [K(18-crown-6)][$L^{tBu}Ni^{II}$(*S*,*S*:η^2-SSO)]·2C_6H_6·C_5H_{12} (**6.12**·2C_6H_6·C_5H_{12}) shown with 50% thermal ellipsoids. Hydrogen atoms, an alternate orientation of SSO^{2-}, and solvate molecules have been omitted for clarity. Selected metrical parameters: S2a-S2b 2.05(1) Å, S1-O1 1.16(2) Å, Ni1-S2a 2.167(7) Å, Ni1-S2b 2.207(8) Å,

Ni1-N1 1.898(8) Å, Ni1-N2 1.895(8) Å, O1a-K1 2.65(2) Å, S2b-K1 3.66(1) Å, N1-Ni1-N2 97.2(3)°, N1-Ni1-S2a 105.5(3)°, N2-Ni1-S2b 101.7(3)°, O1a-S2a-S2b 119.4(11)°.

To account for the presence of **6.12** in the reaction mixture, I hypothesize that [K(18-crown-6)][$L^{tBu}Ni^{II}(\kappa^2\text{-}SOCO_2)$] (**6.11**) transfers a S-atom to unreacted [K(18-crown-6)][$L^{tBu}Ni^{II}(\eta^2\text{-}SO)$] (**6.2**) to form [K(18-crown-6)][$L^{tBu}Ni^{II}(\kappa^2\text{-}CO_3)$] (**6.6**) and **6.12**, however, this does not account for the formation of the other products (Scheme 6.10).

Scheme 6.10 Proposed formation of [K(18-crown-6)][$L^{tBu}Ni^{II}(S,S\text{:}\eta^2\text{-}SSO)$] (**6.12**)

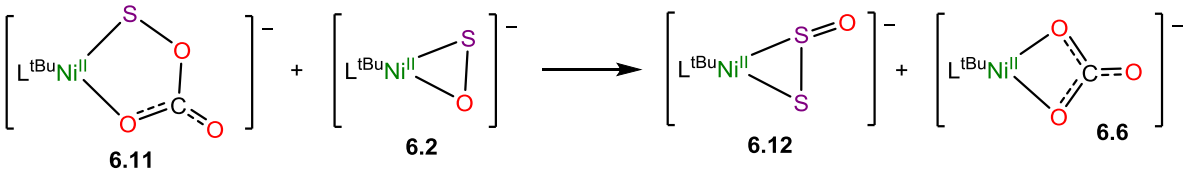

6.2.9 Synthesis of [{$L^{tBu}Ni$}$_2$(μ^2-κ^2-η^2-SNNO)] (6.13)

In order to further explore that reactivity of the $SNNO^{2-}$ ligand, I reacted [K(18-crown-6)][$L^{tBu}Ni^{II}(\kappa^2\text{-}SNNO)$] (**6.1**) with trimethylsilyltriflate (Me_3SiOTf) in an effort to effect silylation or heteroatom abstraction at the $SNNO^{2-}$ moiety. Accordingly, reaction of **6.1** with Me_3SiOTf in C_6D_6 resulted in the formation of [{$L^{tBu}Ni$}$_2$(μ^2-κ^2-η^2-SNNO)] (**6.13**) in 56% yield. Efforts to scale up this reaction were hampered by the limited thermal stability of **6.13**. Notably, storage of solutions of **6.13** results in spontaneous loss of N_2O leading to the formation of [{$L^{tBu}Ni$}$_2$(μ^2-S)] which was identified based on comparison of its ^{1}H NMR spectrum with a reported ^{1}H NMR spectrum of this species (Scheme 6.11).[87]

Scheme 6.11 Synthesis of [{$L^{tBu}Ni$}$_2$(μ^2-κ^2-η^2-SNNO)] (**6.13**)

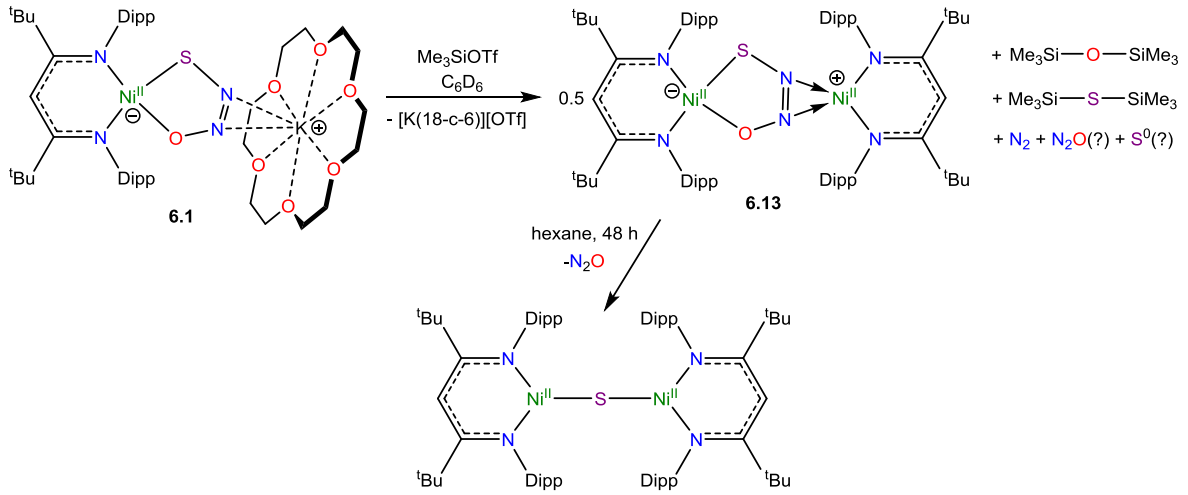

The solid state molecular structure of complex **6.13** is shown in Figure 6.12. Complex **6.13** features an μ^2-κ^2-η^2-thiohyponitrite ($[SNNO]^{2-}$) ligand, which is likely formed by the trapping of $[L^{tBu}Ni^{II}(\kappa^2\text{-SNNO})]^-$ with "$[L^{tBu}Ni^{II}]^+$"; however, the overall mechanism of this transformation is not yet known. The $[SNNO]^{2-}$ ligand in **6.13** is disordered over four positions, related by C_2 rotations about the Ni-Ni vector and an orthogonal vector the bisects the Ni-Ni vector and is contained in the plane of the SNNO ligand. Due to the disorder present in the $[SNNO]^{2-}$ moiety, the bond distances in **6.13** are anomalous, with S-N and O-N bonds of 1.582(1) Å and 1.432(1) Å, which are too short and too long for typical single bonds, respectively, while the N-N bond length of 1.195(9) Å is indicative of a double bond.[16] The ^{1}H NMR spectrum of **6.13** in C_6D_6 is consistent with a diamagnetic, square planar Ni^{II} complex and features one *tert*-butyl resonance at 1.10 ppm and two *i*Pr methyl resonances at 2.09 and 1.46 ppm.

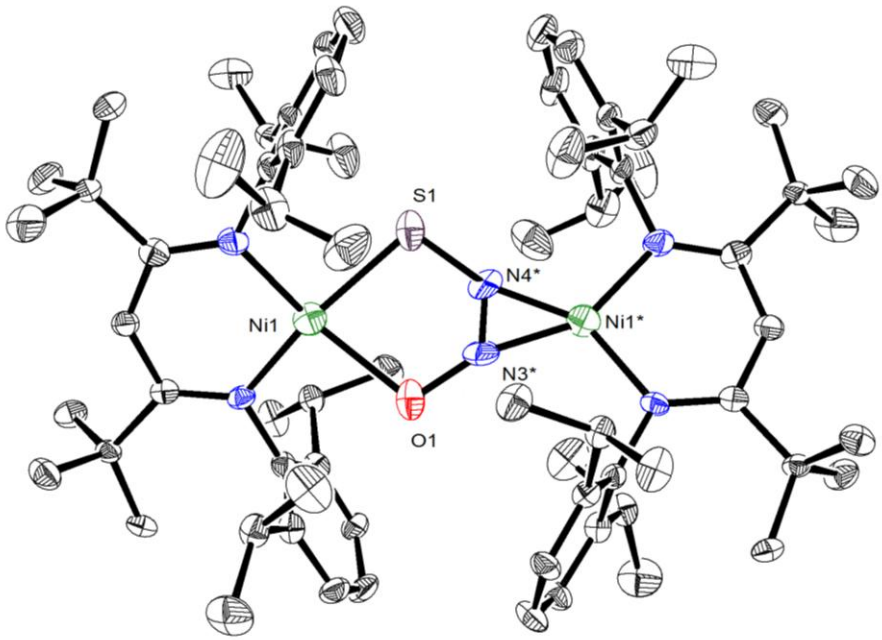

Figure 6.12. ORTEP drawing of [{$L^{tBu}Ni$}$_2$(μ^2-κ^2-η^2-SNNO)]·C_7H_8 (**6.13**·C_7H_8) shown with 50% thermal ellipsoids. Hydrogen atoms, alternate orientations of $SNNO^{2-}$, and a C_7H_8 solvate molecule have been omitted for clarity. Selected metrical parameters: S1-N4* 1.582(1) Å, N4*-N3* 1.195(9) Å, N3*-O1 1.432(1) Å, Ni1-S1 2.296(6) Å, Ni1-O1 2.296(6), Ni1*-N3* 1.83(1) Å, Ni1*-N4* 1.79(1) Å, S1-N4*-N3* 122(1)°, O1-N3*-N4* 126(1)°.

6.3 Summary

In this chapter, I detailed the reaction of [K(18-crown-6)][$L^{tBu}Ni^{II}$(S)] (**2.5**) with N_2O to yield an unprecedented thiohyponitrite complex, [K(18-crown-6)][$L^{tBu}Ni^{II}$(κ^2-SNNO)] (**6.1**).Gentle thermolysis of [K(18-crown-6)][$L^{tBu}Ni^{II}$(κ^2-SNNO)] (**6.1**) results in extrusion of N_2 and formation of [K(18-crown-6)][$L^{tBu}Ni^{II}$(η^2-SO)] (**6.2**), a rare example of a structurally characterized SO complex, along with trace amounts of [K(18-crown-6)][$L^{tBu}Ni^{II}$(η^2-OSSO)] (**6.3**) and [K(18-crown-6)][$L^{tBu}Ni^{II}$(η^2-S_2)] (**6.4**). [K(18-crown-6)][$L^{tBu}Ni^{II}$(η^2-SO)] (**6.2**) reacts rapidly with CO, forming the "masked" terminal Ni(II) sulfide intermediate, [K(18-crown-6)][$L^{tBu}Ni^{II}$(S)] (**2.5**), along with CO_2, via O-atom abstraction. This Ni(II)

sulfide intermediate then reacts with CO or CO_2 to form [K(18-crown-6)][$L^{tBu}Ni^{II}(\eta^2$-SCO)] (**5.1**) and [K(18-crown-6)][$L^{tBu}Ni(S,O{:}\kappa^2$-$SCO_2)$] (**6.5**), respectively. [K(18-crown-6)][$L^{tBu}Ni^{II}(\eta^2$-SO)] (**6.2**) can also react with the newly formed CO_2 to form a putative monothiopercarbonate complex, [K(18-crown-6)][$L^{tBu}Ni^{II}(\kappa^2$-$SOCO_2)$] (**6.11**), which can then transfer an S atom to CO, forming COS (**6.7**) and [K(18-crown-6)][$L^{tBu}Ni^{II}(\kappa^2$-$CO_3)$] (**6.6**).

Significantly, the observation of [K(18-crown-6)][$L^{tBu}Ni^{II}$(S)] (**2.5**) in the reaction mixture, along with the formation of [K(18-crown-6)][$L^{tBu}Ni^{II}(\eta^2$-SCO)] (**5.1**) and [K(18-crown-6)][$L^{tBu}Ni^{II}(S,O{:}\kappa^2$-$SCO_2)$] (**6.5**), confirms that the SO ligand is susceptible to O-atom abstraction, which had not been previously demonstrated. Perhaps more importantly, these reaction products reveal the stepwise conversion of [K(18-crown-6)][$L^{tBu}Ni^{II}(\kappa^2$-SNNO)] (**6.1**) to [K(18-crown-6)][$L^{tBu}Ni^{II}(\eta^2$-SO)] (**6.2**) and then [K(18-crown-6)][$L^{tBu}Ni^{II}$(S)] (**2.5**), which represents a formal reduction of N_2O by CO, forming N_2 and CO_2. While [K(18-crown-6)][$L^{tBu}Ni^{II}$(S)] (**2.5**) could never function as a catalyst for N_2O reduction because it quickly undergoes off-cycle reactivity under the reaction conditions, the stoichiometric transformation parallels the chemistry mediated by nano-particulate Pt/Rh in catalytic converters. In contrast to the metal-centered redox of the catalytic converter example, however, all of the redox chemistry in this system occurs at the sulfide ligand. The nickel center remains in the 2+ oxidation state at every step. The use of ligand-centered redox is an intriguing strategy for N_2O reduction and I suggest that the study of model systems, such as the one presented in this chapter, could inspire the design of a new generation of homogeneous and heterogeneous N_2O reduction catalysts.

6.4 Experimental Procedures

6.4.1 General Methods

All reactions and subsequent manipulations were performed under anaerobic and anhydrous conditions under an atmosphere of nitrogen. Hexanes, Et_2O, and toluene were dried using a Vacuum Atmospheres DRI-SOLV Solvent Purification system and stored over 3Å sieves for 24 h prior to use. Benzene-d_6, toluene-d_8, thf-d_8, pentane, and C_8H_{18} (isooctane) were dried over 3 Å molecular sieves for 24 h prior to use. [L^{tBu}NiCl], and $[K]_6[L^{tBu}Ni(\kappa^2\text{-}CO_3)]_6$ were synthesized according to previously reported procedures.[11,88] All other reagents were purchased from commercial suppliers and used as received.

^1H and $^{13}C\{^1H\}$ NMR spectra were recorded on a Agilent Technologies 400-MR DD2 400 MHz spectrometer or a Varian UNITY INOVA 500 MHz spectrometer. ^1H and $^{13}C\{^1H\}$ NMR spectra were referenced to external $SiMe_4$ using the residual protio solvent peaks as internal standards. The chemical shifts of $^{19}F\{^1H\}$ were referenced indirectly with the ^1H resonance of $SiMe_4$ at 0 ppm, according to IUPAC standard.[89,90] IR spectra were recorded on a Nicolet 6700 FT-IR spectrometer. Elemental analyses were performed by the Micro-Mass Facility at the University of California, Berkeley.

6.4.2 Synthesis of [L^{tBu}Ni(OTf)]

A 20 mL scintillation vial was charged with a dark green solution of [L^{tBu}NiCl] (41 mg, 0.0688 mmol) in THF (3 mL). To this stirring solution was added solid AgOTf (17.8 mg, 0.688 mmol). After addition, the solution gradually transformed from dark green to bright green in color, concomitant with the deposition of a white precipitate (presumably AgCl). This solution was allowed to stir for 12 h, whereupon the reaction mixture was filtered through a Celite column supported on glass wool (0.5 cm × 2 cm). The solution was

concentrated to 0.5 mL *in vacuo*, layered with hexane (2 mL), and stored at -25 °C for 24 h, which resulted in the deposition of bright green needles that were isolated by decanting off the supernatant (40 mg, 82% yield). ^{1}H NMR (400 MHz, 25 °C, benzene-d_6): δ 7.20 (d, $^{3}J_{HH}$, = 7.5 Hz, 4H, m-Ar-**H**), 6.81 (t, $^{3}J_{HH}$, = 7.1 Hz, 2H, o-Ar-**H**), 4.58 (sept, $^{3}J_{HH}$, = 6.3 Hz, 4H, C**H**$(CH_3)_2$), 3.20 (s, 1H, γ-**H**), 2.55 (d, $^{3}J_{HH}$, = 6.2 Hz, 12H, CH(C**H**$_3)_2$), 1.33 (d, $^{3}J_{HH}$, = 6.1 Hz, 12H, CH(C**H**$_3)_2$), 0.83 (s, 18H, C(C**H**$_3)_3$) ppm. ^{19}F{^{1}H} NMR (376 MHz, 25 °C, benzene-d_6): δ -77.98 (s) ppm. Single crystals of [L^{tBu}Ni(OTf)] were analyzed by X-ray diffraction. This analysis unambiguously confirmed the proposed formulation of the complex, however the crystals were badly twinned, which greatly reduced the data quality. Crystallographic details: Monoclinic, $P2_1/n$, a = 25.044(3), b = 10.7335(15), c = 32.146(4), α = 90, β = 96.992(8), γ = 90, V = 8577(2) g/cm^3, Z = 4.

6.4.3 Reaction of [K(18-crown-6)][L^{tBu}Ni(S)] (2.4) with N_2O.

A 50 mL Schlenk flask, equipped with a Teflon rotoflow valve, was charged with a dark brown solution of **2.5** (41.0 mg, 0.0452 mmol) in toluene (1 mL). The headspace was then evacuated and filled with N_2O gas (1 atm). After addition of N_2O, the solution gradually changed from dark brown to a pale yellow color. After stirring for three hours, the reaction mixture was then transferred into a scintillation vial inside a glovebox, filtered through a Celite column supported on glass wool (0.5 cm × 2 cm), and concentrated to 0.5 mL *in vacuo*. Addition of isooctane (0.5 mL) to this solution and subsequent storage at -25 °C for 24 h resulted in the formation of small pale orange plates, which were isolated by decanting off the supernatant (26.3 mg, 62% yield). Anal. Calcd for $C_{47}H_{77}KN_4NiO_7S$: C, 60.05; H, 8.26; N, 5.96; S, 3.41. Found: C, 60.19; H, 8.31; N, 5.59; S, 3.33. ^{1}H NMR (400 MHz, 25 °C, benzene-d_6): 7.05 (6H, Ar-**H**), 5.43 (1H, γ-**H**), 4.48 (sept, $^{3}J_{HH}$, = 6.8 Hz, 4H,

C**H**$(CH_3)_2$), 2.93 (24H, 18-crown-6), 2.01 (d, $^3J_{HH}$, = 6.7 Hz, 12H, CH(C**H**$_3)_2$), 1.52 (d, $^3J_{HH}$, = 6.8 Hz, 12H, CH(C**H**$_3)_2$), 1.29 (18H, C(C**H**$_3)_3$) ppm. ^{13}C NMR (125 MHz, 25 °C, benzene-d_6): 166.67 (Ar-*i*C), 143.72 (Ar-*o*C), 124.08 (Ar-*p*C), 122.19 (Ar-*m*C), 70.37 (18-crown-6), 42.86 (**C**$(CH_3)_3$), 33.89 (C(**C**$H_3)_3$), 28.51 (CH(**C**$H_3)_2$), 26.61 (CH(**C**$H_3)_2$), 24.57 (**C**$H(CH_3)_2$), ppm. γ-**C**H resonance not observed. IR (KBr pellet, cm^{-1}): 1628 (w), 1579 (w), 1537 (m), 1514 (m), 1463 (m), 1442 (m), 1413 (s), 1382 (w), 1365 (m), 1351 (m), 1319 (m), 1284 (w), 1263 (w), 1251 (m), 1218 (m), 1191 (w), 1180 (w), 1160 (m), 1110 (vs), 1056 (m), 1031 (w), 960 (s), 937 (w), 898 (w), 837 (m), 800 (m), 779 (m), 759 (m), 667 (w), 530 (w), 514 (w), 455 (w), 408 (w).

6.4.4 Variable temperature NMR Spectroscopy of 6.1.

To an NMR tube was added a toluene-d_8 (0.5 mL) solution of **6.1** (7.2 mg, 0.0077 mmol). The sample was cooled to -85 °C in a 500 MHz NMR spectrometer. ^{1}H NMR spectra were collected at ca. 20 °C intervals. ^{1}H NMR (500 MHz, 25 °C, toluene-d_8): 6.90-7.10 (6H, Ar-**H**), 5.33 (1H, γ-**H**), 4.39 (sept, $^3J_{HH}$, = 6.8 Hz, 4H, C**H**$(CH_3)_2$), 2.98 (24H, 18-crown-6), 1.93 (d, $^3J_{HH}$, = 6.7 Hz, 12H, CH(C**H**$_3)_2$), 1.49 (d, $^3J_{HH}$, = 6.8 Hz, 12H, CH(C**H**$_3)_2$), 1.23 (18H, C(C**H**$_3)_3$) ppm. ^{1}H NMR (500 MHz, 0 °C, toluene-d_8): 6.90-7.10 (6H, Ar-**H**), 5.39 (1H, γ-**H**), 4.40 (sept, $^3J_{HH}$, = 6.8 Hz, 4H, C**H**$(CH_3)_2$), 2.93 (24H, 18-crown-6), 1.95 (d, $^3J_{HH}$, = 6.7 Hz, 12H, CH(C**H**$_3)_2$), 1.51 (d, $^3J_{HH}$, = 6.8 Hz, 12H, CH(C**H**$_3)_2$), 1.25 (18H, C(C**H**$_3)_3$) ppm. ^{1}H NMR (500 MHz, -20 °C, toluene-d_8): 6.90-7.10 (6H, Ar-**H**), 5.42 (1H, γ-**H**), 4.41 (sept, $^3J_{HH}$, = 6.8 Hz, 4H, C**H**$(CH_3)_2$), 2.90 (24H, 18-crown-6), 1.97 (d, $^3J_{HH}$, = 6.6 Hz, 12H, CH(C**H**$_3)_2$), 1.52 (d, $^3J_{HH}$, = 6.8 Hz, 12H, CH(C**H**$_3)_2$), 1.26 (18H, C(C**H**$_3)_3$) ppm. ^{1}H NMR (500 MHz, -40 °C, toluene-d_8): 6.90-7.10 (6H, Ar-**H**), 5.46 (1H, γ-**H**), 4.42 (sept, $^3J_{HH}$, = 6.7 Hz, 4H, C**H**$(CH_3)_2$), 2.87 (24H, 18-

crown-6), 1.98 (d, $^3J_{HH}$, = 6.5 Hz, 12H, CH(C**H**$_3$)$_2$), 1.52 (d, $^3J_{HH}$, = 6.8 Hz, 12H, CH(C**H**$_3$)$_2$), 1.28 (18H, C(C**H**$_3$)$_3$) ppm. ^{1}H NMR (500 MHz, -65 °C, toluene-d_8): 6.90-7.10 (6H, Ar-**H**), 5.50 (1H, γ-**H**), 4.45 (br s, 4H, C**H**(CH$_3$)$_2$), 2.84 (24H, 18-crown-6), 2.00 (br s, 12H, CH(C**H**$_3$)$_2$), 1.54 (d, $^3J_{HH}$, = 6.0 Hz, 12H, CH(C**H**$_3$)$_2$), 1.31 (18H, C(C**H**$_3$)$_3$) ppm. ^{1}H NMR (500 MHz, -85 °C, toluene-d_8): 6.90-7.10 (6H, Ar-**H**), 5.52 (1H, γ-**H**), 4.47 (br s, 4H C**H**(CH$_3$)$_2$), 2.83 (24H, 18-crown-6), 2.02 (br s, 12H, CH(C**H**$_3$)$_2$), 1.55 (br s, 12H, CH(C**H**$_3$)$_2$), 1.33 (18H, C(C**H**$_3$)$_3$) ppm.

6.4.5 Synthesis of [K(18-crown-6)][L^{tBu}Ni(η^2-SO)] (6.2)

In a glovebox, a J-Young NMR tube was charged with a yellow orange solution of [K(18-crown-6)][L^{tBu}Ni(*S*,*O*:κ$_2$-SNNO)] (**II**) (74 mg, 0.0787 mmol) and toluene-d_8 (1 mL). The NMR tube was then sealed, removed from the glovebox and heated at 45 °C for 6 d in an oil bath, which resulted in a gradual color change from yellow to orange. After 6 d, a ^{1}H NMR spectrum was recorded, which revealed the presence of [K(18-crown-6)][L^{tBu}Ni(η^2-SO)] (**6.2**), along with formation of trace amounts of [K(18-crown-6)][L^{tBu}Ni(η^2-OSSO)] (**6.3**) and [K(18-crown-6)][L^{tBu}Ni(η^2-S$_2$)] (**6.4**). ^{1}H NMR (400 MHz, 25 °C, toluene-d_8): δ 7.01-6.73 (**6.2**, m, 6H, Ar-**H**, dipp), 5.53 (**6.3**, s, γ-**H**), 5.47 (**6.4**, s, γ-**H**), 5.43 (**6.2**, s, 1H, γ-**H**), 4.50 (**6.2**, sept, $^3J_{HH}$, = 6.7 Hz, 2H, C**H**(CH$_3$)$_2$), 4.38 (**6.2**, sept, $^3J_{HH}$, = 6.7 Hz, 2H, C**H**(CH$_3$)$_2$), 3.04 (**6.2**, s, 24H, 18-crown-6), 2.21 (**6.2**, d, $^3J_{HH}$, = 6.7 Hz, 6H, CH(C**H**$_3$)$_2$), 2.05 (**6.2**, d, $^3J_{HH}$, = 6.7 Hz, 6H, CH(C**H**$_3$)$_2$), 1.57 (**6.2**, overlapping doublets, CH(C**H**$_3$)$_2$), 1.30 (**6.2**, s, 9H, C(C**H**$_3$)$_3$), 1.25 (**6.2**, s, 9H, C(C**H**$_3$)$_3$). The NMR tube was then transferred to a glovebox, and the reaction mixture was filtered through a Celite column supported on glass wool (0.5 cm × 2 cm). The volatiles were removed from the filtrate *in vacuo*. The resulting orange residue was extracted into toluene (1 mL), filtered through a Celite column

supported on glass wool (0.5 cm × 2 cm), and concentrated *in vacuo* to ca. 0.5 mL. This solution was then layered with pentane (2 mL) and subsequent storage at -25 °C for 48 h resulted in the deposition of orange plates of [K(18-crown-6)][L^{tBu}Ni(η^2-SO)] (**6.2**), which were isolated by decanting off the supernatant (62 mg, 82% yield). In one instance, a few orange plates of [K(18-crown-6)][L^{tBu}Ni(η^2-OSSO)] (**6.3**) were also isolated from the reaction mixture. These were analyzed by X-ray diffraction. Anal. Calcd for **6.2**: $C_{47}H_{77}KN_2NiO_7S \cdot C_7H_8$: C, 64.59; H, 8.53; N, 2.79. Found: C, 63.68; H, 8.38; N, 3.01. ^{1}H NMR (400 MHz, 25 °C, benzene-d_6): δ 7.01-6.73 (m, 6H, Ar-**H**, dipp), 5.54 (s, 1H, γ-**H**), 4.62 (sept, $^3J_{HH}$, = 6.7 Hz, 2H, C**H**$(CH_3)_2$), 4.48 (sept, $^3J_{HH}$, = 6.7 Hz, 2H, C**H**$(CH_3)_2$), 3.01 (s, 24H, 18-crown-6), 2.31 (d, $^3J_{HH}$, = 6.7 Hz, 6H, CH(C**H**$_3)_2$), 2.15 (d, $^3J_{HH}$, = 6.7 Hz, 6H, CH(C**H**$_3)_2$), 1.57 (overlapping doublets, 12H, CH(C**H**$_3)_2$), 1.37 (s, 9H, C(C**H**$_3)_3$), 1.32 (s, 9H, C(C**H**$_3)_3$). ^{13}C{^{1}H} NMR (125 MHz, 25 °C, benzene-d_6): δ 164.91 (Ar-C), 163.28 (Ar-C), 155.40 (Ar-C), 150.77 (Ar-C), 142.13 (Ar-C), 140.54 (Ar-C), 122.19 (Ar-C), 120.99 (Ar-C), 97.87 (γ-**C**), 69.78 (18-crown-6), 42.34 (**C**$(CH_3)_3$), 42.31 (**C**$(CH_3)_3$), 33.79 (C(**C**$H_3)_3$), 33.66 (C(**C**$H_3)_3$), 28.80 (CH(**C**$H_3)_2$), 28.64 (CH(**C**$H_3)_2$), 26.24 (CH(**C**$H_3)_2$), 25.94 (CH(**C**$H_3)_2$), 24.66 (**C**$H(CH_3)_2$), 23.70 (**C**$H(CH_3)_2$). IR (KBr Pellet, cm^{-1}): 1535 (m), 1519 (s), 1457 (m), 1429 (m), 1412 (m), 1409 (s), 1385 (m), 1365 (m), 1352 (s), 1321 (s), 1284 (w), 1250 (w), 1214 (w), 1192 (w), 1160 (w), 1110 (s), 1056 (w), 964 (s), 937 (w), 902 (s, ν_{SO}), 896 (w), 839 (m), 819 (w) 804 (w), 779 (m), 759 (m), 728 (w), 669(w), 636 (s), 561 (w), 528 (w).

6.4.6 Synthesis of [K(18-crown-6)][L^{tBu}Ni(η^2-S_2)] (6.4)

A 20 mL scintillation vial was charged with a brown solution of [K(18-crown-6)][L^{tBu}Ni(S)] (**2.5**) (29.7 mg, 0.0312 mmol) in toluene (1 mL). S_8 (1.0 mg, 0.0038 mmol)

was then added to the stirring brown solution, which resulted in a gradual color change from brown to dark orange. The reaction mixture was stirred for 30 min. The reaction mixture was then filtered through a Celite column supported on glass wool (0.5 cm × 2 cm), concentrated *in vacuo* to ca. 0.25 mL, and layered with pentane (1.5 mL). Storage of this vial at -25 °C for 24 h resulted in the deposition of dark yellow plates of [K(18-crown-6)][$L^{tBu}Ni(\eta^2\text{-}S_2)$] (**6.4**), which were isolated by decanting off the supernantant (23 mg, 81 %). Anal. Calcd for $C_{47}H_{77}KN_2NiO_6S_2$: C, 60.83; H, 8.36; N, 3.02. Found: C, 60.61; H, 8.18; N, 2.70. ^{1}H NMR (400 MHz, 25 °C, benzene-d_6): δ 7.02-7.00 (m, 6H, Ar-**H**, dipp), 5.56 (s, 1H, γ-**H**), 4.42 (sept, $^3J_{HH}$, = 6.7 Hz, 4H, C**H**$(CH_3)_2$), 3.03 (s, 24H, 18-crown-6), 2.25 (d, $^3J_{HH}$, = 6.8 Hz, 12H, CH(C**H**$_3)_2$), 1.54 (d, $^3J_{HH}$, = 6.8 Hz, 12H, CH(C**H**$_3)_2$), 1.36 (s, 18H, C(C**H**$_3)_3$). ^{1}H NMR (400 MHz, 25 °C, Toluene-d_8): δ 7.09-6.92 (m, 6H, Ar-**H**, dipp), 5.46 (s, 1H, γ-**H**), 4.32 (sept, $^3J_{HH}$, = 6.9 Hz, 4H, C**H**$(CH_3)_2$), 3.05 (s, 24H, 18-crown-6), 2.17 (d, $^3J_{HH}$, = 6.7 Hz, 12H, CH(C**H**$_3)_2$), 1.51 (d, $^3J_{HH}$, = 6.7 Hz, 12H, CH(C**H**$_3)_2$), 1.30 (s, 18H, C(C**H**$_3)_3$). ^{13}C{^{1}H} NMR (125 MHz, 25 °C, benzene-d_6): δ 140.05 (Ar-C), 137.47 (Ar-C), 128.91 (Ar-C), 125.28 (Ar-C), 98.08 (γ-**C**), 69.56 (18-crown-6), 34.03 (**C**$(CH_3)_3$), 33.70 (C(**C**$H_3)_3$), 28.16 (CH(**C**$H_3)_2$), 22.33 (CH(**C**$H_3)_2$), 21.03 (**C**H$(CH_3)_2$). IR (KBr Pellet, cm^{-1}): 1535 (m), 1519 (s), 1457 (m), 1429 (m), 1412 (m), 1409 (s), 1385 (m), 1365 (m), 1352 (s), 1321 (s), 1284 (w), 1250 (w), 1214 (w), 1192 (w), 1160 (w), 1110 (s), 1056 (w), 964 (s), 937 (w), 896 (w), 839 (m), 819 (w) 804 (w), 779 (m), 759 (m), 728 (w), 669(w), 541 (w), 528 (w).

6.4.7 Reaction of [K(18-crown-6)][$L^{tBu}Ni(\eta^2$-SO)] (6.2) with ^{13}CO

In a glovebox, a J-Young NMR tube was charged with a yellow-orange solution of [K(18-crown-6)][$L^{tBu}Ni(\eta^2$-SO)] (12.2 mg, 0.0134 mmol) in C_6D_6 (1 mL). The NMR tube

was then sealed and removed from the glovebox. Its headspace was evacuated and replaced with 1 atm of ^{13}CO. Over the course of the reaction, the color gradually lightens from yellow-orange to yellow. After 1 h, a ^{1}H NMR spectrum was recorded, which revealed the presence of the nickel(II) sulfide **2.5**, ([$L^{tBu}Ni(S)]^-$), an unidentified diamagnetic intermediate, as well as [K(18-crown-6)][$L^{tBu}Ni(\eta^2$-SCO)] (**5.1**), [K(18-crown-6)][$L^{tBu}Ni(\kappa^2$-$SCO_2)$] (**6.5**), [K(18-crown-6)][$L^{tBu}Ni(\kappa^2$-$CO_3)$] (**6.6**), and [K(18-crown-6)][$L^{tBu}Ni(\kappa^2$-$S_2CO)$] (**6.8**). ^{1}H NMR (400 MHz, 25 °C, benzene-d_6, note: spectral data have only been tabulated for the [K(18-crown-6)][$L^{tBu}Ni(S)$] intermediate and the region from 5.00-5.75 ppm, which is diagnostic for the γ-H environment of the β-diketiminate ligand): 32.92 ([$L^{tBu}Ni(S)]^-$), 31.91 ([$L^{tBu}Ni(S)]^-$), 8.50 ([$L^{tBu}Ni(S)]^-$), 5.87 ([$L^{tBu}Ni(S)]^-$), 5.62 (s, 1H, γ-**H**, **6.3**), 5.57 (s, 1H, γ-**H**, **6.8**, tentative assignment), 5.56 (s, 1H, γ-**H**, **6.4**), 5.54 (s, 1H, γ-**H**, **6.2**), 5.48 (s, 1H, γ-**H**, overlapping **5.1** and **6.5**), 5.43 (s, 1H, γ-**H**, unidentified diamagnetic intermediate), 5.42 (s, 1H, γ-**H**, **6.6**), -0.63 ([$L^{tBu}Ni(S)]^-$), -23.24 ([$L^{tBu}Ni(S)]^-$), -130.25 ([$L^{tBu}Ni(S)]^-$). Note that the observation of **6.3** and **6.4** in the reaction mixture can be rationalized by their presence, in small amounts, in the starting material. After 6 h, ^{1}H and ^{13}C NMR spectra were recorded. These spectra revealed the absence of [K(18-crown-6)][$L^{tBu}Ni(S)$] (**2.4**) and the aforementioned unidentified diamagnetic intermediate. The spectrum also reveals the presence of [K(18-crown-6)][$L^{tBu}Ni(\eta^2$-SCO)] (**5.1**), [K(18-crown-6)][$L^{tBu}Ni(\kappa^2$-$SCO_2)$] (**6.5**), [K(18-crown-6)][$L^{tBu}Ni(\kappa^2$-$CO_3)$] (**6.6**), COS (**6.7**), [K(18-crown-6)][$L^{tBu}Ni(\kappa^2$-$S_2CO)$] (**6.8**), as well as two unidentified products. ^{1}H NMR (400 MHz, 25 °C, benzene-d_6, note: spectral data have only been tabulated for the region from 5.00-5.75 ppm, which is diagnostic for the γ-H environment of the β-diketiminate ligand): 5.62 (s, 1H, γ-**H**, **6.3**), 5.57 (s, 1H, γ-**H**, **6.8**, tentative assignment), 5.56 (s, 1H, γ-**H**, **6.4**), 5.48 (s,

1H, γ-**H**, overlapping **5.1** and **6.5**), 5.42 (s, 1H, γ-**H**, **6.6**). $^{13}C\{^{1}H\}$ NMR (125 MHz, 25 °C, benzene-d_6, note: spectral data have only been tabulated for the region from 140-220 ppm, which is diagnostic for the ^{13}C chemical shifts of $[CO_xS_y]^{2-}$–type species): δ 214.72 ($[L^{tBu}Ni(\eta^2\text{-S}\mathbf{C}O)]^-$, **5.1**), 206.88 ($[L^{tBu}Ni(S_2\mathbf{C}O)]^-$, **6.8**, tentative assignment), 191.38 (unassigned), 184.00 (**C**O), 178.47 (unassigned), 177.30 (($[L^{tBu}Ni(\kappa^2\text{-S}\mathbf{C}O_2)]^-$, **6.5**, 165.27 ($[L^{tBu}Ni(\kappa^2\text{-}\mathbf{C}O_3)]^-$, **6.6**), 152.93 (S**C**O, **6.7**).

6.4.8 Reaction of [K(18-crown-6)][$L^{tBu}Ni(\eta^2$-SO)] (6.2) with CO, Monitored by IR Spectroscopy

In a glovebox, a J-Young NMR tube was charged with a yellow-orange solution of [K(18-crown-6)][L^{tBu}Ni(SO)] (10.0 mg, 0.0110 mmol) in C_6D_6 (1 mL). The NMR tube was then sealed and removed from the glovebox. The headspace of the NMR tube was then evacuated and replaced with 1 atm of CO. The reaction was monitored by ^{1}H NMR spectroscopy. During the course of the reaction, the color of the solution gradually lightened to yellow. After 6 h the J-Young tube was then transferred into a glove box, where the solution was transferred into a 20 mL scintillation vial. The volatiles were removed *in vacuo* to yield an orange residue, which was extracted into hexane (0.5 mL) and transferred into a solution IR cell. IR (hexanes solution, cm^{-1}): 2021 (m, $L^{tBu}Ni^{I}$(CO), **6.9**),[57] 1666 (m, $[L^{tBu}Ni^{II}(\eta^2\text{-SCO})]^-$, **5.1**),[53] 1620 (m, $[L^{tBu}Ni^{II}(\kappa^2\text{-}CO_3)]^-$, **6.6**). These assignments were confirmed by comparison with IR spectra of authentic samples in hexane.

6.4.9 Synthesis of [K(18-crown-6)][$L^{tBu}Ni(\kappa_2$-$SCO_2)$] (6.5)

In a glovebox, a J-Young NMR tube was charged with a brown solution of [K(18-crown-6)][L^{tBu}Ni(S)] (**2.5**) (35.0 mg, 0.0391 mmol) dissolved in C_6D_6 (1 mL). The NMR tube was then sealed, removed from the glovebox, and the headspace of the NMR tube was

evacuated and replaced with 1 atm of CO_2. Upon CO_2 addition, the solution quickly changed color to gold. A ^{1}H NMR spectrum was collected, which revealed the clean formation of a new diamagnetic Ni-containing complex. The NMR tube was then transferred to a glove box, and the reaction mixture was transferred into a 20 mL scintillation vial. The volatiles were then removed *in vacuo* to give a pale brown residue. The residue was extracted into toluene (1 mL), filtered through a Celite column supported on glass wool (0.5 cm × 2 cm), and concentrated *in vacuo* to ca. 0.5 mL. This solution was then layered with hexanes (2 mL). Subsequent storage at -25 °C for 48 h resulted in the deposition of pale brown blocks of [K(18-crown-6)][L^{tBu}Ni(η^2-SCO$_2$)] (**6.5**), which were isolated by decanting off the supernatant (21 mg, 57 %). Anal. Calcd for: $C_{48}H_{77}KN_2NiO_8S\cdot1.5C_7H_8$: C, 65.17; H, 8.32; N, 2.60. Found: C, 64.70; H, 8.17; N, 2.61. ^{1}H NMR (400 MHz, 25 °C, benzene-d_6): δ 6.95 (s, 6H, Ar-**H**, dipp), 5.48 (s, 1H, γ-**H**), 4.50 (sept, $^3J_{HH}$, = 6.7 Hz, 4H, C**H**(CH$_3$)$_2$), 3.03 (s, 24H, 18-crown-6), 2.20 (d, $^3J_{HH}$, = 6.8 Hz, 12H, CH(C**H**$_3$)$_2$), 1.51 (d, $^3J_{HH}$, = 6.8 Hz, 12H, CH(C**H**$_3$)$_2$), 1.22 (s, 18H, C(C**H**$_3$)$_3$). ^{13}C{^{1}H} NMR (125 MHz, 25 °C, benzene-d_6): δ 177.31 (S**C**O$_2$), 165.85 (Ar-C) , 142.76 (Ar-C), 123.60 (Ar-C), 121.55 (Ar-C), 98.02 (γ-**C**), 69.61 (18-crown-6), 41.68 (**C**(CH$_3$)$_3$), 33.32 (C(**C**H$_3$)$_3$), 28.34 (CH(**C**H$_3$)$_2$), 25.51 (CH(**C**H$_3$)$_2$), 23.94 (**C**H(CH$_3$)$_2$). IR (KBr Pellet, cm^{-1}): 1606 (s, ν_{CO}), 1535 (m), 1519 (s), 1457 (m), 1429 (m), 1412 (m), 1409 (s), 1385 (m), 1365 (m), 1352 (s), 1321 (s), 1284 (w), 1250 (w), 1214 (w), 1205(m), 1180 (w), 1161 (w), 1110 (s), 1056 (w), 964 (s), 937 (w), 896 (w), 839 (m), 819 (w) 804 (w), 779 (m), 759 (m), 728 (w), 669(w), 582 (w), 532 (w), 503 (m).

6.4.10 Synthesis of [K(18-crown-6)][L^{tBu}Ni(κ^2-CO$_3$)] (6.6)

In a glovebox, a 20 mL scintillation vial was charged with a suspension of [K]$_6$[L^{tBu}Ni(κ^2-CO$_3$)]$_6$ (34 mg, 0.00859 mmol) in toluene (2 mL). To this stirring, pale

brown suspension was added 18-crown-6 (14 mg, 0.0515 mmol). The solution was stirred for 2 h, whereupon the pale brown solid was completely consumed. The volatiles were then removed *in vacuo* from the pale yellow solution to give a yellow solid. The solid was extracted into pentane (1 mL), filtered through a Celite column supported on glass wool (0.5 cm × 2 cm), and concentrated *in vacuo* to ca. 0.25 mL. Addition of hexamethyldisiloxane (0.5 mL) to this solution, followed by storage at -25 °C for 48 h, resulted in the deposition of colorless crystals of 18-crown-6, which were isolated by decanting off the supernatant. The volatiles were then removed from the supernatant *in vacuo* to give a yellow solid. This solid was extracted into pentane (0.5 mL), filtered through a Celite column supported on glass wool (0.5 cm × 2 cm), concentrated *in vacuo* to ca. 0.25 mL, and transferred to a 5 mL vial. This vial was placed inside a 20 mL scintillation vial. Toluene (2 mL) was then added to the outer vial, which was then sealed. Storage of this two vial system at -25 °C for 96 h resulted in the deposition of yellow plates of [K(18-crown-6)][L$^{t\text{Bu}}$Ni(κ^2-CO_3)] (**6.6**), which were isolated by decanting off the supernatant (8.2 mg, 17% yield). The supernatant was then transferred to a 5 mL vial. This vial was placed inside a 20 mL scintillation vial. Toluene (2 mL) was then added to the outer vial, which was then sealed. Storage of this two vial system at -25 °C for 10 d resulted in the deposition of a second crop of yellow plates of **6.6**, which were isolated by decanting off the supernatant (17 mg, overall yield: 52%). ^{1}H NMR (400 MHz, 25 °C, benzene-d_6): δ 6.96-6.88 (m, 6H, Ar-**H**, dipp), 5.42 (s, 1H, γ-**H**), 4.47 (br s, 4H, C**H**(CH_3)$_2$), 3.14 (s, 24H, 18-crown-6), 2.14 (br s, 12H, CH(C**H**$_3$)$_2$), 1.50 (d, $^3J_{HH}$, = 5.5 Hz, 12H, CH(C**H**$_3$)$_2$), 1.15 (s, 18H, C(C**H**$_3$)$_3$). ^{13}C{^{1}H} NMR (125 MHz, 25 °C, benzene-d_6): δ 165.74 (Ar-C), 165.29 (**C**O_3^{2-}), 146.21 (Ar-C), 142.27 (Ar-C), 123.76 (Ar-C), 121.30 (Ar-C),

97.76 (γ-**C**), 69.75 (18-crown-6), 41.09 (**C**$(CH_3)_3$), 32.99 (C(**C**$H_3)_3$), 28.41 (CH(**C**$H_3)_2$), 25.34 (CH(**C**$H_3)_2$), 23.40 (**C**H$(CH_3)_2$). IR (hexanes solution, cm^{-1}): 1620 (ν_{CO}).

6.4.11 Synthesis of [K(18-crown-6)][L^{tBu}Ni(η^2-CO_2)] (6.10)

In a glovebox, a 20 mL scintillation vial was charged with a suspension of [L$^{t\text{Bu}}$Ni(OTf)] (87 mg, 0.113 mmol) in hexane (5 mL). To this stirring bright green suspension was added KC_8 (45.7 mg, 0.338 mmol), which resulted in a rapid color change to deep red and then more slowly to deep purple, concomitant with dissolution of the solid. The deep purple color is indicative of the formation of K_2[{L^{tBu}Ni}$_2$(N_2)].[66] This solution was stirred for 48 h, whereupon it was then filtered through a Celite column supported on glass wool (0.5 cm × 2 cm) into a 50 mL Schlenk flask equipped with a Teflon rotoflow valve, a ground glass joint with a rubber septum, and a magnetic stir bar. The Schlenk flask was then sealed, removed from the glovebox, and attached to a Schlenk line in a fume hood. Carbon dioxide (2.5 mL, 0.113 mmol) was injected into the stirring solution using an airtight syringe. Upon addition, the deep purple reaction mixture quickly changed to deep red and then to pale orange. After 5 min, the Schlenk flask was transferred to a glove box, where a solution of 18-crown-6 (29.8 mg, 0.113 mmol) in hexane (1 mL) was added to the reaction mixture. This addition resulted in the deposition of a small amount of orange solid, but there was no obvious color change. The reaction mixture was then filtered through a Celite column supported on glass wool (0.5 cm × 2 cm) and concentrated *in vacuo* to ca. 1 mL. Benzene (0.25 mL) was then added to this solution as a crystallization aid. Storage of this solution at -25 °C for 48 h resulted in the deposition of a pale orange plates of [K(18-crown-6)][L^{tBu}Ni(η^2-CO_2)] (**6.10**), which were isolated by decanting off the supernatant (33 mg, yield 41%). Anal. Calcd for: $C_{48}H_{77}KN_2NiO_8 \cdot C_6H_6$: C, 65.78; H, 8.48; N, 2.84. Found: C, 65.99; H, 8.68; N, 2.76. ^{1}H

NMR (400 MHz, 25 °C, benzene-d_6): δ 7.11-6.81 (m, 6H, Ar-**H**, dipp), 5.42 (s, 1H, γ-**H**), 4.37 (sept, $^3J_{HH}$, = 6.7 Hz, 2H, C**H**$(CH_3)_2$), 4.26 (sept, $^3J_{HH}$, = 6.7 Hz, 2H, C**H**$(CH_3)_2$), 2.99 (s, 24H, 18-crown-6), 1.96 (d, $^3J_{HH}$, = 6.8 Hz, 6H, CH(C**H**$_3)_2$), 1.86 (d, $^3J_{HH}$, = 6.8 Hz, 6H, CH(C**H**$_3)_2$), 1.56 (overlapping doublets, 12H, CH(C**H**$_3)_2$), 1.42 (s, 9H, C(C**H**$_3)_3$), 1.34 (s, 9H, C(C**H**$_3)_3$). $^{13}C\{^1H\}$ NMR (125 MHz, 25 °C, benzene-d_6): δ 167.23 (**C**O_2) 165.74 (Ar-C), 163.83 (Ar-C), 153.43 (Ar-C), 149.49 (Ar-C), 141.42 (Ar-C), 139.56 (Ar-C), 121.99 (Ar-C), 121.67 (Ar-C), 121.63 (Ar-C), 121.29 (Ar-C), 95.22 (γ-**C**), 69.64 (18-crown-6), 42.47 (**C**$(CH_3)_3$), 42.21 (**C**$(CH_3)_3$), 33.58 (C(**C**$H_3)_3$), 33.08 (C(**C**$H_3)_3$), 28.04 (CH(**C**$H_3)_2$), 27.83 (CH(**C**$H_3)_2$), 26.01 (CH(**C**$H_3)_2$), 24.10 (CH(**C**$H_3)_2$), 23.82 (**C**$H(CH_3)_2$), 23.37 (**C**$H(CH_3)_2$). IR (KBr Pellet, cm^{-1}): 1664 (m, ν_{CO}), 1618 (m), 1514 (m), 1464 (m), 1446 (m), 1433 (m), 1414 (s), 1381 (m), 1365 (m), 1352 (m), 1321 (m), 1284 (w), 1252 (w), 1221 (w), 1196 (w), 1159 (w), 1113 (s), 1055 (w), 1032 (w), 962 (m), 937 (w), 896 (w), 983 (m), 831 (w) 804 (w), 779 (m), 766 (m), 758 (m), 728 (w), 681(w).

6.4.12 Reaction of [K(18-crown-6)][L^{tBu}Ni(η^2-SO)] (6.2) with CO_2, Monitored by ^{1}H NMR Spectroscopy

In a glovebox, a J-Young NMR tube was charged with a yellow-orange solution of [K(18-crown-6)][L^{tBu}Ni(η^2-SO)] (10.0 mg, 0.0110 mmol) in C_6D_6 (0.6 mL). The NMR tube was then sealed and removed from the glovebox. The headspace of the NMR tube was evacuated and replaced with 1 atm of CO_2. Upon addition of CO_2, the color of the solution lightened slightly to pale yellow. A ^{1}H NMR spectrum was taken after 10 min, which revealed complete consumption of complex **6.2** and clean formation of a single new diamagnetic product, which we have tentatively assigned as the monothiopercarbonate complex [K(18-crown-6)][L^{tBu}Ni(κ^2-SOCO_2)] (**6.11**). (400 MHz, 25 °C, benzene-d_6): δ 7.20

(d, $^3J_{HH}$, = 7.6 Hz, 4H, meta-Ar-**H**, dipp), 6.89 (t, $^3J_{HH}$, = 7.5 Hz, 2H, para-Ar-**H**, dipp), 4.62 (sept, $^3J_{HH}$, = 6.6Hz, 4H, C**H**$(CH_3)_2$), 4.49 (s, 1H, γ-**H**), 2.99 (s, 24H, 18-crown-6), 2.37 (d, $^3J_{HH}$, = 6.3 Hz, 12H, CH(C**H**$_3)_2$), 1.52 (d, $^3J_{HH}$, = 6.6 Hz, 12H, CH(C**H**$_3)_2$), 1.20 (s, 18H, C(C**H**$_3)_3$). The NMR tube was then bought into a glove box, where the solution was transferred to a 20 mL vial, the volatiles were removed *in vacuo* to yield an orange residue. This residue was then extracted into pentane (1 mL), filtered through a Celite column supported on glass wool (0.5 cm × 2 cm), and concentrated *in vacuo* to 0.25 mL. Storage of this solution at -25 °C for 48 h resulted in the deposition of a pale orange plates of [K(18-crown-6)][L^{tBu}Ni(η^2-SSO)] (**6.12**), along with other crystalline and solid products. The resulting mixture of solid products was then characterized by ^{1}H NMR spectroscopy in C_6D_6. ^{1}H NMR (400 MHz, 25 °C, benzene-d_6, note: spectral data have only been tabulated for the region from 5.00-5.75 ppm, which is diagnostic for the γ-H environment of the β-diketiminate ligand): 5.62 (s, 1H, γ-**H**, **6.3**), 5.57 (s, 1H, γ-**H**, **6.8**, tentative assignment), 5.56 (s, 1H, γ-**H**, **6.4**), 5.54 (s, 1H, γ-**H**, **6.12**, tentative assignment), 5.42 (s, 1H, γ-**H**, **6.6**), 5.40(s, 1H, γ-**H**, **6.10**) ppm. Crystallographic details for **6.12**: Triclinic, P-1, a = 12.706(9), b = 13.26(1), c = 20.63(1), α = 81.62(2), β = 88.88(2), γ = 63.56(2), V = 3075(4) g/cm^3, Z = 2.

6.4.13 Reaction of [K(18-crown-6)][L^{tBu}Ni(κ^2-SNNO)] (6.1) with Me_3SiOTf to yield [{L^{tBu}Ni}$_2$(μ^2-κ^2-η^2-SNNO)] (6.13)

In a glove box, a NMR tube was charged with a yellow-orange solution of [K(18-crown-6)][L^{tBu}Ni(κ^2-SNNO)] (**6.1**) (13 mg, 0.0136 mmol) in C_6D_6 (0.6 mL). To this solution was added TMSOTf (2.5 μL, 0.0136 mmol). Upon addition, the solution darkens to orange-brown. A ^{1}H NMR spectrum taken after 10 min, revealed complete consumption of complex **6.1** and clean formation of a single new diamagnetic product, [{L^{tBu}Ni}$_2$(μ^2-κ^2-η^2-SNNO)]

(**6.13**). The NMR tube was then bought into a glove box, the solution was transferred to a 20 mL vial and volatiles were removed *in vacuo* to give a brown residue. This residue was extracted into pentane (0.5 mL), filtered through a Celite column supported on glass wool (0.5 cm × 2 cm), concentrated *in vacuo* to ca. 0.1 mL, and stored at -25 °C for 48 h which resulted in the deposition of orange plates of [{L^{tBu}Ni}$_2$(μ^2-κ^2-η^2-SNNO)] (a yield was not determined due to the small amount of product isolated). (400 MHz, 25 °C, benzene-d_6): δ 7.20 (d, $^3J_{HH}$, = 7.50 Hz, 8H, meta-Ar-**H**, dipp), 6.33 (t, $^3J_{HH}$, = 7.5 Hz, 4H, para-Ar-**H**, dipp), 4.74 (sept, $^3J_{HH}$, = 6.7Hz, 8H, C**H**(CH_3)$_2$), 2.13 (d, $^3J_{HH}$, = 6.5 Hz, 24H, CH(C**H**$_3$)$_2$), 1.49 (d, $^3J_{HH}$, = 6.6 Hz, 24H, CH(C**H**$_3$)$_2$), 1.14 (s, 36H, C(C**H**$_3$)$_3$). A ^{1}H NMR spectrum of the supernatant from this reaction revealed the formation of a paramagnetic product which has been identified as [{L^{tBu}Ni}$_2$(μ^2-S)] based on a comparison to the reported ^{1}H NMR spectrum of this complex.[87] Crystallographic details for **6.13**: Monoclinic, C2/c, a = 21.898(3), b = 21.444(3), c = 15.639(2), α = 90, β = 100.825(8), γ = 90, V = 7213.0(15) g/cm^3, Z = 8.

6.4.14 Synthesis of [K(18-crown-6)][C(O)$_2$CPh$_3$]

In a glovebox, a 50 mL bomb fitted with teflon rotoflow valve was charged with a deep red solution of [K(18-crown-6)][CPh_3][60] (130 mg, 0.238 mmol) in THF (3 mL). The bomb was then sealed and removed from the glovebox. The headspace of the bomb was evacuated and replaced with 1 atm of CO_2. Upon addition of CO_2, the solution rapidly became colorless, whereupon the headspace of the bomb was evacuated and the bomb was transferred into a glovebox. The volatiles were then removed from the solution *in vacuo* to give a white solid which was extracted into toluene (2 mL), filtered through a Celite column supported on glass wool (0.5 cm × 2 cm), and layered with hexanes (7 mL) followed by

storage at -25 °C for 24 h. This yields colorless crystals that were isolated by decanting off the supernatant (112 mg, 80%). (400 MHz, 25 °C, benzene-d_6): δ 7.97 (d, 6H, ortho-Ar-**H**), 7.20 (t, 6H, meta-Ar-**H**), 7.10 (t, 3H, para-Ar-**H**), 3.15 (s, 24H, 18-crown-6) ppm.

6.4.15 Synthesis of [$L^{tBu}Ni^{II}$(*O*,*O*:κ^2-C(O)$_2$CPh$_3$)]

A 20 mL scintillation vial was charged with a dark green solution of [$L^{tBu}Ni^{II}Cl$] (50 mg, 0.0849 mmol) in THF/toluene (1 mL:1 mL). To this stirring solution was added solid [K(18-crown-6)][C**(**O)$_2$CPh$_3$] (51 mg, 0.0849 mmol). After addition, the solution gradually transformed from dark green to purple in color, concomitant with the deposition of a white precipitate (KCl). This solution was allowed to stir for 30 min, whereupon the reaction mixture was filtered through a Celite column supported on glass wool (0.5 cm × 2 cm). The volatiles were then removed from the solution *in vacuo* to give a oily purple residue. This residue was extracted into hexane (2 mL), filtered through a Celite column supported on glass wool (0.5 cm × 2 cm), and concentrated *in vacuo* to 0.5 mL. Storage of this solution at -25 °C for 48 h results in the deposition of purple plates which were isolated by decanting off the supernatant. (27 mg, 37% yield). The solid state molecular structure of [$L^{tBu}Ni^{II}$(*O*,*O*:κ^2-C(O)$_2$CPh$_3$)] can be found in . ^{1}H NMR (400 MHz, 25 °C, benzene-d$_6$): δ 7.00-6.80 (m, 19H, Ar-**H**, CPh$_3$ and Dipp), 6.66 (t, 2H, o-Ar-**H**, Dipp), 4.35 (s, 1H, γ-**H**), 4.24 (sept, 4H, C**H**(CH$_3$)$_2$), 2.09 (d, 12H, CH(C**H**$_3$)$_2$), 1.39 (d, 12H, CH(C**H**$_3$)$_2$), 1.00 (s, 18H, C(C**H**$_3$)$_3$) ppm. Crystallographic details: Orthorhombic, $P_{2c\text{-}2ac}$, a = 22.257(2), b = 10.736(1), c = 19.581(2), α = 90, β = 90, γ = 90, V = 4679.2(7) g/cm^3, Z = 6.

6.4.16 Reduction of [$L^{tBu}Ni^{II}$(*O*,*O*:κ^2-C(O)$_2$CPh$_3$)]

To a cold (-25 °C) purple, stirring solution of [$L^{tBu}Ni^{II}$(*O*,*O*:κ^2-C(O)$_2$CPh$_3$)] (27 mg, 0.0318 mmol) and 18-crown-6 (16.8 mg, 0.0637 mmol) in Et$_2$O (2 mL) was added KC$_8$ (8.6

mg, 0.0637 mmol). After addition, the color of the solution rapidly became dark red-orange and some brown precipitate starts to form. The mixture was allowed to stir for 5 min, whereupon 0.5 mL of THF was added to dissolve all of solids that had formed. The reaction mixture was then stirred for another 5 min and no changes were observed. This mixture was filtered through a Celite column supported on glass wool (0.5 cm × 2 cm) to give a black plug and a red-orange filtrate. Volatiles were removed from the filtrate *in vacuo*, and the resulting red residue was extracted into THF-d_8 for ^{1}H NMR spectroscopic analysis. The ^{1}H NMR spectrum reveals the clean formation of a paramagnetic Ni^I product, which has been tentatively identified as [K(18-crown-6)][$L^{tBu}Ni^I$(*O*,*O*:κ^2-C(O)$_2$CPh$_3$)]. However, attempts to isolate and characterize this product have been unsuccessful. ^{1}H NMR (400 MHz, 25 °C, THF-d_8): δ = 24.18 (br s), 21.21 (br s), 13.16 (br s), 7.94 (s), 7.17 (s), 7.10 (br m), 3.96 (br s), 3.08 (s), - 1.48 (br s), -11.91 (br s) ppm.

6.4.17 Reaction of [$L^{tBu}Ni^{II}(OCPh_3)$] (7.2) with KC_8 in the presence of 18-crown 6 and CO_2 to yield [K(18-crown-6)][$L^{tBu}Ni^{II}(\kappa^2\text{-}CO_3)$] (6.6)

In a glovebox, a 50 mL bomb fitted with teflon rotoflow valve and a ground glass joint was charged with a cold (-25 °C) bright green solution of [$L^{tBu}Ni^{II}(OCPh_3)$] (40 mg, 0.0488 mmol) and 18-crown-6 (25.8 mg, 0.0976 mmol) in THF (5 mL). The bomb was then sealed and removed from the glovebox. The headspace of the bomb was evacuated and replaced with 1 atm of CO_2. The stopper was then removed from the ground glass joint, with the bomb under a positive pressure of CO_2 and KC_8 (13.2 mg, 0.0976 mmol) was added, and the stopper was replaced. Upon addition of KC_8, the solution rapidly became red-brown and was allowed for 10 min, no further changes were observed. Next, volatiles were removed from the reaction mixture *in vacuo* to give an orange residue. The bomb is then transferred into a

glovebox. The orange residue was extracted into toluene (2 mL), leaving behind some colorless solid, and filtered through a Celite column supported on glass wool (0.5 cm × 2 cm) to give a pale orange solution. This solution was then concentrated *in vacuo* to 1 mL and stored at - 25 °C for 24 h resulting in the deposition of colorless crystals which appear to contain the -CPh_3 moiety based on their ^{1}H NMR spectrum. (400 MHz, 25 °C, benzene-d_6): δ 7.31-7.03 (m, Ar-**H**, CPh_3), 3.51 (s, 18-crown-6) ppm. The pale orange supernatant was the filtered through a Celite column supported on glass wool (0.5 cm × 2 cm), concentrated *in vacuo* to 0.25 mL, layered with hexane (2 mL) and stored at - 25 °C for 72 h resulting in the deposition of pale brown block crystals of [K(18-crown-6)][$L^{tBu}Ni^{II}(\kappa^2$-$CO_3)$] (**6.6**) which co-crystallized with the clear crystals (due to the fact that [K(18-crown-6)][$L^{tBu}Ni^{II}(\kappa^2$-$CO_3)$] co-crystallized with another product with similar solubility, a yield for this reaction could not be determined). ^{1}H NMR (400 MHz, 25 °C, benzene-d_6): δ 6.90-6.87 (m, 6H, Ar-**H**, dipp), 5.40 (s, 1H, γ-**H**), 4.49 (sept, 4H, C**H**$(CH_3)_2$), 3.40 (s, 24H, 18-crown-6), 2.14 (d, 12H, CH(C**H**$_3)_2$), 1.50 (d, 12H, CH(C**H**$_3)_2$), 1.16 (s, 18H, C(C**H**$_3)_3$). ppm.

6.5 X-ray Crystallography

Data for **6.1-6.4**, **6.5**, **6.6**, and **6.10** were collected on a Bruker KAPPA APEX II diffractometer equipped with an APEX II CCD detector using a TRIUMPH monochromator with a Mo Kα X-ray source (α = 0.71073 Å). The crystals were mounted on a cryoloop under Paratone-N oil, and all data were collected at 100(2) K using an Oxford nitrogen gas cryostream. Data were collected using ω scans with 0.5° frame widths. Frame exposures of 15 seconds were used for all seven crystals. Data collection and cell parameter determinations were conducted using the SMART program.[91] Integration of the data frames and final cell parameter refinements were performed using SAINT software.[92] Absorption

correction of the data was carried out using the multi-scan method SADABS.[93] Subsequent calculations were carried out using SHELXTL.[94] Structure determination was done using direct or Patterson methods and difference Fourier techniques. All hydrogen atom positions were idealized, and rode on the atom of attachment. However, hydrogen atoms were not added to disordered carbon atoms. Structure solution, refinement, graphics, and creation of publication materials were performed using SHELXTL. [94]

In complex **6.1**, the one of the solvate molecule sites was modelled with mixed occupancy, wherein both toluene and C_8H_{18} were present in a 50:50 ratio. The positions of the carbon atoms were constrained using DFIX command in SHELXL. Hydrogen atoms were not added to disordered carbon atoms. Additionally, the $[SN=NO]^{2-}$ ligand was found to be disordered over two orientations, which were related by a C_2 rotation about the Ni-K vector. These two orientations were modelled in a 70:30 ratio using an FVAR command in SHELXL.

For complex **6.2**, the C_7H_8 solvate molecule is disordered over two positions, which were related by a 180° rotation. These two orientations were modeled in a 51:49 ratio using the FVAR command in SHELXL. The C-C bonds in the C_7H_8 molecules were constrained to 1.4 or 1.5 Å, for the double and single bonds, respectively, using the DFIX command. Additionally, one of the O atoms, and the two adjacent C atoms on the 18-crown-6 ring, were found to be disordered over two positions. These disordered atoms were modeled in a 50:50 ratio. Hydrogen atoms were not added to the carbon atoms that were adjacent to the disordered carbons. Additionally, the $[SO]^{2-}$ ligand in **6.2** was found to be disordered over two positions in a 97:3 ratio, which are related by a C_2 rotation about the Ni-K axis. The

relative occupancy of these two orientations was determined with the FVAR command in SHELXL.

For complex **6.3**, one of the C_6H_{14} solvate molecules was found to be disordered over two positions, which were modeled in a 50:50 ratio. In addition, the C-C bonds within the disordered C_6H_{14} molecule were constrained using the SADI command in SHELXL.

For complex **6.4**, both C_7H_8 solvate molecules were all found to be disordered over two positions, which were each modeled in a 50:50 ratio. The C-C bond lengths in these molecules were constrained using the SADI command in SHELXL.

For complex **6.5**, one of the C_7H_8 solvate molecules was found to be disordered over two positions, which were modeled in a 50:50 ratio. The C-C bond lengths in this molecule were constrained using the SADI command in SHELXL. Additionally, the $[SCO_2]^{2-}$ ligand was found to be disordered over two orientations, which were related by a C_2 rotation about the Ni-K vector. These two orientations were modeled in a 87:13 ratio using the FVAR command in SHELXL. The S, C, and O atoms of the $[SCO_2]^{2-}$ ligand were refined isotropically.

For complex **6.6**, the ligand *tert*-butyl groups on the β-diketiminate ligand were found to be disordered over two positions. These disordered groups were modeled in a 50:50 ratio. In addition, the C-C bond lengths within the C_5H_{12} solvate molecule were constrained using the SADI and FLAT commands in SHELXL. The carbon atoms of the C_5H_{12} solvate were refined isotropically.

For complex **6.10**, the 18-crown-6 molecule was found to be disordered over two positions. These two orientations were modeled in a 76:24 ratio using the FVAR command in SHELXL. The C-C and C-O bond lengths in this molecule were constrained using the

SADI command in SHELXL. These C and O atoms were refined isotropically. Additionally, the C-C bonds within the C_6H_6 solvate molecules were constrained using both the SADI and DFIX commands in SHELXL. Additionally, the $[CO_2]^{2-}$ ligand was found to be disordered over two orientations, which were related by a C_2 rotation about the Ni-K vector. These two orientations were modeled in a 53:47 ratio using the FVAR command in SHELXL.

Further crystallographic details for complexes **6.1-6.4, 6.5, 6.6, and 6.10** can be found in Table 6.1 and Table 6.2.

Table 6.1. X-ray Crystallographic Data for Complexes 6.1-6.4

	6.1·1.5C_7H_8·0.5C_8H_{18}	**6.2**·C_7H_8	**6.3**·2C_6H_{14}	**6.4**·2C_7H_8
empirical formula	$C_{47}H_{77}KN_4NiO_7S$ ·1.5C_7H_8·0.5C_8H_{18}	$C_{47}H_{77}KN_2NiO_7S$· C_7H_8	$C_{47}H_{77}KN_2NiO_8S_2$ ·2C_6H_{14}	$C_{47}H_{77}KN_2NiO_6S_2$ ·2C_7H_8
crystal habit, color	Plate, Yellow	Plate, Orange	Plate, Orange	Plate, Yellow
crystal size (mm)	0.2 × 0.15 × 0.05	0.15 × 0.1 × 0.02	0.2 × 0.1 × 0.03	0.2 × 0.1 × 0.02
crystal system	Triclinic	Triclinic	Monoclinic	Triclinic
space group	*P-1*	*P-1*	*C2/c*	*P-1*
volume (Å^3)	3073.9(13)	2743.8(7)	12534.2(2)	3085.8(7)
a (Å)	11.847(3)	12.564(2)	38.446(4)	12.814(2)
b (Å)	13.438(3)	13.325(2)	18.600(2)	13.340 (2)
c (Å)	19.455(5)	17.435(3)	18.970(2)	20.566(3)
α (deg)	94.052(5)	83.702(5)	90	80.905(4)
β (deg)	95.344(6)	82.251(5)	112.480(2)	87.457(4)
γ (deg)	91.766(6)	72.027(5)	90	62.801(4)
Z	1	2	8	2
formula weight (g/mol)	2075.34	1004.10	1132.37	1112.30
density (calculated) (Mg/m^3)	1.167	1.215	1.200	1.197
absorption coefficient (mm^{-1})	0.467	0.517	0.493	0.498
F_{000}	1160	1084	4928	1200
total no. reflections	29005	18945	27994	12552
unique reflections	12584	11164	12832	8893
R_{int}	0.0932	0.0442	0.0616	0.0684
final R indices (I >2σ(I)]	R_1 = 0.0906 wR_2 = 0.2564	R_1 = 0.0730 wR_2 = 0.1674	R_1 = 0.0865 wR_2 = 0.2195	R_1 = 0.0635 wR_2 = 0.1444
largest diff. peak and hole (e$^-$ A^{-3})	1.444 and -0.486	1.585 and -0.961	1.285 and -1.141	2.496 and -0.787
GOF	1.017	1.004	1.029	1.012

Table 6.2. X-ray Crystallographic Data for Complexes 6.5, 6.6, and 6.10.

	6.5·1.5C_7H_8	**6.6**·0.5C_5H_{12}	**6.10**·2C_6H_6
empirical formula	$C_{48}H_{77}KN_2NiO_8S$ ·1.5C_7H_8	$C_{48}H_{77}KN_2NiO_9$ ·0.5C_5H_{12}	$C_{48}H_{77}KN_2NiO_8$·2C_6H_6
crystal habit, color	Block, Pale-Brown	Plate, Yellow	Plate, Orange
crystal size (mm)	0.15 × 0.1 × 0.1	0.2 × 0.2 × 0.05	0.2 × 0.1 × 0.05
crystal system	Monoclinic	Monoclinic	Monoclinic
space group	*P21/n*	*P21/n*	*P21/c*
volume (Å^3)	5851.6(9)	10592.8(1)	5909(3)
a (Å)	12.594 (1)	24.849(2)	20.875(6)
b (Å)	20.265(2)	17.449(1)	11.044(3)
c (Å)	22.942(2)	27.016(2)	26.136(8)
α (deg)	90	90	90
β (deg)	92.030(5)	115.268(3)	101.289(7)
γ (deg)	90	90	90
Z	2	4	4
formula weight (g/mol)	1078.20	1919.99	1064.14
density (calculated) (Mg/m^3)	1.219	1.204	1.196
absorption coefficient (mm^{-1})	0.491	0.497	0.451
F_{000}	2308	4152.0	2296
total no. reflections	35435	47795	24126
unique reflections	12142	21602	11782
R_{int}	0.0980	0.0894	0.0834
final R indices (I >2σ(I)]	R_1 = 0.0582 wR_2 = 0.1176	R_1 = 0.0905 wR_2 = 0.2063	R_1 = 0.1112 wR_2 = 0.2693
largest diff. peak and hole (e$^-$ A^{-3})	0.878 and -0.754	1.776 and -0.986	1.995 and -0.744
GOF	1.009	1.032	1.070

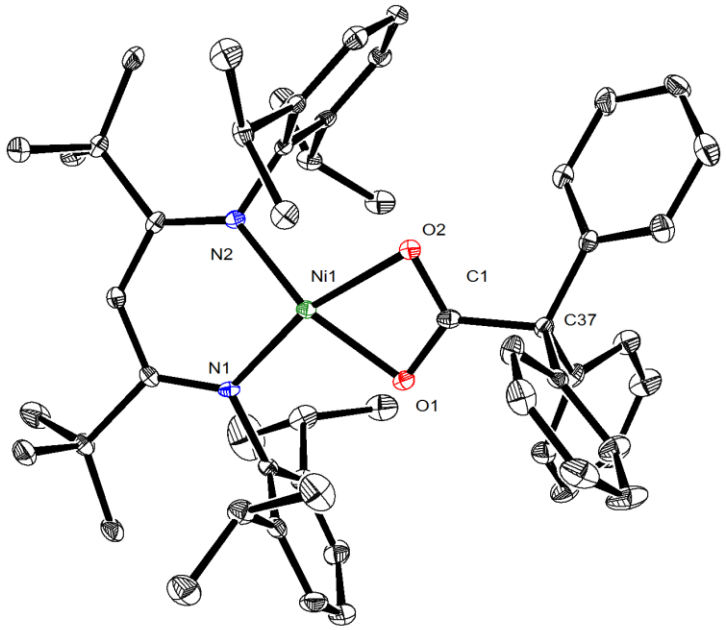

Figure 6.13. ORTEP drawing of [L^{tBu}Ni(*O*,*O*:κ^2-C(O)$_2$CPh$_3$)] shown with 50% thermal ellipsoids. Hydrogen atoms have been omitted for clarity.

6.6 Appendix

6.6.1 NMR Spectra

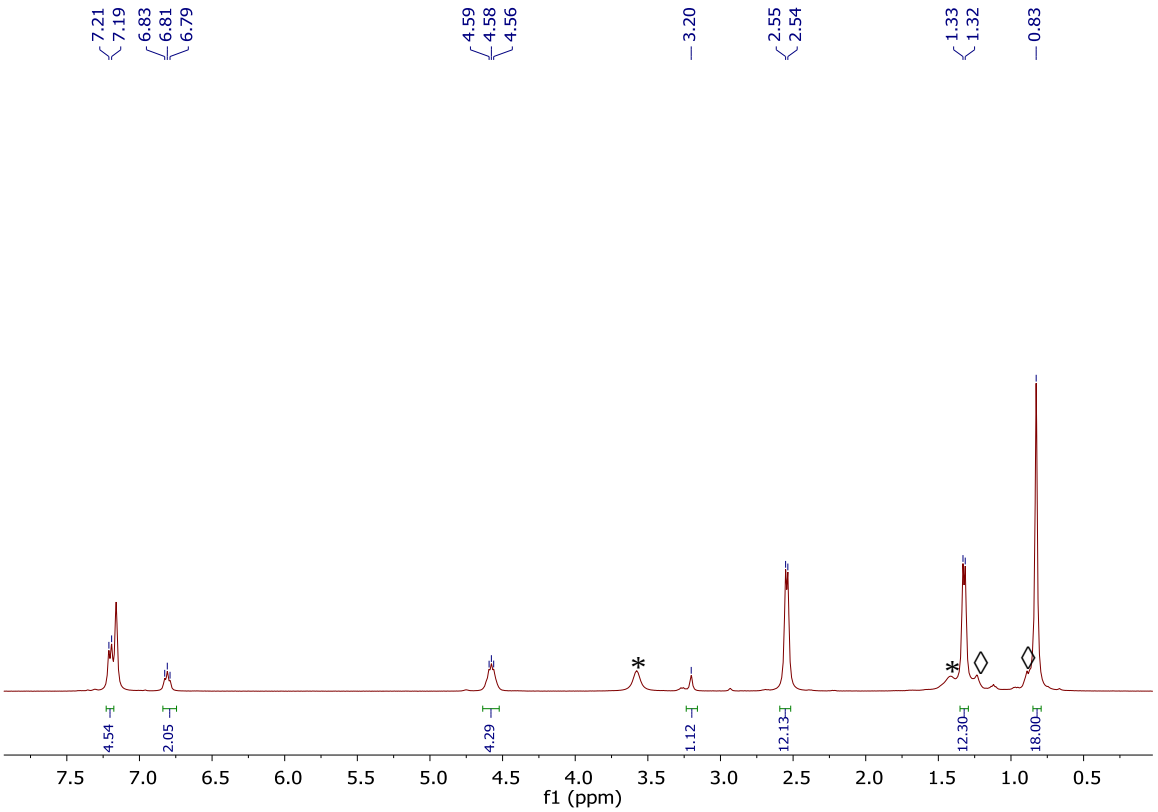

Figure A 6.1. ^{1}H NMR spectrum of [L^{tBu}Ni(OTf)] in benzene-d_6. (*) indicates the presence of THF, (◊) indicates the presence of hexane.

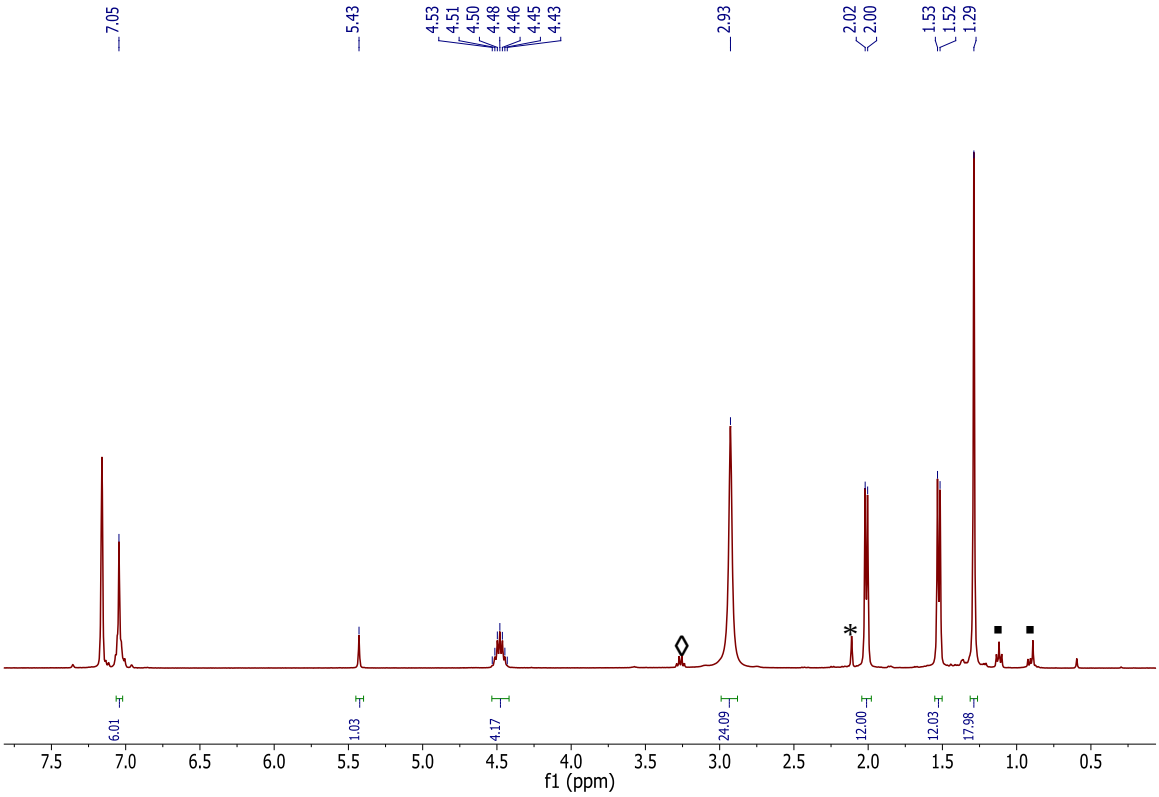

Figure A 6.2. ^{1}H NMR spectrum of [K(18-crown-6)][L^{tBu}Ni(SN=NO)] (**6.1**) in benzene-d_6. (*) indicates the presence of toluene, (▪) indicates the presence of hexanes, (◊) indicates the presence of Et_2O.

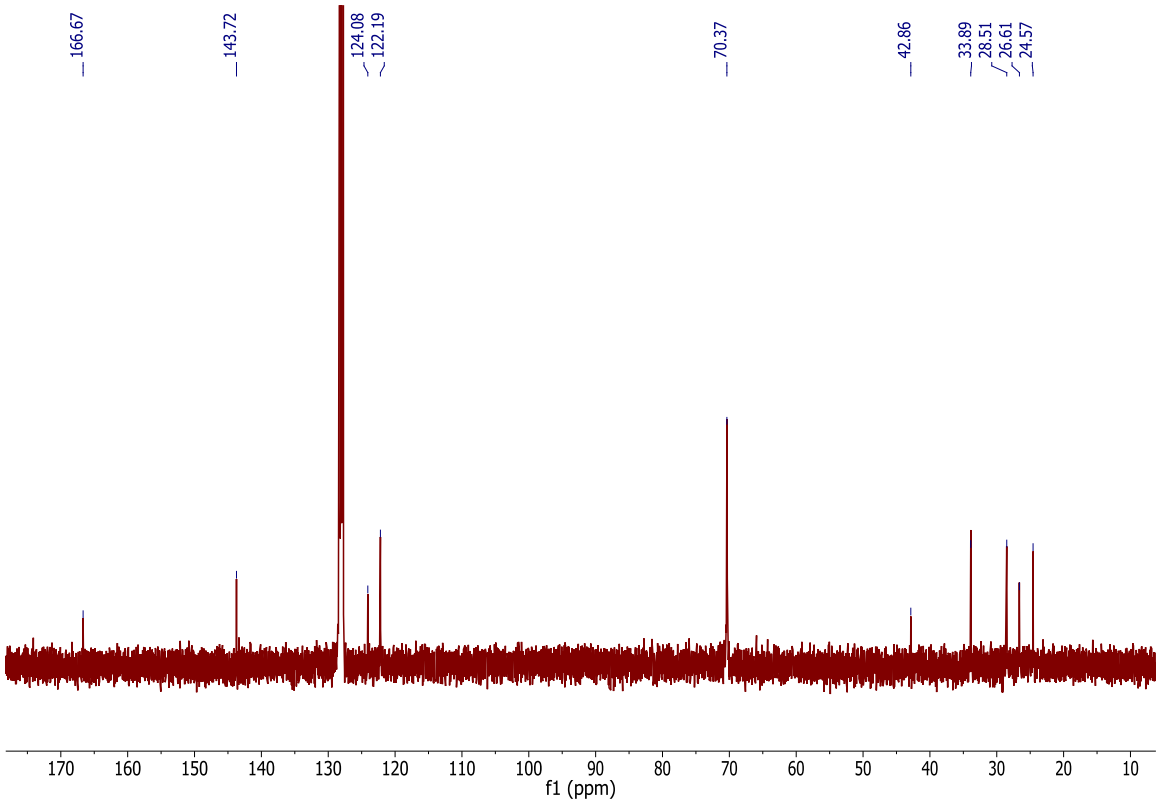

Figure A 6.3. ^{13}C NMR spectrum of [K(18-crown-6)][L^{tBu}Ni(SN=NO)] (**6.1**) in benzene-d_6. The β-diketiminate backbone γ-carbon was not observed. It is expected to appear between 90-100 ppm.[95]

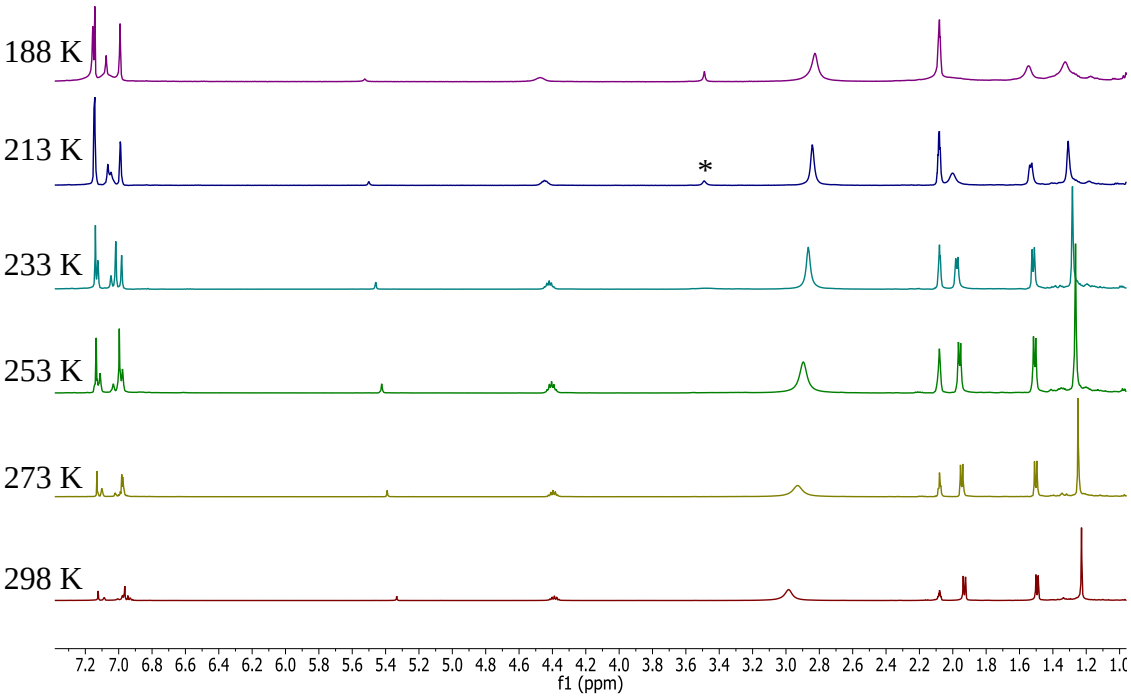

Figure A 6.4. Variable temperature ^{1}H NMR spectra of [K(18-crown-6)][L^{tBu}Ni(SN=NO)] (**6.1**) in toluene-d_8. (*) indicates the presence of free 18-crown-6.

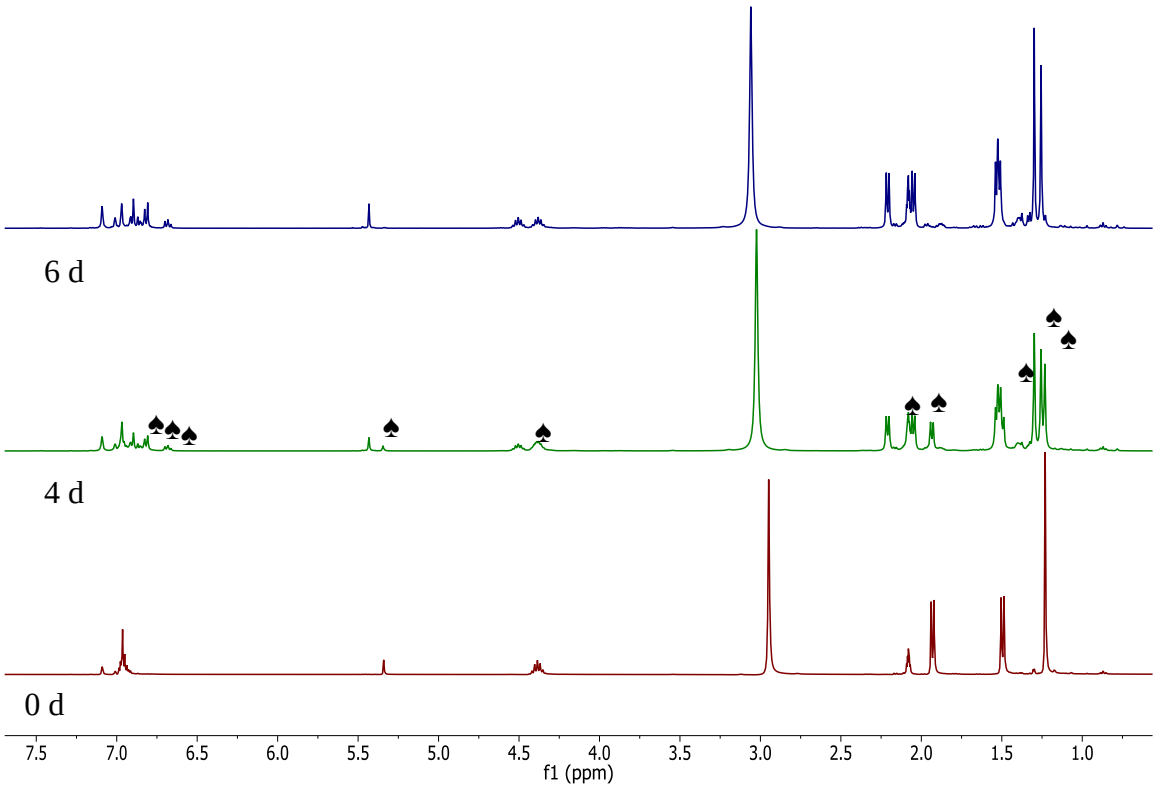

Figure A 6.5. ^{1}H NMR spectra of the thermolysis of [K(18-crown-6)][L^{tBu}Ni(*S*,*O*:κ^{2}-SNNO)] (**6.1**) to form [K(18-crown-6)][L^{tBu}Ni(η^{2}-SO)] (**6.2**) in toluene-d_8 at 45 °C. (♠) indicates the presence of **6.2**.

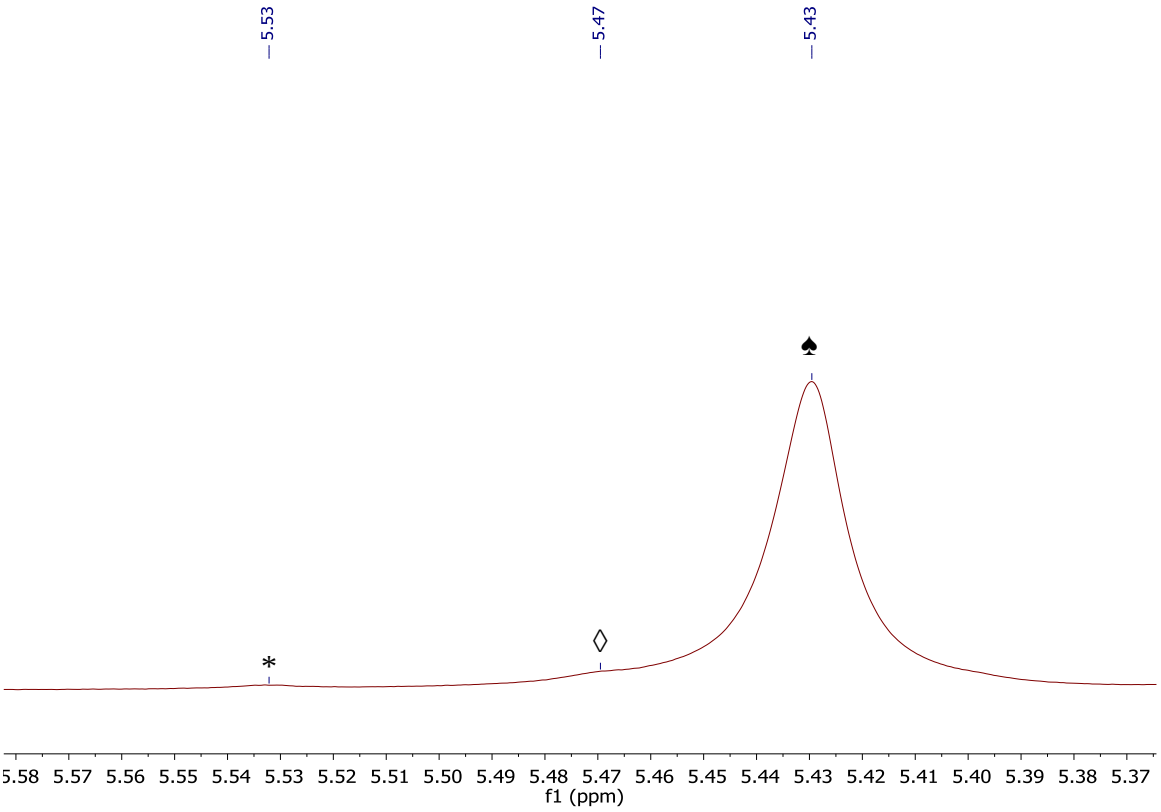

Figure A 6.6. Partial ^{1}H NMR spectra of the thermolysis of [K(18-crown-6)][L^{tBu}Ni(*S,O*:κ^{2}-SNNO)] (**6.1**) to form [K(18-crown-6)][L^{tBu}Ni(η^{2}-SO)] (**6.2**) after 6 days in toluene-d_8. (♠) indicates the presence of **6.2**, (*) indicates the presence of **6.3**, and (◊) indicates the presence of **6.4**.

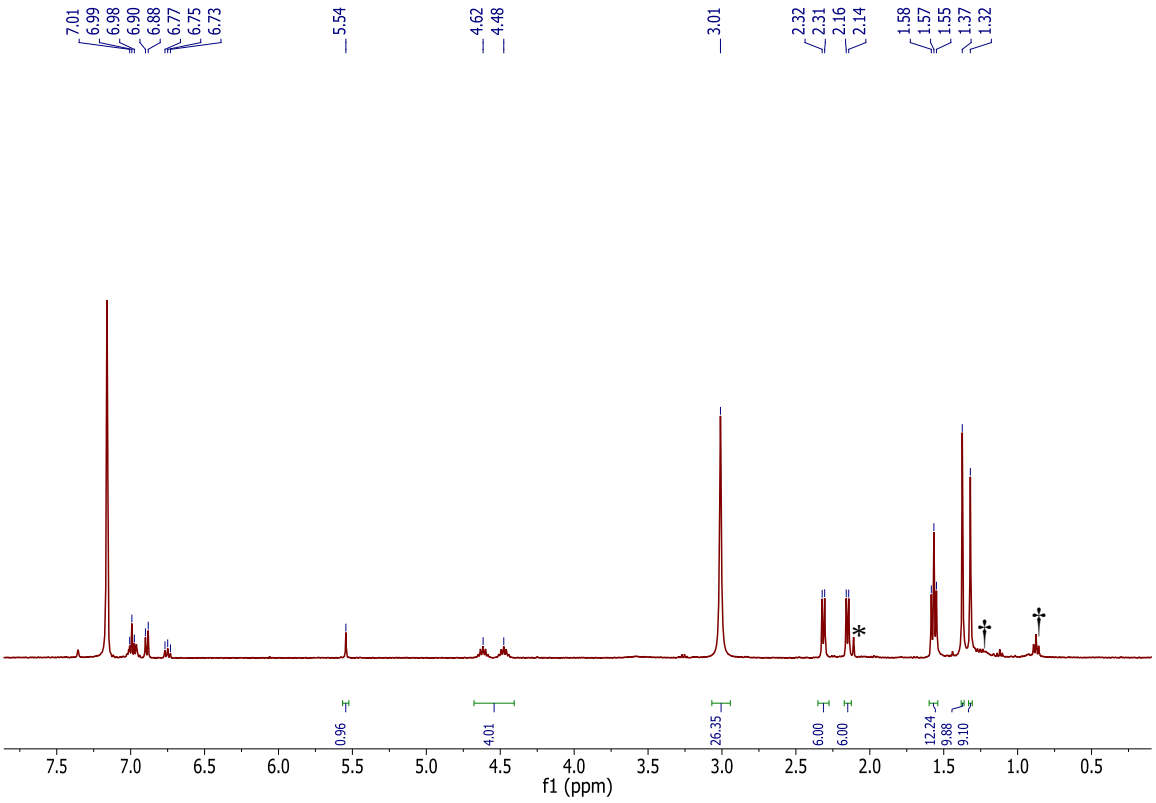

Figure A 6.7. ^{1}H NMR spectrum of [K(18-crown-6)][L^{tBu}Ni(SO)] (**6.2**) in benzene-d_6. (*) indicates the presence of toluene, and (†) indicates the presence of pentane.

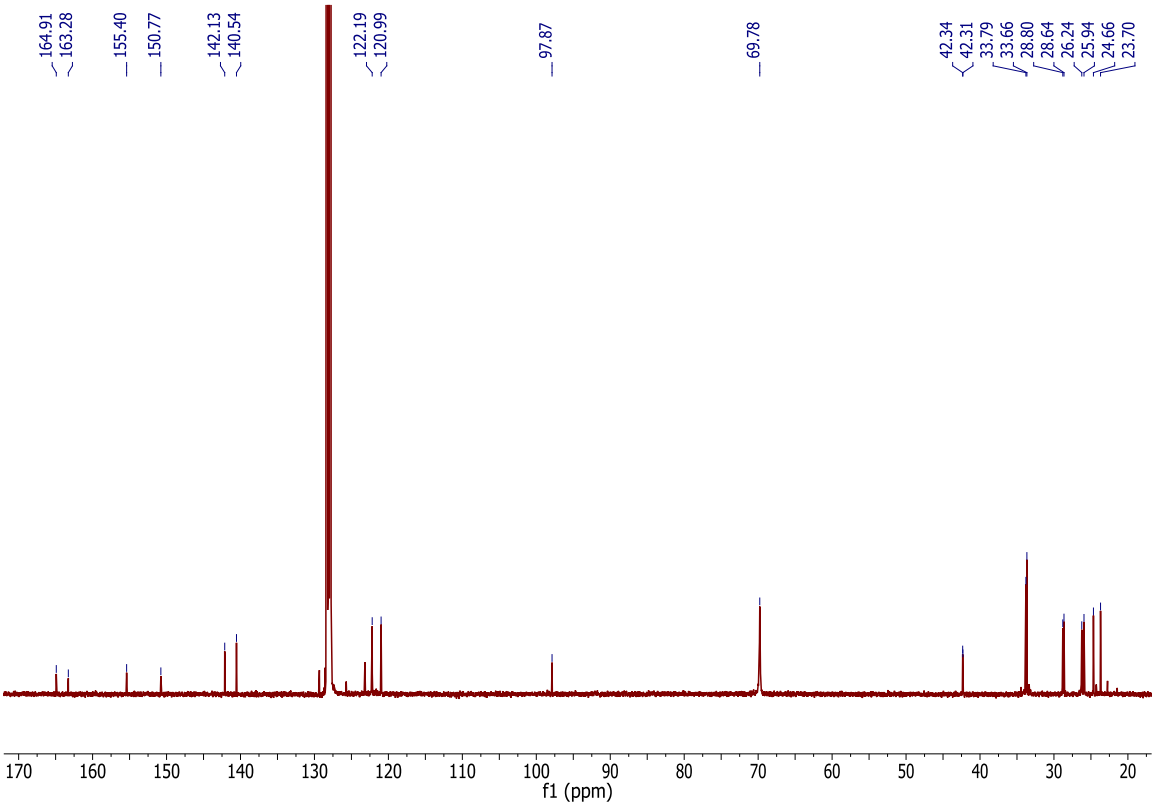

Figure A 6.8. $^{13}C\{^{1}H\}$ NMR spectrum of [K(18-crown-6)][L^{tBu}Ni(η^2-SO)] (**6.2**) in benzene-d_6.

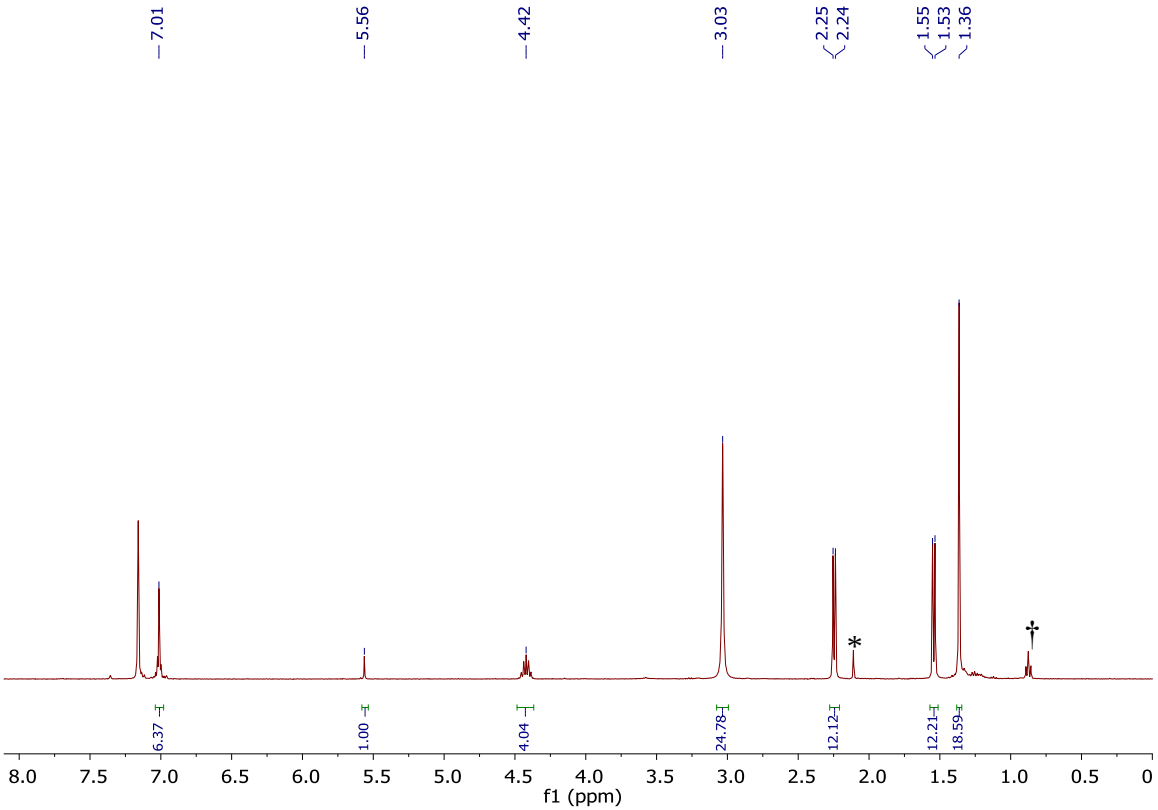

Figure A 6.9. ^{1}H NMR spectrum of [K(18-crown-6)][L^{tBu}Ni(η^2-S$_2$)] (**6.4**) in benzene-d_6. (*) indicates the presence of toluene, and (†) indicates the presence of pentane.

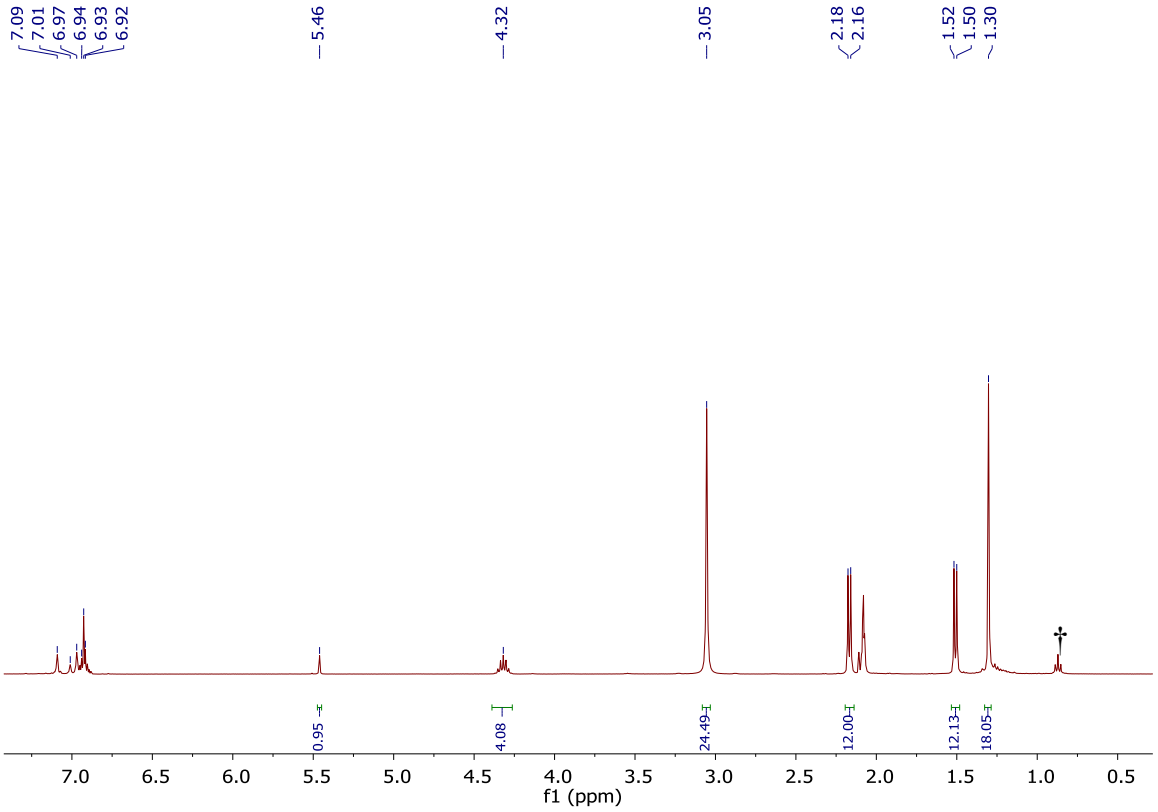

Figure A 6.10. ^{1}H NMR spectrum of [K(18-crown-6)][L^{tBu}Ni(η^2-S_2)] (**6.4**) in toluene-d_8. (†) indicates the presence of pentane.

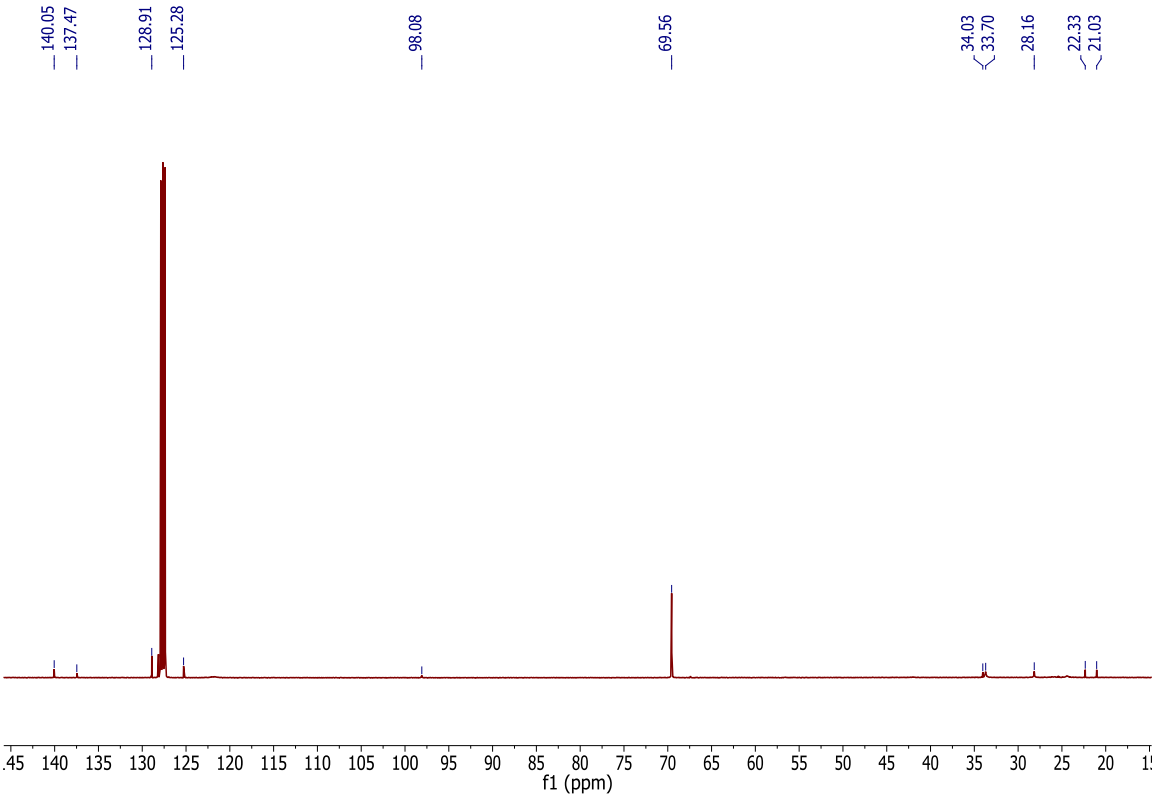

Figure A 6.11. $^{13}C\{^{1}H\}$ NMR spectrum of [K(18-crown-6)][$L^{tBu}Ni(\eta^2\text{-}S_2)$] (**6.4**) in benzene-$d_6$.

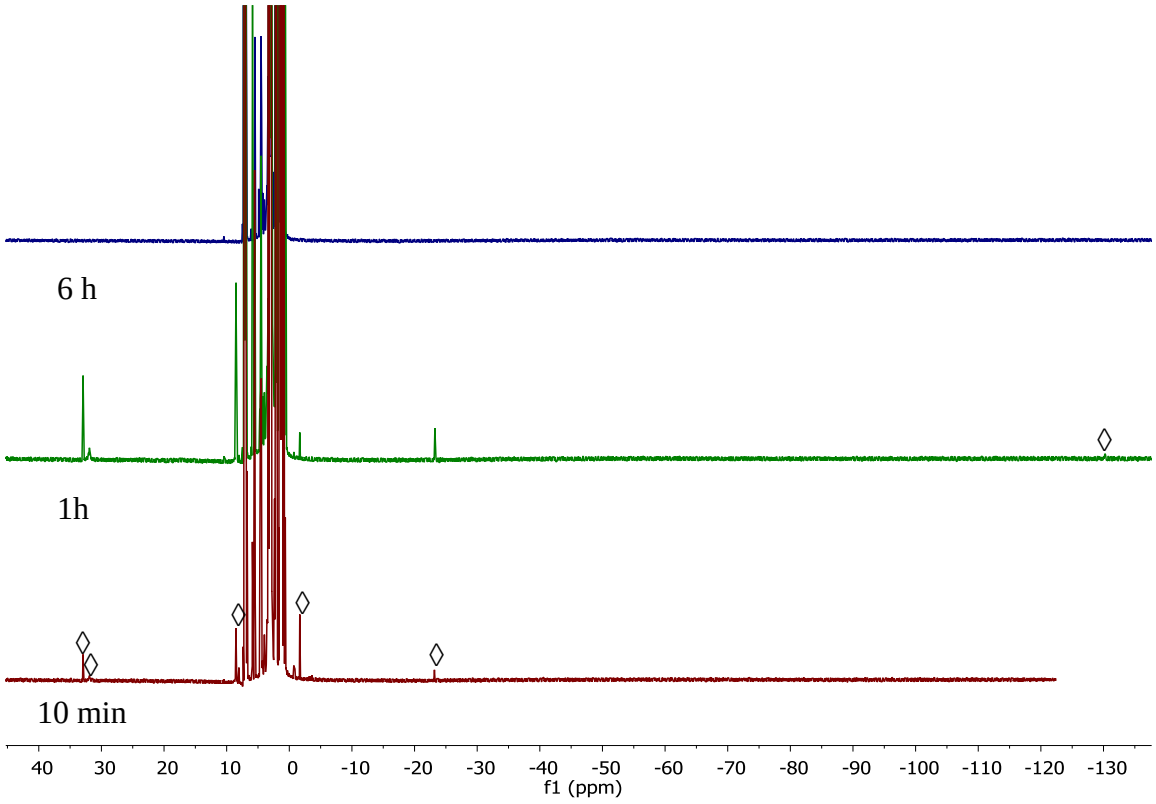

Figure A 6.12. Partial ^{1}H NMR spectra of the reaction of [K(18-crown-6)][L^{tBu}Ni(η^2-SO)] (**6.2**) with ^{13}CO in C_6D_6. (◊) indicates the presence of a [K(18-crown-6)][L^{tBu}Ni(S)] (**2.4**).

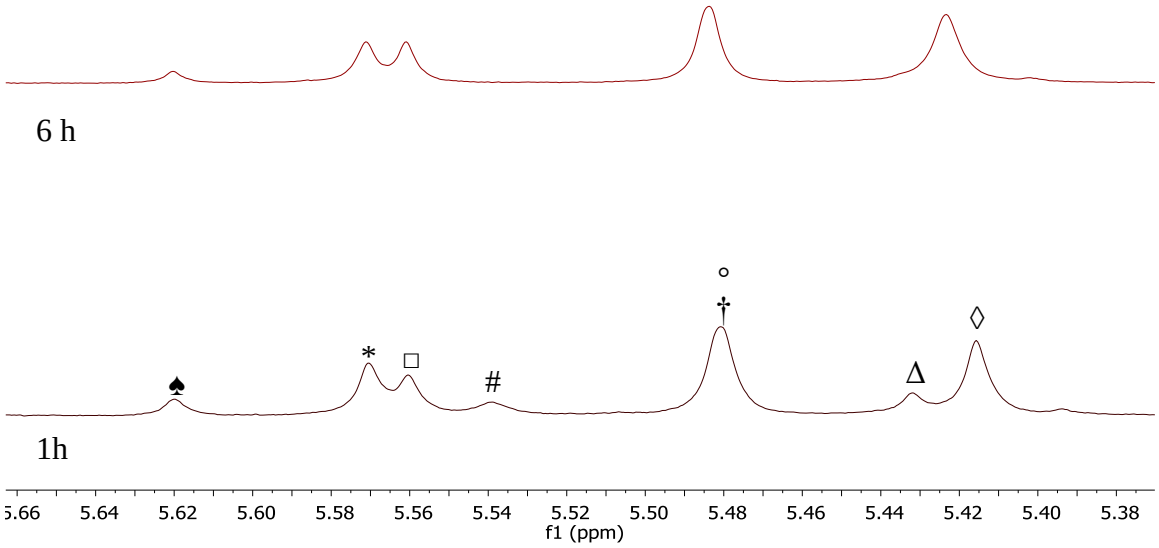

Figure A 6.13. Partial ^{1}H NMR spectra of the reaction of [K(18-crown-6)][L^{tBu}Ni(η^2-SO)] (**6.2**) with ^{13}CO in C_6D_6. (#) indicates the presence of **1**, (♠) indicates the presence of **6.2**, (□) indicates the presence of **6.4**, (°) indicates the presence of [K(18-crown-6)][L^{tBu}Ni(η^2-SCO)] (**5.1**), (†) indicates the presence of [K(18-crown-6)][L^{tBu}Ni(κ^2-SCO$_2$)] (**6.5**), (◊) indicates the presence of [K(18-crown-6)][L^{tBu}Ni(κ^2-CO$_3$)] (**6.6**), (*) has been tentatively assigned to [K(18-crown-6)][L^{tBu}Ni(κ^2-S$_2$CO)] (**6.8**), and (Δ) indicates the presence of an unidentified diamagnetic intermediate.

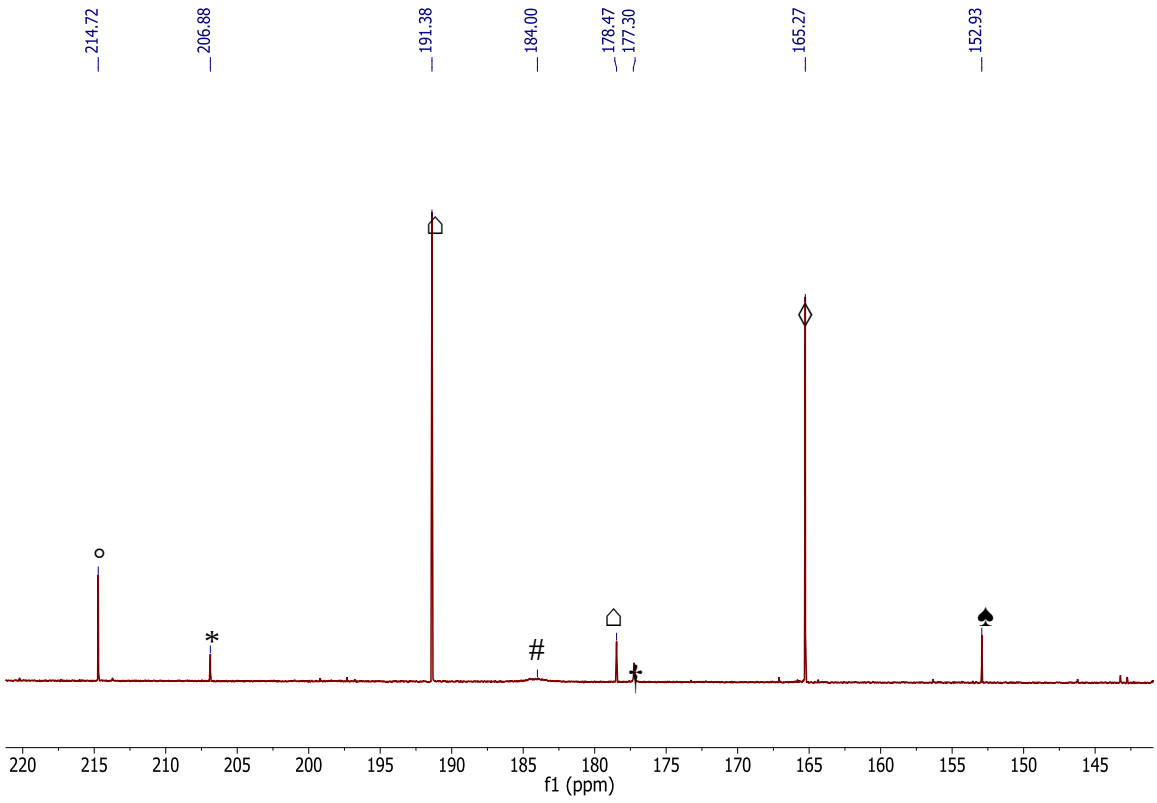

Figure A 6.14. Partial $^{13}C\{^{1}H\}$ NMR spectrum of the reaction of [K(18-crown-6)][$L^{tBu}Ni(\eta^2$-SO)] (**6.2**) with ^{13}CO in C_6D_6 after 6 h. (†) indicates the presence of [K(18-crown-6)][$L^{tBu}Ni(\kappa^2$-SCO_2)] (**6.5**), (◊) indicates the presence of [K(18-crown-6)][$L^{tBu}Ni(\kappa^2$-CO_3)] (**6.6**), (°) indicates the presence of [K(18-crown-6)][$L^{tBu}Ni(\eta^2$-SCO)] (**5.1**), (♠) indicates the presence of SCO (**6.7**),[54] (#) indicates the presence of ^{13}CO, and (⌂) indicates the presence of unidentified products. (*) has been tentatively assigned to [K(18-crown-6)][$L^{tBu}Ni(\kappa^2$-S_2CO)] (**6.8**).

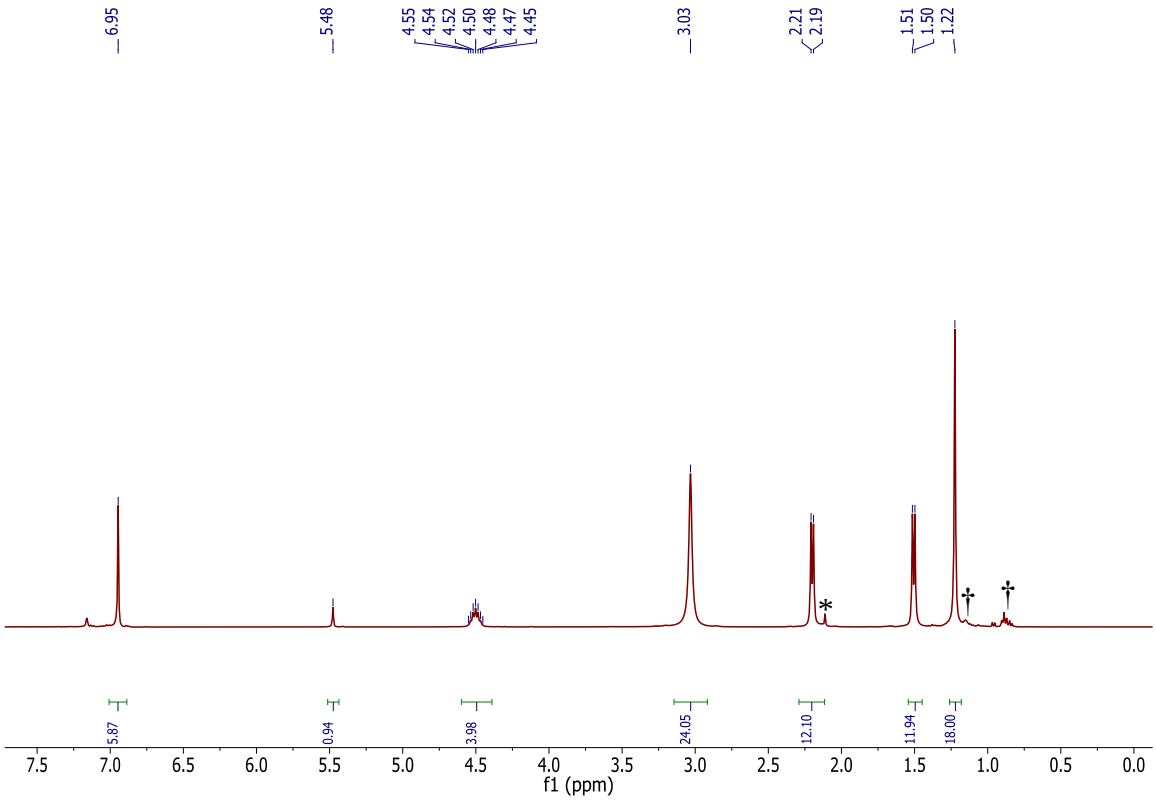

Figure A 6.15. ^{1}H NMR spectrum of [K(18-crown-6)][L^{tBu}Ni(κ^2-SCO$_2$)] (**6.5**) in benzene-d_6. (*) indicates the presence of toluene, and (†) indicates the presence of pentane.

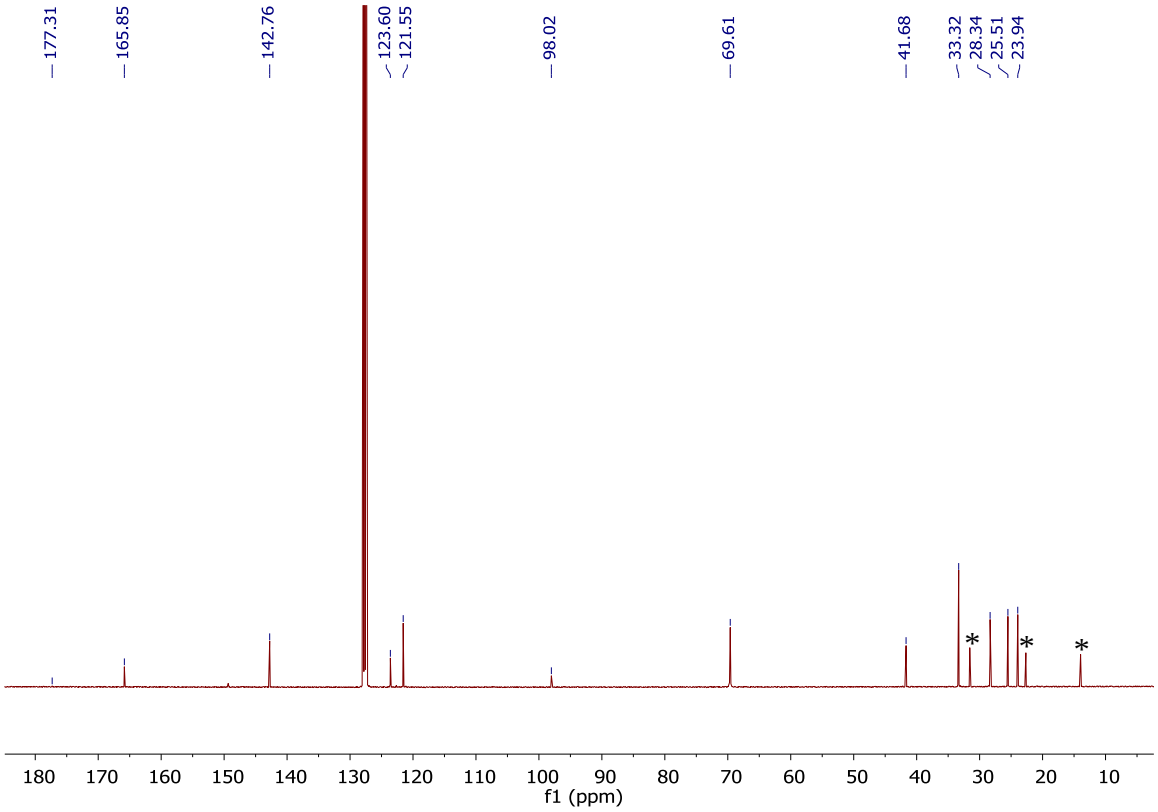

Figure A 6.16. $^{13}C\{^{1}H\}$ NMR spectrum of [K(18-crown-6)][$L^{tBu}Ni(\kappa^2\text{-}SCO_2)$] (**6.5**) in benzene-$d_6$. (*) indicates the presence of hexane.

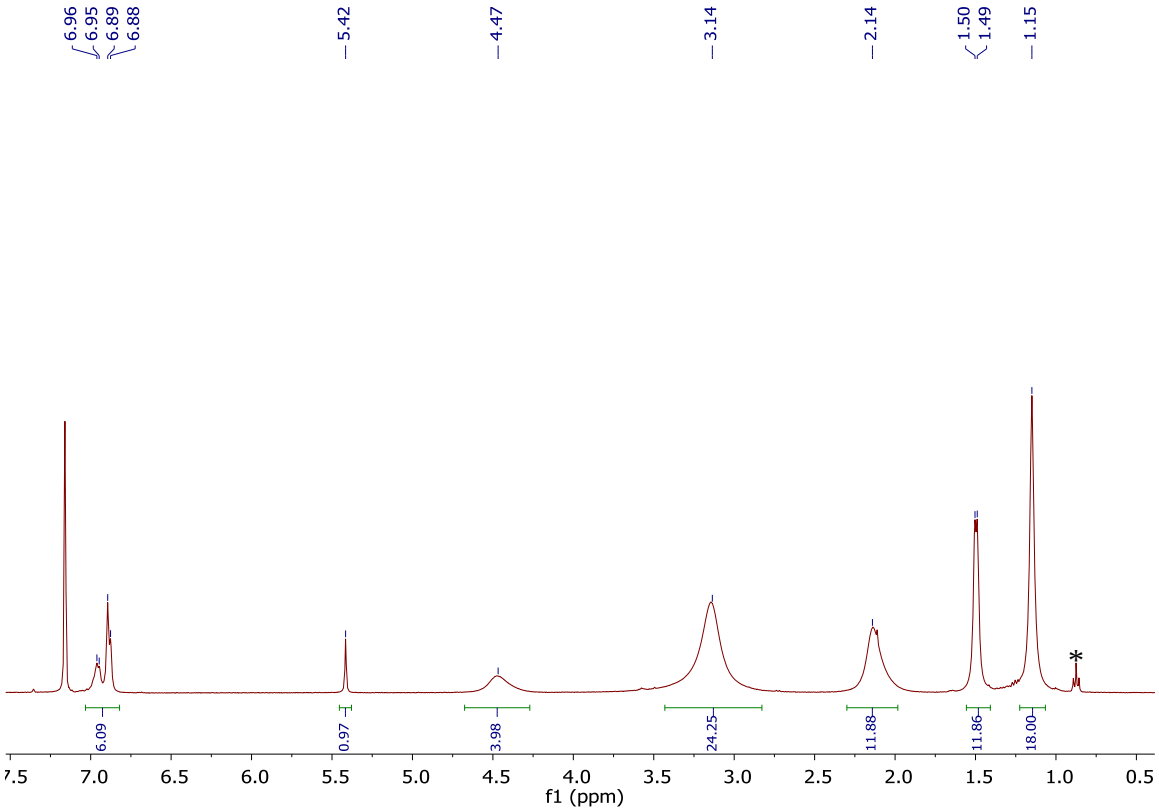

Figure A 6.17. ^{1}H NMR spectrum of [K(18-crown-6)][L^{tBu}Ni(κ^2-CO_3)] (**6.6**) in benzene-d_6. (*) indicates the presence of pentane.

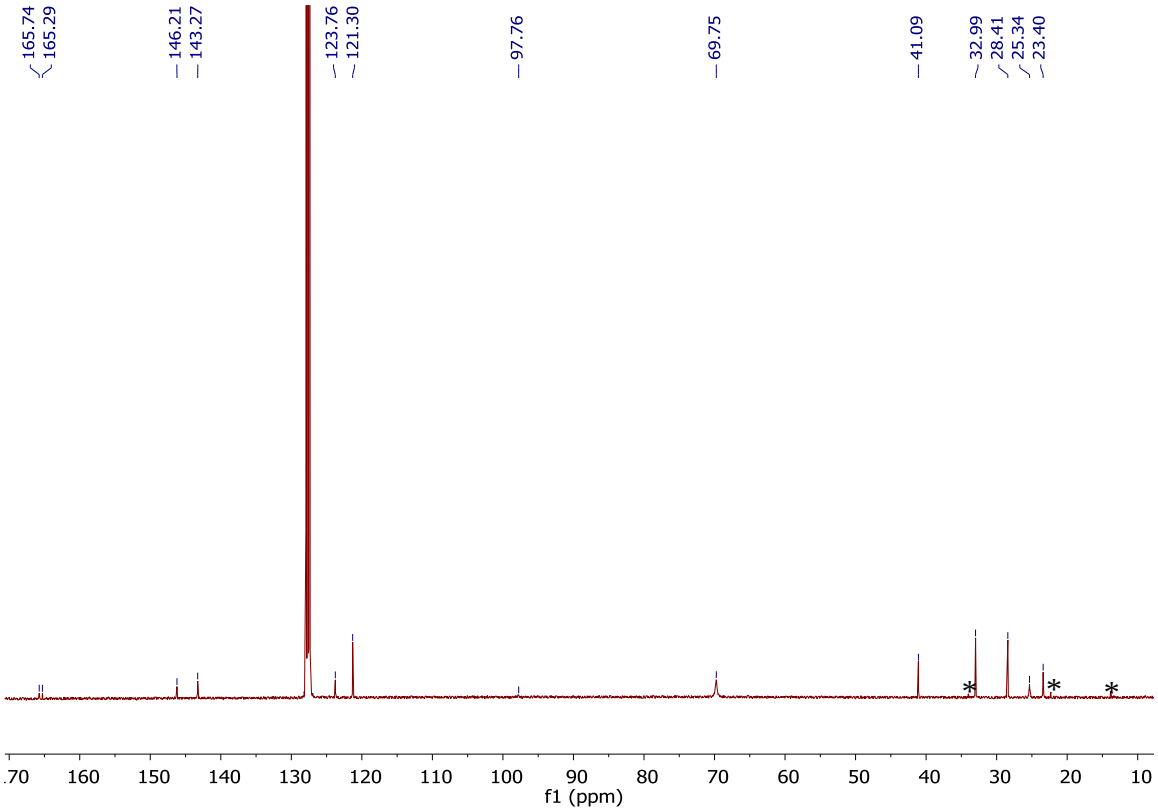

Figure A 6.18. $^{13}C\{^{1}H\}$ NMR spectrum of [K(18-crown-6)][L^{tBu}Ni(κ^2-CO_3)] (**6.6**) in benzene-d_6. (*) indicates the presence of pentane.

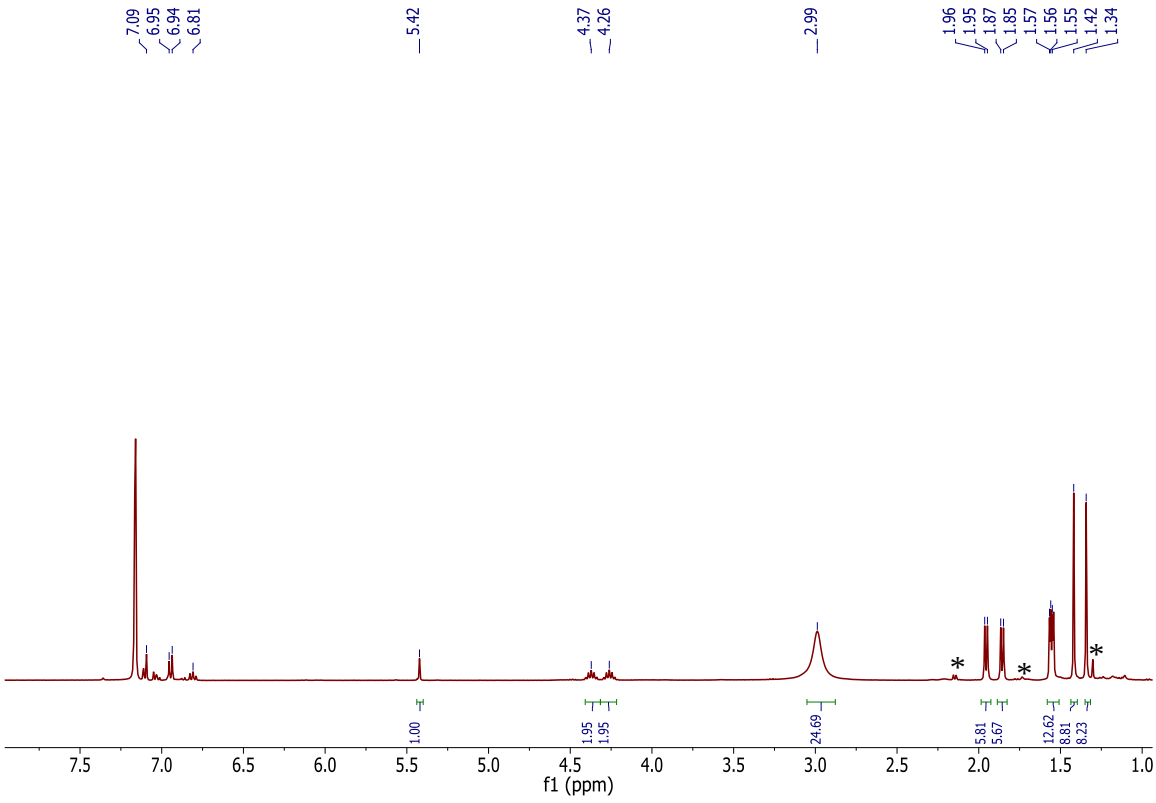

Figure A 6.19. ^{1}H NMR spectrum of [K(18-crown-6)][L^{tBu}Ni(η^2-CO_2)] (**6.10**) in benzene-d_6. (*) indicates the presence of trace unidentified diamagnetic impurities.

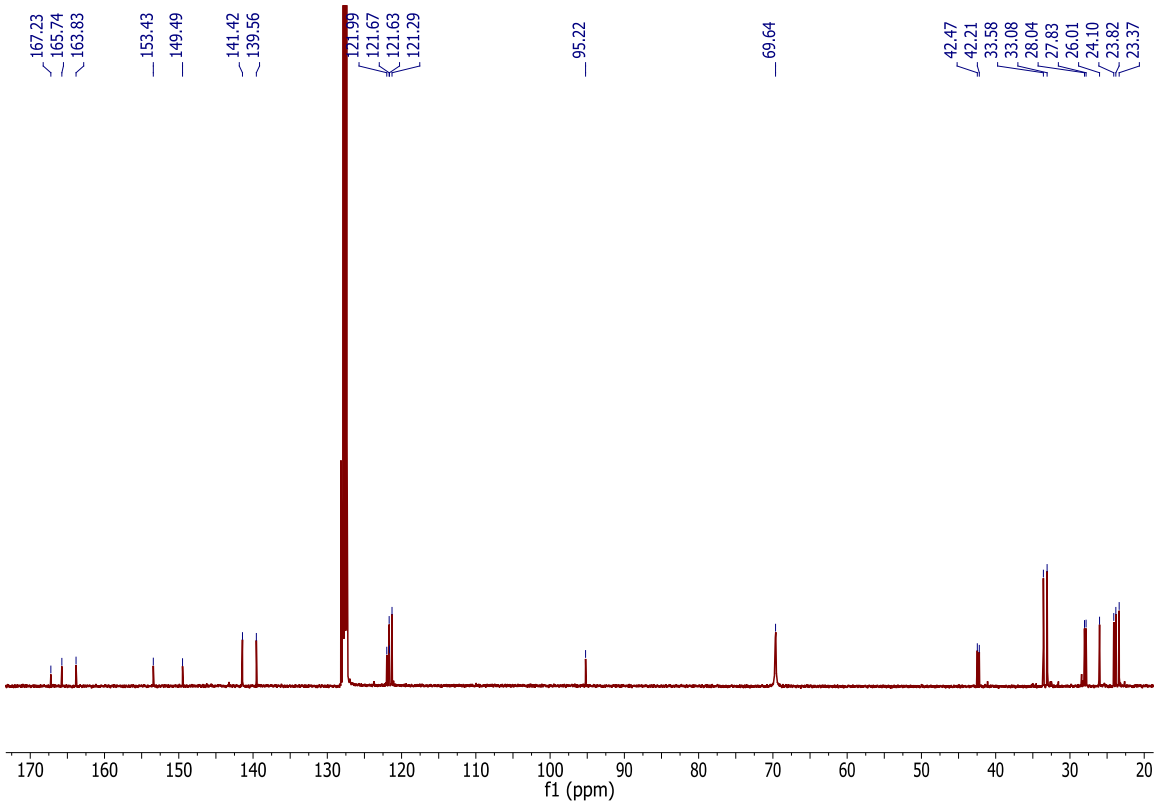

Figure A 6.20. $^{13}C\{^{1}H\}$ NMR spectrum of [K(18-crown-6)][$L^{tBu}Ni(\eta^2\text{-}CO_2)$] (**6.10**) in benzene-$d_6$.

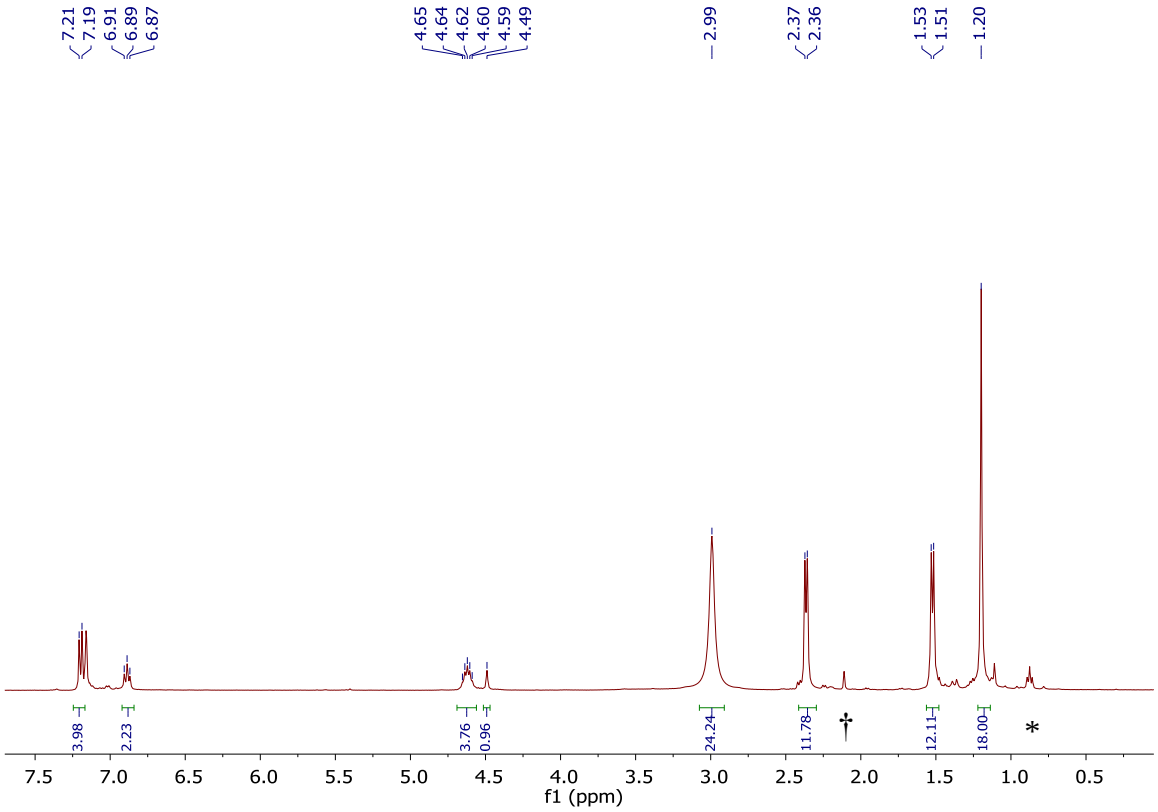

Figure A 6.21. *In situ* ^{1}H NMR spectrum of the reaction of [K(18-crown-6)][L^{tBu}Ni(SO)] (**6.2**) with CO_2 in benzene-d_6. (*) indicates the presence of pentane, (†) indicates the presence of toluene.

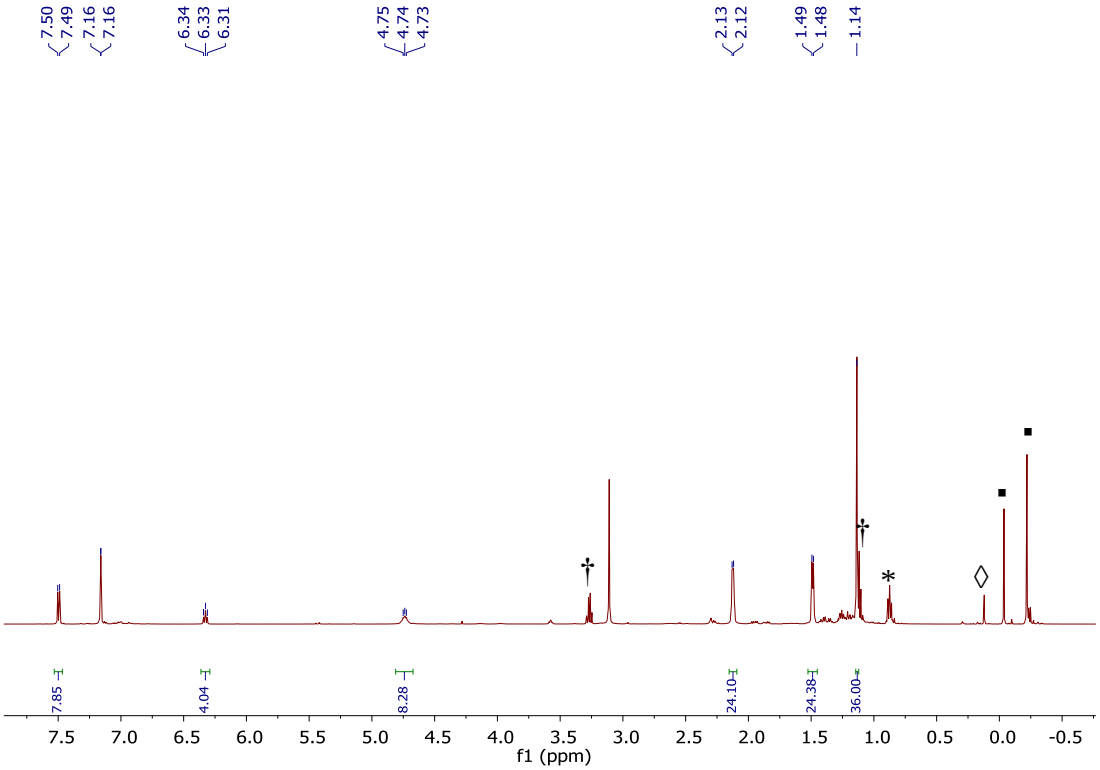

Figure A 6.22. *In situ* ^{1}H NMR spectrum of the reaction of [K(18-crown-6)][L^{tBu}Ni(SNNO)] (**6.1**) with TMSOTf in benzene-d_6. (*) indicates the presence of pentane, (†) indicates the presence of Et_2O, (◊) indicates the presence of hexamethyldisiloxane (HMDSO), and (▪) indicates the presence of unidentified trimethylsilane containing products.

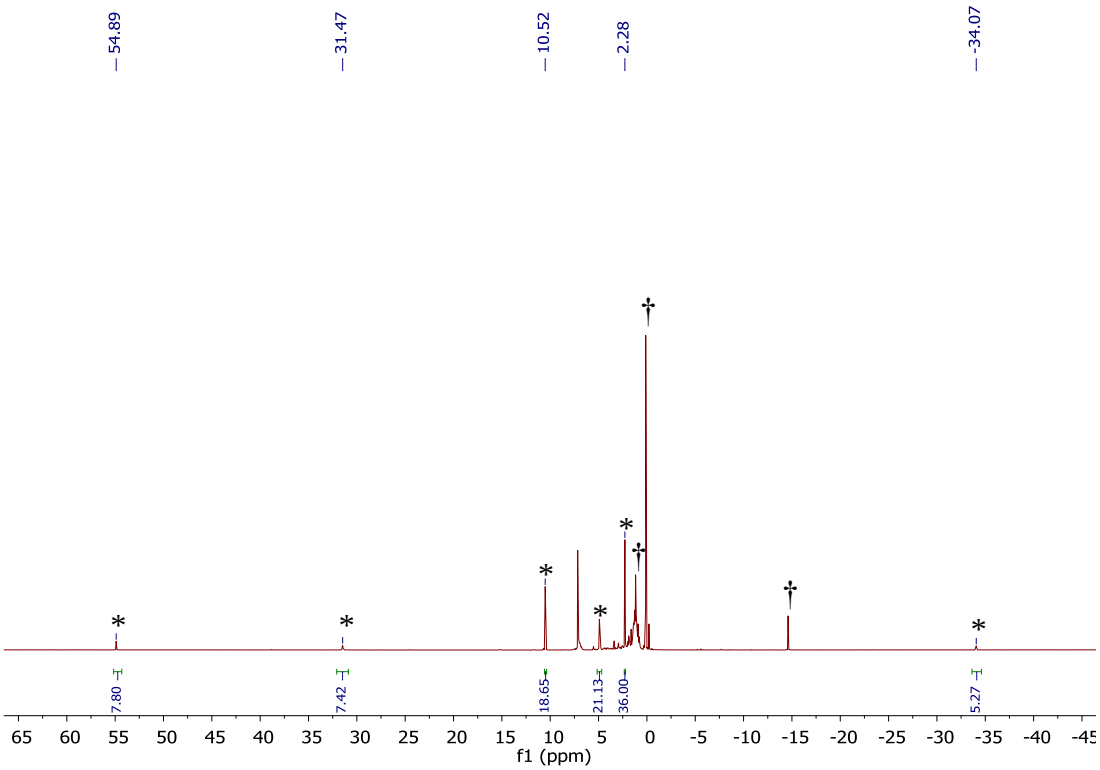

Figure A 6.23. ^{1}H NMR spectrum of products of the decomposition of [{L^{tBu}Ni}$_2$(μ^2-κ^2-η^2-SNNO)] (**6.13**) in benzene-d_6. (*) indicates the presence of [{L^{tBu}Ni}$_2$(μ^2-S)],[87] (†) indicates the presence of unidentified products.

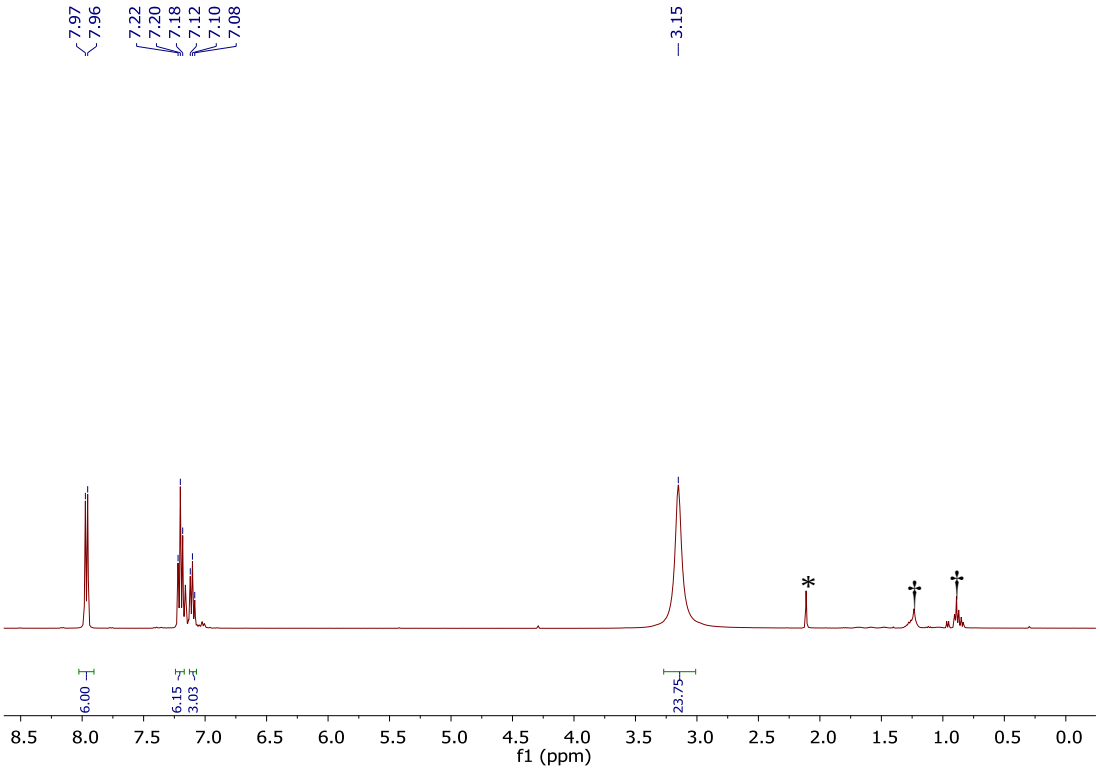

Figure A 6.24. ^{1}H NMR spectrum of [K(18-crown-6)][$C(O)_2CPh_3$] in benzene-d_6. (*) indicates the presence of toluene and (†) indicates the presence of hexane.

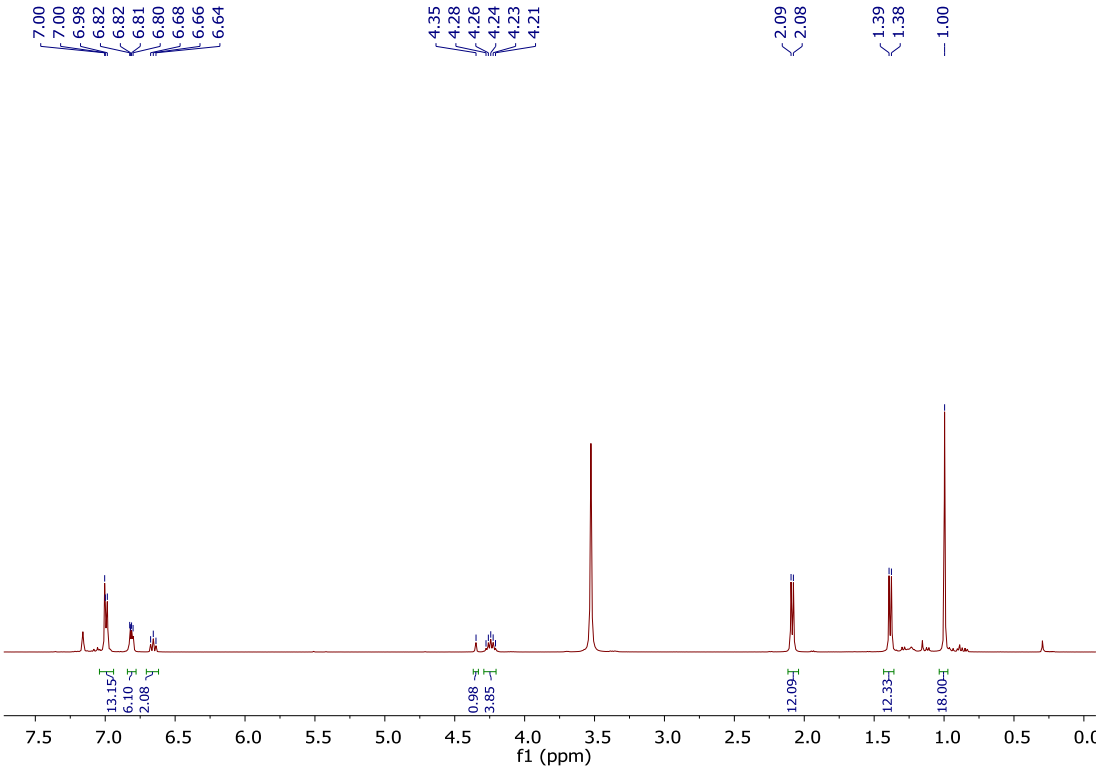

Figure A 6.25. ^{1}H NMR spectrum of [$L^{tBu}Ni^{II}$(*O*,*O*:κ^{2}-C(O)$_2$CPh$_3$)] in benzene-d_6.

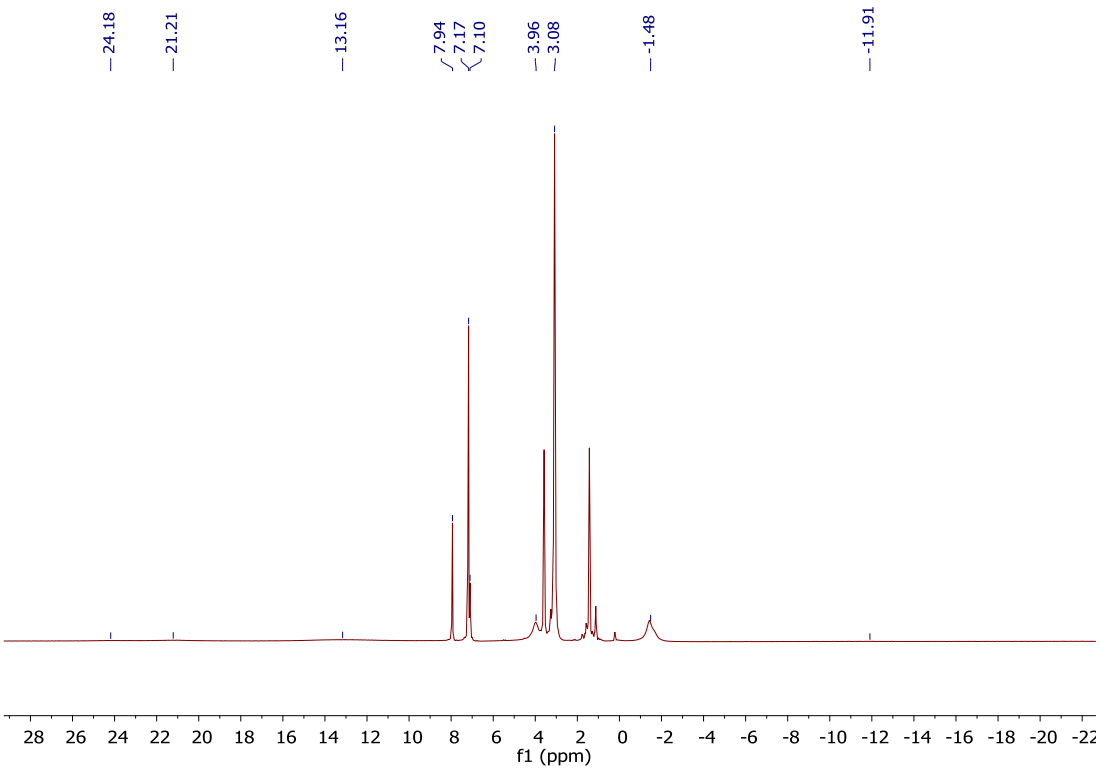

Figure A 6.26. ^{1}H NMR spectrum of the product of the reaction of [$L^{tBu}Ni^{II}$(*O*,*O*:κ^{2}-$C(O)_2CPh_3$)] with KC_8 in the presence of 18-crown-6 taken in THF-d_8.

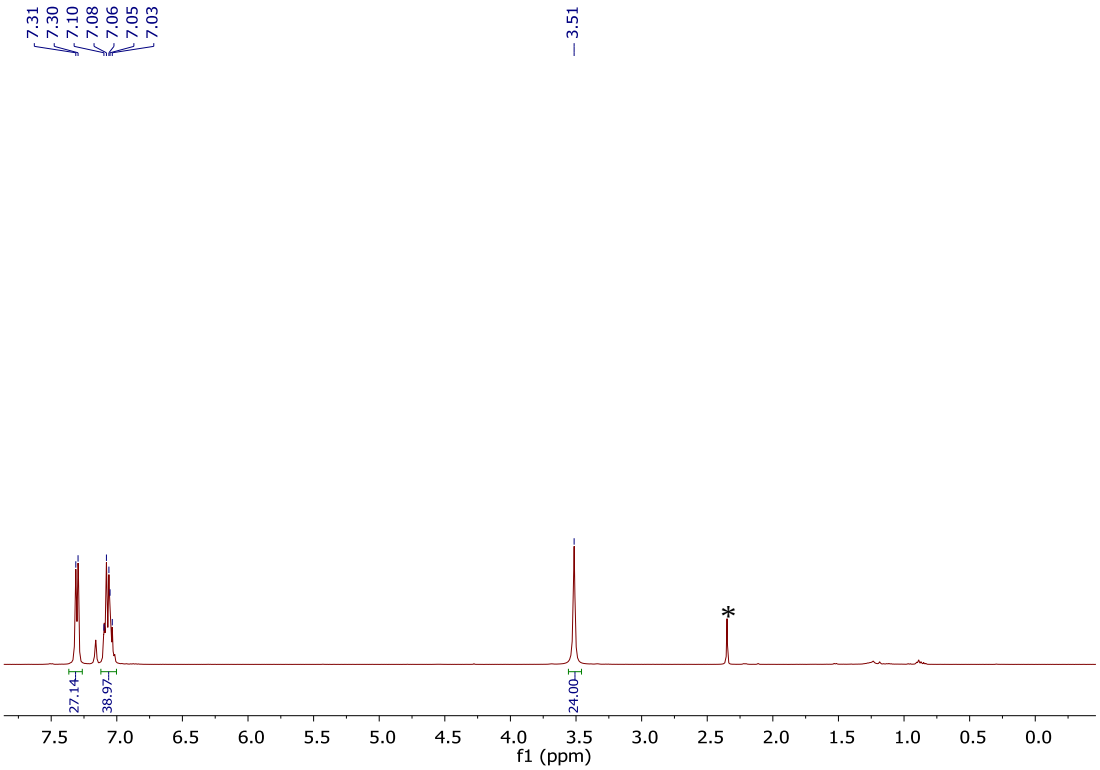

Figure A 6.27. ^{1}H NMR spectrum of the colorless crystals isolated from the reaction of [$L^{tBu}Ni^{II}(OCPh_3)$] with KC_8 in the presence of 18-crown 6 and CO_2 taken in benzene-d_6. (*) indicates the presence of toluene.

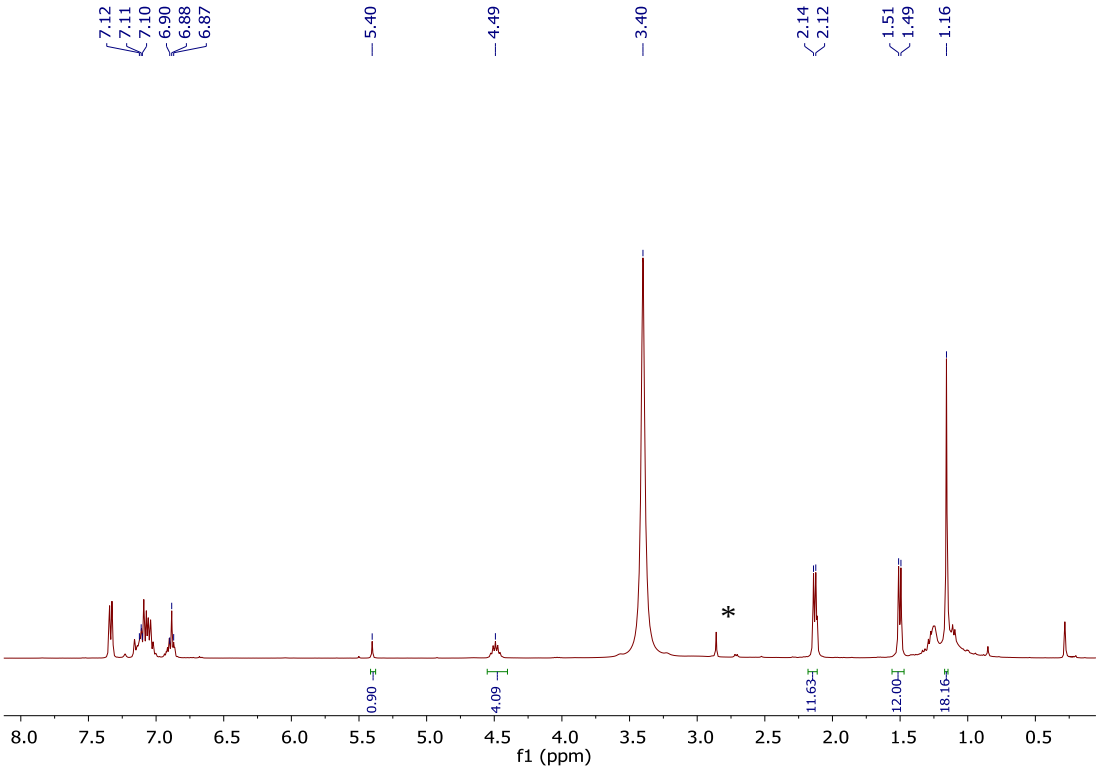

Figure A 6.28. ^{1}H NMR spectrum of [K(18-crown-6)][$L^{tBu}Ni(\kappa^2\text{-}CO_3)$] (**6.6**) isolated from the reaction of [$L^{tBu}Ni^{II}(OCPh_3)$] with KC_8 in the presence of 18-crown-6 and CO_2 taken in benzene-d_6. (*) indicates the presence of toluene.

6.6.2 IR Spectra

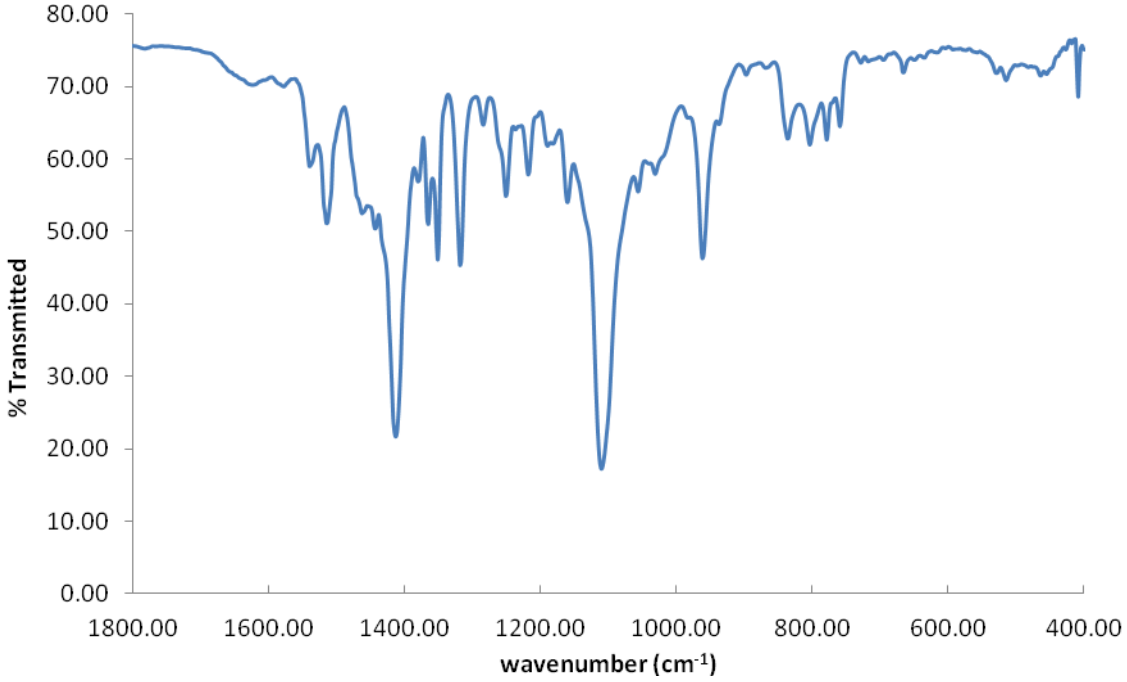

Figure A 6.29. Partial IR spectra of complex **6.1** (KBr pellet).

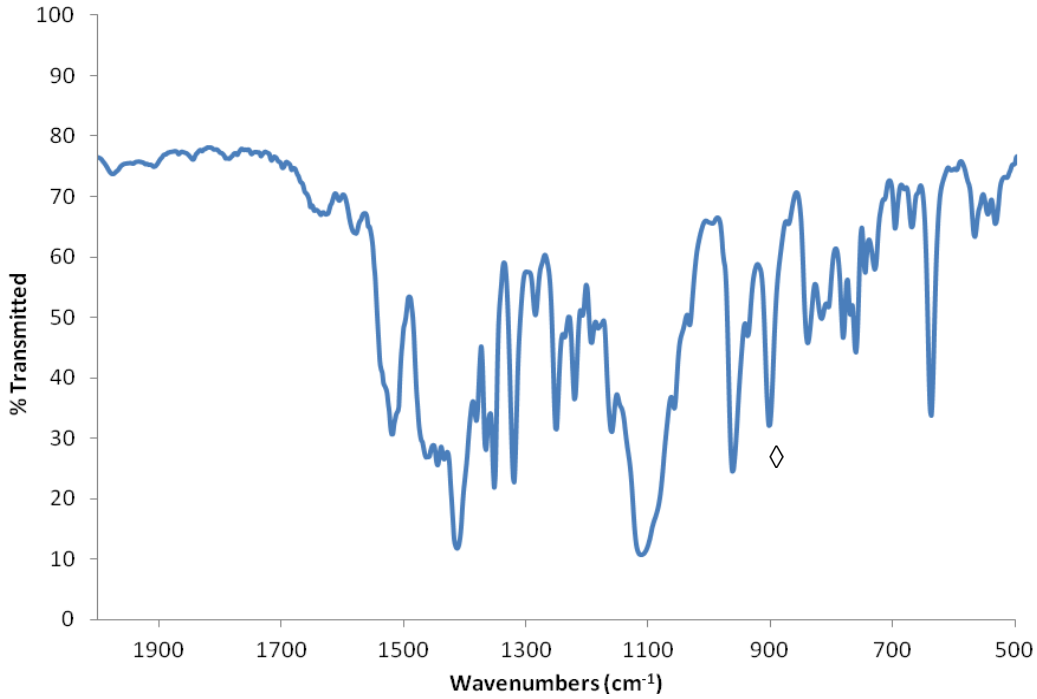

Figure A 6.30. Partial IR spectrum of [K(18-crown-6)][L^{tBu}Ni(η^2-SO)] (**6.2**) (KBr pellet), (◊) indicates the presence of the ν_{SO} mode.

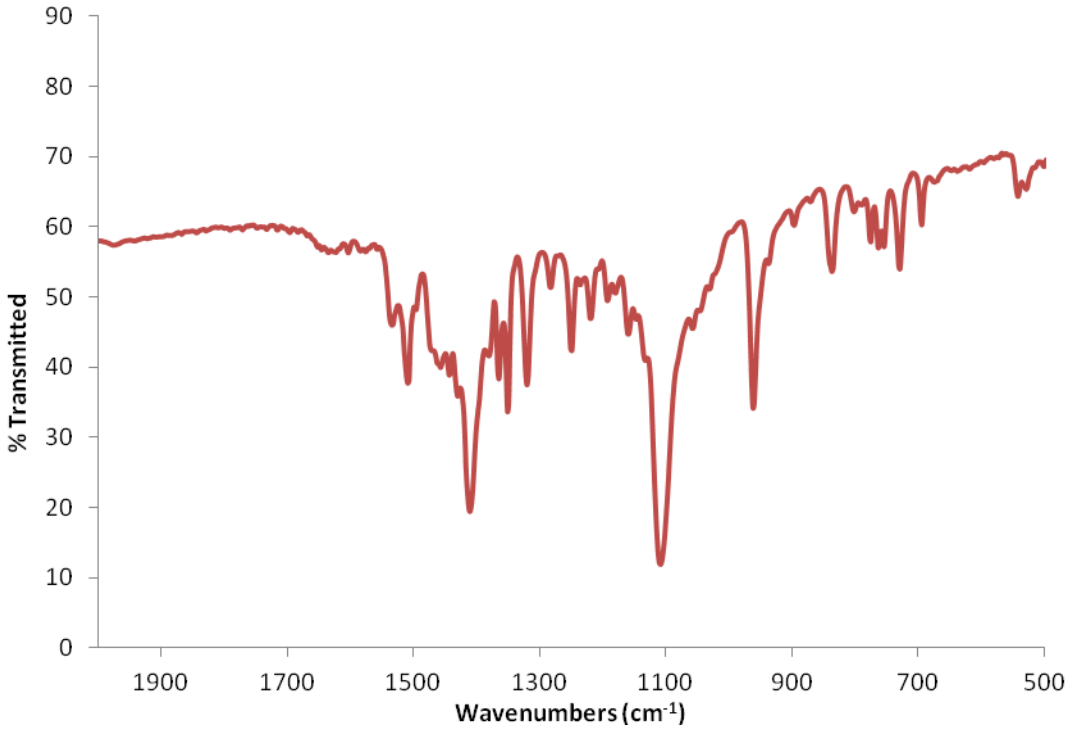

Figure A 6.31. Partial IR spectrum of [K(18-crown-6)][L^{tBu}Ni(η^2-S_2)] (**6.4**) (KBr pellet).

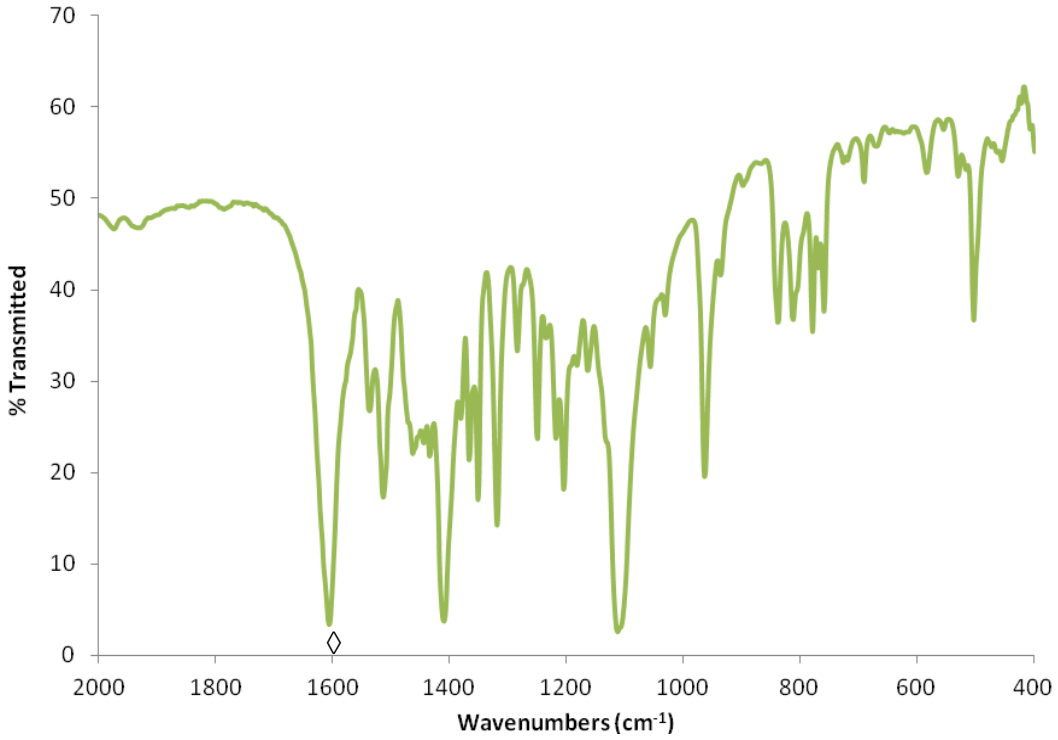

Figure A 6.32. Partial IR spectrum of [K(18-crown-6)][L^{tBu}Ni(κ^2-SCO_2)] (**6.5**) (KBr pellet), (◊) indicates the presence of the ν_{CO} mode.

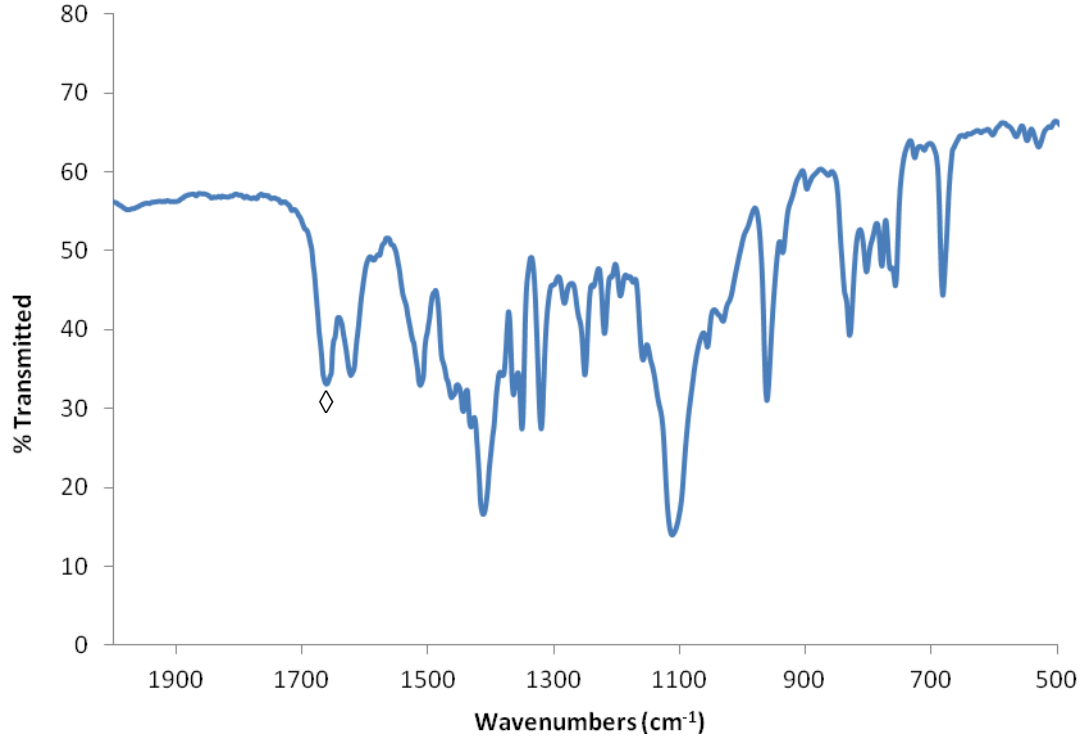

Figure A 6.33. Partial IR spectrum of [K(18-crown-6)][L^{tBu}Ni(η^2-CO_2)] (**6.10**) (KBr pellet) , (◊) indicates the presence of the ν_{CO} mode.

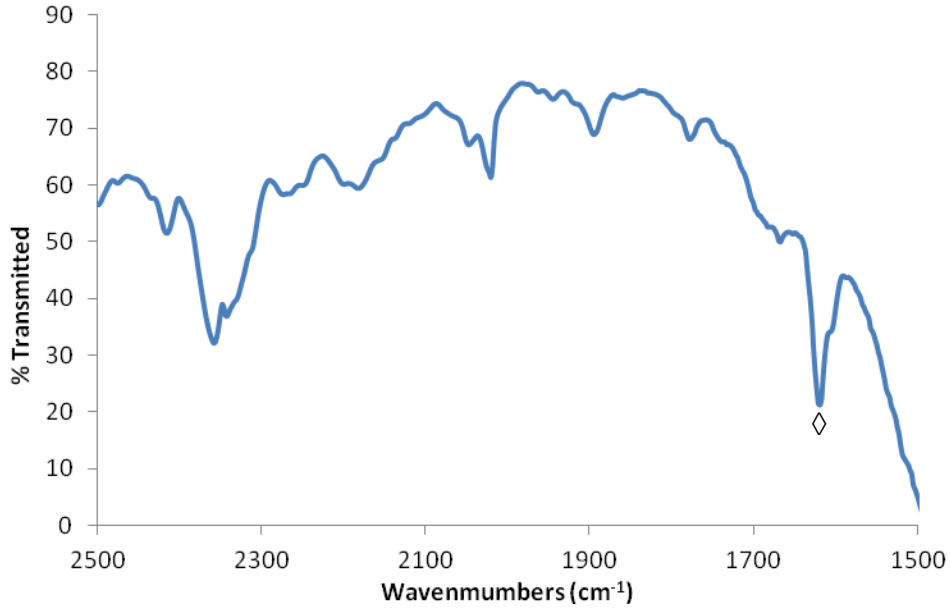

Figure A 6.34. Partial solution IR (hexane) of [K(18-crown-6)][L^{tBu}Ni(κ^2-CO_3)] (**6.6**). (◊) indicates the presence of the ν_{CO} mode.

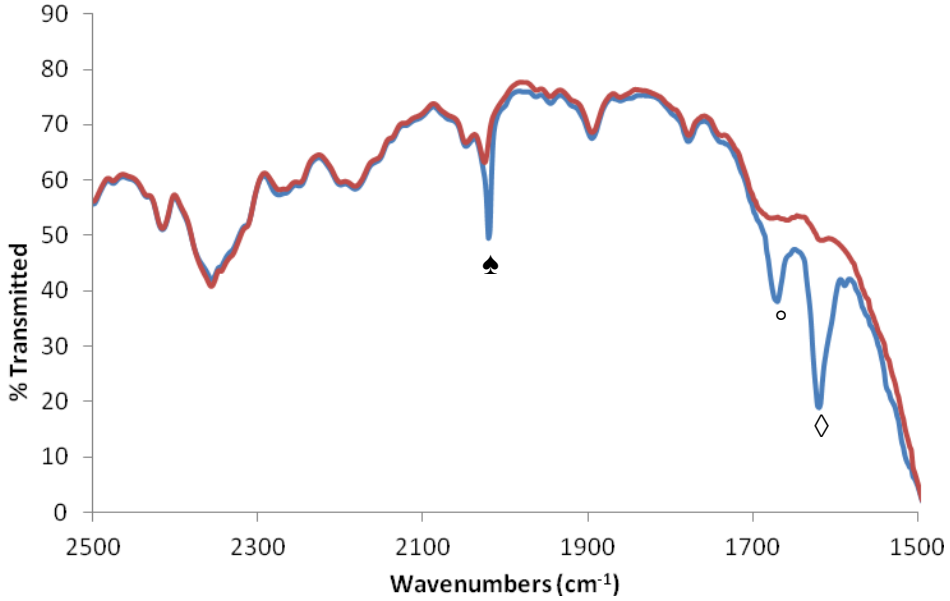

Figure A 6.35. Partial solution IR (hexane) of the reaction of [K(18-crown-6)][L^{tBu}Ni(η^2-SO)] (**6.2**) with CO (blue trace). Hexane background (red trace). (°) indicates the presence of [K(18-crown-6)][L^{tBu}Ni(η^2-SCO)] (**5.1**), (◊) indicates the presence of [K(18-crown-6)][L^{tBu}Ni(κ^2-CO_3)] (**6.6**), (♠) indicates the presence of [L^{tBu}Ni^{I}(CO)] (**6.9**).[57]

6.7 References

(1) Ravishankara, A. R.; Daniel, J. S.; Portmann, R. W. Nitrous Oxide (N_2O): The Dominant Ozone-Depleting Substance Emitted in the 21st Century. *Science (80-.).* **2009**, *326* (5949), 123.

(2) Trogler, W. C. Physical Properties and Mechanisms of Formation of Nitrous Oxide. *Coord. Chem. Rev.* **1999**, *187* (1), 303.

(3) Leontev, A. V; Fomicheva, O. A.; Proskurnina, M. V; Zefirov, N. S. Modern Chemistry of Nitrous Oxide. *Russ. Chem. Rev.* **2001**, *70* (2), 91.

(4) Prather, M. J. Time Scales in Atmospheric Chemistry: Coupled Perturbations to N_2O, NO_y, and O_3. *Science (80-.).* **1998**, *279* (5355), 1339.

(5) Davidson, E. A.; Kanter, D. Inventories and Scenarios of Nitrous Oxide Emissions. *Environ. Res. Lett.* **2014**, *9* (10), 105012.

(6) Konsolakis, M. Recent Advances on Nitrous Oxide (N_2O) Decomposition over Non-Noble-Metal Oxide Catalysts: Catalytic Performance, Mechanistic Considerations, and Surface Chemistry Aspects. *ACS Catal.* **2015**, *5* (11), 6397.

(7) Neuffer, B.; Frank, N.; Desai, M. Available and Emerging Technologies for Reducing Greenhouse Gas Emissions from the Nitric Acid Production Industry. Report of the Office of Air and Radiation; U.S. Environmental Protection Agency: Research Triangle Park, NC.

(8) Dameris, M. Depletion of the Ozone Layer in the 21st Century. *Angew. Chem. Int. Ed.* **2010**, *49* (3), 489.

(9) Granger, P.; Parvulescu, V. I. Catalytic NO_x Abatement Systems for Mobile Sources: From Three-Way to Lean Burn after-Treatment Technologies. *Chem. Rev.* **2011**, *111* (5), 3155.

(10) Reeds, J. P.; Yonke, B. L.; Zavalij, P. Y.; Sita, L. R. Carbon Monoxide-Induced N–N Bond Cleavage of Nitrous Oxide That Is Competitive with Oxygen Atom Transfer to Carbon Monoxide As Mediated by a Mo(II)/Mo(IV) Catalytic Cycle. *J. Am. Chem. Soc.* **2011**, *133* (46), 18602.

(11) Horn, B.; Limberg, C.; Herwig, C.; Feist, M.; Mebs, S. CO Oxidation at Nickel Centres by N_2O or O_2 to Yield a Novel Hexanuclear Carbonate. *Chem. Commun.* **2012**, *48* (66), 8243.

(12) Kaplan, A. W.; Bergman, R. G. Nitrous Oxide Mediated Synthesis of Monomeric Hydroxoruthenium Complexes. Reactivity of $(DMPE)_2Ru(H)(OH)$ and the Synthesis of a Silica-Bound Ruthenium Complex. *Organometallics* **1998**, *17* (23), 5072.

(13) Lee, J.-H.; Pink, M.; Tomaszewski, J.; Fan, H.; Caulton, K. G. Facile Hydrogenation of N_2O by an Operationally Unsaturated Osmium Polyhydride. *J. Am. Chem. Soc.* **2007**, *129* (28), 8706.

(14) Doyle, L. E.; Piers, W. E.; Borau-Garcia, J. Ligand Cooperation in the Formal Hydrogenation of N_2O Using a $PC_{Sp2}P$ Iridium Pincer Complex. *J. Am. Chem. Soc.* **2015**, *137* (6), 2187.

(15) Zeng, R.; Feller, M.; Ben-David, Y.; Milstein, D. Hydrogenation and Hydrosilylation of Nitrous Oxide Homogeneously Catalyzed by a Metal Complex. *J. Am. Chem. Soc.* **2017**, *139* (16), 5720.

(16) Hartmann, N. J.; Wu, G.; Hayton, T. W. Synthesis of a "Masked" Terminal Nickel(II) Sulfide by Reductive Deprotection and Its Reaction with Nitrous Oxide. *Angew.*

Chem. Int. Ed. **2015**, *54* (49), 14956.
(17) Severin, K. Synthetic Chemistry with Nitrous Oxide. *Chem. Soc. Rev.* **2015**, *44* (17), 6375.
(18) Puiu, S. C.; Warren, T. H. Three-Coordinate β-Diketiminato Nickel Nitrosyl Complexes from Nickel(I)−Lutidine and Nickel(II)−Alkyl Precursors. *Organometallics* **2003**, *22* (20), 3974.
(19) Otten, E.; Neu, R. C.; Stephan, D. W. Complexation of Nitrous Oxide by Frustrated Lewis Pairs. *J. Am. Chem. Soc.* **2009**, *131* (29), 9918.
(20) Feldmann, C.; Jansen, M. Cis-Sodium Hyponitrite—A New Preparative Route and a Crystal Structure Analysis. *Angew. Chem. Int. Ed.* **1996**, *35* (15), 1728.
(21) Wright, A. M.; Hayton, T. W. Understanding the Role of Hyponitrite in Nitric Oxide Reduction. *Inorg. Chem.* **2015**, *54*, 9330.
(22) Tskhovrebov, A. G.; Solari, E.; Wodrich, M. D.; Scopelliti, R.; Severin, K. Covalent Capture of Nitrous Oxide by N-Heterocyclic Carbenes. *Angew. Chem. Int. Ed.* **2012**, *51* (1), 232.
(23) Yu, H.; Jia, G.; Lin, Z. Theoretical Studies on O-Insertion Reactions of Nitrous Oxide with Ruthenium Hydride Complexes. *Organometallics* **2008**, *27* (15), 3825.
(24) Pyykkö, P. Additive Covalent Radii for Single-, Double-, and Triple-Bonded Molecules and Tetrahedrally Bonded Crystals: A Summary. *J. Phys. Chem. A* **2015**, *119* (11), 2326.
(25) Powell, F. X.; Lide Jr., D. R. Microwave Spectrum of the SO Radical. *J. Chem. Phys.* **1964**, *41* (5), 1413.
(26) Horn, B.; Limberg, C.; Herwig, C.; Braun, B. Three-Coordinate Nickel(II) and Nickel(I) Thiolate Complexes Based on the β-Diketiminate Ligand System. *Inorg. Chem.* **2014**, *53* (13), 6867.
(27) Bianchini, C.; Mealli, C.; Meli, A.; Sabat, M. Stepwise Metal-Promoted Conversion of η^2-CS_2 into η^2-SO. Synthesis and Crystal Structure of the Complex $[(Triphos)Rh(\mu\text{-}SO)_2Rh(Triphos)][BPh_4]_2 \bullet HCONMe_2$. *J. Chem. Soc., Chem. Commun.* **1985**, No. 15, 1024.
(28) Neher, A.; Heyke, O.; Lorenz, I. P. Rhodium-Komplexe Des A-Frame-Typs $[Rh(CO)Dppm]_2(\mu\text{-}X)$ Mit Den Brückenliganden Schwefel, Schwefelmonoxid Und Schwefeldioxid. *Z. Anorg. Allg. Chem.* **1989**, *578* (1), 185.
(29) Longobardi, L. E.; Wolter, V.; Stephan, D. W. Frustrated Lewis Pair Activation of an N-Sulfinylamine: A Source of Sulfur Monoxide. *Angew. Chem. Int. Ed.* **2015**, *54* (3), 809.
(30) Markó, L.; Markó-Monostory, B.; Madach, T.; Vahrenkamp, H. First Fixation of the Unstable Species Sulfur Monoxide in a Cluster: Synthesis and Structure of $Fe_3(CO)_9(S)SO$. *Angew. Chem. Int. Ed.* **1980**, *19* (3), 226.
(31) Hoots, J. E.; Lesch, D. A.; Rauchfuss, T. B. Peracid Oxidation of Inorganic Chalcogen Ligands in Transition-Metal Complexes. *Inorg. Chem.* **1984**, *23* (20), 3130.
(32) Bagherzadeh, S.; Mankad, N. P. Oxidation of a $[Cu_2S]$ Complex by N_2O and CO_2: Insights into a Role of Tetranuclearity in the CuZ Site of Nitrous Oxide Reductase. *Chem. Commun.* **2018**, *54* (9), 1097.
(33) Lovas, F. J.; Tiemann, E.; Johnson, D. R. Spectroscopic Studies of the SO_2 Discharge System. II. Microwave Spectrum of the SO Dimer. *J. Chem. Phys.* **1974**, *60* (12),

5005.
(34) Harcourt, R. D. Qualitative Valence-Bond Descriptions of Bonding for S-N, S-O, S-F and S-S Compounds via Increased-Valence Structures. *J. Mol. Struct.* **1989**, *186* (Supplement C), 131.
(35) Harcourt, R. D. Increased-Valence Structures for Qualitative Valence-Bond Representations of Electronic Structure for Electron-Rich Molecules. *Eur. J. Inorg. Chem.* **2000**, *2000* (9), 1901.
(36) Martin-Drumel, M. A.; van Wijngaarden, J.; Zingsheim, O.; Lewen, F.; Harding, M. E.; Schlemmer, S.; Thorwirth, S. Millimeter- and Submillimeter-Wave Spectroscopy of Disulfur Dioxide, OSSO. *J. Mol. Spectrosc.* **2015**, *307*, 33.
(37) Marsden, C. J.; Smith, B. J. An Ab Initio Study of Many Isomers of S_2O_2. A Combined Theoretical and Experimental Analysis of the Harmonic Force Field and Molecular Structure of Cis-Planar OSSO. *Chem. Phys.* **1990**, *141* (2), 335.
(38) Schmid, G.; Ritter, G.; Debaerdemaeker, T. Die Komplexchemie Niederer Schwefeloxide, II. Schwefelmonoxid Und Dischwefeldioxid Als Komplexliganden. *Chem. Ber.* **1975**, *108* (9), 3008.
(39) Lorenz, I.-P.; Kull, J. Complex Stabilization of Disulfur Dioxide in the Fragmentation of Thiirane S-Oxide on Bis(Triphenylphosphane)Platinum(0). *Angew. Chem. Int. Ed.* **1986**, *25* (3), 261.
(40) The Other Example, $[(Diphos)_2Ir(OSSO)]Cl$, Features a Trans-OSSO Ligand (Dihedral Angle = 68°) with an S-S Bond Length of 2.041 Å. Curiously, One of Its S-O Bond Lengths (1.21(2) Å) Is Anomalously Short, Which May Indicate Unresolved Disorder.
(41) Smiles, D. E.; Wu, G.; Hayton, T. W. Reversible Chalcogen-Atom Transfer to a Terminal Uranium Sulfide. *Inorg. Chem.* **2014**, *53* (24), 12683.
(42) Sweeney, Z. K.; Polse, J. L.; Andersen, R. A.; Bergman, R. G.; Kubinec, M. G. Synthesis, Structure, and Reactivity of Monomeric Titanocene Sulfido and Disulfide Complexes. Reaction of H_2 with a Terminal MS Bond. *J. Am. Chem. Soc.* **1997**, *119* (19), 4543.
(43) Sweeney, Z. K.; Polse, J. L.; Bergman, R. G.; Andersen, R. A. Dihydrogen Activation by Titanium Sulfide Complexes. *Organometallics* **1999**, *18* (26), 5502.
(44) Mealli, C.; Midollini, S.; Sacconi, L. Transition-Metal Complexes with Sulfur Atom as Ligand. 2. Synthesis, Properties, and Structural Characterization of Thio, Mercapto, and Methylthio Complexes of Cobalt(I) and Nickel(I) and -(II) with Poly(Tertiary Phosphines). *Inorg. Chem.* **1978**, *17* (3), 632.
(45) J. Pleus, R.; Waden, H.; Saak, W.; Haase, D.; Pohl, S. Preparation of the First Sulfur-Containing Cobalt and Nickel Complexes Stabilised by the Macrocyclic Cyclam Ligand; Observation of S-H Bond Activation. *J. Chem. Soc., Dalt. Trans.* **1999**, No. 15, 2601.
(46) Cho, J.; Van Heuvelen, K. M.; Yap, G. P. A.; Brunold, T. C.; Riordan, C. G. New Synthetic Routes to a Disulfidodinickel(II) Complex: Characterization and Reactivity of a $Ni_2(\mu\text{-}\eta^2\text{:}\eta^2\text{-}S_2)$ Core. *Inorg. Chem.* **2008**, *47* (10), 3931.
(47) Yao, S.; Milsmann, C.; Bill, E.; Wieghardt, K.; Driess, M. From a Paramagnetic, Mononuclear Supersulfidonickel(II) Complex to a Diamagnetic Dimer with a Four-Sulfur Two-Electron Bond. *J. Am. Chem. Soc.* **2008**, *130* (41), 13536.
(48) Inosako, M.; Kunishita, A.; Kubo, M.; Ogura, T.; Sugimoto, H.; Itoh, S. ($\mu\text{-}\eta^2\text{:}\eta^2\text{-}$

Disulfido)Dinickel(II) Complexes Supported by 6-Methyl-TPA Ligands. *Dalt. Trans.* **2009**, No. 43, 9410.

(49) Iluc, V. M.; Laskowski, C. A.; Brozek, C. K.; Harrold, N. D.; Hillhouse, G. L. Monomeric and Dimeric Disulfide Complexes of Nickel(II). *Inorg. Chem.* **2010**, *49* (15), 6817.

(50) Olechnowicz, F.; Hillhouse, G. L.; Jordan, R. F. Synthesis and Reactivity of NHC-Supported $Ni_2(\mu^2\text{-}\eta^2,\eta^2\text{-}S_2)$-Bridging Disulfide and $Ni_2(\mu\text{-}S)_2$-Bridging Sulfide Complexes. *Inorg. Chem.* **2015**, *54* (6), 2705.

(51) Yao, S.; Xiong, Y.; Zhang, X.; Schlangen, M.; Schwarz, H.; Milsmann, C.; Driess, M. Facile Dissociation of $[(LNi^{II})_2E_2]$ Dichalcogenides: Evidence for $[LNi^{II}E_2]$ Superselenides and Supertellurides in Solution. *Angew. Chem. Int. Ed.* **2009**, *48* (25), 4551.

(52) Hartmann, N. J.; Wu, G.; Hayton, T. W. Activation of CS_2 by a "Masked" Terminal Nickel Sulfide. *Dalt. Trans.* **2016**, *45*, 14508.

(53) Hartmann, N. J.; Wu, G.; Hayton, T. W. Reactivity of a Nickel Sulfide with Carbon Monoxide and Nitric Oxide. *J. Am. Chem. Soc.* **2016**, *138* (38), 12352.

(54) Farrell, W. S.; Zavalij, P. Y.; Sita, L. R. Metal-Catalyzed "On-Demand" Production of Carbonyl Sulfide from Carbon Monoxide and Elemental Sulfur. *Angew. Chem. Int. Ed.* **2015**, *54* (14), 4269.

(55) Wilton-Ely, J. D. E. T.; Solanki, D.; Hogarth, G. Synthesis and Reactivity of the Ruthenium(II) Dithiocarbonate Complex $[Ru(\kappa^2\text{-}S_2CO)(Dppm)_2]$ (Dppm = Bis(Diphenylphosphino)Methane). *Inorg. Chem.* **2006**, *45* (13), 5210.

(56) Lalrempuia, R.; Stasch, A.; Jones, C. The Reductive Disproportionation of CO_2 Using a Magnesium(I) Complex: Analogies with Low Valent f-Block Chemistry. *Chem. Sci.* **2013**, *4* (12), 4383.

(57) Horn, B.; Pfirrmann, S.; Limberg, C.; Herwig, C.; Braun, B.; Mebs, S.; Metzinger, R. N_2 Activation in Ni^I–NN–Ni^I Units: The Influence of Alkali Metal Cations and CO Reactivity. *Z. Anorg. Allg. Chem.* **2011**, *637* (9), 1169.

(58) Lam, O. P.; Franke, S. M.; Heinemann, F. W.; Meyer, K. Reactivity of U–E–U (E = S, Se) Toward CO_2, C_2, and COS: New Mixed-Carbonate Complexes of the Types U–CO_2E–U (E = S, Se), U–CS_2E–U (E = O, Se), and U–COSSe–U. *J. Am. Chem. Soc.* **2012**, *134* (40), 16877.

(59) Schoo, C.; Klementyeva, S. V; Gamer, M. T.; Konchenko, S. N.; Roesky, P. W. Samarocene Oxide: From an Undesired Decomposition Product to a New Reagent. *Chem. Commun.* **2016**, *52* (40), 6654.

(60) Smiles, D. E.; Wu, G.; Hayton, T. W. Synthesis of Uranium–Ligand Multiple Bonds by Cleavage of a Trityl Protecting Group. *J. Am. Chem. Soc.* **2014**, *136* (1), 96.

(61) Smiles, D. E.; Wu, G.; Kaltsoyannis, N.; Hayton, T. W. Thorium-Ligand Multiple Bonds via Reductive Deprotection of a Trityl Group. *Chem. Sci.* **2015**, *6* (6), 3891.

(62) Döhring, A.; Jolly, P. W.; Krüger, C.; Romão, M. J. The Ni(0)—CO_2 System: Structure and Reactions of $[Ni(PCy_3)_2(\eta^2\text{-}CO_2)]$. *Z. Naturforsch. B* **1985**, *40*, 484.

(63) Beck, R.; Shoshani, M.; Krasinkiewicz, J.; Hatnean, J. A.; Johnson, S. A. Synthesis and Chemistry of Bis(Triisopropylphosphine) Nickel(I) and Nickel(0) Precursors. *Dalt. Trans.* **2013**, *42* (5), 1461.

(64) Kim, Y.-E.; Kim, J.; Lee, Y. Formation of a Nickel Carbon Dioxide Adduct and Its Transformation Mediated by a Lewis Acid. *Chem. Commun.* **2014**, *50* (78), 11458.

(65) Anderson, J. S.; Iluc, V. M.; Hillhouse, G. L. Reactions of CO_2 and CS_2 with 1,2-Bis(Di-Tert-Butylphosphino)Ethane Complexes of Nickel(0) and Nickel(I). *Inorg. Chem.* **2010**, *49* (21), 10203.
(66) Pfirrmann, S.; Limberg, C.; Herwig, C.; Stößer, R.; Ziemer, B. A Dinuclear Nickel(I) Dinitrogen Complex and Its Reduction in Single-Electron Steps. *Angew. Chem. Int. Ed.* **2009**, *48* (18), 3357.
(67) Lee, C. H.; Laitar, D. S.; Mueller, P.; Sadighi, J. P. Generation of a Doubly Bridging CO_2 Ligand and Deoxygenation of CO_2 by an (NHC)Ni(0) Complex. *J. Am. Chem. Soc.* **2007**, *129* (45), 13802.
(68) Sahoo, D.; Yoo, C.; Lee, Y. Direct CO_2 Addition to a Ni(0)–CO Species Allows the Selective Generation of a Nickel(II) Carboxylate with Expulsion of CO. *J. Am. Chem. Soc.* **2018**, *140* (6), 2179.
(69) Hashimoto, K.; Nagatomo, S.; Fujinami, S.; Furutachi, H.; Ogo, S.; Suzuki, M.; Uehara, A.; Maeda, Y.; Watanabe, Y.; Kitagawa, T. A New Mononuclear Iron(III) Complex Containing a Peroxocarbonate Ligand. *Angew. Chem. Int. Ed.* **2002**, *41* (7), 1202.
(70) Meier, G.; Braun, T. Hydrogenation of a Rhodium Peroxido Complex by Formate Derivatives: Mechanistic Studies and the Catalytic Formation of H_2O_2 from O_2. *Angew. Chem. Int. Ed.* **2012**, *51* (50), 12564.
(71) Yamashita, M.; Goto, K.; Kawashima, T. Fixation of Both O_2 and CO_2 from Air by a Crystalline Palladium Complex Bearing N-Heterocyclic Carbene Ligands. *J. Am. Chem. Soc.* **2005**, *127* (20), 7294.
(72) Coucouvanis, D.; Draganjac, M. The Formation of Perthiocarbonate Ligands Following the Addition of CS_2 to Binary Molybdenum-Sulfur Complexes. *J. Am. Chem. Soc.* **1982**, *104* (24), 6820.
(73) Yu, S.-B.; Holm, R. H. Tetrahedral and Square-Pyramidal Sulphur-Rich Complexes of Manganese(II). *Polyhedron* **1993**, *12* (2), 263.
(74) McKillop, A.; Sanderson, W. R. Sodium Perborate and Sodium Percarbonate: Cheap, Safe and Versatile Oxidising Agents for Organic Synthesis. *Tetrahedron* **1995**, *51* (22), 6145.
(75) Tsugawa, T.; Furutachi, H.; Marunaka, M.; Endo, T.; Hashimoto, K.; Fujinami, S.; Akine, S.; Sakata, Y.; Nagatomo, S.; Tosha, T.; et al. Oxidation Reactivity of a Structurally and Spectroscopically Well-Defined Mononuclear Peroxocarbonato–Iron(III) Complex. *Chem. Lett.* **2015**, *44* (3), 330.
(76) Lane, B. S.; Vogt, M.; DeRose, V. J.; Burgess, K. Manganese-Catalyzed Epoxidations of Alkenes in Bicarbonate Solutions. *J. Am. Chem. Soc.* **2002**, *124* (40), 11946.
(77) Yao, H.; Richardson, D. E. Epoxidation of Alkenes with Bicarbonate-Activated Hydrogen Peroxide. *J. Am. Chem. Soc.* **2000**, *122* (13), 3220.
(78) Donahue, J. P. Thermodynamic Scales for Sulfur Atom Transfer and Oxo-for-Sulfido Exchange Reactions. *Chem. Rev.* **2006**, *106* (11), 4747.
(79) Shaver, A.; Mouatassim, B. El; Florent Mortini; Francine Bélanger-Gariépy; Lough, A. Reactions of $(\eta^5\text{-}C(_5Me_5)Ir(PMe_3)(SH)_2$ and $(\eta^5\text{-}C_5Me_5)Ir(PMe_3)(SH)(H)$ with Thionylaniline (PhNSO) to Give Novel Iridium S_3O and S_2O Comp. *Organometallics* **2007**, *26* (17), 4229.
(80) Herberhold, M.; Schmidkonz, B.; Ziegler, M. L.; Zahn, T. Disulfur Monoxide as

Complex Ligand - Preparation and Molecular Structure of [(η^5-C_5Me_5)$Mn(CO)_2(S_2O)$]. *Angew. Chemie Int. Ed. English* **1985**, *24* (6), 515.

(81) Faller, J. W.; Ma, Y. A Mononuclear Oxosulfidomolybdenum(VI) Complex and Other Oxo, Sulfido, and η^2-S_2O Derivatives of (Cp*) Molybdenum and-Tungsten. *Organometallics* **1989**, *8* (3), 609.

(82) Brown, D. S.; Owens, C. F.; Wilson, B. G.; Welker, M. E.; Rheingold, A. L. Synthesis and Reaction Chemistry of the Readily Available Molybdenum S_2O Complex [$MoO(S_2CNEt_2)_2(S_2O)$]. *Organometallics* **1991**, *10* (4), 871.

(83) Halcrow, M. A.; Huffman, J. C.; Christou, G. Synthesis, Characterization, and Molecular Structure of the New S_2O Complex $Mo(S_2O)(S_2CNEt_2)_3 \cdot 1/2Et_2O$. *Inorg. Chem.* **1994**, *33* (17), 3639.

(84) Rys, A. Z.; Lebuis, A.; Shaver, A.; Harpp, D. N. Selective Oxidation of Cp_2MoS_2 and Cp_2MoS_4 To Give Cp_2MoS_2O and Cp_2MoS_4O , Respectively : A Novel Thermally Induced Oxygen Migration Converting 1-Oxo-Cp_2MoS. **1999**, *18* (7), 10.

(85) Suzuki, T.; Tsuji, N.; Kashiwabara, K.; Tatsumi, K. Oxidative Additions of Cyclo-Octasulfur and Cyclo-Octaselenium to the Cobalt(II) Complex of 1,3-Bis(Dimethylphosphino)Propane (Dmpp). *Inorg. Chem.* **2000**, *39* (17), 3938.

(86) Ishii, A.; Murata, M.; Oshida, H.; Matsumoto, K.; Nakayama, J. Oxosulfido Complexes of Platinum — $(Ph_3P)_2Pt(S_2O)$ and $(Ph_3P)_4Pt_2(\mu\text{-}S)(\mu\text{-}SO)$ — Their Formation and Properties. *Eur. J. Inorg. Chem.* **2003**, *2003* (20), 3716.

(87) Holze, P.; Horn, B.; Limberg, C.; Matlachowski, C.; Mebs, S. The Activation of Sulfur Hexafluoride at Highly Reduced Low-Coordinate Nickel Dinitrogen Complexes. *Angew. Chem. Int. Ed.* **2014**, *53* (10), 2750.

(88) Holland, P. L.; Cundari, T. R.; Perez, L. L.; Eckert, N. A.; Lachicotte, R. J. Electronically Unsaturated Three-Coordinate Chloride and Methyl Complexes of Iron, Cobalt, and Nickel. *J. Am. Chem. Soc.* **2002**, *124* (48), 14416.

(89) Harris Robin, K.; Becker Edwin, D.; Cabral de Menezes Sonia, M.; Goodfellow, R.; Granger, P. NMR Nomenclature: Nuclear Spin Properties and Conventions for Chemical Shifts. IUPAC Recommendations 2001. International Union of Pure and Applied Chemistry. Physical Chemistry Division. Commission on Molecular Structure and Spectroscopy. *Pure Appl. Chem.* **2002**, *40* (7), 489.

(90) Harris Robin, K.; Becker Edwin, D.; Cabral De Menezes Sonia, M.; Granger, P.; Hoffman Roy, E.; Zilm Kurt, W. Further Conventions for NMR Shielding and Chemical Shifts. *Pure Appl. Chem.* **2008**, *80*, 59.

(91) SMART Apex II. Bruker AXS Inc.: Madison, WI 2005.

(92) SAINT Software User's Guide. Bruker AXS Inc.: Madison, WI 2005.

(93) Sheldrick, G. M. SADABS. University of Gottingen: Germany 2005.

(94) SHELXTL PC. Bruker AXS Inc.: Madison, WI 2005.

(95) M. Budzelaar, P. H.; van Oort, A. B.; Orpen, A. G. β-Diiminato Complexes of VIII and TiIII – Formation and Structure of Stable Paramagnetic Dialkylmetal Compounds. *Eur. J Inorg. Chem.* **1998**, *1998* (10), 1485.

Chapter 7 Progress Toward the Synthesis of Late Transition Metal Oxo, Sulfide, and Imido Complexes

Table of Contents

7.1 Introduction

In the past 20 years, the library of late transition metal (groups 9, 10, 11) complexes containing metal-ligand multiple bonds has expanded significantly.[1,2] For example, there has been a notable increase in the number of carbene (CR_2^{2-}),[3] nitrene (NR^{2-}),[4–11] nitride (N^{3-}),[12,13] and phosphinidene (PR^{2-})[14,15] complexes.[16,17] Despite these successes, the number of terminal chalcogenide (E^{2-}, E = O, S) complexes has remained nearly stagnant, reflecting the challenges associated with the synthesis of these species. The only two well characterized late metal terminal oxo (O^{2-}) complexes, $[Ir^{V}(O)(Mes)_3]$ (Mes = 2,4,6-$Me_3C_6H_2$) and $[Pt^{IV}(O)(PCN)][BF_4]$ (PCN = $C_6H_3[CH_2P(tBu)_2](CH_2CH_2NMe_2)$),[18,19] both feature 3rd row transition metals in high oxidation states that are not commonly accessible for first row metals and require the use of $2e^-$ oxidants to install the terminal oxo ligands (Figure 7.1).

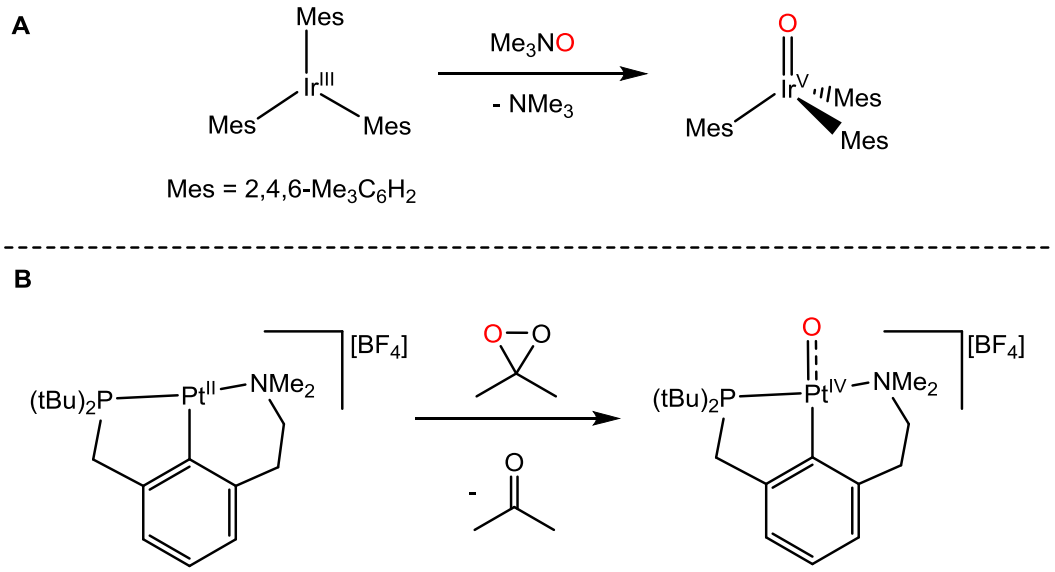

Figure 7.1. The synthesis of late transition metal terminal oxo complexes. **A**, Ref. 18; **B**, Ref. 19.

In chapter 2, I demonstrated that the reductive deprotection of Ni tritylthiolate complexes, [$L^{R}Ni^{II}(SCPh_3)$] (**2.1**, R = Me; **2.2**, R = ^{t}Bu), is an effective route for the synthesis of "masked" terminal sulfides, [K(L)][$L^{R}Ni^{II}(S)$] (**2.4**, R = Me, L = 18-crown-6; **2.5**, R = ^{t}Bu, L = 18-crown-6; **2.6**, R = ^{t}Bu, L = 2,2,2-cryptand).[20] The reductive deprotection strategy is advantageous for first row transition metals because installation of the terminal ligand does not require a change in metal oxidation state. The Hayton group has also recently reported the synthesis of actinide terminal oxos, [K(18-crown-6)][$An(O)(NR_2)_3$] (An = U, Th, R = $SiMe_3$), using reductive deprotection (Scheme 7.1),[21,22] indicating that this strategy may also be generally useful for the synthesis of oxo complexes. In this chapter, I report on my efforts to extend the scope of the 'reductive deprotection' reaction to the synthesis of other late transition metal (Fe, Co, Ni) complexes with oxo, sulfide, and imido ligands.

Scheme 7.1 Synthesis of actinide oxo complexes via reductive deprotection.

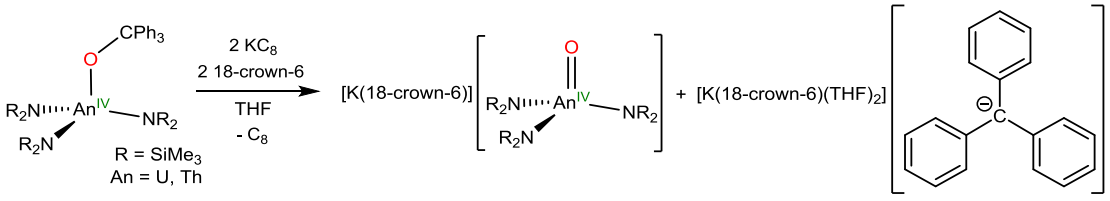

7.2 Results and Discussion

7.2.1 Synthesis and Characterization of [$L^{Me}Ni^{II}(OCPh_3)$] (7.1) and [$L^{tBu}Ni^{II}(OCPh_3)$] (7.2)

Addition of 1 equiv of $KOCPh_3$ to [$L^{R}Ni^{II}Cl$] (R = Me, ^{t}Bu)[23] in C_6H_6 results in the formation of [$L^{R}Ni^{II}(OCPh_3)$] (**7.1**, R = Me; **7.2**, R = ^{t}Bu). Complex **7.1** can be isolated as

deep aqua blocks from hexanes in 72% yield, while complex **7.2** can be isolated as bright green powder in 70% yield (Scheme 7.2).

Scheme 7.2 Synthesis of [$L^{Me}Ni^{II}(OCPh_3)$] (**7.1**) and [$L^{tBu}Ni^{II}(OCPh_3)$] (**7.2**)

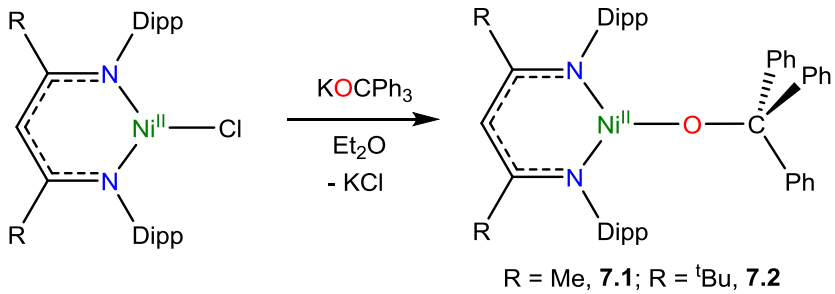

The formulations of **7.1** and **7.2** were confirmed by elemental analysis, however, only **7.1** has been characterized by X -ray crystallography. The solid state molecular structure of **7.1** is shown in Figure 7.2. Complex **7.1** features a three coordinate Ni^{II} center ligated by a tritylalkoxide moiety. The Ni-O and C-O bond lengths in **7.1** are 1.756(1) and 1.400(2) Å, respectively, and are both consistent with single bonds.[20,24,25] The Ni-O-C angle in **7.1** is 150.6(1)° and is larger than the Ni-S-C angles in both **2.1** and **2.2** which could be indicative of the presence of some π character in the Ni-O bond. In contrast to [$L^{Me}Ni^{II}(SCPh_3)$] (**2.1**), the coordination geometry of the Ni center is planar ((Σ(L-Ni-L) = 360.0°) and is best described as distorted T-shaped with N-Ni-O angles of 144.27(7)° and 119.41(7)°.[26,27] Finally, the Ni-N bonds in **7.1** are similar to those found in other Ni^{II} β-diketiminate complexes.[20,28,29] The ^{1}H NMR spectra of complexes **7.1** and **7.2** in C_6D_6 are similar to those reported for other three-coordinate Ni^{II} *β*-diketiminate complexes; **7.1** features one backbone methyl resonance at -69.62 ppm and a single γ-CH resonance at -188.42 ppm and **7.2** features one *tert*-butyl resonance at 2.31 ppm and a single γ-CH resonance at -210.03 ppm.[20,30–33] Additionally, Evans' method determination of the magnetic moment of these

complexes revealed values of 3.09 and 3.08 B.M. for **7.1** and **7.2**, respectively; these values are also consistent with S = 1 Ni^{II} complexes.[32–34]

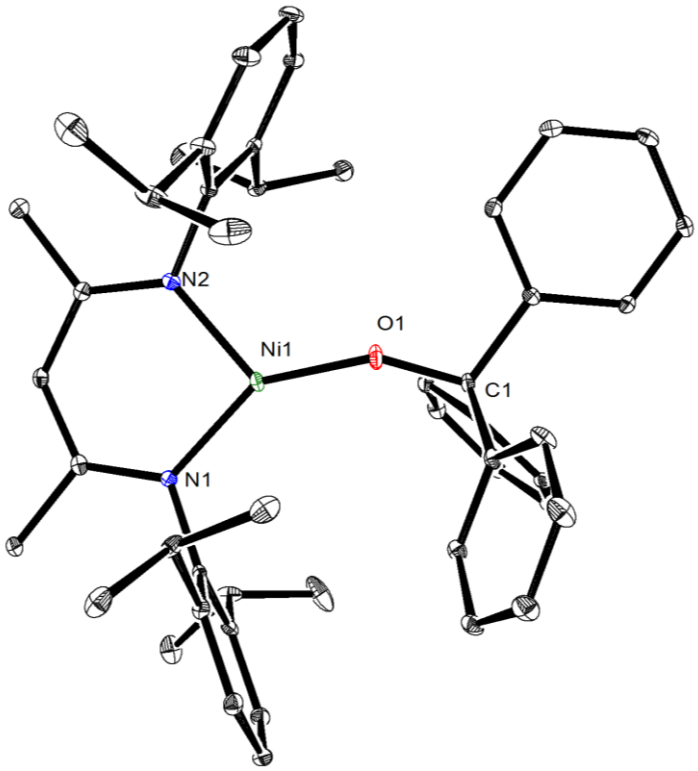

Figure 7.2. ORTEP diagram of [$L^{Me}Ni^{II}(OCPh_3)$] (**7.1**) with 50% probability ellipsoids. Hydrogen atoms have been omitted for clarity. Selected bond lengths and angles: Ni1-O1 1.756(1) Å, C1-O1 1.400(2) Å, Ni1-N1 1.901(2) Å, Ni1-N2 1.918(2) Å, N1-Ni1-N2 96.29(7)°, N1-Ni1-O1 144.27(7)°, N2-Ni1-O1 119.41(7)°, Ni1-O1-C1 150.6(1)°.

7.2.2 Synthesis and Characterization of [K(18-crown-6) $(THF)_2$][$L^{Me}Ni^{I}(OCPh_3)$] (7.3)

Subsequent reduction of **7.1** with 1 equiv of KC_8, in cold (-25 °C) Et_2O, in the presence of 18-crown-6, results in the formation of [K(18-crown-6)$(THF)_2$][$L^{Me}Ni^{I}(OCPh_3)$] (**7.3**). Complex **7.3** can be isolated as deep red needles from THF/hexanes in 82% yield (Scheme 7.3).

Scheme 7.3 Synthesis of [K(18-crown-6)(THF)$_2$][L^{Me}Ni^{I}(OCPh$_3$)] (**7.3**)

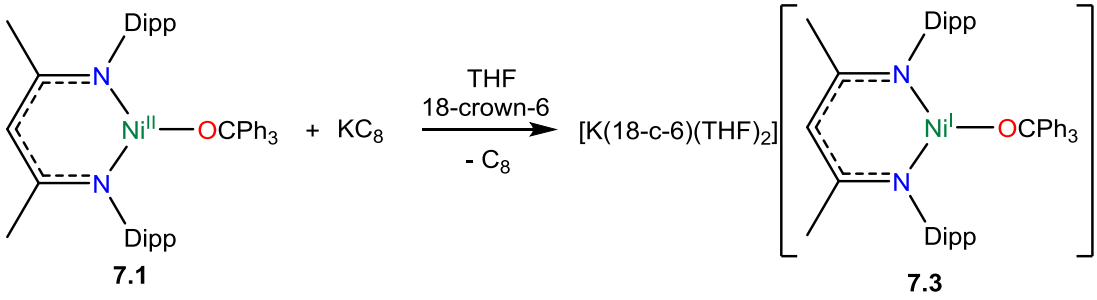

I should also note that the reaction of **7.1** with 2 equiv of KC_8, in the presence of 18-crown-6, still affords **7.3**, indicating that the trityl O-C bond in this complex is too strong to be reduced using KC_8. Additionally, it appears likely that the steric pressure from the β-diketiminate Dipp groups play a role in the outcome of this reaction as O-C bond cleavage is observed in the reduction of complex **7.2**(see below). The formulation of complex **7.3** has been confirmed by X-ray crystallography and elemental analysis. The solid state molecular structure of **7.3** is shown in Figure 7.3. The Ni center in complex **7.3** exhibits a planar (Σ(L-Ni-L) = 357°), Y-shaped coordination geometry. The Ni-O (1.875(2) Å) and Ni-N bond lengths (1.945(2), 1.958(2) Å) in **7.3** are longer than those in **7.1**, consistent with the larger atomic radius of Ni^{I} relative to Ni^{II}.[31,33,35] The Ni-O-C angle in **7.3** is 144.3(2)° and is slightly more acute than that in **7.1**.The ^{1}H NMR spectrum of complex **7.3** in THF-d_8 features broad paramagnetic resonances typical of those observed for other Ni^{I} *β*-diketiminate complexes, for example, **7.3** features one backbone methyl resonance at -41.13 ppm and a two diasterotopic isopropyl-CH$_3$ resonances at 6.82 and 6.72 ppm.[31,33,35,36]

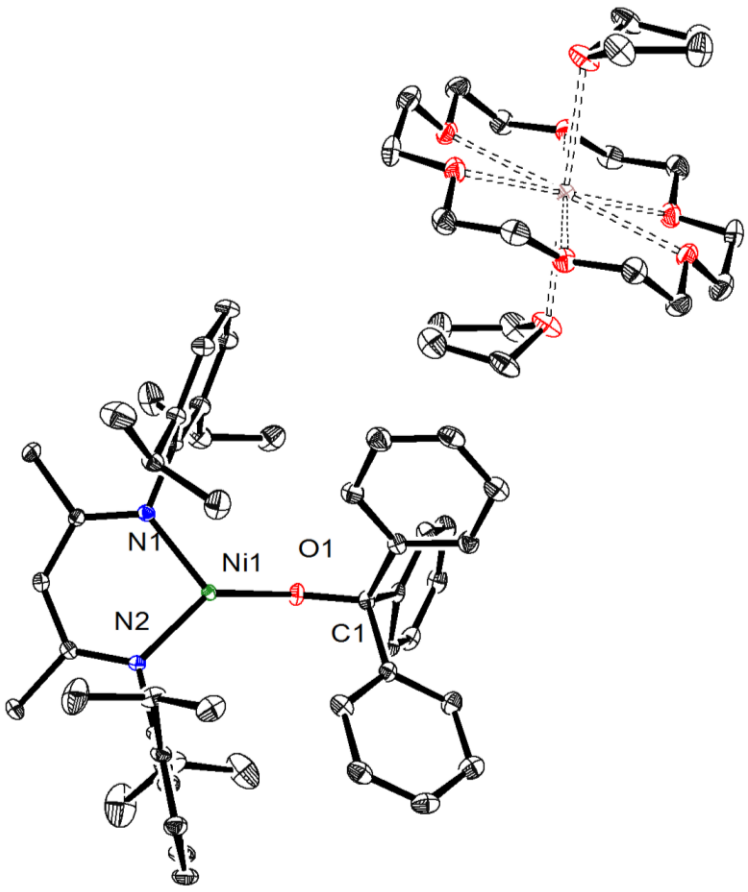

Figure 7.3. ORTEP diagram of $[K(18\text{-crown-6})(THF)_2][L^{Me}Ni^{I}(OCPh_3)]\cdot C_4H_8O$ (**7.3**$\cdot C_4H_8O$) with 50% probability ellipsoids. Hydrogen atoms and a THF solvate molecule have been omitted for clarity. Selected bond lengths and angles: Ni1-O1 1.875(2) Å, C1-O1 1.378(3) Å, Ni1-N1 1.945(2) Å, Ni1-N2 1.958(2) Å, N1-Ni1-N2 94.61(9)°, N1-Ni1-O1 133.15(8)°, N2-Ni1-O1 128.94(9)°, Ni1-O1-C1 144.3(2)°.

7.2.3 Synthesis and Characterization of $[K(18\text{-crown-6})][L^{tBu}Ni^{I}(OH)]$ (7.4)

Reduction of **7.2** with 2 equiv of KC_8, in cold (-25 °C) THF, in the presence of 18-crown-6, results in the formation of $[K(18\text{-crown-6})][L^{tBu}Ni^{I}(OH)]$ (**7.4**). Complex **7.4** can be isolated as red-orange plates from Et_2O in 69% yield (Scheme 7.4).

Scheme 7.4 Synthesis of [K(18-crown-6)][L^{tBu}Ni^{I}(OH)] (**7.4**)

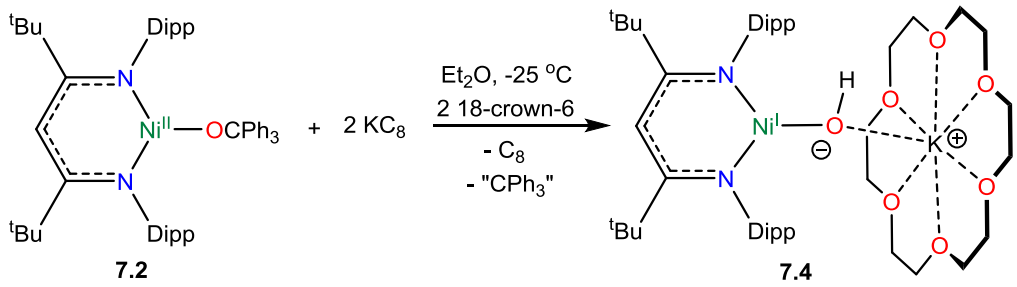

The formulation of complex **7.4** has been confirmed by X-ray crystallography, and its solid state molecular structure is shown in Figure 7.4. Complex **7.4** features a three coordinate Ni^{I} center ligated by a hydroxo (OH^{-}) moiety with a Ni-O bond length of 1.877(4) Å which is longer than that observed in complex **7.1** (1.756(1) Å) and identical to that observed in complex **7.3** (1.875(2) Å). The coordination geometry of the Ni center (Σ(L-Ni-L) = 369.8°) is best described as distorted T-shaped. The ^{1}H NMR spectrum of **7.4** in C_6D_6 contains broad paramagnetic resonances typical of those observed for other Ni^{I} β-diketiminate complexes, for example, **7.3** features one *tert*-butyl resonance at -1.48 ppm and an isopropyl-CH resonance at 12.64 ppm.[31,33,35,36] A resonance assignable to the OH^{-} proton was not observed in this spectrum. To my knowledge, complex **7.4** is the first example of a Ni^{I} hydroxo species. Previously reported Ni OH^{-} complexes have typically been synthesized via metathesis with hydroxide salts.[37–42] For example, reaction of [Ni^{II}($CH_2C_6H_5$)(PMe_3)(Cl)] with NaOH resulted in the formation of [Ni^{II}($CH_2C_6H_5$)(PMe_3)(μ-OH)]$_2$.[37]

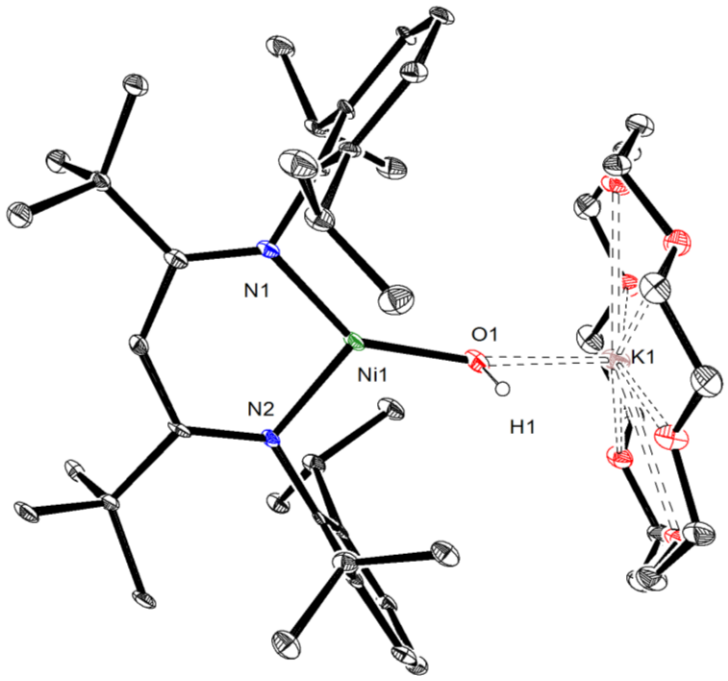

Figure 7.4. ORTEP diagram of [K(18-crown-6)][$L^{tBu}Ni^{I}$(OH)]·$C_4H_{10}O$ (**7.4**·$C_4H_{10}O$) with 50% probability ellipsoids. Hydrogen atoms and an Et_2O solvate molecule omitted for clarity. Selected bond lengths and angles: Ni1-O1 1.877(4) Å, O1-K1 2.574(4) Å, Ni1-N1 1.884(4) Å, Ni1-N2 1.908(4) Å, N1-Ni1-N2 98.6(2)°, N1-Ni1-O1 143.4(2)°, N2-Ni1-O1 117.8(2)°.

A tentative mechanism for the formation of **7.4** can be found in Scheme 7.5. However, this mechanism is definitely not certain as I have not yet been able to identify the trityl containing byproduct(s) of this reaction. Based on my observations and ^{1}H NMR spectra taken of the crude products of this reaction, I can rule out the formation of common triphenylmethyl containing products such as $[CPh_3]^-$, Gomberg's dimer, and triphenylmethane (Ph_3CH). The absence of $[CPh_3]^-$ as a product disfavors the direct reductive deprotection route that was observed in the synthesis of Ni sulfides from [$L^{Me}Ni^{II}(SCPh_3)$] (**2.1**) and [$L^{tBu}Ni^{II}(SCPh_3)$] (**2.2**). While the absence of Gomberg's dimer[43]

and triphenylmethane disfavor spontaneous homolytic pathways such as that observed in the 1 electron reduction of [$L^{tBu}Ni^{II}(SCPh_3)$] (**2.2**) (Scheme 2.5). Scheme 7.5 depicts the formation of an intermediate oxyl radical, which abstracts an H-atom leading to homolysis of the tritylalkoxide O-C bond to yield **7.4** and trityl radical. Oxyls are often implicated as intermediates in H-atom abstraction reactions.[44,45] It is possible that the trityl radical could couple with solvent radicals formed via the initial oxyl H-atom abstraction step. Notably, reductive cleavage of the O-CPh_3 O-C bond has only been observed for complex **7.2**, I can rationalize this difference based on the increased steric pressure on -CP_3 by the β-diketiminate Dipp groups.[46,47] I hypothesize that this steric pressure facilitates O-C bond cleavage in this system.

Scheme 7.5 Possible mechanisms for the formation [K(18-crown-6)][$L^{tBu}Ni^{I}(OH)$] (**7.4**)

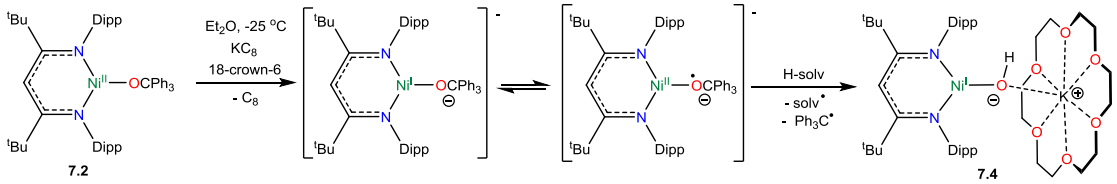

7.2.4 Synthesis and Characterization of [$L^{Me}Fe^{II}(OCPh_3)$] (7.5) [$L^{tBu}Fe^{II}(OCPh_3)(NCCH_3)$] (7.6) and [K(18-crown-6)$(THF)_2$][$L^{Me}Fe^{I}(OCPh_3)$] (7.7)

Addition of 1 equiv of $HOCPh_3$ to [$L^{Me}Fe^{II}(N(TMS)_2)$][48] (TMS = $SiMe_3$) in Et_2O results in the formation of [$L^{Me}Fe^{II}(OCPh_3)$] (**7.5**). Complex **7.5** can be isolated as yellow needles from Et_2O layered with hexanes in 80% yield (Scheme 7.6).

Scheme 7.6 Synthesis of [$L^{Me}Fe^{II}(OCPh_3)$] (**7.5**)

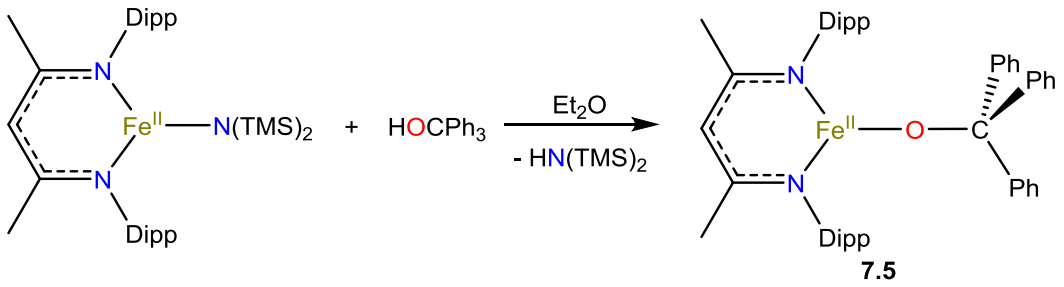

The solid state molecular structure of **7.5** is shown in Figure 7.5. Complex **7.5** features a three coordinate Fe^{II} center ligated by a tritylalkoxide moiety with a Fe-O bond length of 1.806(1) Å which is consistent with a single bond.[49–51] The Fe-O-C angle in **7.5** of 143.53(1)° is similar to that observed in complex **7.1** suggesting that these two complexes have similar M-O bonding interactions. The coordination geometry of Fe center is planar (Σ(L-Fe-L) = 359.9°) and is best described as T-shaped based on the N1-Fe1-O1 angle of 150.11(6)°. Finally, the Fe-N bonds in **7.5** are similar to those found in other Fe^{II} β-diketiminate complexes. [23,46,52,53] The ^1H NMR spectrum of **7.5** in C_6D_6 contains paramagnetically shifted resonances similar to those of other three coordinate Fe^{II} *β*-diketiminate complexes for example, **7.5** features one backbone methyl resonance at 15.25 ppm and a two diasterotopic isopropyl-CH_3 resonances at -15.39 and -90.19 ppm.[23,46,52,53]

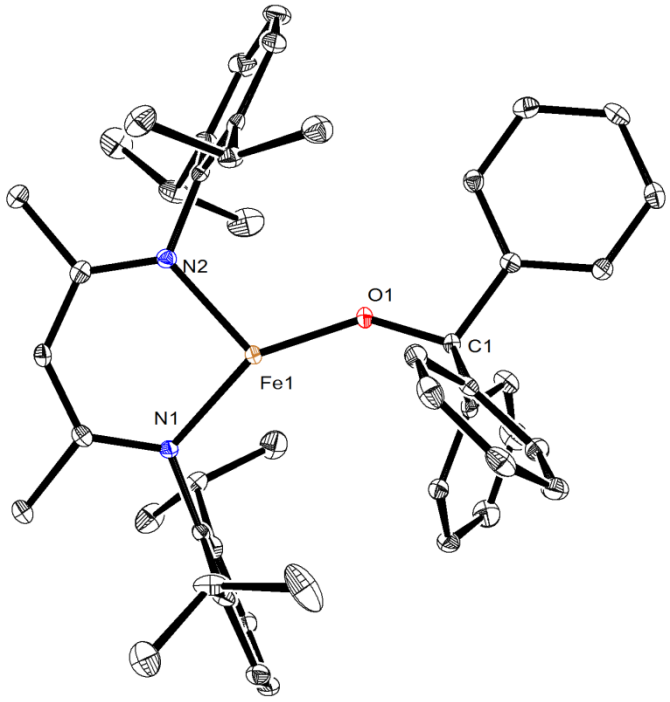

Figure 7.5. ORTEP diagram of [$L^{Me}Fe^{II}(OCPh_3)$] (**7.5**) with 50% probability ellipsoids. Hydrogen atoms omitted for clarity. Selected bond lengths and angles: Fe1-O1 1.806(1) Å, C1-O1 1.404(2) Å, Fe1-N1 1.966(1) Å, Fe1-N2 2.000(1) Å, N1-Fe1-N2 96.58(6)°, N1-Fe1-O1 150.11(6)°, N2-Fe1-O1 113.24(6)°, Fe1-O1-C1 143.53(1)°.

Addition of 1 equiv of $KOCPh_3$ to [$L^{tBu}Fe^{II}Cl$][46] in Et_2O results in the formation of [$L^{tBu}Fe^{II}(OCPh_3)(NCCH_3)$] (**7.6**). Complex **7.6** can be isolated as bright orange plates from Et_2O in 39% yield (Scheme 7.7).

Scheme 7.7 Synthesis of [$L^{tBu}Fe^{II}(OCPh_3)(NCCH_3)$] (**7.6**)

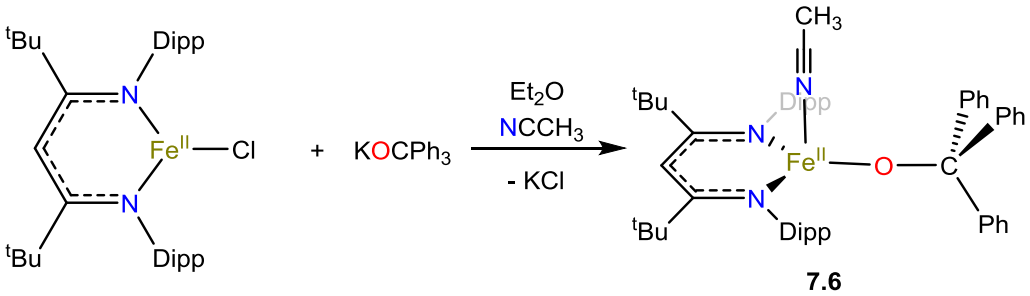

Complex **7.6** was isolated with a coordinated acetonitrile molecule as a crystallization aid due to its high solubility. The solid state molecular structure of **7.6** is shown in Figure 7.6. Complex **7.6** features a trigonal pyramidal Fe^{II} center ligated by tritylalkoxide and acetonitrile moieties with a Fe-O bond length of 1.839(3) Å which is consistent with a single bond.[49–51] The Fe1-N3 bond in **7.6** of 2.134(6) Å and is notably longer than the Fe1-N1 and Fe-N2 bonds as would be expected for the neutral $NCCH_3$ ligand. The ^1H NMR spectrum of **7.6** in C_6D_6 contains paramagnetically shifted resonances similar to those of other Fe^{II} β-diketiminate complexes for example, **7.6** features one *tert*-butyl resonance at 45.49 ppm and two diastereotopic isopropyl-CH_3 resonances at -27.64 and -121.31 ppm. [23,46,52,53]

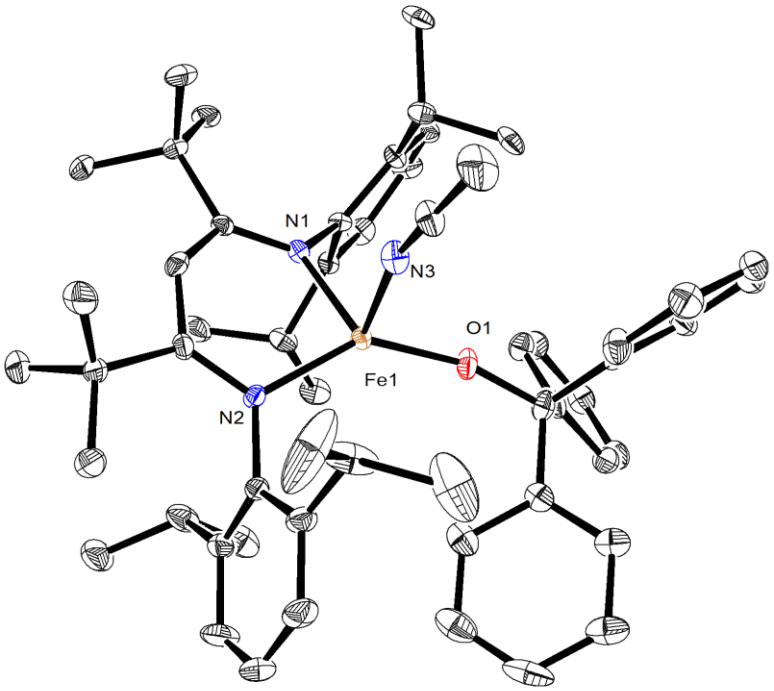

Figure 7.6. ORTEP diagram of [$L^{tBu}Fe^{II}(OCPh_3)(NCCH_3)$] (**7.6**) with 50% probability ellipsoids. Hydrogen atoms omitted for clarity. Selected bond lengths and angles: Fe1-O1 1.839(3) Å, Fe1-N3 2.134(6) Å, Fe1-N1 2.034(4) Å, Fe1-N2 2.033(4) Å, N1-Fe1-N2 96.5(1)°, N1-Fe1-O1 115.2(1)°, N2-Fe1-O1 140.3(1)°, O1-Fe1-N3 100.5(2)°.

With complexes **7.5** and **7.6** in hand, I attempted cleave the O-C bonds in these complexes using the reductive deprotection protocol. Reduction of **7.5** with KC_8, in cold (-25 °C) Et_2O, in the presence of 18-crown-6, results in the formation of $[K(18\text{-crown-}6)(THF)_2][L^{Me}Fe^{I}(OCPh_3)]$ (**7.7**). Complex **7.7** can be isolated as deep green blocks in 19% yield (Scheme 7.8). Reduction of complex **7.6** under the same conditions also appears to form a similar Fe^{I} species, which I hypothesize is $[L^{tBu}Fe^{I}(OCPh_3)]^{-}$; however, I have been unable to isolate this complex due to its high solubility and its tendency to convert back to $[L^{tBu}Fe^{II}(OCPh_3)]$ upon storage in solution. Similar to the attempted reductive deprotection of complex **7.1**, it appears that steric pressure on the -CPh_3 group may also dictate the reaction outcome of the reductive deprotection of **7.5** and **7.6**. Specifically, since the Fe-O bond lengths in **7.5** (1.806(1) Å) and **7.6** (1.839(3) Å) are longer than the Ni-O bond in **7.1** (1.756(1) Å), there is less pressure to drive the C-O bond cleavage.

Scheme 7.8 Synthesis of $[K(18\text{-crown-}6)(THF)_2][L^{Me}Fe^{I}(OCPh_3)]$ (**7.7**)

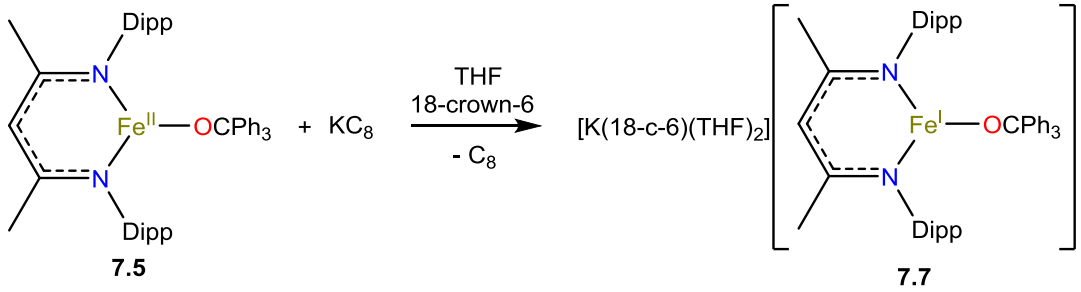

7.5 **7.7**

The reaction of **7.5** with 2 equiv of KC_8, in the presence of 18-crown-6, also affords **7.7**, indicating that, like complex **7.1**, the trityl O-C bond in this complex is too strong to be reduced using KC_8. The formulation of complex **7.7** has been confirmed by X-ray crystallography, its solid state molecular structure is shown in Figure 7.7. The Fe center in **7.7** exhibits a planar (Σ(L-Fe-L) = 360°), T-shaped coordination geometry. The Fe-O bond

length in **7.7** (1.832(3) Å) is longer than that in **7.5** (1.806(1) Å), consistent with the larger atomic radius of Fe^{I} relative to Fe^{II}.[54] The ^{1}H NMR spectrum of complex **7.7** in C_6D_6 features broad paramagnetic resonances typical of those observed for other Fe^{I} β-diketiminate complexes, for example, **7.7** features one backbone methyl resonance at -65.53 ppm and a one diasterotopic isopropyl-CH_3 resonance at -9.73 ppm.[54,55]

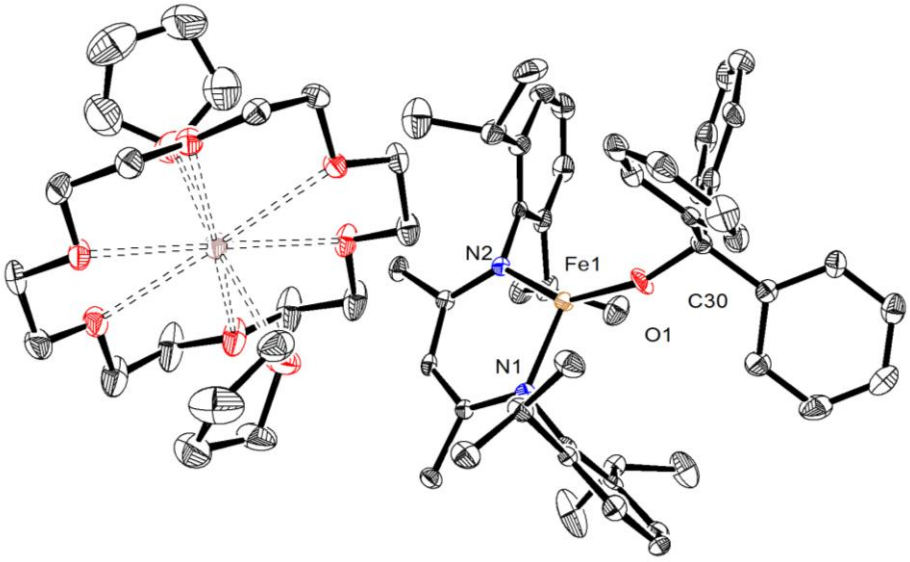

Figure 7.7. ORTEP diagram of [K(18-crown-6)$(THF)_2$][$L^{Me}Fe(OCPh_3)$] (**7.7**) with 50% probability ellipsoids. Hydrogen atoms omitted for clarity. Selected bond lengths and angles: Fe1-O1 1.832(3) Å, O1-C30 1.390(4) Å, Fe1-N1 1.933(3) Å, Fe1-N2 1.915(3) Å, N1-Fe1-N2 98.8(1)°, N1-Fe1-O1 116.7(1)°, N2-Fe1-O1 144.5(1)°, Fe1-O1-C30 157.5(2)°.

7.2.5 Synthesis and Reduction of [$L^{tBu}Ni^{II}$(*O*,*O*:κ^2-PINO)] (7.8)

Due to the challenges associated with the deprotection of the $OCPh_3$ group outlined in the early sections of this chapter, I sought to make use of an alternate oxo protecting group. Recently, Baran and co-workers published a series of reports describing the use of hydroxyphthalimide esters to perform decarboxylative borylation, alkenylation, and cross

coupling reactions.[56–58] Notably, the decarboxylation step in these reactions involves the cleavage of the hydroxyphthalimide ester N-O bond initiated by a one electron reduction (Scheme 7.9). Given this precedent, I pursued the synthesis of a nickel phthalimide *N*-oxide complex in order to determine if reductive deprotection of the phthalimide group could yield an oxo complex.

Scheme 7.9 Reductive decarboxylation of a hydroxyphthalimide ester

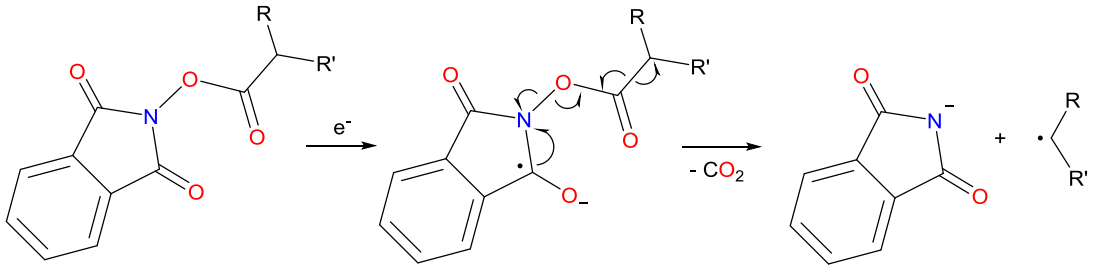

Addition of 1 equiv of potassium phthalimide *N*-oxide (K[PINO], PINO = $C_6H_4(CO)_2NO^-$) to [$L^{tBu}Ni^{II}Cl$][23] in THF results in the formation of[$L^{tBu}Ni^{II}$(*O*,*O*:κ^2-PINO)] (**7.8**). Complex **7.8** can be isolated as red plates from toluene layered with pentane in 91% yield (Scheme 7.10).

Scheme 7.10 Synthesis of [$L^{tBu}Ni^{II}$(*O*,*O*:κ^2-PINO)] (**7.8**)

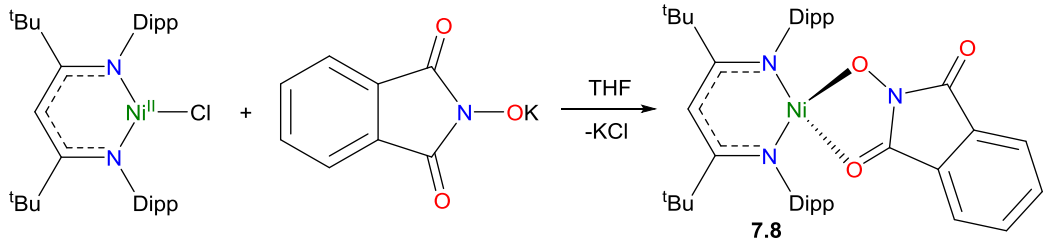

The solid state molecular structure of **7.8** is shown in Figure 7.8. Complex **7.8** features a four coordinate Ni^{II} center ligated in a κ^2 fashion by the PINO moiety with Ni-O bond lengths of 1.921(6) Å and 2.056(6) Å for the *N*-oxide and carbonyl Ni-O bonds, respectively. There is only a slight elongation of the C2-O3 (1.24(1) Å) bond relative to the C1-O2

(1.21(1) Å) bond, indicating minimal activation the coordinated carbonyl C=O bond. While the N1-O1 bond length of 1.353(7) Å is consistent with a single bond. The coordination geometry of the Ni center is best described as pseudo-tetrahedral. The ^{1}H NMR spectrum of **7.8** in C_6D_6 contains paramagnetically shifted resonances similar to those of other Ni^{II} β-diketiminate complexes, for example, **7.8** features one *tert*-butyl resonance at 1.88 ppm and two diastereotopic isopropyl-CH_3 resonances at 8.10 and 6.94 ppm.[20,23,32]

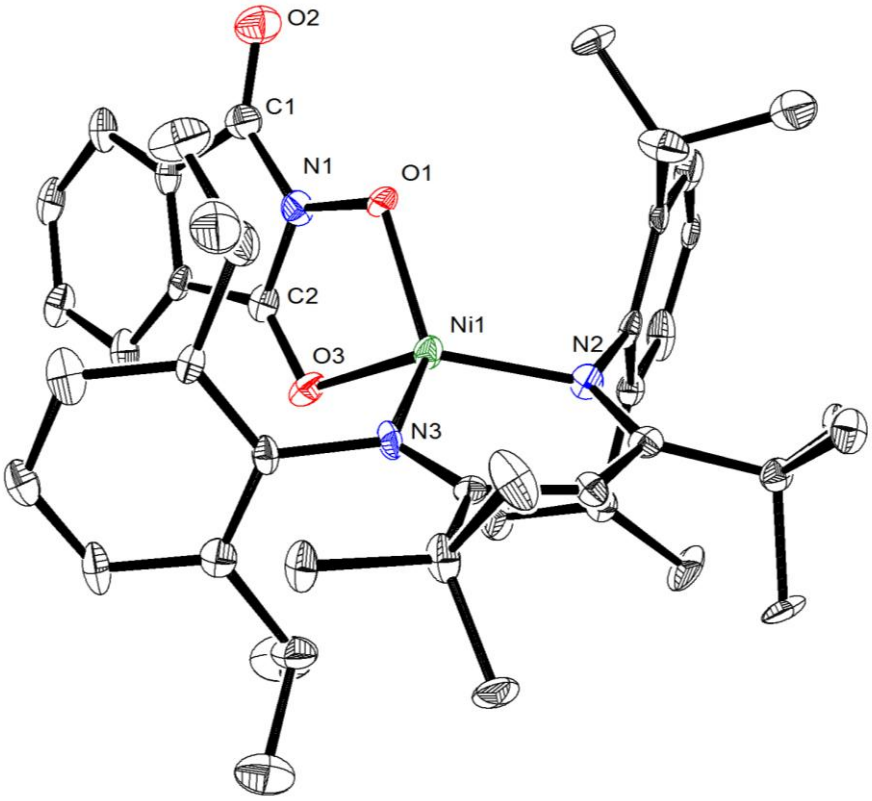

Figure 7.8. ORTEP diagram of [$L^{tBu}Ni^{II}$(*O*,*O*:κ^2-PINO)] (7.8) with 50% probability ellipsoids. Hydrogen atoms omitted for clarity. Selected bond lengths and angles: Ni1-O1 1.921(6) Å, Ni1-O3 2.056(5) Å, N1-O1 1.353(7) Å, C2-O3 1.24(1) Å, C1-O2 1.21(1) Å, Ni1-N2 1.909(6) Å, Ni1-N3 1.918(6) Å, N1-Ni1-N2 96.7(3)°, N2-Ni1-O1 117.0(3)°, N3-Ni1-O1 125.5(3)°, N2-Ni1-O3 132.9(2)°, N3-Ni1-O3 105.3(2)°, N1-Ni1-O3 82.7(2)°.

With complex **7.8** in hand, I endeavored to apply the reductive deprotection protocol to this system. Accordingly, exposure of a THF/Et_2O solution of **7.8** to 2 equiv of KC_8 in the presence of 18-crown-6 resulted in a color change of the solution from red to red-brown along with the deposition of a red-orange solid that I have tentatively identified as [K(18-crown-6)][PIN] (PIN = $C_6H_4(CO)_2N^-$). I have been able to confirm that the identity of the Ni containing product of this reaction as [K(18-crown-6)][$L^{tBu}Ni^{I}$(OH)] (**7.4**), which I had previously characterized, via the isolation of single crystals from the reaction (Scheme 7.11). I was unable to record yields for both of these products.

Scheme 7.11 Reduction of [$L^{tBu}Ni^{II}$(*O*,*O*:κ^2-PINO)] (**7.8**) in the presence of 18-crown-6

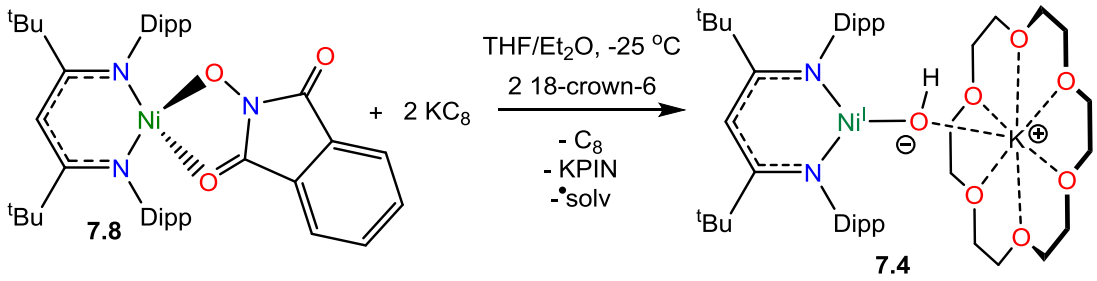

When the reaction of **7.8** with KC_8 was performed in the presence of 2,2,2-cryptand, I observe a color change of the reaction mixture from red to red-brown. However, I do not observe the formation of a significant amount of solids (aside from C_8) in this reaction (Scheme 7.11). Interestingly, I have also observed the formation of a transient, diamagnetic Ni containing species in the ^{1}H NMR spectrum of the crude reaction mixture (Figure 7.9). I have tentatively identified this species as a Ni^{II} oxo, based on the observation that other three coordinate Ni^{II} complexes with metal-ligand multiple bonds to carbon and nitrogen are diamagnetic.[3,14,59,60] For example, the transient diamagnetic product (Ni^{II} oxo) formed in this reaction features one *tert*-butyl resonance at 1.84 ppm and two diastereotopic isopropyl-CH_3 resonances at 1.59 and 1.65 ppm, while the paramagnetic product, "[K(2,2,2-

cryptand)][$L^{tBu}Ni^{I}$(OH)]", of this reaction features a broad *tert*-butyl resonance at -1.43 ppm. Based upon integration of the *tert*-butyl resonances of these two products, it appears that they are present in a roughly 1:1 ratio. Notably, the potassium salt of the ligand, $L^{tBu}K$, is not present in this reaction based on comparison of its reported ^{1}H NMR spectrum with that in Figure 7.9. I was able to isolate and structurally characterize one of the products of this reaction as [K(2,2,2-cryptand)][PIN] (**7.9**) and its solid state molecular structure is shown in Figure 7.10. While, I have been unable to isolate the Ni containing product of this reaction, based on the formation of **7.4** in the reduction of **7.8** in the presence of 18-crown-6 (Scheme 7.10), I propose that [K(2,2,2-cryptand)][$L^{tBu}Ni^{I}$(OH)] is likely the final product of this reaction (Scheme 7.12).

Scheme 7.12 Reduction of [$L^{tBu}Ni^{II}$(*O*,*O*:κ^2-PINO)] (**7.8**) in the presence of 2,2,2-crypand

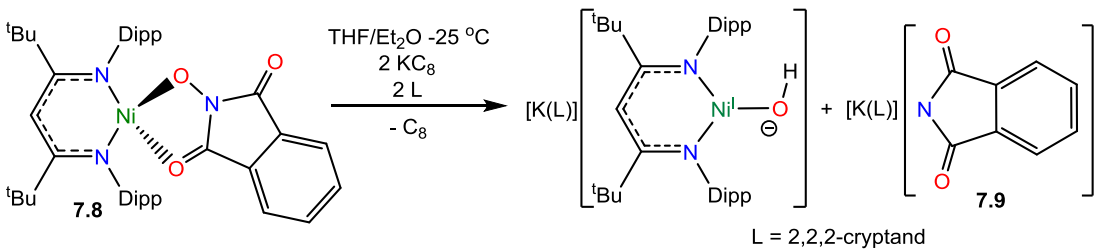

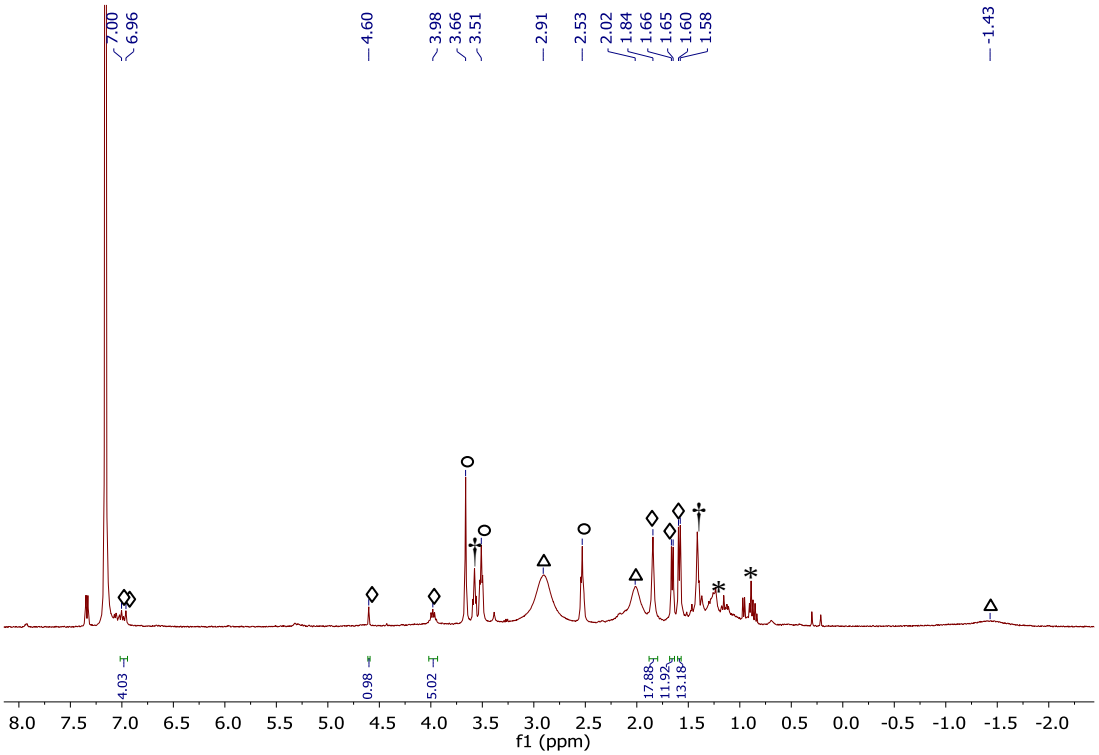

Figure 7.9. ^{1}H NMR spectrum of the crude products of the reaction of [$L^{tBu}Ni^{II}$(PINO)] (**7.8**) with KC_8 in the presence of 2,2,2-cryptand in C_6D_6. (◊) has been tentatively assigned to a Ni^{II} oxo species, (Δ) has been tentatively assigned to a Ni^{I} hydroxide species, (°) indicates the presence of 2,2,2-cryptand, (*) indicates the presence of hexane, and (†) indicates the presence of THF.

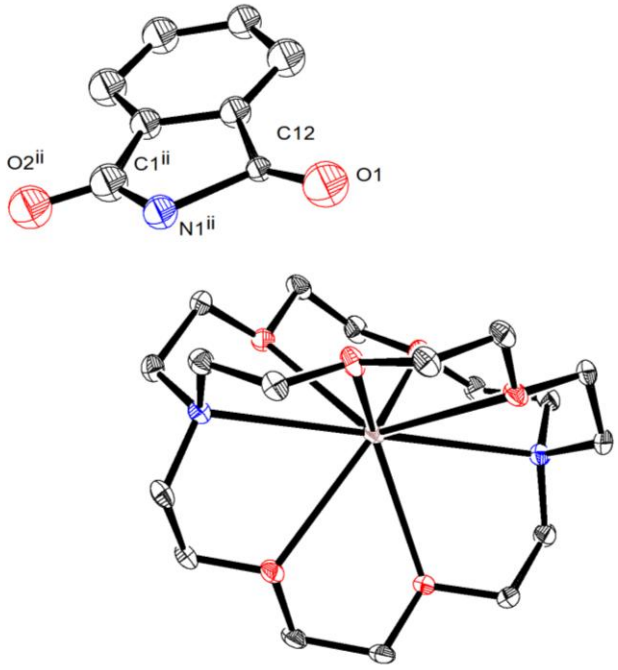

Figure 7.10. ORTEP diagram of [K(2,2,2-cryptand)][PIN] (**7.9**) with 50% probability ellipsoids. Hydrogen atoms and an alternate orientation of $[PIN]^-$ omitted for clarity.

To date, I have been unable to isolate the nickel-containing products of the reaction involving 2,2,2-cryptand. However, based upon the formation of **7.9** and the ^{1}H NMR spectra of the reaction products, it appears to be likely that the ultimate Ni containing product of this reaction is identical to **7.4**. In contrast to the reduction of $[L^{tBu}Ni^{II}(OCPh_3)]$ (**7.2**) to form **7.4**, in which no intermediates assignable to a Ni^{II} oxo species have been observed, optimization of reaction and work-up conditions for the reductive deprotection of **7.8** could lead to the isolation of a Ni^{II} oxo.

7.2.6 Synthesis and Characterization of $[L^{tBu}M^{II}(SCPh_3)]$ (7.10, M = Fe; 7.11, M = Co, 7.12, M = Zn)

Addition of 1 equiv of $KSCPh_3$ to $[L^{tBu}Fe^{II}Cl]$[46], $[L^{tBu}Co^{II}Cl_2Li(THF)_2]$[23], or $[L^{tBu}Fe^{II}Cl]$[61] in benzene results in the formation of $[L^{tBu}M^{II}(SCPh_3)]$ (M = Fe, **7.10**; M = Co, **7.11,** M = Zn, **7.12**). Complex **7.10** can be isolated as orange needles from hexanes in 68%

yield, while complex **7.11** can be isolated as orange needles from hexanes in 53% yield, and complex **7.12** can be isolated as colorless needles in 66% yield (Scheme 7.13).

Scheme 7.13 Synthesis of [$L^{tBu}M^{II}(SCPh_3)$] (M = Fe, **7.10**; M = Co, **7.11**, M = Zn, **7.12**)

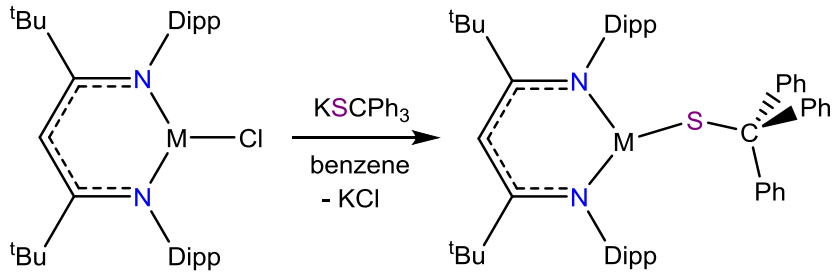

7.10, M = Fe
7.11, M = Co
7.12, M = Zn

The formulation of Complexes **7.10 - 7.12** were confirmed by X-ray crystallography. The solid state molecular structures of **7.10 - 7.12** are shown in Figure 7.11. Complexes **7.10 - 7.12** feature three coordinate M^{II} centers ligated by a tritylthiolate moiety. The M-S and C-S bond lengths in **7.10** (Fe-S = 2.2597(8) and C-S = 1.874(3) Å), **7.11** (Co-S = 2.212(1) and C-S = 1.878(4) Å), **7.12** (Zn-S = 2.220(1) and C-S = 1.876(4) Å) are consistent with single bonds.[62–64] The coordination geometry of these three complexes is nearly identical, and only deviate slightly from planarity (Σ(L-Ni-L) = 352.9°, **7.10**; 350.8°, **7.11**; 354.5°, **7.12**) and the coordination geometry of the metal centers is best described as distorted Y-shaped. The ^{1}H NMR spectra of **7.10** and **7.11** are typical for paramagnetic three coordinate [$L^{tBu}M^{II}(X)$] complexes. For example, **7.10** features one *tert*-butyl resonance at 36.34 ppm and two diastereotopic isopropyl-CH_3 resonances at 7.62 and -14.25 ppm and **7.10** features one *tert*-butyl resonance at 31.50 ppm and two diastereotopic isopropyl-CH_3 resonances at -8.15 and -59.25 ppm.[33] While the ^{1}H NMR spectrum of **7.12** is diamagnetic, as expected for a d^{10} complex and features one *tert*-butyl resonance at 1.16 ppm and two diastereotopic isopropyl-CH_3 resonances at 1.25 and 1.46 ppm.[64–66]

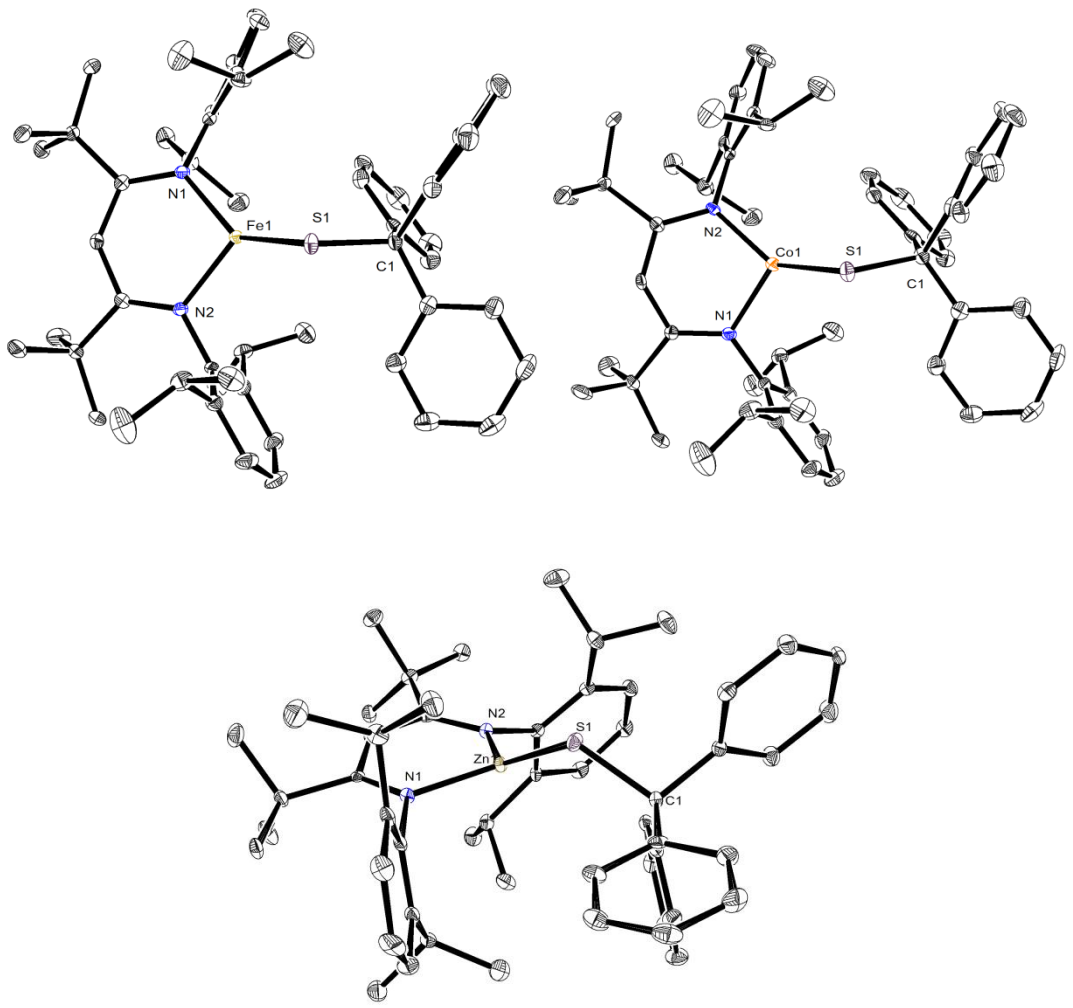

Figure 7.11. ORTEP diagrams of $[L^{tBu}Fe^{II}(SCPh_3)]\cdot C_6H_{14}$ (7.10·C_6H_{14}, top left), $[L^{tBu}Co^{II}(SCPh_3)]\cdot C_6H_{14}$ (**7.11**·C_6H_{14}, top right), and $[L^{tBu}Zn^{II}(SCPh_3)]\cdot C_4H_{10}O$ (**7.12**·$C_4H_{10}O$, bottom) with 50% probability ellipsoids. Hydrogen atoms and solvate molecules omitted for clarity. Selected bond lengths and angles: (**7.10**) Fe1-S1 2.2597(8) Å, C1-S1 1.874(3) Å, Fe1-N1 1.993(2) Å, Fe1-N2 2.003(2) Å, N1-Fe1-N2 98.01(9)°, N1-Fe1-S1 136.29(7)°, N2-Fe1-S1 118.64(7)°, Fe1-S1-C1 116.50(9)°; (**7.11**) Co1-S1 2.212(1) Å, C1-S1 1.878(4) Å, Co1-N1 1.963(3) Å, Co1-N2 1.944(3) Å, N1-Co1-N2 99.3(1)°, N1-Co1-S1 115.67(9)°, N2-Co1-S1 135.8(1)°, Co1-S1-C1 115.1(1)°; (**7.12**) Zn1-S1 2.220(1) Å, C1-

S1 1.876(4) Å, Zn1-N1 1.969(3) Å, Zn1-N2 1.953(3) Å, N1-Zn1-N2 101.2(1)°, N1-Zn1-S1 117.4(1)°, N2-Zn1-S1 135.9(1)°, Zn1-S1-C1 117.70(15)°.

7.2.7 Synthesis of [K(18-crown-6)][L^{tBu}Fe(X)(SCPh$_3$)] (X = S^{2-}, 7.13a; X = SH$^-$, 7.13b)

With [L^{tBu}Fe^{II}(SCPh$_3$)] (**7.10**) in hand, I attempted to cleave the C-S bond in **7.10** using the reductive deprotection protocol. Accordingly, addition of two equiv of KC_8 to a cold Et_2O solution of **7.10** in the presence of 18-crown-6 resulted in the apparent cleavage of the C-S, as indicated by my observation of the formation of trityl anion in the reaction. However, a solid state molecular structure of crystalline material isolated from this reaction reveals what appears to be either a Fe^{III} "masked" sulfide tritylthiolate complex, [K(18-crown-6)][L^{tBu}Fe^{III}(S)(SCPh$_3$)] (**7.13a**) or a Fe^{II} hydrosulfide (SH$^-$) tritylthiolate complex, [K(18-crown-6)][L^{tBu}Fe^{II}(SH)(SCPh$_3$)] (**7.13b**) (Scheme 7.14). A yield for this reaction was not determined as the crystallization method resulted in the deposition of a mixture of products. I was also unable to determine the other Fe containing product of this reaction.

Scheme 7.14 Reduction of (**7.10**) to yield [K(18-crown-6)][L^{tBu}Fe(X)(SCPh$_3$)] (**7.13**)

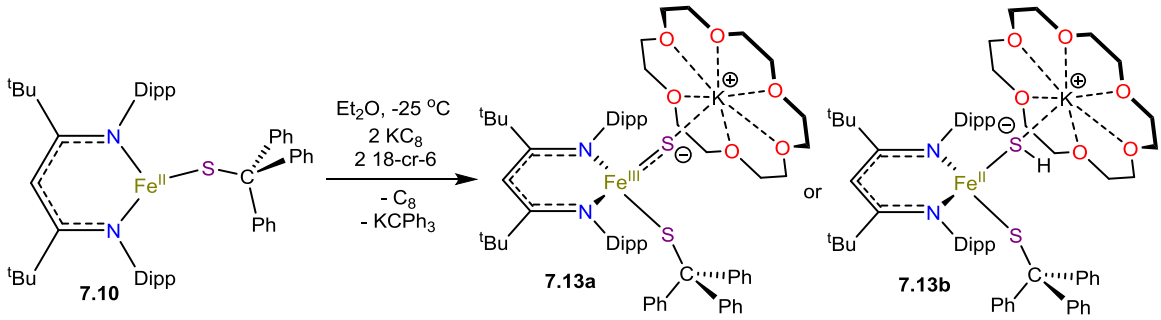

Unfortunately, the structural data for **7.13** contains too much disorder to afford any meaningful structural analysis beyond the tentative evaluation of the Fe ligand environment. Promisingly, the ^{1}H NMR spectrum of crystals of this product in C_6D_6 appears to contain one major paramagnetic species (Figure 7.12). Containing one *tert*-butyl resonance at 12.50

ppm and two diastereotopic isopropyl-CH_3 resonances at -2.35 and -19.28 ppm. Due to my uncertainty about the formulation of **7.13**, I am unable to draw any firm conclusions about its mechanism of formation aside from the probable intermediacy of an iron sulfide complex, based on my observation of the formation of trityl anion as a byproduct of the reduction.

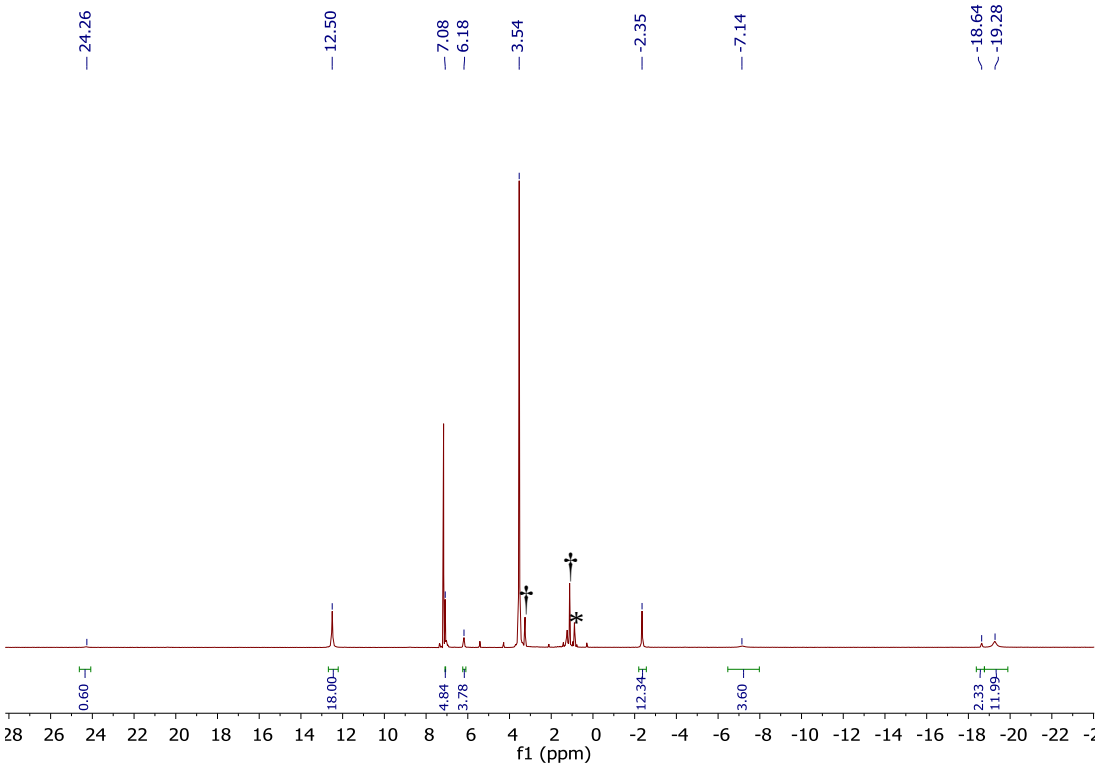

Figure 7.12. ^{1}H NMR spectrum of complex **7.13** in C_6D_6. (*) indicates the presence of hexane and (†) indicates the presence of Et_2O.

7.2.8 Synthesis of [K(18-crown-6)][L^{tBu}Co^{I}(SH)] (7.14)

Subsequent reduction of [L^{tBu}Co^{II}(SCPh$_3$)] (**7.11**) with 2 equiv of KC_8, in cold (-25 °C) Et_2O, in the presence of 18-crown-6, results in the formation of [K(18-crown-6)][L^{tBu}Co^{I}(SH)] (**7.14**) (Scheme 7.15). I should also note that trityl anion was observed as a byproduct in this reaction, indicating the intermediacy of a Co "masked" terminal sulfide in this reaction.[20–22]

Scheme 7.15 Reduction of (**7.11**) to yield [K(18-crown-6)][L^{tBu}Co^{I}(SH)] (**7.14**)

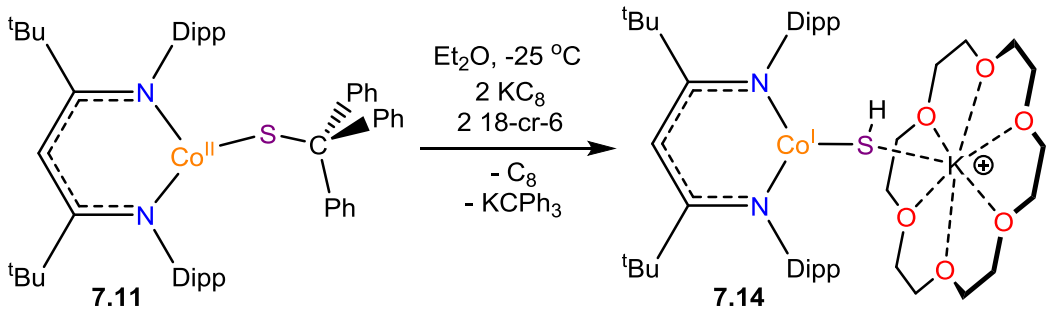

Further optimization of this reaction is required for the clean isolation of **7.14**, as significant decomposition occurred during the work up. Nevertheless a single crystal suitable for X-ray crystallography was obtained from the products of this reaction. The solid state molecular structure of **7.14** is shown in Figure 7.13. Complex **7.14** features a three coordinate Co^{I} center ligated by a hydrosulfide (SH^{-}) moiety with a Co-S bond length of 2.207(3) Å which is identical to the Co-S bond in the starting material, **7.11** (2.212(1) Å), and is consistent with a single bond.[63] My observation that the Co-S interaction does not appear to have any multiple bonding character combined with the Co-S-K bond angle of 136.4(1)°, which is more acute than the Ni-S-K angle for the closely related complex, [K(18-crown-6)][L^{tBu}Ni^{I}(SH)] (**2.11**, 142.3(1)°), supports my formulation of **7.14** as a Co^{I} hydrosulfide complex. The coordination geometry of the Co center in **7.14** is planar (Σ(L-Co-L) = 359.9°) and is best described as Y-shaped. Unfortunately, I was unable to record a ^{1}H NMR spectrum of this material. That said, **7.14** does represents only the second structurally characterized Co hydrosulfide complex.[67] It is possible that further optimization of the reaction and work-up conditions for this reaction could yield the desired Co "masked" terminal sulfide [L^{tBu}Co^{II}(S)]$^{-}$.

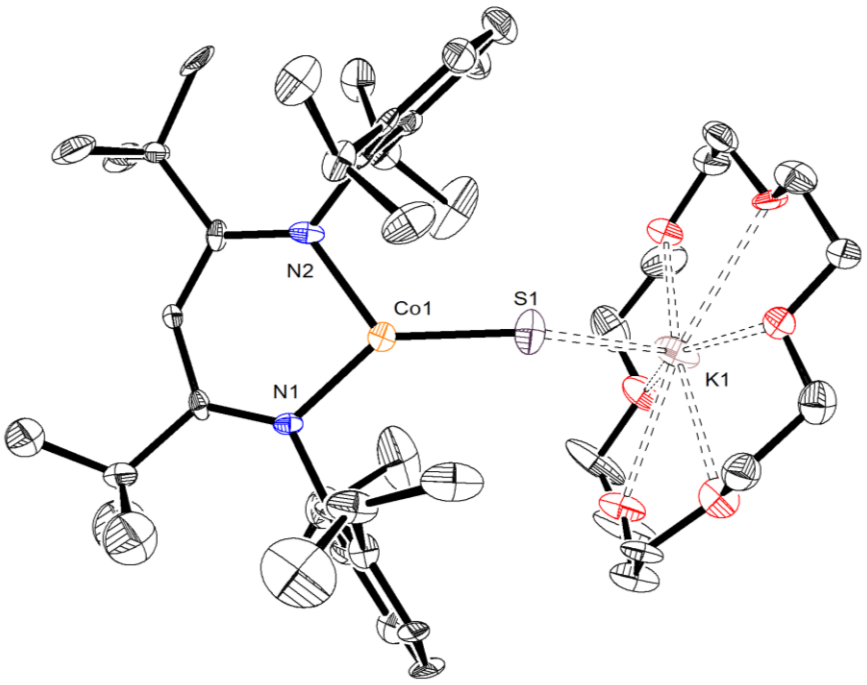

Figure 7.13 ORTEP diagram of [K(18-crown-6)][$L^{tBu}Co^{I}(SH)$]·$C_4H_{10}O$ (**7.14**·$C_4H_{10}O$) with 50% probability ellipsoids. Hydrogen atoms and Et_2O solvate molecule omitted for clarity. Selected bond lengths and angles: Co1-S1 2.207(3) Å, Co1-N1 1.916(6) Å, Co1-N2 1.929(6) Å, N1-Co1-N2 97.4(3)°, N1-Co1-S1 138.8(2)°, N2-Co1-S1 123.7(2)°.

7.2.9 Synthesis of [K(18-crown-6)][$L^{tBu}Ni^{I}$(*N*,*O*:κ^2-NHTs)] (7.15)

In the final portions of this chapter, I will focus on two attempts to extend the reductive deprotection protocol to the synthesis of Ni imido (NR^{2-}) complexes. The tosyl ($S(O)_2C_6H_4$-*p*-CH_3) group has been shown to be versatile protecting group for amines in organic synthesis.[68] Moreover, in 2008, Ankner and Hilmersson reported a reductive protocol for the facile deprotection of tosylamides via S-N bond cleavage (scheme 7.16).[69] Given this precedent, I pursued the synthesis of a nickel tosylamide complex in order to determine if reductive deprotection of the tosyl group could yield an imido complex.

Scheme 7.16 Reductive cleavage of the tosylamide S-N bond

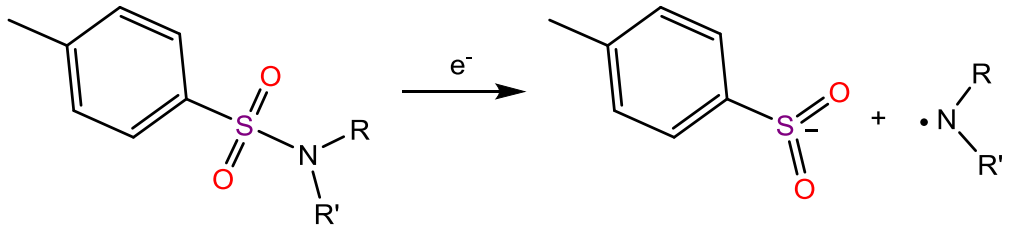

Accordingly, I synthesized the Ni^{II} tosylamide ($NHTs^{-}$ = $[NHS(O)_2C_6H_4$-*p*-$CH_3]^{-}$) complex via the reaction of 1 equiv of K[NHTs] with $[L^{tBu}Ni^{II}Cl]$[23] in Et_2O/THF resulting in the formation of $[L^{tBu}Ni^{II}(N,O{:}\kappa^2$-NHTs)] (**7.15**). Complex **7.15** can be isolated as purple plates in 32% yield (Scheme 7.17).

Scheme 7.17 Synthesis of $[L^{tBu}Ni^{II}(N,O{:}\kappa^2$-NHTs)] (**7.15**)

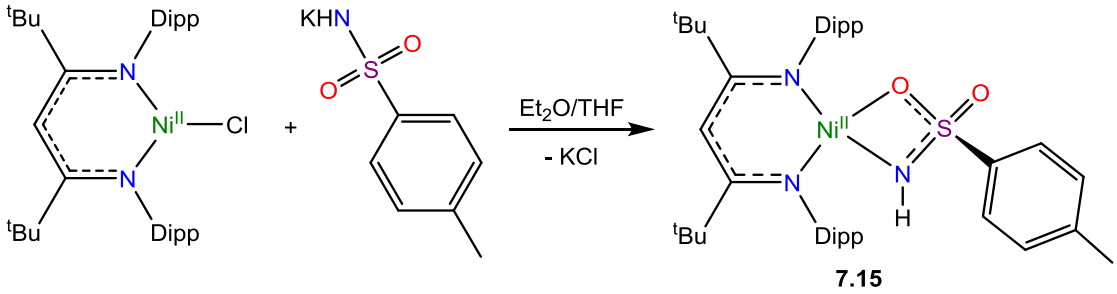

Complex **7.15** was characterized by X-ray crystallography and ^{1}H NMR spectroscopy. The solid state molecular structure of **7.15** is shown in Figure 7.14. Complex **7.15** features a square planar (Σ(L-Ni-L) = 360.5°) Ni^{II} center ligated in a bidentate κ^2-*N*,*O* fashion by the NHTs moiety with Ni-N and Ni-O bond lengths of 1.967(2) and 1.989(1) Å, respectively, which are consistent with a single bonds.[31] The ^{1}H NMR spectrum of **7.15** in C_6D_6 is consistent with a diamagnetic, square planar Ni^{II} *β*-diketiminate complex. For example, **7.15** features one *tert*-butyl resonance at 1.05 ppm and two diastereotopic isopropyl-CH_3 resonances at 2.64 and 1.62 ppm.[23,31]

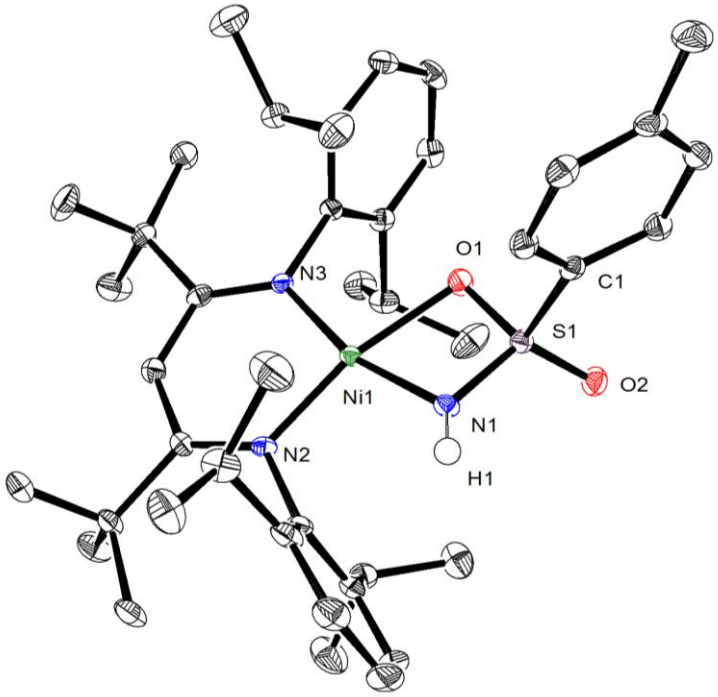

Figure 7.14. ORTEP diagram of [$L^{tBu}Ni^{II}$(*N*,*O*:κ^2-NHTs)] (**7.15**) with 50% probability ellipsoids. Hydrogen atoms omitted for clarity. Selected bond lengths and angles: Ni1-N1 1.967(2) Å, Ni1-O1 1.989(1) Å, Ni1-N2 1.875(2) Å, Ni1-N3 1.878(2) Å, N1-S1 1.550(2) Å, O1-S1 1.501(2) Å, N2-Ni1-N3 96.71(7)°, N1-Ni1-N2 98.06(7)°, N3-Ni1-O1 94.92(6)°, N1-Ni1-O1 70.79(6)°.

With complex **7.15** in hand, I attempted to apply the reductive deprotection protocol in order to cleave the N-S bond. Accordingly, addition of two equiv of KC_8 to a solution of **7.15** in cold (-25 °C) THF, in the presence of 18-crown-6, results in a rapid color change of the solution from purple to dark red. Workup of the reaction products resulted in the isolation of [K(18-crown-6)][$L^{tBu}Ni^{I}$(NHTs)] (**7.16**) as dark red plates in 38% yield (Scheme 7.18).

Scheme 7.18 Synthesis of [K(18-crown-6)][L^{tBu}Ni^{I}(NHTs)] (**7.16**)

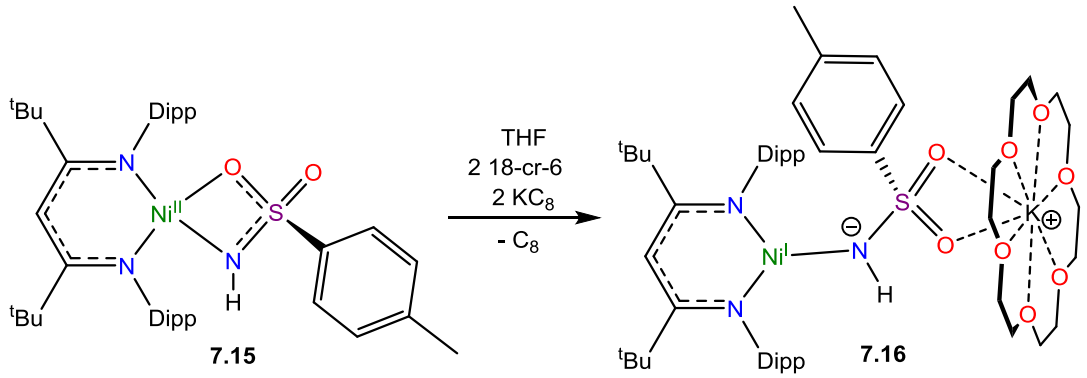

The formulation of complex **7.16** was confirmed by X-ray crystallography. The solid state molecular structure of **7.16** is shown in Figure 7.15. Complex **7.16** features a three coordinate Ni^{I} center ligated by the NHTs moiety with Ni-N bond length 1.947(2) Å which is only slightly shorter than that in the starting material, complex **7.15**. While the *β*-diketiminate Ni-N bonds are elongated from 1.875(2) and 1.878(2) Å to 1.884(2) and 1.929(2) Å consistent with increased iconic radius of Ni(I) relative to Ni(II). The ^{1}H NMR spectrum of **7.16** in C_6D_6 is consistent with a Ni^{I} *β*-diketiminate complex, for example, **7.16** features one broad *tert*-butyl resonance at -1.06 ppm.[31,33,35,36] The change in coordination geometry relative to **7.15** is attributable to the coordination of the sulfonyl O-atoms to the [K(18-crown-6)]$^{+}$ countercation and the increased electron density at the Ni center. This result demonstrates that the NHTs^{-} ligand is not suitable for reductive deprotection as the Ni center is reduced instead of the N-S bond, indicating that the N-S bond in this ligand is too strong.

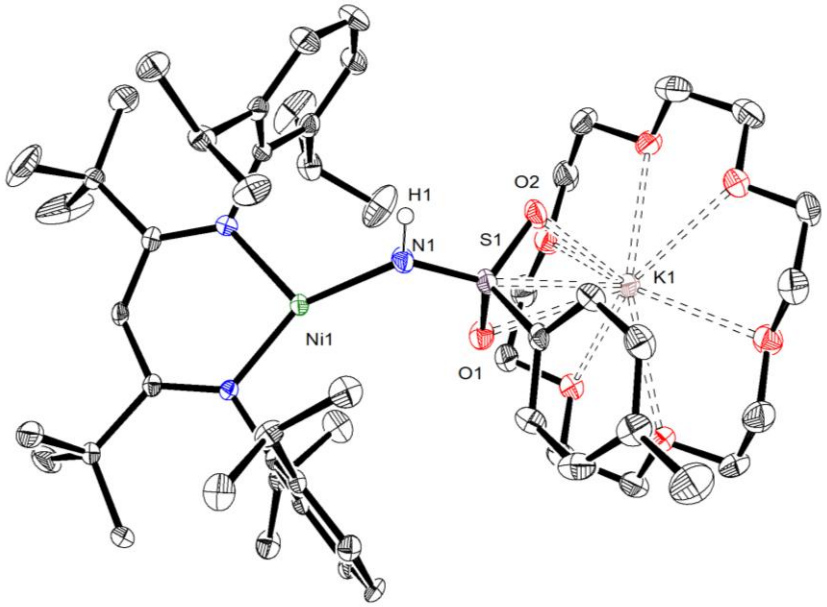

Figure 7.15. ORTEP diagram of [K(18-crown-6)][$L^{tBu}Ni^{I}$(NHTs)] (**7.16**) with 50% probability ellipsoids. Hydrogen atoms omitted for clarity. Selected bond lengths and angles: Ni1-N1 1.947(2) Å, Ni1-N2 1.884(2) Å, Ni1-N3 1.929(2) Å, N1-S1 1.560(2) Å, N2-Ni1-N3 98.32(9)°, N1-Ni1-N2 149.5(1)°, N3-Ni1-N1 111.3(1)°.

7.2.10 Synthesis and Reduction of [{L^{tBu}(PhNCO)}Ni^{II}(*N*,*O*:κ^2-PhNC(O)OCPh$_3$)] (7.17)

Addition of two equiv of phenyl isocyanate (PhNCO) to a C_6D_6 solution of [L^{tBu}Ni^{II}(OCPh$_3$)] (**7.2**) results in the formation of [{L^{tBu}(PhNCO)}Ni^{II}(*N*,*O*:κ^2-PhNC(O)OCPh$_3$)] (**7.17**). Complex **7.17** can be isolated as brown plates in 57% yield (Scheme 7.19).

Scheme 7.19 Synthesis of [{L^{tBu}(PhNCO)}Ni^{II}(*N*,*O*:κ^2-PhNC(O)OCPh$_3$)] (**7.17**)

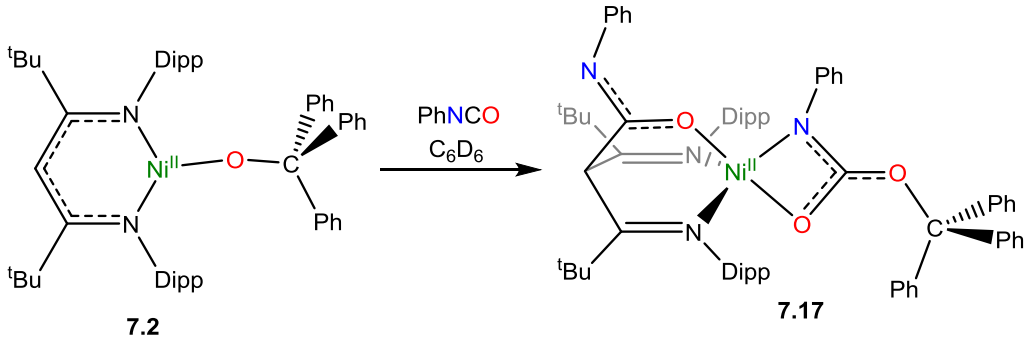

7.2 **7.17**

The formulation of complex **7.17** was confirmed by X-ray crystallography and its solid state molecular structure is shown in Figure 7.16. Complex **7.17** features a κ^2-carbamate, [κ^2-*N*,*O*-PhNC(O)OCPh$_3$]$^-$, ligand which is the result of insertion of PhNCO into the Ni-O bond. Insertion of isocyanate into metal alkoxide bonds has been previously reported. For example, Tam and co-workers demonstrated that a lead alkoxide complex, [L^{Me}Pb(O^{i}Pr)], reacts with PhNCO to yield [L^{tBu}Pb{(Ph)NC(O)O^{i}Pr}].[70] An additional equivalent of PhNCO has also been incorporated into the product via a nucleophilic attack on the electrophilic PhNCO carbon atom by the β-diketiminate γ-carbon. While, insertion of PhNCO into the Ni-O bond was the intended outcome for this reaction, the incorporation of the second equivalent was unexpected. Nucleophilic bond forming reactions involving the β-diketiminate γ-carbon have been reported previously for CS_2, O_2, NO, $OCCPh_2$, nitriles,

and diazoacetate.[29,71–75] However, to my knowledge, this is the first example involving PhNCO.

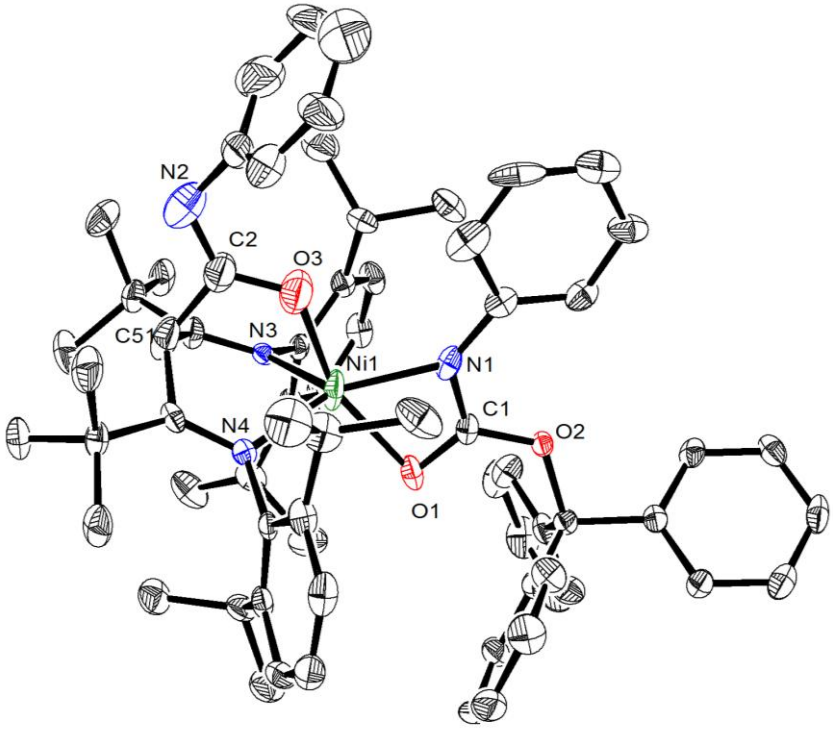

Figure 7.16. ORTEP diagram of [{L^{tBu}(PhNCO)}Ni^{II}(*N*,*O*:κ^2-PhNC(O)OCPh$_3$)] (**7.17**) with 50% probability ellipsoids. Hydrogen atoms omitted for clarity. Selected bond lengths and angles: Ni1-N1 1.995(4) Å, Ni1-O1 2.149(4) Å, Ni1-N3 2.023(4) Å, Ni1-N4 2.015(4) Å, Ni1-O3 1.989(1) Å, N1-C1 1.336(7) Å, C1-O1 1.252(6) Å, C1-O2 1.348(6) Å, O3-C2 1.295(7) Å, C2-C51 1.65(1) Å, N1-C1-O1 117.0(5)°, N1-C1-O2 120.0(5)°.

Reductive deprotection of this complex is intended to result in the cleavage of the O-CPh$_3$ bond yielding $[CPh_3]^-$ and $[PhNCO_2]^{2-}$. It is hypothesized that the $[PhNCO_2]^{2-}$ moiety could then undergo spontaneous release of CO_2 to yield the desired imido ($[NPh]^{2-}$) ligand (Scheme 7.20). Subsequent addition of two equiv of KC_8 to a solution of **7.17** in cold (-25 °C) Et_2O/THF, in the presence of 18-crown-6, results in a rapid color change of the solution from brown to dark red. While I have been unable to characterize the product of this

reaction, I do not observe the formation of the trityl anion in this reaction, leading me to conclude that the reduction of **7.17** did not result in the desired bond cleavage. Curiously, the product of this reaction is diamagnetic, indicating the presence of either Ni^{II} or Ni^{0} (Figure 7.17).

Scheme 7.20 Proposed reduction of **7.17**

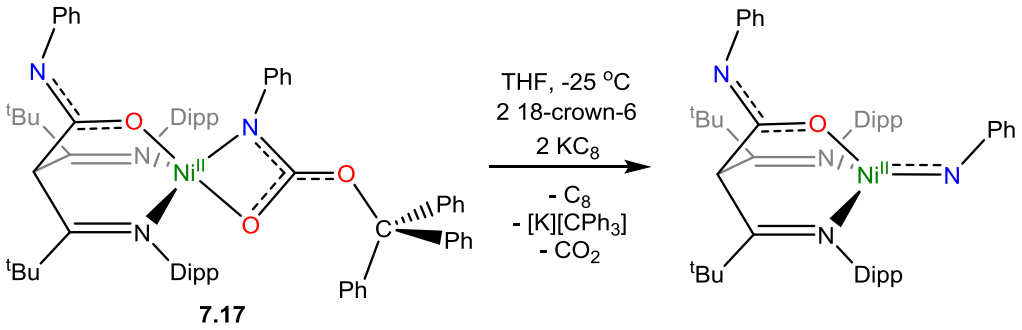

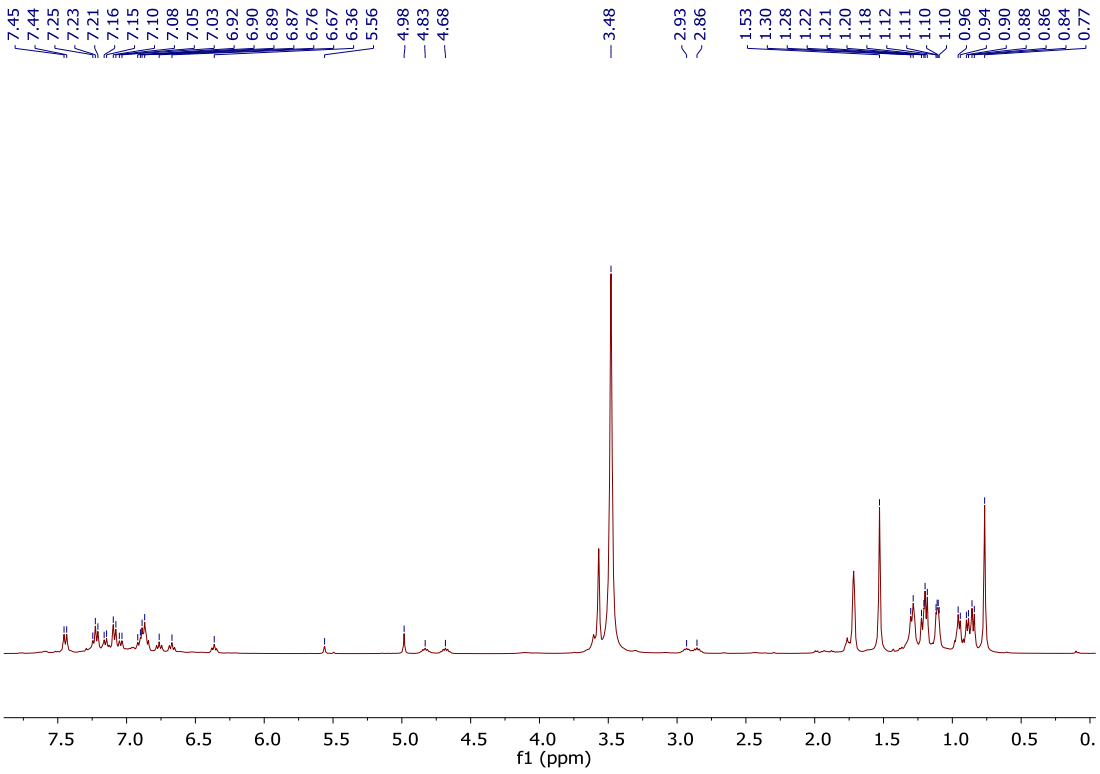

Figure 7.17. ^{1}H NMR spectrum of the product of the reduction of [{L^{tBu}(PhNCO)}Ni^{II}(*N*,*O*:κ^{2}-PhNC(O)OCPh$_3$)] (**7.17**) with KC8 in the presence of 18-crown-6 in THF-d_8.

7.3 Summary

The results outlined in Chapter 7 demonstrate the challenges related to the application of the reductive deprotection protocol for the synthesis of late transition metal complexes with terminal chalcogenide and imido. First, it appears that the O-C bond in the tritylalkoxide ($OCPh_3^-$) ligand is too strong to be preferentially reduced in complexes **7.1**, **7.2**, **7.5**, and **7.6** based on the formation of metal centered reduction products in these reactions, and precluding the formation of the desired "M^{II}=O" products. While, in the case of [L^{tBu}Ni^{II}(OCPh$_3$)] (**7.2**), reduction leads to the isolation of [K(18-crown-6)][L^{tBu}Ni^{I}(OH)] (**7.4**), it is not clear if this reaction proceeds through a Ni oxo intermediate. In contrast, reductive deprotection of the Ni pthalimide *N*-oxide complex, [L^{tBu}Ni^{II}(*O*,*O*:κ^{2}-PINO)]

(**7.8**), appears to be more promising, due my the observation of [K(L)][PIN] and [K(L)][$L^{tBu}Ni^{I}(OH)$] (L = 18-crown-6, 2,2,2-cryptand) as the products of this reaction. Promisingly, I also observed a transient intermediate by ^{1}H NMR spectroscopy that I have tentatively identified as a Ni oxo species. The reductive deprotection of Fe and Co tritylthiolates, also presented some unexpected challenges. While there is preliminary evidence that reductive cleavage of the tritylthiolate C-S bonds in [$L^{tBu}M^{II}(SCPh_3)$] (**7.10**, **7.11**) was successful. The final products isolated from these reactions were not the anticipated "masked" terminal sulfides. Further work is needed in order to determine what is occurring in these reactions. Finally, attempts to access Ni imidos via the reductive deprotection of tosylamide, [$L^{tBu}Ni^{II}(N,O{:}\kappa^2\text{-NHTs})$] (**7.15**), and carbamate, [{L^{tBu}(PhNCO)}$Ni^{II}(N,O{:}\kappa^2\text{-PhNC(O)OCPh}_3)$] (**7.17**), complexes resulted in reduction of the Ni center and formation of an unidentified diamagnetic product, respectively. While some of these approaches appear to show promise, this work demonstrates that the success of these reactions is dictated by a number of different factors, of which, relative bond strengths, metal/bond redox potentials, and the steric/electronic properties of the supporting β-diketiminate ligand appear to be the most important.

7.4 Experimental Procedures

7.4.1 General Methods

All reactions and subsequent manipulations were performed under anaerobic and anhydrous conditions under an atmosphere of nitrogen. Hexanes, diethyl ether (Et_2O), toluene, and tetrahydrofuran (THF) were dried using a Vacuum Atmospheres DRI-SOLV Solvent Purification system and stored over 3Å sieves for 24 h prior to use. Benzene-d_6, tetrahydrofuran-d_8, toluene-d_8, and C_8H_{18} (isooctane) were dried over 3Å molecular sieves

for 24 h prior to use. [$L^{Me}Ni^{II}Cl$],[32] [$L^{tBu}Ni^{II}Cl$],[23] [$L^{Me}Fe^{II}(N(TMS)_2)$],[48] [$L^{tBu}Fe^{II}Cl$],[46] [$L^{tBu}Co^{II}Cl_2Li(THF)_2$],[23] $KSCPh_3$,[76] and $KOCPh_3$[77] were synthesized according to the previously reported procedures. All other reagents were purchased from commercial suppliers and used as received.

^1H and $^{13}C\{^1H\}$ NMR spectra and Evans' method determinations[34] were recorded on a Agilent Technologies 400-MR DD2 400 MHz spectrometer or a Varian UNITY INOVA 500 MHz spectrometer. ^1H and $^{13}C\{^1H\}$ NMR spectra were referenced to external $SiMe_4$ using the residual protio solvent peaks as internal standards.[78,79] IR spectra were recorded on a Nicolet 6700 FT-IR spectrometer with a NXR FT Raman Module. Elemental analyses were performed by the Micro-Mass Facility at the University of California, Berkeley.

7.4.2 Synthesis of [$L^{Me}Ni^{II}(OCPh_3)$] (7.1)

To a dark blue, stirring suspension of [$L^{Me}Ni^{II}Cl$] (84.4 mg, 0.165 mmol) in C_6H_6 (1.5 mL) was added solid $KOCPh_3$ (49.2 mg, 0.165 mmol). After addition, the color of the solution gradually transformed from dark blue to a dichroic solution which is turquoise to reflected light and maroon to transmitted light concomitant with the deposition of a fine white precipitate (KCl). This solution was allowed to stir for 15 min, whereupon the reaction mixture was filtered through a Celite column supported on glass wool (0.5 cm × 2 cm). The volatiles were removed from the filtrate *in vacuo*, and the turquoise residue was extracted into hexanes (2 mL) and filtered through a Celite column supported on glass wool (0.5 cm × 2 cm) yielding a turquoise filtrate. The volume of this solution was reduced *in vacuo* to 1 mL. Storage of the solution at -25 °C for 24 h resulted in the deposition of dark aqua blocks of [$L^{Me}Ni^{II}(OCPh_3)$], which were isolated by decanting off the supernatnat (87 mg, 72%). Anal. Calcd for: $C_{48}H_{56}N_2NiO$: C, 78.37; H, 7.67; N, 3.81. Found: C, 78.20; H, 7.56; N,

3.79. ^{1}H NMR (400 MHz, 25 °C, benzene-d_6): δ = 43.50 (s, 4H, Ar-*m***H**, dipp), 33.83 (s, 4H, C**H**$(CH_3)_2$), 9.33 (d, 6H, Ar-*m***H**, CPh_3), 9.16 (s, 12H, $CH(CH_3)_2$), 6.69 (s, 12H, $CH(CH_3)_2$), 6.27 (s, 6H, Ar-*o***H**, CPh_3), 5.56 (t, $^{3}J_{HH}$, = 7.0 Hz, 3H, Ar-*p***H**, CPh_3), -17.55 (s, 2H, Ar-*p***H**, dipp), -69.62 (s, 6H, $C(CH_3)$), -188.42 (s, 1H, γ-**H**) ppm. Evans' method (C_6D_6, 400 MHz, 25 °C, 0.031 M): 3.09 B.M. Crystallographic details: Triclinic, P-1, a = 11.942(2), b = 12.785(2), c = 14.589(2), α = 94.222(5), β = 90.744(5), γ = 115.716(5), V = 1998.7(5) g/cm^3, Z = 2.

7.4.3 Synthesis of [$L^{tBu}Ni^{II}(OCPh_3)$] (7.2)

To a dark green, stirring suspension of [$L^{tBu}Ni^{II}Cl$] (130 mg, 0.218 mmol) in C_6H_6 (3 mL) was added solid $KOCPh_3$ (65.1 mg, 0.218 mmol). After addition, the color of the solution gradually transformed from dark green to bright green, concomitant with the deposition of a fine white precipitate (KCl). This solution was allowed to stir for 2 hours, whereupon the reaction mixture was filtered through a Celite column supported on glass wool (0.5 cm × 2 cm). Then, volatiles were removed from the filtrate *in vacuo*, and the resulting green residue was extracted into pentane (3 mL) and filtered through a Celite column supported on glass wool (0.5 cm × 2 cm) yielding a bright green filtrate. Volatiles were removed from the filtrate *in vacuo* to yield [$L^{tBu}Ni^{II}(OCPh_3)$] as a bright green powder (126 mg, 70%). ^{1}H NMR (400 MHz, 25 °C, benzene-d_6): δ = 47.83 (s, 4H, Ar-*m***H**, dipp), 37.69 (s, 4H, C**H**$(CH_3)_2$), 9.50 (d, $^{3}J_{HH}$, = 5.1 Hz, 6H, Ar-*m***H**, CPh_3), 8.99 (s, 12H, $CH(CH_3)_2$), 7.94 (s, 12H, $CH(CH_3)_2$), 4.63 (t, $^{3}J_{HH}$, = 7.1 Hz, 3H, Ar-*p***H**, CPh_3), 2.31 (s, 18H, $C(CH_3)_3$), 1.71 (s, 6H, Ar-*o***H**, CPh_3), -25.08 (s, 2H, Ar-*p***H**, dipp), -210.03 (s, 1H, γ-**H**) ppm. Evans' method (C_6D_6, 400 MHz, 25 °C, 0.034 M): 3.08 B.M.

7.4.4 Synthesis of [K(18-crown-6)(THF)$_2$][L^{Me}Ni^{I}(OCPh$_3$)] (7.3)

To a deep aqua, cold (-25 °C), stirring solution of [L^{Me}Ni^{II}(OCPh$_3$)] (**7.1**) (42 mg, 0.0571 mmol) and 18-crown-6 (15.1 mg, 0.0571 mmol), in Et_2O (2 mL), was added KC_8 (7.8 mg, 0.0577 mmol). This resulted in immediate formation of a dark red-brown mixture. This mixture was allowed to warm to room temperature and stir overnight. After stirring overnight, a red powder had precipitated out of the reaction mixture. The pale gold supernatant was decanted and the volatiles were removed from the remaining red powder *in vacuo*. The resulting dark red powder was then extracted into THF (1 mL) and filtered through a Celite column supported on glass wool (0.5 cm × 2 cm), which afforded a black plug (C_8) and a dark red filtrate. This filtrate was then concentrated to 0.25 mL *in vacuo*, layered with hexanes (1 mL), and stored at -25 °C for 24 h. This resulted in the deposition of dark red needles, which were isolated by decanting off the supernatant (55.4 mg, 82% yield). Anal. Calcd for $C_{68}H_{96}KN_2NiO_9$: C, 69.02; H, 8.18; N, 2.37. Found: C, 68.99; H, 8.02; N, 2.30. ^{1}H NMR (400 MHz, 25 °C, THF-d_8): δ = 23.15 (br s, Ar-*m***H**), 16.97 (br s, C**H**(CH$_3$)$_2$), 6.82 (br s, CH(C**H**$_3$)$_2$), 6.72 (br s, CH(C**H**$_3$)$_2$), 3.70 (br s, 18-crown-6), -24.31 (br s, Ar-*p***H**), -41.13 (br s, C(C**H**$_3$)) ppm. Crystallographic details: Triclinic, P-1, a = 11.995(2), b = 12.785(3), c = 24.637(5), α = 84.129(3), β = 89.750(3), γ = 64.814(3), V = 3397.6(1) g/cm^3, Z = 2.

7.4.5 Synthesis of [K(18-crown-6)][L^{tBu}Ni^{I}(OH)] (7.4)

To a bright green, cold (-25 °C), stirring solution of [L^{tBu}Ni^{II}(OCPh$_3$)] (**7.2**) (70 mg, 0.0911 mmol) in THF (2 mL), was added KC_8 (24.6 mg, 0.182 mmol). This resulted in the immediate formation of a dark red-brown mixture. This mixture was allowed to stir for 3 min, after which a cold solution of 18-crown-6 (44.2 mg, 0.182 mmol) in THF (1 mL) was

added drop wise. No color change is observed upon addition of 18-crown-6, the mixture was then allowed to stir for another 5 min. The reaction mixture was then stored at - 25 °C for 30 min, after which it was filtered through a Celite column supported on glass wool (0.5 cm × 2 cm), which afforded a black plug (C_8) and a deep red-brown filtrate. The volatiles were removed from the filtrate *in vacuo* to produce a dark red-brown residue. This residue was extracted into Et_2O (2 mL) and the resulting solution was filtered through a Celite column supported on glass wool (0.5 cm × 2 cm), which afforded a deep red-brown filtrate. This solution was then concentrated *in vacuo* to 1 mL and stored at -25 °C for 24 h. This resulted in the deposition of a mixture of colorless (18-crown-6) and red-orange plates. The red-orange plates (26 mg) were isolated by washing the material with small (0.5 mL × 2) portions of Et_2O to remove the 18-crown-6. A second crop of crystals was isolated by layering of the Et_2O supernatant with pentane (2 mL) followed by storage at -25 °C for 48 h. This material was isolated by decanting off the supernatant (29 mg, total yield: 55 mg, 69% yield). ^{1}H NMR (400 MHz, 25 °C, benzene-d_6): δ = 19.73 (br s, Ar-*m***H**), 12.64 (br s, C**H**$(CH_3)_2$), 4.03 (br s, CH(C**H**$_3)_2$), 3.55 (br s, CH(C**H**$_3)_2$), 2.37 (br s, 18-crown-6), -1.48 (br s, C(C**H**$_3)_3$), -11.40 (br s, Ar-*p***H**). ppm. Crystallographic details: Triclinic, P-1, a = 12.314(5), b = 13.252(5), c = 18.671(7), α = 69.929(8), β = 87.468(8), γ = 69.247(8), V = 2665.7(2) g/cm^3, Z = 2.

7.4.6 Synthesis of [L^{Me}Fe^{II}(OCPh$_3$)] (7.5)

To an orange, stirring solution of [L^{Me}Fe^{II}N(TMS)$_2$][48] (100 mg, 0.158 mmol) in Et_2O (3 mL) was added a solution of $HOCPh_3$ (41.1 mg, 0.158 mmol) in Et_2O (1 mL). After addition, the color of the solution gradually transformed from orange to yellow. This solution was allowed to stir for 45 min, whereupon the reaction mixture was filtered through

a Celite column supported on glass wool (0.5 cm × 2 cm) to give a yellow filtrate. This solution was then concentrated *in vacuo* to 0.25 mL, layered with hexane (2 mL), and stored at - 25 °C for 72 h resulting in the deposition of yellow needles which were isolated by decanting off the supernatant (93.4 mg, 80% yield). ^{1}H NMR (400 MHz, 25 °C, benzene-d_6): δ = 87.10 (s, 1H, γ-**H**), 71.88 (s, 4H, C**H**$(CH_3)_2$), 15.25 (c), 12.92 (s, 3H, Ar-*p***H**, CPh_3), -12.40 (s, 4H, Ar-*m***H**, dipp), -15.39 (s, 12H, CH(C**H**$_3)_2$), -61.59 (s, 2H, Ar-*p***H**, dipp), -90.19 (s, 12H, CH(C**H**$_3)_2$) ppm. Crystallographic details: Triclinic, P-1, a = 11.941(2), b = 12.789(2), c = 14.543(3), α = 94.025(4), β = 91.325(4), γ = 115.050(4), V = 2003.7(6) g/cm^3, Z = 2.

7.4.7 Synthesis of [L^{tBu}Fe^{II}(OCPh$_3$)(NCCH$_3$)] (7.6)

To a cold (-25 °C), stirring suspension of $KOCPh_3$ (36.4 mg, 0.122 mmol) in Et_2O (2 mL) was added a cold bright red solution of [L^{tBu}Fe^{II}Cl][46] (72.3 mg, 0.122 mmol) in Et_2O (2 mL). After addition, the color of the solution quickly changed from red to bright orange. This solution was allowed to stir for 1h, during which a white precipitate (KCl) crashes out of the reaction mixture. The mixture was then filtered through a Celite column supported on glass wool (0.5 cm × 2 cm) to give an off-white plug and a bright orange filtrate. This solution was then concentrated *in vacuo* to 1 mL and transferred to a 5 mL vial. This vial was then placed into a 20 mL vial containing hexamethyldisiloxide (HMDSO, 3 mL) this two vial system was then sealed and stored at -25 °C for 72 h resulting in the deposition of bright orange plates which were isolated by decanting off the supernatant (23 mg). A second crop of crystals was obtained by adding one drop of acetonitrile to the Et_2O supernatant followed by storage at -25 °C for 24 h (16 mg; total yield: 39 mg, 39%) ^{1}H NMR (400 MHz, 25 °C, benzene-d_6): δ = 45.49 (s, 18H, C(C**H**$_3)_3$), 21.04 (s, 6H, Ar-**H**, CPh_3), 15.23 (s,

6H, Ar-**H**, CPh_3), 4.27 (s, 4H, Ar-*m***H**, dipp), 0.55 (s, 3H, $NCCH_3$), -13.29 (s, 4H, C**H**$(CH_3)_2$), -27.64 (s, 12H, CH(C**H**$_3)_2$), -82.96 (s, 2H, Ar-*p***H**, dipp), -121.31 (s, 12H, CH(C**H**$_3)_2$) ppm. Crystallographic details: Monoclinic, C2/c, a = 9.803(3), b = 40.09(1), c = 13.175(5), α = 90, β = 110.150(4), γ = 90, V = 4860(3) g/cm^3, Z = 4.

7.4.8 Synthesis of [K(18-crown-6)(THF)$_2$][L^{Me}Fe^{I}(OCPh$_3$)] (7.7)

To an orange, stirring solution of [L^{Me}Fe^{II}(OCPh$_3$)] (40 mg, 0.0546 mmol) in THF (2 mL) was added KC_8 (14.8 mg, 0.1091 mmol). After addition, the color of the solution quickly transformed to dark green, then 18-crown-6 (26.5 mg, 0.1091 mmol) was added, no color change was observed upon this addition. This solution was allowed to stir for 15 min, whereupon the reaction mixture was filtered through a Celite column supported on glass wool (0.5 cm × 2 cm) to give a black plug and a deep green filtrate. The volume of the filtrate was reduced *in vacuo* to 0.5 mL and transferred to a 5 mL vial. This vial was then placed inside a 20 mL vial containing 3 mL of pentane. This two vial system was then sealed and stored at - 25 °C for 24 h resulting in the deposition of green blocks of [K(18-crown-6)(THF)$_2$][L^{Me}Fe^{I}(OCPh$_3$)] which were isolated by decanting off the supernatant (12 mg, 19% yield). Note: prolonged storage of this species in solution, results in reformation of the starting material via oxidation. ^{1}H NMR (400 MHz, 25 °C, benzene-d_6): δ = 13.43 (br s), 11.32 (br s), 9.62 (br s), 8.03 (s), 3.57 (s, THF), 3.30 (s), 1.47 (s, THF), -4.23 (br s), -9.73 (br s, 12H, CH(C**H**$_3)_2$), -65.53 (br s, 12H, CH(C**H**$_3)_2$) ppm. Crystallographic details: Monoclinic, P21/n, a = 17.093(1), b = 19.187(2), c = 20.213(2), α = 90, β = 96.674(6), γ = 90, V = 6584(1) g/cm^3, Z = 4.

7.4.9 Synthesis of K[PINO]

The preparation of K[PINO] was adapted from a previously reported method which used KOH to deprotonate PINOH.[80] To a colorless stirring solution of hydroxypthalimide (PINOH) (92 mg, 0.564 mmol) in toluene (5 mL), was added a solution of potassium bistrimethylsilylamide ($KN(TMS)_2$, 118 mg, 0.592 mmol) in toluene (1 mL) drop wise. This resulted in immediate formation of a dark maroon mixture. This mixture was allowed to stir for 2 hr. After stirring for 2 h, the stir bar was removed and the volatiles were removed *in vacuo* to provide a maroon residue. This residue was washed with THF (1 mL × 2) and hexanes (1 mL × 2) and the washings were discarded. K[PINO] was isolated as a dark red powder (96 mg, 85% yield). ^{1}H NMR (400 MHz, 25 °C, DMSO-d_6): δ = 7.38 (doublet of doublets, 2H, Ar-**H**), 7.23 (doublet of doublets, 2H, Ar-**H**) ppm.

7.4.10 Synthesis of [$L^{tBu}Ni^{II}$(*O*,*O*:κ^2-PINO)] (7.8)

To a dark green, stirring solution of [$L^{tBu}Ni^{II}Cl$] (57 mg, 0.956 mmol) in THF (2 mL) was added solid K[PINO] (19.2 mg, 0.0956 mmol). After addition, the color of the solution gradually transformed from dark green to dark red-purple, concomitant with the deposition of a fine white precipitate (KCl). This solution was allowed to stir for 2 hours, whereupon the reaction mixture was filtered through a Celite column supported on glass wool (0.5 cm × 2 cm) to give a deep red-purple filtrate. Volatiles were removed from the filtrate *in vacuo*, and the resulting red-purple residue was extracted into toluene (2 mL) and filtered through a Celite column supported on glass wool (0.5 cm × 2 cm) yielding a red-purple filtrate. This solution was the concentrated *in vacuo* to 1 mL, layered with pentane (3 mL), and stored at -25 °C for 24 h resulting in the deposition of red-purple plates which were isolated by decanting off the supernatant (36 mg). A second crop of crystals was obtained by removing

the volitles from the supernatant *in vacuo* followed by extraction into toluene (0.5 mL), layering with pentane (2 mL), and storage at -25 °C for 72 h. This crop was isolated by decanting off the supernatant (27 mg, total: 63 mg, 91% yield). ^{1}H NMR (400 MHz, 25 °C, benzene-d_6): δ = 38.98 (s, 4H, Ar-*m***H**, dipp), 29.11 (s, 4H, C**H**$(CH_3)_2$), 8.10 (s, 12H, CH(C**H**$_3)_2$), 6.94 (s, 12H, CH(C**H**$_3)_2$), 5.03 (s, 2H, PINO, Ar-**H**), 4.15 (s, 2H, PINO, Ar-**H**), 1.88 (s, 18H, C(C**H**$_3)_3$), -35.01 (s, 2H, Ar-*p***H**, dipp) ppm. Crystallographic details: Monoclinic, $P2_1/n$, a = 10.422(9), b = 14.941(1), c = 25.023(2), α = 90, β = 95.85(2), γ = 90, V = 3876(5) g/cm^3, Z = 4.

7.4.11 Reaction of [LtBuNiII(O,O:κ2-PINO)] (7.8) with KC8 in the presence of 18-crown-6

To a dark red, cold (-25 °C), stirring solution of [L^{tBu}Ni^{II}(*O*,*O*:κ^2-PINO)] (**7.8**) (36 mg, 0.0498 mmol) and 18-crown-6 (13.2 mg, 0.0498 mmol) in THF/Et_2O (1:2 mL), was added KC_8 (16.8 mg, 0.125 mmol). This resulted in the rapid formation of a dark red-brown mixture. This mixture was allowed to stir for 30 min. During this time some dark red precipitate forms. The reaction mixture was then filtered through a Celite column supported on glass wool (0.5 cm × 2 cm), which afforded a dark plug and a deep red-brown filtrate. The plug was washed with pyridine to give a pale brown-orange solution which I have tentatively identified as [K(18-crown-6)][PIN]. The volatiles were removed from the main filtrate solution *in vacuo* to produce a dark red-brown residue. This residue was extracted into Et_2O (2 mL) and the resulting solution was filtered through a Celite column supported on glass wool (0.5 cm × 2 cm), which afforded a deep red-brown filtrate. The volatiles were removed from this solution *in vacuo* to yield a red-brown residue. This residue was then extracted into toluene (1 mL), storage of this solution at -25 °C for 2 m resulted in the

deposition of red-orange plates. The red-orange plates were identified as [K(18-crown-6)][$L^{tBu}Ni^{I}$(OH)] (**7.4**) by X-ray crystallography and ^{1}H NMR spectroscopy. ^{1}H NMR (400 MHz, 25 °C, benzene-d_6): δ = 19.65 (br s), 12.81 (br s), 3.58 (br s), 3.08 (br s), 2.99 (br s), 2.36 (br s), 0.91 (br s), -1.48 (br s) ppm. Crystallographic details: Monoclinic, C2/c, a = 40.65(1), b = 20.531(7), c = 14.677(4), α = 90, β = 98.74(1), γ = 90, V = 12108(7) g/cm^3, Z = 8.

7.4.12 Reaction of [$L^{tBu}N^{iII}$(O,O:κ^2-PINO)] (7.8) with KC_8 in the presence of 2,2,2-cryptand

To a dark red, cold (-25 °C), stirring solution of [$L^{tBu}Ni^{II}$(*O*,*O*:κ^2-PINO)] (**7.8**) (27 mg, 0.0373 mmol) and 2,2,2-cryptand (14 mg, 0.0373 mmol) in THF/Et_2O (1:1 mL), was added KC_8 (10.1 mg, 0.0747 mmol). This resulted in immediate formation of a dark red-brown mixture. This mixture was allowed to stir for 30 min. The reaction mixture was then filtered through a Celite column supported on glass wool (0.5 cm × 2 cm), which afforded a black plug (C_8) and a red-brown filtrate. The volatiles were removed from the filtrate *in vacuo* to produce a dark red-brown residue. A ^{1}H NMR spectrum of a reaction aliquot in C_6D_6 reveals the presence of both diamagnetic and a paramagnetic products. ^{1}H NMR (400 MHz, 25 °C, benzene-d_6): δ = 7.05-6.96 (m, diamagnetic product), 4.60 (s, diamagnetic product), 3.98 (sept, diamagnetic product), 3.66 (s, 2,2,2-cryptand), 3.51 (t, 2,2,2-cryptand), 2.91(br s, paramagnetic product), 2.53 (t, 2,2,2-cryptand), 2.02 (br s, paramagnetic product), 1.83 (s, diamagnetic product), 1.65 (d, diamagnetic product), 1.59 (d, diamagnetic product), -1.43 (br s, paramagnetic product) ppm. This residue was extracted into Et_2O (1 mL), filtered through a Celite column supported on glass wool (0.5 cm × 2 cm), and transferred into a 5 mL vial. This vial was then placed inside of a 20 mL containing 3 mL of toluene. The two

vial system was then sealed and stored at -25 °C for 24 h resulting in the deposition of brown-orange plates of [K(2,2,2-cryptand)][PIN] which were isolated by decanting off the supernatant. Crystallographic details: Monoclinic, C2/c, a = 12.598(2), b = 16.300(2), c = 14.378(2), α = 90, β = 97.181(7), γ = 90, V = 2929.3(7) g/cm^3, Z = 4. The supernatant of the crystallization mixture appears to contain a Ni^I containing product which has been tentatively assigned as [K(2,2,2-cryptand)][$L^{tBu}Ni^I$(OH)]. ^{1}H NMR (400 MHz, 25 °C, benzene-d_6, all [K(2,2,2-cryptand)][$L^{tBu}Ni^I$(OH)] assignments are tentative): δ = 21.05 (br s, [K(2,2,2-cryptand)][$L^{tBu}Ni^I$(OH)]), 13.19 (br s, [K(2,2,2-cryptand)][$L^{tBu}Ni^I$(OH)]), 3.93 (br s, [K(2,2,2-cryptand)][$L^{tBu}Ni^I$(OH)]), 3.66 (s, 2,2,2-cryptand), 3.50 (s, 2,2,2-cryptand), 2.53 (s, 2,2,2-cryptand), 2.23 (br s, [K(2,2,2-cryptand)][$L^{tBu}Ni^I$(OH)]), 2.02 (br s, [K(2,2,2-cryptand)][$L^{tBu}Ni^I$(OH)]), 1.43 (br s, [K(2,2,2-cryptand)][$L^{tBu}Ni^I$(OH)]), -1.46 (br s, [K(2,2,2-cryptand)][$L^{tBu}Ni^I$(OH)]) ppm.

7.4.13 Synthesis of [$L^{tBu}Fe^{II}(SCPh_3)$] (7.10)

To a bright red, stirring solution of [$L^{tBu}Fe^{II}Cl$] (63 mg, 0.106 mmol) in C_6H_6 (3 mL) was added solid $KSCPh_3$ (33.4 mg, 0.218 mmol). After addition, the color of the solution quickly transformed to red-orange, concomitant with the deposition of a fine white precipitate (KCl). This solution was allowed to stir for 15 min, whereupon the reaction mixture was filtered through a Celite column supported on glass wool (0.5 cm × 2 cm). Volatiles were removed from the filtrate *in vacuo*, and the orange residue was extracted into hexanes (2 mL) and filtered through a Celite column supported on glass wool (0.5 cm × 2 cm) yielding a red-orange filtrate. The volume of this filtrate was reduced to 0.5 mL *in vacuo* and the resulting solution was stored at - 25 °C for 48 h resulting in the deposition of orange needles which were isolated by decanting off the supernatant (60 mg, 68% yield). ^{1}H

NMR (400 MHz, 25 °C, benzene-d_6): δ = 71.31 (s, 6H, Ar-**H**, CPh_3), 52.17 (s, 1H, γ-**H**), 36.34 (s, 18H, $C(C\mathbf{H}_3)_3$), 15.21 (s, 6H, Ar-**H**, CPh_3), 12.15 (s, Ar-**H**, CPh_3 or Ar-*m***H**, dipp), 9.50 (s, Ar-**H**, CPh_3 or Ar-*m***H**, dipp), 7.62 (s, 12H, $CH(C\mathbf{H}_3)_2$), -14.25 (s, 12H, $CH(C\mathbf{H}_3)_2$), -67.48 (s), -79.78 (s, 2H, Ar-*p***H**, dipp), -80.34 (s, 4H, $C\mathbf{H}(CH_3)_2$) ppm. Crystallographic details: Triclinic, P-1, a = 12.070(1), b = 12.194(1), c = 18.365(2), α = 95.465(2), β = 104.714(2), γ = 108.568(2), V = 2432.1(4) g/cm^3, Z = 2.

7.4.14 Synthesis of [$L^{tBu}Co^{II}(SCPh_3)$] (7.11)

To a dark green, stirring solution of [$L^{tBu}Co^{II}Cl_2Li(THF)_2$] (65 mg, 0.103 mmol) in C_6H_6 (3 mL) was added solid $KSCPh_3$ (32.6 mg, 0.103 mmol). After addition, the color of the solution quickly transformed to red-orange, concomitant with the deposition of a fine white precipitate (KCl). This solution was allowed to stir for 30 min, whereupon the reaction mixture was filtered through a Celite column supported on glass wool (0.5 cm × 2 cm). Volatiles were removed from the filtrate *in vacuo*, and the orange residue was extracted into hexanes (2 mL) and filtered through a Celite column supported on glass wool (0.5 cm × 2 cm) yielding a red-orange filtrate. The volume of this filtrate was reduced to 0.25 mL *in vacuo* and the resulting solution was stored at - 25 °C for 24 h resulting in the deposition of orange needles which were isolated by decanting off the supernatant (46 mg, 53% yield). ^{1}H NMR (400 MHz, 25 °C, benzene-d_6): δ = 59.80 (s, 6H, Ar-**H**, CPh_3), 31.50 (s, 18H, $C(C\mathbf{H}_3)_3$), 19.12 (s, 3H, Ar-**H**, CPh_3), 4.50 (s, 6H, Ar-**H**, CPh_3), 3.55 (s, 4H, Ar-*m***H**, dipp), -8.15 (s, 12H, $CH(C\mathbf{H}_3)_2$), -49.85 (s, 2H, Ar-*p***H**, dipp), -55.56 (s, 4H, $C\mathbf{H}(CH_3)_2$), -59.25 (s, 12H, $CH(C\mathbf{H}_3)_2$) ppm. Crystallographic details: Triclinic, P-1, a = 12.008(1), b = 12.182(1), c = 18.394(2), α = 95.698(3), β = 104.610(3), γ = 108.973(2), V = 2413.3(5) g/cm^3, Z = 2.

7.4.15 Synthesis of [$L^{tBu}Zn^{II}(SCPh_3)$] (7.12)

To a colorless, stirring solution of [$L^{tBu}Zn^{II}Cl$][61] (50 mg, 0.0830 mmol) in THF (3 mL) was added solid $KSCPh_3$ (26 mg, 0.0830 mmol). This solution was allowed to stir for 24 h, during this time the deposition of some fine white precipitate (KCl) was observed. The reaction mixture was then filtered through a Celite column supported on glass wool (0.5 cm × 2 cm), the volatiles were removed from the filtrate *in vacuo*, and the white residue was extracted into Et_2O (2 mL) and filtered through a Celite column supported on glass wool (0.5 cm × 2 cm) yielding a colorless filtrate. The volume of this filtrate was reduced to 0.25 mL *in vacuo* and the resulting solution was stored at - 25 °C for 48 h resulting in the deposition of colorless needles which were isolated by decanting off the supernatant (33 mg, 66% yield). ^{1}H NMR (400 MHz, 25 °C, benzene-d_6): δ = 7.44-6.99 (m, 21H, Ar-**H**, Dipp and CPh_3), 5.59 (s, 1H, γ-**H**), 3.20 (sept, 4H, C**H**$(CH_3)_2$), 1.45 (d, 12H, CH(C**H**$_3)_2$), 1.25 (d, 12H, CH(C**H**$_3)_2$), 1.16 (s, 18H, C(C**H**$_3)_3$), ppm. Crystallographic details: Triclinic, P-1, a = 12.064(3), b = 12.102(3), c = 18.443(4), α = 95.063(6), β = 105.096(5), γ = 108.896(6), V = 2415.4(9) g/cm^3, Z = 2.

7.4.16 Reaction of [$L^{tBu}Fe^{II}(SCPh_3)$] (7.10) with KC_8 in the presence of 18-crown-6

To an orange, cold (-25 °C), stirring solution of [$L^{tBu}Fe^{II}(SCPh_3)$] (**7.10**) (112 mg, 0.134 mmol) and 18-crown-6 (71.1 mg, 0.269 mmol) in Et_2O (2 mL), was added KC_8 (36.3 mg, 0.269 mmol). This resulted in the rapid formation of a dark red mixture. This mixture was allowed to stir for 5 min, after which 1 mL of hexanes was added, resulting in the precipitation of a red solid ($KCPh_3$). The mixture was then allowed to stir for another 5 min after which it was filtered through a Celite column supported on glass wool (0.5 cm × 2 cm), which afforded a dark plug and a dark red filtrate. The volatiles were removed from the

filtrate *in vacuo* to produce a dark red-brown residue. This residue was extracted into hexanes (2 mL) and the resulting mixture was filtered through a Celite column supported on glass wool (0.5 cm × 2 cm), which afforded a dark red filtrate. This solution was then concentrated *in vacuo* to 0.5 mL and stored at -25 °C for 72 h. This resulted in the deposition red-brown plates mixed with an oil and other solids. The red-brown plates characterized by X-ray crystallography and ^{1}H NMR spectroscopy. ^{1}H NMR (400 MHz, 25 °C, benzene-d_6): δ = 24.26 (s, 1H, γ-**H**), 12.50 (s, 18H, C(C**H**$_3$)$_3$), 7.08 (s), 6.18 (s, 4H, Ar-*m***H**, dipp), 3.54 (br s, 18-crown-6), -2.35 (s, 12H, CH(C**H**$_3$)$_2$), -7.14 (s, 4H, C**H**(CH$_3$)$_2$ s), -18.64 (s, 2H, Ar-*p***H**, dipp), -19.28 (s, 12H, CH(C**H**$_3$)$_2$) ppm. Crystallographic details: Monoclinic, P21, a = 22.114(5), b = 12.907(3), c = 23.386(6), α = 90, β = 95.92(2), γ = 90, V = 6639(3) g/cm^3, Z = 6.

7.4.17 Synthesis of [K(18-crown-6)][L^{tBu}Co^{I}(SH)] (7.14)

To an orange-red, cold (-25 °C), stirring solution of [L^{tBu}Co^{II}(SCPh$_3$)] (**7.11**) (46 mg, 0.0550 mmol) and 18-crown-6 (29.1 mg, 0.110 mmol) in Et$_2$O (2 mL), was added KC$_8$ (14.9 mg, 0.110 mmol). This resulted in immediate formation of a dark red mixture. This mixture was allowed to stir for 20 min, after which the mixture was filtered through a Celite column supported on glass wool (0.5 cm × 2 cm), which afforded a dark plug and a dark red filtrate. This solution was then concentrated *in vacuo* to 1 mL and 0.5 mL of hex was added. The resulting mixture was filtered through a Celite column supported on glass wool (0.5 cm × 2 cm), which afforded a dark red filtrate. This solution was then stored at -25 °C for 72 h which did not result in the formation of any solids. The volatiles were removed from this solution *in vacuo* to produce a dark red-brown residue. This residue was extracted into Et$_2$O (1 mL), filtered through a Celite column supported on glass wool (0.5 cm × 2 cm), and

concentrated *in vacuo* to 0.25 mL and stored at -25 °C for 48 h. This resulted in the deposition of a mixture of solids including some red plates. The red plates were characterized by X-ray crystallography, a ^{1}H NMR of the product mixture reveals a complicated mixture of paramagnetic products. Crystallographic details: Triclinic, P-1, a = 12.713(3), b = 13.040(4), c = 17.790(5), α = 78.256(8), β = 83.082(7), γ = 70.806(8), V = 2722 (1) g/cm^3, Z = 2.

7.4.18 Synthesis of K[NHTs]

The preparation of K[NHTs] was adapted from a previously reported method which used NaOEt to deprotonate $NH_2S(O)_2C_6H_4$-*p*-CH_3.[81] To a colorless stirring solution of tosylamine ($NH_2S(O)_2C_6H_4$-*p*-CH_3, 151 mg, 0.882 mmol) in THF (5 mL) was added a solution of potassium bistrimethylsilylamide ($KN(TMS)_2$, 176 mg, 0.882 mmol) in THF (2 mL). Upon addition, a white solid immediately began to form and the mixture was allowed to stir for 20 min. After stirring for 20 min, the volitiles were removed from the mixture *in vacuo* to yield a fine white powder. This powder was then washed with THF (1 mL × 1) and Et_2O (1 mL × 2). Volitiles were removed from the remaining solid *in vacuo* to yield K[NHTs], a white powder that is insoluble in organic solvents (179 mg, 98% yield).

7.4.19 Synthesis of [L^{tBu}Ni^{II}(*N*,*O*:κ^2-NHTs)] (7.15)

To a dark green, stirring suspension of [L^{tBu}Ni^{II}Cl] (51.3 mg, 0.0860 mmol) in Et_2O (3 mL) was added solid K[NHTs] (18 mg, 0.0860 mmol). After addition, the color of the solution gradually transformed from dark green to pale purple, concomitant with the deposition of a fine white precipitate (KCl). Then, 0.25 mL of THF were added and the solution was allowed to stir for another 25 min, during which the color of the solution changed to magenta. The reaction mixture was then filtered through a Celite column

supported on glass wool (0.5 cm × 2 cm) to give a deep purple filtrate. Volatiles were removed from the filtrate *in vacuo*, and the resulting magenta residue was extracted into Et_2O/Hex (2:1 mL) and filtered through a Celite column supported on glass wool (0.5 cm × 2 cm) yielding a purple filtrate. This solution was then stored at - 25 °C for 48 h resulting in the deposition of purple plates which were isolated by decanting off the supernatant (20 mg, 32% yield). ^{1}H NMR (400 MHz, 25 °C, benzene-d_6): δ = 8.19 (d, 4H, *m*-Ar-**H**, Dipp), 6.75 (d, 2H, Ar-**H**, NHTs), 6.56 (d, 2H, Ar-**H**, NHTs), 5.43 (t, 2H, *m*-Ar-**H**, Dipp), 5.26 (sept, 4H, C**H**$(CH_3)_2$), 2.63 (d, 12H, CH(C**H**$_3)_2$), 1.91 (s, 3H, C**H**$_3$, NHTs), 1.62 (d, 12H, CH(C**H**$_3)_2$), 1.05 (s, 18H, C(C**H**$_3)_3$), 0.27 (s, 1H, γ-**H** or N-**H**), -1.62 (s, 1H, γ-**H** or N-**H**) ppm. Crystallographic details: Triclinic, P-1, a = 10.417(1), b = 12.457(2), c = 16.298(2), α = 98.336(3), β = 94.103(3), γ = 108.770(3), V = 1965.5(4) g/cm^3, Z = 2.

7.4.20 Synthesis of [K(18-crown-6)][L^{tBu}Ni^{II}(*N*,*O*:κ^2-NHTs)] (7.16)

To a purple, stirring solution of [L^{tBu}Ni^{II}(*N*,*O*:κ^2-NHTs)] (20 mg, 0.0289 mmol) and 18-crown-6 (15.3 mg, 0.0578 mmol) in THF (1 mL) was added KC_8 (7.8 mg, 0.0578 mmol). After addition, the color of the solution rapidly transformed from purple to dark red. This solution was allowed to stir for 30 min, whereupon the reaction mixture was filtered through a Celite column supported on glass wool (0.5 cm × 2 cm) to give a deep red filtrate. Volatiles were removed from the filtrate *in vacuo*, and the resulting red residue was extracted into Et_2O (1 mL) and filtered through a Celite column supported on glass wool (0.5 cm × 2 cm) yielding a red filtrate. This solution was then transferred to a 5 mL vial. This vial was then placed inside a 20 mL vial containing 3 mL of toluene. This two vial system was then sealed and stored at - 25 °C for 24 h resulting in the deposition of red plates of [K(18-crown-6)][L^{tBu}Ni^{I}(NHTs)] which were isolated by decanting off the supernatant

(11 mg, 38% yield). ^{1}H NMR (400 MHz, 25 °C, benzene-d_6): δ = 21.25 (br s), 11.61 (br s), 3.61 (br s), 3.16 (br s), 2.63 (br s), -1.06 (br s) ppm. Crystallographic details: Triclinic, P-1, a = 12.920(1), b = 14.091(2), c = 17.146(2), α = 70.283(3), β = 74.811(3), γ = 82.629(3), V = 2833.1(6) g/cm^3, Z = 2.

7.4.21 Synthesis of [{L^{tBu}(PhNCO)}Ni^{II}(*N*,*O*:κ^2-PhNC(O)OCPh$_3$)] (7.17)

To a green, stirring solution of [L^{tBu}Ni^{II}OCPh$_3$] (36.5 mg, 0.0445 mmol) in C_6H_6 (1 mL) was added phenyl isocyanate (PhNCO, 9.73 μL, 0.0890 mmol). After addition, the color of the solution gradually transformed from bright green to brown. This solution was allowed to stir for 1 h, whereupon the volatiles were removed from the solution *in vacuo*. The resulting pale brown residue was extracted into pentane (2 mL) and filtered through a Celite column supported on glass wool (0.5 cm × 2 cm) yielding a brown filtrate. This solution was then concentrated *in vacuo* to 1 mL and transferred to a 5 mL vial. This vial was then placed inside a 20 mL vial containing 3 mL of toluene. This two vial system was then sealed and stored at - 25 °C for 48 h resulting in the deposition of brown plates of [{L^{tBu}(PhNCO)}Ni^{II}(*N*,*O*:κ^2-PhNC(O)OCPh$_3$)] which were isolated by decanting off the supernatant (27 mg, 57% yield). ^{1}H NMR (400 MHz, 25 °C, benzene-d_6): δ = 30.05 (br s), 26.98 (s), 20.42 (s), 19.78 (s), 17.08 (s), 12.68 (s), 9.14 (s), 7.91 (s), 7.75 (s), 7.37 (s), 7.30 (s), 6.58 (s), 3.53 (s), 2.31 (s), 1.18 (s), -10.00 (s), -11.27 (br s), -19.70 (s), -46.40 (br s) ppm. Crystallographic details: Triclinic, P-1, a = 12.274(4), b = 13.969(5), c = 17.189(7), α = 76.71(1), β = 87.25(1), γ = 88.91(1), V = 2865(2) g/cm^3, Z = 4.

7.4.22 Reaction of [{L^{tBu}(PhNCO)}Ni^{II}(*N*,*O*:κ^2-PhNC(O)OCPh$_3$)] (7.17) with KC_8 in the presence of 18-crown-6

To a brown, stirring solution of [{L^{tBu}(PhNCO)}Ni^{II}(*N*,*O*:κ^2-PhNC(O)OCPh$_3$)] (27 mg, 0.0255 mmol) and 18-crown-6 (13.5 mg, 0.0510 mmol) in Et_2O/THF (2:1 mL) was added KC_8 (6.9 mg, 0.0255 mmol). After addition, the color of the solution rapidly became red-orange. The mixture was allowed to stir for 3 min, whereupon the reaction mixture was filtered through a Celite column supported on glass wool (0.5 cm × 2 cm) to give a red-orange filtrate. Volatiles were removed from the filtrate *in vacuo*, and the resulting red residue was extracted into THF-d_8 for ^{1}H NMR spectroscopic analysis. The ^{1}H NMR spectrum reveals the clean formation of a diamagnetic product, however, attempts to isolate and characterize this product have been unsuccessful. ^{1}H NMR (400 MHz, 25 °C, THF-d_8): δ = 7.45 (d), 7.23 (t), 7.16 (d), 7.09 (d), 7.04 (d), 6.92-6.87 (m), 6.76 (t), 6.67 (t), 6.63 (t), 5.56 (s), 4.98 (s), 4.83 (sept), 4.68 (sept), 3.48 (s), 2.93 (sept), 2.86 (sept), 1.53 (s), 1.29 (d), 1.22 (d), 1.19 (d), 1.11 (doublet of doublets), 0.95 (d), 0.89 (d), 0.85 (d), 0.77 (s) ppm.

7.4.23 X-ray Crystallography

Data for solid state molecular structures were collected on a Bruker KAPPA APEX II diffractometer equipped with an APEX II CCD detector using a TRIUMPH monochromator with a Mo Kα X-ray source (α = 0.71073 Å). The crystals were mounted on a cryoloop under Paratone-N oil, and all data were collected at 100(2) K using an Oxford nitrogen gas cryostream. Data were collected using ω scans with 0.5° frame widths. Data collection and cell parameter determination were conducted using the SMART program.[82] Integration of the data frames and final cell parameter refinement were performed using SAINT software.[83] Absorption correction of the data was carried out using the multi-scan method

SADABS.[84] Subsequent calculations were carried out using SHELXTL.[85] Structure determination was done using direct or Patterson methods and difference Fourier techniques. All hydrogen atom positions were idealized, and rode on the atom of attachment. Structure solution, refinement, graphics, and creation of publication materials were performed using SHELXTL.[85]

7.5 Appendix

7.5.1 NMR Spectra

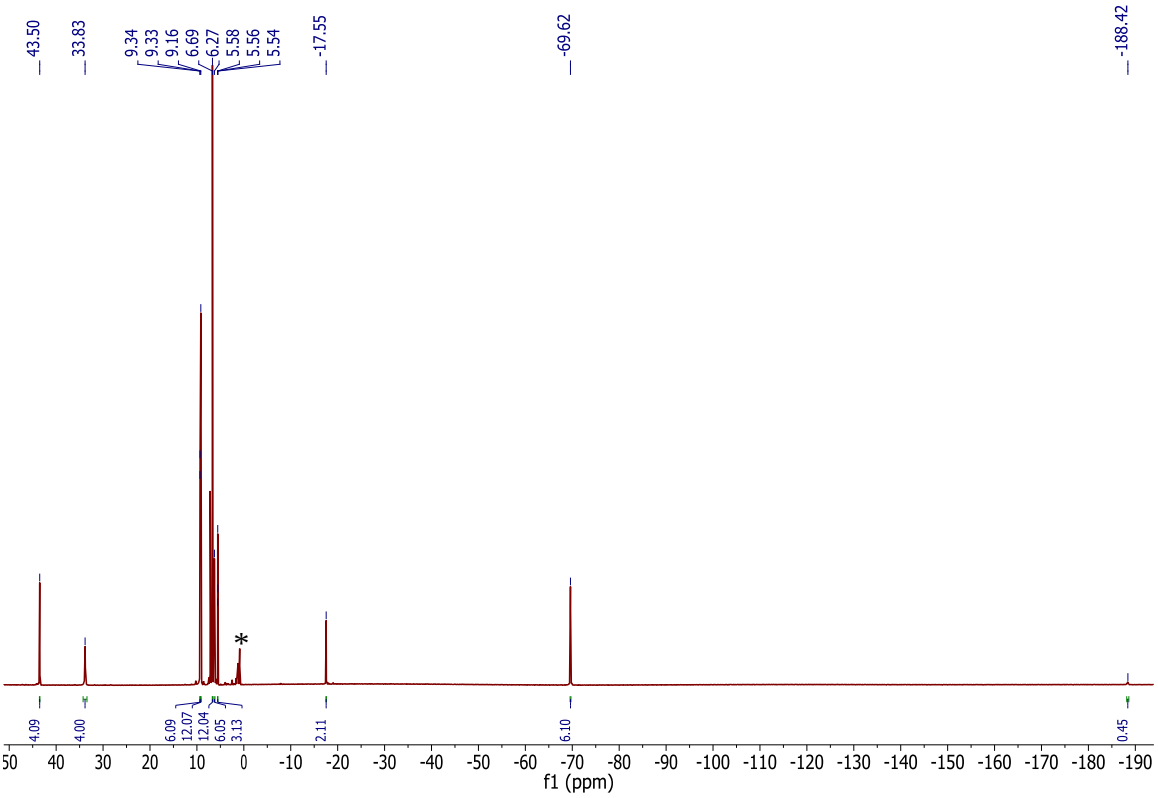

Figure A 7.1. ^{1}H NMR spectrum of [$L^{Me}Ni^{II}(OCPh_3)$] (**7.1**) in benzene-d_6. (*) indicates the presence of hexanes.

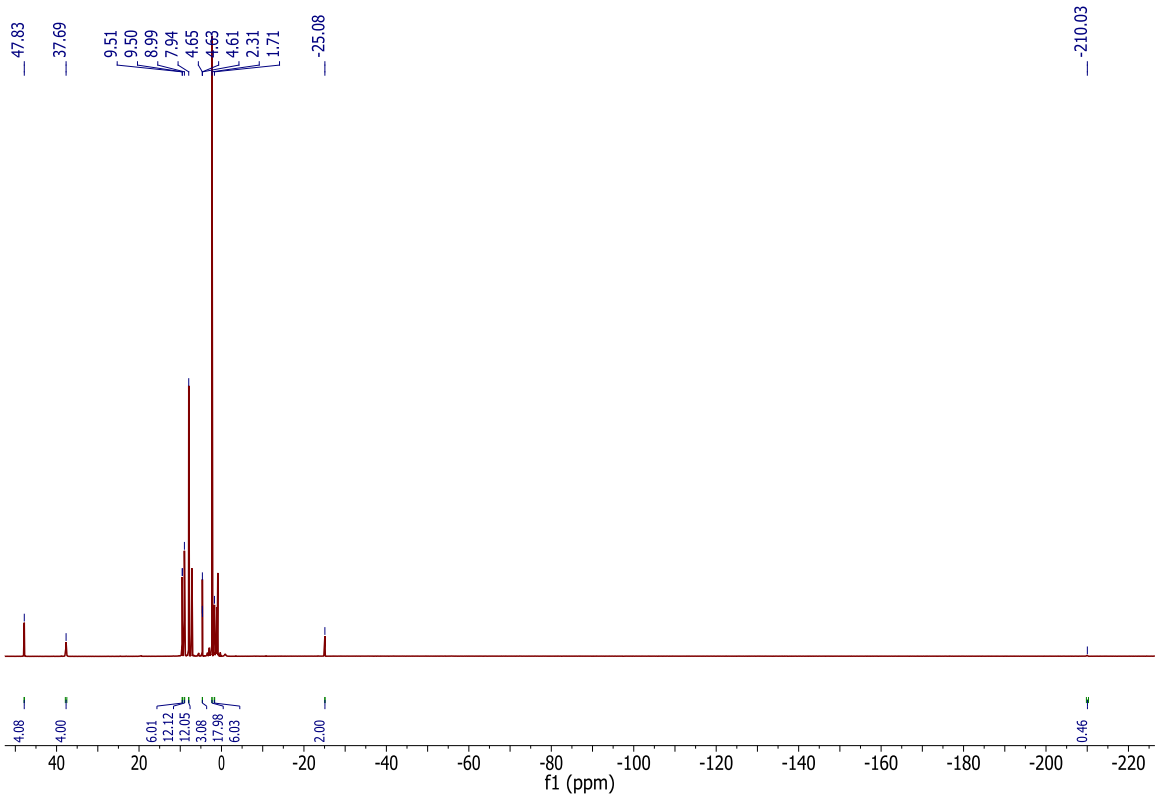

Figure A 7.2. ^{1}H NMR spectrum of [$L^{tBu}Ni^{II}(OCPh_3)$] (**7.2**) in benzene-d_6. (*) indicates the presence of pentane.

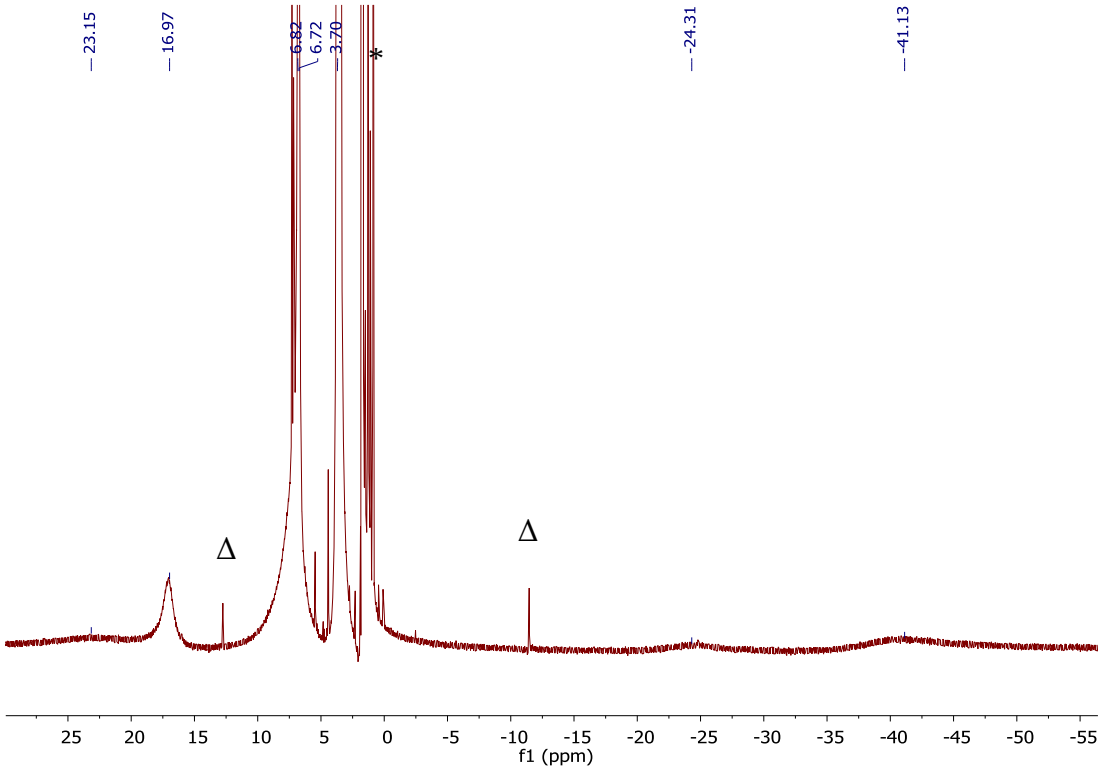

Figure A 7.3. ^{1}H NMR spectrum of [K(18-crown-6)(THF)$_2$][L^{Me}Ni^{II}(OCPh$_3$)] (**7.3**) in THF-d_8. (*) indicates the presence of hexanes, (Δ) indicates the presence of an unidentified impurity.

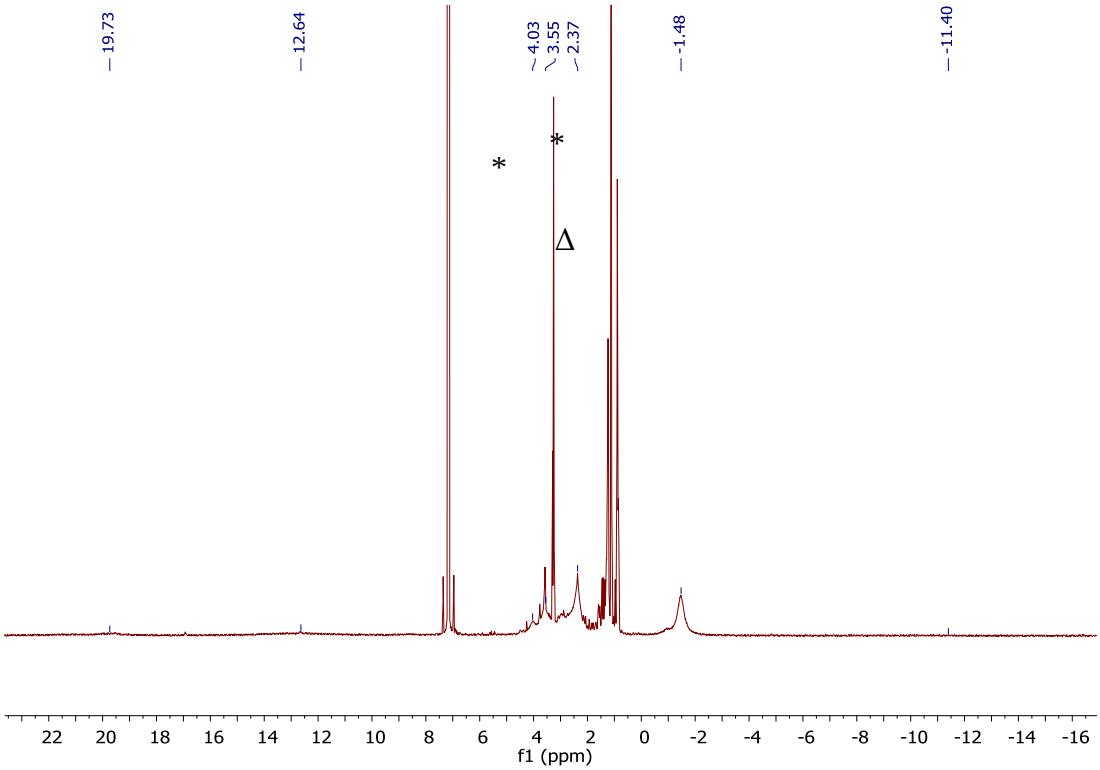

Figure A 7.4. ^{1}H NMR spectrum of [K(18-crown-6)][L^{tBu}Ni^{I}(OH)] (**7.4**) in benzene-d_6. (*) indicates the presence of Et_2O, (Δ) indicates the presence of pentane.

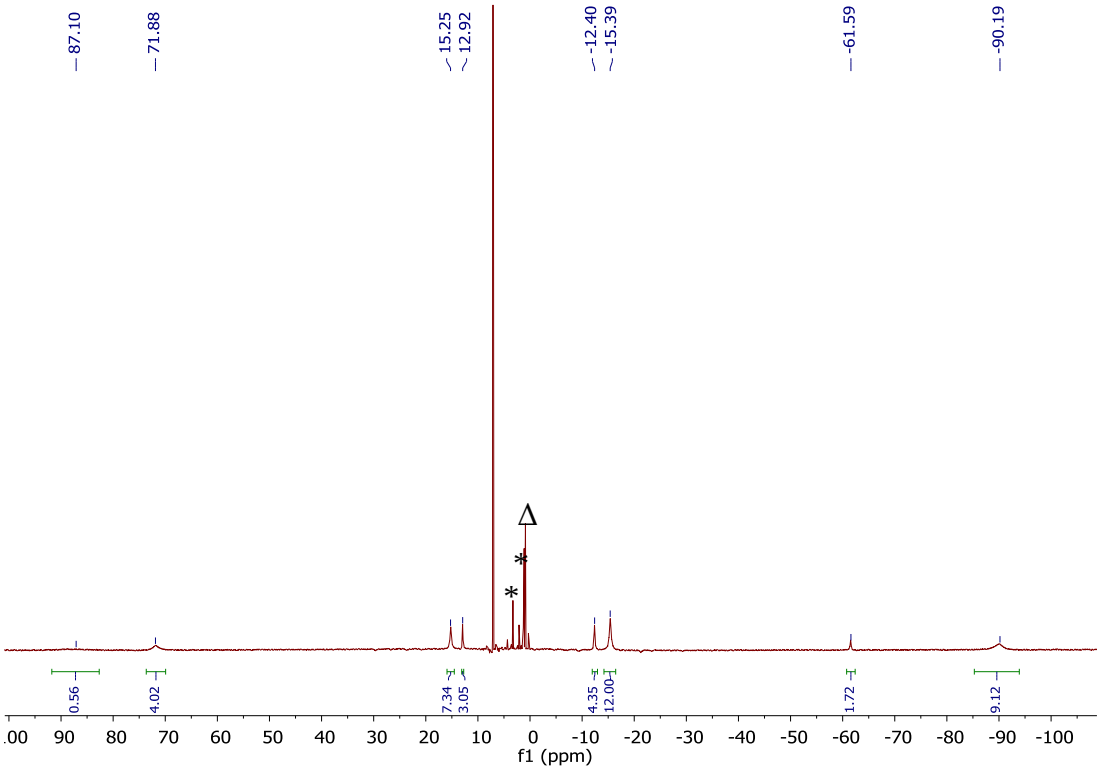

Figure A 7.5. ^{1}H NMR spectrum of [$L^{Me}Fe^{II}(OCPh_3)$] (**7.5**) in C_6D_6. (*) indicates the presence of Et_2O and (Δ) indicates the presence of hexanes.

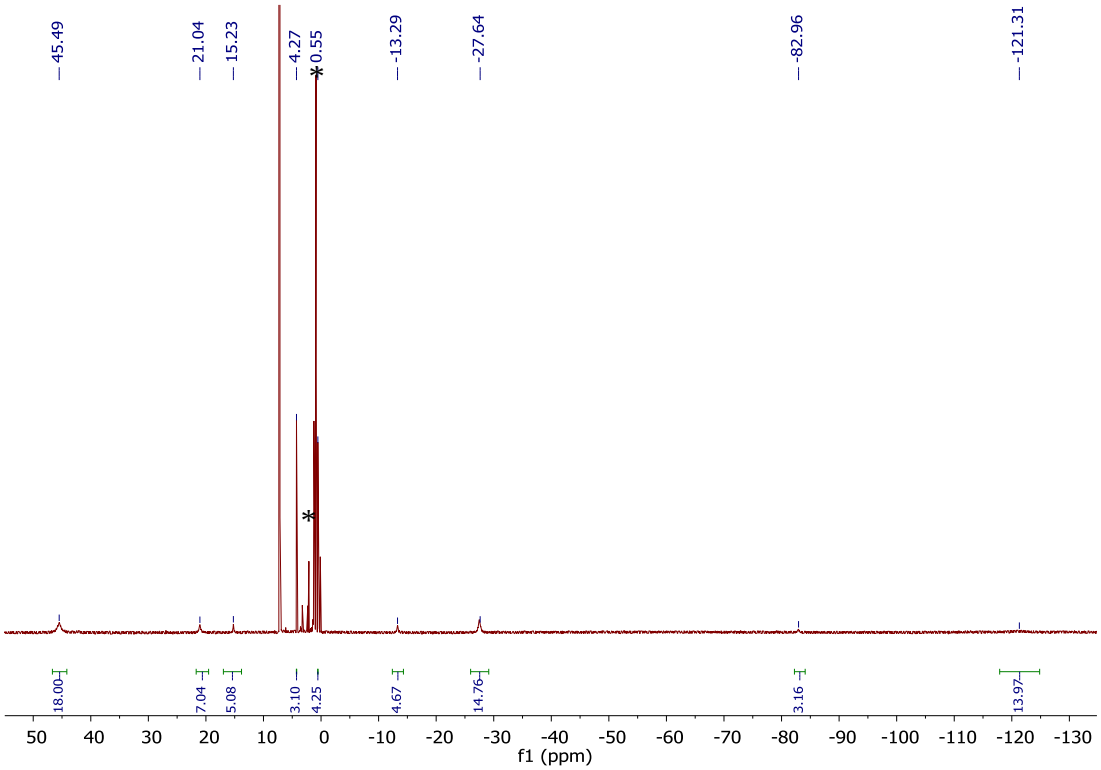

Figure A 7.6. ^{1}H NMR spectrum of [$L^{tBu}Fe^{II}(OCPh_3)(NCCH_3)$] (**7.6**) in C_6D_6. (*) indicates the presence of Et_2O.

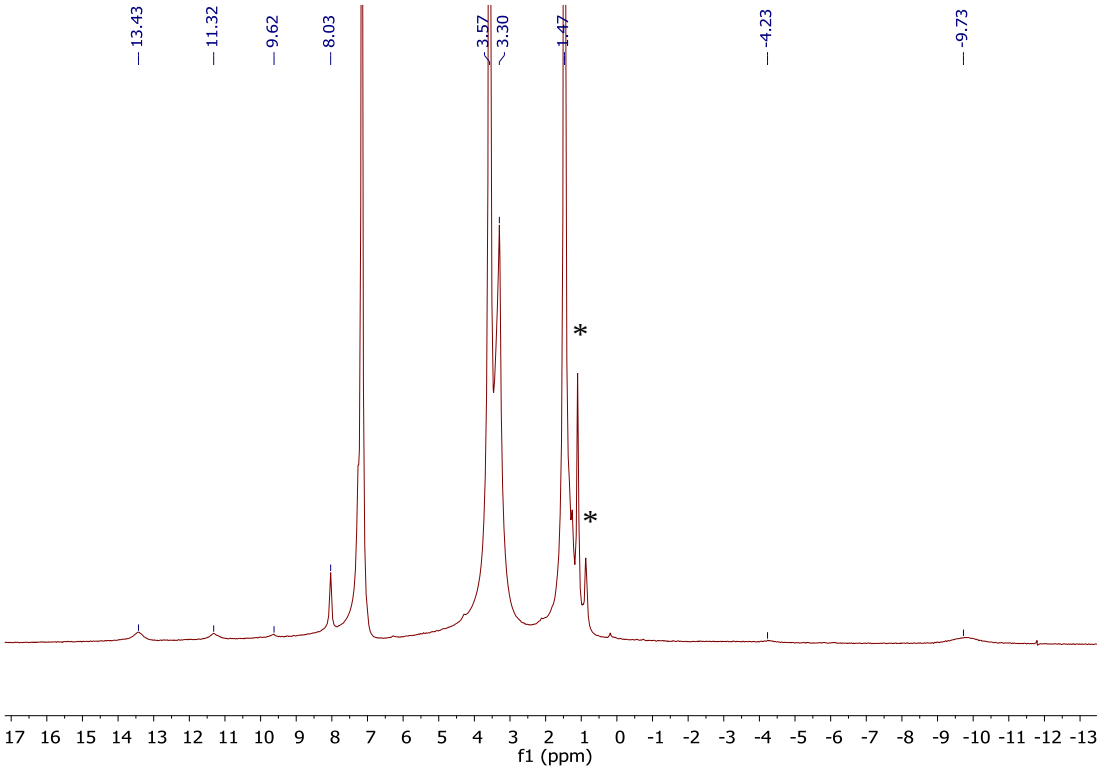

Figure A 7.7. ^{1}H NMR spectrum of [K(18-crown-6)(THF)$_2$][L^{Me}Fe^{I}(OCPh$_3$)] (**7.7**) in C_6D_6. (*) indicates the presence of pentane.

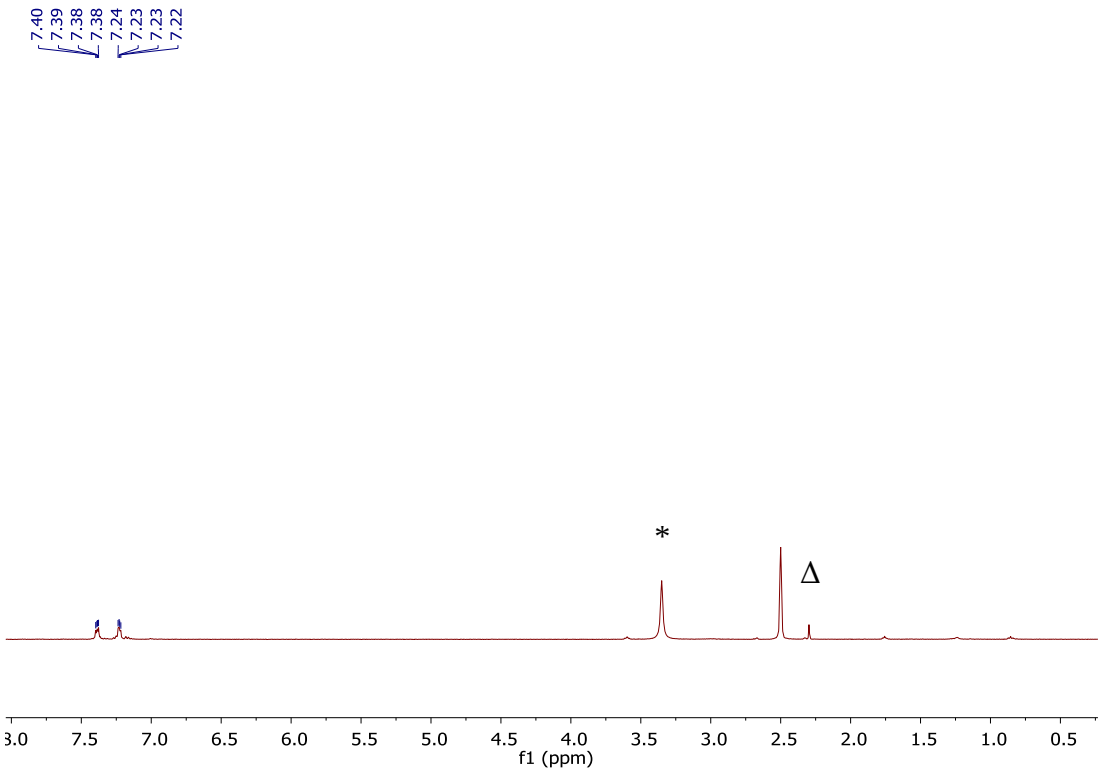

Figure A 7.8. ^{1}H NMR spectrum of K[PINO] in DMSO-d_6. (*) indicates the presence of H_2O and (Δ) indicates the presence of toluene.

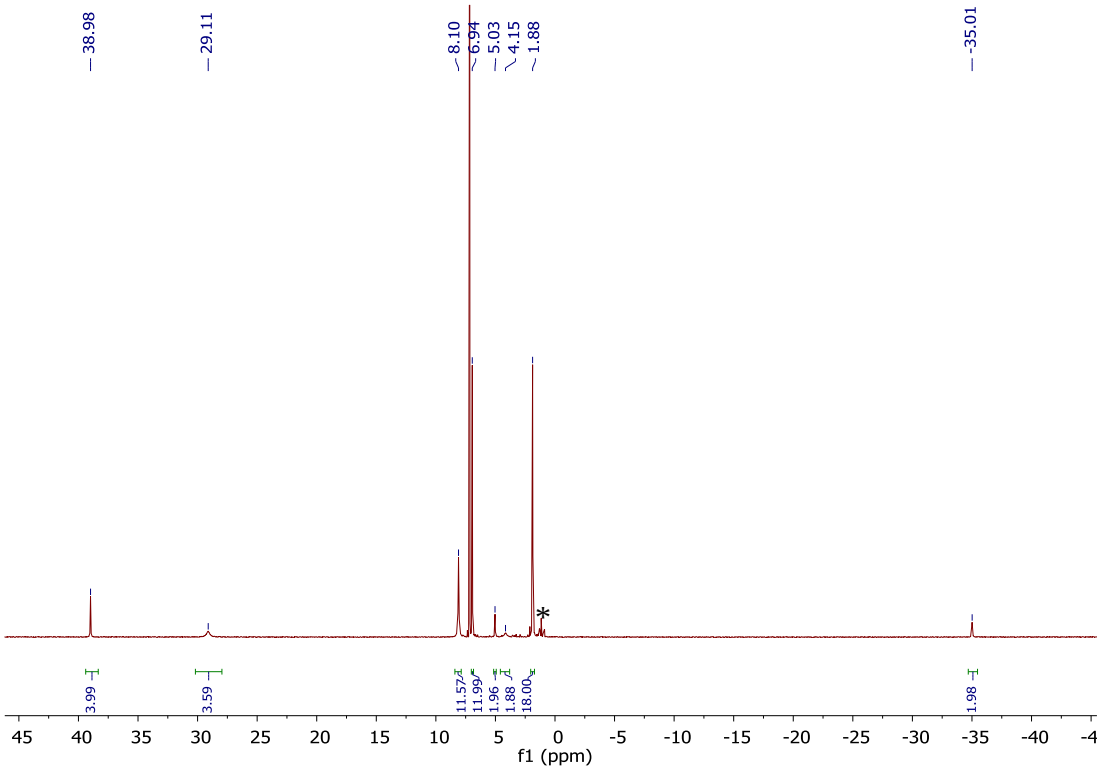

Figure A 7.9. ^{1}H NMR spectrum of [L^{tBu}Ni^{II}(*O*,*O*:κ^{2}-PINO)] (**7.8**) in benzene-d_6. (*) indicates the presence of pentane.

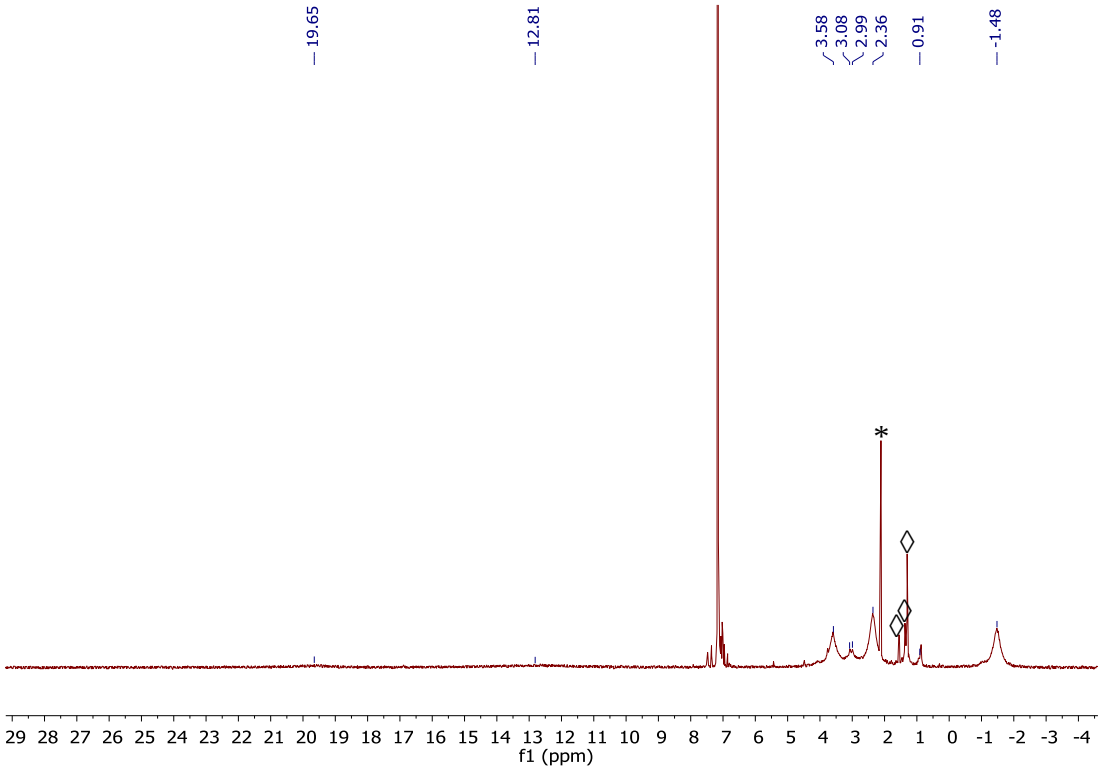

Figure A 7.10. ^{1}H NMR spectrum of [K(18-crown-6)][L^{tBu}Ni^{I}(OH)] (**7.4**) isolated from the reduction of [L^{tBu}Ni^{II}(*O*,*O*:κ^{2}-PINO)] (**7.8**) with KC_8 in the presence of 18-crown-6 in benzene-d_6. (*) indicates the presence of toluene and (◊) indicates the presence of an unidentified diamagnetic impurity.

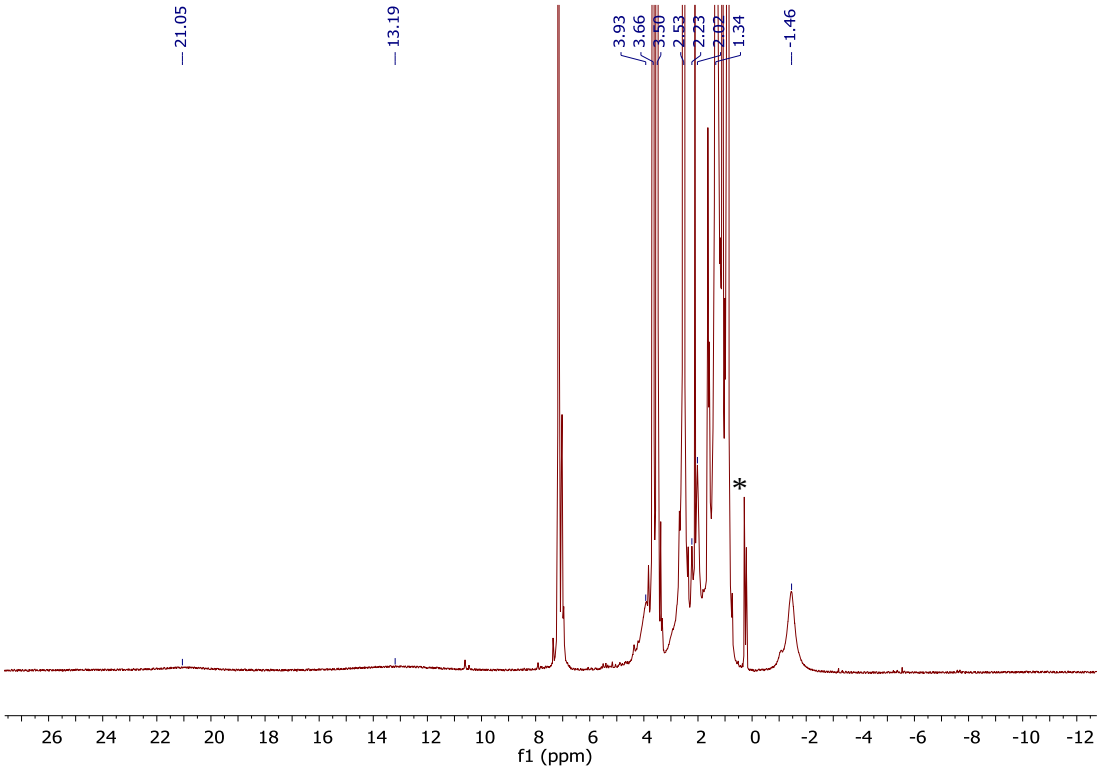

Figure A 7.11. ^{1}H NMR spectrum of the crude products of the reaction of [$L^{tBu}Ni^{II}$(*O*,*O*:κ^{2}-PINO)] (**7.8**) with KC_8 in the presence of 2,2,2-cryptand in benzene-d_6. (*) indicates the presence of pentane.

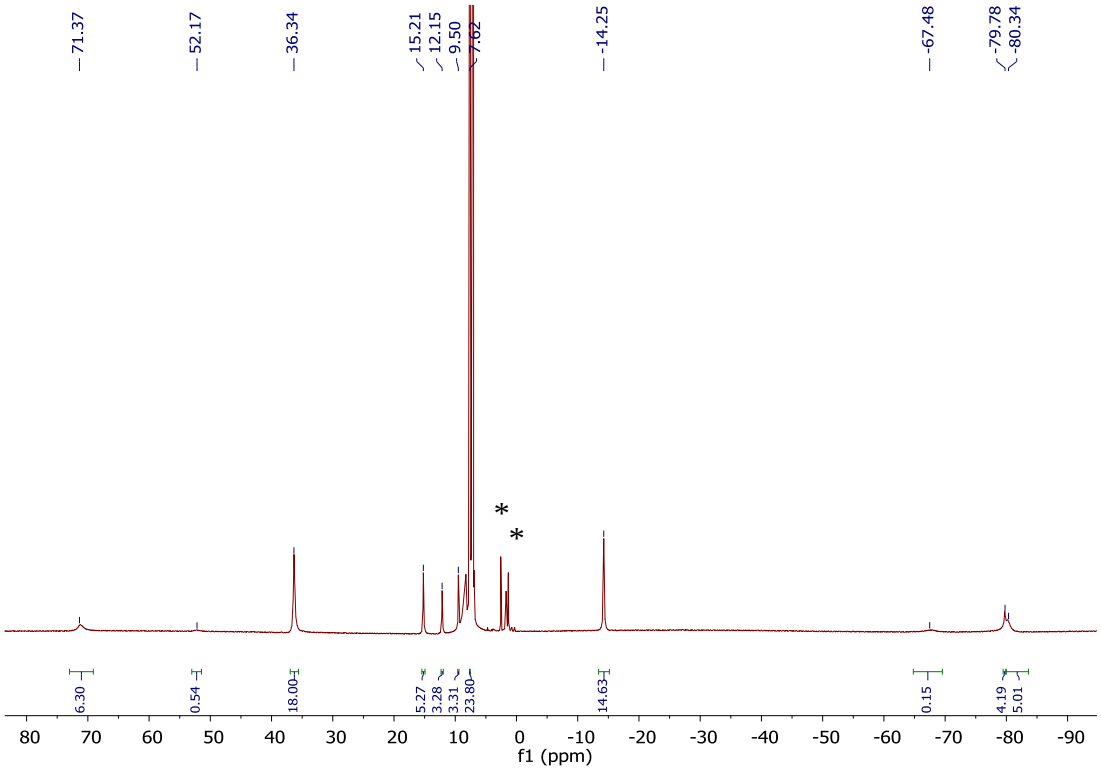

Figure A 7.12. ^{1}H NMR spectrum of [$L^{tBu}Fe^{II}(SCPh_3)$] (**7.10**) in benzene-d_6. (*) indicates the presence of hexane.

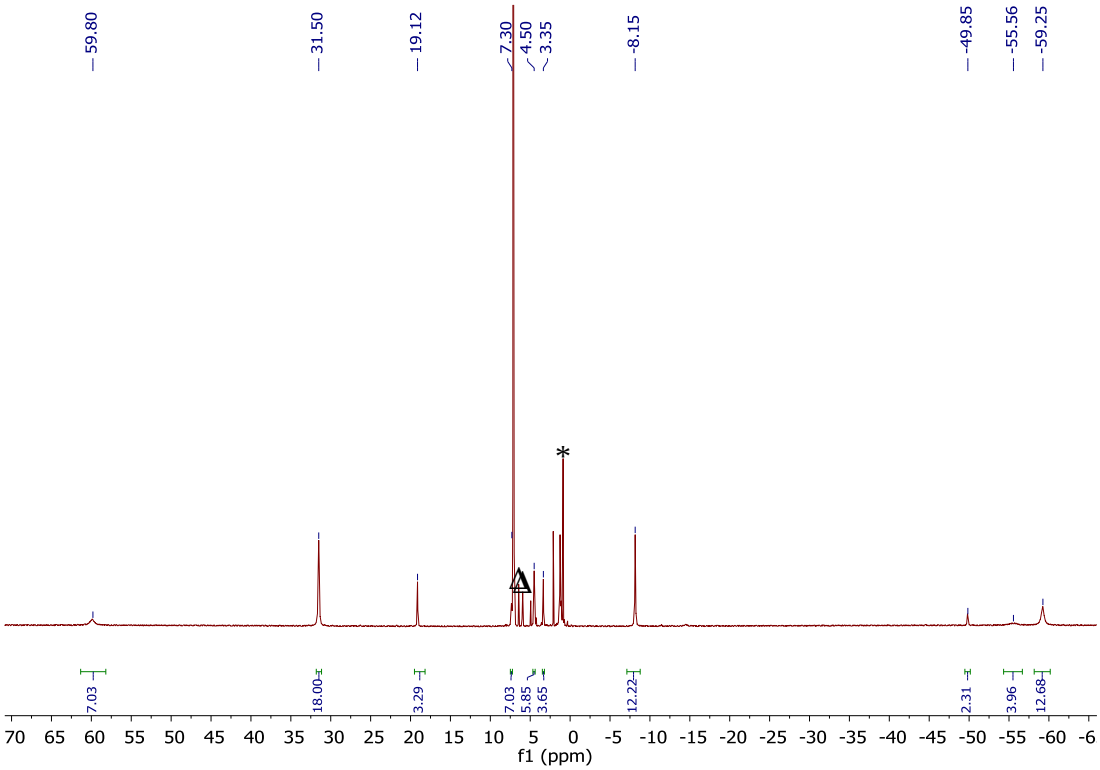

Figure A 7.13. ^{1}H NMR spectrum of [$L^{tBu}Co^{II}(SCPh_3)$] (**7.11**) in benzene-d_6. (*) indicates the presence of hexane and (Δ) indicates the presence of gomberg's dimer.[43]

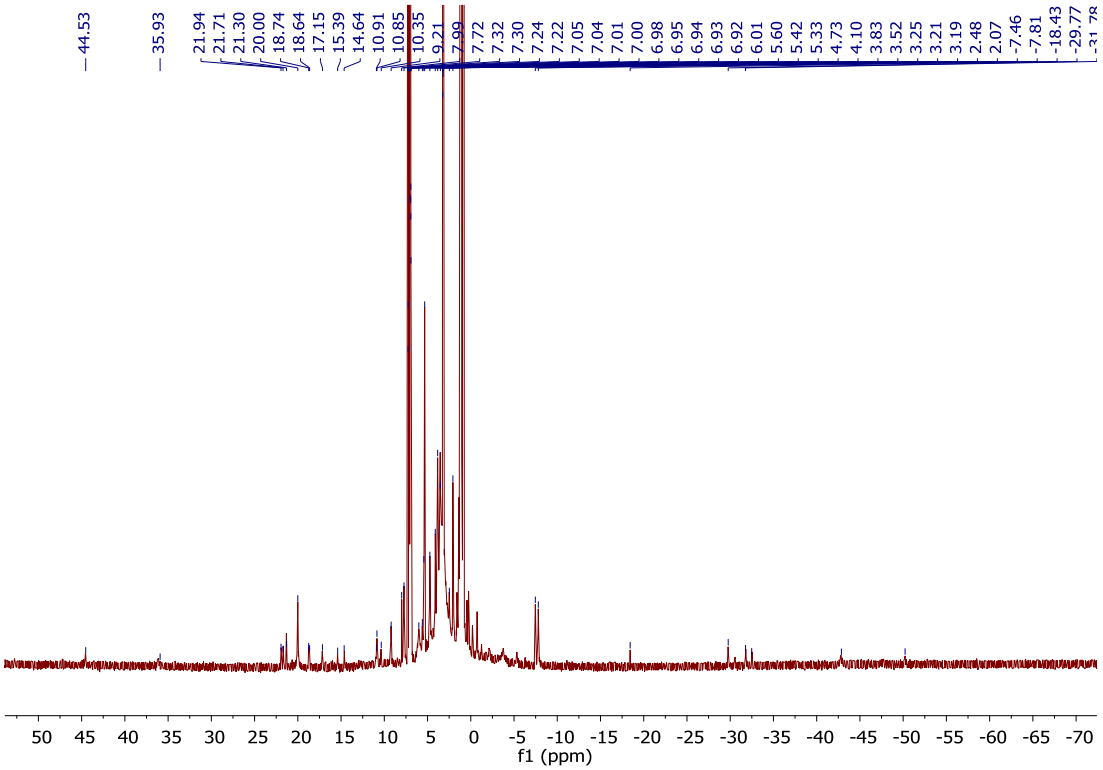

Figure A 7.14. ^{1}H NMR spectrum of the products of the reduction of [$L^{tBu}Co^{II}(SCPh_3)$] (**7.11**) with KC_8 in the presence of 18-crown-6 in C_6D_6.

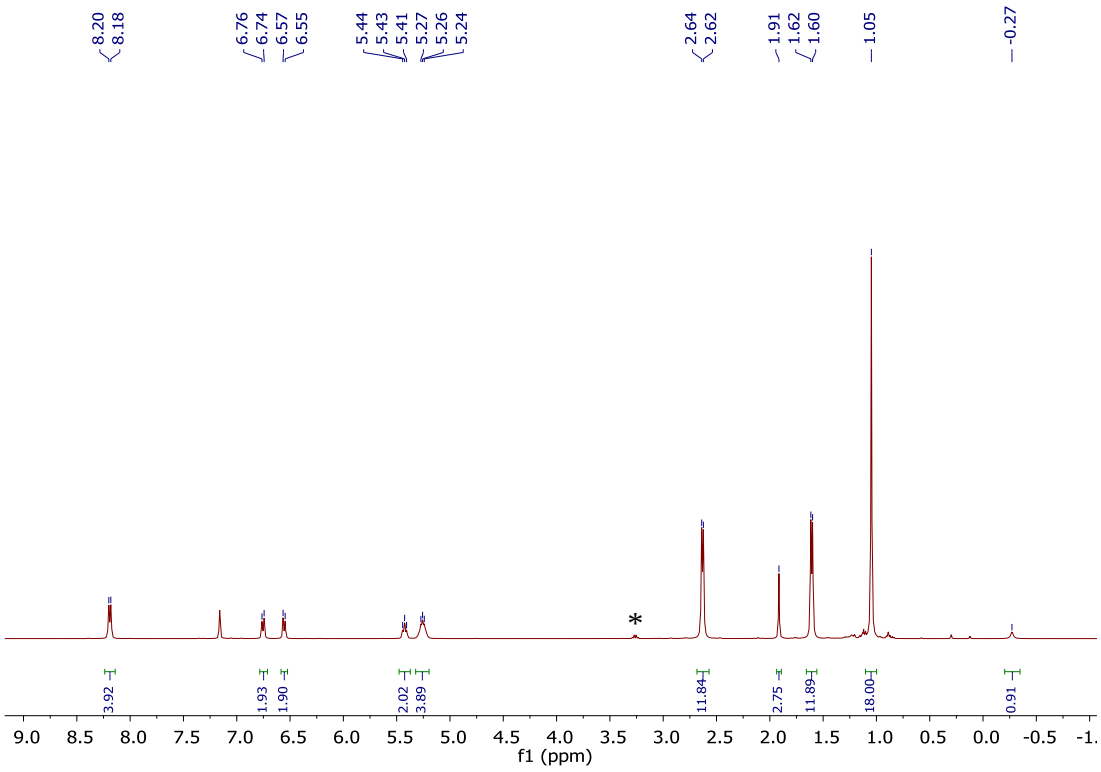

Figure A 7.15. ^{1}H NMR spectrum of [$L^{tBu}Ni^{II}$(*N*,*O*:κ^{2}-NHTs)] (**7.15**) in C_6D_6. (*) indicates the presence of Et_2O.

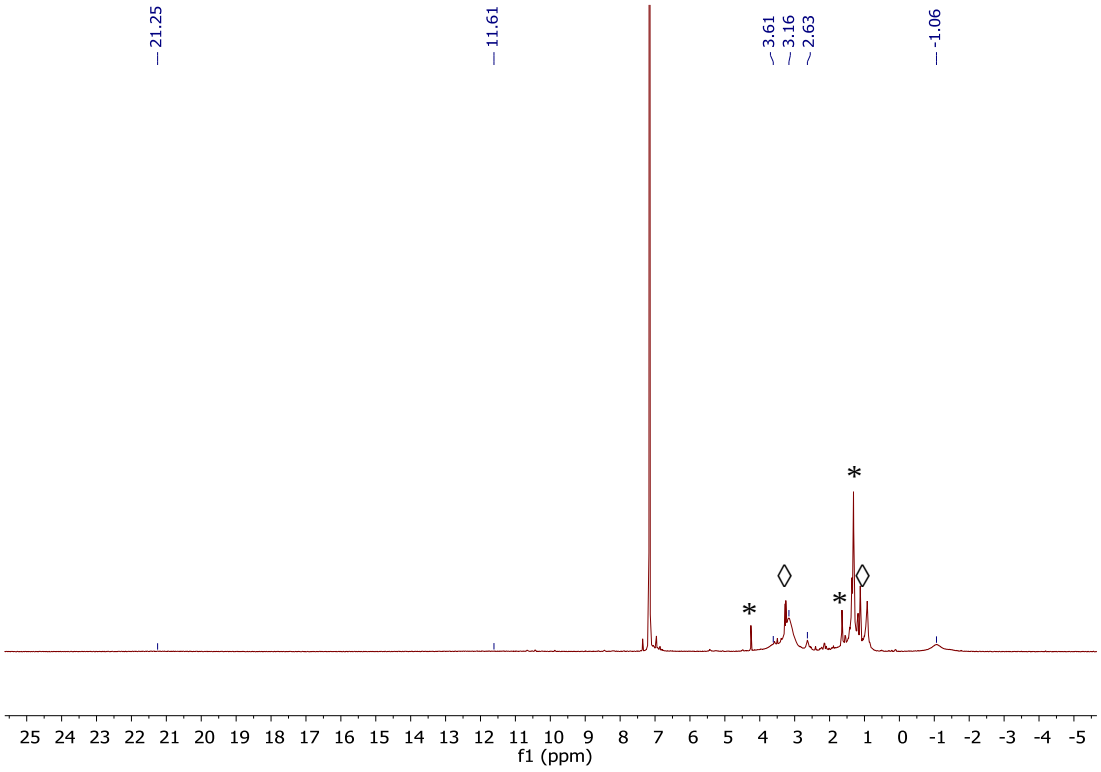

Figure A 7.16. ^{1}H NMR spectrum of [K(18-crown-6)][L^{tBu}Ni^{I}(NHTs)] (**7.16**) in C_6D_6. (*) indicates the presence of unidentified diamagnetic impurity and (◊) indicates the presence of Et_2O.

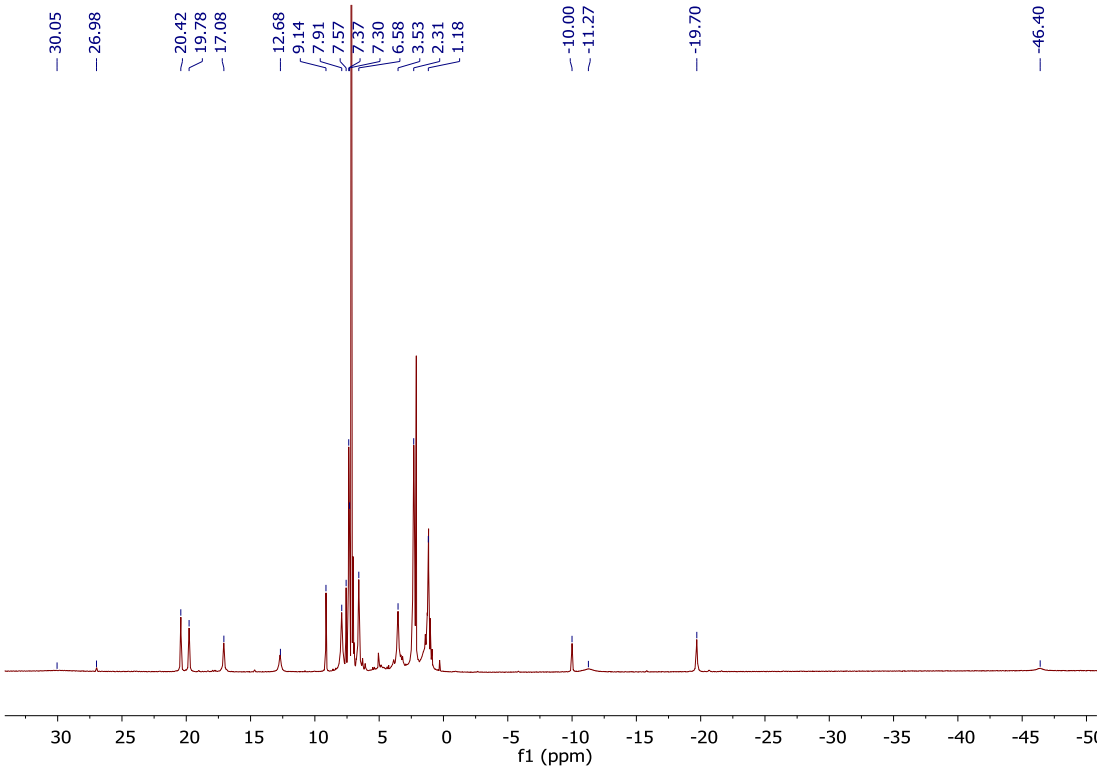

Figure A 7.17. ^{1}H NMR spectrum of [{L^{tBu}(PhNCO)}Ni^{II}(*N*,*O*:κ^{2}-PhNC(O)OCPh$_3$)] (**7.17**) in C_6D_6.

7.6 References

(1) Berry, J. F. Terminal Nitrido and Imido Complexes of the Late Transition Metals. *Comments Inorg. Chem.* **2009**, *30* (1–2), 28.

(2) Ray, K.; Heims, F.; Pfaff, F. F. Terminal Oxo and Imido Transition-Metal Complexes of Groups 9–11. *Eur. J Inorg. Chem.* **2013**, 3784.

(3) Iluc, V. M.; Hillhouse, G. L. Three-Coordinate Nickel Carbene Complexes and Their One-Electron Oxidation Products. *J. Am. Chem. Soc.* **2014**, *136* (17), 6479.

(4) Jenkins, D. M.; Betley, T. A.; Peters, J. C. Oxidative Group Transfer to Co(I) Affords a Terminal Co(III) Imido Complex. *J. Am. Chem. Soc.* **2002**, *124* (38), 11238.

(5) Shay, D. T.; Yap, G. P. A.; Zakharov, L. N.; Rheingold, A. L.; Theopold, K. H. Intramolecular CH Activation by an Open-Shell Cobalt(III) Imido Complex. *Angew. Chem. Int. Ed.* **2005**, *44* (10), 1508.

(6) Mindiola, D. J.; Hillhouse, G. L. Isocyanate and Carbodiimide Synthesis by Nitrene-Group-Transfer from a Nickel(II) Imido Complex. *Chem. Commun.* **2002**, No. 17, 1840.

(7) Jones, C.; Schulten, C.; Rose, R. P.; Stasch, A.; Aldridge, S.; Woodul, W. D.; Murray, K. S.; Moubaraki, B.; Brynda, M.; La Macchia, G.; et al. Amidinato– and Guanidinato–Cobalt(I) Complexes: Characterization of Exceptionally Short Co–Co Interactions. *Angew. Chem. Int. Ed.* **2009**, *48* (40), 7406.

(8) Mindiola, D. J.; Waterman, R.; Iluc, V. M.; Cundari, T. R.; Hillhouse, G. L. Carbon–Hydrogen Bond Activation, C–N Bond Coupling, and Cycloaddition Reactivity of a Three-Coordinate Nickel Complex Featuring a Terminal Imido Ligand. *Inorg. Chem.* **2014**, *53* (24), 13227.

(9) King, E. R.; Sazama, G. T.; Betley, T. A. Co(III) Imidos Exhibiting Spin Crossover and C–H Bond Activation. *J. Am. Chem. Soc.* **2012**, *134* (43), 17858.

(10) Iluc, V. M.; Miller, A. J. M.; Anderson, J. S.; Monreal, M. J.; Mehn, M. P.; Hillhouse, G. L. Synthesis and Characterization of Three-Coordinate Ni(III)-Imide Complexes. *J. Am. Chem. Soc.* **2011**, *133* (33), 13055.

(11) Kogut, E.; Wiencko, H. L.; Zhang, L.; Cordeau, D. E.; Warren, T. H. A Terminal Ni(III)-Imide with Diverse Reactivity Pathways. *J. Am. Chem. Soc.* **2005**, *127* (32), 11248.

(12) Schöffel, J.; Rogachev, A. Y.; DeBeer George, S.; Burger, P. Isolation and Hydrogenation of a Complex with a Terminal Iridium–Nitrido Bond. *Angew. Chem. Int. Ed.* **2009**, *48* (26), 4734.

(13) Scheibel, M. G.; Askevold, B.; Heinemann, F. W.; Reijerse, E. J.; de Bruin, B.; Schneider, S. Closed-Shell and Open-Shell Square-Planar Iridium Nitrido Complexes. *Nat. Chem.* **2012**, *4* (7), 552.

(14) Melenkivitz, R.; Mindiola, D. J.; Hillhouse, G. L. Monomeric Phosphido and Phosphinidene Complexes of Nickel. *J. Am. Chem. Soc.* **2002**, *124* (15), 3846.

(15) Cundari, T. R.; Jimenez-Halla, J. O. C.; Morello, G. R.; Vaddadi, S. Catalytic Tuning of a Phosphinoethane Ligand for Enhanced C−H Activation. *J. Am. Chem. Soc.* **2008**, *130* (39), 13051.

(16) Waterman, R.; Hillhouse, G. L. Group Transfer from Nickel Imido, Phosphinidene, and Carbene Complexes to Ethylene with Formation of Aziridine, Phosphirane, and Cyclopropane Products. *J. Am. Chem. Soc.* **2003**, *125* (44), 13350.

(17) Iluc, V. M.; Hillhouse, G. L. Hydrogen-Atom Abstraction from Ni(I) Phosphido and Amido Complexes Gives Phosphinidene and Imide Ligands. *J. Am. Chem. Soc.* **2010**, *132* (43), 15148.
(18) Hay-Motherwell, R. S.; Wilkinson, G.; Hussain-Bates, B.; Hursthouse, M. B. Synthesis and X-Ray Crystal Structure of Oxotrimesityliridium(V). *Polyhedron* **1993**, *12* (16), 2009.
(19) Poverenov, E.; Efremenko, I.; Frenkel, A. I.; Ben-David, Y.; Shimon, L. J. W.; Leitus, G.; Konstantinovski, L.; Martin, J. M. L.; Milstein, D. Evidence for a Terminal Pt(IV)-Oxo Complex Exhibiting Diverse Reactivity. *Nature* **2008**, *455* (7216), 1093.
(20) Hartmann, N. J.; Wu, G.; Hayton, T. W. Synthesis of a "Masked" Terminal Nickel(II) Sulfide by Reductive Deprotection and Its Reaction with Nitrous Oxide. *Angew. Chem. Int. Ed.* **2015**, *54* (49), 14956.
(21) Smiles, D. E.; Wu, G.; Hayton, T. W. Synthesis of Uranium–Ligand Multiple Bonds by Cleavage of a Trityl Protecting Group. *J. Am. Chem. Soc.* **2014**, *136* (1), 96.
(22) Smiles, D. E.; Wu, G.; Kaltsoyannis, N.; Hayton, T. W. Thorium-Ligand Multiple Bonds via Reductive Deprotection of a Trityl Group. *Chem. Sci.* **2015**, *6* (6), 3891.
(23) Holland, P. L.; Cundari, T. R.; Perez, L. L.; Eckert, N. A.; Lachicotte, R. J. Electronically Unsaturated Three-Coordinate Chloride and Methyl Complexes of Iron, Cobalt, and Nickel. *J. Am. Chem. Soc.* **2002**, *124* (48), 14416.
(24) Hartmann, N. J.; Wu, G.; Hayton, T. W. Reactivity of a Nickel Sulfide with Carbon Monoxide and Nitric Oxide. *J. Am. Chem. Soc.* **2016**, *138* (38), 12352.
(25) Melzer, M. M.; Jarchow-Choy, S.; Kogut, E.; Warren, T. H. Reductive Cleavage of O-, S-, and N-Organonitroso Compounds by Nickel(I) β-Diketiminates. *Inorg. Chem.* **2008**, *47* (22), 10187.
(26) Fan, H.; Adhikari, D.; Saleh, A. a; Clark, R. L.; Zuno-Cruz, F. J.; Sanchez Cabrera, G.; Huffman, J. C.; Pink, M.; Mindiola, D. J.; Baik, M.-H. Understanding and Predicting Distorted T- versus Y-Geometries for Neutral Chromous Complexes Supported by a Sterically Encumbering Beta-Diketiminate Ligand. *J. Am. Chem. Soc.* **2008**, *130* (51), 17351.
(27) Eckert, N. A.; Dinescu, A.; Cundari, T. R.; Holland, P. L. A T-Shaped Three-Coordinate Nickel(I) Carbonyl Complex and the Geometric Preferences of Three-Coordinate D9 Complexes. *Inorg. Chem.* **2005**, *44* (22), 7702.
(28) Yao, S.; Xiong, Y.; Zhang, X.; Schlangen, M.; Schwarz, H.; Milsmann, C.; Driess, M. Facile Dissociation of $[(LNi^{II})_2E_2]$ Dichalcogenides: Evidence for $[LNi^{II}E_2]$ Superselenides and Supertellurides in Solution. *Angew. Chem. Int. Ed.* **2009**, *48* (25), 4551.
(29) Hartmann, N. J.; Wu, G.; Hayton, T. W. Activation of CS_2 by a "Masked" Terminal Nickel Sulfide. *Dalt. Trans.* **2016**, *45*, 14508.
(30) Holze, P.; Horn, B.; Limberg, C.; Matlachowski, C.; Mebs, S. The Activation of Sulfur Hexafluoride at Highly Reduced Low-Coordinate Nickel Dinitrogen Complexes. *Angew. Chem. Int. Ed.* **2014**, *53* (10), 2750.
(31) Horn, B.; Limberg, C.; Herwig, C.; Braun, B. Three-Coordinate Nickel(II) and Nickel(I) Thiolate Complexes Based on the β-Diketiminate Ligand System. *Inorg. Chem.* **2014**, *53* (13), 6867.
(32) Eckert, N. A.; Bones, E. M.; Lachicotte, R. J.; Holland, P. L. Nickel Complexes of a

Bulky Beta-Diketiminate Ligand. *Inorg. Chem.* **2003**, *42* (5), 1720.
(33) Holland, P. L.; Cundari, T. R.; Perez, L. L.; Eckert, N. a; Lachicotte, R. J. Electronically Unsaturated Three-Coordinate Chloride and Methyl Complexes of Iron, Cobalt, and Nickel. *J. Am. Chem. Soc.* **2002**, *124* (48), 14416.
(34) Evans, D. F. The Determination of the Paramagnetic Susceptibility of Substances in Solution by Nuclear Magnetic Resonance. *J. Chem. Soc.* **1959**, 2003.
(35) Hartmann, N. J.; Wu, G.; Hayton, T. W. Trapping of an Ni^{II} Sulfide by a Co^{I} Fulvene Complex. *Organometallics* **2017**, *36* (9), 1765.
(36) Köthe, C.; Braun, B.; Herwig, C.; Limberg, C. Synthesis, Characterization, and Interconversion of β-Diketiminato Nickel N_xH_y Complexes. *Eur. J Inorg. Chem.* **2014**, *2014* (31), 5296.
(37) Carmona, E.; Marín, J. M.; Palma, P.; Paneque, M.; Poveda, M. L. Pyrrolyl, Hydroxo, and Carbonate Organometallic Derivatives of Nickel(II). Crystal and Molecular Structure of $[Ni(CH_2C_6H_4\text{-}o\text{-}Me)(PMe_3)(\mu\text{-}OH)]2\bullet 2,5\text{-}HNC_4H_2Me_2$. *Inorg. Chem.* **1989**, *28* (10), 1895.
(38) Kitajima, N.; Hikichi, S.; Tanaka, M.; Morooka, Y. Fixation of Atmospheric Carbon Dioxide by a Series of Hydroxo Complexes of Divalent Metal Ions and the Implication for the Catalytic Role of Metal Ion in Carbonic Anhydrase. Synthesis, Characterization, and Molecular Structure of $[LM(OH)]_n$ (n =. *J. Am. Chem. Soc.* **1993**, *115* (13), 5496.
(39) Lozano, A. A.; Sáez, M.; Pérez, J.; García, L.; Lezama, L.; Rojo, T.; López, G.; García, G.; Santana, M. D. Structure and Magnetic Properties of Carbonate-Bridged Five-Coordinate Nickel(II) Complexes Controlled by Solvent Effect. *Dalt. Trans.* **2006**, *0* (32), 3906.
(40) Huang, D.; Holm, R. H. Reactions of the Terminal $Ni^{II}-OH$ Group in Substitution and Electrophilic Reactions with Carbon Dioxide and Other Substrates: Structural Definition of Binding Modes in an Intramolecular $Ni^{II}\cdots Fe^{II}$ Bridged Site. *J. Am. Chem. Soc.* **2010**, *132* (13), 4693.
(41) Huang, D.; Makhlynets, O. V.; Tan, L. L.; Lee, S. C.; Rybak-Akimova, E. V.; Holm, R. H. Fast Carbon Dioxide Fixation by 2,6-Pyridinedicarboxamidato-Nickel(II)-Hydroxide Complexes: Influence of Changes in Reactive Site Environment on Reaction Rates. *Inorg. Chem.* **2011**, *50* (20), 10070.
(42) Schmeier, T. J.; Nova, A.; Hazari, N.; Maseras, F. Synthesis of PCP-Supported Nickel Complexes and Their Reactivity with Carbon Dioxide. *Chem. - A Eur. J.* **2012**, *18* (22), 6915.
(43) Gomberg, M. An Instance of Trivalent Carbon: Triphenylmethyl. *J. Am. Chem. Soc.* **1900**, *22* (11), 757.
(44) Ye, S.; Neese, F. Nonheme Oxo-Iron(IV) Intermediates Form an Oxyl Radical upon Approaching the C-H Bond Activation Transition State. *Proc. Natl. Acad. Sci. U. S. A.* **2011**, *108* (4), 1228.
(45) Shimoyama, Y.; Ishizuka, T.; Kotani, H.; Shiota, Y.; Yoshizawa, K.; Mieda, K.; Ogura, T.; Okajima, T.; Nozawa, S.; Kojima, T. A Ruthenium(III)-Oxyl Complex Bearing Strong Radical Character. *Angew. Chemie Int. Ed.* **2016**, *55* (45), 14041.
(46) Smith, J. M.; Lachicotte, R. J.; Holland, P. L. Tuning Metal Coordination Number by Ancillary Ligand Steric Effects: Synthesis of a Three-Coordinate Iron(II) Complex. *Chem. Commun.* **2001**, *0* (17), 1542.

(47) Chen, C.; Bellows, S. M.; Holland, P. L. Tuning Steric and Electronic Effects in Transition-Metal [Small Beta]-Diketiminate Complexes. *Dalt. Trans.* **2015**.
(48) Panda, A.; Stender, M.; Wright, R. J.; Olmstead, M. M.; Klavins, P.; Power, P. P. Synthesis and Characterization of Three-Coordinate and Related Beta-Diketiminate Derivatives of Manganese, Iron, and Cobalt. *Inorg. Chem.* **2002**, *41*, 3909.
(49) Javier Vela; Vaddadi, S.; Cundari, T. R.; Smith, J. M.; Gregory, E. A.; Lachicotte, R. J.; Flaschenriem, C. J.; Holland, P. L. Reversible Beta-Hydrogen Elimination of Three-Coordinate Iron(II) Alkyl Complexes: Mechanistic and Thermodynamic Studies. *Organometallics* **2004**, *23* (22), 5226.
(50) Eckert, N. A.; Smith, J. M.; Lachicotte, R. J.; Holland, P. L. Low-Coordinate Iron(II) Amido Complexes of Beta-Diketiminates: Synthesis, Structure, and Reactivity. *Inorg. Chem.* **2004**, *43* (10), 3306.
(51) Eckert, N. A.; Stoian, S.; Smith, J. M.; Bominaar, E. L.; Münck, E.; Holland, P. L. Synthesis, Structure, and Spectroscopy of an Oxodiiron(II) Complex. *J. Am. Chem. Soc.* **2005**, *127* (26), 9344.
(52) Eckert, N. A.; Stoian, S.; Smith, J. M.; Bominaar, E. L.; Münck, E.; Holland, P. L. Synthesis, Structure, and Spectroscopy of an Oxodiiron(II) Complex. *J. Am. Chem. Soc.* **2005**, *127* (26), 9344.
(53) Holland, P. L. Electronic Structure and Reactivity of Three-Coordinate Iron Complexes. *Acc. Chem. Res.* **2008**, *41* (8), 905.
(54) Chiang, K. P.; Bellows, S. M.; Brennessel, W. W.; Holland, P. L. Multimetallic Cooperativity in Activation of Dinitrogen at Iron–potassium Sites. *Chem. Sci.* **2014**, *5* (1), 267.
(55) Chiang, K. P.; Scarborough, C. C.; Horitani, M.; Lees, N. S.; Ding, K.; Dugan, T. R.; Brennessel, W. W.; Bill, E.; Hoffman, B. M.; Holland, P. L. Characterization of the Fe-H Bond in a Three-Coordinate Terminal Hydride Complex of Iron(I). *Angew. Chem. Int. Ed.* **2012**, *51* (15), 3658.
(56) Cornella, J.; Edwards, J. T.; Qin, T.; Kawamura, S.; Wang, J.; Pan, C. M.; Gianatassio, R.; Schmidt, M.; Eastgate, M. D.; Baran, P. S. Practical Ni-Catalyzed Aryl-Alkyl Cross-Coupling of Secondary Redox-Active Esters. *J. Am. Chem. Soc.* **2016**, *138* (7), 2174.
(57) Edwards, J. T.; Merchant, R. R.; McClymont, K. S.; Knouse, K. W.; Qin, T.; Malins, L. R.; Vokits, B.; Shaw, S. A.; Bao, D. H.; Wei, F. L.; et al. Decarboxylative Alkenylation. *Nature* **2017**, *545* (7653), 213.
(58) Li, C.; Wang, J.; Barton, L. M.; Yu, S.; Tian, M.; Peters, D. S.; Kumar, M.; Yu, A. W.; Johnson, K. A.; Chatterjee, A. K.; et al. Decarboxylative Borylation. *Science (80-.).* **2017**, *356* (6342), eaam7355.
(59) Mindiola, D. J.; Hillhouse, G. L. Synthesis, Structure, and Reactions of a Three-Coordinate Nickel-Carbene Complex, {1,2-Bis(Di-Tert-Butylphosphino)Ethane}NiCPh$_2$. *J. Am. Chem. Soc.* **2002**, *124* (34), 9976.
(60) Mindiola, D. J.; Hillhouse, G. L. Terminal Amido and Imido Complexes of Three-Coordinate Nickel. *J. Am. Chem. Soc.* **2001**, *123* (19), 4623.
(61) Ayala, C. N.; Chisholm, M. H.; Gallucci, J. C.; Krempner, C. Chemistry of BDI*M(2+) Complexes (M = Mg, Zn) and Their Role in Lactide Polymerization Where BDI* Is the Anion Derived from Methylenebis(C-TBu, N-2,6-Diisopropylphenyl)Imine BDI*H. *Dalt. Trans.* **2009**, *0* (42), 9237.

(62) Chiang, K. P.; Barrett, P. M.; Ding, F.; Smith, J. M.; Kingsley, S.; Brennessel, W. W.; Clark, M. M.; Lachicotte, R. J.; Holland, P. L. Ligand Dependence of Binding to Three-Coordinate Fe(II) Complexes. *Inorg. Chem.* **2009**, *48* (12), 5106.
(63) Power, P. P.; Shoner, S. C. The Neutral Transition Metal Thiolates$[M(SAr)_2]_2$ (M = Mn, Fe or Co, Ar = 2,4,6-t-$Bu_3C_6H_2$). *Angew. Chemie Int. Ed. English* **1991**, *30* (3), 330.
(64) Varonka, M. S.; Warren, T. H. S-Nitrosothiol and Nitric Oxide Reactivity at β-Diketiminato Zinc Thiolates. *Inorg. Chim. Acta* **2007**, *360* (1), 317.
(65) Ayala, C. N.; Chisholm, M. H.; Gallucci, J. C.; Krempner, C. Chemistry of BDI*M(2+) Complexes (M = Mg, Zn) and Their Role in Lactide Polymerization Where BDI* Is the Anion Derived from Methylenebis(C-TBu, N-2,6-Diisopropylphenyl)Imine BDI*H. *Dalt. Trans.* **2009**, No. 42, 9237.
(66) Chisholm, M. H.; Gallucci, J.; Phomphrai, K. Coordination Chemistry and Reactivity of Monomeric Alkoxides and Amides of Magnesium and Zinc Supported by the Diiminato Ligand CH(CMeNC6H3-2,6-i Pr2)2. A Comparative Study. *Inorg. Chem.* **2002**, *41* (10), 2785.
(67) Anacona, J. R.; Azocar, M.; Nusetti, O.; Rodriguez-Barbarin, C. Crystal Structure of the First SH-Containing Tetrahedral Cobalt(II) Complex, $[Co(Quinoline)_2(SH)_2]$. Superoxide Dismutase Activity. *Transit. Met. Chem.* **2003**, *28* (1), 24.
(68) Wuts, P. G. M.; Greene, T. W. *Greene's Protective Groups in Organic Synthesis*; John Wiley & Sons, Inc.: Hoboken, NJ, USA, 2006.
(69) Ankner, T.; Hilmersson, G. Instantaneous Deprotection of Tosylamides and Esters with SmI_2/Amine/Water. *Org. Lett.* **2009**, *11* (3), 503.
(70) Tam, E. C. Y.; Johnstone, N. C.; Ferro, L.; Hitchcock, P. B.; Fulton, J. R. Carbon Dioxide Activation by "Non-Nucleophilic" Lead Alkoxides. *Inorg. Chem.* **2009**, *48* (18), 8971.
(71) Scheuermann, M. L.; Luedtke, A. T.; Hanson, S. K.; Fekl, U.; Kaminsky, W.; Goldberg, K. I. Reactions of Five-Coordinate Platinum(IV) Complexes with Molecular Oxygen. *Organometallics* **2013**, *32* (17), 4752.
(72) Kalita, A.; Kumar, V.; Mondal, B. C-Nitrosation of a β-Diketiminate Ligand in Copper(II) Complex. *RSC Adv.* **2015**, *5* (1), 643.
(73) Basuli, F.; Huffman, J. C.; Mindiola, D. J. Reactivity at the β-Diketiminate Ligand Nacnac$^-$ on Titanium(IV). Diimine-Alkoxo and Bis-Anilido Ligands Stemming from the Nacnac$^-$ Skeleton. *Inorg. Chem.* **2003**, *42* (24), 8003.
(74) Yempally, V.; Fan, W. Y.; Arndtsen, B. A.; Bengali, A. A. Intramolecular C–C Bond Coupling of Nitriles to a Diimine Ligand in Group 7 Metal Tricarbonyl Complexes. *Inorg. Chem.* **2015**, *54* (23), 11441.
(75) Gregory, E. A.; Lachicotte, R. J.; Holland, P. L. A Cationic Three-Coordinate Iron(II) Complex and the Reaction of β-Diketiminate with Ethyl Diazoacetate. *Organometallics* **2005**, *24* (8), 1803.
(76) Chadwick, S.; Englich, U.; Ruhlandt-Senge, K. Lewis Base Coordination versus Cation−π Interaction in Monomeric and Hexameric Potassium Thiolates. *Organometallics* **1997**, *16* (26), 5792.
(77) Poulton, J. T.; Sigalas, M. P.; Folting, K.; Streib, W. E.; Eisenstein, O.; Caulton, K. G. $RuHX(CO)(PR_3)_2$: Can ν_{CO} Be a Probe for the Nature of the Ru-X Bond? *Inorg. Chem.* **1994**, *33* (7), 1476.

(78) Harris Robin, K.; Becker Edwin, D.; Cabral de Menezes Sonia, M.; Goodfellow, R.; Granger, P. NMR Nomenclature: Nuclear Spin Properties and Conventions for Chemical Shifts. IUPAC Recommendations 2001. International Union of Pure and Applied Chemistry. Physical Chemistry Division. Commission on Molecular Structure and Spectroscopy. *Pure Appl. Chem.* **2002**, *40* (7), 489.
(79) Harris Robin, K.; Becker Edwin, D.; Cabral De Menezes Sonia, M.; Granger, P.; Hoffman Roy, E.; Zilm Kurt, W. Further Conventions for NMR Shielding and Chemical Shifts. *Pure Appl. Chem.* **2008**, *80*, 59.
(80) Dekamin, M. G.; Peyman, S. Z. Phthalimide-N-Oxyl Salts: Efficient Organocatalysts for Facile Synthesis of (Z)-3-Methyl-4-(Arylmethylene)-Isoxazole-5(4H)-One Derivatives in Water. *Monatshefte für Chemie - Chem. Mon.* **2016**, *147* (2), 445.
(81) Bottino, F.; Di Grazia, M.; Pappalardo, S.; Finocchiaro, P.; Mamo, A.; Fronczek, F. R. Reaction of Tosylamide Monosodium Salt with Bis(Halomethyl) Compounds: An Easy Entry to Symmetrical N-Tosyl Aza Macrocycles. *J. Org. Chem.* **1988**, *53* (15), 3521.
(82) SMART Apex II. Bruker AXS Inc.: Madison, WI 2005.
(83) SAINT Software User's Guide. Bruker AXS Inc.: Madison, WI 2005.
(84) Sheldrick, G. M. SADABS. University of Gottingen: Germany 2005.
(85) SHELXTL PC. Bruker AXS Inc.: Madison, WI 2005.